

**Die Expeditionen ANTARKTIS IX/1-4
des Forschungsschiffes „POLARSTERN“ 1990/91**

**The Expeditions ANTARKTIS IX/1-4
of the Research Vessel “POLARSTERN“ in 1990/91**

**Herausgegeben von / Edited by
Ulrich Bathmann, Meinhard Schulz-Baldes,
Eberhard Fahrbach, Victor Smetacek,
Hans-Wolfgang Hubberten
unter Mitarbeit der Fahrtteilnehmer /
with contributions of the participants**

**Ber. Polarforsch. 100 (1992)
ISSN 0176 - 5027**

ANTARKTIS IX/1-4

20 October 1990 - 13 May 1991

KOORDINATOR/COORDINATOR

Victor Smetacek

ANT IX/1: Bremerhaven - Punta Arenas
FAHRTLEITER/CHIEF SCIENTIST
Meinhard Schulz-Baldes

ANT IX/2: Punta Arenas - Cape Town
FAHRTLEITER/CHIEF SCIENTIST
Eberhard Fahrbach

ANT IX/3: Cape Town - Cape Town
FAHRTLEITER/CHIEF SCIENTIST
Victor Smetacek

ANT IX/4: Cape Town - Bremerhaven
FAHRTLEITER/CHIEF SCIENTIST
Hans-Wolfgang Hubberten

Landgestützte Arbeiten auf der König-Georg-Insel
M. Rauschert

The coordinator appreciates the skilful technical assistance
of Ingrid Lukait during the edition of this cruise report.

INHALT / CONTENTS

EINLEITUNG	1
FOREWORD	2
Fahrtabschnitt ANT IX/1.....	4
1. Schwermetalle in diversen Kompartimenten	5
1.1. Zielsetzung.....	5
1.2. Oberflächenwasser	5
1.3. Tiefenwasser	5
1.4. Voltammetrische Analysen von Oberflächenwasser	6
1.5. Spurenmetalle in marinem Regen	6
1.6. Extraktion und AAS-Analyse	7
1.7. Partikuläre Substanz.....	7
1.8. Neuston	7
1.9. Tiefenplankton.....	10
2. Chlorophyll im Phytoplankton und DMSP in Phytoplankton und Neuston	11
3. Mikrozooplankton und Nannoplankton	12
3.1. Tiefenstationen.....	12
3.1.1. Phytoplanktonproben.....	12
3.1.2. Nährstoff-Proben.....	14
3.1.3. Oberflächenwasserproben	14
3.2. Lebendkulturen und Proben von Coccolithophoriden	17
3.3. Mikrozooplanktonproben	18
3.4. Hydrologie.....	20
3.5. Vorläufige Beobachtungen und Ergebnisse	21
4. Gasförmige Salpetersäure, Ammoniak und partikelförmiges Ammoniumnitrat in der Atmosphäre.....	22
5. Biogene Schwefelverbindungen und deren Reaktionsprodukte in Seewasser und mariner Atmosphäre.....	23
6. Polychlorbiphenyle (PCB), Hexachlorcyclohexan-Isomeren (HCH) und Hexachlorbenzols (HCB) in der Grundsicht der Troposphäre und im ozeanischen Oberflächenwasser.....	24
7. Organobromverbindungen in der marinen Troposphäre und im atlantischen Oberflächenwasser	26
8. Messungen von atmosphärischem Quecksilber über dem Atlantik.....	27
9. Messungen zur spektralen optischen Dicke des Aerosols über Meer	28
10. Fernerkundung stratosphärischer Spurenstoffe mit Absorptions-Spektroskopie im ultravioletten und sichtbaren Spektralbereich	29
11. Aktivitäten am neuen Bordrechnersystem während ANT IX/1	30

Fahrtabschnitt ANT IX/2.....	31
1. Fahrtverlauf und Zusammenfassung	31
1. Itinerary and summary	36
2. Physical Oceanography	39
2.1 Water masses and circulation	39
2.2. Distribution of dissolved inorganic nutrients in the water column	54
2.3. Tritium and Helium measurements	56
2.4. Water level measurements	56
2.5. Optical properties of sea water.....	58
2.6. Underway measurements of current profiles, XBTs and the thermosalinograph	58
3. Chemistry	65
3.1. Measurements of biogenic sulfur compounds and their reaction products in sea water and the marine atmosphere	65
3.2. Measurements of the concentration of Nitric acid, Ammonia and Ammonium Nitrate in the marine atmosphere.....	66
3.3. Organobromine compounds in the ocean and atmosphere.....	66
3.4. Biogeochemistry of Silica.....	68
3.5. Biogeochemistry of Barium.....	70
4. Marine Biology	71
4.1. Energy flux at the base of the Antarctic food web.....	71
4.2. Phytoplankton biomass and species distribution	72
4.3. DMS - Production by Antarctic phytoplankton species.....	73
4.4. Effect of dissolved organic compounds derived from "brown ice" on the development of surface phytoplankton in the Weddell Sea.....	75
4.5. Reproduction and life cycles of dominant copepods in the Weddell Sea.....	80
4.6. Comparative studies on the temperature dependence and kinetics of digestive enzymes in crustaceans.....	82
4.7. ³² Si applied to marine biology.....	83
5. Marine Geology.....	84
5.1. Bathymetry	84
5.2. Sediment distribution	86
5.3. Particle flux in the water column	88
5.4. Stable isotopes in the water column	90
5.5. Natural radioactive isotopes in the water column.....	90
6. Postinstallation work on the computer system	91
7. Weather conditions.....	92
8. Ice conditions.....	93
9. Acknowledgements.....	94

Fahrtabschnitt ANT IX/3.....	95
1. Einleitung	95
1. Introduction	101
2. Weather conditions.....	105
3. Ice observations in the eastern Weddell and Lazarev Seas.....	107
4. Water column studies.....	125
4.1. Physical oceanography.....	125
4.1.1 Oceanographic tracer studies	142
4.1.2. Measurements of turbulent fluctuations of temperature and current velocity at long ice stations.....	143
4.1.3. Sea ice motion and mixed layer dynamics by meteorological ARGOS buoys.....	143
4.2. Sea ice and plankton ecology.....	143
4.2.1. Sea ice physics and chemistry.....	144
4.2.2 Sea ice ecology	146
4.2.3. Water column ecology	163
4.3. Plankton experiments	180
4.3.1. Experiments with natural algal populations from water and sea ice.....	180
4.3.2. Zooplankton.....	182
5. Benthos.....	185
5.1. Macrozoobenthos ecology.....	185
5.1.1. The use of Hydrosweep data for biological sampling activities.....	188
5.1.2. Faunistic-ecological investigations by means of underwater photography.....	189
5.1.3. Macrofauna sampling and <i>in-situ</i> observation with the multibox corer	192
5.1.4. Preliminary subsample evaluation from AGT and GSN catches.....	193
5.1.5. Studies on the benthic molluscs (Gastropoda and Bivalvia).....	196
5.1.6. Amphipod biology.....	199
5.1.7. Distribution and reproductive biology of caridean shrimps (Decapoda: <i>Natantia</i>) in the Lazarev Sea, and comparisons with the Weddell Sea	200
5.1.8. Ecohistological studies on Antarctic benthic invertebrates.....	204
5.2. Meiofauna and microfauna.....	206
5.2.1. Rhizopodan protists and nematodes at the sediment surface and in sea ice.....	206
5.3. Comparative investigations on fishes of the Weddell and the Lazarev Seas.....	208
6. Geology	223
6.1. Marine-geological and geophysical investigations.....	223
6.1.1. Glaciomarine sedimentary processes in the Weddell and Lazarev Seas.....	223
6.1.2. Physical properties of the sediments and other geophysical investigations.....	245
6.2. Bathymetry and Seafloor Mapping by Hydrosweep	246
6.2.1. Depth and Navigation Data Evaluation, Processing and Seafloor Mapping.....	246
6.2.2. Sea Floor Topography in Selected Areas (Examples).....	248

6.2.3.	Future Research and Development Work.....	254
6.3.	Geochemistry.....	257
6.3.1.	Uranium-series radionuclides in the water column.....	257
6.3.2.	The carbonate system.....	258

Fahrtabschnitt ANT IX/4..... 262

1.	Zusammenfassung und Fahrtverlauf	262
2.	Summary and Itinerary	269
3.	Das Wetter während ANT-IX/4	272
4.	Bathymetrische und sedimentechographische Profilmessungen.....	274
4.1	Bathymetrie und Meeresbodenkartierung mit Hydrosweep.....	274
4.2.	Sedimentechographie.....	279
5.	Marin-geologische und sedimentphysikalische Arbeiten.....	285
5.1.	Geräteeinsatz und Probennahme	285
5.2.	Sedimentphysikalische Untersuchungen.....	288
5.2.1.	Messung der magnetischen Suszeptibilität.....	288
5.2.2.	Messung des elektrischen Widerstandes	289
5.3.	Sedimentologische Untersuchungen.....	292
5.3.1	Beprobung von Sedimentkernen	292
5.3.2	Sedimentbeschreibung	293
5.3.3	Porzellanitbeprobung	301
5.3.4	Tonmineralogie	301
5.3.5	Barytakkumulation im Oberflächensediment.....	302
5.3.6	Rekonstruktion von Oberflächentemperaturen mit Hilfe von Ketonen	303
5.4.	Paläontologische Bearbeitung von Sedimentproben	303
5.4.1.	Diatomeen und Radiolarien.....	303
5.4.2	Benthische Foraminiferen und stabile Isotope.....	305
5.5.	Stratigraphische Ergebnisse.....	307
6.	Untersuchungen in der Wassersäule	311
6.1	CTD-Messungen.....	311
6.2.	Plankton.....	313
6.2.1.	Planktonuntersuchungen	313
6.2.2.	Mikrozooplankton und Nannoplankton	317
6.3.	Verankerungsarbeiten und Sedimentfallen	325
7.	Spurenstoffe in der maritimen Atmosphäre und Hydrosphäre.....	327
7.1.	Schwerflüchtige Organochlorverbindungen in der troposphärischen Grundsicht und im Oberflächenwasser.....	327
7.2.	Organobromverbindungen in der marinen Troposphäre und im atlantischen Oberflächenwasser	328
8.	Untersuchungen zum Nahrungsverhalten und zur Aktivität hochantarktischer Garnelen (Decapoda: <i>Natantia</i>).....	329

Landgestützte biologische Arbeiten auf der König-Georg-Insel (Südshetlandinseln, Antarktis)	333
1. Einleitung.....	333
2. Summary.....	333
3. Faunistisch/ökologische Arbeiten im Benthal der Maxwellbucht und der Fildes-Straße.....	335
3.1 Technik, Methodik	335
3.2 Quantitative Probennahmen	335
3.3. Qualitative Probennahmen.....	336
3.4. Bodenmorphologie und Bodenbesiedlung.....	336
3.5 Sapropel-Indikator	337
3.6 Bemerkungen zur Polychaetenfauna.....	338
3.7 Bemerkungen zur Amphipodenfauna	339
4. Untersuchungen am Adeliepinguin (<i>Pygoscelis adeliae</i>) und am Eselspinguin (<i>Pygoscelis papua</i>) auf Ardley Island (King George Island, Antarktis) im Südsommer 1990/91.....	343
 Anhang 1: Station lists	 345
ANT IX/1	345
ANT IX/2	345
ANT IX/3	349
ANT IX/4	358
 Anhang 2: Core descriptions	 361
ANT IX/3	362
ANT IX/4	379
Anhang 3: Participating Institutions	397
Anhang 4: Ship's Crew.....	400
Anhang 5: Participants.....	401

EINLEITUNG

V.Smetacek, U. Bathmann (AWI)

Die neunte Expedition mit FS 'Polarstern' in die Antarktis, ANT IX, begann am 20. Oktober 1990, setzte sich aus vier Fahrtabschnitten zusammen und war am 13. Mai 1991 beendet. Die Überfahrt durch den Atlantik während des ersten Fahrtabschnittes war vorwiegend chemischen Untersuchungen der Atmosphäre und des Ozeans gewidmet. Auf dem zweiten Abschnitt erfolgte die ozeanographische Erfassung des Weddellwirbels im Rahmen des World Ocean Circulation Experiments (WOCE). Der dritte Fahrtabschnitt sollte ursprünglich ins südwestliche Weddellmeer führen, mußte dann jedoch aufgrund der extrem schwierigen Eisverhältnisse mit neuen Arbeitsplänen für alle Gruppen der physikalischen Ozeanographie, der Biologie und der Geologie in die Lazarev See umgelenkt werden. Während des vierten Abschnitts wurde ein vorwiegend geologisches Arbeitsprogramm auf dem Rückweg im Südatlantik absolviert.

Auf dem Abschnitt Bremerhaven - Punta Arenas setzten Chemiker ihre umfangreichen langjährigen Untersuchungen über Nord-Süd-Unterschiede der Konzentrationen verschiedener organischer und anorganischer Stoffe in der Atmosphäre und deren Wechselwirkung mit dem Ozean fort. Am 14. November traf FS "Polarstern" in Punta Arenas ein.

Am 17. November 1990 verließ "Polarstern" Punta Arenas mit Kurs auf King George Island. Dort wurden 3 Wissenschaftler mit Ausrüstung auf der russischen Station Bellingshausen abgesetzt. Auf der sich daran anschließenden ozeanographisch-biologischen Profildfahrt quer durch das Weddellmeer wurden 21 Verankerungen ausgebracht und 7 aufgenommen, die Daten zur Bilanzierung der Strömungsverhältnisse und zum vertikalen Stofftransport im Ozean liefern. Flankierende Profile von CTD, Nährsalzen, Organismenverteilung und deren Produktion haben verschiedenen Wassermassen charakterisiert. Ein Besuch der Georg-von-Neumayer-Station (GvN) zwecks Entladung von Ausrüstungsgegenständen erfolgte kurz vor Abschluß dieses Abschnittes, der am 30. 12. 1990 in Kapstadt beendet war.

Drei Tage später, am 3. Januar 1991, verließ FS 'Polarstern' Kapstadt, um Personal und weitere wissenschaftliche und Versorgungsgüter zur GvN zu transportieren. Kurz nach Verlassen von GvN gelang die Bergung von 5 mit einem Hubschrauber verunglückten Südafrikanern, die 300 km von der Küste entfernt gestrandet waren. Im Anschluß erfolgte der Vorstoß in das bisher unbekannte südwestliche Weddellmeer, der Anfang Februar nach mehrmaligem Festsitzen von FS 'Polarstern' im aufgetürmten Eisbrei des süd-östlichen Weddellmeeres abgebrochen wurde. Während der Drift im Eisbrei wurden biologischen Prozesse zum Stoffumsatz im Eis und im oberen Pelagial und die Strömungsverhältnisse unter dem Eis verfolgt. Die Besiedlung des Meeresbodens wurde dort auf dem Schelf und entlang des Kontinentalhanges ebenso aufgenommen, wie anschließend auf dem Schelf der Lazarev See. Wie die anderen Arbeitsgruppen für ihren Bereich, hatten auch die Geologen ein Alternativprogramm zur Meeresbodenbeprobung und -vermessung für die Rekonstruktion der rezenten Geschichte dieses Gebietes entwickelt, das sowohl Transekte über das Schelf als auch in die Tiefsee des nord-östlichen Weddellmeeres und bis zur untermeerischen Erhebung der Maudkuppe einschloß. Nach der Aufnahme von Personal von GvN sowie von der

weiter östlich gelegenen Georg-Forster-Station traf "Polarstern" am 28. März 1991 in Kapstadt ein.

Der vierte Fahrtabschnitt, der nach zwei Hafentagen am 30. März 1991 begann, führte eine geologische Forschergruppe aus dem Sonderforschungsbereich 216 der Universität Bremen und aus dem AWI zur Bouvet Insel. Die Beprobung und Vermessung submariner Erhebungen bildeten das wissenschaftliche Hauptinteresse dieses Abschnittes mit FS "Polarstern", das am 13. Mai 1991 nach Bremerhaven zurückkehrte.

FOREWORD

V.Smetacek, U. Bathmann (AWI)

The ninth research cruise of RV "Polarstern" to the Antarctic (ANT IX) consisted of 4 Legs. The first Leg addressed chemical interactions between ocean and atmosphere during the southward voyage. The second Leg carried out investigations of the Weddell Gyre within the framework of the World Ocean Circulation Experiment (WOCE). The third Leg was planned as a broad-based, interdisciplinary study of the hitherto unexplored southwestern Weddell Sea but had to be reorganized with a new scientific program for the Lazarev Sea because of exceptionally heavy ice conditions in the Weddell Sea. The fourth Leg was the return journey and was primarily devoted to the geology of the South Atlantic.

RV "Polarstern" departed from Bremerhaven on October 20, 1990 and arrived in Punta Arenas on November 14. The intensive chemical research programme was a continuation of previous Atlantic crossings and addressed hemispheric variability of metals and various natural and anthropogenic compounds in atmosphere and ocean.

The second Leg commenced on November 17 and proceeded first to King George Island where personnel and supplies were dropped off at the Bellingshausen station. From there, the transect across the Weddell Gyre first performed in the winter of 1989, was repeated. Twenty one current meter moorings were deployed and the 7 in the field since 1989 were successfully recovered and equipped with new instruments. Water column measurements of physical, chemical and biological parameters were carried out; the data will aid in assessing seasonal differences in hydrography and their influence on the ecology of the Gyre. The current meter data will enable quantification of bottom water formation and transport of water out of and into the Gyre. Sediment traps attached to three of the current meter moorings were also serviced. The data obtained from them, together with results of specific studies on silica cycling, will further our knowledge on vertical particle flux and cycling of matter in the Weddell Sea. At the end of the cruise, equipment was dropped at the Georg-von-Neumeyer Station (GvN). Cape Town was reached on December 30, 1990.

The third leg left Cape Town on January 3, 1991 with personnel and equipment for GvN on board. Shortly after disembarkation and unloading of supplies at GvN, "Polarstern" helicopters rescued 5 South-African personnel who were stranded at 3,000 m elevation and 300 km inland. The unusually heavy and extensive ice cover prevented "Polarstern"'s southward journey and the ship was forced to drift for 2 weeks entrapped in thick, soft ice named

"porridge ice" by Capt. Lawrence of RRS "Bransfield". Ice and under-ice physics and biology was investigated during the period of drift, and as ice conditions did not improve till the beginning of February alternate plans had to be made for work in the Lazarev Sea between GvN and Georg-Forster stations. On several transects along the shelf and into the deep-sea, all disciplines participating on this cruise - oceanography, biology and geology - investigated in closely interlocked programmes water mass distribution, water chemistry as well as the morphology of the sea floor and composition of the sediments. GvN was visited on the return journey and personnel from here as well as the Georg-Forster-Station further to the East transported to Cape Town where 'Polarstern' arrived on March 28, 1991.

The fourth Leg departed from Cape Town on March 30 and proceeded to Bouvet Island. The aim of this predominantly geological Leg was to map and sample submarine elevations - the Agulhas Ridge, the Meteor Rise and the eastern flank of the southernmost Mid-Atlantic Ridge - in order to refine existing models of the paleoceanography of the South Atlantic. "Polarstern" arrived in Bremerhaven on May 13, 1991.

FAHRTABSCHNITT ANT IX/1

(Bremerhaven - Punta Arenas 20.10.1990 - 14.11.1990)

M. Schulz-Baldes (AWI)

Einführung

Auf dem Fahrtabschnitt zwischen Bremerhaven und Punta Arenas, Chile, wurden im wesentlichen Spurenstoffe in Atmosphäre, Wasser und Organismen untersucht. Dabei wurden Einblicke in die von der geographischen Breite abhängige Verteilung, in die Bildungsweise und in das Schicksal natürlicher und anthropogener Spurenstoffe gewonnen. "Polarstern" verließ am 20.10.1990 um 0.00 Uhr Bremerhaven und erreichte am 14.11.1990 um 12.00 Uhr die Reede von Punta Arenas. Die Reise verlief für die luftchemischen Gruppen planmäßig, erfreulich waren ergiebige Regenproben in der Intertropischen Konvergenzzone (ITCZ). Die Stationsarbeit mit Neustonschlitzen und Rosettenkranzwasserschöpfer litt teilweise unter den widrigen Witterungsverhältnissen. So mußten 2 der geplanten 8 Tiefenstationen und 4 Neustonstationen wegen zu hohen Seegangs und Starkwind abgesagt werden. Schwerpunkte der Untersuchungen waren:

- Schwermetalle in Oberflächenwasser, Tiefenwasser, Regenwasser, partikulärer Substanz, Neuston und Tiefenplankton
- Bestimmung des Chlorophyll- und des DMSP-Gehaltes im Phytoplankton und Bestimmung des DMSP-Gehaltes im Neustontfang.
- Mikrozooplankton und Nannoplankton während ANT IX/1
- Messung der Konzentrationen an gasförmiger Salpetersäure, gasförmigem Ammoniak und partikelförmigem Ammoniumnitrat in der Atmosphäre
- Messungen biogener Schwefelverbindungen und deren Reaktionsprodukte in Seewasser und mariner Atmosphäre
- Muster und Gehalte der Polychlorbiphenyle (PCB), der Hexachlorcyclohexan-Isomeren (HCH) und des Hexachlorbenzols (HCB) in der Grundschicht der Troposphäre und im ozeanischen Oberflächenwasser
- Organobromverbindungen in der marinen Troposphäre und im atlantischen Oberflächenwasser
- Messungen von atmosphärischem Quecksilber über dem Atlantik
- Messungen zur spektralen optischen Dicke des Aerosols über Meer
- Fernerkundung stratosphärischer Spurenstoffe mittels Absorptions-
- Aktivitäten am neuen Bordrechnersystem während ANT IX/1

Introduction

On the first leg of ANT IX between Bremerhaven and Punta Arenas, the main scientific issues were the determination of trace substances in the atmosphere, the water and the organisms. We concentrated on investigations of production, concentration, and fate of natural and anthropogenic substances in relation to geographical regions.

'Polarstern' left Bremerhaven at midnight on 20 October 1990 and arrived at Punta Arenas on 14 November 1990 noon. All investigations for air chemistry were successful especially rain sampling near the Intertropical Convergence Zone (ITCZ). Because of rough weather two stations for deep water sampling by means of the CTD and 4 stations for neuston sampling had to be canceled. The main topics of investigation during our cruise leg are listed below:

- Heavy metals in surface waters, deep waters and rain water, in particulate matter (especially neuston and deep-sea plankton)
- Concentrations of chlorophyll and DMSP in phytoplankton and neuston

- Distribution of microplankton and nannoplankton
- Concentrations of gaseous HNO_3 , ammonium and particulate NH_4NO_3 in the atmosphere
- Biogenic sulfur components and their reaction products in seawater and atmosphere
- Polychlorbiphenyls (PCB), Hexachlorcyclohexan-Isomers (HCH) and Hexachlorbenzol (HCB) in the troposphere and ocean surface waters
- Organochroms in the troposphere and the ocean surface waters
- Atmospheric mercury in the atmosphere
- Spectral optical density of aerosols in the atmosphere
- Remote sensing of stratospheric trace substances
- Installation of a new main frame computer on 'Polarstern'

1. SCHWERMETALLE IN OBERFLÄCHENWASSER, TIEFENWASSER, REGENWASSER, PARTIKULÄRE SUBSTANZ, NEUSTON UND TIEFENPLANKTON
H. Hamann, E. Helmers, J. Modersitzki, M. Schulz-Baldes (AWI)

1.1. Zielsetzung

Auf dem Schnitt Bremerhaven - Punta Arenas sollen in verschiedenen Kompartimenten (Oberflächenwasser, Tiefenwasser, Regenwasser, partikulärer Substanz, Neuston, Tiefenplankton) Schwermetallgehalte analysiert werden. Sie sollen mit weiteren chemischen Parametern, die von anderen Arbeitsgruppen bestimmt wurden, verglichen und korreliert werden, wie z. B. Nährstoffen und Chlorophyll. Schwerpunktmäßig werden die Metalle Cadmium, Kupfer und Blei bearbeitet, in ausgewählten Kompartimenten auch zusätzlich Aluminium.

1.2. Oberflächenwasser

An 146 Positionen wurden Oberflächenwasserproben gewonnen. Das Meerwasser wurde während der Fahrt mit Hilfe eines Schnorchels, der im hydrographischen Schacht in ca. 12 m Wassertiefe installiert war, einer Kunststoffleitung und einer Teflon-Pumpe direkt in eine Cleanbench geleitet und dort unter sorgfältiger Kontaminationsminimierung abgefüllt.

1.3. Tiefenwasser

An insgesamt 6 Stationen wurden Vertikalprofile mit der Rosette in 12 Tiefen gefahren (Tab. 1.1). Mit einer Speichersonde wurden die ozeanographischen Parameter Druck, Salzgehalt und Temperatur ermittelt; Nährstoffgehalte der Proben werden im Heimatlabor bestimmt. Diese Meßdaten dienen zur Charakterisierung der Wasserkörper und als Begleitdaten für die Spurenmetall-Konzentrationen von Al, Cd, Co, Cu, Fe, Mn, Ni, Pb und Zn, deren vertikale Verteilung studiert werden soll.

Tab. 1.1: Tiefenstationen

Station	Datum	Breite		Länge	
		Grad	min	Grad	min
Höhe Gibraltar	25.10.90	34	26,8 N	22	41,8 W
nördlich Kapverden	28.10.90	20	50,2 N	27	57,4 W
südlich Kapverden	31.10.90	4	15,8 N	28	27,4 W
Höhe Salvador	4.11.90	14	10,5 S	33	5,6 W
Höhe Rio de Janeiro	7.11.90	27	36,1 S	40	37,7 W
Höhe Rio de la Plata	9.11.90	34	49,7 S	47	30,0 W

Tiefen bei allen Stationen: 20, 50, 70, 100, 200, 300, 500, 750, 1000, 1500, 2000, 3000 m

1.4. Voltammetrische Analysen von Oberflächenwasser

Aus der Vielzahl der gewonnenen Oberflächenwasserproben wurden bereits an Bord stichprobenartig einzelne mit Hilfe der differentiellen anodischen Pulsinversvoltammetrie (DPASV) an einer Quecksilberfilmelektrode (MFE) analysiert. Der Elektrodenstand ("Rotel 2", EG & G GmbH) wurde in der Clean-bench des Reinraumlaborcontainers betrieben.

Cadmium

Erste Analysen bestätigen eine Anbindung dieses Metalls an die ozeanischen Zirkulationssysteme und biochemische Zyklen. Niedrige Konzentrationen (um 1 ng/kg) wurden im Einflußbereich von Strömungssystemen mit relativ geringer Bioproduktivität (Südäquatorialstrom/Brasilstrom) gefunden, höhere Gehalte (um 5 ng/kg) wiesen schelfbeeinflusste Oberflächenstromgebiete (Falklandstrom) mit höherer Produktivität aus.

Blei

Auf dem Fahrtabschnitt ANT VIII/7 wurde mit Hilfe der Schnorchelprobennahme und nachfolgender voltammetrischen Analytik ein Datensatz von Oberflächenwasser-Bleigehalten in hoher horizontaler Auflösung gewonnen. Hierbei gelang die Auflösung von Ereignissen im Konzentrationsbereich zwischen 1 und 10 ng/kg. Die erzielten Ergebnisse sollten auf ANT IX/1 nach Möglichkeit reproduziert werden, was für die Intertropische Konvergenzzone (ITCZ), die auf ANT VIII/7 einen Anstieg der Bleigehalte um den Faktor 10 aufwies, gelungen zu sein scheint. Darüber hinaus scheinen die Bleigehalte im südwestlichen Atlantik mit bis zu 10 ng/kg höher zu sein als im südöstlichen Atlantik, vielleicht bedingt durch die Nähe industrieller Ballungszentren in Südamerika.

Kupfer

Die Kupfergehalte der bisher vermessenen Proben schwanken um einen Mittelwert von etwa 50 ng/kg und weisen damit auf ein relativ stabiles Gleichgewicht bei der Austauschbilanz dieses Metalls hin.

1.5. Spurenmetalle in marinem Regen

Unsere Untersuchungen vergangener Expeditionen deuten an, daß die Naßdeposition von Metallen (insbesondere Blei) aus der Atmosphäre eine größere Bedeutung für den Metallhaushalt des Oberflächenwassers zu haben scheint als die Trockendeposition dieser Metalle (z.B. im Saharastaub-Eintragsgebiet des Nordost-Atlantiks). Das Metallbudget im Oberflächenwassers wird daher wahrscheinlich zum Großteil aus den durch Regen

eingetragenen Frachten aufrechterhalten. Dieses gilt im Besonderen für die regenreiche ITCZ. Auf ANT IX/1 wurde insgesamt 9 Regenwasserproben gewonnen, davon 4 Doppelproben mit Hilfe zweier nebeneinander installierter Sammelapparaturen. Die voltammetrisch gemessenen Bleigehalte schwanken zwischen 90 und 500 ng/kg. Hierbei gab es gute Übereinstimmungen in den parallel gesammelten Proben. Die erhaltenen Daten sollen für eine Modellierung des Bleiflusses im System Atmosphäre-Meerwasser genutzt werden.

1.6. Extraktion und AAS-Analyse

Wie schon bei ANT VII/5 sind auch diesmal Konzentrationen für Cd zwischen <1-5 ng/kg, Pb <10 ng/kg, Cu 40-60 ng/kg und Zn 30-60 ng/kg zu erwarten. Für Co, Fe und Mn als terrigene Metalle sind vor allem im Bereich der Saharastaubeinträge höhere Fluktuationen möglich. Aufgrund dieser niedrigen Konzentrationsbereiche ist es nicht möglich, die Metallkonzentrationen direkt im Meerwasser zu bestimmen, mit Ausnahme der voltammetrisch zugänglichen Metalle. Deshalb werden die Wasserproben in einem Reinraumlabor an Land mit Hilfe der Flüssig-flüssig-Extraktion aufgearbeitet. Zum einen wird dabei die bei der Messung störende Salzkomponente eliminiert, zum anderen können die Wasserproben um den Faktor 100:1 angereichert werden. Die eigentliche Messung der Metalle erfolgt dann mit der Graphitrohr-AAS. Aluminium wird fluorimetrisch bestimmt.

1.7. Partikuläre Substanz

Eine Durchlaufzentrifuge mit Titanrotor konnte direkt an das Schnorchelsystem angeschlossen werden. Der kontinuierliche Betrieb ermöglichte die Ablagerung des Schwebstoffs bei einer Flußrate von 400 - 700 ml Seewasser pro Minute im Rotor bei 17.000 U/min. Je nach Bioproduktivität der beprobten Wasserkörper wurde der Schwebstoff nach einer Laufzeit von 8 bis 40 Stunden entnommen und auf Polykarbonat- und Glasfaserfiltern für die nachfolgende Analyse seiner Spurenmetall- und POC- Gehalte und für die Wägung gesammelt. Die Aufarbeitung der Filter erfolgt mit gleicher Methodik wie bei den Neustonproben. Die Spurenmetallgehalte der Schwebstoffe sollen mit dem Gehalt an gelösten Metallen (s.o.), den Ergebnissen der Chlorophyllmessungen im Oberflächenwasser (Arbeitsgruppe Meeresbotanik, Universität Bremen) sowie mit den Arbeiten über die Planktonzusammensetzung (Institut für Erdwissenschaften, Freie Universität Amsterdam) verglichen werden.

1.8. Neuston

Der Neustonschlitten, bestückt mit 8 Netzen von 300 bzw. 500 µm Maschenweite, wurde täglich eine halbe Stunde vor Sonnenaufgang und eine halbe Stunde nach Sonnenuntergang bei einer Schiffsgeschwindigkeit von 4 kn für 15 min seitlich vom Schiff geschleppt. Tab. 1.2 enthält die Stationsliste.

Tab. 1.2: Neustonstationen

Sta.-Nr.	Datum	Uhrzeit UTC	Breite			Länge		
			Grad	min	N	Grad	min	W
1	22.10.90	18.30	47	14,4	N	11	18,9	W
2	24.10.90	18:07	38	59,9	N	20	12,8	W
3	25.10.90	7.24	36	25,9	N	21	52,9	W
4	25.10.90	19.51	34	23	N	22	43,6	W
5	26.10.90	7.30	31	44	N	23	49,8	W
6	26.10.90	19.45	28	54,1	N	24	57,2	W
7	27.10.90	7.30	31	44	N	23	49,8	W
8	27.10.90	19.55	23	27,6	N	26	59,7	W
9	28.10.90	7.26	20	48,5	N	27	58,3	W
10	28.10.90	20.05	18	53,8	N	28	36	W
11	29.10.90	7.25	16	32,3	N	28	6	W
12	29.10.90	20.15	13	51,6	N	28	50	W
13	30.10.90	7.25	11	31,3	N	28	44,9	W
14	30.10.90	20.15	8	41,8	N	28	38,1	W
15	31.10.90	7.25	6	18,1	N	28	33,6	W
16	31.10.90	20.19	4	15,2	N	28	26,2	W
17	1.11.90	22.08	2	15,2	S	28	17	W
18	2.11.90	7.17	4	15,5	S	28	54,1	W
19	2.11.90	20.35	7	16,7	S	30	8,9	W
20	3.11.90	7.06	9	22,2	S	31	2,7	W
21	4.11.90	7.05	14	12,4	S	33	7,8	W
22	4.11.90	21.15	16	25,2	S	34	6,2	W
23	5.11.90	7.15	18	29,3	S	34	49,8	W
24	5.11.90	21.28	21	29,9	S	36	7,1	W
25	6.11.90	7.23	23	34,8	S	37	16,9	W
26	7.11.90	7.30	27	35,1	S	40	43,5	W
27	8.11.90	7.35	30	53,3	S	43	46,5	W
28	8.11.90	22.25	33	20,9	S	46	10	W
29	9.11.90	7.45	34	50,4	S	47	34,1	W
30	9.11.90	22.45	36	47,2	S	49	30,6	W
31	10.11.90	7.45	38	18,7	S	51	7,6	W
32	10.11.90	23.10	41	3,3	S	53	56,1	W
33	11.11.90	23.35	44	59,7	S	58	25,7	W
34	12.11.90	8.05	46	21,2	S	59	59,4	W

Die Fänge wurden vereinigt und sofort sortiert. Dabei erfolgte eine Zuordnung zu insgesamt 40 Taxa. Tab. 1.3 zeigt nicht die Präsenz eines Taxons an bestimmten Stationen, sondern gibt die Probenzahl an, die unter der Voraussetzung genügender Biomasse erhalten wurde. Da häufig innerhalb eines Taxons mehrere Arten unterschieden und getrennt aussortiert wurden, wird die Gesamtzahl der gewonnenen Proben sehr viel höher liegen.

1.9. Tiefenplankton

Zur Gewinnung von Tiefenplanktonproben wurde ein Bongonetz (500 µm Maschenweite) mit einem Scherkörper auf den 6 Vertikalstationen eingesetzt. Während das Schiff mit 2 kn Geschwindigkeit lief, wurden 1000 m Seil ausgesteckt bei ca. 0,6 m/sec Fiergeschwindigkeit. Nach 15 min Schlepp wurde dann mit gleicher Geschwindigkeit gehievt, während das Schiff aufstoppte. Insgesamt wurde damit etwa 75 min gefischt, die erreichte Tiefe dürfte bei 400 - 500 m liegen. Auf allen Stationen wurden gute Ausbeuten an Copepoden, Euphausiaceen, Chaetognathen und Pteropoden erzielt (Tab. 1.4). Auch in den Tiefenplanktonproben sollen nach Gefriertrocknung und Säureaufschluß die Metallkonzentrationen bestimmt und mit den Konzentrationen im Seewasser aus den vertikalen Rosettenprofile korreliert werden.

Tab. 1.4: Tiefenplankton-Taxa

	1	2	3	4	5	6	Summe
CNIDARIA							
Siphonophora			1	1	1	1	4
MOLLUSCA							
Heteropoda				1	1	1	3
Pteropoda, thecosomat		1	1	1	1		4
andere Gastropoda				1		1	2
Cephalopoda	1				1		2
CRUSTACEA							
Copepoda	1	1	1	1	1	1	6
Ostracoda		1	1	1			3
Hyperiidae	1	1	1	1	1	1	6
Phronima						1	1
Euphausiacea	1	1	1	1	1	1	6
Decapoda natantia	1						1
Decapoda reptantia					1		1
Stomatopoda			1			1	2
CHAETOGNATHA	1	1	1	1	1	1	6
TUNICATA							
Thaliacea						1	1
Pyrosoma	1						1
VERTEBRATA							
Myctophida	1						1
Glasaal	1				1		2
andere Fischlarven	1	1	1	1	1	1	6

2. BESTIMMUNG DES CHLOROPHYLL- UND DES DMSP-GEHALTES IM PHYTOPLANKTON UND BESTIMMUNG DES DMSP-GEHALTES IM NEUSTONFANG.

C. Thiel, H. Wolff (FBB)

Zielsetzung

Ziel dieser Expedition ist die Untersuchung des Chl- und DMSP- Gehaltes des Oberflächenwassers (Schöpfproben), des DMSP-Gehaltes des Neustons, sowie Bestimmung der Artenzusammensetzung des Phytoplanktons.

Der Chlorophyllgehalt ist ein Maß für die in Seewasserproben vorhandene Menge an Phytoplankton. Schöpfproben wurden auf Glasfaserfilter angereichert und ihr Chl_a -Gehalt im Impulsfluorometer gemessen. Da jedoch die Fluoreszenz des Phytoplanktons vom physiologischen Zustand und der dominierenden Art abhängig ist, werden Parallelbestimmungen mit herkömmlichen Extraktionsverfahren im Heimatlabor gemacht, um die relativen Fluoreszenzwerte in absolute Konzentration umrechnen zu können.

Die schwefelhaltige Substanz Dimethylsulfoniumpropionat =DMSP ist die quantitativ bedeutendste Quelle natürlicher Schwefelverbindungen. Circa 25% der globalen Schwefelemissionen gelangen als Dimethylsulfid =DMS, einem Spaltprodukt des DMSP, in die Atmosphäre. Hauptsächliche Produzenten des DMSP sind die Mikroalgen des marinen Planktons und benthische grüne Makroalgen der Küste. Der DMSP-Gehalt des Phytoplanktons ist wesentlich von der Artenzusammensetzung abhängig. Erstmals haben wir regelmäßig Proben vom Neuston-Schlitten genommen. Darüberhinaus soll versucht werden, den DMSP-Gehalt vom Zooplankton mit Hilfe der Gaschromatographie zu bestimmen.

Arbeitsprogramm

Während dieser Reise wurden von den Breitengraden 47°Nord bis 44°Süd täglich jeweils um 8.30 Uhr, 12.30 Uhr, 16.30 Uhr und um 18.30 Uhr Schöpfproben des Oberflächenwassers vom Arbeitsdeck des Schiffes genommen. Vier mal drei Liter des durch das 200 Mikrometer-Netz vorfiltrierten Meerwassers wurden über Whatmann GF/C Glasfaserfilter filtriert. Je zwei Liter wurden für die DMSP-Bestimmung in Alufolie bzw. für die Chlorophyllmessungen in Greiner-Röhrchen verpackt, und bei einer Temperatur von -30°C tiefgefroren. Die Untersuchung der DMSP-Konzentration erfolgt im Heimatlabor der Universität Bremen mittels Gaschromatographie, diejenige des Chlorophylls, nach Extraktion in 90%igem Aceton, auf fluorometrischen und photometrischen Wege. Zur Beurteilung der Artenzusammensetzung des Phytoplanktons wurden 220 ml Seewasser mit 4 ml 37%igem Formaldehyd fixiert und in Braunglasflaschen abgefüllt. Die taxonomischen Großgruppen werden im Heimatlabor mikroskopisch ermittelt. Außerdem wurden noch zweimal täglich Proben vom Neustonfang genommen. Morgens, jeweils 1/2 Std vor Sonnenaufgang bzw. Abends 1/2 Std nach Sonnenuntergang. Der Fang wurde artspezifisch sortiert und in Glasröhrchen mit 0,1 N HCL aufbewahrt und tiefgefroren (-30°C). Es wurden jeweils noch 200 ml und 400 ml Seewasser filtriert. Anschließend wurde mit dem Fluorometer die Chl_a-Fluoreszenz ermittelt. Des weiteren haben wir einen Vergleich mit verschiedenen Glasfaser-Filtertypen vorgenommen (GF/C 2,7 µm GF/F 0,45 µm).

3. MIKROZOOPLANKTON UND NANNOPLANKTON G. Bos, M. Knappertsbusch (VUA)

Während der Überfahrt des Forschungsschiffes "Polarstern" von Bremerhaven nach Punta Arenas, vom 20.10.90 bis zum 14.11.90, sammelten wir 55 Mikrozooplankton Netzproben im Oberflächenwasser kombiniert mit 55 Oberflächenwasser Isotopen-Proben, und 102 Oberflächenproben für kalkiges Nannoplankton. An insgesamt 7 Tiefenstationen sammelten wir in den obersten 300 m der Wassersäule 81 Phytoplanktonproben und 81 Nährstoffproben in 13 Standard-Wassertiefen. Gleichzeitig wurden Temperatur- und Salinitäts-Tiefenprofile (300 m) gemessen. Weiterhin wurden Proben für Immunolabelling Experimente an Coccolithophoriden und für Coccolithophoriden Lebendkulturen gesammelt.

Mit unseren Untersuchungen möchten wir einerseits horizontale und vertikale Diversitätsgradienten planktonischer Foraminiferen und Coccolithophoriden in Abhängigkeit der durchfahrenen Wassermassen dokumentieren, andererseits soll aufgrund der an den Tiefenstationen gesammelten Proben die Coccolithen-Karbonat Exportproduktion abgeschätzt werden. Die durchfahrene Strecke reiht sich in idealer Weise an das im Nordatlantik durchgeführte niederländische JGOFS-Programm an (JGOFS Leg 4, Reykjavik-Galway, Juni 1990). Um Vergleiche anstellen zu können, wurden die Oberflächenwasser Phytoplanktonproben mit jenen der anderen "Wassergruppen" zeitlich koordiniert (C. Thiel & H. Wolff: DMSP, Diatomeen, Chlorophyll-Messungen; E. Helmers: Schwermetalle, Nährstoffe im Oberflächenwasser; R. Staubes: DMS-Messungen).

3.1. Tiefenstationen

3.1.1. Phytoplanktonproben

Von insgesamt 7 Stationen (Tab. 1.5) wurden jeweils 13 Wasserproben aus den folgenden Tiefen gesammelt: 3 m, 10 m (von der Seewasserpumpe des Schiffes), 20 m, 30 m, 40 m, 50 m, 60 m, 75 m, 100 m, 150 m, 200 m, 250 m und 300 m. Die Proben stehen in Tab. 1.6. Die Tiefenintervalle stimmen mit jenen der im Juni 1990 durchgeführten JGOFS Leg 4- Expedition im Nordatlantik überein. Die Probenentnahme erfolgte mit einem 12 Flaschen-Rosettensamplern, welcher mit einer CTD-Sonde bestückt war. Die Wasserschöpfer waren 12-Liter Niskin-Flaschen.

Das Wasser von jedem Schöpfer wurde in Plastik-Containern zwischengespeichert (ohne Vergiften) und danach sofort durch ein Vakuum Millipore System filtriert (Vakuum ca. 32 cm Hg-Säule). Es wurden Zellulose-Azetat Membranfilter (Typ HA) von Millipore (Porengröße 0.45 µm, Filterdurchmesser 47 mm) verwendet. Alle Filter waren zuvor gewogen, damit später über das Trockengewicht die Phytoplankton-Biomasse abgeschätzt werden kann. Die Menge des filtrierten Wassers variierte zwischen 2 und 9 Litern, meistens waren es 8 Liter. Um das Meersalz auszuwaschen, verwendeten wir deionisiertes Wasser von der schiffseigenen Millipore-Wasserreinigungs Anlage. Um der Karbonatlösung vorzubeugen, wurden einige Tropfen NH_3 -Lösung hinzugefügt bis sich der pH auf 9 eingestellt hatte. Nach der Filtration wurden alle Filter zuerst luftgetrocknet und dann in Plastik-Dosen verpackt bei 4°C im Kühlraum aufbewahrt.

Tab. 1.5: 300 m CTD - Tiefenstationen

Station	Breite	Länge	Datum	Zeit (GMT)	Data Files
Station 1	34° 24.944' N	22° 41.992' W	25.10.90	18.30 h	IX_1.dat
Station 2	26° 11.086' N	25° 58.213' W	27.10.90	08.00 h	Mich_1.dat
Station 3	20° 48.638' N	27° 58.247' W	28.10.90	07.30 h	Mich_2.dat
Station 4	04° 16.639' N	28° 29.873' W	31.10.90	17.00 h	Mich_3.dat
Station 5	14° 12.343' S	33° 07.754' W	04.11.90	07.00 h	Mich_4.dat
Station 6	27° 36.323' S	40° 43.469' W	07.11.90	07.35 h	Mich_5.dat
Station 7	34° 50.387' S	47° 33.943' W	09.11.90	05.50 h	Mich_6.dat

Tab. 1.6: Phytoplanktonproben an den Stationen

Station	Probe	Breite (Grad)	Länge (Grad)	Tiefe (m)	Liter filtriert
ST 1	FB1	34.416	22.67	0	9
ST 1	FB2	34.416	22.67	10	10
ST 1	FB3	34.416	22.67	20	6
ST 1	FB4	34.416	22.67	100	8
ST 1	FB5	34.416	22.67	200	7
ST 1	FB6	34.416	22.67	300	8
ST 1	FB7	34.416	22.67	500	8
ST 2	FB8	26.185	25.97	3	8
ST 2	FH 33	26.185	25.97	10	7
ST 2	FB9	26.185	25.97	20	8
ST 2	FB 10	26.185	25.97	30	8
ST 2	FB 11	26.185	25.97	40	8
ST 2	FB 12	26.185	25.97	50	8
ST 2	FB 13	26.185	25.97	60	8
ST 2	FB 14	26.185	25.97	75	7
ST 2	FB 15	26.185	25.97	100	8
ST 2	FB 16	26.185	25.97	150	8
ST 2	FB 17	26.185	25.97	200	8
ST 2	FB 18	26.185	25.97	250	8
ST 2	FB 19	26.185	25.97	300	9
ST 3	FB 20	20.811	27.971	3	9
ST 3	FH 38	20.811	27.971	10	9
ST 3	FB 21	20.811	27.971	20	9
ST 3	FB 22	20.811	27.971	30	10
ST 3	FB 23	20.811	27.971	40	9
ST 3	FB 24	20.811	27.971	50	10
ST 3	FB 25	20.811	27.971	75	8
ST 3	FB 26	20.811	27.971	100	10
ST 3	FB 27	20.811	27.971	150	11
ST 3	FB 28	20.811	27.971	200	10
ST 3	FB 29	20.811	27.971	250	10
ST 3	FB 30	20.811	27.971	300	10
ST 4	FB 31	4.277	28.498	3	8
ST 4	FH 56	4.277	28.498	10	8
ST 4	FB 32	4.277	28.498	20	8
ST 4	FB 33	4.277	28.498	30	8
ST 4	FB 34	4.277	28.498	40	8
ST 4	FB 35	4.277	28.498	50	8
ST 4	FB 36	4.277	28.498	60	9
ST 4	FB 37	4.277	28.498	75	10
ST 4	FB 38	4.277	28.498	100	9
ST 4	FB 39	4.277	28.498	150	9
ST 4	FB 40	4.277	28.498	200	9

Station	Probe	Breite (Grad)	Länge (Grad)	Tiefe (m)	Liter filtriert
ST 4	FB 41	4.277	28.498	250	8
ST 4	FB 42	4.277	28.498	300	8
ST 5	FB 43	-14.206	33.129	3	7
ST 5	FB 44	-14.206	33.129	10	8
ST 5	FB 45	-14.206	33.129	20	9
ST 5	FB 46	-14.206	33.129	30	8
ST 5	FB 47	-14.206	33.129	40	7
ST 5	FB 48	-14.206	33.129	50	7
ST 5	FB 49	-14.206	33.129	60	7
ST 5	FB 50	-14.206	33.129	75	7
ST 5	FB 51	-14.206	33.129	100	8
ST 5	FB 52	-14.206	33.129	150	4.7
ST 5	FB 53	-14.206	33.129	200	8
ST 5	FB 54	-14.206	33.129	250	8
ST 5	FB 55	-14.206	33.129	300	9.4
ST 6	FB 56	-27.605	40.724	3	8
ST 6	FB 57	-27.605	40.724	10	8
ST 6	FB 58	-27.605	40.724	20	9
ST 6	FB 59	-27.605	40.724	30	9
ST 6	FB 60	-27.605	40.724	40	9
ST 6	FB 61	-27.605	40.724	50	9
ST 6	FB 62	-27.605	40.724	60	8
ST 6	FB 63	-27.605	40.724	75	9
ST 6	FB 64	-27.605	40.724	100	7
ST 6	FB 65	-27.605	40.724	150	9
ST 6	FB 66	-27.605	40.724	200	10
ST 6	FB 67	-27.605	40.724	250	10
ST 6	FB 68	-27.605	40.724	300	11
ST 7	FB 69	-34.844	7.566	3	9
ST 7	FB 70	-34.844	7.566	10	9
ST 7	FB 71	-34.844	7.566	20	8
ST 7	FB 72	-34.844	7.566	30	8
ST 7	FB 73	-34.844	7.566	40	8
ST 7	FB 74	-34.844	7.566	50	9
ST 7	FB 75	-34.844	7.566	60	9
ST 7	FB 76	-34.844	7.566	75	9
ST 7	FB 77	-34.844	7.566	100	9.3
ST 7	FB 78	-34.844	7.566	150	9.2
ST 7	FB 79	-34.844	7.566	200	10
ST 7	FB 80	-34.844	7.566	250	10
ST 7	FB 81	-34.844	7.566	300	10

3.1.2. Nährstoff-Proben

Von jeder Schöpfprobe wurden ca. 200 ml Wasser für die Nährstoff-Analyse gesammelt. Für Nitrat- und Phosphat wurden 100 ml in PVC-Flaschen abgefüllt und (ohne Vergiften) sofort bei minus 20°C eingefroren. Für die Silikat-Analyse wurden 100 ml Wasser gesammelt und bei plus 4°C aufbewahrt (ohne Vergiften).

3.1.3. Oberflächenwasserproben

Die Oberflächenwasserproben für Phytoplankton stammen aus 10 m Tiefe und wurden via Membranpumpe über eine Schlauchleitung in ein Auffanggefäß geleitet und dort gesammelt. Die Phytoplanktonproben stammen damit exakt aus derselben Leitung wie die Mikrozooplanktonproben von Gerard Bos. Die Probeentnahme erfolgte meistens alle 6 Stunden, um 00.30, 06.30, 12.30 und 18.30 Uhr Schiffszeit. Es wurden jeweils 10 Liter entnom-

men und mit der in 1.1 beschriebenen Methode filtriert und aufbewahrt. Die Probedaten sind in Tab. 1.7 aufgelistet. Schiffszeit und GMT sind in Tab. 1.8 gegenübergestellt. Für alle Proben wurden die Temperatur (beidseits des Schiffes sowie am Bug (THS)), und Salinität notiert.

Tab. 1.7: Oberflächen-Phytoplanktonproben (10 m)

Probe No.	Datum	GMT	Schiffszeit	Breite	Länge	Temperatur(°C)	Salinität(‰)	Liter
FH 1	20.10.	20.43	21.43	51.643	02.291	15.79	35.26	1.35
FH 2	20.10.	23.28	00.28	51.093	01.574	15.92	35.30	2
FH 3	21.10.	12.03	13.03	50.039	02.572	15.97	35.32	3
FH 4	21.10.	18.06	19.06	49.436	04.650	13.83	35.34	4.8
FH 5	22.10.	00.09	00.09	48.816	06.581	15.61	35.56	6
FH 6	22.10.	07.20	07.20	48.172	08.479	15.14	35.64	6
FH 7	22.10.	12.15	12.15	47.710	09.903	16.20	35.72	8
FH 8	22.10.	14.54	14.54	47.445	10.698	16.15	35.71	6
FH 9	22.10.	18.25	18.25	47.242	11.305	16.04	35.68	9
FH 10	22.10.	20.20	20.20	46.956	11.623	16.31	35.72	7
FH 11	22.10.	24.00	24.00	46.322	12.320	16.57	35.79	7
FH 12	23.10.	06.03	06.03	45.254	13.559	16.93	35.87	8
FH 13	23.10.	10.12	10.12	44.572	14.273	17.23	35.94	8
FH 14	23.10.	13	13	44.095	14.765	17.32	35.87	6
FH 15	23.10.	19.07	19.07	43.185	15.818	17.35	36.03	6
FH 18	24.10.	6.16	5.16	41.329	17.796	17.58	35.94	8
FH 19	24.10.	12.32	11.32	40.218	18.977	18.09	36.09	9
FH 20	24.10.	12.32	11.32	40.218	18.977	18.48	36.05	6
FH 21	24.10.	19.3	18.3	38.910	20.287	18.48	36.05	8
FH 22	25.10.	1.3	0.3	37.677	21.339	19.25	36.33	10
FH 23	25.10.	8.15	7.15	36.245	21.951	20.34	36.49	9
FH 24	25.10.	13.3	12.3	34.959	22.491	20.74	36.22	7
FH 25	25.10.	13.3	12.3	34.959	22.491	20.74	36.22	7
FH 26	25.10.	19.3	18.3	34.402	22.712	21.16	36.4	7
FH 27	26.10.	1.35	0.35	33.02	23.283	23.06	37.11	9
FH 28	26.10.	9.3	8.3	31.26	23.998	23.37	37.07	9
FH 29	26.10.	13.3	12.3	30.26	24.396	23.45	37.01	8
FH 30	26.10.	9.3	8.3	31.26	23.998	23.37	37.07	7
FH 31	26.10.	19.5	18.5	28.887	24.961	24.19	37.2	10
FH 32	27.10.	1.4	0.4	27.447	25.497	24.49	37.39	6
FH 33	27.10.	8	7	26.181	25.971	25.13	37.51	7
FH 34	27.10.	13.37	12.37	24.870	26.485	25.4	37.4	5
FH 35	27.10.	19.32	18.32	23.451	27.001	25.56	37.39	7
FH 36	27.10.	13.37	12.37	24.870	26.485	25.4	37.4	7
FH 37	28.10.	1.35	0.35	22.119	27.502	25.27	37.42	9
FH 38	28.10.	7.3	6.3	20.811	27.971	26.08	26.08	9
FH 39	28.10.	13.5	12.5	20.138	28.074	26.34	36.86	8
FH 40	28.10.	19.35	18.35	18.891	28.613	26.49	36.82	8
FH 41	29.10.	1.3	0.3	17.777	28.991	26.92	36.55	9
FH 42	29.10.	9.2	8.2	16.139	28.929	27.37	36.28	9
FH 43	29.10.	13.4	12.4	15.153	28.892	27.57	36.24	8
FH 44	29.10.	19.35	18.35	18.891	28.613	26.49	36.82	9
FH 45	29.10.	19.32	18.32	23.451	27.001	25.56	37.39	9
FH 46	29.10.	19.3	18.3	13.888	28.846	27.7	36.21	8
FH 47	30.10.	1.3	0.3	12.701	28.807	27.73	36.16	9
FH 48	30.10.	9.3	8.3	11.084	28.748	27.88	35.75	9
FH 49	30.10.	13.3	12.3	10.118	28.71	28.36	35.74	5
FH 50	30.10.	13.3	12.3	10.118	28.71	28.36	35.74	9
FH 51	30.10.	19.3	18.3	8.753	28.66	28.62	34.47	8
FH 52	31.10.	1.3	0.3	7.513	28.603	28.76	34.66	8
FH 53	31.10.	9.3	8.3	5.837	28.541	28.1	35.49	5
FH 54	31.10.	9.3	8.3	5.837	28.541	28.1	35.49	4.4
FH 55	31.10.	13.3	12.3	4.974	28.525	28.41	35.37	7

Probe No.	Datum	GMT	Schiffszeit	Breite	Länge	Temperatur(°C)	Salinität(‰)	Liter
FH 56	31.10.	17	16	4.277	28.498	28.39	35.25	8
FH 57	01.11.	1.3	0.3	2.949	28.478	28.26	35.56	6
FH 58	01.11.	9.3	8.3	0.958	28.402	27.2	36.05	8
FH 59	01.11.	13.3	12.3	-0.135	28.369	26.93	36.18	9
FH 60	01.11.	21	20	-2.01	28.297	26.78	36.27	7
FH 61	02.11.	1.3	0.3	-2.949	28.524	26.26	36.24	8
FH 62	02.11.	9.3	8.3	-5.023	29.226	26.18	36.25	8
FH 63	02.11.	14	13	-5.844	29.565	26.26	36.25	8
FH 64	02.11.	20	19	-7.234	30.153	26.68	36.23	7
FH 65	03.11.	1.3	0.3	-8.273	30.596	26.9	36.53	8
FH 66	03.11.	9.1	8.1	-9.786	31.229	26.89	36.52	9
FH 67	03.11.	15.25	14.25	-11	31.761	26.9	36.79	9
FH 68	03.11.	19.3	18.3	-11.855	32.125	26.97	36.79	8
FH 69	04.11.	1.3	0.3	-13.137	32.674	26.82	36.76	8
FH 70	04.11.	13.45	12.45	-14.911	33.442	26.82	36.85	9
FH 71	04.11.	19.3	18.3	-16.152	33.987	26.34	37.23	8
FH 72	05.11.	9.3	8.3	-18.938	35.003	25.54	37.34	8
FH 73	05.11.	13.3	12.3	-19.097	35.063	25.69	37.36	9
FH 74	05.11.	19.3	18.3	-21.198	35.937	25.34	37.29	9
FH 75	06.11.	1.3	0.3	-22.393	36.599	24.68	37.1	10
FH 76	06.11.	9.3	8.3	-24.064	37.553	23.6	36.81	9
FH 77	06.11.	12	11	-24.546	37.991	23.43	36.92	7
FH 78	06.11.	13.3	12.3	-24.862	38.268	22.94	36.77	9
FH 79	06.11.	19.3	18.3	-25.756	39.062	22.01	36.5	9
FH 80	07.11.	1.3	0.3	-26.667	39.891	21.89	36.49	8
FH 81	07.11.	13.3	12.3	-28.023	41.09	21.76	36.56	9
FH 82	07.11.	19.3	18.3	-28.965	41.997	21.4	36.54	9
FH 83	08.11.	1.3	0.3	-29.933	42.901	21.49	36.47	9
FH 84	08.11.	10.3	8.3	-31.395	44.28	19.93	36.07	9
FH 85	08.11.	14.3	12.3	-32.102	44.953	20.41	35.79	6
FH 86	08.11.	19.3	18.3	-33.12	45.928	18.66	35.86	2.5
FH 88	09.11.	2.3	0.3	-34.036	46.819	18.87	36.01	5
FH 89	09.11.	15	13	-35.538	48.296	17.86	35.79	4
FH 90	09.11.	20.3	18.3	-36.509	49.267	15.01	34.79	4
FH 91	09.11.	23.05	21.05	-36.892	49.619	13.22	33.94	3
FH 92	10.11.	3.55	1.55	-37.689	50.479	17.43	35.34	3
FH 93	10.11.	10.3	8.3	-38.838	51.648	17.86	33.98	7
FH 94	10.11.	14.4	12.4	-39.647	52.498	17.5	35.75	5
FH 95	10.11.	20.3	18.3	-40.667	53.575	11.32	34.45	3
FH 96	11.11.	3.2	1.2	-41.732	54.733	11.69	34.48	3.2
FH 97	11.11.	11.2	9.2	-43.075	56.082	9.55	34.10	2
FH 98	11.11.	14.30	12.30	-43.570	56.757	9.54	34.12	3
FH 99	11.11.	21.00	19.00	-44.657	57.981	9.23	34.13	3
FH100	12.11.	02.30	00.30	-45.517	58.974	6.26	34.11	7
FH101	12.11.	10.45	08.45	-45.751	60.410	7.59	33.82	2
FH102	12.11.	14.30	12.30	-47.404	61.184	7.54	33.71	
FH103	12.11.	18.20	20.20	-48.405	62.403	8.21	33.70	

Tab. 1.8: Zeit-Schema Schiffszeit-GMT

GMT	0	1	2	3	4	5	6	7	8	9	10	11	12	13	14	15	16	17	18	19	20	21	22	23	24	
LT 21.10.90																										
LT	1	2	3	4	5	6	7	8	9	10	11	12	13	14	15	16	17	18	19	20	21	22	23	24	1	
Wechsel in der Nacht vom 21.10.90 auf 22.10.90:																										
LT	0	1	2	3	4	5	6	7	8	9	10	11	12	13	14	15	16	17	18	19	20	21	22	23	24	
Wechsel in der Nacht vom 23.10.90 auf 24.10.90:																										
LT	23	0	1	2	3	4	5	6	7	8	9	10	11	12	13	14	15	16	17	18	19	20	21	22	23	
Wechsel in der Nacht vom 7.11.90 auf 8.11.90																										
LT	22	23	0	1	2	3	4	5	6	7	8	9	10	11	12	13	14	15	16	17	18	19	20	21	22	
Wechsel in der Nacht vom 12.11.90 auf 13.11.90:																										
LT	21	22	23	0	1	2	3	4	5	6	7	8	9	10	11	12	13	14	15	16	17	18	19	20	21	

3.2. Lebendkulturen von Coccolithophoriden und Proben für Immunolabelling

Um Coccolithophoriden anzureichern, wurden zwischen 1 und 6 Liter Meerwasser über einen 1.0 mm Polycarbonat-Nucleopore Filter filtriert. Der Filter wurde danach in 15 ml Meerwasser in einem Reagenzglas geschüttelt, und so das Filtergut von der Filteroberfläche gewaschen. Etwa 7.5 ml wurde bei Zimmertemperatur im abgedunkelten Licht belassen und dient als Ausgangsmaterial für Coccolithophoriden Zellkulturen. Die andere Hälfte wurde mit ca. 7 ml 4%-iger gepufferter Paraformaldehyd fixiert. Als Puffer diente 0.2 M tris, pH zwischen 8 und 9. Eine Auflistung der gesammelten Proben findet sich in Tab. 1.9. Das Material soll von Paul van der Wal am NIOZ für Kulturexperimente und Immunolabelling weiterverwendet werden.

Tab. 1.9: Proben für Zellkulturen und Immunolabelling

FixiertesKultur Material	v/d Wal	Kultur M. K.	Liter	Tiefe (m)	Breite	Länge	pH 4% P.F.+tris
F-FH8	CL-FH8	CLM-FH8	4	10	47.445	10.698	6.5
F-FH12	CL-FH12	CLM-FH12	2	10	45.254	13.559	6.5
F-FH14	CL-FH14	CLM-FH14	4	10	44.096	14.765	9.2
F-FH19	CL-FH19	CLM-FH19	5	10	40.218	18.977	9.2
F-FH22	CL-FH22	CLM-FH22	5	10	37.683	21.339	8.2
F-FH24	CL-FH24	CLM-FH24	5	10	34.959	22.491	8.1
F-FB02	CL-FB02	-	1	10	Stat. 1		8.1
F-FB03	CL-FB03	CLM-FB03	2.8	50	Stat. 1		8.1
F-FB04	CL-FB04	-	2.45	100	Stat. 1		8.1
F-FB05	CL-FB05	-	2.0	200	Stat. 1		8.1
F-FB06	CL-FB06	-	2.25	300	Stat. 1		8.1
F-FB07	CL-FB07	-	2.3	500	Stat. 1		8.1
F-FH29	CL-FH29	CLM-FH29	5	10	30.260	24.396	8.1
F-FH34	CL-FH34	CLM-FH34	5	10	24.869	25.970	8.1
F-FB08	CL-FB08	-	2.7	3	Stat. 2		8.1
F-FB09	CL-FB09	-	2.6	20	Stat. 2		8.1
F-FB12	CL-FB12	-	2.4	50	Stat. 2		8.1
F-FB15	CL-FB15	-	2.5	100	Stat. 2		8.1
F-FB17	CL-FB17	-	2.6	200	Stat. 2		8.1
F-FH43	CL-FH43	CLM-FH43	6	10	15.153	28.892	8.6
F-FH49	CL-FH49	CLM-FH49	5	10	10.118	28.709	8.6
F-FH40	CL-FH40	CLM-FH40	3	10	18.891	28.613	8.6
F-FH46	CL-FH46	CLM-FH46	6	10	13.888	28.846	8.6
F-FH39	CL-FH39	CLM-FH39	6	10	20.138	28.074	8.6
F-FH53	CL-FH53	CLM-FH53	3	10	05.837	28.541	8.1
-	-	CLM-FH53/2	3	10	05.837	28.541	8.1
F-FH55	CL-FH55	CLM-FH55	2.55	10			8.1
F-FH55	CL-FH55	CLM-FH55	3	10			8.1
F-FH59	CL-FH59	CLM-FH59	7	10			7.9
F-FH63	CL-FH63	CLM-FH63	5	10			8.1
F-FB43	CL-FB43	-	3	3			9.0
F-FB44	CL-FB44	-	2	10			9.0
F-FB45	CL-FB45	-	1.4	20			9.0
F-FB46	CL-FB46	-	2.3	30			9.0
F-FB47	CL-FB47	-	2.5	40			9.0
F-FB48	CL-FB48	-	3.3	50			9.0
F-FB50	CL-FB50	-	1.4	75			9.0
F-FB51	CL-FB51	-	2.2	100			9.0
F-FB53	CL-FB53	-	2.4	200			9.0
F-FB54	CL-FB54	-	2.2	250			9.0
F-FH85	CL-FH85	CLM-FH85	5	10			8.5

3.3. Mikrozooplanktonproben

Während ANT IX/1 wurden insgesamt 53 Mikrozooplankton Proben gesammelt. Unser Ziel ist festzustellen, in wieweit Wassermassen über die Diversitätsgradienten planktonischer Foraminiferen identifizierbar sind. Die Foraminiferenfauna im Oberflächenwasser soll später mit den fossilen Foraminiferen-Vergesellschaftungen in holozänen Tiefseesedimenten verglichen werden. Isotopenproben wurden gesammelt, um die $^{18}\text{O}/^{16}\text{O}$ Isotopenverhältnisse im Wasser mit jenen der Foraminiferenschalen zu vergleichen. Alle Netzproben sind in Tab. 1.10 aufgelistet, die zugehörigen Daten für die Isotopenproben stehen in Tab. 1.11.

Tab. 1.10: Oberflächenwasser Foraminiferen-Proben (10 m)

Probe	Datum	GMT	Schiffs-Zeit	Breite (Grad)	Länge °West	Temp, THS(°C)	Salin, (‰)	Wassermenge m ³
PL 00	22.10.	11,15	11,15	47,787	9,675	16,08	35,73	0,27
PL 01	22.10.	18,25	18,25	47,242	11,305	16,03	35,68	5,98
PL 02	22.10.	24	24	46,322	12,32	16,57	35,79	5,42
PL 03	23.10.	6,03	6,03	45,253	13,559	16,93	35,87	5,78
PL 04	23.10.	13	13	44,096	14,765	17,32	35,87	6,18
PL 05	23.10.	21,06	21,06	42,881	16,153	17,77	36,01	8,18
PL 06	24.10.	6,16	5,16	41,329	17,796	17,58	35,94	9,24
PL 07	24.10.	15,57	14,57	39,539	19,651	18,43	36,04	9,74
PL 08	24.10.	23,53	22,53	38,084	21,116	19,09	36,38	6,99
PL 09	25.10.	9	8	36,102	22,012	20,5	36,48	9,15
PL 10	25.10.	18,14	17,14	34,428	22,685	21,43	36,38	8,99
PL 11	26.10.	3,02	2,02	32,701	23,422	22,43	36,68	8,8
PL 12	26.10.	12,05	11,05	30,652	24,243	23,62	37,08	9,29
PL 13	26.10.	21	20	28,613	25,045	24,25	37,29	9,51
PL 14	27.10.	6,1	5,1	26,377	25,905	25,05	37,52	9,98
PL 15	27.10.	15	14	24,526	26,6	25,36	37,24	9,76
PL 16	27.10.	23,58	22,58	22,506	27,362		37,51	10,08
PL 17	28.10.	9,04	8,04	20,836	27,956	25,98	36,87	10,3
PL 18	28.10.	18,01	17,01	19,238	28,46	26,2	36,79	10,11
PL 19	29.10.	3,04	2,04	17,433	28,979	26,96	36,48	11,24
PL 20	29.10.	12,01	11,01	15,568	28,915	27,44	36,29	11,11
PL 21	29.10.	21,01	20,01	13,725	28,832	27,6	36,2	11,66
PL 22	30.10.	6,07	5,07	11,713	28,77	27,93	35,83	11,85
PL 23	30.10.	15,03	14,03	9,795	28,7	28,42	35,75	11,68
PL 24	30.10.	23,58	22,58	7,882	28,6	28,76	34,16	11,61
PL 25	31.10.	9,06	8,06	5,952	28,546	28,26	35,65	11,98
PL 26	31.10.	18,05	17,05	4,266	28,465	28,49	35,27	11,5
PL 27	01.11.	3,06	2,06	2,55	28,458	28,23	35,66	11,33
PL 28	01.11.	12,02	11,02	0,299	28,384	26,97	36,12	10,64
PL 29	01.11.	21,05	20,05	-1,993	28,298	26,76	36,28	10,28
PL 30	02.11.	6,02	5,02	-4,067	28,868	26,32	36,26	10,51
PL 31	02.11.	15,01	14,01	-6,065	29,66	26,26	36,16	10,21
PL 32	02.11.	0,02	23,02	-7,974	30,468	26,9	36,46	10,37
PL 33	03.11.	9,15	8,15	-9,758	31,216	26,89	36,51	10,35
PL 34	03.11.	17,59	16,59	-11,524	31,979	27,16	36,75	9,71
PL 35	04.11.	6,08	5,08	-14,111	33,1	26,55	36,78	13,87
PL 36	04.11.	17,58	16,58	-15,8	33,83	26,69	37,2	13,37
PL 37	05.11.	6,08	5,08	-18,353	34,793	25,59	37,34	13,93
PL 38	05.11.	18,03	17,03	-20,866	35,752	25,29	37,27	13,5
PL 39	06.11.	6,17	5,17	-23,444	3737,2	24,34	37,3	13,74
PL 40	06.11.	18,01	17,01	-25,502	38,841	22,12	36,53	12,63
PL 41	07.11.	6,1	5,1	-27,433	40,581	22,48	36,79	13,45
PL 42	07.11.	17,59	16,59	-28,694	41,745	21,65	36,59	13,11
PL 43	08.11.	6,16	4,16	-30,729	43,648	21,1	36,41	13,98

Probe	Datum	GMT	Schiffs- Zeit	Breite (Grad)	Länge °West	Temp. THS(°C)	Salin, (‰)	Wasser- menge m ³
PL 44	08.11.	14,58	12,58	-32,156	45	20,2	35,89	9,81
PL 45	09.11.	3	1	-34,183	46,964	18,55	35,99	13,92
PL 46	09.11.	15,1	13,1	-35,54	48,298	17,86	35,79	13,68
PL 47	09.11.	0,01	22,01	-37,009	49,743	13,53	34,18	10,06
PL 48	10.11.	6,12	4,12	-38,132	50,921	15,69	35,16	7,01
PL 49	10.11.	12,04	10,04	-39,108	51,949	17,5	34,04	6,49
PL 50	10.11.	18,05	16,05	-40,241	53,082	13,02	33,78	6,77
PL 51	11.11.	3,25	1,25	-41,76	54,762	11,67	36,46	10,30
PL 52	11.11.	12,06	10,06	-43,183	56,223	9,62	34,09	9,44
PL 53	11.11.	19,12	17,12	-44,315	57,596	9,20	34,11	7,62
PL 54	11.11.	01,09	23,09	-45,267	58,684	7,17	34,09	7,00
PL 55	12.11.	10,58	08,58	-46,751	60,410	7,59	33,82	10,69

Tab. 1.11: Oberflächenwasser Isotopen-Proben

Probe	Datum	GMT	Schiffs- Zeit	Breite (Grad)	Länge (Grad)	Temp. THS(°C)	Salinität (‰)
I00	22.10.	8,17	8,17	48,083	8,763	16,65	35,82
I01	22.10.	12,22	12,22	47,7	9,935	16,08	35,72
I02	22.10.	18,37	18,37	47,236	11,32	16,03	35,68
I03	23.10.	0,2	0,2	46,253	12,401	16,3	35,71
I04	23.10.	6,41	6,41	45,163	13,653	16,49	35,76
I05	23.10.	13,05	13,05	44,096	14,765	17,32	35,87
I06	23.10.	21,06	21,06	42,881	16,153	17,77	36,01
I07	24.10.	6,24	5,24	41,329	17,796	17,58	35,94
I08	24.10.	16,07	15,07	39,504	19,684	18,53	36,05
I09	24.10.	24,05	23,05	38,036	21,164	19,09	36,38
I10	25.10.	9,07	8,07	35,963	22,075	20,81	36,41
I11	25.10.	18,21	17,21	34,425	22,688	21,39	36,37
I12	26.10.	3,1	2,1	32,651	23,437	22,42	36,70
I13	26.10.	12,1	11,1	30,621	24,255	23,61	37,07
I14	26.10.	21,08	20,08	28,59	25,053	24,3	37,28
I15	27.10.	6,21	5,21	26,344	25,917	25,05	37,52
I16	27.10.	15,07	14,07	24,499	26,611	25,34	37,23
I17	27.10.	0,07	23,07	22,477	27,374	25,65	37,51
I18	28.10.	9,12	8,12	20,836	27,956	25,98	36,87
I19	28.10.	18,08	17,08	19,212	28,471	26,19	36,78
I20	29.10.	3,25	2,25	17,36	28,976	26,96	36,48
I21	29.10.	12,08	11,08	15,542	28,915	27,44	36,29
I22	29.10.	21,08	20,08	13,7	28,833	27,58	36,2
I23	30.10.	6,15	5,15	11,68	28,769	27,9	35,83
I24	30.10.	15,09	14,09	9,77	28,699	28,51	35,79
I25	30.10.	0,04	23,04	7,85	28,6	28,75	34,23
I26	31.10.	9,14	8,14	5,925	28,545	28,26	35,65
I27	31.10.	18,12	17,12	4,266	28,463	28,52	35,27
I28	01.11.	3,15	2,15	2,515	28,457	28,22	35,64
I29	01.11.	12,22	11,22	0,211	28,38	26,95	36,14
I30	01.11.	21,05	20,1	-2,023	28,296	26,78	36,27
I31	02.11.	6,13	5,13	-4,105	28,879	26,31	36,26
I32	02.11.	15,08	14,08	-6,095	29,673	26,29	36,16
I33	02.11.	0,1	23,1	-7,995	30,477	26,9	36,47
I34	03.11.	9,24	8,24	-9,788	31,23	26,89	36,52
I35	03.11.	18,06	17,06	-11,553	31,992	27,15	36,75
I36	04.11.	6,21	5,21	-14,15	33,117	26,59	36,79
I37	04.11.	18,05	17,05	-15,821	33,839	26,72	37,20
I38	05.11.	6,18	5,18	-18,388	34,806	25,58	37,35
I39	05.11.	18,11	17,11	-20,895	35,769	25,27	37,27
I40	06.11.	6,26	5,26	-23,482	37,482	24,36	37,06
I41	06.11.	18,09	17,09	-25,523	38,859	22,11	36,54
I42	07.11.	6,17	5,17	-27,455	40,603	22,52	36,8

Probe	Datum	GMT	Schiffs- Zeit	Breite (Grad)	Länge (Grad)	Temp. THS(°C)	Salinität (‰)
I43	07.11.	18,07	17,07	-28,711	41,769	21,65	36,59
I44	08.11.	6,27	4,27	-30,758	43,674	20,94	36,38
I45	08.11.	15,07	13,07	-32,21	45,052	20,33	35,95
I46	09.11.	3,2	1,2	-34,191	46,971	18,53	35,98
I47	09.11.	15,19	13,19	-35,567	48,325	17,88	35,8
I48	09.11.	0,09	22,09	-37,035	49,774	13,53	34,18
I49	10.11.	6,21	4,21	-38,168	50,949	15,64	35,13
I50	10.11.	12,1	10,1	-39,108	51,949	17,5	34,04
I51	10.11.	18,13	16,13	-40,267	53,093	11,13	33,83
I52	11.11.	3,45	1,45	-41,797	54,802	11,6	34,45
I53	11.11.	12,13	10,13	-43,199	56,246	9,62	34,09
I54	11.11.	19,31	17,31	-46,379	57,669	9,28	34,11
I55	11.11.	01,15	23,15	-45,287	58,706	7,14	34,09

Methodik

Oberflächenwasser aus einer Tiefe von 10 m wurde via Planktonpumpe des Schiffes (Membranpumpe) und einer Schlauchleitung kontinuierlich durch ein 75 µm Netz geleitet. Um das Netz vor mechanischer Beschädigung zu schützen (Schlingerbewegungen) wurde es in einer grossen, meerwassergefüllten Wanne aufgehängt. Damit wurde das Netz auch vor zu starker Sonneneinstrahlungen geschützt. Die Durchfluß-Wassermenge wurde mit einem Flow-Meter gemessen, welches Dank der spontanen Hilfe der Techniker an Bord an die lokalen Verhältnisse angepasst wurde. Der mittlere Wasserfluß war 18 Liter pro Minute. In den meisten Fällen wechselten wir die Netze alle 9 Stunden aus. Bei geringeren Planktoninhalten verlängerten wir die Dauer auf 12 Stunden, bei erhöhter Produktivität reduzierten wir die Zeit auf 3 oder 6 Stunden. Bei jedem Wechsel wurden Zeit, Position, Wassertemperatur, und Salinität registriert und eine Isotopenprobe entnommen. Der Netzinhalt wurde in 250 ml PVC-Flaschen gespült, mit gepufferter (Borax-Puffer, pH 8.2-8.5) Formaldehyd-Lösung fixiert und dann bei +4°C im Kühlraum aufbewahrt. Die Isotopenproben wurden in Glas-Flaschen gesammelt und mit 2-3 Tropfen einer gesättigten KJ-Lösung versetzt.

3.4. Hydrologie

An den Tiefenstationen wurden Temperatur und Salinitätsprofile in den obersten 300 m der Wassersäule erstellt. Die Meßsonde war eine CTD von Seabird Electronics (Modell SBE), mit einer Meßrate von 2 Scans pro Sekunde. Die Absenkgeschwindigkeit war zwischen 1 bis 1.4 Meter pro Sekunde. Die Sonde funktionierte einwandfrei; einzig die End-Tiefenanzeige der Seilwinde stimmte nicht vollständig mit den End-Tiefen der Profile überein, was auf Strömungen in der Wassersäule zurückzuführen ist (Abweichung des Kabels von der lotrechten Richtung). Der Fehler bei den 300 m Casts beträgt bis zu 30 m. In der folgenden Liste sind die Datenfiles für die 300 m und 3000 m Casts aufgereiht (Die geographischen Positionen sind in Tab. 1.5 aufgelistet)

Station	Cast 300 m	Cast 3000 m
Sta. 1	-	-
Sta. 2	Mich_1.dat	IX_1.dat
Sta. 3	Mich_2.dat	IX_2.dat
Sta. 4	Mich_3.dat	IX_3.dat
Sta. 5	Mich_4.dat	IX_4.dat
Sta. 6	Mich_5.dat	IX_5.dat
Sta. 7	Mich_6.dat	IX_6.dat

3.5. Vorläufige Beobachtungen und Ergebnisse

Im Ganzen konnten wir unser Foraminiferen- und Phytoplankton-Programm wie geplant durchführen: Zwei von acht Tiefenstationen mussten jedoch schlechten Wetters wegen gestrichen werden. Die durchfahrenen Wassermassen lassen sich gut anhand der Temperatur- und Salinitäts Signatur im Oberflächenwasser identifizieren. Die Werte sind symmetrisch bezüglich 8° nördlicher Breite. Zwischen 50°N und 8°N erreicht die Salinität ihr Maximum (37.5‰) bei 25°N, während die Temperatur graduell ansteigt. Diese Muster bildet die zentralen Wassermassen der Nord-Atlantischen Wirbel ab. Im Nordäquatorialstrom beobachteten wir bei 8° nördlicher Breite das absolute Temperatur Maximum und ein ausgeprägtes Salinitäts-Minimum. Zwischen 8°N und 36°S fällt die Temperatur wieder ab, wobei bei 12°S der Brasilstrom für ein sekundäres Temperaturmaximum sorgt. Das Salinitätsmaximum der südatlantischen Wirbel wurde bei 20°S erreicht. Bei 36°S beschreibt die Oberflächentemperatur ein kräftiges Minimum, verbunden mit einem starken Abfall der Salinität. Vermutlich ist dieses Muster weniger durch die nahegelegene Mündung des Rio de la Plata verursacht, sondern durch die in dieser Gegend typischerweise etwas nach Norden verlagerte Ozeanische Front der Subtropischen Konvergenz. Zwischen 38°S und 42°S beobachteten wir starke Fluktuationen der Salinität, und bei 40°S machen sich die Ausläufer des Falklandstroms mit einem Temperatursturz im Oberflächenwasser von mehr als 5°C überdeutlich bemerkbar. Die starken Fluktuationen könnten durch kleine, lokale Eddies im Grenzbereich zwischen Falklandstrom und dem südlichen Brasilstrom verursacht sein. Im südlichsten Abschnitt unserer Fahrt, zwischen 40°S und 50°S, sinkt die Temperatur weiterhin und pegelt sich um 7.5°C ein. Die Salinität liegt hier lediglich bei 34‰.

In den nördlichen und südlichen zentralen Wassermassen waren die Planktonbestände erwartungsgemäss sehr niedrig. Unsere Netze mussten daher meistens ganze 9 Stunden oder mehr ausgesetzt werden, um eine vernünftige Probenmenge an planktonischen Foraminiferen zu erhalten. In den meisten Fällen beobachteten wir kleine, juvenile Stadien von Planktonforaminiferen häufiger als grosse, adulte Stadien. In solch tiefproduktiven Gebieten wären zusätzlich Netze mit kleineren Maschenweiten (z.B. 30 µm) sehr nützlich gewesen. Auch die Phytoplankton-Filtrationen waren sehr zeitaufwendig, da aus demselben Grunde große Wassermengen filtriert werden mußten. Meistens fanden wir kleine Globigerinen, Dinoflagellaten (*Ceratium*), Tintinniden und Copepoden. In den nördlichen Subtropen fanden wir eine grosse Artenvielfalt im kalkigen Nannoplankton: zahlreiche *Schyplosphaera apsteinii*, viele *Helicopontosphaera carteri*, *Umbellosphaera tenuis*, *Rhabdosphaera clavigera*, *Calcidiscus leptoporus*, *Syracospharta pulchra*, *Thoracosphaera heimii*, und *Emiliana huxleyi*. In den äquatorialen Breiten erhöhte sich die Artenzahl der Foraminiferen und bei 6°N fanden wir *Globigerina* sp., *Globigerinoides ruber*, *Globorotalia menardii*, viele Radiolarien und Dinoflagellaten. Besonders formenreich präsentierten sich die Radiolarien im Brasilstrom. Im Nordäquatorialstrom erhöhten sich die Bestände, zeigten jedoch grosse Fluktuationen. In der äquatorialen Auftriebszone beobachteten wir eine grosse Menge brauner, haariger, chlorophyllhaltiger Organismen (Dinoflagellaten), welche unser Netz zeitweilig verstopften. Radiolarien, sehr viele Diatomeen, Ceratium-ähnliche Dinoflagellaten, und viele Coccolithophoriden waren ebenfalls zu verzeichnen. Über dem Äquator selbst und in den südlich davon gelegenen zentralen Wassermassen fanden wir ent-

täuschend wenig Plankton: einige kleine Foraminiferen, Dinoflagellaten, dafür sehr schöne Radiolarien und Ostracoden. Zwischen 8°S und 11°S beobachteten wir viele isolierte Stacheln, vermutlich von spinosen Foraminiferen. (Da zu dieser Zeit Vollmond war, vermuteten wir den Einsatz des monatlichen Reproduktionszyklus (Gametogenesis) einer oberflächennahen Foraminiferenart).

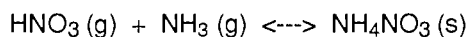
Die subtropische Konvergenz machte sich durch einen gewaltigen Anstieg an Biomasse bemerkbar: Riesige Mengen an dicken roten Copepoden und eine enorme Anzahl pennater Diatomeen füllten Netze und Filter. Immer noch waren Foraminiferen eher selten. Wir sahen aber erste Kaltwasser-Indikatoren wie *Neogloboquadrina pachyderma*. Auf dem Schelf angelangt, wurden unsere Netze so stark gefüllt, dass sie verstopften. Das Meerwasser war braungrau, und durch unsere Phytoplankton Filter liefen nur noch 2 Liter.

Da unsere Filter erst an Land gewogen und ausgezählt wurden, ließen sich nur einige sehr vorläufige Abschätzungen der Phytoplanktonbiomasse machen. Aufgrund der Anzahl Liter, die filtriert wurden und der Verfärbungen der Filter schlossen wir, daß Stationen 4 und 7 die höchsten Biomassen aufwiesen. In unseren Tiefenproben fanden wir erwartungsgemäss eine starke Abnahme an Chlorophyll unterhalb 75 m. Die größten Chlorophyll-Gehalte befanden sich nicht direkt an der Oberfläche, sondern in den obersten 10 bis 20 Metern. Besonders viel Chlorophyll beobachteten wir bei Sta. 4 in 75 m. Unterhalb 100 m sank der Gehalt an allen Stationen stark ab. Sta. 5 zeigte die geringsten Konzentrationen; selbst das Oberflächenwasser war sehr arm an Chlorophyll.

Zum Schluss möchten wir unsere Bewunderung über die Ausstattung der "Polarstern" ausdrücken. Ganz herzlich möchten wir uns für die grossartige Hilfe der Besatzung bedanken. Dank sei auch unserem Fahrleiter, Dr. Schulz-Baldes, für die Gelegenheit an ANT IX/1 teilnehmen zu dürfen.

4. **MESSUNG DER KONZENTRATIONEN AN GASFÖRMIGER SALPETERSÄURE, GASFÖRMIGEM AMMONIAK UND PARTIKELFÖRMIGEM AMMONIUMNITRAT IN DER ATMOSPHERE**
Th. Papenbrock (RUB)

Salpetersäure (HNO₃) ist ein stabiles Endprodukt der atmosphärischen NO_x- und HO_x-Chemie. Zu einem Drittel ist Salpetersäure am sauren Regen als Verursacher beteiligt und stellt somit ein wichtiges Spurengas in der Luft dar. Ammoniak (NH₃) ist die wichtigste Base in der Luft und wird besonders durch biologische Prozesse freigesetzt. Es wird in sauberer und verschmutzter Luft gefunden, gerade auch in mariner Atmosphäre. Beide Substanzen stehen mit dem partikelförmigen Ammoniumnitrat in folgendem Gleichgewicht:



Mit unserer Methode, der Laserphotolyse, haben wir kontinuierlich die Konzentration von HNO₃ und NH₃ mit einer Integrationszeit von einer Stunde ermittelt. Die Nachweisgrenze lag bei 40 pptv für HNO₃ und bei 0,3 ppbv für NH₃.

Wie schon bei früheren Reisen, wurde ein Nordsüdgefälle registriert. Maximale Konzentrationen wurden im Englischen Kanal ermittelt. Hier lagen die Salpetersäurekonzentrationen bei maximal 1,2 ppbv. Ähnliche Werte wurden für die NH_3 -Konzentrationen bestimmt. Mit Hilfe der Denuder-Technik wurden 18 Denuderproben mit einer Sammelzeit von 24 bzw. 48 Stunden (ab 30°Süd) genommen. Die Bestimmung der Konzentrationen von gasförmiger HNO_3 und partikelförmigem Ammoniumnitrat erfolgt nach der Reise im Heimatlabor. Salpetersäure wurde in einem kalten Denuderrohr gesammelt, Ammoniumnitrat in einem geheizten Rohr bei Temperaturen zwischen 140°C und 160°C. Durch die gleichzeitige Konzentrationsbestimmung von Salpetersäure, Ammoniak und Ammoniumnitrat sollen Zusammenhänge über das oben genannte temperatur- und feuchteabhängige Gleichgewicht aufgeklärt werden. In Verbindung mit der Teilnahme an ARK VII/2 bzw. ANT IX/2 versuchen wir gleichzeitig, einen Konzentrationschnitt der drei Substanzen von 80°N bis 70°S zu ermitteln.

5. MESSUNGEN BIOGENER SCHWEFELVERBINDUNGEN UND DEREN REAKTIONSPRODUKTE IN SEEWASSER UND MARINER ATMOSPHERE

R. Staubes, B. Schäfer (IfMG)

Während des Fahrtabschnittes ANT IX/1 wurden simultane Messungen von Dimethylsulfid (DMS), Carbonylsulfid (COS), Schwefelkohlenstoff (CS_2) und Methylmercaptan (MeSH) in Seewasser und der marinen Grenzschicht durchgeführt. Als wichtigste Reaktionsprodukte dieser Verbindungen in der Troposphäre, wurden die Konzentrationen von Sulfat und Methansulfonat im Aerosol bestimmt.

Atmosphärische Proben wurden auf dem Peildeck genommen; um den Einfluß des Schiffes zu minimieren, wurden zu diesem Zweck zwei Ausleger an der vorderen Reling des Peildecks befestigt. Aerosole wurden auf Delbag-Filtern angereichert, die Analyse der jeweiligen Ionenkonzentrationen im Aerosol wird ionenchromatographisch im Frankfurter Labor durchgeführt. Das untersuchte Seewasser wurde dem Seewasser-Pumpensystem des Schiffes entnommen. Die Konzentrationen von atmosphärischen sowie im Seewasser gelösten DMS, COS, CS_2 und MeSH wurden mit Hilfe eines Gaschromatographen mit flammenphotometrischen Detektor analysiert. Die Resultate bestätigen, daß DMS das dominierende Schwefelgas im Seewasser darstellt; COS, CS_2 und MeSH tragen insgesamt nur höchstens 20% zum beobachteten Schwefelgas-Gehalt des Seewassers bei. Atmosphärisches DMS in der marinen Grenzschicht zeigte eine signifikante räumliche Variabilität, während COS entlang der Fahrtroute nahezu homogen verteilt war. Spuren weiterer biogener Schwefelgase wurden nur in einer begrenzten Anzahl in atmosphärischen Proben gefunden.

Parallel dazu wurde die Konzentration von Wolkenkondensationskernen bestimmt, die als atmosphärisches Reaktionsprodukt von DMS gebildet werden können. Die Gesamtpartikelkonzentration wurde mit einem Kernzähler TSI 3020 gemessen. Um die Wolkenkondensationskernzahl zu bestimmen, wurde die Anzahl der aktivierten Partikel mit Hilfe einer thermischen Diffusionskammer gemessen.

6. **MUSTER UND GEHALTE DER POLYCHLORBI-
PHENYLE (PCB), DER HEXACHLORCYCLOHEXAN-
ISOMEREN (HCH) UND DES HEXACHLORBENZOLS
(HCB) IN DER GRUNDSCHICHT DER TROPOSPHÄRE
UND IM OZEANISCHEN OBERFLÄCHENWASSER**
R. Bacher, O. Luxenhofer, J. Schreitmüller (UU)

Zielsetzungen

Die Arbeiten erfolgten im Rahmen der schon seit mehreren Jahren durchgeführten Untersuchungen über Beziehungen zwischen chemischer Struktur und globalen Umweltverhalten von Xenobiotika. Es wurden Luft- und Wasserproben für Messungen umweltrelevanter C1-C14-Organohalogenverbindungen während der Traverse von 50 N bis 50 S genommen. Es sollten u.a. Nord-Süd-Profile für folgende Substanzen erstellt werden:

- Chloroform, Tetrachlormethan
- Trichlorethen, Tetrachlorethen, Methylchloroform
- Hexachlorbutadien
- Hexachlorbenzol
- HCH-Gruppe
- Polychlorbiphenyle
- DDT-Gruppe
- Chlordan-Gruppe

Die großen Variationen in physikochemischen Parametern (Dampfdruck, Wasserlöslichkeit, Henry-Konstante), im Transportverhalten (Depositionsverhalten, Transport an Partikeln gebunden oder in der Gasphase) und in den Abbaueigenschaften, die mit der Summe dieser Verbindungen erfaßt werden, lassen wertvolle Erkenntnisse über das allgemeine Verteilungsverhalten von Xenobiotika in verschiedenen Umweltkompartimenten erwarten.

Der direkte Einfluß der für die untersuchten Xenobiotika relevanten Emissionsquellen ist bei einer Beprobung im marinen Bereich minimiert. So können vor allem die Mechanismen des Ferntransports (Interhemisphären-austausch) auf dieser Fahrtroute gut untersucht werden. Die Produktions- und Anwendungsstätten der Großzahl der beprobten Substanzen liegen überwiegend in der Nordhemisphäre (Ausnahme: Pestizide). Die Korrelationen der Analysenwerte zwischen der Nord- und Südhemisphäre sind deswegen von besonderem Interesse. Ein gemessener Eintrag vieler der diskutierten Substanzen in die Südhemisphäre erfolgt überwiegend über die globalen Austauschprozesse aus der Nordhemisphäre. Der Vergleich der zu erstellenden Analysendaten mit entsprechenden Werten einer früheren Fahrt unserer Arbeitsgruppe (ANT III/4- Kapstadt-Bremerhaven-1985) soll Erkenntnisse über Zu- bzw. Abnahmetrends für die untersuchten Substanzen in den verschiedenen Umweltkompartimenten erbringen.

Arbeitsprogramm

Die Probenahme wurde nach Ausfahrt aus dem Ärmelkanal aufgenommen. Zuvor war aufgrund des starken Schiffsverkehrs und vom Festland kommender Winde mit zu starken direkten anthropogenen Einträgen zu rechnen. Die Luftprobenahme auf leicht- bis mittelflüchtige CKW (C1-C6) wurde durch adsorptive Anreicherung dieser Substanzen auf Tenax durchgeführt (Probevolumina: 1-500 l Luft). Entsprechend den zu erwartenden Konzentrationen der

Zielkomponenten im ppt-ppq-Bereich (pg-ng/m³) und den Erfordernissen der Minimierung des Durchbruchs wurde die beprobte Luftmenge auf bestimmte Untergruppen der genannten Substanzklasse ausgerichtet. Als Probenahmeort für die leichtflüchtigen CKW (Probenvolumen: <15 l) diente bei schlechter Witterung das Peildeck. Ansonsten konnte für diesen Zweck auch der Bugausleger genutzt werden, der den für diese Fragestellung geringsten Kontaminationseinfluß durch das Schiff selbst erwarten läßt. Die Probenahme der mittelflüchtigen CKW (-> C6) wurde auf dem Peildeck durchgeführt (Probenvolumen 200-500 l). Es wurden für jeden Probentyp im Tagesverlauf mindestens zwei Probennahmen durchgeführt und dabei stets Parallelproben gezogen. Zusätzlich wurden CKW in Wasserproben durch Auspurgen mit gereinigter Luft und anschließender adsorptiver Anreicherung auf Tenax erfaßt.

Für die Probenahme von Luft in Blickrichtung auf die schwerflüchtigen CKW (vor allem der PCBs) wurde ein High-Volume-Sampler eingesetzt. Die kontinuierlich geförderten Luftmengen für die Einzelproben betragen hier zwischen 500-1000 m³. Die adsorptive Anreicherung der Organohalogenverbindungen erfolgte hierbei auf Kieselgel, wobei außerdem eine Separation des partikel- und gasförmigen Anteils des Eintrages über einen Glasfaserfilter erfolgt. Der Durchbruch wird durch eine zweite separate Kieselgelschicht in der Sammelapparatur beprobt. Als Probenahmeort diente während der ganzen Reise das Peildeck. Bei ungünstiger Windlage (achterliche Winde) wurde der High-Volume-Sampler während einiger Stationsstops des Schiffes kurzzeitig abgestellt. Außerdem wurden noch für alle untersuchten Substanzgruppen einige zusätzliche Luftproben auf dem Helikopter- und dem Arbeitsdeck parallel zu den üblichen Probenahmeorten genommen, um den Einfluß von Kontaminationen durch das Schiff erkennen zu können. Die Probenahme von schwerflüchtigen Organohalogenverbindungen im Wasser erfolgte durch täglich mehrmalige Entnahme von Oberflächwasser mit Edelstahlheimern aus der schiffseigenen Förderpumpe am Achterdeck (Probenvolumina ca. 80 l). Die so gewonnenen Wasserproben wurden mittels einer Pumpe durch eine XAD-Kartusche (Divinylbenzol-Polystyrol-Copolymer) gefördert, wobei eine adsorptive Anreicherung der Organohalogenverbindungen erfolgt. So wurden über einen Arbeitstag integrierte vorfraktionierte Wasserproben gewonnen. Sämtliche erwähnten Adsorptionsmittel wurden für den Transport luftdicht in geeignete Glasgeräte eingeschmolzen.

Geplante Messungen am Heimatinstitut

Die über Adsorption auf Tenax gewonnenen Proben (C1-C6-CKW) werden nach bereits ausgearbeiteten Methoden thermisch desorbiert. Nach einer Fokussierung durch eine Kältefalle (flüssiger Stickstoff) erfolgt die Eingabe und Trennung in einem gaschromatographischen System. Die Desorption erfolgt im Falle von Kieselgel und XAD mittels organischer Laufmittel. Vor der eigentlichen Injektion am Gaschromatographen wird weiterhin ein Clean-up mit verschiedenen adsorptionschromatographischen Methoden durchgeführt, um interferierende Begleitkomponenten von interessierenden Substanzen abzutrennen. Die Detektion für alle zu messenden Proben soll mit dem für Halogenverbindungen sehr empfindlichen Elektroneneinfangdetektor (ECD) erfolgen. Zusätzlich sollen einige Proben der schwerflüchtigen Organohalogenverbindungen mit einem massenspektrometrischen Detektor (MSD) gemessen und ausgewertet werden.

**7. ORGANOBROMVERBINDUNGEN IN DER MARINEN
TROPOSPHÄRE UND IM ATLANTISCHEN
OBERFLÄCHENWASSER**
Th. Oertel, R. Weller (AWI)

Ziel der Messungen während der Überfahrt von Bremerhaven nach Punta Arenas war es, horizontale Verteilungsprofile verschiedener leichtflüchtiger bromierter Kohlenwasserstoffe in der marinen Troposphäre zu messen. Zu diesen Verbindungen zählt Methylbromid (CH_3Br), das hauptsächlich von Makroalgen produziert wird sowie die fluorierten Verbindungen Trifluorbrommethan (CF_3Br) und Difluorchlorbrommethan (CF_2ClBr), die beide anthropogenen Ursprungs sind. Die letzteren gelten wegen ihrer chemischen und photolytischen Stabilität in der Troposphäre als langfristige, potentielle Quelle für Br-Atome in der Stratosphäre und sind dort in den katalytischen Ozonabbau involviert. Ein signifikantes Ozonzerstörungspotential der biogenen Organobromverbindungen wird in der Literatur diskutiert. Aus den gemessenen Profilen dieses und vorangegangener Fahrtabschnitte, ergänzt durch Laborexperimente, werden Aussagen über den biogenen Beitrag auf den bromkatalysierten stratosphärischen Ozonabbau erwartet. Zur Untersuchung des Austausches mit der Hydrosphäre wurden die luftchemischen Daten durch Messungen der Organobromverbindungen im Oberflächenwasser ergänzt.

Luftprobennahme und gaschromatographische Analytik erfolgte 20 m über dem Meeresspiegel im Luftchemiecontainer auf der vorderen Steuerbordseite des Peildecks durch eine ca. 5 m lange Edelstahlleitung. Die Windrichtung wurde ständig überwacht und die Messung bei ungünstigen Verhältnissen abgebrochen, um eine Kontaminierung durch Schiffsabgase o.ä. zu vermeiden. Die Spurengase wurden durch Ausfrieren in flüssigem Argon angereichert (flüssiges Argon verhindert im Gegensatz zu flüssigem Stickstoff das Auskondensieren von Sauerstoff, der die Messungen empfindlich stören könnte). Dabei saugte eine Membranpumpe die Luft bei konstantem Fluß (50 ccm/min) durch ein U-förmiges Stahlrohr, gepackt mit silylierter Glaswolle. Vor der Kühlfalle wurde der Wassergehalt der Luft mit Hilfe eines Permeations-Gastrockners entfernt. Mit dieser Methode wurden ca. 120 Luftproben zwischen 15°N und 50°S gesammelt und unmittelbar danach gaschromatographisch analysiert (aufgrund technischer Probleme war eine kontinuierliche Probenahme erst ab 15°N möglich). Da der Gaschromatograph mit einem zwar hochempfindlichen aber nur bedingt selektiven Elektroneneinfang-Detektor (ECD) ausgestattet war, wurden ca. 30 Luftproben getrennt gesammelt und in einer Tiefkühltruhe bei -30°C gelagert. Diese Proben sollen am AWI durch aufwendigere Methoden wie Gaschromatographie-Massenspektroskopie-Kopplung (GC-MS), Gaschromatographie-Iontrap oder Gaschromatographie-FTIR-Kopplung analysiert werden, um die in den Chromatogrammen detektierten Peaks möglichst vollständig zuzuordnen.

An Bord ließen sich durch Vergleiche mit Standards CH_3Br , CF_3Br und CF_2ClBr direkt auswerten und eine vorläufige Quantifizierung ergab, daß die Konzentrationen dieser Verbindungen im unteren pptv - Bereich liegen und keine signifikanten Gradienten gemessen werden konnten, ein Befund, der typisch ist für Verbindungen mit einer langen troposphärischen Verweildauer. Eine zuverlässige Quantifizierung und statistische Aufarbeitung der Daten erfolgt am AWI.

Zur Untersuchung des Austausches der leichtflüchtigen Bromverbindungen im System Ozean/Luft wurden ca. 40 Wasserproben zwischen 31°N und 50°S in Glasampullen gesammelt, die ebenfalls erst am AWI analysiert werden können.

**8. MESSUNGEN VON ATMOSPHERISCHEM
QUECKSILBER ÜBER DEM ATLANTIK**
F. Slemr, E. Langer (IFUG)

Das Ziel der geplanten Messungen war es, die Entwicklung des Quecksilbergehalts der Atmosphäre weiterzuverfolgen, deren Messungen vor zehn Jahren begonnen wurden. Dazu wurden insgesamt etwa 300 Analysen des Gesamtquecksilbers in der Luft mit gleicher Technik durchgeführt, mit der vor zehn Jahren bei Fahrten mit FFS "Walther Herwig" und FS "Meteor" Quecksilber über den nahezu gleichen Gebieten des Atlantiks und zu gleicher Jahreszeit gemessen worden ist. Die erste Durchsicht der Daten ergibt, daß die Gesamtquecksilber-Konzentrationen in der Luft gegenüber den Messungen aus den Jahren 1977 bis 1980 um etwa 20% angestiegen sind. Der geschätzte Anstieg in beiden Hemisphären ist etwa gleich groß. Die Messungen ergeben somit den ersten Hinweis auf den ansteigenden Trend der Quecksilberkonzentrationen in der Atmosphäre. Die Versuche, diesen durchaus zu erwartenden Trend mit Analysen der Eisbohrkerne nachzuweisen, schlugen bisher unseres Wissens wegen Kontaminationsproblemen fehl.

Dieser erste Eindruck muß allerdings noch durch detaillierte Analyse der Daten verifiziert werden. Aus dem Datensatz müssen die durch Schiffsabgase oder durch Schiffskörper kontaminierten Proben ausgeschlossen werden. Obwohl die Windverhältnisse insgesamt für die Luftprobennahme durchaus günstig waren, wurden die Proben bei den Stationen, bei denen sich das Schiff gedreht hat, nahezu regelmäßig kontaminiert. Im Gegensatz zu den früheren Messungen ist die Interpretation der Daten dadurch erschwert, daß die ITCZ diesmal anhand der Quecksilberdaten definiert werden konnten. Damit lassen sich die Daten zum Teil nicht eindeutig zu nord- oder südhemisphärischen Luftmassen zuordnen. Eindeutige Zuordnung wird vielleicht mit Hilfe der Daten über Kohlenmonoxid-Konzentrationen und mit der Analyse der meteorologischen Situation zum Zeitpunkt des Überquerens der ITCZ möglich.

Ergänzend zu diesen Messungen wurden Luftproben für die Bestimmung von Methylquecksilber gezogen, die vom N. Bloom in Seattle analysiert werden. Die Ergebnisse dieser Messungen könnten zu der Lösung der umstrittenen Frage beitragen, ob die Ozeane biogenes Quecksilber, u.a. als Methylquecksilber, emittieren können. Unabhängig von den Messungen, die auf die Aufklärung des globalen Quecksilberkreislaufs gerichtet waren, wurde kontinuierlich Ozon und Wasserstoffperoxid registriert. Das Wasserstoffperoxid wurde mit fluorimetrischer Methode nach Lazrus et al. gemessen, die auch Hinweise über das Gehalt der organischen Peroxide in der Luft liefert. Die Konzentrationen des Wasserstoffperoxids und der organischen Peroxide zeigten ein Maximum in der Äquatorregion an, die von den Modellen der troposphärischen Chemie vorausgesagt wird. Detaillierte Auswertung dieser Daten steht noch aus.

9. MESSUNGEN ZUR SPEKTRALEN OPTISCHEN DICKE DES AEROSOLS ÜBER MEER

A. Herber (ULP)

Die spektrale optische Dicke des Aerosols wird durch Messungen der direkten Sonnenstrahlung mit einem Sonnenfotometer (Typ ABAS - AOL) im Wellenlängenbereich von 400 bis 1100 nm bestimmt. Mit diesen Messungen im Oktober/November 1990 wurde nach den Messungen im Juni 1991 ein zweiter Meridionalschnitt der optischen Dicke des Aerosols vorgenommen. Die ersten Messungen wurden auf dem Fahrtabschnitt von Puerto Madryn (Argentinien) nach Rostock auf dem sowjetischen Forschungsschiff A. Fedorov durchgeführt. Damit war die Möglichkeit gegeben, innerhalb eines Jahres saisonale Besonderheiten im Nord - Süd Schnitt zu untersuchen. Mit diesen Messungen kann das Wissen über die globale Verteilung des Aerosols vertieft werden. Aus früheren Messungen ist bekannt, daß die spektrale optische Dicke des Aerosols auf der Nordhemisphäre höher ist als auf der Südhemisphäre, da durch die Verteilung der Landmassen auf der Erde und die erhöhte Konzentration der Industrie wesentlich mehr natürliche und anthropogene Quellen auf der Nordhalbkugel vorhanden sind. Bei dem über Meer gemessenen Aerosol handelt es sich in erster Linie um marines Aerosol (Sea spray) mit der Hauptkomponente NaCl. Über Luftmassentransporte können aber auch andere Aerosoltypen herangeführt werden.

Für ein marines Aerosolspektrum ist im Wellenlängenbereich von 400 bis 1100 nm ein neutrales Extinktionsverhalten charakteristisch, das heißt, die optische Dicke des Aerosols ist fast wellenlängenunabhängig. Eine genaue Beschreibung der aerosoloptischen Dicke und damit eine Charakterisierung des Aerosols ist nicht ohne Beschreibung der meteorologischen Randbedingungen möglich. Auf der Reise Ant IX/1 wurde zwischen 48°N und 48°S pro Breitengrad eine Radiosonde gestartet. Damit war die Möglichkeit gegeben, für die Aerosolmessungen Informationen über die Höhenverteilung von Temperatur und Wind zu erhalten. Bei den Messungen im Juni ist eine klare Nord - Süd Abhängigkeit der Aerosoloptischen Dicke Delta festzustellen, wobei wegen der ITCZ im Juni (2°N - 2°S) nicht der Äquator die Trennlinie ist. Für die Nordhemisphäre ist eine starke Variabilität zu beobachten, mit Deltawerten der optischen Dicke des Aerosols von 0.178 ± 0.089 bei einer Wellenlänge von 1000 nm. Für die Südhemisphäre wurden deutlich geringere Deltawerte von 0.065 ± 0.028 gemessen.

Beim zweiten Meridionalschnitt wurden zwischen dem 22. Oktober und 11. November (48°N - 45°S) über 40 Messungen zur spektralen optischen Dicke des Aerosols durchgeführt. Für die Nordhemisphäre sind ähnliche Ergebnisse zu verzeichnen, wie bei den Messungen im Juni. Der mittlere Deltawert beträgt 0.183 ± 0.073 bei 1000 nm. Die ITCZ lag im Oktober zwischen 9 und 5°N. Etwas überraschend ist, daß die optische Dicke des Aerosols der Südhemisphäre wesentlich höher liegt als im Juni. Der mittlere Deltawert beträgt 0.100 ± 0.030 . Ob es sich dabei um einen jahreszeitlichen Effekt handelt oder es andere Ursachen hat ist unklar. Auch ein systematischer Meßfehler ist nicht ausgeschlossen. Bei den vorgestellten Meßdaten handelt es sich um vorläufige Ergebnisse.

**10. FERNERKUNDUNG STRATOSPHERISCHER
SPURENSTOFFE MITTELS ABSORPTIONS-SPEK-
TOSKOPIE IM ULTRAVIOLETTEN UND SICHTBAREN
SPEKTRALBEREICH**
K. Kreher (UH)

Zielsetzung

Auf dem Fahrabschnitt ANT IX/1 (Bremerhaven - Punta Arenas) wurden Streulichtmessungen zur simultanen Konzentrationsbestimmung von Ozon und einigen mit dem Ozonabbau-Mechanismus eng verknüpften stratosphärischen Spurenstoffen (Stickoxid- und Halogenverbindungen) durchgeführt. Die ungefähr 2.000 gewonnenen Spektren enthalten Informationen über die Breitenabhängigkeit der Säulendichten dieser Spurenstoffe. Die Fahrt diente sowohl zum Datensammeln, d.h. zur Aufnahme der Streulichtspektren, als auch zur generellen Erprobung des Meßaufbaus (Schiffstauglichkeit). Im Anschluß an den Fahrabschnitt ANT IX/1 soll diese Apparatur zu den selben Messungen in der meteorologischen Station der GvN eingesetzt werden. Um eine Aussage bezüglich der Güte der Spektrennahme zu machen, muß erst eine entsprechende Auswertung am Institut für Umweltphysik in Heidelberg erfolgen.

Arbeitsprogramm

Über eine 8m lange Quarzfaser wurde das im Zenit gestreute Sonnenlicht in einen Spektrographen geleitet, dort mit einem holographischen Gitter spektral zerlegt und mit einer Photodiodenzeile analysiert. Aufgenommen wurden die Meßspektren vorwiegend bei Zenitwinkeln von 80-95°, d.h. bei Sonnenauf- und -untergang. In diesem Fall ist der Lichtweg durch die Atmosphäre, und somit auch die Wegstrecke, auf der die atmosphärischen Spurengase das Licht absorbieren können, besonders groß. Die so gewonnenen Spektren weisen charakteristische Absorptionsbanden der in der Atmosphäre vorhandenen Spurengase auf, die nach Entfernung der dominierenden Fraunhoferlinien mit bei möglichst kleinen Zenitwinkeln aufgenommenen Referenzspektren zur Berechnung von vertikalen Säulendichten benutzt werden können. Die Bestimmung der optischen Dichten von Ozon (O_2 und Stickstoffdioxid (NO_2)) konnte mit einem einfachen Auswertalgorithmus schon teilweise an Bord der Polarstern geschehen. Die weitere Auswertung - d.h. die eigentliche Berechnung der Konzentrationen - kann erst in Heidelberg vorgenommen werden, da zu ihrer Durchführung ein Computermodell benötigt wird, das den Strahlungstransport in der Atmosphäre simuliert. Von der Gruppe der im Ozonabbau involvierten Halogenverbindungen können aus den aufgenommenen Spektren die Konzentrationen von Bromoxid (BrO) und Chlordioxid (OCIO) bestimmt werden. Auch diese Auswertung erfordert einen erheblichen rechnerischen Aufwand und wird deshalb erst am Heimatinstitut vorgenommen werden können.

Die bis jetzt aus den Spektren bestimmten optischen Dichten für Ozon und Stickstoffdioxid zeigen jedoch, daß die gemessenen Konzentrationen in den erwarteten Größenordnungen liegen.

11. AKTIVITÄTEN AM NEUEN BORDRECHNERSYSTEM WÄHREND ANT IX/1

J-M. Schlüter, P. Gerchow (AWI)

Während des Werftaufenthalts im November 1990 von FS Polarstern in Bremerhaven, wurde der wissenschaftliche Bordrechner durch ein neues Bordrechnersystem von Digital Equipment ausgetauscht. Das Bordrechnersystem besteht nun aus einer Maschine für die Benutzer und vier sogenannten Servern, welche unterschiedliche Aufgaben wahrnehmen:

- Datenbankserver für die Nutzung von wissenschaftlichen Datenbanken.
- Datalogger zur Aufzeichnung der wissenschaftlichen und navigatorischen Daten.
- Server für die Vernetzung von Apple Macintosh Computern.
- Server für die Vernetzung von IBM-kompatiblen Personal Computern.

Während ANT IX/1 sind folgende Tätigkeiten am neuen Bordrechnersystem durchgeführt worden :

- Modifizieren und Überprüfen der von Digital vorgegebenen Benutzerschnittstellen.
- Einstellungen am Bordrechnersystem verändert, damit ein möglichst sicherer Betrieb gewährleistet wird.
- Modifizieren der wissenschaftlichen und navigatorischen Datenaufzeichnungs- und Verarbeitungsprozesse.
- Konfigurieren des Apple-Netzwerkes für Print- und Fileservices.
- Installieren des PCLAN-Servers zur Einbindung von IBM-PCs in das VAX-Bordrechnersystem.
- Erstellen von Dokumentation und Schulungsunterlagen für das System-Management.
- Erstellen von Dokumentation für die Wissenschaftler.

FAHRTABSCHNITT ANT IX/2

(Punta Arenas - Kapstadt - 16.11.90 - 30.12.90)

1. FAHRTVERLAUF UND ZUSAMMENFASSUNG
E. Fahrbach (AWI)

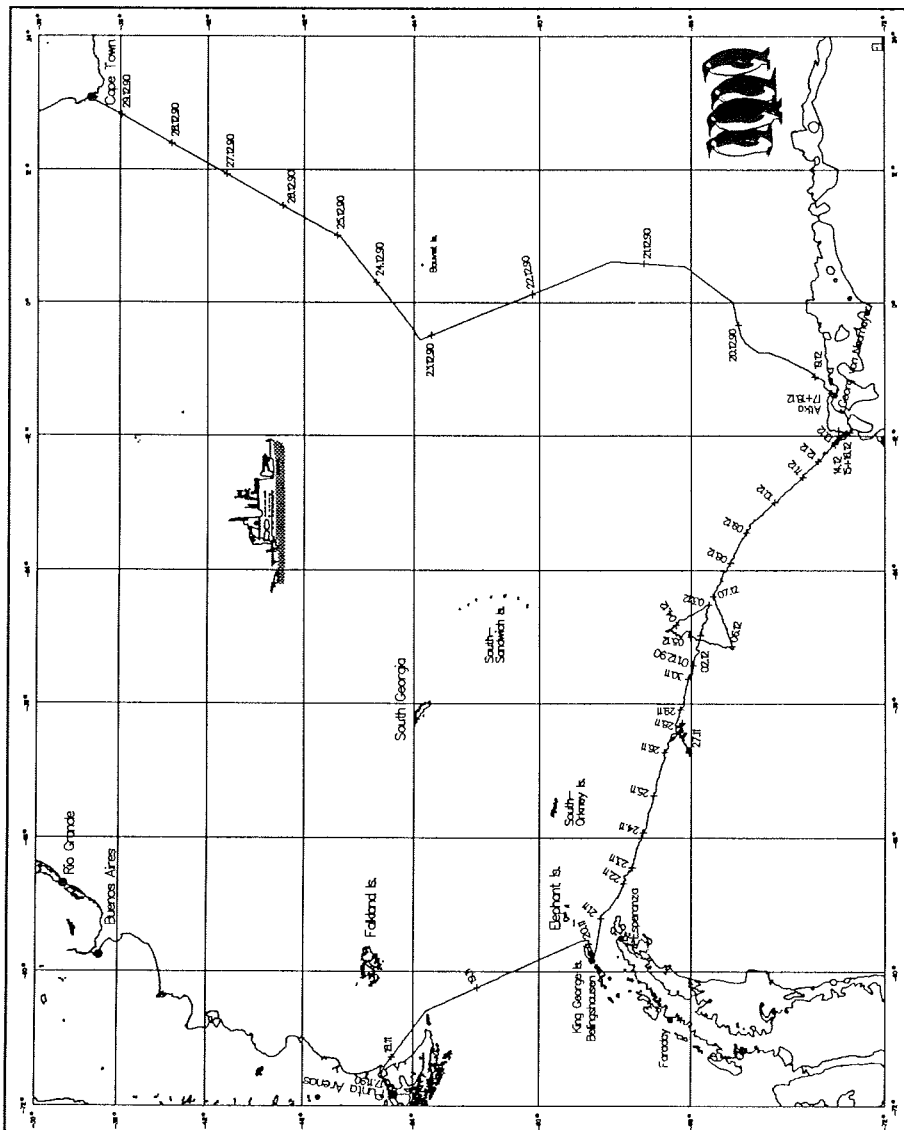
Am 17. November 1990 um 23.00 Uhr verließ "Polarstern" die Bunkerpier von Cabo Negro bei Punta Arenas. Durch die Magellanstraße liefen wir in den Atlantik, dann entlang der Ostküste Feuerlands zur Drake Passage. Den Kontinentalabhang bei 54°54'S, 63°19'W erreichten wir am 19. November und begannen die Arbeiten zur physikalischen Ozeanographie des Antarktischen Zirkumpolarstroms mit einem XBT-Schnitt (Expendable Bathythermograph). Die XBT-Profile wurden zur Verwendung im Rahmen des IGOS-Programmes (Integrated Global Ocean Services System) in das Global Telecommunication System (GTS) eingespeist. Zur Erfassung des Strömungsfeldes wurde ein Akustischer Strömungsprofilmesser (ADCP) eingesetzt. Die Untersuchungen der Luftchemie wurden in Fortsetzung der Arbeiten vom vergangenen Fahrtabschnitt weitergeführt. Es wurden Messungen zum marinen Schwefelkreislauf, in dem DMS (Dimethylsulfid) eine besondere Rolle spielt, zu reaktiven atmosphärischen Stickstoffverbindungen und den Organobromverbindungen ausgeführt. Sie stehen im Zusammenhang mit der Untersuchung anthropogener Einflüsse auf die Zusammensetzung der Atmosphäre und deren Folgeerscheinungen.

Die Polarfront erreichten wir bei 57°23'S, 61°14'W. Dort begannen die Hydrosweep- und Parasoundvermessungen, die während der ganzen Reise fortgesetzt wurden. Am 20. November passierten wir kurz nach Mitternacht auf 58°55'W den 60sten Breitengrad und hatten damit die Antarktis erreicht. Unser erstes Ziel war die sowjetische Forschungsstation "Bellingshausen" auf der King-George-Insel, wo wir drei deutsche Wissenschaftler zu einem viermonatigen Forschungsaufenthalt ablieferten. Sie sind die ersten Bundesbürger, die Forschungsarbeiten auf einer sowjetischen Polarstation ausführen. Als "Polarstern" in die Maxwellbucht, an der die Station liegt, einlief, wurden wir bereits erwartet. Fertig gepackt stand ein Schwimmpanzer mit Geräten und etwa 1,5 Tonnen zu entsorgendem Abfall bereit. Aus Sicherheitsgründen von unserem Schlauchboot eskortiert, ging das Amphibienfahrzeug bei "Polarstern" längsseits und wurde entladen. Anschließend wurden mehr als acht Tonnen Versorgungsgüter für die Durchführung eines biologischen Forschungsprojektes von "Polarstern" angelandet. Die fünf Stunden für das Lademanoöver nutzten wir über einen Pendelverkehr mit dem Helikopter zur Völkerbegegnung. Während wir sowohl die sowjetische wie auch die benachbarte chilenische Station "Teniente Marsh" besuchen konnten, folgten etwa 50 sowjetische, chilenische und ein deutscher Stationsbewohner unserer Einladung zu einer Besichtigung des Schiffes. Mit Abschluß der Ladearbeiten traten unsere Gäste ihren Rückweg an. Ein deutscher Wissenschaftler ging nach einem elfmonatigen Aufenthalt mit uns auf die Rückreise. Nach der Messung eines hydrographischen Vertikalprofils mit der CTD-Sonde (conductivity, temperature, depth) sowie einem Fang mit dem Multinetz verließen wir die Bucht. Von der King-George-Insel dampften wir bei mäßigem Wind über die Bransfieldstraße zur nordöstlich der Antarktischen Halbinsel gelegenen Joinvilleinsel. Hier begann die Forschungsarbeit auf dem Schelf mit den ersten Hols des Agassiz-Trawls. Der reichliche Fang verschaffte den Biologen lebende Krebse für Hälterungsversuche, bei denen

die Temperaturabhängigkeit und die Kinetik der Verdauungsenzyme von Crustaceen untersucht wird.

Im offenen Wasser erreichten wir den westlichen Fußpunkt unseres Schnittes, der quer durch das Weddellmeer nach Kapp Norvegia verläuft und auf dem das Hauptarbeitsprogramm stattfand (Fig. 2.1). Die physikalischen Ozeanographen begannen mit der Auslegung der Verankerung 215. Die ausgebrachten Geräte sollen zwei Jahre lang, bis sie wieder eingeholt werden, Geschwindigkeit und Richtung von Meeresströmungen, die Temperatur des Wassers und den Wasserstand messen.

Fig. 2.1: Die Fahrtroute von "Polarstern" während ANT IX/2
 Fig. 2.1: Cruise track of "Polarstern" during ANT IX/2



Im Anschluß wurde auf dem Schelf im freien Wasser die erste Biologiestation ausgeführt, auf der zweimal das CTD mit Kranzwasserschöpfer, Multinetz, Bongonetz, Planktonnetz, Quantameter und Secchischeibe eingesetzt wurde. Die biogeochemischen Arbeiten waren besonders auf den Silikat- und Stickstoffhaushalt ausgerichtet. Dazu wurden Inkubationen an Deck und im Labor ausgeführt, wobei die Aufnahme von radioaktivem ^{14}C , ^{32}Si , und ^{32}P , sowie stabilem ^{15}N bestimmt wurde. Der Stickstofffluß im antarktischen Nährstoffkreislauf wurde von der Wassersäule bis zum Zooplankton verfolgt. In diesem Rahmen wurde die Zusammensetzung und die Biomasse des Phytoplankton sowie die Reproduktion und die Entwicklung dominanter Copepoden untersucht.

Im offenen Wasser wurde die Verankerung 206 aufgenommen, die vor einem Jahr ausgebracht worden war. Bei der Auslegung der Fortsetzungsverankerung brach ein Drehwirbel, was wegen der notwendigen Aufnahme des abgerissenen Teils und der anschließenden Neuauslegung zu einer Verzögerung führte.

Unter günstigen Bedingungen ging es zügig nach Südosten. Bei $63^{\circ}30'\text{S}$, $51^{\circ}30'\text{W}$ erreichten wir am 22. November in etwa 150 km Entfernung von der Küste das Eis, das sich schon von der Ferne durch den Eisblink am Himmel angemeldet hatte. Gleichmäßige Winde hatten zur Ausbildung einer scharfen Kante geführt. Schnell verwandelte sich die kannelige See in ein sanft wiegendes Feld aus Trümmereis und Schollen. Bei Wassertemperaturen über dem Gefrierpunkt waren deutliche Spuren des Schmelzens zu erkennen. Mit zunehmender Entfernung von der Küste nahm der Wind ab, und es begleitete uns eine ruhige Wetterlage mit schwachen Winden und milden Lufttemperaturen, die nur ausnahmsweise unter -4°C fielen. Beim weiteren Vordringen ins Eis vergrößerten sich die Schollen auf mehrere Kilometer Durchmesser, waren aber meist durch breite Rinnen getrennt. Diese gestatteten uns zwar zügiges Fahren, doch erzwangen sie einen Kurs in Schlangenlinien, um zur gewünschten Position zu gelangen.

Unter der CTD mit dem Kranzwasserschöpfer wurde ein neuentwickelter "Minimulticorer" aufgehängt, der jeweils zwei Sedimentproben mit an die Oberfläche brachte. Ohne wesentlichen zusätzlichen Zeitaufwand konnte so ein Profil des Oberflächensediments durch das Weddellmeer aufgenommen werden. Am 26. November begann bei $65^{\circ}34'\text{S}$, $38^{\circ}52'\text{W}$ die Hydrosweep- und Parasoundvermessung eines Rinnensystems, das sich durch das Weddellmeer schlängelt. Auf einem 500 km langen Vermessungskurs wurde jeweils ein 10 km breiter Streifen des Meeresbodens unter dem Schiff mit dem Fächerlot erfasst. Damit wird der Verlauf und die Struktur dieser Rinne bestimmt, die bei einer Wassertiefe von über 4650 m bis zu 100 m tief in den Boden einschneidet. Die schwierigen Eisverhältnisse, gekennzeichnet durch mehrere Kilometer große Schollen von bis zu einem Meter Dicke machten allerdings das Abfahren eines regelmäßigen Vermessungsnetzes unmöglich, so daß mit weniger günstigen Kursen vorlieb genommen werden mußte. Die Vermessung wurde am 28. November abgeschlossen.

Im Anschluß wurde die erste Verankerung (208) im Eis bei einer Bedeckung von etwa 70% aufgenommen. Dazu wurden vor der Auslösung auf mehreren Kursen die bis zu 500 m großen Schollen zerfahren, um den Auftriebskörpern die Möglichkeit zu geben, zwischen den Trümmern an die Oberfläche zu

kommen. Erst 40 Minuten nach der Auslösung wurde ein Auftriebskörper gesichtet. Dann allerdings konnte die weitere Aufnahme zügig erfolgen. Bei der Verankerung 209 am 3. Dezember gestaltete sich die Aufnahme durch die Eisverhältnisse noch schwieriger, da kein Auftriebskörper mehr an die Wasseroberfläche aufschwimmen konnte. Deshalb mußte der Auslöser akustisch angepeilt werden, was die absolute Stilllegung des Schiffes erfordert und sehr aufwendig war. Nach Lokalisierung der Verankerung konnte sie durch gezieltes Brechen der Scholle, unter der sie lag, erreicht und aufgenommen werden. Die Arbeiten erstreckten sich über 8 Stunden. Diese Technik mußte bei allen weiteren Verankerungen angewendet werden, wogegen sich die Auslegung im Eis grundsätzlich als unproblematisch erwies. Das Zentrum des Weddellwirbels, durch eine relativ dünne Deckschicht gekennzeichnet, wurde am 2. Dezember bei $66^{\circ}16'S$, $30^{\circ}18'W$ erreicht. Zur genaueren Lokalisierung des Zentrums wurden auf einem zum Hauptkurs senkrecht liegenden Schnitt 7 CTD-Stationen über eine Entfernung von 150 m ausgeführt. Da es beabsichtigt ist, mit einer derartigen Anordnung der CTD-Profile absolute Strömungsgeschwindigkeiten nach dem Prinzip der sogenannten Beta-Spirale zu berechnen, wurde die Anordnung Beta-Kreuz genannt. Im Vorjahr war während der Winter Weddell Gyre Study (WWGS '89) in diesem Bereich, verbunden mit höheren Wassertemperaturen, auch erhöhte biologische Aktivität gefunden worden. Dies konnte auf unserer Reise nicht bestätigt werden. Die Untersuchungen in diesem Gebiet waren am 7. Dezember abgeschlossen und die Arbeiten auf dem Hauptschnitt mit Kurs Südosten wurden mit CTD-Profilen, Biologiestationen, Verankerungsaufnahmen und -auslegungen fortgesetzt. Die Eisverhältnisse gestalteten sich bei weiterem Vordringen nach Südosten schwieriger, da die Schollen ausgedehnter und weniger durch Anschmelzen versprödet waren. Die Rinnen schlossen sich bei abnehmenden Temperaturen durch Neueisbildung. Das Ende des Schnittes bei Kapp Norvegia wurde am 15. Dezember erreicht. Die Küstenpolynya war nur sehr schwach ausgebildet und stark veränderlich. Bei schwachem Wind bewirkten nur die Gezeiten durch das Zusammenschieben des Eises die Ausbildung offener Wasserstellen. Die Biologen mußten erkennen, daß immer noch keine Frühlingsblüte zu sehen war, und die erhofften Untersuchungen am Eisrand nicht möglich waren. Allerdings stand die wüstenhafte Wassersäule mit 54 m Secchitiefe im krassen Gegensatz zum üppigen Algenwachstum im Eis, das gelblich über ocker bis tiefbraun gefärbt war. Die Polynya war zwar schmal, doch das offene Wasser reichte aus, um ein Agassiz-Trawl zu fahren. Der seewärtige Eisgürtel der Polynya bestätigte deren Ruf als Eisfabrik. Von Wind und Strom zusammengeschoben, hat sich hier ein viele Kilometer breites Feld von zerbrochenen und aufgetürmten Eisschollen verfestigt. Dadurch entstanden Eisverhältnisse, die zu den schwersten unserer Reise zählten und für Fahren und Forschung hinderlich waren. So mußten wir auf die Aufnahme der letzten Verankerung (214) verzichten, da sie kaum eine Chance gehabt hätte, unter den meterhohen Eisrücken aufzutauchen. Nachdem schon über längere Zeit Funkkontakt mit den Frauen der Georg-von-Neumayer-Station (GvN) bestanden hatte, besuchte am 13. Dezember eine kleine Vorhut mit dem Helikopter die Station. Nach neun Monaten waren wir der erste Besuch. Wir waren gespannt, ob wir als Eindringlinge empfangen, oder das willkommene Ende der Abgeschlossenheit darstellen würden. Der herzliche Empfang entsprach mehr der zweiten Möglichkeit.

Die letzte Station auf unserem Schnitt durch das Weddellmeer lag in einem "Inlet", einer kleinen etwa 1000 m langen und 400 m breiten Bucht im Schelfeis, in der "Polarstern" im eisfreien Wasser vor der 25 m hohen Schelfeiskante lag, die eine grandiose Kulisse für Kranzwasserschöpfer, Bongonetz und Multinetz bot. Die Zeit, die uns blieb, um auf bessere Eisverhältnisse zur Aufnahme der Verankerung 214 zu warten, nutzten wir zu einer Hydrosweepvermessung des Kontinentalabhanges, die sich wegen des Eises allerdings sehr schwierig gestaltete. Dabei fiel auf, daß sich dort hangparallel Rinnen im Eis ausbildeten, wo sich die Tiefe stark änderte, wie über dem oberen Kontinentalabhang und dem Explorer-Escarpment. Nachdem keine Besserung der Eisverhältnisse zu erkennen war, liefen wir am 16. Dezember ab zur GvN-Station. Mit dem Abschluß der Stationsarbeiten auf dem Hauptschnitt ging ein wichtiger Teil unserer Reise zu Ende. Zwischen der Joinvilleinsel und Kapp Norvegia hatten wir 82 mal mit CTD-Sonde und dem Kranzwasserschöpfer die Wassermassen beprobt, 21 Strömungsmesserverankerungen ausgebracht und 7 aufgenommen. Mit unseren Verankerungen haben wir den größten Heizungszähler der Welt installiert. Der Weddellwirbel wirkt wie ein riesiger Wärmetauscher, bei dem das warme Wasser im Osten von Norden her einströmt, und das abgekühlte Wasser, das seine Wärme an die Luft abgegeben hat, wieder im Westen ausströmt. Die Abkühlung verursacht Absinkbewegungen, die durch Meereisbildung mit Salzfreisetzung verstärkt werden. Die Wechselwirkung mit dem angrenzenden Schelfeis spielt für den Wärme- und Salzhaushalt ebenfalls eine Rolle. Durch diese Vorgänge wird ein riesiges Wasservolumen durchmischt, was dem Wärmetauscher im Weddellmeer einen hohen Wirkungsgrad verschafft und seine Bedeutung bei der Untersuchung weltweiter Klimaveränderungen bedingt. Deshalb ist dieser Teil unserer Arbeit ein Beitrag zum internationalen World Ocean Circulation Experiment (WOCE). Die biologischen Arbeiten sind als Untersuchungen des Stoffkreislaufs im Ozean im Rahmen der internationalen Joint Global Ocean Flux Study (JGOFS) zu sehen. Die besondere Rolle des Weddellmeers im "Südlichen Ozean" soll erklärt und ein Beitrag zur Abschätzung der Bedeutung dieses Seegebietes für den globalen Kohlenstoffkreislauf geleistet werden. Hier steht der Gegensatz zwischen hohem Nährstoffangebot und geringer Produktion im Vordergrund. In einem chemisch-biologischen Projekt konnte erstmals die DMS-Produktion von antarktischem Phytoplankton gemessen und damit bestimmten Arten zugeordnet werden.

Am 17. Dezember erreichten wir die Atkabucht. In den frühen Morgenstunden hatten wir eine Rinne ins Festeis gebrochen, um eine solide Plattform zur Entladung von rund 100 Tonnen Versorgungsgütern zu haben. Verzurrungen wurden gelöst, Luken geöffnet und Schlitten, Schneefahrzeuge und Container auf dem Eis abgesetzt. Inzwischen waren die Überwinterinnen und die Sommergäste mit ihren Fahrzeugen angekommen, und der erste Treck konnte sich über das Meereis in Richtung Schelfeiskante auf den Weg machen. Von dort aus ging es über eine Schneerampe auf das Schelfeis und weiter zur Station. Nach Abschluß der Versorgung zog "Polarstern" in der Nacht vom 18. auf den 19. Dezember aus dem Festeis heraus und dampfte in Richtung Kapstadt. Auf dem Peildeck in den Luftchemiecontainern, im Hydrosweepraum und am XBT-Werfer gingen die Messungen weiter. Ansonsten wurde an der Terminals und PCs gearbeitet, um Messdaten aufzubereiten und Listen, Tabellen oder Berichte zu erstellen. Wegen der Eisverhältnisse wurde ein östlicher Kurs gewählt, wodurch noch eine Hydrosweepvermessung über die Maud Kuppe abefahren werden konnte. Am Eisrand bei

68°00'S, 3°58'W fand die letzte Biologiestation statt. Über eine Entfernung von etwa 30 sm war die Eisbedeckung von 70% auf 10% zurückgegangen.

Am 23. Dezember erreichten wir die Position 54°20'S, 3°23'W etwa 200 sm westlich der Bouvetinsel, wo eine Verankerung mit Sedimentfallen ausgebracht wurde (BO1). Die Polarfront überquerten wir am 24. Dezember bei 51°45'S, 2°24'E. Der Weihnachtsabend wurde mit einer Feier im "Blauen Salon" und einem kalten Buffet zelebriert. Nach einer kurzen Nacht wurde am 25. Dezember die letzte Verankerung aufgenommen (PF3) und wieder ausgelegt (PF4). Die Wetterverhältnisse verschlechterten sich während der Arbeiten derart, daß die CTD-Messung nach der Verankerung ausfallen mußte. Beim Erreichen der 200 Meilengrenze wurden die Forschungsarbeiten eingestellt. Am 30. Dezember 1990 um 01.00 Uhr lief Polarstern in Kapstadt an der Bunkerpier ein.

1. ITINERARY AND SUMMARY

E. Fahrbach (AWI)

On 17 November 1990 "Polarstern" left Punta Arenas. In Drake Passage physical oceanography work was started with an XBT-transect (Expendable Bathythermograph) across the Antarctic Circumpolar Current. An Acoustic Doppler Current Profiler (ADCP) recorded the current field in the upper few hundred meters. The bathymetry and geology programmes began with soundings of Hydrosweep and Parasound which were continued during the complete cruise. Chemical investigations from the first leg were continued with underway measurements. They concentrated on biogenic sulfur compounds and their reaction products in sea water and the marine atmosphere with particular interest in DMS (dimethyl sulfide). Concentrations of nitric acid, ammonia and ammonium nitrate and organobromine compounds were investigated in the marine atmosphere.

We reached the Polar Front on 19 November at 57°23'S, 61°14'W. The first logistic task of the cruise was to deposit three German scientists with more than 8 tons of supply goods at the Soviet station "Bellingshausen" on King George Island. One scientist returned with us after an eleven months stay. After measuring the first CTD-profile (conductivity, temperature, depth) and making a catch with the multinet, we approached Joinville Island at the north-eastern tip of the Antarctic Peninsula. There, two hauls with the Agassiz-trawl provided material for comparative studies on the temperature dependence and kinetics of digestive enzymes in crustaceans.

Still in open water we reached the western end of our main hydrographic transect crossing the Weddell Gyre towards Kapp Norvegia (Fig. 2.1) where the first of 21 current meter moorings was deployed and the first of seven recovered. On the shelf the first biology station took place including measurements with quantameter and Secchi disk, two CTD casts combined with a rosette water sampler and catches with multinet, bongo net, and plankton net. The water samples were used for biogeochemical investigations with special emphasis on the silica and nitrogen cycles. For this reason incubations were carried out to measure the uptake of radioactive ^{14}C , ^{32}Si and ^{32}P and stable ^{15}N . The nitrogen flux in the Antarctic food web could be determined from the water column to the zooplankton. In this context the phytoplankton biomass

and species distribution as well as reproduction and life cycles of dominant copepods were studied.

On 22 November at about 150 km from the coast we met at 63° 30'S, 51°30'W the ice edge. The winds calmed down with increasing distance from the coast and air temperatures did not drop below -4°C. Rather quickly the swell disappeared and the floes increased in size. However, due to a system of leads, we could proceed along our course as planned.

On 26 November at 65°34'S, 38°52'W we reached a deep sea channel which was surveyed with hydrosweep and parasound along 500-km profiles over a distance of 144 km. The structure is 1 to 3 km wide with a depth of 60 to 100 m below the adjacent sea level of about 4650 m. It extends with large meanders from westnorthwest to eastnortheast. Due to the heavy ice cover, consisting of floes a few kilometers in diameter and up to a meter thick, the track line could not be maintained as straight as desirable. Bottom samples were collected with a minicorer which was hung under the CTD. This instrument was newly developed. During initial trials a procedure was achieved which allowed its use without significant additional shiptime. After this phase it was used routinely on 37 stations.

The first recovery of a current meter mooring (208) within the ice (70% ice cover) occurred on 29 November. Before the acoustic release of the mooring the floes of up to 500 m in diameter were broken into smaller pieces to allow the floats to reach the surface. After the release 40 minutes of intensive search were necessary to sight a float before the recovery could be successfully finished. At mooring 209 on 3 December no float reached the surface and a time consuming acoustic ranging and breaking of ice floes finally permitted the detection and consequent recovery after 8 hours. This tedious technique had to be applied during all further recoveries, whereas the deployment of moorings could be accomplished without any problem.

The center of the Weddell Gyre at about 66°16'S, 30°18'W is marked by a relatively shallow surface mixed layer. It was reached on 2 December. For a better localization of the center a transect of 150 nm length consisting of 7 CTD-stations perpendicular to the main transect was carried out. On the basis of those data absolute velocities will be determined using the Beta spiral concept. During the Winter Weddell Gyre Study (WWGS) '89 higher mixed layer temperatures and more intense biological activity were found in that area. This was not observed during the present cruise possibly due to the different season. On 7 December the investigations in the "beta cross" area were terminated and the main transect was continued to the southeast with CTD-profiles, biology stations, mooring recoveries and deployments. The ice conditions became less favourable due to larger floes of less friable ice and closed leads because of colder temperatures. The transect was finished on 15 December. The coastal polynya was only poorly established and highly variable. Because the biologists noted that there was no sign of a spring bloom, the planned stations were cancelled. The desert-like conditions in the water column, evidenced by a Secchi depth of 54 m were in sharp contrast to the abundant algae growth in the ice which gave rise to all colors from yellow to brown. Although small the narrow polynya was large enough for a haul with the Agassiz-trawl. The offshore ice belt of the polynya confirmed the term "ice-factory". It provided the heaviest ice conditions during the cruise and made the

recovery of mooring 214 impossible. The last station on the transect was located in an inlet of 1 km length and 400 m width. In this inlet casts with CTD, multi- and bongo net were carried out in open water in the vicinity of the 25 m high shelf ice front. After a hydrosweep survey of the continental slope in the area of the Explorer-Escarpement we left on 16 December towards the Georg-von-Neumayer-Station (GvN). The work along the transect between Joinville Island and Kapp Norvegia amounted to 82 CTD and rosette stations, 7 biology stations, 21 mooring deployments and 7 recoveries. The established mooring network represents a gigantic flow meter which measures the volume of water and its heat content entering the Weddell Gyre in the northeast and leaving it in the northwest. South of our transect, cooling due to contact with the atmosphere and the shelf ice, together with salt release through ice formation, induces vertical descent of water masses to the bottom. Glacial meltwater has to be taken into account for a quantitative understanding of those processes. Because of the significance of deep reaching vertical mixing for the global abyssal circulation, our measurements are part of the World Ocean Circulation Experiment (WOCE).

The biogeochemical investigations of the cycles and budgets of various constituents represent a contribution to the international Joint Global Ocean Flux Study (JGOFS). They aim to explain the special role of the Weddell Gyre in the Southern Ocean and to estimate the significance of this area to the global carbon cycle. The contrast between the high nutrient availability and the low production remains unresolved. A chemical-biological project allowed for the first time, direct measurement of DMS-production of Antarctic phytoplankton and determination of the contributions of different species. On 17 December we reached Atka-Bight. In the early morning "Polarstern" rammed into the fast ice to provide a safe platform for the unloading of about 100 tons of supply goods for the GvN-Station. First contacts with the female overwintering team had been established by a helicopter visit on 13 December to prepare the unloading procedure. The first trek with unloaded material left in the early afternoon towards the shelf ice edge and the station. Due to favourable conditions all loading was finished in the evening. "Polarstern" left the Atka-Bight at midnight of 18 December. On the way north air chemistry, XBT, hydrosweep and parasound measurements were continued. The ice edge was met at 68°00'S, 3°58'W where the ice concentration dropped within 30 nm from 70% to 10%. Here the last biology station was carried out. On 23 December we reached 54°20'S, 3°23'W about 200 nm west of Bouvet Island where mooring BO1 was deployed with two sediment traps. The Polar Front was crossed on 24 December at 51°45'S, 2°24'E. Christmas Eve was celebrated with a merry ceremony in the "Blue Saloon" and a delightful buffet. The recovery of the last mooring PF 3 and deployment of PF4 was achieved in the morning of the 25 December. When we reached the 200 nm limit research was terminated. On 30 December 1990 at 01.00 "Polarstern" reached the bunker pier of Cape Town.

2. PHYSICAL OCEANOGRAPHY

2.1 Water masses and circulation

T. Behmann, E. Fahrbach, J. Dehn, M. Knoche, T. Markus, R. Plugge, V. Strass, (AWI); C. Buxhoeveden, (ITBA); M. Harder, H.-H. Hinrichsen, H. Schäfer, U. Sterr, A. Wisotzki (FPB); E. Schütt, (FGB); H.-J. Brosin, M. Schmidt, (IfMW)

Objectives

The aim of the physical oceanography programme is to further understand the circulation in the Weddell Gyre and the related distribution of water masses. The operations contribute to a multiyear project, the Weddell Gyre Study, which is part of the World Ocean Circulation Experiment (WOCE). During this period a hydrographic survey along a transect from the northern tip of the Antarctic Peninsula to Kapp Norvegia (Fig. 2.2) will be repeated four times, twice in summer and twice in winter, to measure the water mass distribution with its seasonal and interannual variability. The programme was initiated with a winter survey in 1989, the Winter Weddell Gyre Study (WWGS) '89, and will be continued with further surveys in austral winter 1992 and summer 1992/1993.

Simultaneously an extensive current meter mooring programme began with the deployment of seven current meter moorings. The data from those moorings will be used to estimate the volume transport in the Weddell Gyre. Direct current measurements are essential because they are the only way to obtain the barotropic flow which determines the net volume transport. From the measured mass, heat, and salt transports across the transect we can derive water mass formation rates.

The transformation of Winter Water (WW) and Warm Deep Water (WDW) in the inflow to Antarctic and Weddell Sea Bottom Water (AABW, WSBW) in the outflow is of special interest, because it results from a deep vertical exchange which is relevant to the large scale abyssal circulation of the world ocean. Present estimates show that about 70% of the Antarctic Bottom Water spreading into the world ocean obtains its water mass characteristics in the Weddell Sea. Because the salt budget of the area is strongly influenced by ice formation and melting, special interest is focussed on the ice transport across the transect. Interaction with the ice shelves has to be taken into account for a quantitative understanding.

Fig. 2.2: Schematic representation of the Weddell Gyre and the transect from Joinville Island to Kapp Norvegia (KN).

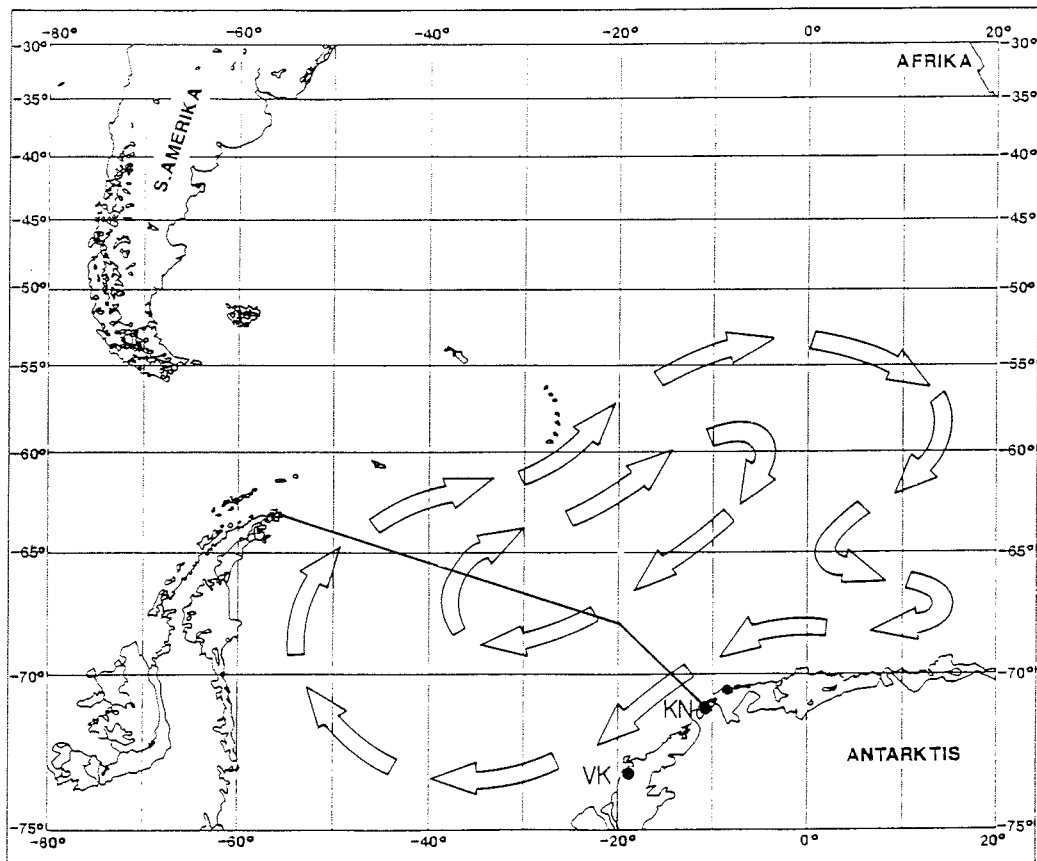
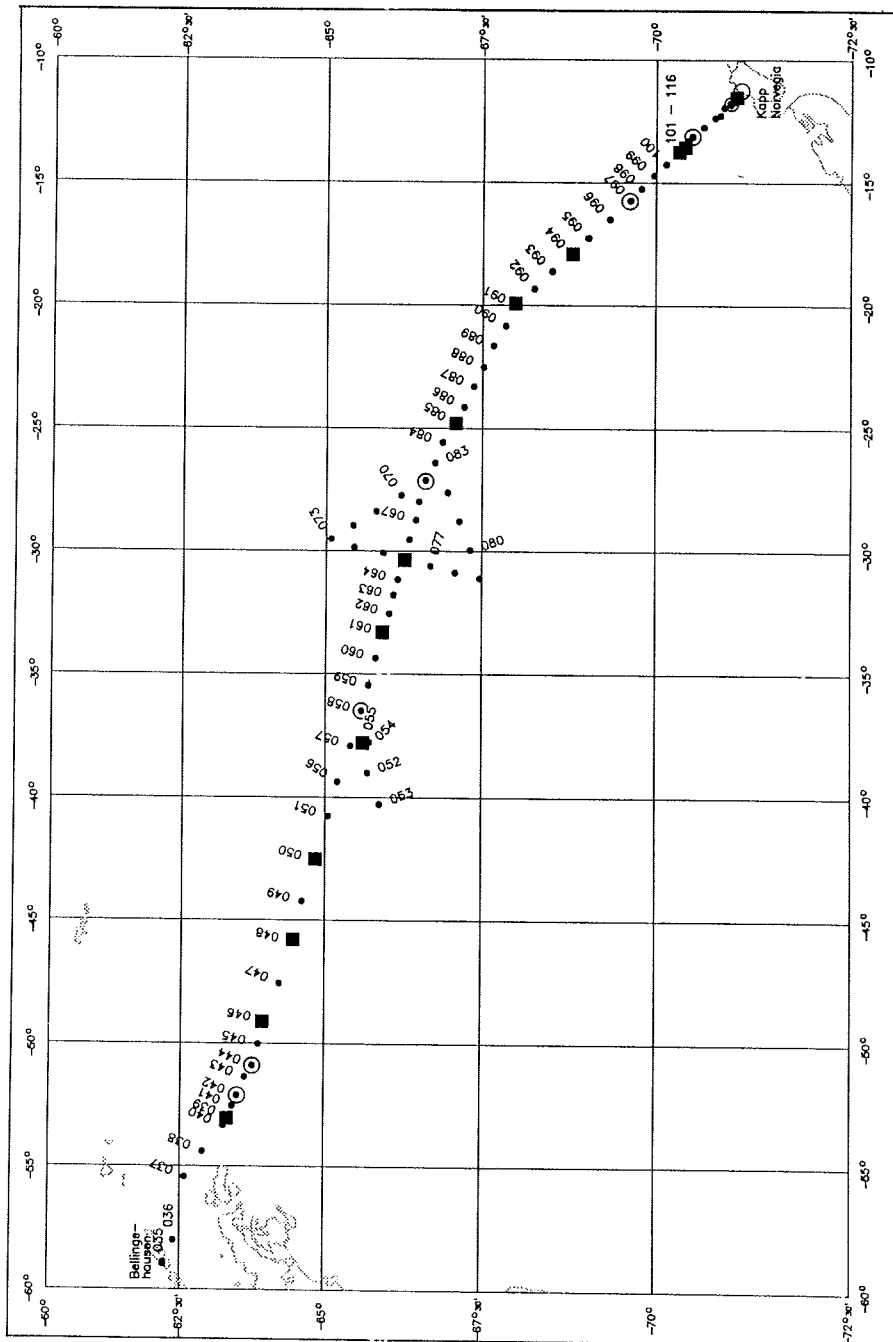


Fig. 2.3: Station map of "Polarstern"-cruise ANT IX/2. Small dots stand for CTD-stations, circles for recovered and squares for deployed moorings.



Work at sea

In order to obtain the water mass distribution, a hydrographic section was carried out with 74 CTD-profiles (conductivity, temperature, depth) and discrete casts for temperature, salinity, oxygen, nutrients and tracers (helium, tritium and ^{18}O). For the location of the stations see Fig. 2.3 and the station list (Anhang 1). On the eastern slope the station distance was small enough (Fig. 2.4) to resolve topographic features such as the Explorer-Escarpement. Seven current meter moorings were recovered and 21 were laid (Tab. 2.1 and 2.2, Fig. 2.3). On six of them ice thickness will be measured by upward-looking sonars (ULS). The moorings will stay in position for two years. Vertical temperature and electrical conductivity profiles were measured with a Neil Brown Mark III B CTD. The quality of the CTD-measurements was assured by reference measurements with a rosette sampler. Water samples were taken with a General Oceanic rosette composed of 24 bottles with 12 l volume each. Each time a water bottle was closed 50 cycles of pressure, temperature and conductivity were recorded with the CTD, quality controlled and averaged.

Pressure and temperature measurements were corrected by means of a laboratory calibration carried out in the Scripps Institution of Oceanography before the cruise. A second calibration will be done after the cruise. Both calibrations will lead to a more elaborate correction of the data. However, the control by electronic as well as mercury reversing thermometers and pressure meters gives us confidence that the preliminary data have errors of less than 5 mK in temperature and 5 db in pressure.

The salinity data are given in PSU. They are based on the CTD conductivity measurements from which salinity was calculated using the Unesco Practical Salinity Scale (PSS78). The values were compared with salinities from water bottle samples measured with a Guildline Autosol 8400 A in reference to I.A.P.S.O. Standard Seawater. The number of samples per profile, the mean difference between the samples and the CTD measurements as well as its standard deviation are shown in Fig. 2.5. Preliminary data presented in this report were corrected with a constant offset of 0.023 to an accuracy of 0.005. The final data will be corrected in conductivity for time and depth dependence of the deviations. Afterwards salinity will be recalculated.

Oxygen was determined with an automatic titration unit, using the Winkler method with a photometric endpoint determination. The error in the oxygen determination is estimated to 1%. This results from intercomparisons at selected stations between the chemical oceanography group from the Oregon State University and the AWI group both using different instruments. Duplicate samples from the same water bottle were analysed during the complete cruise as a measure of precision. The obtained data are given in ml/l.

Tab. 2.1: Moorings recovered during "Polarstern"-cruise ANT IX/2

Mooring	Latitude Longitude	Date Time	Water Depth (m,corr.)	Instrument Type	Depth
206	63°29.6' S 52°07.4' W	13.09.89	946	AVT	229
		11.13		S	349
		22.11.90		AVT	876
207	63°45.8' S 50°54.3' W	08.52	2503	AVT	263
		14.09.89		AVTPC	952
		10.39		AVT	2162
		23.11.90		AVT	2410
208	65°36.3' S 36°29.9' W	00.41	4768	AVTPC	288
		24.09.89		AVTPC	1037
		18.30		S	1090
		29.11.90		(AVT)	2610
		13.00		S	4122
209	66°36.8' S 27°07.4' W		4863	AVT	4631
		01.10.89		AVTC	293
		10.28		AVTPC	993
		03.12.90		(AVT)	2653
		09.16		(AVT)	4725
210	69°38.9' S 15°44.5' W	05.10.89	4751	AVTC	289
		21.11		AVTPC	988
		11.12.90		AVT	2547
		14.29		AVT	4617
211	70°29.5' S 13°07.0' W	6./7.10.89	2402	AVTC	247
		00.13		AVTPC	856
		14.12.90		AVT	2066
		14.28		AVT	2313
212	70°59.2' S 11°49.4' W	08.10.89	1069	AVTPC	309
		16.55		AVT	999
		13.12.90			
		22.50			
PF3	50°07.6' S 05°50.0' E	09.11.89	3785	S	625
		10.34		AVT	645
		25.12.90		S	3200
		08.30		AVT	3220

AVTPC: Aanderaa current meter with temperature, pressure and conductivity sensor. In brackets instruments with poor data quality.

S: Sediment trap

Tab. 2.2: Moorings deployed during "Polarstern"-cruise ANT IX/2.

Mooring	Latitude (S)		Date Time	Water depth (m, uncorr.)	Type	Instrument		
	Longitude (W)					No.	Depth	
215	63°19.89'		21.11.90	448	AVTP	10001	291	
	52°59.07'		20:14		AVTP	9996	396	
					WLR	1155	447	
206/2	63°29.55'		22.11.90	942	AVTP	8402	253	
	52°06.27'		14:54		AVTP	9786	891	
207/2	63°45.05'		23.11.90	2498	ULS	9/90	165	
	50°54.32'		06:52		AVTP	9206	326	
					TK	1569		
					ATR	1100	578	
					AVTPC	8395	1037	
					AVT	8417	2187	
					TK	1570		
216	63°56.96'		24.11.90	3477	AVT	1102	2439	
			49°09.21'		00:34	AVT	8418	2447
						AVT	9182	2968
217	64°25.10'		24.11.90	4424	AVT	9184	3426	
			45°50.97'		21:26	ULS	13/90	141
218	64°48.87'		25.11.90	4688	AVTPC	9192	250	
			42°29.28'		21:15	S	890107	796
						AVTC	9211	1010
						AVT	9185	2510
						ACM-2	1281	4373
						AVTP	10005	252
						TK	1427	
219	65°39.87'		28.11.90	4732	ATR	944	505	
			37°42.45'		13:36	AVTP	9212	993
						AVT	9186	2503
						ACM-2	1284	4636
						AVT	9187	4226
208/2	65°38.14'		29.11.90	4776	AVT	9188	4674	
			36°30.20'		18:27	AVT	9190	4722
						ULS	11/90	171
						AVTPC	9194	281
						AVTPC	9213	1040
						S	890106	1123
						AVT	9191	2533
220	65°58.19'		30.11.90	4799	S	890108	4165	
			33°20.33'		15:43	ACM-2	1285	4725
						AVT	9767	4300
221	66°16.63'		02.12.90	4784	AVT	9768	4748	
			30°17.78'		10:49	ADCP		236
209/2	66°37.35'		03.12.90	4862	AVTPC	9195	247	
			27°07.10'		20:50	TK	1426	
						ATR	943	499
						AVTPC	9214	985
						AVTPC	9215	2499
						ACM-2	1288	4732
						ULS	14/90	147
						AVTP	9202	279
						AVTPC	9216	1015
						AVTPC	9217	2526
222	67°03.56'		07.12.90	4836	ACM-2	1289	4809	
			24°52.11'		22:54	AVT	9769	4336
223	67°59.84'		09.12.90	4885	ACM-2	1282	4785	
			19°57.64'		17:24	AVTPC	9205	251
						AVTPC	9218	1010
					AVT	9208	2520	
					ACM-2	1290	4834	

Mooring	Latitude (S)		Date Time	Water depth (m, uncorr.)	Type	Instrument	
	Longitude (W)					No.	Depth
224	68°49.65'		10.12.90	4740	AVT	9770	4239
			17°54.49'	13:38	ACM-2	1291	4689
210/2	69°39.63'		11.12.90	4745	ULS	10/90	151
			15°42.90'	16:50	AVTP	9201	270
					TK	1571	
					ATR	1103	523
					AVTP	9995	1012
					AVT	9391	2521
225	70°19.11'		12.12.90	4329	ACM-2	1297	4694
			13°39.61'	18:19	AVTP	10002	275
					AVT	9783	1124
					AVT	9997	2625
226	70°22.84'		13.12.90	2943	AVT	9782	4278
			13°32.53'	00:57	AVTP	10003	231
					AVTP	9998	980
212/2	70°54.67'		14.12.90	1555	AVT	9207	2892
			11°57.80'	07:34	ULS	12/90	135
					AVTP	8367	254
					AVTC	9401	759
211/2	70°29.67'		14.12.90	2381	AVT	9402	1504
			13°08.85'	22:17	AVTP	10004	270
					TK	1572	
					ATR	1104	523
					AVTP	8396	1012
					AVT	9999	2222
KN4	70°59.51'		15.12.90	892	AVT	9392	2329
			11°46.86'	09:55	S	860019	328
					AVTP	9209	333
					S	860020	782
					AVTPC	9210	810
214/2	71°02.93'		15.12.90	378	UCM		811
			11°41.25'	12:56	AVTP	8370	213
					AVT	9403	318
					WLR	1044	377
BO1	54°20.3' S		23.12.90	2734	S	860024	423
	03°22.6' W		16.43		AVT	7727	474
					S	890005	2196
					AVT	8037	2217
PF4	50°07.6' S		25.12.90	3807	S	860038	625
	05°52.0' E		10.31		AVT	9803	646
					S	890009	3267
					AVT	9805	3290

Abbreviations:

ACM-2	Acoustic current meter, Neil Brown
ADCP	Acoustic doppler current meter
ATR	Recording unit for thermistor chain
AVTPC	Aanderaa current meter with temperature, pressure and conductivity sensor
S	Sediment trap
UCM	Acoustic current meter, Simtronics
ULS	Upward looking sonar
WLR	Water level recorder

Fig. 2.4: Cruise-track and location of CTD-stations off Kapp Norvegia during "Polarstern"-cruise ANT IX/2.

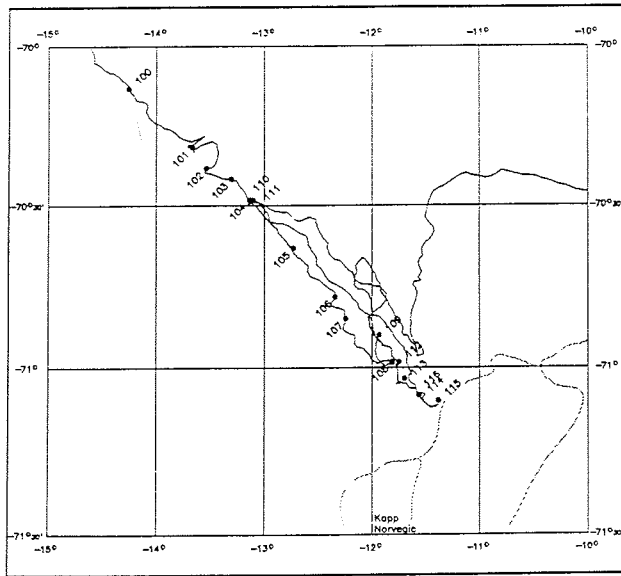
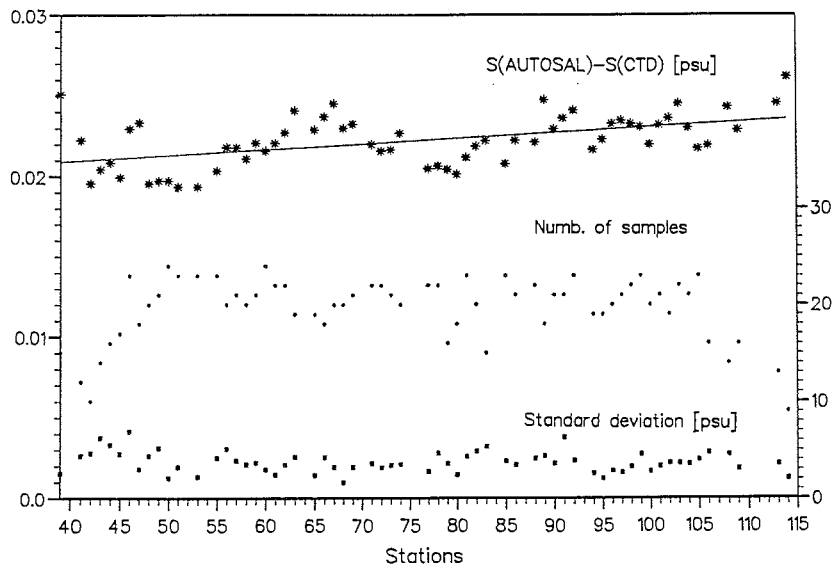


Fig. 2.5: Comparison between salinity measurements from water bottles with those from the CTD. Stars give the mean difference for each station between the bottle and CTD salinities, squares the standard deviation, and dots the number of samples per station.



Preliminary results

The hydrographic features measured along the transect are presented as sections of potential temperature and salinity (Fig. 2.6). Below a shallow surface layer of WW which deepens significantly towards the shelf edge, a temperature and salinity maximum due to the WDW is found. It is more pronounced at the boundaries than in the interior with temperatures up to 0.8°C in the east and 0.4°C in the west evidencing the inflow in the east and the outflow in the west. The largest part of the water column with potential temperatures between 0 and -0.8°C and salinities from 34.67 to 34.64 is classified as AABW. Below we find WSBW with temperatures colder than -0.8°C which extends in the west in a shallow layer over the continental slope indicating the outflow of this freshly formed water mass. The young age of this water mass is suggested by the high oxygen content (Fig. 2.7). In the forthcoming analysis we will quantify the transformation which occurs south of our transect of inflowing water masses in the east into the outflowing ones in the west.

Seasonal changes on that transect are most evident in the near surface layers. Relatively warm air temperatures (Fig. 2.8 top) and weak winds (Fig. 2.8 bottom) indicate the onset of spring.

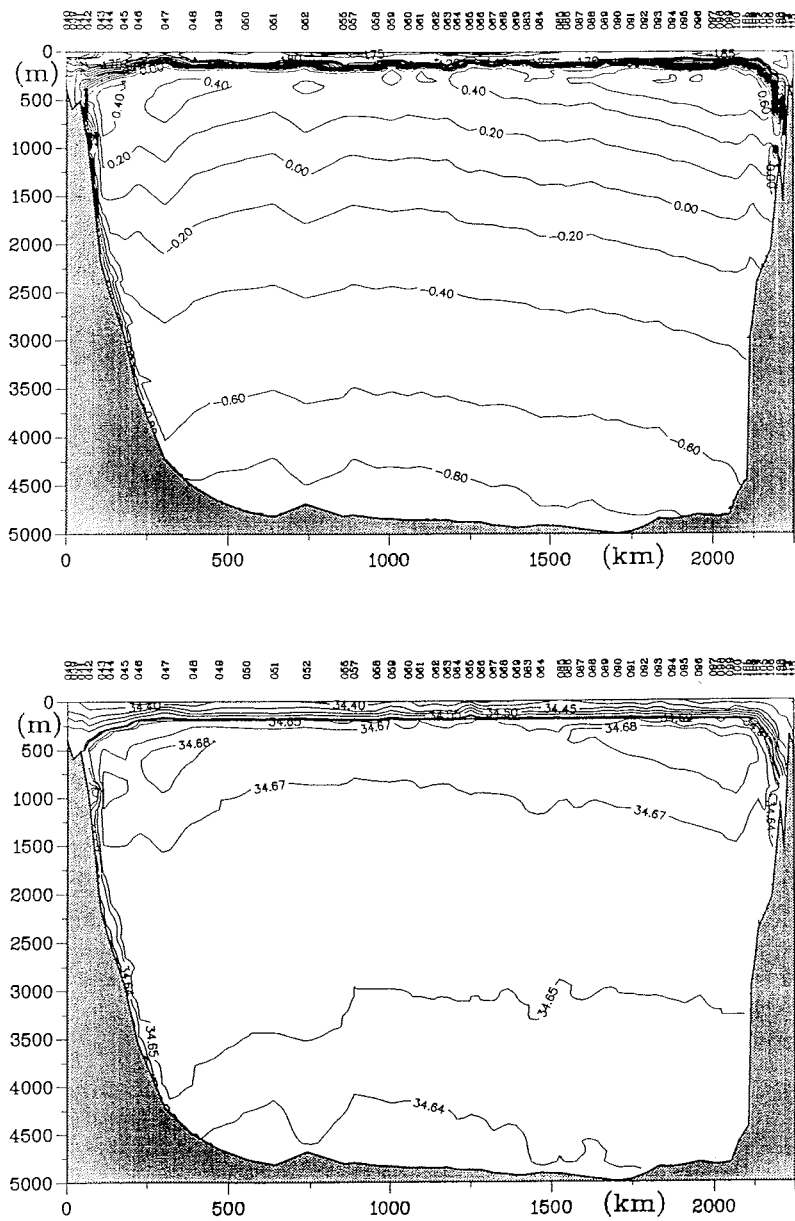
A comparison of surface layer temperatures and salinities measured in September and October during WWGS '89 with the ones obtained during the present cruise indicates a much more pronounced springtime warming in the west than in the east (Fig. 2.9 top). The salinity decrease due to ice melting was more intense in the east than in the west (Fig. 2.9 bottom). In the deeper layers fluctuations of a wide spectral range are expected to be at least as intense as the seasonal cycle. Consequently no seasonal change can be identified in the comparison of the two sections.

From CTD data on a straight section only geostrophic current shear can be estimated. Absolute currents can be obtained by the use of mass conservation of geostrophic currents in and out of a closed area or by the Beta-spiral method. Therefore, in the area of the gyre centre, which is indicated by the doming of the isotherms, a second section normal to the main section was carried out with a length of about 275 km (Fig. 2.10, top).

The estimate of absolute geostrophic current velocities by use of the Beta-spiral method will yield additional information on the location of the gyre center complementary to the moored current meter data. However, this method requires the calculation of the second derivative of isopycnals with respect to horizontal and vertical coordinates and is very sensitive to fluctuations. Thus, quantitative estimates need to be carried out with the final data.

The transects of the potential temperature along the Beta-cross (Fig. 2.10, top) show smoothly inclined isolines which seem to reflect the doming of the Weddell Gyre. The temperature maximum of the WDW increases towards the north. This can be taken as an indication that there is a southward component in this level and consequently the center of the gyre has to be located further to the west.

Fig. 2.6: Vertical section of potential temperature (top) and salinity (bottom) from Joinville Island (left) to Kapp Norvegia (right) carried out during "Polarstern"-cruise ANT IX/2.



The interaction with the ice shelf was studied by means of a CTD profile which was measured in an inlet of the Quarisen northeast of Kapp Norvegia (Fig. 2.11, top). The temperature profile shows cold WW above a slightly warmer layer centered at 200 m depth which tops a colder bottom layer (Fig. 2.11, bottom). The salinity increases from top to bottom. Presently it is not possible to conclude if the deeper layer is the remnant of a WW-layer which reached to the bottom and is separated from a slightly warmed surface layer by an intrusion of warmer water from offshore, or if it represents water which emanates from under the ice shelf. Tracer data measured from the water samples will be used to answer this question.

Fig. 2.7: Vertical section of dissolved oxygen from Joinville Island (left) to Kapp Norvegia (right) carried out during "Polarstern"-cruise ANT IX/2.

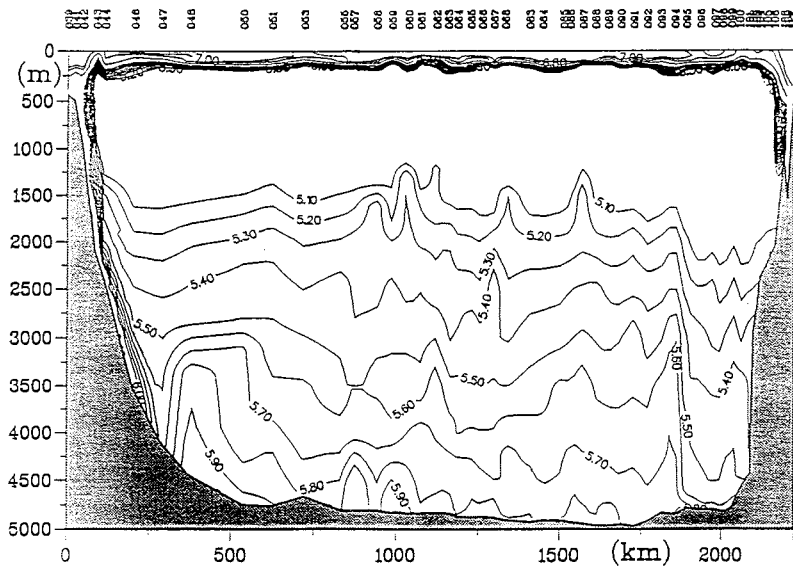


Fig. 2.8.: Three-hour averages of air temperature (top) and wind speed (bottom) measured during CTD-stations on "Polarstern" during ANT IX/2.

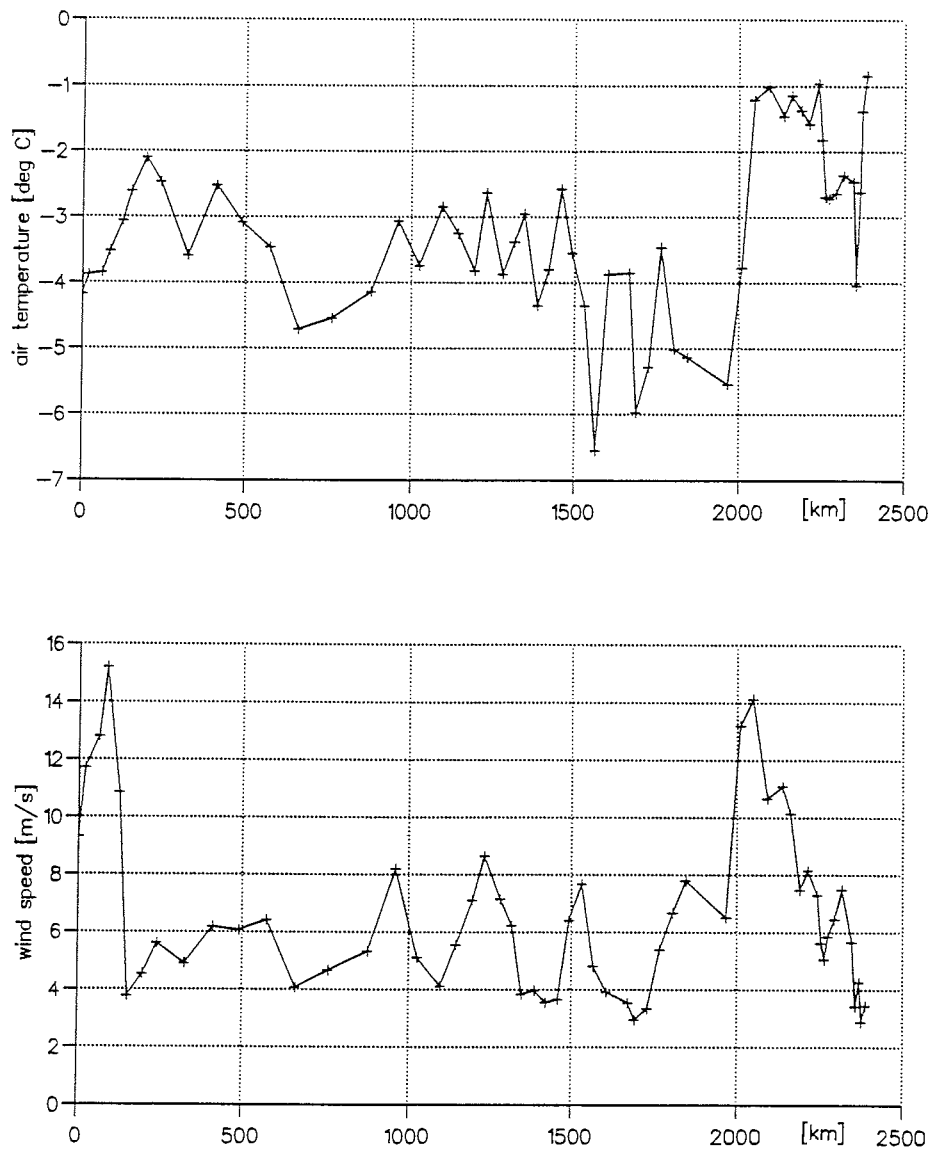


Fig. 2.9: Surface layer temperatures (top) and salinities (bottom) measured with the CTD in 10 m water depths during winter 1989 (WWGS '89, dotted line) and spring 1990 (ANT IX/2, solid line).

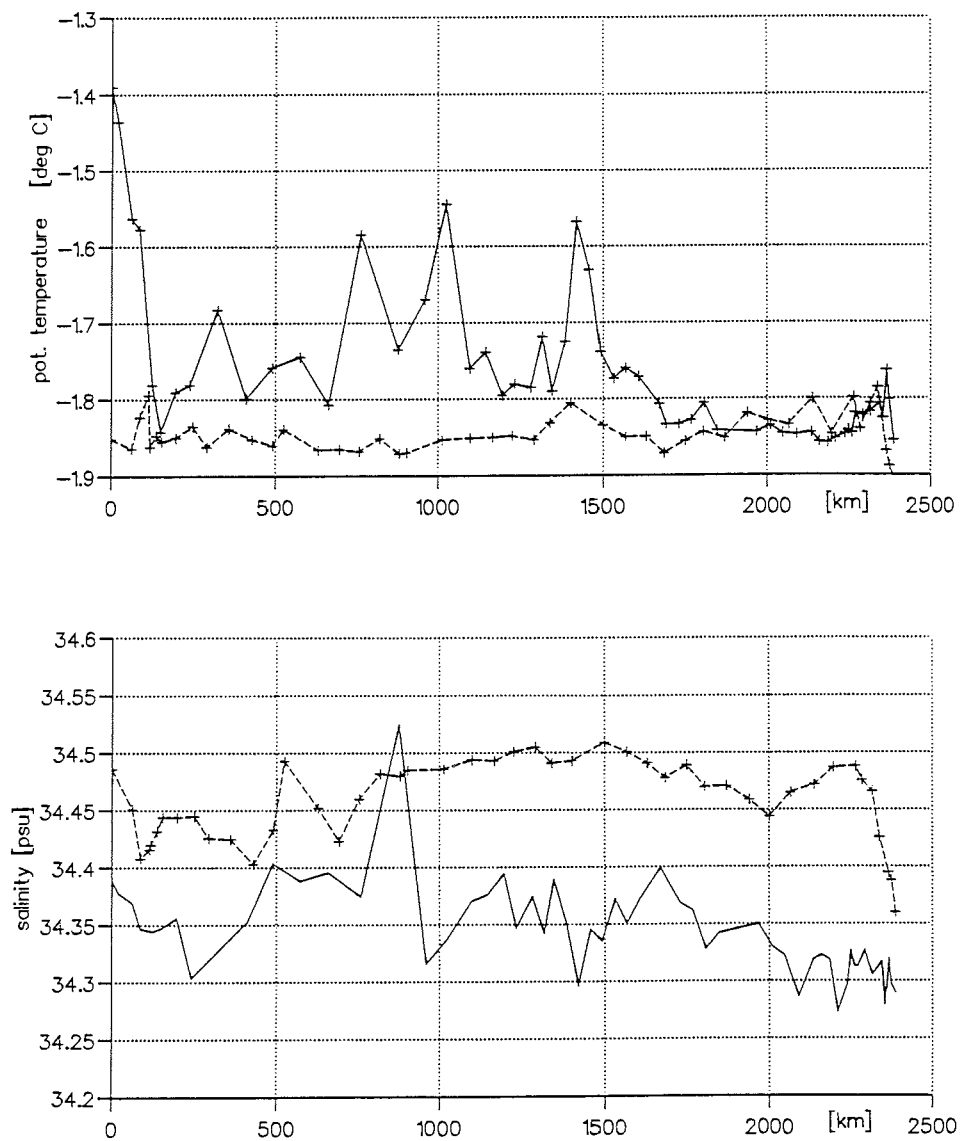


Fig. 2.10: Cruise track and station locations in the "Beta-cross" area during "Polarstern"-cruise ANT IX/2 (top) and vertical sections of potential temperature (bottom) along the track lines.

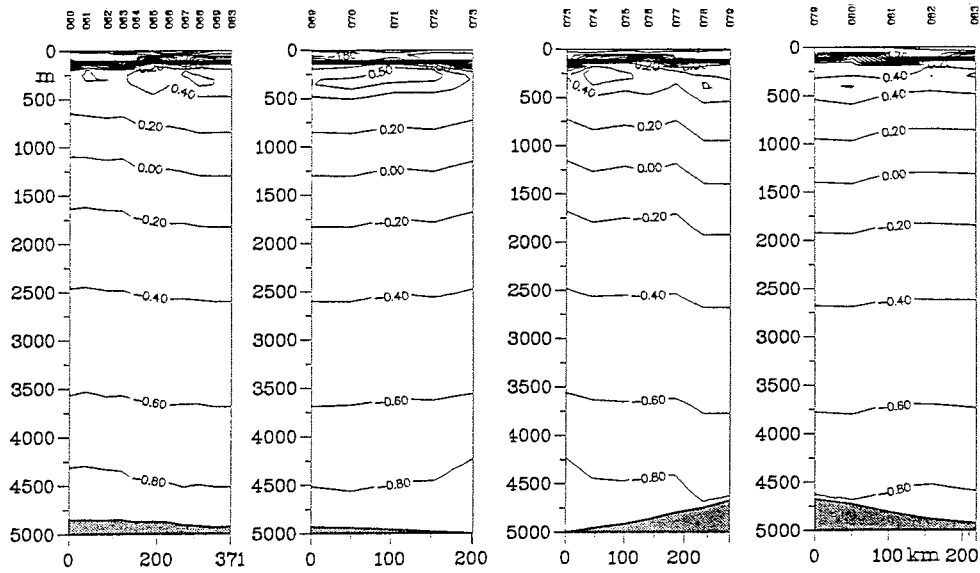
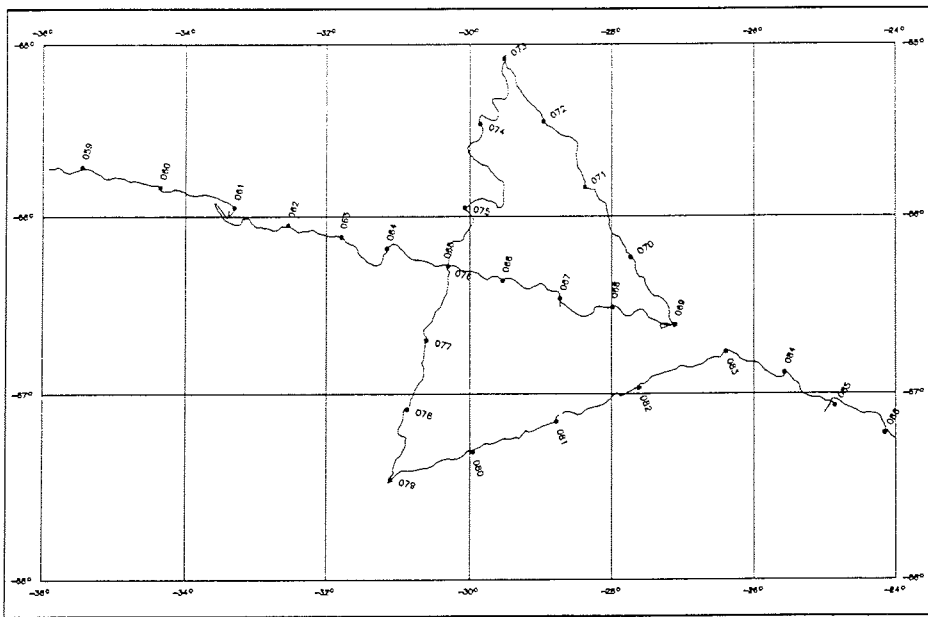
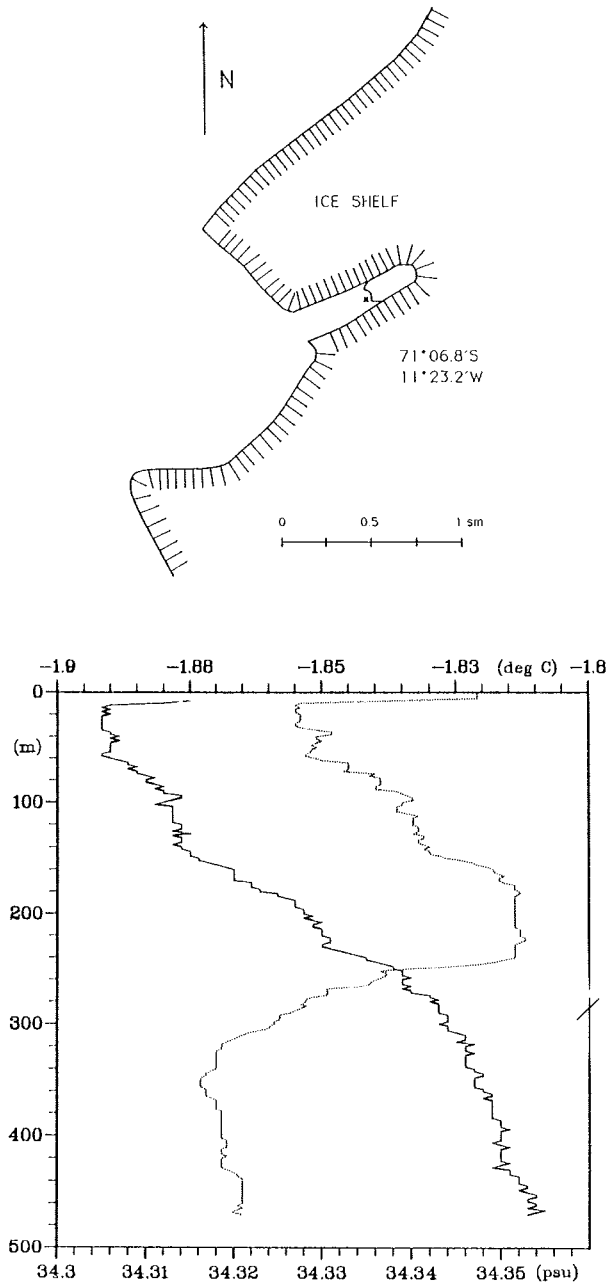


Fig. 2.11: Location of the station in the inlet of the Quarisen during "Polarstern"-cruise ANT IX/2 (top) and vertical profiles of potential temperature (stippled line) and salinity (solid line) in the inlet (bottom).



2.2. Distribution of dissolved inorganic nutrients in the water column

J. M. Krest, A. A. Ross (OSU)

Objectives

By obtaining high quality nutrient data from late winter and early spring, we will improve on the sparse historical data set of the central Weddell Sea. The repeated "Polarstern" transects should permit the seasonal and interannual variability of the major water masses to be assessed. This data set will be used to study the evolution of WW which is the mixed layer beneath the seasonal pack ice. WW properties change with length of time under the ice due to continuous mixing of warmer, higher nutrient waters (WDW) from just below the pycnocline. From the analysis of nutrients in this surface layer, we plan to extend and refine our earlier estimates of net primary productivity in the Weddell Sea.

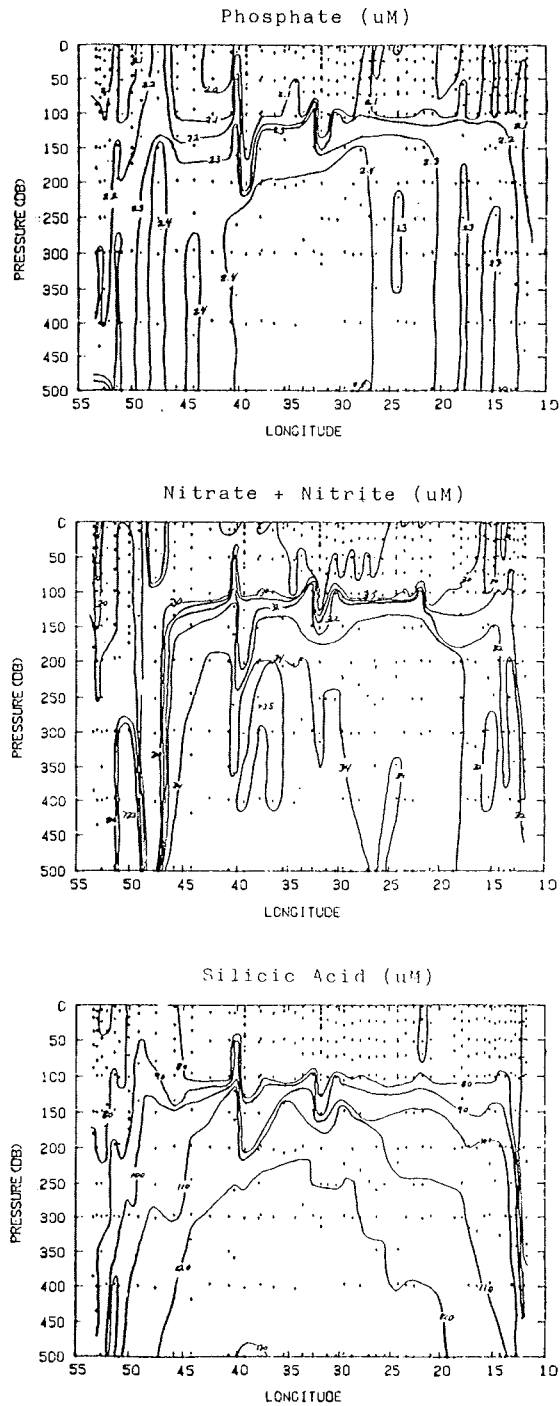
Work at sea

At 88 CTD casts, water samples were taken and analyzed for silicic acid, phosphate (Ortho-Phosphate), nitrate + nitrite (N+N), nitrite, and ammonium. Analyses were performed using the ALPKEM RFA-300 continuous flow analysis system. The entire water column was sampled for nutrients, but at this time, only the surface water in the primary northwest-to-southeast transect has been examined for silicic acid, phosphate and N+N.

Preliminary Results

Contour plots of nutrients in the upper 500 meters (Fig. 2.12) show a fairly well defined layer of WW from approximately 50°W to 14°W. In the WW-layer which occupies the top 100 meters of the water column silicic acid concentrations range from 70 to 80 μM , N+N concentrations from 28 to 30 μM , and phosphate concentrations from about 2.0 to 2.1 μM . Underlying this WW-layer is a reasonably strong nutricline, varying in depth from 100 to 150 meters. In this nutricline, silicic acid increases in concentration to 110 micromolar, N+N increases to 33 μM , and phosphate increases to 2.3 μM . For all three nutrients, concentrations are most elevated in the center of this gyre, indicating a general upwelling trend. At two locations, 40° and 32°W, the contour plots for all three nutrients indicate strong vertical mixing between the WW and the underlying water mass. At the western and eastern boundaries, intense vertical mixing causes nearly vertical nutrient isolines. In the WSBW a tongue of low concentration silicic acid can be seen which extends laterally more than halfway across the Weddell Sea Basin at a depth of approximately 4500 to 5000 meters. Initial comparisons were made with data obtained by Oregon State University's group during WWGS '89 and show good agreement.

Fig. 2.12: Vertical sections of nutrients from Joinville Island to Kapp Norvegia carried out during "Polarstern"-cruise ANT IX/2.



2.3. Tritium and Helium measurements R. Well (FPB)

Objectives

Within the scope of the physical oceanography programme the tritium and helium-isotope contents of the water samples serve as tracers for water mass characteristics. In addition, they can yield information about the time scales of exchange of the water masses within the Weddell Gyre. On this cruise - for the first time - we degassed water samples at sea. This procedure is expected to reduce the contamination caused by longtime storage and can simplify the handling of the sample containers. For this purpose we tested new degassing equipment on board and will compare the results with those obtained with the traditional method.

Work at sea

We took water samples at 6 CTD-stations on the shelf and continental slope of the Antarctic Peninsula in water depths of about 400, 1000, 2200, 2500, 3550 and 4200 m, at 3 CTD-stations in the central Weddell Sea at water depths of about 4700, 4760 and 4860 m and at 4 CTD-stations on the eastern continental slope off Kapp Norvegia in water depths of about 4400, 2400, 1600 and 500 m. Altogether about 50 double-samples were taken. One half of them were degassed on board, the other half will be degassed after our return in the laboratory, the helium- and neon-isotope contents will be compared.

Preliminary Results

As the measurements of the samples have to be done with a mass spectrometer in the laboratory we can not present data or quantitative results of the intercomparison here. The degassing technique on board did not show serious technical problems. Some problems occurred with the melting off procedure of the glass ampoules so that presently we can not generally guarantee that the extracted gas is well caught in the glass ampoule.

2.4. Water level measurements C. Buxhoeveden, (ITBA); E. Fahrbach, R. Plugge, (AWI); E. Schütt (FGB)

Objectives

Water level measurements and deployments of water level recorders were carried out during ANT IX/2 for two reasons: to obtain further information on the tides in the Weddell Sea and to study low frequency fluctuations such as coastal trapped waves or basin modes, for a better understanding of the fluctuations observed in the moored current meter records.

Work at sea

To obtain time series long enough for a detailed tidal analysis and to study lower period fluctuations, two current meter moorings on the western and the eastern shelf respectively (215, 214/2) were equipped with Aanderaa water level recorders (WLR). It was planned to recover mooring 214/1 with a WLR, but due to the heavy ice conditions off the eastern shelf, this was not possible and the mooring had to be recovered during the following leg. During the stay in the Atka-Bight a short period study took place to check a tidal prediction made by members of the Meeresphysik section at AWI on the basis of previous measurements. With this aim soundings of the navigational echo

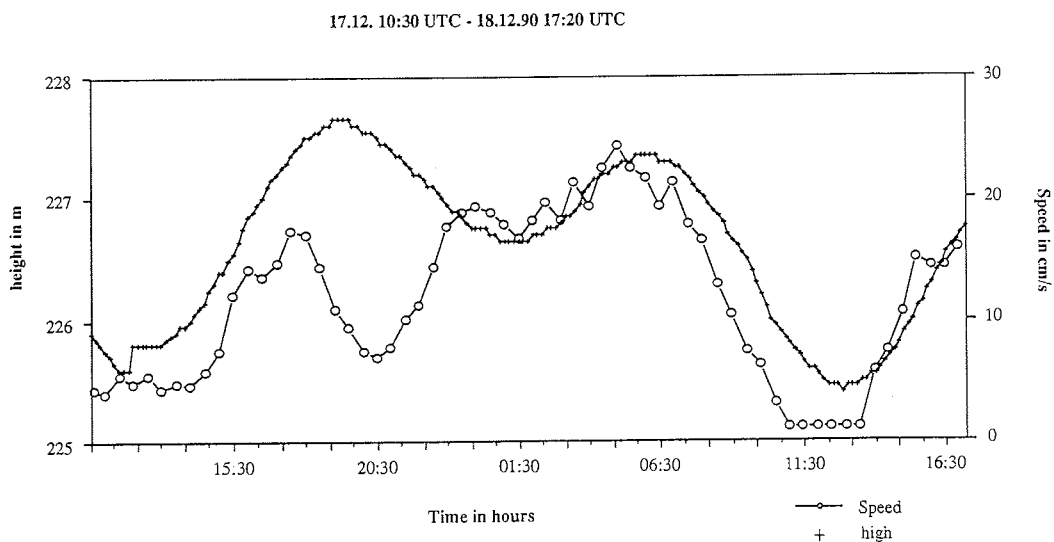
sounder were evaluated and a current meter was moored 50m below the hull of "Polarstern" through the moon pool (Fig. 2.13).

Preliminary results

The short term study over 36 hours allowed us to compare the predicted and observed tidal range as well as the times of high and low water. It appears that they agree to the accuracy of the measurements. The times of the extrema can be determined to about 10 min which corresponds to the difference in the predictions. The determination of the tidal range is affected by the influence of lower period fluctuations of the sea level and the motion of the ship due to the unloading and later ballasting which changes the location and inclination of the echosounder. Both effects add up to an uncertainty of about 15 cm in the determination of the tidal range which is about 10% of the observed range.

Within this range predicted and measured data correlate. The correlation between tidal current and sea level is less clear. Whereas during 18 December high and low water seems to correlate with maximum and minimum tidal current, on the 17th no correlation is found. This agrees with observations from moored current meters where nontidal current variability is as strong as the tidal one.

Fig. 2.13: Records of the current speed (open circles) in 50 m water depth and the navigational echo sounder from "Polarstern" during the visit to Atka-Bight.



2.5. **Optical properties of sea water**

R. Plugge, V. Strass (AWI)

Objectives

The optical properties of sea water vary with its constituents of biological origin. Observational methods based on the variations of the optical properties allow measurements of biological variables at the same high sampling rate as temperature and salinity, and thus can be used for underway data recording. Data sets including both biological and physical variables collected in this way allow for statistical studies of the dependency of the biological realm on the physical environment. During the present cruise a sensor package for measuring temperature, salinity, chlorophyll, fluorescence, Mie backscatter and yellow substance was employed; the optical measurements allow determination of the concentration of phytoplankton biomass and particles and zooplankton concentration/activity.

Work at sea

The hydrographic-optical sensor package (named COMED, developed in the Meeresphysik section at the AWI) was mounted in the ship's well at hull depth (11 m), where the data were collected at a rate of 1 cycle per 10 seconds. Measurements were taken during two periods: the first starting on 18 November and ending on 22 November, the second period starting on 20 December and ending on 29 December. During both periods the ship crossed the Antarctic Circumpolar Current with the Polar Front: the first time on the southward leg from Punta Arenas towards Bellingshausen-Station, the second time on the northward leg from GvN-Station towards Cape Town. During the period in between the ice conditions required the COMED System to be switched off and to cover the sensor package with a protective lid in order to avoid damages.

2.6. **Underway measurements of current profiles, XBTs and the thermosalinograph**

T. Behmann, J. Dehn, E. Fahrbach, M. Knoche, T. Markus, V. Strass, (AWI); H.-J. Brosin, M. Schmidt, (IfMW); C. Buxhoeveden, (ITBA); M. Harder, H.-H. Hinrichsen, H. Schäfer, U. Sterr, A. Wisotzki (FPB)

Objectives

The Antarctic Circumpolar Current is subject to a wide range of temporal and spatial variability. The repeated crossings of "Polarstern" are used to obtain a data set which is suitable to address longer term variability of the thermal field and spatial variability of the velocity field. The temperature profiles are inserted in the Integrated Global Ocean Services System (IGOSS).

Work at sea

This goal is approached by usage of the Vessel Mounted Acoustic Doppler Current Profiler (VM-ADCP, manufactured by RD Instruments, San Diego) which allows us to monitor the current profile in the upper 350m of the water column from the ship moving at full speed. The corresponding thermal structures were measured by means of XBTs using T-7 probes. Sea surface temperature and salinity is recorded by a thermosalinograph.

By use of the ADCP a cross section of the upper ocean velocity profile through the Circumpolar Current was recorded through Drake Passage to the Antarctic Peninsula. A set of calibration data were collected by running a cross-shaped course pattern on the shelf of the Antarctic Peninsula. During the calibration courses the ADCP was operated in its bottom track mode; a variety of control parameter settings were used during the measurements in order to optimise the instrument's performance. The data sampled were transferred to the ship's VAX computer for processing and plotting. During the measurements the ADCP was run without the occurrence of major problems. However, during a later phase of the cruise no more data were obtained for two reasons. First, in its mode of operation the ADCP's transducer sits at hull depth (approx. 11 m) in the ship's well without any protection against mechanical damage by ice floes pushed under the ship. When the ship moves through the ice the transducer is protected by a lid consisting of two stainless steel sheets of 8 mm thickness. With the transducer behind the protective lid the ADCP not able to function. Consequently, no ADCP measurements of current profiles could be obtained along the Weddell Sea cross section. Second, it appeared that the protective lid was not strong enough to withstand the collisions with ice floes. When we tried to reactivate the ADCP in ice-free waters after having left the GvN-Station, we noticed that the lid was deformed by the impacts from ice floes and the transducer assembly was severely damaged. All four transducer heads were scoured off at their outer periphery, and in one case the metal cage embedding the transducer face was torn. Moreover, two of the transducer heads were loosened from their proper connection to the transducer electronics housing because the connecting bolts had been lengthened by leverage, leading to gaps of up to 3 mm wide between the transducer heads and the electronics housing. Through these gaps sea water flooded the electronics housing. Because of the severeness of the damages, there was no way of repairing the transducer assembly on board of the ship and to employ the ADCP during the further parts of the cruise.

The thermal structure of the upper 700 to 800 meters was measured by 194 XBT-profiles which were recorded with a Nautilus-system. Times and locations of the individual profiles are given in Tab. 2.3 and 2.4. Comparison between 8 XBT and CTD measurements at the same stations confirmed the accuracy of 0.2 K given by the manufacturer. The data obtained are depicted as vertical sections in Fig. 2.14.

Sea surface temperature and salinity were recorded continuously in the bow thruster channel at about 5 m depth with a thermosalinograph supplied by Meerestechnik-Electronik (ME). The data were controlled by salinity samples taken at the inlet to the instrument and the temperature measurements of the CTD. The following corrections have to be applied to the recorded data:

$$\begin{aligned}T_{\text{true}} &= 0.921 T_{\text{recorded}} - 0.253 \\S_{\text{true}} &= 0.949 S_{\text{recorded}} - 1.772\end{aligned}$$

The corrected data will then be accurate to 0.03 K and 0.03. However, it has to be taken into account that occasionally a water-ice mixture is flowing in sensor head which results in erroneous data. The error is obvious by the reduced conductivity due to the ice. Therefore we do not use the thermosalinograph data along the transect but refer to the CTD-data in 10 m depth (Fig. 2.9). The T/S-profiles across Drake Passage and from Antarctica to South Africa are shown in Fig. 2.15.

Tab. 2.3: XBT-Section C. San Juan - King George Island

Station No.	Date (GMT) (uncorr.)	Time	Position S	W	Depth (m)
1	18.11.90	23:57	54°39'	63°31'	122
2	19.11.90	01:12	54°54'	63°19'	>1800
3		02:03	55°07'	63°08'	2639
4		03:07	55°20'	62°57'	4171
5		04:03	55°34'	62°48'	4141
6		05:18	55°48'	62°35'	4090
7		06:25	56°01'	62°25'	3953
8		07:45	56°15'	62°11'	4040
9		08:50	56°29'	62°00'	4100
10		09:58	56°42'	61°48'	3000
11		10:58	56°56'	61°39'	>3000
12		11:58	57°09'	61°27'	3819
13		12:58	57°23'	61°14'	3845
14		14:05	57°38'	61°02'	3631
15		14:56	57°50'	60°52'	3601
16		16:01	58°04'	60°42'	4305
17		17:39	58°28'	60°21'	3073
18		18:31	58°31'	60°12'	3600
19		19:30	58°44'	60°03'	3715
20		20:35	58°58'	59°50'	6428
21		21:35	59°11'	59°39'	4090
22		22:50	59°25'	59°27'	4298
23	20.11.90	00:04	59°40'	59°13'	2142
24		01:08	59°52'	59°02'	5930
25		02:09	60°06'	58°49'	3490
26		03:21	60°20'	58°36'	3868
27		04:21	60°33'	58°23'	3912
28		05:26	60°47'	58°11'	4266
29		06:33	61°00'	57°58'	4910
30		07:39	61°14'	57°45'	2499
31		08:40	61°27'	57°33'	903
32		09:45	61°41'	57°18'	399
33		10:42	61°54'	57°10'	259
34		12:01	62°06'	57°26'	743
35		13:15	62°13'	58°02'	1280
36		14:03	62°17'	58°24'	1100
37		15:01	62°17'	58°44'	464

Tab 2.4: XBT-Section Antarctica - South Africa

Station	Date	Time (GMT)	Latitude	Longitude	Depth (m, uncorr.)
106	20.12.90	04:06	68°11' S	04°28' W	4086
107		10:00	67°45' S	03°09' W	4283
108		14:35	67°32' S	01°04' W	> 4000
109		17:17	67°15' S	00°24' E	3451
110		19:20	67°00' S	00°52' E	> 4500
111		22:20	66°30' S	01°49' E	4080
112	21.12.90	00:05	66°15' S	02°21' E	3680
113		01:55	66°00' S	02°51' E	3390
114		03:40	65°45' S	03°17' E	3669
115		06:25	65°15' S	03°21' E	2627
116		07:44	65°00' S	03°23' E	2530
117		09:06	64°45' S	03°26' E	
118		10:31	64°30' S	03°29' E	2177
119		11:57	64°15' S	03°31' E	2600
120		13:16	64°00' S	03°34' E	3159
121		14:11	63°45' S	03°36' E	4365
122		16:01	63°30' S	03°37' E	4940
123		17:22	63°15' S	03°41' E	5055
124		18:44	63°00' S	03°44' E	5360
125		20:01	62°45' S	03°31' E	5340
126		21:25	62°30' S	03°16' E	5378
127		22:40	62°15' S	03°02' E	5372
128		23:55	62°00' S	02°49' E	5380
129	22.12.90	01:20	61°45' S	02°34' E	5378
130		02:30	61°30' S	02°20' E	5376
131		03:50	61°15' S	02°07' E	5122
132		05:10	61°00' S	01°53' E	3341
133		06:07	60°48' S	01°42' E	5400
134		07:45	60°30' S	01°27' E	4181
135		09:02	60°15' S	01°15' E	4303
136		11:36	59°45' S	00°51' E	4924
137		12:45	59°30' S	00°39' E	> 4200
138		15:17	59°00' S	00°14' E	4488
139		16:37	58°45' S	00°02' E	4599
140		18:00	58°29' S	00°12' W	4428
141		19:05	58°15' S	00°22' W	3885
142		20:10	58°00' S	00°34' W	3900
143		21:35	57°45' S	00°45' W	4210
144		22:50	57°30' S	00°58' W	3905
145	23.11.90	00:06	57°15' S	01°10' W	3368
146		02:35	56°45' S	01°33' W	3563
147		03:50	56°30' S	01°44' W	4187
148		05:04	56°15' S	01°55' W	4045
149		06:40	55°58' S	02°09' W	3386
150		07:45	55°44' S	02°18' W	3371
151		08:55	55°30' S	02°29' W	2640
152		10:13	55°15' S	02°41' W	2460
153		11:24	55°01' S	02°51' W	3143
154		12:44	54°45' S	03°03' W	2645
155		13:56	54°30' S	03°14' W	2606
156		18:35	54°20' S	03°24' W	2702
157		19:15	54°15' S	03°15' W	2400
156		21:20	54°00' S	02°36' W	2495
157		23:17	53°45' S	01°59' W	2040
158	24.12.90	01:10	53°30' S	01°25' W	2658
159		03:05	53°15' S	00°50' W	2358
160		04:16	53°05' S	00°29' W	2600
161		04:54	53°00' S	00°19' W	2481
162		06:45	52°45' S	00°15' E	2720
163		08:20	52°30' S	00°46' W	2800

Station	Date	Time (GMT)	Latitude	Longitude	Depth (m,uncorr.)
164		10:15	52°15' S	01°19' E	2800
165		12:04	52°00' S	01°52' E	2600
166		13:55	51°45' S	02°24' E	3053
167		15:45	51°30' S	02°57' E	3485
168		17:35	51°15' S	03°28' E	3390
169		18:25	51°00' S	04°00' E	3608
170		19:50	50°57' S	04°06' E	3553
171		21:25	50°45' S	04°30' E	3231
172		23:14	50°30' S	05°02' E	3349
173	25.12.90	01:45	50°15' S	05°33' E	3659
174		11:20	50°00' S	05°58' E	3711
175		13:00	49°45' S	06°11' E	3519
176		14:40	49°30' S	06°23' E	3500
177		16:25	49°13' S	06°37' E	3464
178		18:30	49°00' S	06°48' E	3684
179		20:36	48°45' S	07°02' E	3890
180		22:45	48°29' S	07°15' E	2182
181	26.12.90	00:39	48°15' S	07°27' E	2465
182		02:47	47°59' S	07°43' E	4158
183		04:30	47°45' S	07°53' E	3090
184		06:30	47°30' S	08°05' E	2550
185		08:19	47°15' S	08°18' E	1837
186		10:04	47°00' S	08°31' E	3452
187		11:52	46°45' S	08°43' E	3685
188		13:37	46°30' S	08°55' E	4420
189		15:20	46°15' S	09°07' E	4680
190		16:55	46°01' S	09°19' E	4650
191		18:50	45°45' S	09°32' E	4563
192		20:30	45°30' S	09°43' E	4513
193		22:20	45°15' S	09°55' E	4610
194	27.12.90	00:05	45°00' S	10°08' E	4710
195		01:44	44°45' S	10°20' E	4748
196		03:21	44°30' S	10°31' E	4981
197		05:09	44°15' S	10°43' E	4231
198		06:47	44°00' S	10°55' E	4305
199		09:30	43°45' S	11°07' E	4409
200		11:20	43°28' S	11°19' E	4980
201		12:50	43°15' S	11°31' E	4591
202		14:30	43°00' S	11°43' E	4703
203		16:10	42°45' S	11°55' E	4505
204		17:42	42°30' S	12°06' E	4606
205		19:33	42°13' S	12°20' E	3239
206		20:48	42°00' S	12°29' E	5102
207		22:17	41°45' S	12°40' E	3329
208		23:49	41°30' S	12°51' E	2980
209	28.12.90	00:13	41°15' S	13°02' E	2100
210		01:40	41°00' S	13°10' E	4500
211		03:22	40°45' S	13°22' E	4626
212		05:06	40°30' S	13°36' E	4934
213		06:52	40°15' S	13°48' E	4842
214		08:35	40°00' S	13°59' E	4135
215		10:10	39°45' S	14°10' E	4679
216		13:21	39°29' S	14°21' E	4760
217		14:53	39°13' S	14°31' E	4730
218		15:14	39°00' S	14°40' E	4744
219		16:57	38°45' S	14°51' E	4853
220		18:30	38°29' S	15°04' E	4856
221		22:53	37°51' S	15°33' E	4866
222		23:35	37°45' S	15°37' E	4396
223	29.12.90	01:04	37°30' S	15°49' E	4788
224		02:29	37°15' S	15°58' E	4708

Fig. 2.14: XBT sections across Drake Passage (top) and from Antarctica to South Africa (bottom) carried out during ANT IX/2. For location see see Fig. 2.1.

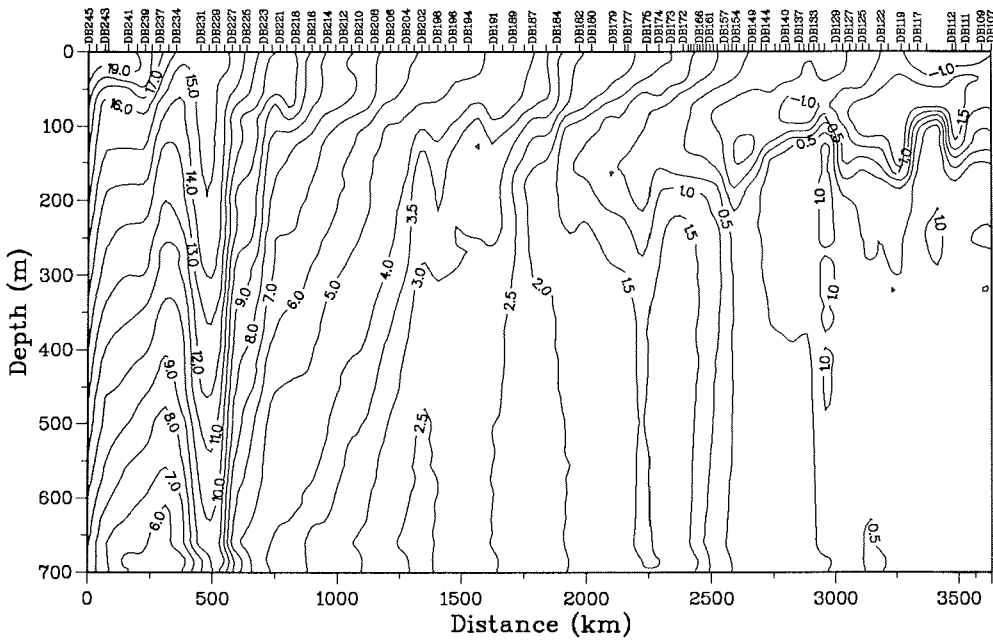
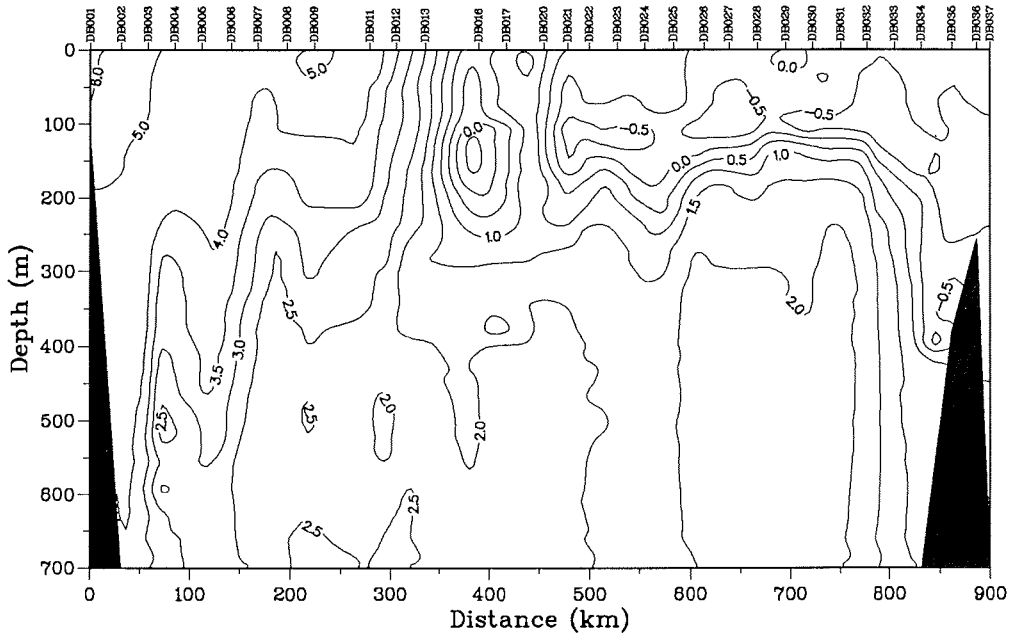
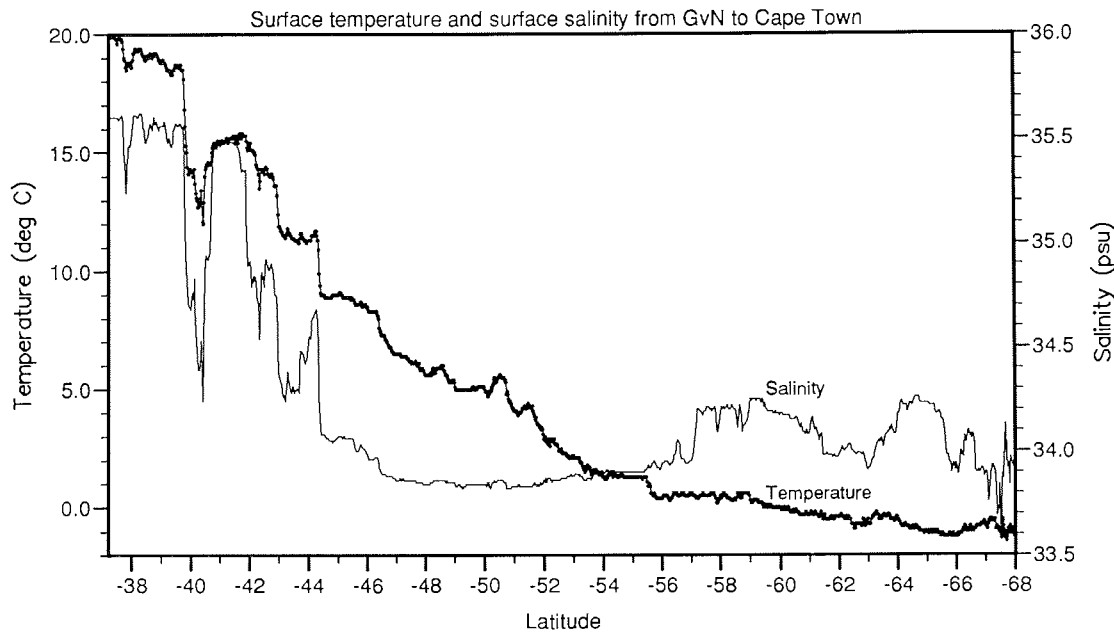
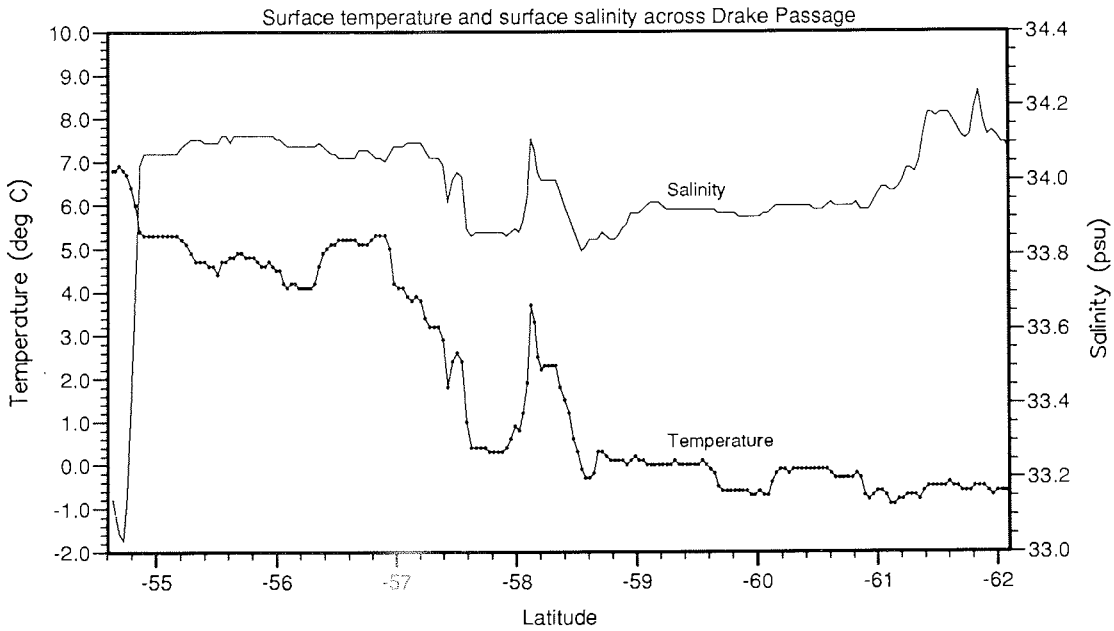


Fig. 2.15: T/S-profiles across Drake Passage (top) and from Antarctica to South Africa (bottom) measured with a thermosalinograph during ANT IX/2. For location see Fig. 2.1.



3. CHEMISTRY

3.1. Measurements of biogenic sulfur compounds and their reaction products in sea water and the marine atmosphere

R. Staubes (IfMG)

Objectives

Oceanic emissions of biogenic sulfur gases like dimethyl sulfide (DMS), carbonyl sulfide (COS), carbon disulfide (CS₂) and methyl mercaptan (CH₃SH) constitute a major flux of sulfur to the atmosphere, a source which is believed to be responsible for the background levels of SO₂, non-sea salt sulfate and methanesulfonic acid. These compounds are important factors in cloud chemistry and global climate as contributors to cloud condensation nuclei. The dominant sulfur compound released from the oceans and thus the most important precursor of non-sea salt sulfate is considered to be DMS which is produced from metabolic processes in certain algae.

Work at sea

During ANT IX/2 we performed simultaneous measurements of dimethyl sulfide (DMS), carbonyl sulfide (COS), carbon disulfide (CS₂) and methyl mercaptan (MeSH) in sea water and the atmospheric boundary layer. The concentrations of the main reaction products sulfate and methanesulfonate in aerosols in the atmosphere were determined. The air samples were collected at the front of the ship's upper deck; to minimize the influence of the ship two outriggers were fixed at the rail. Aerosols were sampled on filters; the analysis of the ion concentration in the aerosols will be carried out in the laboratory in Frankfurt. The seawater samples were taken from the ship's continuous seawater pumping system. The concentration of atmospheric and dissolved DMS, COS, CS₂ and MeSH were analyzed by means of a gas chromatographic system equipped with a flame photometric detector. Biological data of the seawater have been collected during the cruise to aid the interpretation of the findings. Due to our participation in the cruise legs ARK VII/2, ANT IX/1 and ANT IX/2 of "Polarstern" the concentration profiles of atmospheric and dissolved DMS, COS, CS₂ and MeSH could be examined from 82°N to 71°S.

Preliminary results

The data show that DMS is the dominant sulfur gas in all sea water samples examined, with smaller amounts of COS, CS₂ and MeSH in sum accounting for less than 20% of the observed sulfur in seawater. Atmospheric DMS in the boundary layer was characterized by a significant spatial variability, while COS was distributed fairly homogeneously along the cruise. Traces of biogenic sulfur gases other than DMS and COS were found only in a limited number of atmospheric samples.

3.2. **Measurements of the concentration of Nitric acid, Ammonia and Ammonium Nitrate in the marine atmosphere**

T. Papenbrock (RUB)

Objectives

Nitric acid (HNO_3) is a final, stable product of atmospheric NO_x and HO_x chemistry. One third of the acid rain is caused by nitric acid. Hence, nitric acid is an important indicator for two of the most important cycles in clean and polluted air. Ammonia (NH_3), one of the most important bases in air, is mainly produced by biological processes. It has been found in clean and polluted air, even in the marine atmosphere, for example in the Sargasso Sea. Ammonium nitrate participates in the acid-base equilibrium with gaseous nitric acid and ammonia. This equilibrium depends on temperature and relative humidity of the air masses. For a better understanding of the concentration distribution of these three components and the equilibrium in the atmosphere, it is important to do simultaneous measurements.

Work at sea

Our method for measuring the concentration of nitric acid and ammonia in air is based on laser photolysis yielding excited OH and NH radicals. The fluorescence intensities of the two species are taken as a measure for the nitric acid and ammonia mixing ratios in the atmosphere. At present the detection limits for long integration times (one hour) is 0.04 ppbv for nitric acid and 0.3 ppbv for ammonia, respectively. Our method allows direct and continuous measurements. To examine the concentration of ammonium nitrate in air we took Denuder probes with sampling times between 40 and 64 hours. The air was sampled at the front of the ship's upper deck and pumped through an 8-meter long teflon tube to the photolysis cell. The analysis of the samples will be performed in our home laboratory after the cruise.

Preliminary results

The highest nitric acid and ammonia concentrations were measured in the Strait of Magellan after leaving Punta Arenas. The maximum values were 250 pptv for nitric acid and 600 pptv for ammonia, respectively. During the following days the concentrations slowly decreased with north-westerly winds. Then the wind changed direction and we measured air masses coming from the east. The concentrations decreased very quickly with the values often below the detection limits. Due to our participation in the cruise legs ARK VII/2 and ANT IX/1 und 2 of "Polarstern" in 1990, the concentration profiles of atmospheric gaseous nitric acid and ammonia could be examined from 82°N to 70°S.

3.3. **Organobromine compounds in the ocean and atmosphere**

T. Bluszcz, O. Schrems (AWI)

Objectives

A considerable amount of the bromine which is present in the atmosphere originates from natural sources. The oceans are important sources for methyl bromide (CH_3Br) and bromoform (CHBr_3). These are compounds which are produced by marine macro-algae. Anthropogenic emissions of organobromine compounds like the halons 1301 (CF_3Br) and 1211 (CF_2ClBr), how-

ever, are responsible for the increase of the bromine concentration in the stratosphere due to their long life times. So far, halons have very low concentrations in the atmosphere, but show an increasing tendency. Increasing production and emission rates of these chemicals can be expected in the future. Therefore, these anthropogenic source gases are a potential reservoir for stratospheric bromine radicals which are efficiently involved in the catalytic ozone depletion cycles. On the other hand a significant ozone depletion potential of the biogenic organobromine compounds has to be considered for the lower stratosphere. The objective of our work is to obtain horizontal concentration profiles of various volatile organobromine compounds during legs 1, 2 and 4 of the "Polarstern"-cruise ANT/IX. The profiles will provide information about the global distribution of these compounds, as well as information about the biogenic and anthropogenic contributions to stratospheric ozone depletion catalyzed by bromine radicals. In order to investigate the air-sea exchange of bromine compounds we collected also surface water samples for later analysis.

Work at sea

The air samples were taken 20 m above sea level through a short 1/4" teflon tube. Gas chromatographic analyses of the samples were performed in the air chemistry container at the upper deck of the ship. During sampling the wind direction was carefully checked in order to avoid contamination of the air samples by the ship. The applied sampling method was cryogenic pre-concentration of the samples by means of liquid argon as coolant. The air was pumped at a constant flow rate through a U-tube (filled with silylated glass wool) which was kept in a dewar containing liquid argon. In this way the trace gases were frozen out inside the U-tube. Prior to the condensation of the trace gases the air moisture was removed by means of a permeation gas dryer or a cold trap kept at -20°C . The samples were transferred from the U-tube to a focussing column and from there injected into the GC. The gas chromatographic separation of the components was achieved with a fused silica capillary column. For the analyses of these halogen-containing samples the GC was equipped with a highly sensitive electron capture detector (ECD). During the leg ANT IX/2 about 120 air samples were directly measured with the gaschromatograph installed in the air chemistry container. For control measurements and application of other analytical methods in the home laboratories an additional air sample was collected daily, sealed and stored at low temperature. Gas chromatography-mass spectrometry (GC-MS) coupling and GC-FTIR coupling will be applied at home for the complete identification of the peaks in the gaschromatogrammes. For the investigation of the air-sea exchange of the bromine species water samples have been taken from the seawater line at about 60 stations and also kept at low temperature. These samples will also be analysed in the home laboratory.

Preliminary results

At the beginning of the cruise we tested several variations of our air sampling technique. Removal of the air moisture by means of a cold trap (-20°C) prior to the condensation of the trace gases turned out to be the most suitable procedure for preparing the air samples. By comparison with calibrated standards of CH_3Br , CHBr_3 , CF_3Br and CF_2ClBr we could perform a preliminary quantification of the samples. It was found that these compounds are present in the marine troposphere at concentrations in the low pptv range. A listing of the compounds according increasing concentrations provides the

following order: $\text{CF}_3\text{Br} < \text{CF}_2\text{ClBr} < \text{CH}_3\text{Br} < \text{CHBr}_3$. The final evaluation and statistical treatment of the gaschromatogrammes will be performed in the home laboratory.

3.4. Biogeochemistry of Silica

L. Goeyens, (VUB); J. Krest, A. Ross, (OSU); A. Leynaert, B. Quéguiner, O. Ragueneau, (IEM); L. Lindner, (RUU)

Objectives

During EPOS Leg 2, high biogenic silica production rates have been measured in the marginal ice zone of the western part of the Weddell Sea and at one station in the Scotia Sea. Comparison with previous studies conducted in the Antarctic Circumpolar Current and in the Ross Sea indicated that the dynamics of silicon in the above mentioned subsystems are quite different. The present study was initiated to bring more information on the importance of the Weddell Sea ecosystem in the silicon budget of the Southern Ocean.

Work at sea

Eleven stations were sampled in the Weddell Sea (from $63^{\circ}12'S$, $53^{\circ}41'W$ to $71^{\circ}06'S$, $11^{\circ}23'W$) at depths ranging from 0 to 300 m. For production experiments, sampling depths were determined with reference to quantummeter profiles (respectively 100%, 25%, 10%, 3%, 1% and 0.1% of surface incident light measured as PAR). 24h incubations were conducted in a deckincubator where *in situ* light was simulated by using different transmission neutral filters. The deck-incubator was cooled by running surface water.

Additional depths were sampled to obtain complete profiles of particulate organic carbon, particulate organic nitrogen, biogenic silica, chlorophyll *a* and nutrients (silicate, nitrate, nitrite, ammonium, phosphate) in the upper 300 m at each station. At each photometric depth the production of biogenic silica was measured by means of stable silicon (^{30}Si) and radioactive silicon (^{32}Si) uptake experiments. For the latter, size-fractionation (on 0.4 and 10 μm filters) was performed at the 25% light level. The radioactive ^{32}Si -silicate enables us to measure phosphorus uptake rates also because it decays into radioactive ^{32}P -phosphate. Dissolution rates of biogenic silica were followed in parallel with production measurements by using the stable ^{29}Si method. The carbon production was measured with the classical ^{14}C method. The nitrogen production was measured only in surface water using the ^{15}N procedure. Phytoplankton samples were collected (lugol fixation) only at depths where production experiments were done and further phytoplankton samples were taken by means of a vertical net in order to estimate the Al/Si content of diatoms.

Preliminary results

For most of the stations production results must be considered as maximum potential production rates because of the importance of ice cover during the cruise (especially for Sta. B3 to B9). In those conditions natural phytoplankton populations experience a different light regime (with periods of darkness under ice) from the one used during incubations.

The distribution of major nutrients indicates weak biological activity during the study period. Surface water silicate, nitrate and phosphate concentrations were respectively about $80 \mu\text{M Si-Si}(\text{OH})_4$, $30 \mu\text{M N-NO}_3$, $2 \mu\text{M P-PO}_4$. As far

as ammonium is concerned the measured concentrations were always very low. They almost never amount more than $0.2 \mu\text{M N-NO}_4$; some stations, near $65^\circ\text{S} - 66^\circ\text{S}$, show, however, a slight increase in ammonium concentration and a corresponding decrease in surface nitrate. But still nitrate concentrations are as high as $27 \mu\text{M N-NO}_3$ in this area. In general these stations were also characterized by a slightly increased phytoplankton production. Preliminary results of ^{14}C uptake experiments indicate low levels of primary production. Maximum uptake rates in a given depth were encountered in surface waters (range : $0.15\text{-}0.54 \text{ mmol C.m}^{-3}\text{d}^{-1}$). The lowest rates were observed at the ice-shelf station where the euphotic layer reached down to 138 m. Maximum rates were measured at station B5 ($31^\circ 47' \text{ W}$, $66^\circ 07' \text{ S}$) and ice-edge station B11 ($03^\circ 57' \text{ W}$, $68^\circ 00' \text{ S}$). Depth-integrated production rates (Tab. 2.5) ranged between 12.2 and $26.2 \text{ mmol C m}^{-2}\text{d}^{-1}$ ($146\text{-}314 \text{ mg C m}^{-2} \text{ d}^{-1}$). These low values can be related both to the importance of the ice cover and the low temperatures which must prevent the emergence of large phytoplankton developments at this period of the year. First results obtained by the ^{32}Si method indicate low uptake rates both for phosphorus and silicon (Tab. 2.5), as well as for carbon uptake. Silica production rates range between $0.62\text{-}8.02 \text{ mmol Si m}^{-2}\text{d}^{-1}$. The highest rate was observed at station B1 and must be taken as characteristic of coastal water rather than the Weddell Sea. At this station the $>10 \mu\text{m}$ fraction accounted for 86.1% of silica uptake rates. The other stations fall within the lower part of the range of production rates that were measured during EPOS Leg 2. The same trend is observed for phosphorus for which the uptake rates range between $0.08\text{-}0.61 \text{ mmol P m}^{-2}\text{d}^{-1}$. At station B7 the $^{32}\text{Si}/^{32}\text{P}$ uptake experiment was conducted on brine (incubated under daylight conditions) and indicated uptake rates one order of magnitude higher than in the water column. Preliminary assimilation ratios, calculated from depth-integrated production rates, are given in Tab. 2.6. With the exception of station B4, C/P ratios range between $101.5\text{-}168.8$, close to the Redfield ratio (C/P = 106). Sta. B1 to B3 exhibit the highest Si/P ratios which suggest the dominance of diatoms in phytoplankton populations. This is also indicated by the high Si/C ratios measured at Sta. B2 and B3. Sta. B5 and B6 are quite different with regards to the three ratios and exhibit low silicon uptake as compared to carbon and phosphorus which can be related to different phytoplankton populations (dominance of non-siliceous phytoplankton). Sta. B4 is different from the other stations, showing high phosphorus uptake relative to carbon and silicon but the high Si/C ratio which suggests the dominance of diatoms in phytoplankton as for the first stations.

Tab. 2.5: Depth-integrated carbon, silicon and phosphorus production rates (in $\text{mmol C m}^{-2}\text{d}^{-1}$, $\text{mmol Si m}^{-2}\text{d}^{-1}$, $\text{mmol P m}^{-2}\text{d}^{-1}$, respectively)

N° Sta.	C prod.	Si prod.*	P prod.* (* data from ^{32}Si method)
B1	-	8.02	-
B2	13.9	1.64	0.14
B3	13.0	1.11	0.08
B4	17.9	2.35	0.38
B5	22.0	1.17	0.19
B6	18.1	0.62	0.11
B7	13.1	-	-
B8	22.5		0.33
B9	26.2		0.33
B10	19.8		0.38
B11	12.2		

Tab. 2.6: C/Si/P assimilation ratios calculated from depth-integrated production rates

N° Sta.	Si/C	Si/P	C/P
B1	-	13.0	-
B2	0.12	12.0	101.5
B3	0.09	14.4	168.8
B4	0.13	6.1	46.5
B5	0.05	6.1	115.8
B6	0.03	5.4	157.4

3.5. Biogeochemistry of Barium

L. Goeyens (VUB)

Objectives

Particulate Ba, as well as other elements like Ca, Sr and Si, trace former biological activity in the marine environment. More than for particulate carbon or nitrogen, the longer turnover time of particulate barium is of interest for its tracer properties. Whether Ba is taken up by organisms in an active or passive way is still a matter of debate. On the one hand active uptake was described in the literature, but on the other hand it was stressed that Ba precipitates in small microenvironments of cell and detritus aggregates as barite crystals. In any case barite crystals represent the major part of particulate Ba in the total suspended matter. During the remineralization process the organic matrix (of cells and/or aggregates) decays and sets the barite crystals free in the sea water, where sedimentation and slow dissolution take place. The presence and distribution of particulate Ba in the marine environment is however very dependent on assimilation and break down processes. In general a vertical Ba profile shows peak concentrations in the surface water and very often secondary peaks near the oxygen minimum. For this reason the study of the biogeochemical cycle of Ba is of interest for other parameters such as nutrients, oxygen, particulate carbon and nitrogen, chlorophyll *a*, and species distributions, but also for flux studies such as nutrient assimilation and regeneration.

Work at sea

The filtration of total suspended matter for particulate Ba, Ca, Sr, Al and Si analysis demands large amounts of sea water. Normally 10 liters are filtered; on previous cruises even more than 20 l were filtered. The total suspended matter (TSM) is collected on membrane filters, Millipore cellulose acetate filters or Nuclepore polycarbonate filters. They are simply dried at 60°C on board and stored in petri dishes until analysis in the home lab.

During the ANT IX/2 cruise samples for TSM were taken at 9 stations. At every station the samples were selected according to the plankton distribution study, carried out by Baumann and Brandini. In general sampling covered the upper 500 to 600 m. The analyses will be carried out in the home lab by dissolution of the samples (filters) after LiBO₂ fusion and determination of the Ba (Ca, Sr, Al and Si) concentrations by ICP.

4. MARINE BIOLOGY

4.1. Energy flux at the base of the Antarctic food web

M. Baumann, F. Brandini, F. Kurbjeweit, (AWI) L. Goeyens, (VUB);
J. Krest, A. Ross, (OSU); B. Quéguiner, (IEM)

Objectives

The information concerning the Antarctic food web is mostly based on descriptive work such as spatiotemporal distributions of nutrients, primary production, phytoplankton biomass (chlorophyll), and zooplankton. To our knowledge, the energy flux from the primary producers to the primary consumers within the pelagic ecosystem is estimated only by means of such a descriptive approach. As an attempt to gain a more precise picture of the trophic relationships among the planktonic communities in Antarctic regions, we focussed on the quantitative nitrogen transfer at the first and second trophic level using the stable isotope ^{15}N as a tracer. This study was carried out in terms of unialgal culture experiments using the common Antarctic copepod *Metridia gerlachei* as a primary consumer and six ^{15}N -labelled algal species as primary producers.

Work at sea

Five diatoms (*Thalassiosira* spp., *Nitzschia curta*, *Porosira glacialis*, *Rhizosolenia alata*, *Chaetoceros socialis*) and a prymnesiophyte (*Phaeocystis* spp.) were isolated from the plankton in the Weddell Sea. The species were grown in natural sea water without the addition of nutrients etc., except EDTA as a chelator. To one liter of 0.2 μm filtered sea water, 3.72 mg of EDTA were added. The stock cultures were stored at 1°C and 30 $\mu\text{Em}^{-2}\text{s}^{-1}$ continuous light. The copepod *Metridia gerlachei* was caught by means of a bongo net with mesh width of 100 μm . The animals were transferred by pipette into filtered seawater and allowed to starve for 48 hours before starting the experiments. The experiments were carried out in 5-l Duran flasks at 1°C and 30 $\mu\text{E m}^{-2}\text{s}^{-1}$ continuous light. Every 24 hours the unialgal cultures were spiked with about four micromoles of $^{15}\text{NH}_4^+$ (97% ^{15}N). It was assumed that after three days the algae were labelled through out. A mixture of 500-ml aliquots of each experimental vessel served as a seventh culture. For the grazing experiment, 20 female copepods were added to each bottle. Sampling was performed according to Tab. 2.7.

Tab. 2.7: Sampling scheme during the phytoplankton grazing experiment

Parameter	0h	24h	48h	72h ¹⁾	96h	120h
POC/PON, NH_4^+	x			x		x
nutrients	x	x	x	x	x	x
cell number	x	x	x	x	x	x
Chl a				x		x
^{15}N in PON				x		x
^{15}N in NH_4^+				x		x
^{14}C - Assimilation				x		x
$^{15}\text{NH}_4^+$ - Addition	x	x	x	x		

¹⁾ Addition of 20 animals to each culture.

Due to the fact that most of the analyses will be done in the home labs, no results can be given here. However, we hope that the experiments will provide information on the ammonia uptake of 6 of the common Antarctic phytoplankton species and on the extent *Metridia gerlachei* feeds on these species.

4.2. Phytoplankton biomass and species distribution

M. Baumann, F. Brandini (AWI)

Objectives

In marine environments, the availability of light and nutrients are important preconditions for the onset of phytoplankton development. The melting of ice along the marginal ice zones of the Weddell Sea during the spring/summer period increases both the mean light penetration and the vertical stability of the water column. Therefore, phytoplankton cells are maintained within the euphotic layer for longer periods, increasing the primary production along the receding ice edge. Moreover due to intense upwelling of the Warm Deep Water, the Weddell Sea is considered as one of the nutrient-richer waters of the World Ocean and there seems to be no evidence that the macro-nutrient concentrations may ever limit phytoplankton growth. During ANT IX/2 our objective was to examine the distributions of phytoplankton, chlorophyll, and particulate organic carbon and nitrogen (PON and POC) on a large-scale northeast-southwest transect across the Weddell Sea with special regard to the marginal ice zone. Due to the almost complete ice cover in the area of the transect we could not perform more stations within the ice edge in order to resolve precisely the spatial gradients of biological parameters usually observed in these areas. Most of our stations were located in heavily ice covered areas (8/10 to 10/10) with very low biological activity in the water column compared to the ice edge zones and to the ice associated communities.

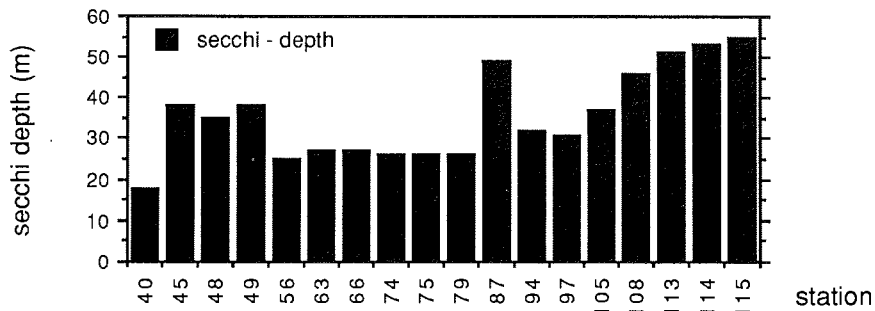
Work at sea

A total of 21 stations were vertically sampled (10 depths) by means of a rosette sampler with an integrated CTD system, to determine phytoplankton biomass in terms of chlorophyll, cell counts, and PON/POC measurements. For the microscopical analyses of species composition, samples were obtained by vertical net hauls, with a mesh size of 20 μm . The microscopic analyses of unpreserved net samples were performed immediately after sampling. Light attenuation was estimated at each station with the Secchi-disk, not in order to determine the euphotic zone, but to get an idea about cell abundance.

Preliminary results

At three stations (39, 43 and 101) no meaningful estimate of the Secchi depth could be determined due to darkness and/or rough sea. The lowest value (17 m) was obtained on the western shelf at station 40, indicating a more developed state of the phytoplankton community, and the highest (55 m) was found on the shelf off the Antarctic Peninsula (Fig. 2.16). Net samples were very poor during the whole transect and usually dominated by diatoms. At the first stations of the northeastern part (e.g. Sta. 40, 45), species were dominated by *Corethron criophilum*, *Thalassiosira*, *Odontella*, *Nitzschia*, *Porosira glacialis*, *Rhizosolenia*, *Chaetoceros*, and *Coscinodiscus*. In the deep waters of the gyre, *Nitzschia* spp, *Rhizosolenia alata*, *Chaetoceros socialis* and dinoflagellates, such as *Gyrodinium* and *Gymnodinium*, were most frequent, whereas in the southeastern sector mainly *Coscinodiscus*, *Chaetoceros* and *Rhizosolenia* appeared.

Fig. 2.16: Secchi depths measured during ANT IX/2.



The nano-size cells were observed in the middle of the gyre (Sta. 66 and 75) after filtration of 500 ml of seawater from the euphotic zone on membrane filters (Sartorius Inc., 0.8 μm). The material was transferred to microscopic slides and observed under $\times 1000$ magnification. It turned out that mainly phytoflagellates of different groups (dinoflagellates, cryptophycean, prasino-phycean) but also zooflagellates (choanoflagellates) dominated the samples. Within the smaller size category ($< 10 \mu\text{m}$) the diatoms were dominated by *Nitzschia cylindrus*. Ice algae samples were obtained at three different stations located in deep, near -slope, and the shelf areas along the cruise track. Ice algal communities over deep water were totally dominated by *Phaeocystis* spec. - no other algae could be found. The near-slope sample contained both *Phaeocystis* and diatoms, mainly *Nitzschia longissima*, *N. curta*, and other pennate species; the shelf sample was dominated by diatoms, the most characteristic species being *N. stellata*, *N. curta*, *N. closterium*, *Odontella weissflogii*, *Amphiprora* spec.. *Phaeocystis* could not be found in this sample. It might be suggested that species composition in the ice algae assemblages are related to depth of the water column, but this should be confirmed in further investigations.

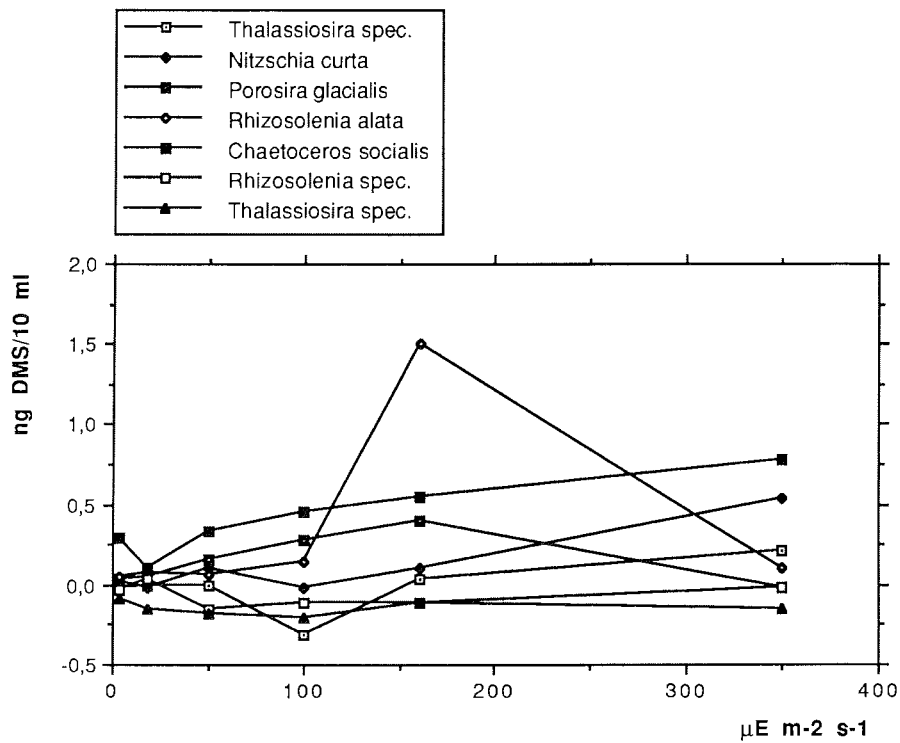
4.3. DMS - Production by Antarctic phytoplankton species

M. Baumann, F. Brandini (AWI); R. Staubes (IfMG)

Objectives

It is well established that the oceans are a significant source of organic sulfur compounds, which are largely biogenic. The most important one is probably dimethyl sulfide (DMS), which is also produced by marine phytoplankton. It is suggested that DMS production is due mainly to dinophyceae and prymnesiophyceae. However, the importance of diatoms in this connection is still unclear and especially in polar regions has this aspect not been investigated. During ANT IX/2 the DMS production of eight dominant Antarctic phytoplankton species under several light- and temperature conditions was tested.

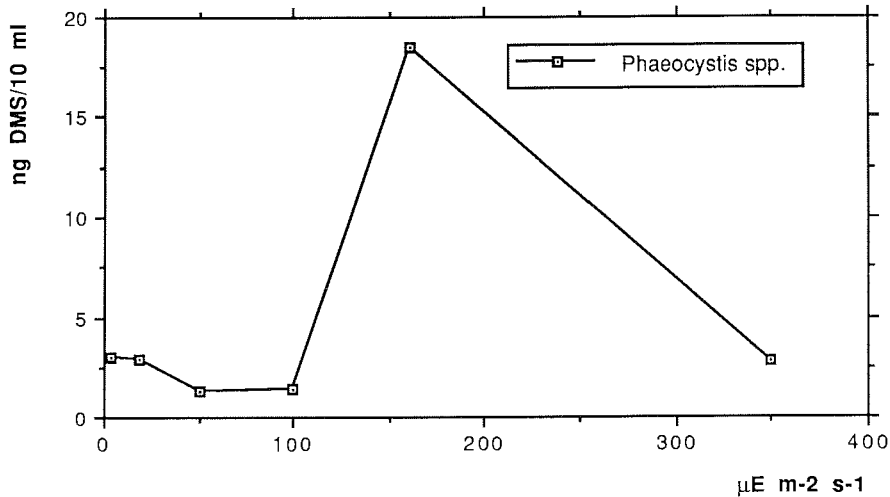
Fig 2.17: Production of DMS by 7 Antarctic diatom species at 1°C and 6 different light conditions in 36 h. Because the initial value was subtracted, negative values occur in those samples where DMS was not produced.



Work at sea

Seven diatom species (two *Thalassiosira* spp., *Nitzschia curta*, *Porosira glacialis*, *Rhizosolenia alata*, *Rhizosolenia* spp, *Chaetoceros socialis*) and a prymnesiophyte (*Phaeocystis* spp.) were isolated from the plankton of the Weddell Sea. The species were grown in natural seawater without the addition of nutrients etc., except EDTA as a chelator. 3.72 mg of EDTA were added to one liter of seawater filtered with 0.2 μm . The stock cultures were stored at 1°C and 30 $\mu\text{E m}^{-2} \text{s}^{-1}$ continuous light. For the experiments, a 2 l culture medium with cells was shaken vigorously and distributed in 100 ml flasks. One aliquot was kept for a quantitative cell analysis and another for the determination of the initial DMS content. The experiments were carried out in an incubator which allowed the choice of six light conditions (350, 160, 100, 50, 18, and 3.5 $\mu\text{E m}^{-2} \text{s}^{-1}$) and two temperatures (1°C and -1.6°C) The DMS released by the algae after three days was analyzed according to the method described in 1.3.1.

Fig 2.18: Production of DMS by *Phaeocystis* spp. at 1°C and six different light conditions.



Preliminary results

Fig. 2.17 shows the preliminary results of DMS produced by the diatoms at 1°C. Although the values still have to be related to cell numbers, one can see that except *Thalassiosira*- and the *Rhizosolenia* spp., all diatoms produced DMS; *Rhizosolenia alata* obviously released the greatest amount. Compared to diatoms, the prymnesiophyte *Phaeocystis* sp. produces significantly more DMS (Fig. 2.18). While values for the diatoms range from 0.1 to 1.5 ng DMS / 10 ml, the *Phaeocystis* culture produced up to 20 ng DMS/10 ml. Later we intend to express the results as DMS production per cell surface for better comparisons of production rates among species.

4.4. Effect of dissolved organic compounds derived from "brown ice" on the development of surface phytoplankton in the Weddell Sea

M. Baumann, F. Brandini, (AWI); J. Krest, A. Ross (OSU)

Objectives

The blooming of phytoplankton cells in the ice edge zones of the Antarctic Ocean has been associated with a vertical stabilization of the surface water layers during ice melting. More recently, the seeding hypothesis has been claimed to be crucial for increasing phytoplankton biomass in the near surface layers, as algae from the brown ice are released in great quantities during the receding of the ice in early spring. However, it should be mentioned that the water column not only receives particulate material from the ice but also dissolved organic compounds making the seeding process much more complex than it is assumed.

According to recent studies on spatial distribution of phytoplankton in the ice edge zones, the dynamics of the blooming should be analyzed at two consecutive stages, starting with the ice associated species (*Nitzschia spp.*, *Navicula spp.*, *Amphiprora spp.*, and *Fragillaria spp.*) immediately after the melting of the ice. Due to grazing pressure and the rapid sinking of cells - ice algae are strongly silicified and therefore heavier than planktonic species - the phytoplankton composition in the ice edge shifts from an ice algae characterized community to a more holoplanktonic community (*Thalassiosira spp.*, *Rhizosolenia spp.*, *Chaetoceros spp.*, and *Corethron criophilum*). We believe that the development of this second stage is strongly related to the input of great amounts of dissolved organic compounds, derived from the "brown ice" community, into the surface water. The dissolved organic material possibly acts as chelators for essential trace metals (Fe, Mn, etc.), improving the development of planktonic diatoms. Although the stimulating effect of the melted "brown ice" on the phytoplankton development was previously mentioned, it seems that hitherto no proper attention has been paid to this. Therefore, during ANT IX/2 we decided to test the potential stimulating effect of dissolved organic material from "brown ice" on the development of the natural phytoplankton of the Weddell Sea.

Work at sea

For testing the effect of DOM from melted ice samples on the potential growth of natural phytoplankton populations, two different "brown ice" (BI 1, BI 2) samples were taken. The analysis of species composition and the contents of the macro-nutrients revealed that they differed both in microalgal community structure and nutrient contents. BI 1 was totally dominated by *Phaeocystis* colonies and BI 2 by a mixture of *Phaeocystis* and diatoms. The growth potential of natural phytoplankton from surface seawater was experimentally tested as follows:

1:	800 ml SSW ¹⁾	+	200 ml FSW ²⁾		
2:	800 ml SSW	+	200 ml FSW	+	EDTA
3:	800 ml SSW	+	200 ml melted BI 1		
4:	800 ml SSW	+	200 ml melted BI 2		

- 1) surface seawater
2) filtered seawater

All experiments were done in duplicates (A, B). 200 ml of SSW were added to the control (1 A/B) and EDTA flasks to avoid dilution effects of initial cell concentrations. The experimental flasks were kept at 1°C and 30 $\mu\text{E m}^{-2}\text{s}^{-1}$. Sampling for cell counts and nutrient concentrations (nitrate, phosphate and silicate) was performed every two days for two weeks. Cell numbers were estimated on board after filtration of 50 ml culture medium on cellulose acetate filters (pore size 0,8 μm). If performed very gently, the cells are not destroyed by this procedure and can be counted with a standard microscope directly on the filters. Total nano-size and macro-size diatoms were counted in the same unit area of the filters and hence results are expressed on a relative basis. Nutrient analyses were carried out on board with the aid of an autoanalyzer.

Preliminary results

Initial cell concentrations in all experimental flasks averaged 200 relative units, and were dominated by *Nitzschia curta*, *N. cylindrus*, *N. kerguelensis*, *Chaetoceros dictyota*, *Chaetoceros* spp., *Pseudonitzschia* spp., *Corethron criophilum*, unidentified centric and pennate diatoms. Total diatoms and two different size classes of *Nitzschia* spp. were considered to represent biomass development. The nano-size *Nitzschia cylindrus* numerically dominated all the experimental approaches. Fig. 2.19 shows clearly the stimulating effect of DOM, derived from both melted BI 1 and BI 2 on growth rates in comparison with the control and EDTA-added flasks. From the differences between cell concentrations after 12 days it might be assumed that DOM derived from diatom - dominated "brown ice" (4 A,B) had a stronger effect on cell doubling rates than DOM from *Phaeocystis* - dominated "brown ice". In contrast to that no significant differences can be observed when the control and the EDTA added bottles are compared.

Initial nutrient concentrations (Fig. 2.20) may not be considered limiting for phytoplankton growth as phosphate, silicate, and total inorganic nitrogen averaged respectively 2.0, 66.9, and 27.8 $\mu\text{mol l}^{-1}$. Ammonium was significantly higher in the DOM/B II- flasks (4 A,B), but decreased to comparatively low concentrations in all experiments after 48 hours.

From these preliminary results it may be concluded that DOM released from the "brown ice" of the Weddell Sea certainly has a stimulating effect on cell growth that hitherto has been neglected. We believe that these results represent baselines for future experimental approaches to provide a more detailed picture of the seeding mechanism and its impact on the blooming of the phytoplankton along the receding ice edge zones of polar seas.

Fig. 2.19: Cell increase during the DOM - experiment

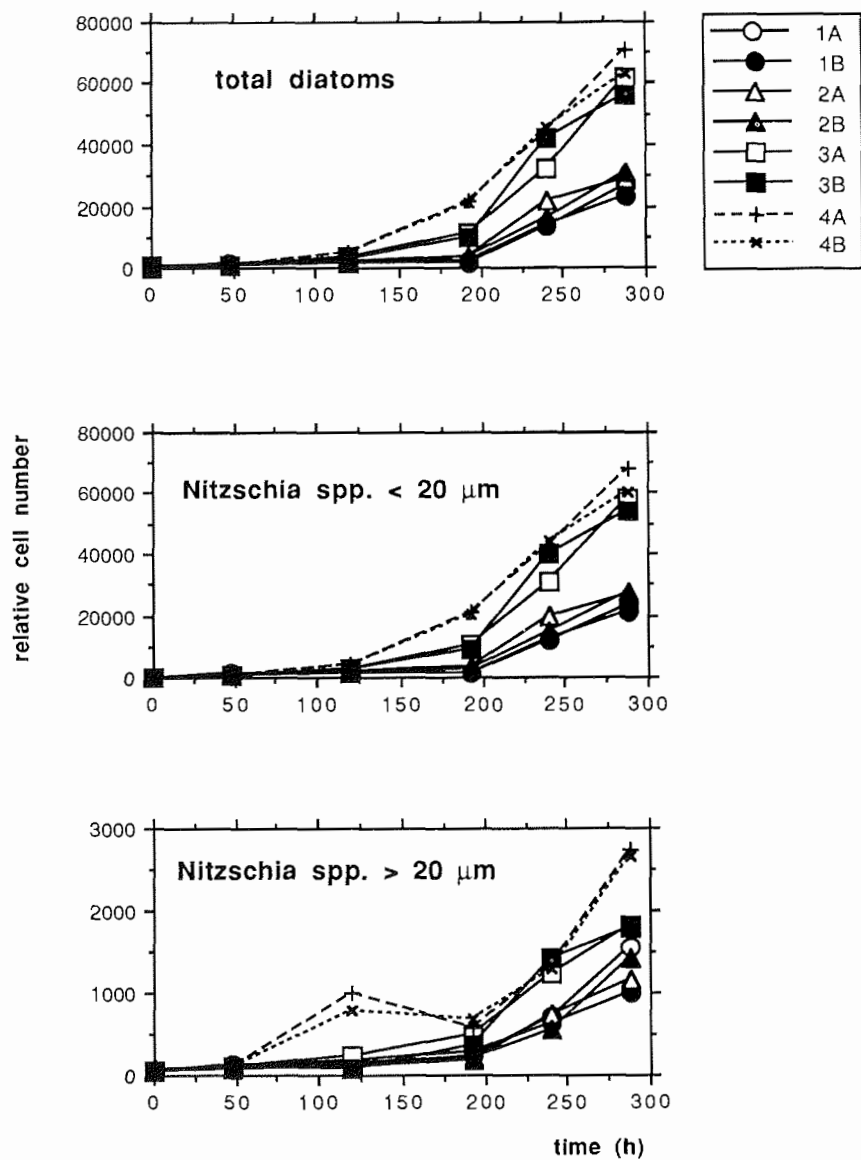
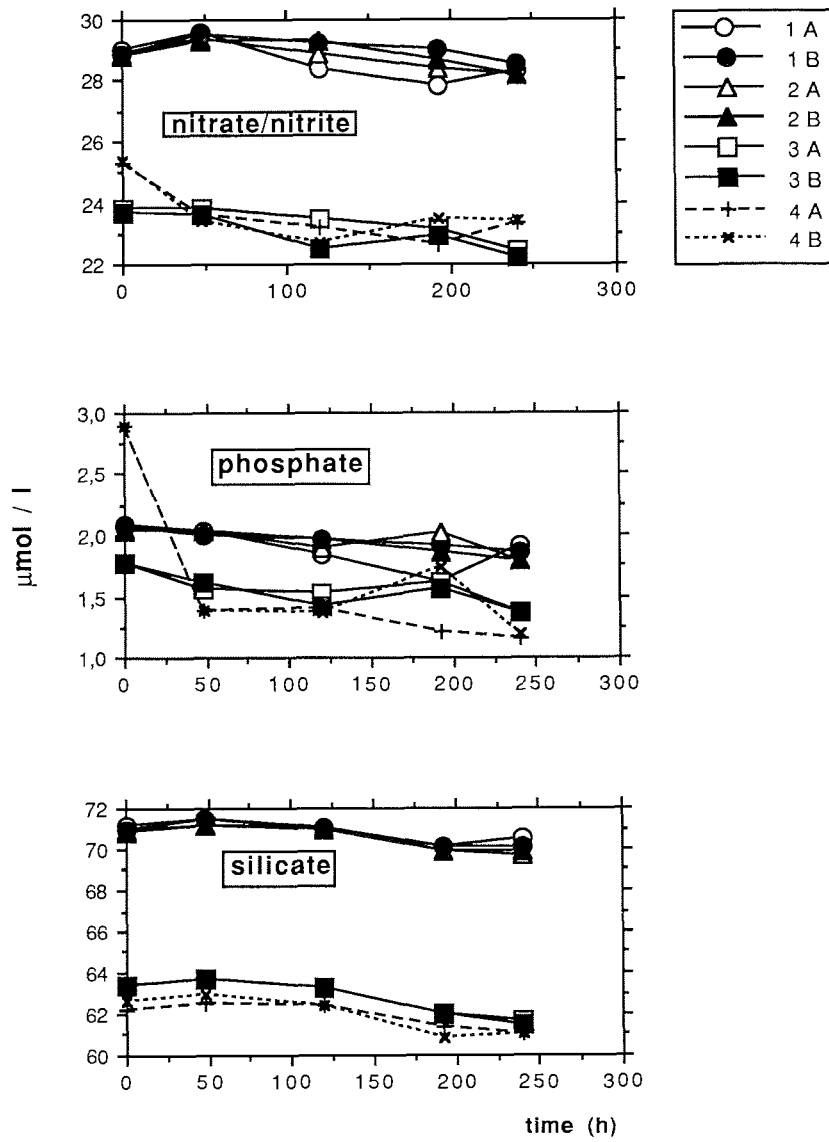


Fig. 2.20: Changes in nutrient concentrations during the DOM-experiment



4.5. Reproduction and life cycles of dominant copepods in the Weddell Sea

F. Kurbjeweit (AWI)

Objectives

Besides krill (i.e. *Euphausia superba*) and salps, copepods play the most important role as secondary producers in the pelagic system of the Antarctic and the Weddell Sea. Several papers have dealt with the distribution and abundance of calanoid copepods in the Antarctic in general, but our knowledge about their distribution, abundance, reproduction and their life cycles are sparse concerning the Weddell Sea. The first aim of this investigation is to examine the distribution and abundance of dominant calanoid copepods such as *Metridia gerlachei*, *Microcalanus pygmaeus*, *Stephos longipes*, *Calanus propinquus* and *Calanoides acutus* in space and time in the Weddell Sea during spring and summer. Due to the short period of primary production in this area, it is of major interest to investigate their reproduction pattern and to obtain if their reproduction is food limited quantitatively as well as qualitatively. With additional biochemical parameters and information about the hydrography it might be possible to develop schemes for their life cycles and their role as secondary producers in the pelagic system.

Work at sea

During ANT IX/2 on the transect from the Antarctic Peninsula to Atka Bay the distribution and abundance of dominant copepods in the upper 1000m of the water column was examined on 13 stations by means of a multinet (100µm mesh size, 0.25m² opening area). Samples from five depth strata at each station were preserved in 4% buffered formaldehyde for future investigation of stage distribution of the above mentioned copepod species and the examination of gonadal development of their females. For the second part of the investigation a bongo net (100µm mesh size; 60cm diameter) was lowered on 10 stations to 300m for getting undamaged females for reproduction experiments. Females from the most abundant copepod species were incubated on four stations under in situ conditions in surface water. In addition females of *C. acutus*, *M. gerlachei* and *S. longipes* were starved in 0.2 µm Nucleopore filtered seawater for up to two weeks. Later on, enhancement of reproduction was attempted with high concentrations of mixed algae, mainly diatoms and the prymnesiophyte *Phaeocystis* sp.. On two stations respiration of female copepods of *S. longipes*, *C. acutus*, *C. propinquus* and *M. gerlachei* were measured to evaluate their metabolic demands. As additional parameters for the interpretation of the reproductive potential of the animals under investigation, samples were taken for dryweight, C/N-content, digestive enzymes (trypsin and amylase) and lipids, which will be examined in the laboratory at home.

Preliminary results

The small copepod species *S. longipes* was found on merely three stations in high numbers, namely on the first station (station 40) on the shelf of the Antarctic Peninsula and on the last two stations close to the ice shelf in the southeast (Sta. 108, 115). *M. pygmaeus*, the other small calanoid copepod of about one millimeter in length, was found only on two stations in low numbers (63 and 94), while *C. acutus* and *M. gerlachei* were abundant on almost all stations. *C. propinquus* was dominant only on stations in the central part of the Weddell Gyre. Besides these copepods on almost all stations cyclopoid

copepods of the genera *Oncaea* spp. and *Oithona* spp. were predominant in the micro- and smaller meso-zooplankton size classes. However, radiolarians were also important on all stations, partly clogging nets and acting as a trap for most of the other zooplankton organisms. On station 115 in an inlet at the ice shelf juveniles of *Pleuragramma antarcticum* (pers. comm. Kellermann) dominated the haul.

In situ egg production experiments on five stations (63, 87, 94, 108, 115) carried out for over 24hrs in ambient surface water showed that *C. acutus*, *C. propinquus* and *M. gerlachei* produced well in the southeastern Weddell Sea close to the ice shelf (Sta. 108 and 115), whereas the reproduction of these species decreased with increasing distance from it (Fig. 1.22). Except on station 63, where none of the four incubated copepod species reproduced (*M. longipes* was used only here) *C. propinquus* laid the most eggs followed by *C. acutus* and *M. gerlachei* (Fig. 2.21). The maximum egg production per day of *C. propinquus* was 15.8, of *C. acutus* 10.1 and for *M. gerlachei* 7.6, respectively. Whether a correlation with chlorophyll concentrations in the water column exists, still has to be proved.

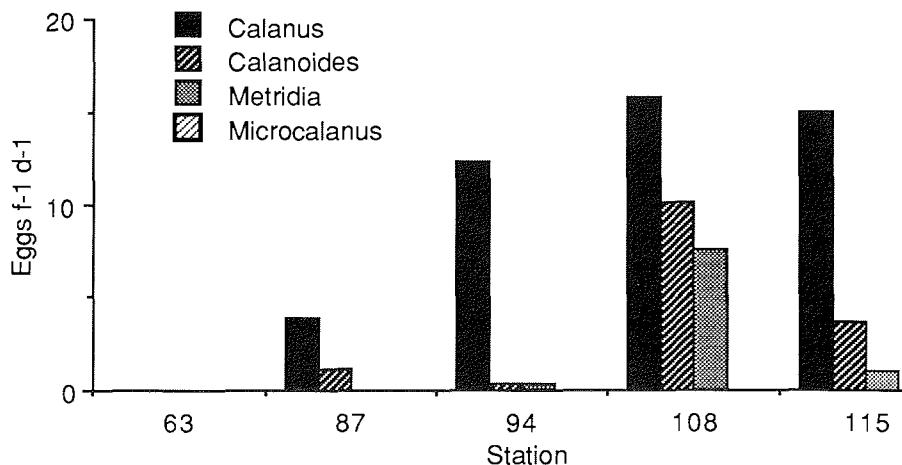


Fig. 2.21: Incubation of the four dominant copepods *Calanus propinquus*, *Calanoides acutus*, *Metridia gerlachei* and *Microcalanus pygmaeus* (only on Sta. 63) on a transect from the central part (Sta. 63) of the Weddell Sea to Atka Bay in the southeast (Sta. 115).

Egg production experiments with *S. longipes* (station 40) under starvation in egg separation chambers showed no significant egg production within 7 days. After the addition of mixed algae, mainly diatoms a) without and b) with *Phaeocystis* sp., the mortality rate was higher in the latter one, but in both incubation series no eggs were laid. In contrast, *S. longipes* was able to produce 2.8 eggs per day (sd = ± 2.0) in tissue culture vessels of only about 3ml volume for three days with *Chaetoceros socialis* as food source. Its maximum clutch size was 8. Furthermore, *Microcalanus pygmaeus* produced an average of 7.5 eggs per day (sd = ± 3.0) even without food supply to the culture vessels for four days. After that time the mortality rate increased dramatically and no eggs were produced anymore. Its maximum clutch size was 11.

On two stations, 45 and 48, 16 females of *C. acutus* were incubated in 0.2 μm Nucleopore filtered seawater to see for how long they could sustain egg production from preconsumed energy reserves. Although variability in egg production was high on both stations, the cumulative egg production for all females combined for each station leveled off after 10 to 11 days (Fig. 2.22). The maximum number of eggs produced on station 45 and 48 was 1355 and 955, or 253 and 195 as maximum numbers for a single female, respectively.

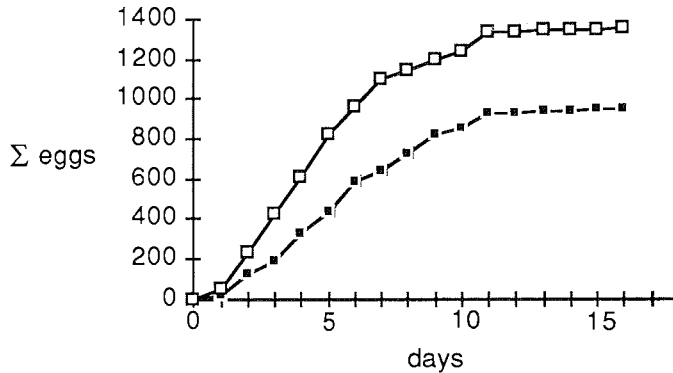


Fig. 2.22: Cumulative egg production of pooled females of *Calanoides acutus* on Sta. 45 (open squares) and 48 (filled squares).

The respiration measurements showed that small calanoid copepods such as *S. longipes* respired between 0.065 and 0.081 $\mu\text{l O}_2$ per animal per hour, while large animals as *C. acutus* respired between 0.244 and 0.456 $\mu\text{l O}_2$ per animal and hour. Respiration of *C. propinquus* and *M. gerlachei* ranged somewhere in between.

Eggs from all five copepod species under investigation, incubated in filtered seawater at 0°C under dim light conditions ($5\mu\text{Em}^{-2}\text{s}^{-1}$) showed quite different developments. While eggs of *C. acutus* needed 8 to 10 days to reach 50% of the NI population, those of *M. gerlachei* needed 3 to 4, and *M. pygmaeus* only 1 to 2 days. Eggs of *C. propinquus* from several hatches did not develop at all.

4.6. Comparative studies on the temperature dependence and kinetics of digestive enzymes in crustaceans

B. Dittrich (AWI)

Objectives

As mediators between food uptake and metabolic turn-over, enzymes play a decisive role in ensuring long-term survival of a species as well as of an individual. As highly sensitive proteins their functioning depends not only on nutritional factors but also directly on environmental conditions. Although a variety of investigations has been devoted to nutritional adaptations in zooplankton organisms, few studies have been carried out on thermal acclimation of their digestive enzymes. Most of the proteases known today show an optimum of activity at about 40-50°C. Generally, increasing as well as decreasing temperatures result in a decrease of activity which is - in

temperate and tropical species - about zero when approaching the freezing-point of water and when exceeding 60°C. The main interest of the present study is focussed on the question of how polar species cope with these extreme unfavourable conditions that exert a lethal effect on all other, not cold-adapted species. The postulation that the nutritional adaptability is a function of the metabolic needs is obviously valid also for thermal adaptability.

Work at sea

Crustaceans from different systematic groups - decapods, isopods and amphipods - as well as pantopods were obtained by means of an Agassiz-trawl, towed at a depth of 140 - 270 m near King George Island (62°35'S, 55°25'W and 62°54'S, 54°24'W) and near Kapp Norvegia (71°05'S, 11°32'W). After collecting and sorting the animals, a large portion was dissected immediately; their midgut glands and gastric fluids were deep-frozen at -80°C and will remain stored at this temperature until further analyses on temperature dependence and kinetics will be carried out at the AWI. After arrival at Cape Town, some of the samples were transported on dry-ice to Germany while the others remained on board "Polarstern". Several individuals of isopods, collected from the Agassiz-trawl off King George Island, were kept individually without any food supply in a temperature-controlled container at 0°C; a small number of them was prepared after each week to obtain information on the resistance to starvation and the influence of such unfavourable nutritional conditions on the enzymatic equipment and activity.

Preliminary Results

Analysis on midgut glands and digestive fluids in the stomachs of crustaceans collected in the course of EPOS 3 in Austral summer 1988/89, were supplemented by samples from the Skagerrak, the German Bight and the coast of Kenya. The results indicate - at least in the trypsin-like protease - characteristic differences in the temperature dependence and kinetics, which become obvious especially in the low-temperature range. Temperature optima of the investigated enzymes do not differ significantly from each other and were found at about 40-50°C. However, the most striking mechanisms of adaptation to permanent low temperatures in the predominantly cold-stenothermic Antarctic species were found to be (1) the high activity even at temperatures near freezing-point which may amount up to 15% of the maximum activity at the temperature optimum and (2) the reduction of activation energy which was found to be only a third of that in temperate and tropical species. Distinct species-specific changes in the enzyme activity after application of selected effectors suggest decisive alterations in the molecular structure of the enzyme protein. However, further detailed analyses on Antarctic species will prove if the results characterize a general phenomenon.

4.7. ³²Si applied to marine biology

M. Baumann, B. Dittrich, F. Kurbjewit, (AWI); L. Lindner (RUU)

Objectives

During EPOS leg 2, pilot experiments had already been carried out to underscore the potential of radioactive ³²Si. This is a follow-up on the previous studies. ³²Si is a weak beta emitter (t_{1/2}=174 y) and is the parent of radioactive ³²P (t_{1/2}=14 d).

Work at sea

Part of the ^{32}Si waste (^{32}Si -silicate in radioactive equilibrium with daughter ^{32}P -phosphate contained in filtered sea water) produced in the course of the ^{32}Si uptake experiments (c.f. section 3.4) was used for labeling of a mixed culture of sea algae. This ^{32}Si - ^{32}P -labelled culture was subsequently used for grazing studies with an amphipod, an isopod and a copepod, respectively.

Preliminary results

After 11 days of incubation, the first culture had taken up about one third of the available ^{32}P ; the uptake of ^{32}Si was considerably less. A second culture (the first one with additional, nutrient rich, waste water) had after several days of incubation two thirds of the ^{32}P incorporated (and seemingly also more ^{32}Si than in case of the first culture). The results show again that with an adequate selection of the type of culture (preferably of diatoms only) ^{32}Si can be recovered from its waste solutions (however, with a lower specific activity). The previous EPOS experiments with krill had shown them to be a nearly ideal specimen for ^{32}Si studies. Unfortunately, due to the lack of krill during this cruise three other animals were tested. Instead we used an amphipod, an isopod and a copepod.

Contrary to all expectations, both starved benthic animals were happily feeding on (labelled) phytoplankton. Dissection of the animals after several days of grazing, was followed by radioactive counting of the different tissues. The activities measured in the digestive systems were low, in contrast to that in the exoskeleton and the muscles combined. Only the amphipod produced several greenish slimy faecal pellets with considerable activity, much of it ^{32}P but also ^{32}Si .

The copepod (*Calanoides acutus*, 8 mm) was measured alive at regular intervals during the grazing/fasting cycles, counting the Cerenkov radiation of ^{32}P taken in. This made it possible to estimate the uptake of phytoplankton (on the order of 1% of the available biomass during a period of a week). No faecal pellets were observed to be produced.

The earlier hypothesis, given in the above mentioned krill studies, that the mechanical and physiological digestive processes of diatoms being grazed form a first and possibly important step in the remineralization of silicon, seems to find additional support in the present observations.

5. MARINE GEOLOGY

5.1. Bathymetry

U. Goldkamp, J. Monk, S. Vucelic (AWI)

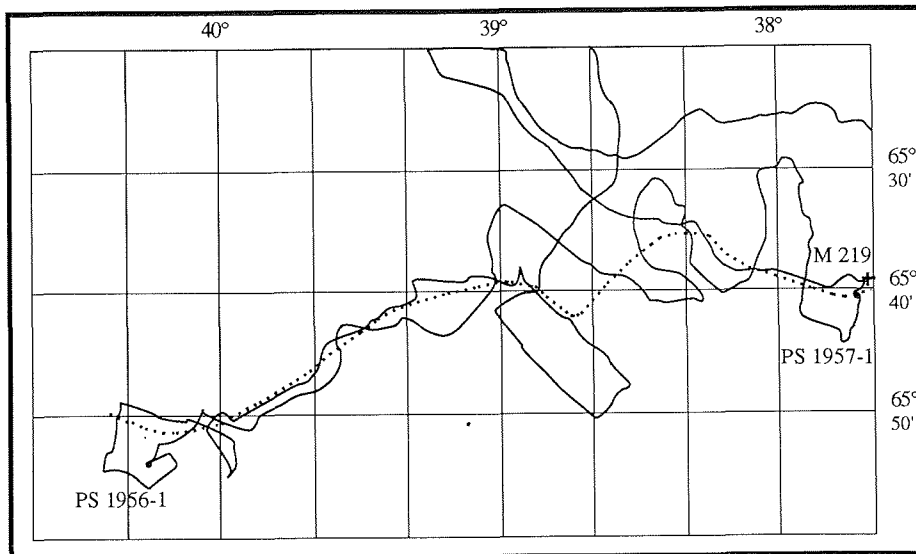
Objectives

During "Polarstern"-cruise ANT V/4 in 1987 a channel-like structure was discovered at 65°40'S, 38°45'W by means of Seabeam fansweep system. The course of the channel was expected to run from SW to NE; accordingly, a rectangular pattern of measurements was planned to investigate the extent and the shape of the channel over a larger distance. From these data the origin of and significance to northeastward bottom water transport will be derived. In addition to this area of special interest, the cruise track was used to continue charting the Weddell Sea.

Work at sea

Starting November 19th the Hydrosweep system was put in operation and worked for more than 9000 profile-kilometers. Due to technical problems, no hydrosweep data were recorded from 29 November, 12.00 until 30 November, 21.30. After leaving the Georg-von-Neumayer-Station measurements were continued while passing Maud Rise and heading for Cape Town until the end of the leg. After reaching the known position of the channel at $65^{\circ}40'S$ and $38^{\circ}45'W$ and passing the first turning points of the survey pattern, the track had to be modified, because the ice conditions made it impossible to follow a prescribed course. Nevertheless, the width of the channel was recorded in its whole extent along the channel axis from east to west which was possible because frequently leads were aligned along the channel axis. At the eastern part of the survey, large ice floes prohibited following the course of the channel. The hydrosweep screen on the bridge allowed changes in the course to be made in a way, that the survey of this part of the channel was achieved despite the ice cover. The channel was surveyed over a total length of 144 kilometers with a track line of 500 kilometers.

Fig. 2.23: Ships track (heavy line) and axis of the deep sea channel in the northwestern Weddell Sea M219 indicates the location of a current meter mooring and PS stand for minicorer samples.



On the shelf and the continental slope off Kapp Norvegia, several hydrosweep profiles could be run in spite of unfavourable ice-conditions to supplement data in the area east of the Wegener Canyon. The route to Atka Bight was used to run a profile parallel to former courses. For the passage to Cape Town a course crossing over the eastern slope of Maud Rise from south to north was chosen. The online constructed isoline-plot showed small cone-like structures in this area, even above Maud Rise. During the complete leg, GPS-satellites could be used for positioning. Offsets, positioning errors and failing data were recorded, which were due to changes in position of the satellite, inter-satellite constellation and the time free of GPS. Offsets and positioning errors were corrected within one day. Therefore, postprocessing resulted in an exact positioning of the fansweep profiles and isobaths crossings of Hydrosweep profiles.

5.2. Sediment distribution

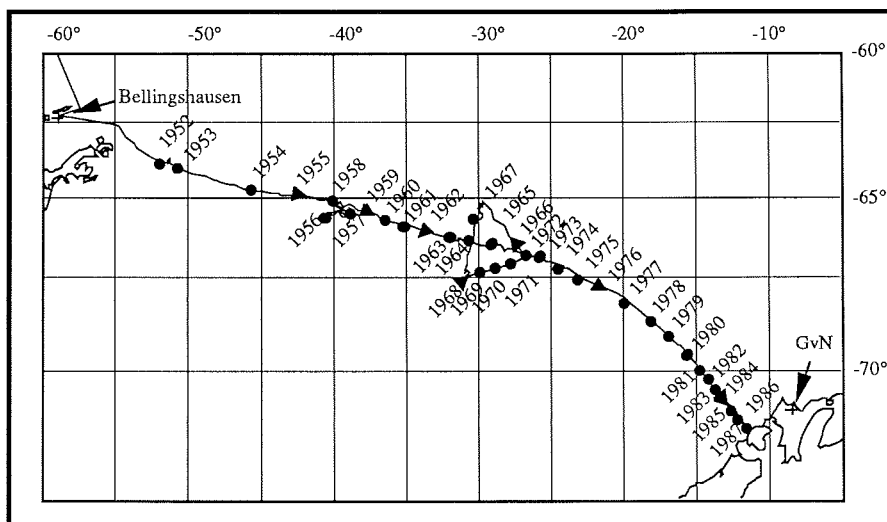
M. Weber (AWI)

Objectives

The program can be subdivided in three parts:

- a Parasound survey, carried out jointly with the bathymetric group, from Bellingshausen to the Agulhas Basin.
- the investigation of the structure, origin and significance of a deep sea channel at $65^{\circ}40'S$, $38^{\circ}45'W$ in the northwestern Weddell Sea with Hydrosweep and Parasound.
- the development of a minicorer based on the principle of a multicorer, which is fixed under the CTD with a 20 m stainless steel wire, to obtain a large number of geological samples in combination with the oceanographic station with no need of additional ship time.

Fig. 2.24: Minicorer sampling stations during ANT IX/2. Circles stand for geological and triangles for geochemical sampling



Work at sea

Parasound and Hydrosweep surveys were carried out in cooperation with the bathymetry group. In addition to the acoustic measurements, two sediment samples were taken using the minicorer and also the current meter mooring 219 was deployed in the center of the channel to get information about the flow velocity (Fig. 2.23). This minicorer enabled us to take 37 samples from the sediment surface (Fig. 2.24, Tab. 2.8), mostly on the transect between Bellingshausen and Kapp Norvegia. The use of the minicorer combined with the CTD saved more than four days of ship time normally needed for extra geological stations.

Preliminary results

Over the length of 144 km (Fig. 2.23) the structure occurs at a water depth of about 4650 m. The channel depth relative to its surroundings increases from 60 m up to 100 m. Most of the channel has an asymmetric geometry with a steep and a smooth slope. In the middle and eastern part of the studied area it is a rather small meandering feature (1 to 3 km wide). In the western part, the channel axis straightens and the channel widens to more than 10 km. The quality of the surface samples from the minicorer is the same as from the multicorer. Further investigations including sedimentological, palaeontological and geochemical analysis will be done in the AWI.

Tab. 2.8: Geological sampling during ANT IX/2

Station-Nb. Cruise 18/	AWIGEO Nb.	Date	Time	geogr. Latitude	geogr. Longitude	Water- depth (m)	MIC Penetra- tion (m)	MIC Length (m)	MIC stored (m)
042	PS 1952-1	22.11.90	13:40	63°29,92' S	52°08,02' W	924	0,02	0,00	0,00
044	PS 1953-1	23.11.90	09:33	63°44,59' S	50°55,36' W	2413	0,20	0,20	0,04
048	PS 1954-1	24.11.90	23:30	64°24,37' S	45°48,21' W	4434	0,28	0,25	0,04
050	PS 1955-1	25.11.90	22:39	64°49,21' S	42°30,22' W	4684	0,26	0,25	0,25
053	PS 1956-1	27.11.90	15:07	65°54,32' S	40°15,47' W	4607	0,10	0,01	0,01
055	PS 1957-1	28.11.90	09:48	65°40,29' S	37°44,63' W	4727	0,12	0,12	0,04
056	PS 1958-1	28.11.90	20:48	65°11,99' S	39°22,31' W	4757	0,32	0,31	0,04
057	PS 1959-1	29.11.90	06:38	65°24,71' S	37°54,80' W	4736	0,28	0,25	0,25
058	PS 1960-1	29.11.90	19:52	65°38,27' S	36°28,42' W	4770	0,24	0,24	0,04
059	PS 1961-1	30.11.90	02:41	65°43,18' S	35°26,86' W	4777	0,25	0,24	0,04
061	PS 1962-1	30.11.90	22:34	65°59,51' S	33°24,71' W	4760	0,26	0,25	0,25
063	PS 1963-1	01.12.90	17:40	66°07,27' S	31°47,09' W	4786	0,25	0,24	0,04
065	PS 1964-1	02.12.90	06:26	66°16,60' S	30°17,80' W	4800	0,25	0,25	0,04
067	PS 1965-1	02.12.90	19:46	66°27,98' S	28°45,30' W	4850	0,25	0,25	0,04
069	PS 1966-1	03.12.90	06:15	66°37,58' S	27°07,48' W	4860	0,25	0,25	0,25
075	PS 1967-1	05.12.90	10:10	65°57,41' S	30°04,25' W	4847	0,21	0,20	0,04
079	PS 1968-1	06.12.90	09:31	67°28,70' S	31°06,61' W	4625	0,29	0,25	0,25
080	PS 1969-1	06.12.90	15:39	67°18,95' S	29°57,50' W	4682	0,25	0,24	0,04
081	PS 1970-1	06.12.90	22:10	67°08,54' S	28°47,76' W	4815	0,25	0,22	0,04
082	PS 1971-1	07.12.90	04:46	66°57,20' S	27°36,63' W	4819	0,24	0,23	0,04
083	PS 1972-1	07.12.90	11:19	66°45,47' S	26°24,15' W	4854	0,18	0,14	0,04
084	PS 1973-1	07.12.90	17:18	66°53,47' S	25°32,89' W	4841	0,25	0,25	0,04
086	PS 1974-1	08.12.90	06:59	67°13,33' S	24°08,78' W	4857	0,12	0,11	0,04
088	PS 1975-1	08.12.90	21:04	67°30,49' S	22°31,29' W	4893	0,27	0,26	0,04
090	PS 1976-1	09.12.90	09:41	67°50,47' S	20°50,65' W	4919	0,27	0,25	0,25
092	PS 1977-1	09.12.90	00:40	68°17,06' S	19°20,42' W	4838	0,27	0,25	0,04
094	PS 1978-1	10.12.90	15:28	68°50,37' S	17°53,60' W	4795	0,10	0,09	0,04
096	PS 1979-1	11.12.90	04:30	69°22,01' S	16°29,80' W	4735	0,08	0,07	0,04
098	PS 1980-1	12.12.90	02:29	69°48,23' S	15°14,07' W	4741	0,04	0,00	0,00
100	PS 1981-1	12.12.90	11:35	70°07,90' S	14°15,21' W	4526	0,26	0,25	0,04
101	PS 1982-1	12.12.90	19:53	70°18,75' S	13°42,09' W	4366	0,26	0,25	0,04
102	PS 1983-1	13.12.90	02:16	70°23,27' S	13°32,57' W	2968	0,26	0,25	0,04
104	PS 1984-1	13.12.90	08:09	70°29,80' S	13°08,31' W	2407	0,26	0,25	0,25
106	PS 1985-1	13.12.90	16:38	70°47,72' S	12°22,24' W	2074	0,22	0,20	0,04
108	PS 1986-1	14.12.90	00:25	70°59,39' S	11°50,73' W	1135	0,23	0,21	0,04
114	PS 1987-1	15.12.90	14:37	71°04,87' S	11°33,72' W	273	0,20	0,19	0,04
118	PS 1988-1	23.12.90	17:42	54°19,84' S	03°24,10' W	2704	0,17	0,17	0,17

5.3. Particle flux in the water column

E. Schöffmann, M. Segl (FGB)

Objectives

To quantify the particle flux from the photic layer to the sediment and to monitor the seasonality of sediment build-up over several years.

Work at sea

At five positions moorings with sediment traps were deployed; two on the western and eastern slope (206 and KN4), one in the center of the Weddell Sea (208), west of Bouvet Island (BO 1) and in the area of the Polar Front (PF 4) (Fig. 2.25). Three sediment trap moorings were recovered in the western and the central Weddell Sea and at the Polar Front (Fig. 2.26).

Fig. 2.25: Schematic representation of the mooring recovered in the Polar Front

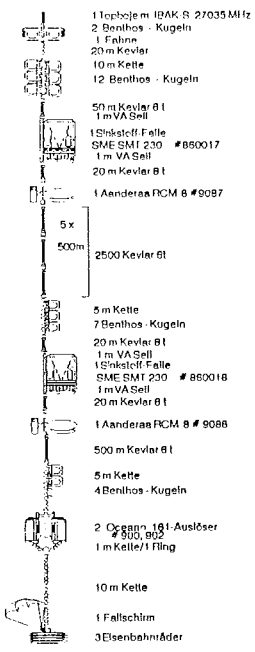
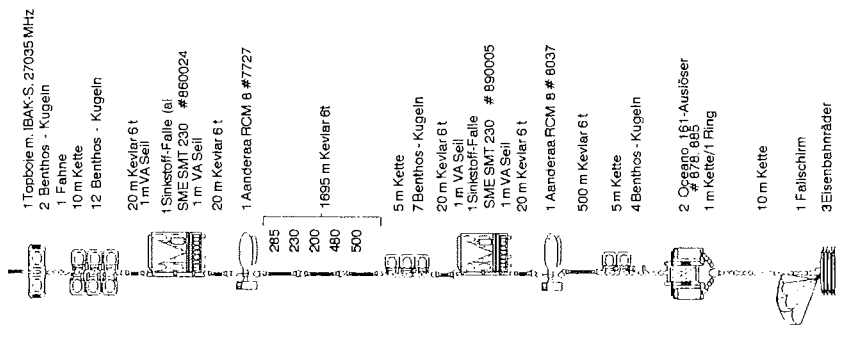
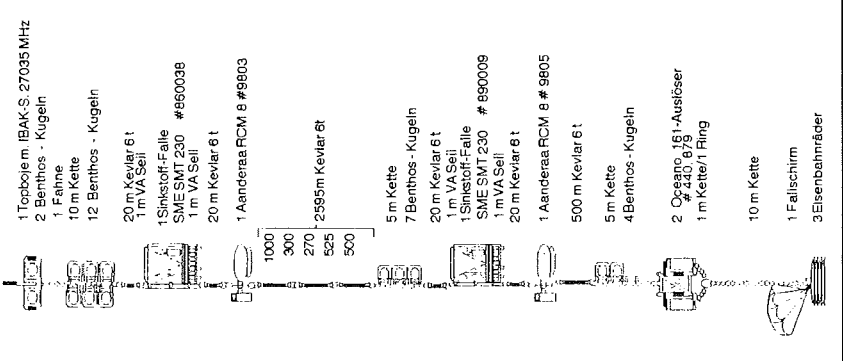
Gerätetyp	Einsatztiefe (m)
 <ul style="list-style-type: none"> 1 Topboje m IDAK S 27035 MHz 2 Benthos - Kugeln 1 Fahne 20 m Kevlar 10 m Kette 12 Benthos - Kugeln 	545
<ul style="list-style-type: none"> 50 m Kevlar 8 t 1 m VASeil 1 Sinterstoff Falle SME SMT 230 # 860017 1 m VASeil 20 m Kevlar 8 t 	825
<ul style="list-style-type: none"> 1 Aanderaa PCM 8 # 9087 	845
<ul style="list-style-type: none"> 5 x 500 m 2500 Kevlar 6t 	
<ul style="list-style-type: none"> 5 m Kette 7 Benthos - Kugeln 20 m Kevlar 8 t 1 m VASeil 1 Sinterstoff Falle SME SMT 230 # 860018 1 m VASeil 20 m Kevlar 8 t 	3200
<ul style="list-style-type: none"> 1 Aanderaa PCM 8 # 9088 500 m Kevlar 8 t 5 m Kette 4 Benthos - Kugeln 	3220
<ul style="list-style-type: none"> 2 Ocean 161-Auslöser # 900, 902 1 m Kette/1 Ring 	3775
<ul style="list-style-type: none"> 10 m Kette 1 Fallschirm 3 Eisenbahnräder 	3785
Verankerung Nr.: PF-3 Schiff: POLARSTERN Expedition: ANT IX/2 Seegebiet: Polarfront Wassertiefe: 3785m Auslegedatum: 09.11.89 Aufnahmedatum: 25.12.90	Position: 50°07,6' S 05°50 0' O

Fig. 2.26: Schematic representation of moorings deployed in the Polar Front and west of Bouvet Island

Gerätetyp	Einsatztiefe (m)	Gerätetyp	Einsatztiefe (m)
 <p>1 Topboiem IBAK-S, 27035 MHz 2 Benthos - Kugeln 1 Fahne 10 m Kette 12 Benthos - Kugeln 20 m Kevlar 6 t 1 m VA Seil 1 Sinkstoff-Falle SME SMT 230 # 860024 1 m VA Seil 20 m Kevlar 6 t 1 Aanderaa RCM 8 # 7727</p> <p>285 230 200 480 500</p> <p>1695 m Kevlar 6t</p> <p>5 m Kette 7 Benthos - Kugeln 20 m Kevlar 6 t 1 m VA Seil 1 Sinkstoff-Falle SME SMT 230 # 890005 1 m VA Seil 20 m Kevlar 6 t 1 Aanderaa RCM 8 # 8037</p> <p>500 m Kevlar 6 t 5 m Kette 4 Benthos - Kugeln</p> <p>2 Oceano 161-Auslöser # 878 885 1 m Kette/1 Ring</p> <p>10 m Kette 1 Fallschirm 3 Eisenbahnräder</p>	480	 <p>1 Topboiem IBAK-S, 27035 MHz 2 Benthos - Kugeln 1 Fahne 10 m Kette 12 Benthos - Kugeln 20 m Kevlar 6 t 1 m VA Seil 1 Sinkstoff-Falle SME SMT 230 # 860038 1 m VA Seil 20 m Kevlar 6 t 1 Aanderaa RCM 8 # 9603</p> <p>1000 300 270 525 500</p> <p>2595 m Kevlar 6t</p> <p>5 m Kette 7 Benthos - Kugeln 20 m Kevlar 6 t 1 m VA Seil 1 Sinkstoff-Falle SME SMT 230 # 890009 1 m VA Seil 20 m Kevlar 6 t 1 Aanderaa RCM 8 # 9605</p> <p>500 m Kevlar 6 t 5 m Kette 4 Benthos - Kugeln</p> <p>2 Oceano 161-Auslöser # 240 879 1 m Kette/1 Ring</p> <p>10 m Kette 1 Fallschirm 3 Eisenbahnräder</p>	3907
<p>Verankerung Nr.: BO-1 Schiff: POLARSTERN Expedition: ANT IX/2 Seegebiet: Westl. Bouvet Island Wassertiefe: 2734 m Auslegedatum: 23.12.90 Aufnahmetermin:</p>	<p>Position: 54°20,3' S 03°22,6' W</p>	<p>Verankerung Nr.: PF-4 Schiff: POLARSTERN Expedition: ANT IX/2 Seegebiet: Polarfront Wassertiefe: 3807 m Auslegedatum: 25.12.90 Aufnahmetermin:</p>	<p>Position: 50°07,6' S 05°52,0' O</p>

On board, smear slides were prepared from the trap samples. The samples were then stored in a cool room at 4°C. Further investigations on the sediment trap material including biological, geological and isotopic analysis will be carried out at the AWI and at the FGB.

Preliminary results

The sediment traps in the Weddell Sea operated since 20 September 1989 (mooring 206) and 5 November 1989 (mooring 208), respectively. The sample bottles were changed every 15 days in spring and summer and every 30 days during the winter. The trap in mooring 206 sampled only until May 1990 because of electronic problems. The upper trap in mooring 208 worked well, the lower trap did not work at all. The flux to the traps showed a maximum during February and March. The traps in the Polar Front operated since November 1989. The maximum flux was in March. In the upper trap, the cups from the winter months contained about 1/8 to 1/4 of the material that was collected in the summer months. In the lower trap the winter cups were nearly empty. This leads to the conclusion that in winter most of the material present in the photic zone is reworked in the water column and does not reach the sediment.

5.4. Stable isotopes in the water column

E. Schöffmann, M. Segl (FGB)

Objectives

Stable oxygen and carbon isotopes are used in marine geology to reconstruct the paleoceanographic history by measuring the $^{18}\text{O}/^{16}\text{O}$ and $^{13}\text{C}/^{12}\text{C}$ in the shells of marine organisms and the $^{13}\text{C}/^{12}\text{C}$ in the organic material, and to quantify the influence of bio-activity.

Work at sea

Samples to determine the isotopic composition of the dissolved CO_2 ($^{13}\text{C}/^{12}\text{C}$) and of the water itself ($^{18}\text{O}/^{16}\text{O}$) were taken from the rosette on all biological stations. Samples of 250 ml and 100ml were put into glass bottles, avoiding air bubbles in the sample. The 250 ml samples for ^{13}C measurements were poisoned with HgCl_2 to avoid further CO_2 production. These samples, as well as the 100 ml samples, were then sealed with wax and stored in a cool room at 4°C. The isotopic composition of the samples will be measured at the stable isotope laboratory of the AWI.

5.5. Natural radioactive isotopes in the water column

E. Schöffmann, M. Segl (FGB)

Objectives

Investigations on sediment samples from the area off West Africa and from the Polar Front show that in areas with high biological activity, the flux of radioisotopes such as ^{10}Be and ^{230}Th to the sediments increases the production of the isotopes. This is due to scavenging of the isotopes by settling particles. This causes a concentration gradient of the isotopes from high to less productive areas which might allow former biological activity to be deduced.

Work at sea

To quantify these effects, samples for ^{10}Be measurements were taken on 4 stations of the Weddell Sea transect. The investigations on these samples will be linked to investigations on ^{230}Th in the Weddell Sea by the geochemistry group of the AWI, and to results of measurements of ^{10}Be and ^{230}Th in the South Atlantic by the FBG. To get the 30 l of water needed for a ^{10}Be analysis, water from different depths within the same water layer was combined. A well known amount of ^9Be carrier was added and Be, together with Mg and other elements, was precipitated at a pH of 8 - 9. The water was decanted, and the precipitate will be prepared for measurements with the accelerator mass spectrometer of the ETH Zürich. Additionally at all the minicorer-stations ^{10}Be samples have been taken from the sediment surface.

6. POSTINSTALLATION WORK ON THE COMPUTER SYSTEM

H. Pfeiffenberger-Pertl (AWI)

Objectives

A new central computer system and two local area networks were installed aboard "Polarstern" in October 1990. Five VAX-VMS systems of different capabilities, configured as a cluster, replace one older VAX-VMS computer. The local area networks, using ethernet and localtalk cabling, provide the possibility to connect PCs and Workstations in all locations used for scientific purposes to each other, the central system and its resources, i.e. printers, plotters, etc. The most important objective of the work at sea was to observe this rather complex system under real conditions, in order to see

- if the concepts leading to its hardware and software configuration do work,
- how the system is utilized by the scientists, how its utility could be improved,
- which problems are encountered and how to fix them.

The result of this work should be a users manual for scientists and support personnel on board that provides advice on this specific installation in the most compact way possible.

Work at sea

The information necessary to meet the objectives was collected while giving advice or help to scientific users and support personnel. Some programming was necessary to fix problems, support routine operation of the system and to meet requests from scientists for access to specific data. The documentation most urgently needed was written.

Preliminary results

In general the VAX systems worked as planned. The most important task, the quasi-realtime data logging and processing on one of these machines, worked without problems. The disc and file services for PCs were made available on board in the same way as at the institute. Due to a much higher data transfer demand between VAX-, IBM-compatible and Macintosh-systems, yet unknown problems appeared. They could be solved by a file conversion utility and some documentation giving recipes. Observations on the use of publicly available PCs led to the conclusion that these will produce more work for the support personnel (or less utility to the scientists) than the VAX-systems, if

- their users are not very disciplined and
- they are managed as personal PCs

Further work has to be done on this problem.

7. WEATHER CONDITIONS

H. Erdmann, H. Köhler, H. Sonnabend (DWD)

At the beginning of the cruise the main cyclonic activity was located west of the Antarctic Peninsula. On 17 November, the steering cyclone moved slowly eastward with a minimum pressure below 960 hPa. Secondary lows passed the Drake Passage quickly and affected "Polarstern" with northwesterly winds Bft 8 and seas up to 5 m. South of the Polar Frontal Zone, visibility deteriorated due to northerly winds Bft 7. On 20 November, "Polarstern" reached Bellingshausen Station with northwesterly winds Bft 7 and snow showers. Due to catabatic influence, the wind increased up to Bft 9 near the station; in spite of the unfavourable weather conditions, helicopter service was possible. Due to the permanent influence of the wide-spread and stable low-pressure system with minimum pressure still below 960 hPa at the southwestern part of Bransfield Strait, wind turned from northwest to southeast Bft 5 on 21 November, while "Polarstern" left Bransfield Strait heading for the Weddell Sea. Snowfall coming up caused bad visibility later on and a decrease of air temperature down to -4°C . In the early evening, "Polarstern" approached an area densely covered with sea ice. During the following next four days, the ship operated within a low pressure area between the steering Weddell Sea cyclone and secondary lows in the north and northeast. Therefore, the pressure gradient as well as the winds were generally weak. Cold air mass advection gave rise to good visibility but was accompanied by some snow showers. On 26 and 27 November, the dominant cyclone remained stable over the northwestern part of the Weddell Sea and began to fill slowly. Therefore, "Polarstern" was affected by stronger cold air advection in the northwestern section accompanied by numerous polar cumulonimbus clouds and heavy snow showers.

On 28 November a new gale center developed in the western part of the Drake Passage and moved to the South Shetlands. On 29 November its frontal systems approached "Polarstern" near 66°S , 37°W while activity was decreasing. Therefore, wind turned northeasterly while decreasing to Bft 3 to 4. Occasionally occurring snowfall diminished visibility until the end of November. At the beginning of December, a flat high developed in the central Weddell Sea. Therefore, the wind was light and varying, the visibility very good and the clouds dissolved. A small-ranged but heavy cyclonic development north of "Polarstern's" operating area caused heavy snowfall on 3 December, which was accompanied by strong easterly winds up to force Bft 7. Therefore helicopter service was not possible on this day. During the night of 4 December, the cyclone moved south while decreasing and crossed the position of "Polarstern" to the west. The wind was backing to the north and caused low level warm air advection with rising dew point near 0°C . As a consequence, fog persisted for about 4 hours. On the same day, another but stronger cyclonic development evolved near South Georgia. This new storm center moved quickly southeast; with its rear and southerly gales up to force Bft 9 it affected "Polarstern" in the central Weddell Sea during 4 December. The maximum wind speed measured on board at the marine meteorological station was 55 knots within gusts. The chill temperature was -27°C and rendered open air work almost impossible. A small wedge within the advanced polar air gave rise to better weather conditions on 5 December but caused decreasing temperatures with morning minimum temperatures near -8°C . In the course of the next 3 days, weather remained fair, sometimes even

sunny with only light winds generally from west, due to the influence of a relatively high pressure center north of the ship's position. During the night hours, ice covering fog patches developed due to heat loss and disappeared when sun rose.

In the eastern section of a quasi-stationary but developing low, strong warm air advection mainly in the upper troposphere produced widespread snowfall also in the operation area of "Polarstern" near 67°S, 23°W on 9 December. During the next 24 hours, temperatures rose to 0°C and wind turned northerly with force up to Bft 7. From 10 to 14 December, a dynamic high developed above the northern part of the Antarctic continent with its center (1004 hPa) near 70°S, 05°W. Therefore, a strong inversion near 1000 m-level caused overcast stratocumuli with some snow showers and light winds. On 15 December "Polarstern" reached Kapp Norvegia in sunshine and light winds produced by the still stationary high near Neuschwabenland.

The weather conditions were still good when "Polarstern" was stationed at the shelf ice near Georg-von-Neumayer-Station for unloading. In spite of overcast sky with a ceiling near 800 feet and occasional "whiteout" conditions, helicopter service was not affected. When "Polarstern" left for Cape Town on 19 December, the synoptic situation changed. The dominant high at Neuschwabenland moved southwest while weakening and the low system east of South Georgia moved east. Therefore an easterly wind increased up to force Bft 6 accompanied with some snowfall and bad visibility.

On 20 December "Polarstern" left the closely packed sea ice near 68°S, 03°W. On the southern edge of a heavy steering low near 60°S, 05°W (958 hPa), which moved east-southeast very slowly, wind increased up to force Bft 7 to 8 while turning from east to southeast for some hours. Next day wind turned southwest while decreasing slowly. Wind seas and swell of about 3 m affected the voyage of "Polarstern" only little. On 24 December a new low developed northeast of South Georgia moving southeast slowly. Its frontal systems affected "Polarstern" on 25 December north of Bouvet Island with northerly gales Bft 8 to 9 turning northwest but decreasing slowly. Shortly before arrival in Cape Town, light winds, sunshine and warm temperatures were encountered.

8. ICE CONDITIONS

H.-J. Brosin, D. Zippel (IfMW)

Visual observations of the ice conditions were performed between 22 November and 20 December according to instructions given by the Glaciological Section of the Alfred-Wegener-Institute. Altogether 236 observations were realized together with an additional 70 observations on the distribution of algae in the ice.

The first iceberg was observed on 20 November at the position 62°12'S, 57°56'W, the last one on 23 December. The ice edge was crossed at 63°30'S, 51°30'W 150 km distant from the nearest shoreline on 22 November. It was passed again at the position 68°S, 04°W on 20 December. The shelf ice edge was reached for the first time at 71°07'S, 11°23'W on 15 December.

The portion of white ice amounted to 40 to 100% of the total ice cover. The thickness mostly varied between 0.5 and 1.5 m and was estimated to be up to

2 m in a few cases. A distinct increase of the size of ice floes to a diameter of more than 1 km was observed at the position 65°39'S, 39°W, an evident reduction of the floe size occurred only close to the end of the observations at 70°25'S, 13°25'W. The thickness of the snow cover on the ice varied between 20 and 50 cm. Marked melting effects at the bottom layers of ice floes were observed for the first time at the position 66°22'S, 29°32'W on 2 December. Local new ice formation (nilas, grey-white ice) were repeatedly observed after a larger decrease in air temperature.

A wide spread occurrence of icebergs was observed particularly at the western edge of the working area between 64° and 65°50'S, 49° and 40°W (up to 41 icebergs within the field of view) and at the southeastern edge from 69°15' to 70°30'S, 16°45' to 10°W (up to 52 icebergs seen simultaneously).

9. ACKNOWLEDGEMENTS

When we left "Polarstern" in Cape Town, we felt that we had had an extremely successful cruise and an enjoyable life on board. We are aware that master Jonas together with officers and crew took good care of our needs with a dedication and patience which guaranteed efficient work and good humour.

FAHRTABSCHNITT ANT IX/3

(Kapstadt - Kapstadt - 03.01.91 - 28.03.91)

1. EINLEITUNG
V. Smetacek, U. Bathmann (AWI)

Am 3. Januar um 8:30 verließ Polarstern den Hafen von Kapstadt mit einem ehrgeizigen Forschungsvorhaben im bislang unerforschten südwestlichen Weddellmeer. Aus Satellitenaufnahmen des vorangegangenen Sommers wußten wir, daß die Eisbedeckung dieses Gebietes sehr gering war, und hofften eine ähnliche Situation auch im Sommer 1991 anzutreffen. Da das Fahrtprogramm multi-disziplinäre Untersuchungen vorsah, hatten wir ein bunt zusammengesetztes Team von Wissenschaftlern an Bord, die sich der Biologie des mehrjährigen Meereises, der Physik, Chemie und Biologie der Wassersäule - unter besonderer Berücksichtigung der antarktischen Bodenwasserbildung - sowie Benthos- und Sedimentuntersuchungen widmen wollten. Eine zusätzliche Aufgabe der Fahrt war die Entsorgung der Antarktisstation 'Georg-von-Neumayer' und der ehemaligen DDR-Station 'Georg Forster'.

Auf der Anfahrt wurde ein kleines wissenschaftliches Programm durchgeführt mit der Aufnahme der Oberflächen- bzw. Tiefenbeschaffenheit der Sedimente durch Hydrosweep and Parasound und regelmäßige XBT-Würfe zur Wassermassencharakterisierung. Auch der Phytoplanktongehalt des Oberflächenwassers wurde erfaßt. Am 13. Januar übergaben wir dem Forschungsschiff "Agulhas", das am südlichen Rande des Packeisstreifens auf uns wartete, verabredungsgemäß Proviant und Ersatzteile und erreichten am Abend die Atka Bucht. Schneetreiben verhinderte die Löscharbeiten bis zum Nachmittag des 14. Januars, dann verlief alles planmäßig schnell. Am nächsten Morgen umrundeten wir Kapp Norvegia, bargen eine Verankerung mit Strommessern und nahmen eine CTD. Zwei Agassiz Trawls brachten zwar Mengen von Benthosorganismen an Deck, unter denen sich jedoch nicht die gesuchte interessante Schneckenart befand.

Unser Südkurs wurde am 15. Januar unterbrochen (Fig. 3.1), da wir 5 Personen retten mußten, die bei einem Inlandflug eines Südafrikanischen Hubschraubers auf einem 3000 m hohen Plateau 300 km landeinwärts von 'Sanae' notgelandet waren. Unsere 2 Polarhubschrauber führten die Rettungsaktion durch, in deren Verlauf alle Personen wohlbehalten geborgen wurden, aber ein Helikopter auf dem Plateau aufgrund von Turbinenschaden zurückgelassen werden mußte. Polarstern war mittlerweile wieder in die Atka Bucht zurückgekehrt und es wurden fieberhaft mehrere Alternativen zur Rettung der beiden gestrandeten Hubschrauber entwickelt und verworfen. Ein gewaltiger Sturm, der sich auf die Notlandestelle zubewegte, führte dann zu der Entscheidung, daß die Südafrikaner ein Schiff mit neuen Hubschraubern von Kapstadt losschickten, um ihren und auch unseren Hubschrauber zu bergen. Dies gelang einige Wochen später, nachdem zwei zusätzliche Hubschrauber in 'Sanae' eingetroffen waren. Die Rettungsaktion verschlang 3 Forschungstage. Die Fahrt nach Süden verlief dank der schmalen Kanäle im Meereis schnell, und wir erreichten Halley Bay am 20. Januar. Dort übernahmen wir von der "Bransfield" 170 Tonnen Treibstoff. Während des Bunkerns besuchten der Direktor und weitere verantwortliche Persönlichkeiten des "British Antarctic Survey" "Polarstern". Wenige Stunden später fuhren wir weiter Richtung

Süden und mußten bald erstmals wieder Eis brechen. Je weiter wir nach Süden drangen, desto weicher wurde die Eisdecke; sie bestand nun aus dünnen, übereinander gestapelten Schollen, deren Hohlräume mit Schnee und Plättcheneis gefüllt waren, in denen die Algen besonders üppig wucherten. Obendrauf lag eine dicke Schneeschicht. Dieses Schollen-Schneegemisch verhielt sich der Wucht des Schiffes gegenüber wie ein zäher Brei, der am Schiffsrumpf klebte und sich kaum beiseite schieben ließ. Als wir nur noch wenige hundert Meter pro Stunde schafften, beschlossen wir, liegen zu bleiben und auf eine Änderung der Windrichtung und Geschwindigkeit zu warten. Der Kapitän der "Bransfield" riet uns über Funk auch dazu: Er kannte diesen Eistyp und nannte ihn "porridge".

Vier Tage lang steckten wir in dem Eisbrei. Während dieser Zeit drifteten wir zusammen mit dem umgebenden Eis insgesamt 21 km nach Südwesten. Währenddessen entstand eine Forschungsstelle auf einer grossen, flachen Eisscholle in 3 km Entfernung vom Schiff, auf der Untereisprofile der Strömung, der Verteilung von Temperatur, Salzgehalt und biologischen Parametern genommen wurden. Eiskernproben ergänzten diese Untersuchungen, deren Teilnehmer regelmäßig im Helicoptershuttle ausgetauscht wurden. Währenddessen wurden vom Schiff die CTD, das Multinetz, eine Videokamera, die viele Stunden lang dicht über dem 330 m tiefen Boden hing, und mehrere Sedimententnahmegeräte eingesetzt, wobei letztere wegen der harten Sedimente keine Kerngewinne erbrachten.

Auf einem Erkundungsflug mit dem Hubschrauber entdeckten wir am 28. Januar einen Riß parallel zum Schelfeis, der mehrere Meter breit und viele Meilen lang war. Nach einigen Stunden Kampf im Eisbrei, währenddessen die Eisschollenstation abgebaut und per Hubschrauber zum Schiff transportiert wurde, erreichten wir den Riß und dampften erleichtert nach Süden. Nach nur 18 km war der Riß bereits wieder verschlossen und wir steckten genau so fest wie zuvor. Aufgrund der vorliegenden Eisinformationen aus Satellitenbildern, die die schwersten Eisverhältnisse seit 17 Jahren dokumentierten, beschlossen wir, das vorgesehene Programm abzubrechen und bei nächster Gelegenheit ein Ausweichprogramm in der Lazarev See zu beginnen. Da die Geologen für die Fahrt nach Norden Sedimentproben und Reliefaufzeichnungen vom Polarstern Sea Mount erbateten, Ozeanographen und Planktologen an küstensenkrechten Schnitten interessiert waren und die Eiskarten keine Küstenpolynya aufzeigten, wollten wir die schweren Packeisverhältnisse entlang der Küste meiden.

Diesmal sorgten jedoch sanfte, aber beständige Winde aus nordöstlicher Richtung dafür, daß das Eis uns noch stärker umklammerte als zuvor. Unsere Ausbruchsversuche endeten, als wir uns nur noch wenige 100 m pro Stunde durch den Eisbrei wühlen konnten. Auf einer nahen etwa 500 m großen und 1 - 2 m dicken Scholle fanden Ozeanographen und Biologen gute Arbeitsbedingungen. Am 30. Januar erschien ein Riß in der Eisdecke, der vom Hubschrauber aus gesichtet wurde. In fiebriger Eile wurde der "Biohausgarten" abgebaut, während "Polarstern" die Motoren anwarf. Nach einiger Mühe erreichten wir den Riß und konnten für einige Kilometer relativ zügig vorankommen, steckten aber bald wieder im Eisbrei fest. Diesesmal waren wir vom Brei vollständig umgeben, selbst die kleinen Schollen in der Umgebung waren für uns so gut wie unerreichbar. Während der Nacht nahm der Druck zu, und der hellbraune Brei wurde zwischen den kleinen Schollen zu unregel-

mäßigen krümeligen Mauern von 2 - 3 m Höhe emporgequetscht (Fig. 3.2). Der Brei war für herkömmliche Eisbohrgeräte schwer zu beproben, aber mit Hilfe der Geologen konnte ein Schwerelotkern von 1,5 m Länge gezogen werden.

Trotz ruhiger Bedingungen öffnete sich am 2. Februar ein 50 m breiter und ca. 10 Meilen langer, küstenparalleler Riß nur 1 km vom Schiff entfernt. Überraschend leicht hatten wir den Riß in nur einer Stunde erreicht. Im schnurgeraden Kanal brausten wir mit zeitweilig 12 Knoten voran. Nach 10 Meilen schneller Fahrt nahm die Eisdichte zu, obwohl die Kanalränder immer noch deutlich zu erkennen waren und darauf hindeuteten, daß sich der Kanal schon mehrfach geöffnet und geschlossen hatte. Wahrscheinlich fungierte das landfeste Packeis als Widerlager gegen das sich durch Tiden und den Strom getrieben das seewärtige Packeis nach Süden bewegte. Wir vermuteten, daß sich bei Flut der Kanal schloß und das komprimierte Porridge-Eis eine Durchfahrt vereitelte. Bei Ebbe verringerte sich der Pressdruck und so war es möglich, unter gelegentlichem Rammen nach ca. 8 Stunden offenes Wasser in der Halley Bucht zu erreichen.

Gleich nach unserer Ankunft wurden Agassiztrawl, Fotoschlitten und Mehrfachgreifer mit Erfolg eingesetzt, darauf folgten zwei Hols mit dem Bodenschleppnetz. Bevor wir zur "Polarsternkuppe" aufbrachen, meldete die "Bransfield", daß sie seit zwei Wochen im Eis am "Kap der Tränen" stecken geblieben war und beim Eisrammen ihre Treibstoffreserven aufgebraucht hatte, und so die 170 Tonnen, die sie uns zur Zeit der offenen Polynyas überlassen hatte, zurückverlangen mußte. Frühmorgens am 5. Februar trafen wir die "Bransfield" am Eisrand und übergaben den Treibstoff. Danach stießen wir ins Packeis Richtung Nord-Nordwest, um das Kap der Tränen zu meiden. Das Packeis des offenen Weddellmeeres war zwar dick, wies aber viele Risse auf, denen wir nach Möglichkeit folgten. Auf dem Weg zur "Polarsternkuppe" nahmen wir CTD-Proben und führten parallel dazu Eisarbeiten aus.

Vom 6. bis 10. Februar wurde die Polarsternkuppe mit Hydrosweep- und Parasound vermessen und durch den Einsatz der verschiedenster Geräte Sedimente bis zu 9 m Kernlänge entnommen. Nach Beendigung der geologischen Arbeiten führten wir einen hydrographischen Schnitt bis zum Schelf südlich von Kapp Norvegia durch. Auf diesem Transekt bargen wir mit Hilfe von Koppelnavigation vom Helikopter aus in fast geschlossener Eisdecke eine Strommesser-Verankerung, deren Bergung auf dem vorangegangenen Fahrtabschnitt unmöglich gewesen war. Argosbojen für Langzeitdriftstudien wurden entlang des gesamten Transektes auf geeigneten Eisschollen ausgebracht. Nach Ankunft auf dem Ostschelf wurden Fisch- und Benthosfänge mit entsprechenden Netzen durchgeführt.

Eine Aufgabe dieser Fahrt war der Personentransport von 'GvN' nach 'Forster', und nach Abschluß aller Arbeiten der Transport der Überwinterungsteams nach Kapstadt. Dies erforderte das mehrmalige Queren der südlichen Lazarev See - unser neues Forschungsgebiet - und so wurde ein komplizierter Arbeitsplan entwickelt, um die Alternativprogramme der einzelnen Arbeitsgruppen optimal aufeinander abzustimmen. Erschwerend bei der Planung kam dabei hinzu, daß wir mit den schweren Geräten, die mehrere Gruppen einsetzen mußten, nicht rund um die Uhr arbeiten konnten. Die Nachtstunden wurden demzufolge zum Dampfen verwendet, wobei

entstehende Sammellücken auf dem ersten Transekt entlang der Küste durch Probennahme während nachfolgender Routen geschlossen wurden.

Am 15. Februar erreichten wir GvN nachdem wir frühere Vermessungsarbeiten auf dem Explorer Escarpment ergänzt hatten. Am nächsten Morgen brachen wir mit Personal für die 'Georg-Forster' Station an Bord auf. Auf dem Weg zogen wir in 700 m Tiefe vor der Atka Bucht ein Grundschieppnetz und nahmen dann in 1° Intervallen Bodenproben für Geologen und Benthologen. Die Planktologen entdeckten eine immense Phytoplanktonblüte im Küstenstrom, die gemeinsam mit den Ozeanographen durch gelegentliche CTD-Einsätze beprobt wurde. Ein mittelschwerer Sturm verhinderte zeitweilig den Einsatz schweren Gerätes; die entsprechenden Proben wurden während der Rückfahrt genommen. In der Bucht vor Forster trafen wir am 21. Februar den schwedischen Frachter "Thuleland", der seit Jahren von Indien zur Versorgung der Stationen eingesetzt wird. Wegen des ungünstigen Flugwetters war ein Transfer unserer drei Passagiere nach Forster an dem Tag nicht möglich - unseren zweiten Hubschrauber hatten wir repariert während der Passage von 'Sanae' wieder an Bord nehmen können. Die Inder stimmten nach Anfrage zu, mit ihren Hubschraubern von der "Thuleland" unsere Passagiere zur indischen Station Matri zu fliegen, die nur 8 km von 'Forster' entfernt liegt. So konnten wir am gleichen Abend unser Forschungsprogramm mit einem Westschnitt fortsetzen.

Am 23. Februar begann der geplante Nordschnitt entlang des 6° Meridians. Eines Sturm mit Windstärken bis 11 zwang uns am 25. 2. zum Schelf zurückzukehren. Auf dem Weg nach Westen wurden auf dem Schelf die noch ausstehenden Stationen beprobt. Am 27. Februar begann dann der 0° Schnitt nach Norden, in dessen Verlauf alle Arbeitsgruppen zu Einsatz kamen. Nachdem am 3. März die Stationen abgearbeitet waren, fuhren wir auf dem 6° Meridian Richtung Süden, um auch diesen Schnitt zu vervollständigen. Zum Leidwesen der Ozeanographen konnten wir aus Zeitgründen diesen Schnitt im Norden nicht auf der Maudkuppe beginnen; die nördlichste Station lag über der größten Wassertiefe zwischen Kuppe und Küste, einer Wunschstation der Geochemiker. Im Anschluß an den Schnitt sollte am 7. März ein Bodenschleppnetz am Schelfhang gefahren werden, das dann auf Grund der unerwartet schweren Eisverhältnisse spontan auf dem Schelf in nur 300 m Tiefe eingesetzt und durch den steinigen Untergrund fast vollständig zerrissen wurde. Die Decks Mannschaft begann sofort mit der Reparatur, so daß das Netz später wieder eingesetzt werden konnte. Die Bucht vor der 'Forster' Station erreichten wir am frühen Morgen des 8. März.

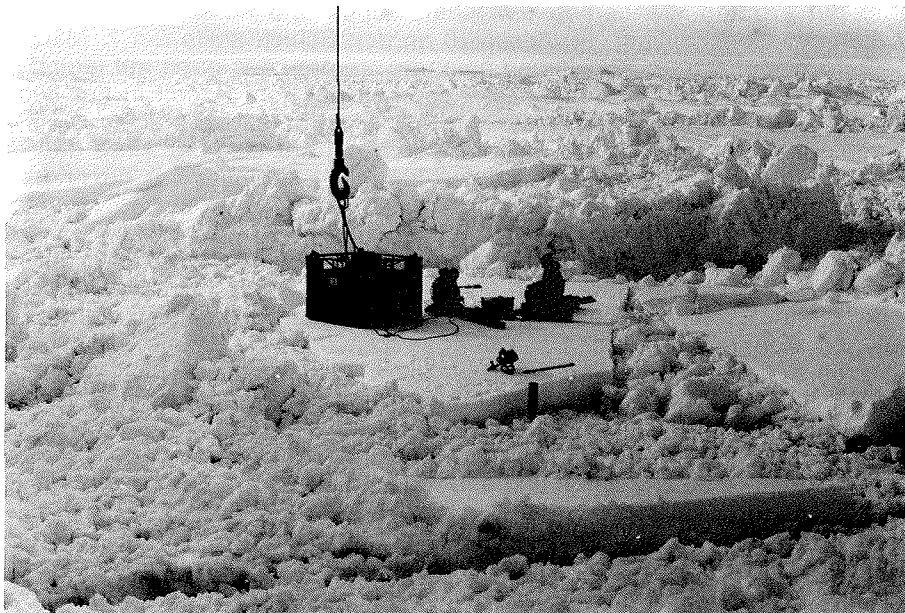
Da mit schlechtem Flugwetter zu rechnen war und der enge Zeitplan zur Eile drängte, baten wir die Sowjets in Novolazarevskaya, die Forster-Gruppe mit Hilfe eines Schlittenzuges an die Schelfeiskante zu transportieren. Im heftigen Schneesturm über schwieriges zerklüftetes Terrain gelang dies unseren Kollegen einen Tag schneller als erwartet. Erst gegen Nachmittag am 8.3. ließ der Wind nach, und die Übernahme der Personen sowie Be- und Entladung konnte beginnen. Abends feierten wir die Ankunft der Forsteraner, die die Vereinigung Deutschlands auf der Polarstation erlebt hatten, zusammen mit 7 sowjetischen und 4 indischen Gästen bis spät in die Nacht.

Am Morgen des 9.3. konnte bei gutem Flugwetter eine kleine Delegation von "Polarstern" die 3 Stationen in der Schirmacher-Oase besuchen. Mittlerweile absolvierte Polarstern Stationsarbeit in der Bucht. Am Nachmittag, nach

Beendigung der Probenahmen, setzten wir unsere Fahrt Richtung 'GvN' fort. Alle Stationslücken der vorangegangenen Transekte inklusive eines ausstehenden Bodenschleppnetzes wurden beprobt und wir erreichten die Atka Bucht in Morgenrauen des 14. März. Die sturmgepeitschte See hatte inzwischen die ehemals glatte Kante zu einem Sägezahnmuster zerfranst und ausgehöhlt; unterhalb der Wasserlinie schimmerte ein mehrere Meter breiter Eisvorsprung hervor. Die ehemals weiche Schneeschicht am Rande der Eiskante war durch Gischtfontänen zu einer harten, glasigen Gebirgslandschaft in Miniatur erstarrt; für die vorgesehenen Arbeiten war dies ein Alptraum. Doch Dank des Geschicks des Kapitäns und der Anstrengungen der Mannschaft waren die Arbeiten am Abend des 16.3. beendet, so daß wir mit den jetzt 68 Eingeschiffen an Bord Richtung Maudkuppe ablegten.

Nach dem Sedimentgewinn auf der Maudkuppe, bei der wir das einzige Gerät der Fahrt (ein Kolbenlot) verloren, beprobten die Geochemiker am 20. 3. eine 5200 m tiefe Wassersäule nördlich der Kuppe. Eine Sinkstoffallen- und Strommesserverankerung wurde als letzte Forschungsstat dieser Fahrt am 21. 3. ausgebracht. Am 28. März beendete "Polarstern" in Kapstadt eine ereignisreiche Fahrt, die dann doch erfolgreich und ohne ernsthafte Probleme abgelaufen ist. Das dies so war, haben wir dem Kapitän und der Besatzung zu verdanken. Sie haben ihre Aufgaben mit einem Höchstmaß an Professionalität erledigt. Stets gut gelaunten, haben sie uns mit ihrer Hilfsbereitschaft den wissenschaftlichen Erfolg ermöglicht.

Fig. 3.2. Aufgetürmte und mit Schnee bedeckte Eisschollen umschließen "Polarstern" und verhindern die Weiterfahrt für mehrere Wochen
Pressure rafted ice floes with snow cover surround the ship enforcing a stop in the porridge ice



1. INTRODUCTION

RV 'Polarstern' left Cape Town in the early morning of 3 January 1991 with the ambitious plan to conduct research in the previously unexplored southwestern corner of the Weddell Sea. Satellite images had revealed extensive retreat of the ice cover during previous summers; we were therefore hopeful that the same conditions would prevail during 1991 as well. The cruise programme comprised multidisciplinary studies of the biology of multiyear sea ice, the physics, chemistry and biology of the water column - in particular the processes leading to Antarctic Bottom Water formation - as well as the benthos and sediments of this area. Accordingly, the scientific contingent on board consisted of large groups representing oceanography, sea ice and pelagic biology, geochemistry, benthology, geodesy and geology. Relief of the stations 'Georg-von-Neumayer' (GvN) and 'Georg Forster' - the latter a station of the former GDR - were additional tasks.

The southward trip was uneventful except for XBT measurements and monitoring of surface phytoplankton that were carried out at regular intervals. We met RV 'Algulhas' on 13 January at the pack ice rim and transferred supplies and spare parts as per request. GvN station was reached the same evening. Poor visibility caused by snow drift prevented unloading of supplies and disembarkation of the overwintering crew until the afternoon of the 14th. These tasks were carried out rapidly following a sudden cessation of wind and, by evening of the same day, 'Polarstern' left Atka Bay on her way to the southern Weddell Sea (Fig. 3.1). On the morning of January 15 a current meter mooring was recovered off Kapp Norvegia followed by a CTD cast and two hauls with the Agassiz trawl. The latter were requested by the benthologists who had found an interesting snail in the area during an earlier cruise. Unfortunately, the particular species was not present amongst the masses of benthos deposited on the deck.

The same evening we interrupted the southward journey to rescue 5 persons on board a South African helicopter that was stranded at 3,000 m elevation 300 km inland from their station SANAE. Both our helicopters participated in the mission which succeeded in saving all personnel but at the cost of one of our helicopters which developed turbine trouble at the rescue site. In the meantime 'Polarstern' steamed back to Atka Bay. After considering various alternatives to salvage the 2 machines (the back-up machine at SANAE was also unable to fly) an approaching storm helped us decide that any attempts would be foolhardy given the means at our disposal. We therefore left the South Africans the task of salvaging both their's and our machines. This was accomplished some weeks later following arrival of 2 additional helicopters at SANAE. The rescue action cost us 3 days and we finally reached Halley Bay on 20 January.

The trip south was rapid as narrow channels in the ice could be used throughout. On arrival at Halley Bay we asked for and received 170 tonnes of fuel from RV 'Bransfield' that was anchored there. During fuel transfer 'Polarstern' was visited by the Director and senior staff of the British Antarctic Survey who had come to oversee construction of the new base. We headed south a few hours later and soon entered closed pack ice at the rim of Halley Bay. Transit was reasonably rapid during the first few hours but became slower as the pack ice became softer. After progress was reduced to a few

100 m/hr in spite of full power, we decided to stop and await better conditions as fuel consumption was very high. Satellite images indicated the presence of polynyas along the Filchner and Ronne ice shelves which we hoped to reach soon. The same images also showed an unusually extensive ice cover in the Weddell Sea for this time of the year. The captain of the 'Bransfield', who was acquainted with the ice type around us and which he aptly called "porridge ice", advised us to wait for wind which would loosen the ice cover and permit considerable saving of fuel.

The composition of the ice indicated that it had formed by rafting of relatively thin floes after they had acquired a thick snow cover. Layers of platelet ice were also involved. This rendered the ice watery and hence soft. The ice cover was pushed apart rather than broken by passage of the ship. As the ship's wake closed almost immediately, ramming was of little use. The porridge ice was coloured brown by algae. The time spent in waiting was utilised by various groups. A time station established on a large floe a few kms from the ship was serviced by helicopter. Biologists and oceanographers carried out measurements and collected samples. The CTD rosette and multinet were also deployed from the ship. Bait attached to the multigrab observed with its video camera was deployed just above the bottom for a night. Although no fish were attracted, the camera provided continuous information of the bottom fauna as the ship drifted with ideal speed. Four days were spent at this site in the ice during which the ship drifted 21 km to the southwest. Various attempts by the geologists to take sediment samples with the box and gravity corers were foiled by the hard substrate. Horizontal net hauls for the zoologists were, of course, out of the question. These 2 groups were understandably frustrated by our enforced sojourn in the porridge ice.

Helicopter reconnaissance revealed the presence of a canal some distance from the ship and on 26 January we decided to plough our way towards it. After several hours of struggle, we finally reached the canal and steamed southwestward for 18 km till the last traces of it vanished and progress in the porridge ice became extremely slow. Based on satellite pictures of the Weddell Sea which indicated that 1991 was the year with the most extensive summer ice cover recorded in the last 17 years, we decided to give up the plan to proceed southwestward and made an alternate plan to work in the Lazarev Sea between GvN and the Forster station. We also decided to take the first opportunity to steam north. For the return journey, the geologists requested samples from the Polarstern Sea Mount. This suggestion was seconded by the water column and ice groups who were interested in carrying out sections from the coastal current into the gyre and back. As satellite images indicated the absence of coastal polynyas and massive build up of ice just north of Halley Bay we thought it futile to attempt to steam north along the coast.

However, we were still stuck in the ice and awaiting the arrival of more favourable conditions. This time "Polarstern" lay alongside a 500 m diameter floe on which time stations were established. Oceanographic and biological measurements were conducted at opposite ends of the floe. On 30 January a canal again appeared on the horizon and the ship again attempted to reach it but after a few hours we were forced to give up. The ice around the ship was composed of small floes with 2 - 3 m high "walls" of soft ice that had been squeezed upward by horizontal pressure (Fig. 3.2).

Despite continuous calm conditions, the canal inexplicably appeared again some kms from the ship on 2 February and we at once made our way towards it. This time, unexpectedly, progress was reasonably fast and we reached it within an hour. The canal appeared as a perfectly straight lead in the ice which stretched to the horizon. This time we steamed north with full steam and made rapid progress. After some hours of steaming, the canal showed signs of closing again but we nevertheless managed to reach open water in Halley Bay by the evening of 2 February. Striations along the canal border indicated that it had previously opened and closed along the same seam. We assume that this was due to tidal action whereby the landward ice pack functioned as stationary fast ice and the seaward pack was transported southward more rapidly by the currents. We assume that at high tide the canal closed and the porridge ice was compressed rendering progress very difficult. Low tide resulted in slackening of pressure, not necessarily visible in the immediate surroundings of the ship, and opening of the canal. Under these conditions, progress by the ship was reasonably fast. Apparently, future navigation in porridge ice should be attempted only in conjunction with the tides.

Immediately after arrival in Halley Bay, the zoology programme was started with Agassiz and bottom trawls combined with photosledge and multibox corer. On 4 February, the northward transect was commenced with CTD casts in Halley Bay. RV 'Bransfield' had left Halley Bay some days before but was unable to make her way north of the Cape of Tears. She had used up much fuel during various futile attempts and now requested back the 170 tonnes she had lent us earlier. We accordingly arranged a rendezvous and returned the fuel on the morning of 5 February on our way north. Passage through the ice was easier than expected. Although the floes were thick, we were able to use leads most of the time. Stations were located next to suitable ice floes so that the ice biologists could take samples during the CTD casts.

The Polarstern Seamount was reached on 6 February and sediment samples were taken with various gear around its top and its eastern flank till 10 February. We then proceeded with the eastward hydrography/planktology transect to the shelf and were able to recover a current meter mooring (in spite of closed ice cover) on the way. Argos buoys had been deployed on suitable ice floes during both the northward as well as eastward transects. Unfortunately, it was difficult to deploy these in a set pattern as suitable ice floes were not always available. On arrival at the eastern shelf, fish and benthos were sampled with Agassiz and bottom trawls accompanied by various other gear.

One of our tasks was to transfer personnel from GvN to Forster station and then collect overwintering crews from both stations for the return journey to Cape Town. Because the Lazarev Sea was now our main research area, we devised a complicated plan to make optimal use of the restricted time at our disposal. This entailed a brief visit to GvN followed by an even shorter stopover at Forster to disembark personnel. We then had a few weeks time for research after which we intended picking up the crew from Forster and then working our way back to GvN to collect the crew from there. On the way to Cape Town we intended taking sediment samples from Maud Rise followed by water samples for the geochemists from deep water north of the Rise. As it was not possible to work round the clock with heavy gear (trawls, corers and grabs), we used the nights for steaming; the gaps left in the transects were to be filled on subsequent to and fro passages.

On 15 February we arrived at the GvN station after making a detour over the Explorer Escarpment to complement earlier measurements by means of Hydrosweep and Parasound profiles. We left the next morning with personnel on board for the Georg Forster station. Our intention was to collect samples at fixed intervals on the shelf and slope for the geologists and zoologists. Transects along the 6°E and Greenwich meridians to Maud Rise and back had been requested by geologists and water column scientists. A bottom trawl taken at 700 m depth off the Atka Bay commenced the transect along the shelf of the Lazarev Sea. We worked our way east taking geology and benthology samples at 1° intervals. As the planktologists had discovered an intense phytoplankton bloom on the shelf, the bottom work was supplemented with occasional CTD casts. A short storm interrupted deployment of heavy gear leaving behind additional gaps to be filled subsequently. We reached the bay in front of Forster Station on 21 February. Poor visibility prevented our helicopters (we had collected the "lost" helicopter from SANAE when passing the station) from transporting our personnel to Forster station which lies about 80 km inland. As the Swedish freighter "Thuleland", chartered by the Indian Antarctic expedition, was lying in the bay, we requested the Indians to transport our personnel to Forster at the next occasion, which they agreed to do. This saved us time and we returned westward the same evening.

We began the transect northward along the 6° meridian on 23 February. We had completed the stations on the shelf and slope and were working in the open sea when a severe storm forced us on 25 February to retreat to the shelf. We now worked our way westward along the shelf, filling gaps left from the previous passage, with the intention of commencing the 0° transect which we started on 27 February. This transect, in which all disciplines participated, was completed on 3 March following which we cut across eastward to the 6° meridian and continued working southward to complete the transect interrupted by the storm. Lack of time prevented us from starting the transect at Maud Rise, much to the disappointment of the oceanographers. Instead, we started at the deepest point between the Rise and the coast where samples were collected by the geochemists. The transect was completed on 7 March; our next intention was to take a bottom trawl on the shelf slope but extensive pack ice which had unexpectedly appeared from the east prevented this undertaking. A spontaneous decision to trawl in an ice-free patch over a depth of only 300 m resulted in a poor catch and considerable damage to the net. The crew immediately started repairing the net so that it could be used again later on, but much further to the west, which was still ice free. We then left for the bay in front of Forster station where we arrived early in the morning of 8 March. Because of our tight schedule, we were not willing to risk waiting for good flight conditions to relieve the Forster crew. We therefore requested the Soviet station Novolazarevskaya to contribute vehicles to transport the men to the coast. The request was spontaneously granted and a convoy of heavy vehicles negotiated the difficult terrain with great success. On arrival of 'Polarstern', a strong wind reduced visibility to near-zero and it was not possible to position the ship to permit embarkation of the men waiting on the ice. The wind slackened by afternoon, permitting transfer of personnel and equipment. That evening, the 10 Forster overwinterers who had spent the period of German unification in the station, were welcomed on board 'Polarstern' with a party in their honour. Soviet and Indian guests were also present.

The morning of 9 March dawned clear so a small delegation from Polarstern set off by helicopter to visit the German, Soviet and Indian stations. During this time, station work was carried out in the bay. By afternoon, the station work was completed and 'Polarstern' commenced her final trip west to GvN. All the gaps left during previous passages along the shelf, including a deep bottom trawl, were successfully closed and we arrived at Atka Bay on the morning of 14 March. The last storm had turned the shelf ice into a jagged, saw-toothed monstrosity and this, combined with a strong swell, made it very difficult to position the ship and carry out loading operations. Thanks to the skill of the captain and hard work by the crews of 'Polarstern' and GvN the operation was completed in time and we left Atka Bay headed for Maud Rise on the evening of 16 March. We now had 68 persons in addition to the crew on board.

After collecting sediment cores on the Rise, during which we lost the only gear of the entire cruise (a piston corer), we carried out a deep water geochemistry station north of the rise on 20 March and deployed a current meter and sediment trap mooring on the 21st further north. We arrived in Cape Town on 28 March, not much the worse for wear in spite of a difficult cruise. The fact that all the groups on board managed to collect interesting data and sample sets even though we suffered a major setback at the outset of the cruise is due to the dedication and professionalise of the captain and crew of 'Polarstern'. We take this opportunity to express our heartfelt thanks for the trouble they took to satisfy our demands.

2. WEATHER CONDITIONS

H.-A. Pols (DWD)

The voyage commenced under high pressure influence and the ship reached the zone of westerly winds in three days. Cyclones between 45° and 65°S normally move eastwards. At this time an intense low pressure system between Bouvet-Island, Marion-Island and Antarctica was the dominating feature. To the rear of this system strong southwesterly winds caused a corresponding high swell. We encountered wind forces of Bft. 7 to 8, sometimes also 9. On 12 January the ship reached the border of drifting sea-ice north of the SANAE Station. The above mentioned cyclone moved eastward and a ridge of high pressure formed over the northeastern Weddell Sea. On 13 January RV 'Polarstern' entered Atka Bay. The following day a frontal system crossed the eastern Weddell Sea with snowfall from low stratus clouds and east to northeasterly winds with speeds around force Bft. 8.

While marked low pressure systems moved across the Drake Passage to the southern Atlantic, only small-scale lows developed over the southeastern Weddell Sea. Here light to moderate, dry and cold, easterly winds were experienced off the shelf-ice until the middle of February. During this time closed cloud cover with low ceiling often caused marginal flight conditions. Wind force bft. 5 to 6 was the maximum wind speed.

Because an improvement of ice conditions by favorable weather conditions could not be expected, the plan to reach the southwesterly edge of the Weddell Sea was given up. So the ship headed north and reached open water on 2 February. The plans were changed and research was now concentrated first on a region west of 'Vestkapp' in the vicinity of Polarstern Seamount (71.25°S/24.5°W) and later in the 'Lazarev Sea' northeast of 'SANAE'.

On arrival in the Lazarev Sea, the weather situation was dominated by a slowly moving intense low pressure system. Other lows coming from the west were included. One wave depression had surrounded a gale center and moved from east to west along the coast of the Lazarev Sea. On the way eastward wind forces of Bft. 9 to 10 were encountered in this depression. In the shelter of the shelf ice and with a swell stabilized by drifting ice, research could be carried out. On 21 February RV 'Polarstern' reached the shelf ice barrier below the Georg-Forster Station. The following day the intense depression moved eastward and weakened.

Research was next carried out along 6°E. Another low tracked eastward and crossed the north of the Weddell Sea and intensified. Ahead of this intense cyclone a strong east to northeasterly flow developed. During the afternoon of 25 February research had to be interrupted because of gales and high seas. The storm center only moved slowly from the northern Weddell Sea to the east and other lows coming from the west were included. For several days north-east to easterly gales persisted. Until early March this depression was the dominant feature, but weakened later. During this time research could be carried out along the Greenwich Meridian, from 3 March onward the investigations interrupted along the 6°E meridian could be continued after the advent of relatively calm conditions.

On 8 March the ship reached the shelf ice border below the Forster Station to pick up 10 overwinterers. At that time mean values of windspeed between Bft. 8 and 10 with gusts up to Bft. 11 and drifting snow dominated the weather situation.

Some small-scale lows had developed along the coast of the Lazarev Sea. Above the relatively warm water, scattered snow showers developed in the unstable layers of the lower atmosphere and intensified those small-scale lows, which showed several similarities to so called 'Polar Lows' observed in the northern hemisphere. The following day fair weather conditions returned, to the relief of many ANT IX/3 participants.

On the way back to GvN the ship entered the influence of an eastward moving intense low, which moved to the Lazarev Sea and weakened. To the rear of the system a ridge of high pressure formed over the northeastern Weddell Sea. The ship, therefore, could start its journey from GvN back to Cape Town in conditions of light to moderate northwesterly winds. On 21 March a depression crossed the path of RV 'Polarstern'. Ahead of this low, northeast to easterly wind intensified and reached gale force during the night. A marked pressure rise with only moderate to fresh northwesterly winds prevailed to the rear of that low, so the work at the last station was not disturbed. Afterwards the RV 'Polarstern' made her way in front of another east-moving low, but was affected by the belt of strong winds associated with that low only for a short time.

3. ICE OBSERVATIONS IN THE EASTERN WEDDELL AND LAZAREV SEAS, JANUARY-MARCH 1991

V. Lukin, A. Provorkin (AARI)

Introduction

The third leg of the ninth research cruise of RV *Polarstern* to Antarctica (ANT IX/3) was planned as a broad-based, interdisciplinary study of the hitherto unexplored southwestern Weddell Sea continental shelf and margin. The successful execution of this project depended upon favourable ice conditions in this area.

The traditional shipping routes to the southern Weddell Sea have generally approached the area between 10° and 30°W, and utilised the strip of relatively open water along the eastern coast. The critical factor for shipping in the lead is an ice cape in longitude 41°W where the Soviet station Druzhnaya-2 was located. During the summer, coastal polynyas tend to be quasi-stationary along the Ronne Ice Shelf, Luitpold Coast and Caird Coast. According to the data of T. Vinje of the Norsk Polarinstitut, the probability of free access during January and February is close to 100% in the region of Kapp Norvegia, declining to about 70-80% along the Filchner Ice Shelf, although a higher probability of access in the latter area, 85%, occurs in the second half of February.

According to the data of K. Strübing, the pack ice concentration along the Antarctic coastline between 10° and 30°W has varied from 0 to 6 tenths in the period from late December to the end of February. Similar conditions are met between 30° and 40°W until the second part of February. From this time onwards, the ice concentration may increase to 8 tenths, reducing the accessibility of these waters, at least temporarily. To the west of 41°W, the ice concentration rises. Naturally, the pack ice not only has seasonal fluctuations, but varies from year to year. However, the shore polynyas are a constant feature of ice conditions in the Weddell Sea during the summer.

G. Kukla and J. Gavin analysed the changes in ice concentration in the Weddell Sea from 1967 - 1977, using satellite data. They found a seemingly periodic fluctuation in the ice cover lasting about eight years. However, this information is only relevant for climatic research. For navigation it is more important to use synoptic time change data. Ice concentrations may fluctuate considerably in response to large changes in atmospheric conditions, such as the passage of depressions, atmospheric fronts, or by remaining for a long period under areas of high atmospheric pressure. Yet there is a big difference for navigators between concentrations of 8-10 tenths first year ice and multi-year ice. The first serious investigation of multi-year ice in the Weddell Sea was carried out by an American expedition from the Cold Regions Research and Engineering Laboratory (CRREL) in February and March 1980 on board USCGC *Polar Sea*. These studies showed that the physical properties of first-year and multi-year ice in the Weddell Sea have considerable differences from Arctic sea ice. This is associated with different hydrophysical behaviour of the upper levels of the ice floes, the meteorological regime and intense biological activity in the Weddell Sea pack ice.

In February 1992 the USSR and USA will organise the first scientific drifting station in the southwestern Weddell Sea. Therefore sea ice investigations in

this area (ice concentration for navigation and the physical properties of multi-year ice floes and their suitability for establishing a drifting station) were of special interest. In the beginning, this research planned by the ice group tallied with the main objectives of other groups on board 'Polarstern'. However, as the route changed from that planned, the objectives of the ice group also had to change.

Sources of ice information

Normally, the Antarctic cruises of 'Polarstern' receive ice information in the form of ice charts from the Joint Ice Center NAVY/NOAA (USA) and the German Hydrographic Institute (FRG). In addition, the ship's meteorological observatory is equipped with a satellite image receiver (type: Dornier, Wefax), which enabled us to receive images of the US (NOAA) and Soviet (Meteor) satellites. If necessary, the ship can also receive facsimile ice charts from the Soviet Antarctic stations Bellingshausen and Molodezhnaya. However, ordinary ice information from the USA, FRG and Soviet Antarctic stations is plotted at a small scale (about 1:20,000,000) and shows only the broad-scale characteristics, whilst the transfer of this ice information takes as much as 7-10 days. In addition to this normal supply of ice information, the Canadian Microwave Group of York University, Ottawa River, twice a week sent to Polarstern ice and wind charts from SSM/1 data during the period of ANT IX/3. These data provide better resolution than small-scale ice charts, as each data-point on the SSM-1 chart represents a satellite measurement on a grid spacing of 25x25 km. However, this chart does not give any information within 45 km of land, and only shows a large space for ice-free areas measuring more than 25x25 km. These constraints limit the value of using SSM-1 data for ice navigation. Thus, the most meaningful data for ice navigation in Antarctic waters comes from a combined analysis of data received from satellites and direct shipboard observations. The use of satellite data, together with ice observations from a helicopter, has proved to be a particularly effective tool in providing the best route for a ship-borne expedition in Antarctic waters. However, the effective use of satellite data is only possible if a skilled ice expert is on board.

Ice observations

During Polarstern cruise ANT IX/3, ice observations consisted of the analysis of satellite data and visual observations from the ship. Satellite data provides the most important and most detailed information concerning ice cover in the Antarctic seas. For research on Antarctic sea ice the most widely used satellites are the US NOAA and Soviet Meteor instruments. Typical data provided by satellites that is useful in sea ice research is summarised in Tab. 3.1. It demonstrates that during the summer season the best ice information comes from the Soviet Meteor satellites. The American SSM-1 has considerable possibilities for future research, but we cannot yet comment about the precision of measurement by this method. Large specially designed experiments are necessary if these aims are to be achieved. The resolution of the image from Meteor permits polynyas, single vast ice floes, very big icebergs, ice concentrations and the age of the ice to be determined. The satellite image receiver "Dornier, Wefax" has a program for positioning latitudes and longitudes only for NOAA satellite pictures. This limited the use of the image from Meteor on board Polarstern. However, we have defined a scale on different parts of the satellite picture in association with the hydrography group. H. Hinze derived by computer a special chart of the Weddell Sea at a

scale of 1:8,800,000 (polar projection at latitude 70°S), which approximately corresponds to the Meteor-3 image. Throughout the period of receipt of Meteor images (6 January to 20 March 1991) one of the Soviet ice experts defined the ice conditions as revealed by the images. The ice group drew seventeen ice charts of the Weddell Sea and twelve supplementary ice charts of the eastern Weddell Sea and the Lazarev Sea during this period. An example of such ice charts is given in Fig. 3.3.

Visual observations were made from the ship throughout the period that Polarstern was having to navigate through ice. The ice experts made the following observations every hour, or when the ice conditions changed: ice type, concentration, floe size, hummocking, thickness of snow and ice. Every 20 nautical miles the ship was underway, observations about icebergs (visual and radar), including the number, type, mean distance between single icebergs and size, were made.

The Soviet ice group furthermore made the following additional observations every four hours for German colleagues:

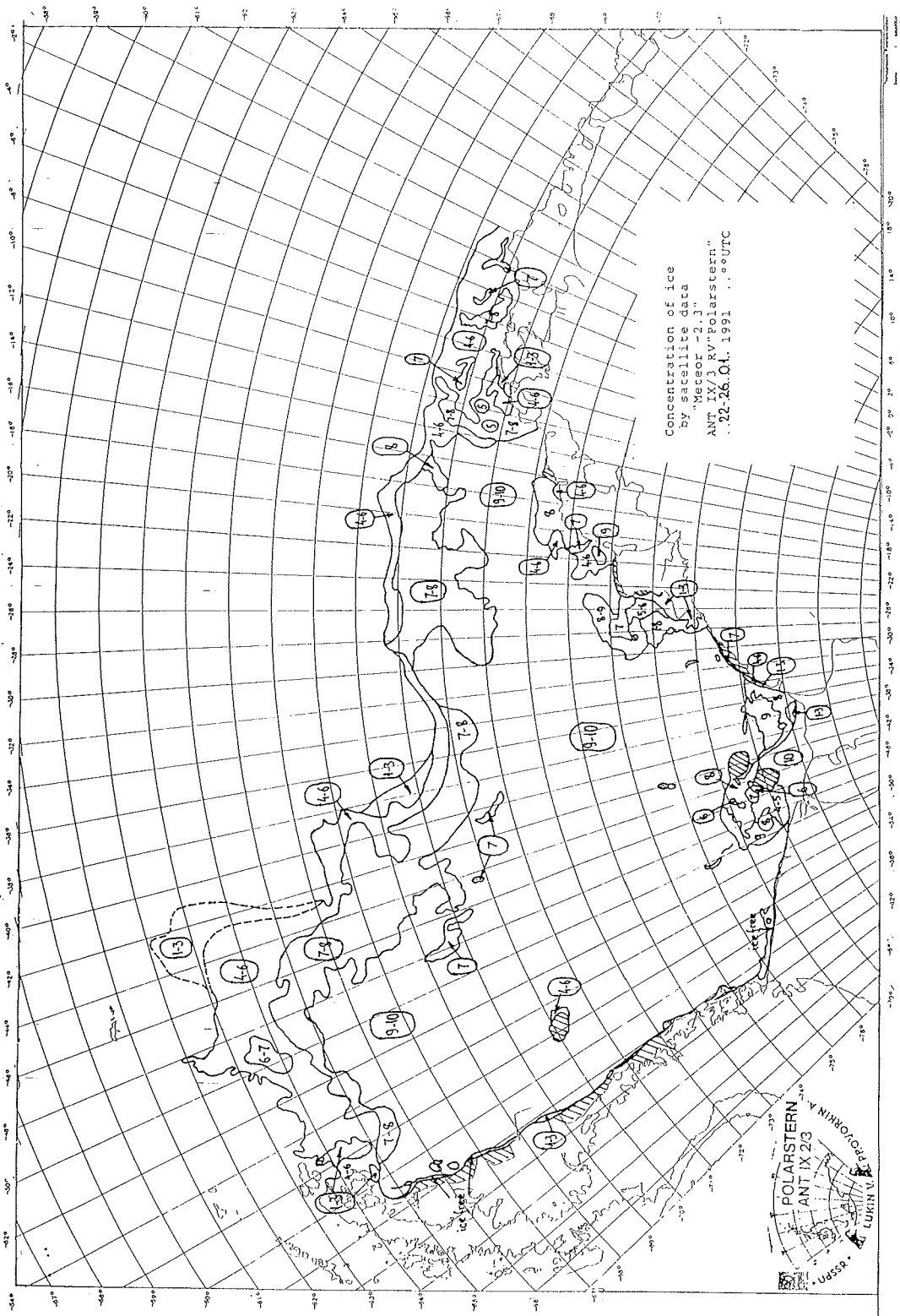
- (1) Weather etc.: air temperature, air pressure, water temperature, wind velocity and direction, visibility.
- (2) Sea ice conditions: ice type, concentration, thickness, snow thickness, floe size, rifting and ridging.
- (3) Presence of krill, brown ice and brown water.
- (4) Additional iceberg information (radar and visual observations): distance and bearings to iceberg.

The main results from shipboard visual observations are shown in Tab. 2 and 3. Every single area where ice conditions were recorded (denoted by a number in the tables) is defined by a change in the ice concentration (Tab. 2). The characteristics of ice floes are defined for each of these areas accordingly. Note that the numbers in each table correspond with one another.

Tab. 3.1. Characteristics of data for ice observations according to satellite type.
IR = infrared

Data	Name of satellite			
	Meteor-2	Meteor-3	NOAA	F-8
Sensor	TV	TV, IR	TV, IR	SSM-1
Width in km of observed area	2400	3000	3000	?
Resolution (km)	2-2.5	2.5-3	4	25
Influence of clouds	Yes	Yes	Yes	No
Precision in defining ice concentration	± 10%	± 10%	± 20%	± 1%
Definition of age of sea ice	To first-year ice	To first-year ice	To first-year ice	First-year and old ice
Contrast between snow, ice and open water in summer	Maximum	Max./Min.	Max./Min.	?

Fig. 3.3. Concentration of ice by satellite data "Meteor - 2.3" ANT IX/3 RV "Polarstern" 22.-26.01.1991



No.	Total ice concn.	First year ice			Young ice		From: Grease ice	To:		Date		
		Thick	Medium	Thin (white)	Nilas	Pancake ice		Lat.°S	Long.°		Lat.°S	Long.°
38	ice free	-	-	-	-	-	-	73°57.0'	22°59.0'w	74°09.2'	24°59.1'w	19.01
39	50-60	40	10-20	-	-	-	-	74°09.2'	24°59.1'w	74°15.6'	26°02.2'w	19.01
40	90-100	80	10-20	-	-	-	-	74°15.6'	26°02.2'w	74°27.3'	25°49.3'w	19-20.01
41	70-80	60	10-20	-	-	-	-	74°27.3'	25°49.3'w	74°30.0'	25°48.1'w	20.01
42	20-30	20	0-10	-	-	-	-	74°30.0'	25°48.1'w	74°34.3'	25°48.2'w	20.01
43	0-10	0-10	-	-	-	-	-	74°34.3'	25°48.2'w	74°43.0'	25°38.2'w	20.01
44	40-50	30	10-20	-	-	-	-	74°43.0'	25°38.2'w	74°51.1'	25°24.0'w	20.01
45	ice free	-	-	-	-	-	-	74°51.1'	25°24.0'w	75°26.0'	27°03.2'w	20.01
46	50-60	50	0-10	-	-	-	-	75°26.0'	27°23.2'w	75°38.8'	27°15.0'w	20.01
47	10-20	10-20	-	-	-	-	-	75°38.8'	27°15.0'w	75°50.7'	27°34.6'w	20.01
48	70-80	50-60	20	-	-	-	-	75°50.7'	27°34.6'w	75°52.5'	27°41.5'w	20.01
49	20-40	20-30	0-10	-	-	-	-	75°52.5'	27°41.5'w	76°06.8'	28°47.2'w	20.01
50	90-100	60	30-40	-	-	-	-	76°06.8'	28°47.2'w	76°20.0'	29°50.3'w	20-21.01
51	100	80	20	-	-	-	-	76°20.0'	29°50.3'w	76°28.4'	30°47.5'w	21-26.01 IS-1
52	100	80	20	-	-	-	-	76°28.4'	30°47.5'w	76°36.4'	31°18.0'w	26-28.01 IS-2
53	100	80	20	-	-	-	-	76°36.4'	31°18.0'w	76°36.7'	31°22.6'w	28-30.01
54	100	80	20	-	-	-	-	76°36.7'	31°22.6'w	75°08.2'	28°36.3'w	30.01-02.02
55	ice free	-	-	-	-	-	-	75°08.2'	28°36.3'w	74°29.9'	26°18.2'w	02-05.02
56	80	40	40	-	-	-	-	74°29.9'	26°18.2'w	74°26.2'	26°38.0'w	05.02
57	90	50	40	-	-	-	-	74°26.2'	26°38.0'w	74°16.4'	26°26.6'w	05.02
58	90-100	50-70	30-50	-	-	-	-	76°16.4'	26°26.6'w	72°32.0'	25°29.8'w	05-07.02
59	90-100	10-30	60	10-30	-	-	-	72°32.0'	25°29.8'w	72°12.5'	25°11.0'w	07.02
60	90	-	50	40	-	-	-	72°12.5'	25°11.0'w	71°44.0'	24°48.0'w	07-08.02
61	90-100	-	40	40	10-20	-	-	71°44.0'	24°48.0'w	71°24.9'	24°46.2'w	08.02
62	70-80	-	30	30-40	10-20	-	-	71°24.9'	24°46.2'w	70°59.7'	25°21.0'w	08-09.02
63	90	-	30	40	20	-	-	70°59.7'	25°21.0'w	71°08.2'	25°17.2'w	09.02
64	70-80	-	30	30	10-20	-	-	71°08.2'	25°17.2'w	71°24.9'	24°46.5'w	09.02
65	70-80	10	30	20-30	10-20	-	-	71°24.9'	24°46.5'w	71°29.8'	24°03.0'w	09-10.02
66	80-90	10	30	30-40	10-20	-	-	71°29.8'	24°03.0'w	71°21.5'	24°14.0'w	10.02
67	90	-	40	40	10	-	-	71°21.5'	24°14.0'w	71°18.3'	23°06.2'w	10-11.02
68	90-100	0-10	40	40	10-20	-	-	71°18.3'	23°06.2'w	71°10.5'	21°27.1'w	11.02
69	90-100	-	50-70	10-30	0-10	-	-	71°10.5'	21°27.1'w	71°15.0'	20°20.7'w	11-12.02
70	90-100	10	60-70	10-20	10-20	-	-	71°15.0'	20°22.7'w	71°27.8'	19°44.2'w	12.02
71	90-100	-	70	10	10-20	-	-	71°27.8'	19°44.2'w	72°04.2'	17°41.0'w	12-13.02
72	90-100	10	60	10	10-20	-	-	72°04.2'	17°41.0'w	72°11.0'	17°17.5'w	13.02
73	80-100	-	30-40	50	0-20	-	-	72°11.0'	17°17.5'w	72°21.9'	16°51.6'w	13.02
74	90	-	-	-	90	-	-	72°21.9'	16°51.6'w	72°21.1'	16°33.5'w	13.02
75	ice free	-	-	-	-	-	-	72°21.1'	16°33.5'w	72°08.0'	16°27.7'w	13.02
76	10-30	10-30	-	-	-	-	-	72°08.0'	16°27.7'w	72°07.1'	16°23.9'w	13.02
77	50	30	-	-	20	-	-	72°07.1'	16°23.9'w	72°06.2'	16°24.1'w	13.02
78	100	-	-	-	100	-	-	72°06.2'	16°24.1'w	71°56.0'	15°51.5'w	13.02

ANT IX/3

112

No.	Total ice concn.	First year ice			Young ice			From:		To:		Date
		Thick	Medium	Thin (white)	Nilas	Pancake ice	Grease ice	Lat.°S	Long.°	Lat.°S	Long.°	
79	60-70	30	30	-	0-10	-	-	71°56.0'	15°51.5'w	71°55.5'	15°37.4'w	13.02
80	90	40-50	30-40	-	10	-	-	71°55.5'	15°37.4'w	71°31.2'	14°43.2'w	13-14.02
81	30	20	10	-	-	-	-	71°31.2'	14°43.2'w	71°26.0'	14°29.0'w	14.02
82	40-60	30	10-30	-	-	-	-	71°26.0'	14°29.0'w	71°06.0'	13°47.1'w	14.02
83	30-40	20	10-20	-	-	-	-	71°06.0'	13°47.1'w	70°54.2'	13°22.3'w	14.02
84	50-60	20-30	20-30	-	-	-	-	70°54.2'	13°22.3'w	70°37.3'	12°44.6'w	14.02
85	20-40	10-20	10-20	-	-	-	-	70°37.3'	12°44.6'w	70°07.2'	12°37.6'w	14.02
86	10-20	0-10	10	-	-	-	-	70°07.2'	12°37.6'w	69°25.5'	11°18.7'w	14.02
87	40-50	20	20-30	-	-	-	-	69°25.5'	11°18.7'w	70°34.2'	09°30.5'w	14-15.02
88	30	10	20	-	-	-	-	70°34.2'	09°30.5'w	70°34.0'	08°07.1'w	15.02 GvN
89	ice free	-	-	-	-	-	-	70°34.0'	08°07.1'w	70°33.4'	08°06.9'w	15.02
90	80-90	80	-	-	0-10	-	-	70°33.4'	08°06.9'w	70°31.0'	07°57.0'w	15-16.02
91	10-20	10	0-10	-	-	-	-	70°31.0'	07°57.0'w	70°29.0'	07°42.0'w	16.02
92	ice free	-	-	-	-	-	-	70°29.0'	07°42.0'w	69°59.8'	05°38.2'E	16-20.02
93	50-60	30	20-30	-	-	-	-	69°59.8'	05°38.2'E	69°59.2'	05°40.5'E	20.02
94	100	80	20	-	-	-	-	69°59.2'	05°40.5'E	69°58.6'	05°56.7'E	20.02
95	50-60	40	10-20	-	-	-	-	69°58.6'	05°56.7'E	69°53.4'	05°51.1'E	20.02
96	40-50	30	10-20	-	-	-	-	69°53.4'	05°51.1'E	69°58.2'	06°03.8'E	20.02
97	90-100	50	40-50	-	-	-	-	69°58.2'	06°03.8'E	69°57.3'	06°16.8'E	20.02
98	50-60	30	20-30	-	-	-	-	69°57.3'	06°16.8'E	69°59.0'	06°29.3'E	20.02
99	90-100	50	40-50	-	-	-	-	69°59.0'	06°29.3'E	70°02.2'	06°39.8'E	20.02
100	ice free	-	-	-	-	-	-	70°02.2'	06°39.8'E	69°59.4'	07°11.0'E	20.02
101	90-100	50	40-50	-	-	-	-	69°59.4'	07°11.0'E	69°58.9'	07°12.0'E	20.02
102	ice free	-	-	-	-	-	-	69°58.9'	07°12.0'E	69°46.2'	09°29.4'E	20-21.02
103	40-50	30	10-20	-	-	-	-	69°46.2'	09°29.4'E	69°44.6'	10°31.5'E	21.02
104	ice free	-	-	-	-	-	-	69°44.6'	10°31.5'E	69°38.7'	11°32.8'E	21.02
105	20-30	20	0-10	-	-	-	-	69°38.7'	11°32.8'E	69°39.0'	11°05.4'E	21.02
106	60	40	20	-	-	-	-	69°39.0'	11°05.4'E	68°38.9'	11°01.6'E	21.02
107	20-30	20	0-10	-	-	-	-	69°38.9'	11°01.6'E	69°39.0'	10°07.8'E	21.02
108	40	30	10	-	-	-	-	69°39.0'	10°07.8'E	69°46.0'	09°47.6'E	21-22.02
109	80	50	30	-	-	-	-	69°46.0'	09°47.6'E	69°47.0'	09°31.1'E	22.02
110	ice free	-	-	-	-	-	-	69°47.0'	09°31.1'E	69°52.7'	08°14.2'E	22.02
111	50	30	20	-	-	-	-	69°52.7'	08°14.2'E	69°41.7'	06°36.6'E	22-23.02
112	30-40	20	10-20	-	-	-	-	69°41.7'	06°36.6'E	69°48.5'	06°17.7'E	23.02
113	10-20	10	0-10	-	-	-	-	69°48.5'	06°17.7'E	69°57.2'	06°18.9'E	23.02
114	ice free	-	-	-	-	-	-	69°57.2'	06°18.9'E	69°53.4'	06°14.6'E	23.02
115	20-30	20	0-10	-	-	-	-	69°53.4'	06°14.6'E	69°51.9'	06°16.8'E	23.02
116	0-10	0-10	-	-	-	-	-	69°51.9'	06°16.8'E	69°50.0'	06°13.0'E	23.02
117	ice free	-	-	-	-	-	-	69°50.0'	06°13.0'E	70°06.1'	05°11.0'E	23-26.02
118	70	40	30	-	-	-	-	70°06.1'	05°11.0'E	70°05.0'	04°56.4'E	26.02
119	100	70	30	-	-	-	-	70°05.0'	04°56.4'E	70°03.4'	04°24.3'E	26-27.02

No.	Total ice concn.	First year ice			Young ice			From:		To:		Date
		Thick	Medium	Thin (white)	Nilas	Pancake ice	Grease ice	Lat.°S	Long.°	Lat.°S	Long.°	
120	60	40	20	-	-	-	-	70°03.4'	04°24.3'E	70°01.9'	04°02.5'E	27.02
121	ice free	-	-	-	-	-	-	70°01.9'	04°02.5'E	69°33.9'	09°41.6'E	27.02-07.03
122	40-60	40-60	-	-	-	-	-	69°33.9'	09°41.6'E	69°40.7'	09°55.4'E	07.03
123	90-100	-	40	-	-	50-60	-	69°40.7'	09°55.4'E	69°42.6'	10°06.4'E	07.03
124	90-100	20	60	-	-	10-20	-	69°42.6'	10°06.4'E	69°46.6'	10°04.3'E	07.03
125	60	20	20	-	20	-	-	69°46.6'	10°04.3'E	69°47.0'	09°56.6'E	07.03
126	70-80	40	20	-	10-20	-	-	69°47.0'	09°56.6'E	69°46.6'	09°48.0'E	07.03
127	90-100	50	30	-	10-20	-	-	69°46.6'	09°48.0'E	69°49.4'	09°58.0'E	07.03
128	40-50	20	20	-	0-10	-	-	69°49.4'	09°58.0'E	69°39.0'	10°16.0'E	07.03
129	80	30-40	30	-	20	-	-	69°39.0'	10°16.0'E	69°44.8'	12°05.2'E	07-08.03
130	30	20	10	-	-	-	-	69°44.8'	12°15.2'E	69°49.9'	12°04.4'E	08.03
131	ice free	-	-	-	-	-	-	69°49.9'	12°04.4'E	69°58.4'	12°10.4'E	09.03
132	100	-	-	-	-	100	-	69°58.4'	12°10.4'E	69°45.0'	10°42.0'E	09.03
133	100	40	20	-	-	40	-	69°45.0'	10°42.0'E	69°43.0'	10°40.0'E	09.03
134	90-100	50-60	10	-	-	20-30	-	69°43.0'	10°40.0'E	69°36.5'	10°35.1'E	09.03
135	50-60	20-30	10	-	-	10-20	-	69°36.5'	10°35.1'E	69°46.0'	06°37.0'E	09-10.03
136	70-80	40	10	-	-	20-30	-	69°46.0'	06°37.0'E	69°55.3'	05°57.0'E	10.03
137	90-100	50	20	-	-	20-30	-	69°55.3'	05°57.0'E	70°00.3'	05°25.4'E	10.03
138	40	-	-	-	-	30	10	70°00.3'	05°25.4'E	69°56.0'	04°35.2'E	10.03
139	90-100	20	20-30	-	-	40-50	-	69°56.0'	04°35.2'E	69°43.0'	04°28.9'E	10.03
140	60	10	10	-	-	40	-	69°43.0'	04°28.9'E	69°45.8'	04°29.4'E	10.03
141	100	20	20	-	-	60	-	69°45.8'	04°29.4'E	70°01.1'	04°01.9'E	10-11.03
142	100	40	10	-	-	50	-	70°01.1'	04°01.9'E	70°01.1'	03°39.6'E	11.03
143	100	50	20	-	-	30	-	70°01.1'	03°39.6'E	70°01.7'	03°21.0'E	11.03
144	90-100	40	20-40	-	-	20-30	-	70°01.7'	03°21.0'E	70°01.5'	02°43.4'E	11.03
145	50-60	20	10	-	-	20-30	-	70°01.5'	02°43.4'E	69°58.8'	02°28.0'E	11.03
146	20	10	10	-	-	-	-	69°58.8'	02°28.0'E	69°56.2'	02°21.0'E	11.03
147	10	10	-	-	-	-	-	69°56.2'	02°21.0'E	69°54.7'	02°20.0'E	11.03
148	60-70	30	20	-	-	10-20	-	69°54.7'	02°20.0'E	69°53.0'	02°18.0'E	11.03
149	ice free	-	-	-	-	-	-	69°53.0'	02°18.0'E	69°44.6'	00°51.5'E	11-12.03
150	100	50-60	40	-	-	0-10	-	69°44.6'	00°51.5'E	69°43.4'	00°41.2'E	12.03
151	ice free	-	-	-	-	-	-	69°43.4'	00°41.2'E	69°37.0'	00°12.5'E	12.03
152	00 60	-	40	-	-	-	-	69°37.0'	00°12.5'E	69°37.5'	01°18.7'E	12-13.03
153	70-90	40	20	-	-	10-30	-	69°37.5'	01°18.7'E	69°49.2'	02°54.7'w	13.03
154	50-60	30	10-20	-	-	10	-	69°49.2'	02°54.7'w	70°06.4'	03°54.0'w	13.03
155	40	20	20	-	-	-	-	70°06.4'	03°54.0'w	70°07.2'	03°55.0'w	13.03
156	ice free	-	-	-	-	-	-	70°07.2'	03°55.0'w	-	-	13.03

Tab. 3.3. Characteristics of ice floes in the eastern Weddell and Lazarev seas

No.	Forms of floating ice				Hummocking %	Thickness snow/ice (cm)				Date	
	Big floe	Medium floe	Small floe	Ice cake		Young ice					
						Thick	Medium	Thin (white)	Nilas		Pancake ice
1	-	-	-	+	20	-	-	-	-	-	12.01
2	-	-	-	+	20	10-20 / 180-200	-	-	-	-	12.01
3	-	-	-	+	20-40	30-40 / 180-200	-	-	-	-	12.01
4	-	-	-	+	40-60	20-30 / 180-200	30-40 / 80-120	-	-	-	12.01
5	-	-	+	+	40-60	30-40 / 120-150	30 / 80-100	-	-	-	12-13.01
6	-	-	+	+	40-60	30-40 / 150-170	30 / 80-100	-	-	-	13.01
7	-	-	+	+	20-40	30-40 / 150	30 / 100	-	-	-	13.01
8	-	-	+	+	20-40	30-40 / 150	20 / 100	-	-	-	13.01
9	-	-	+	+	40-60	30-40 / 150	20 / 100	-	-	-	13.01
10	-	-	+	+	40-60	30-40 / 150	30 / 100	-	-	-	13.01
11	-	-	+	+	40-60	40 / 150	20 / 100	-	-	-	13.01
12	-	-	+	+	20-40	40 / 150	20 / 100	-	-	-	13.01
13	-	-	+	+	20-40	50 / 160	20 / 100	-	-	-	13-14.01
14	-	-	+	+	20-40	50 / 160	-	-	-	-	14.01
15	-	-	-	-	-	-	-	-	-	-	14.01
16	-	-	-	+	40-60	40 / 150	30 / 100	-	-	-	14.01
17	-	-	-	+	40-60	40 / 150	30 / 100	-	-	-	14.01
18	-	-	-	+	40-60	30 / 160	30 / 90	-	-	-	14.01
19	-	-	-	+	60	50 / 150	-	-	-	-	14.01
20	-	-	-	+	40-60	30 / 150	-	-	-	-	15.01
21	-	-	+	+	40-60	50 / 150	30 / 90	-	-	-	15.01
22	-	-	+	+	40-60	40 / 150	20 / 100	-	-	-	15.01
23	-	-	-	-	-	-	-	-	-	-	15.01
24	-	-	-	+	20-40	30 / 180	15 / 110	-	-	-	15-17.01
25	-	-	-	-	-	-	-	-	-	-	17.01
26	-	-	+	+	20-40	40 / 190	30 / 120	-	-	-	17.01
27	-	-	-	+	20	-	20 / 110	-	-	-	17.01
28	-	-	+	+	60-80	40 / 180	30 / 110	-	-	-	18.01
29	-	-	-	-	-	-	-	-	-	-	18.01
30	-	-	+	+	40-60	40 / 190	30 / 120	-	-	-	18.01
31	-	-	+	+	40-60	40 / 190	30 / 120	-	-	-	18.01
32	-	-	+	+	40-60	30 / 190	20 / 120	-	-	-	18.01
33	-	-	-	-	-	-	-	-	-	-	18-19.01
34	-	-	-	+	60	30 / 160	20 / 100	-	-	-	19.01
35	-	-	+	+	60-80	30 / 190	20 / 120	-	-	-	19.01
36	-	-	+	+	60	40 / 190	20 / 120	-	-	-	19.01
37	-	-	+	+	60	40 / 190	20 / 120	-	-	-	19.01
38	-	-	-	-	-	-	-	-	-	-	19.01
39	-	-	+	+	60	30 / 200	30 / 120	-	-	-	19.01

No.	Forms of floating ice				Hummocking %	First year ice			Young ice		Date	
	Big floe	Medium floe	Small floe	Ice cake		Thick	Medium		Thin (white)	Nilas		Pancake ice
							30 / 100	30 / 100				
40	-	-	+	+	60	50 / 160	30 / 100	-	-	-	19-20.01	
41	-	-	+	+	60	50 / 160	30 / 100	-	-	-	20.01	
42	-	-	+	+	60	50 / 160	30 / 100	-	-	-	20.01	
43	-	-	+	+	60	50 / 150	-	-	-	-	20.01	
44	-	-	+	+	60	50 / 150	30 / 100	-	-	-	20.01	
45	-	-	-	-	-	-	-	-	-	-	20.01	
46	-	-	+	+	60	40 / 150	30 / 100	-	-	-	20.01	
47	-	-	+	+	60	30 / 150	-	-	-	-	20.01	
48	-	-	+	+	60	40 / 150	20 / 100	-	-	-	20.01	
49	-	-	+	+	60	40 / 150	20 / 100	-	-	-	20.01	
50	-	+	+	+	60	40-50 / 160	20-30 / 100	-	-	-	20-21.01	
51	-	+	+	-	60	50 / 170	30 / 110	-	-	-	21-26.01	
52	+	+	-	-	60	40 / 180	20 / 120	-	-	-	26-28.01	
53	+	+	+	-	80	50 / 200	30 / 140	-	-	-	28-30.01	
54	+	+	+	+	60-80	40-50 / 200	30 / 160	-	-	-	30.01-02.02	
55	-	-	-	-	-	-	-	-	-	-	02-05.02	
56	-	+	+	+	60-80	40 / 180	30 / 140	-	-	-	05.02	
57	-	+	+	-	60	40 / 180	30 / 140	-	-	-	05.02	
58	+	+	+	-	60-80	40-50 / 190	30 / 120	-	-	-	05-07.02	
59	-	+	+	-	40	40 / 180-200	30 / 120	15 / 40	-	-	07.02	
60	-	+	+	+	20-40	-	30 / 100	20 / 40	-	-	07-08.02	
61	-	-	+	+	40-60	-	30 / 100	20 / 40	-	-	08.02	
62	-	-	+	+	20	-	30-40 / 100	20 / 50	-	-	08-09.02	
63	-	-	+	+	40	-	30 / 110	20 / 50	-	-	09.02	
64	-	-	+	+	20-40	-	30 / 110	15 / 50	-	-	09.02	
65	-	-	+	+	20-40	30 / 150	20 / 100	10 / 40	-	-	09-10.02	
66	-	-	+	+	20-40	30 / 150	20 / 100	10 / 40	-	-	10.02	
67	-	-	+	+	20-40	30-40 / 210	20-30 / 150	15 / 60	-	-	10-11.02	
68	-	+	+	+	20-40	30 / 160	30 / 110	20 / 50	-	-	11.02	
69	+	+	+	-	20-40	-	30-40 / 80	20 / 60	-	-	11-12.02	
70	-	+	+	+	40	40 / 180	30 / 90	20 / 40	-	-	12.02	
71	-	+	+	+	40-60	-	30-40 / 120	20 / 60	-	-	12-13.02	
72	-	+	+	+	40-60	50 / 170	30 / 120	15 / 50	-	-	13.02	
73	-	+	+	+	60-80	-	50 / 120	20 / 70	-	-	13.02	
74	-	-	-	-	-	-	-	-	-	-	13.02	
75	-	-	-	-	-	-	-	-	-	-	13.02	
76	-	+	-	-	0-20	50 / 200	-	-	-	-	13.02	
77	-	+	-	-	60-80	50-60 / 200	-	-	-	-	13.02	
78	-	-	-	-	-	-	-	-	-	-	13.02	
79	-	+	+	+	40	40-50 / 200	30 / 110	-	-	-	13.02	
80	-	+	+	+	40-60	50 / 200	30 / 110	-	-	-	13-14.02	

Ice conditions

During the summer of 1990-91, ice conditions in the eastern Weddell Sea were the heaviest reported in the 17 years since records have been made. The ice belt around Antarctica in the area of the Greenwich Meridian was not breached until 28 January, whereas the mean date for this process to take place is 1 January. The ice edge was further to the north and east than the mean position for multi-year ice in the summer period. The seasonal reduction of the ice-covered area in the Weddell Sea was easily documented, but the speed of the reduction was less easy to determine. In the south and eastern parts of the Weddell Sea, ice conditions were near to normal for multi-year ice. The size of the polynyas along the Ronne-Filchner Ice Shelf and the Antarctic Peninsula were near to their mean multi-year ice condition. The edge of the very close pack ice area (9-10 tenths ice concentration) was developed to the east, and the area covered by this pack ice was more than the multi-year mean (Fig. 3.4).

The change in ice conditions is dependent to a considerable extent on the barometric situation, especially in the area of the ice edge. At times, good ice conditions for navigation prevailed along the coastline of the SE part of the Weddell Sea, but these periods were short-lived (3-4 days). In January, the dominant wind direction was ENE (29.29%) and NE (17.93%) (Tab. 3.4) in the SE Weddell Sea. As a result, sea ice was pressed against the coastline, creating the difficult ice conditions that were experienced during the cruise.

The wind system and large-scale oceanic currents define the general ice drift pattern in the Weddell Sea. Dr. A. Provorkin has derived a method of defining the drift of ice in the Weddell Sea using satellite imagery (Fig. 3.5). In January, a circular system of ice drift was well-developed. The centre of this circulation was at the point 68°30'S, 45°W. The mean speed of ice drift was near to the multi-year mean. However, in the northern part of the Weddell Sea, the mean speed of ice drift was less (by approximately 20%) than during the winter season of 1989, when a joint expedition of Polarstern and the Soviet icebreaker Akademik Fedorov took place.

Sea water in the Weddell Sea began freezing, according to our observations, on 7 February, when nilas was seen forming in Halley Bay. On 12 February we noted the appearance of nilas in the polynyas along the Ronne Ice Shelf in satellite images. By 20 February we recorded grey ice in polynyas along the Filchner Ice Shelf and in Halley Bay. On 1 March grey-white ice was forming in polynyas along the Filchner Ice Shelf and Ronne Ice Shelf (Fig. 3.6). Pancake ice was recorded in the Kapp Norvegia area on 3 March, and by 21 March an unbroken strip of pancake ice, 100 km wide was evident between 20°W and 0°. The ice conditions in the Lazarev Sea were near to the multi-year mean. However, during January the ice concentration here was less than normal, but in March it was more than the mean. The ice distribution in the Lazarev Sea was controlled by ice drift from the east and the positions of large groups of grounded icebergs. The strips showing different ice concentrations are narrow. The ice in the Lazarev Sea is highly dynamic, and this is reflected in rapid and large changes of ice conditions. The freezing process began in the Lazarev Sea on 15 February with formation of nilas, but became especially active after 7 March; this date being earlier than the multi-year mean. The results of statistical analysis of visual ship observations are shown in Tab. 3.5. The calculation of the means has been undertaken only for a single wide area

each time and only within the ice regions of the Weddell and Lazarev seas for the period of the cruise. Tab. 3.5 shows that ice conditions in the Weddell and Lazarev seas are very different. We consider this a result of geographical setting, and not the time difference of observation, since the latter was small, whilst the difference in thickness of the snow and ice between the two regions was much more important. In conclusion, we provide some information concerning a preliminary comparison of SSM-1 and TV satellite data (Fig. 3.7). Here it is demonstrated that not only are there common characteristics, but also some essential differences. Why? The answer to this question we hope to obtain after a special joint research programme has been undertaken.

Tab. 3.4. Statistics concerning wind direction in the eastern Weddell Sea, from observations made by the meteorological station on board "Polarstern". (Figures are in percent)

Speed (knots)	N	NNE	NE	ENE	E	ESE	SE	SSE	S	SSW	SW	WSW	W	WNW	NW	NNW
0-9.8 (5 m/s)	0.8	1.59	9.76	10.56	3.98	0.99	0.99	0.60	1.19	1.79	3.39	4.38	4.58	1.39	1.99	1.79
9.9-19.6 (10 m/s)	2.39	0.41	7.37	15.94	1.19	0.20	0.41	0.20	0.60	0.41	2.59	1.19	0.99	3.58	0.60	0.41
19.7-29.4 (15 m/s)	-	-	0.80	2.79	1.79	0.80	0.20	-	-	-	1.79	0.20	0.20	-	-	-
29.4 (>15 m/s)	-	-	-	-	1.59	1.59	-	-	-	-	-	-	-	-	-	-
TOTALS	3.19	2.00	17.93	29.29	8.55	3.58	1.60	0.80	1.79	2.20	7.77	5.77	5.77	4.97	2.59	2.20

Tab. 3.5. Mean ice conditions in the Weddell Sea and Lazarev Sea from visual ship observations, January to March 1991.

Ice conditions	Weddell Sea	Lazarev Sea
<i>Ice concentrations</i>		
0-10% open water	19.4)	35.3)
10-30% very open pack ice	17.4)	6.4)
40-60% open pack ice	16.5) 100%	26.2) 100%
70-80% close pack ice	9.3)	10.3)
90-100% very close pack ice	37.4)	21.8)
Thick first year ice	41.4)	32.2)
Medium first-year ice	34.2)	17.3)
Thin first-year ice	5.8)	-)
Nilas	3.4) 100%	0.8) 100%
Pancake ice	-)	14.3)
Grease	-)	0.6)
Ice-free	15.2)	34.8)
<i>Forms of floating ice</i>		
Big floe	4.8)	-)
Medium floe	8.9)	-)
Small floe	30.7) 100%	-) 100%
Ice cake	42.0)	51.0)
Small ice cake	13.6)	49.0)
Mean hummocking	49.0%	43.0%
<i>Mean thickness of snow/ice (cm)</i>		
Thick first-year ice	39.6 / 171.7	34.4 / 161.7
Medium first-year ice	24.4 / 108.5	21.8 / 102.4
Thin first-year ice	18.1 / 50.1	- / -
Nilas	- / 5.	- / 5.2
Pancake ice	- / -	4.5 / 13.8

Fig. 3.4. The positions of edge of very close pack-ice in period January - March 1991

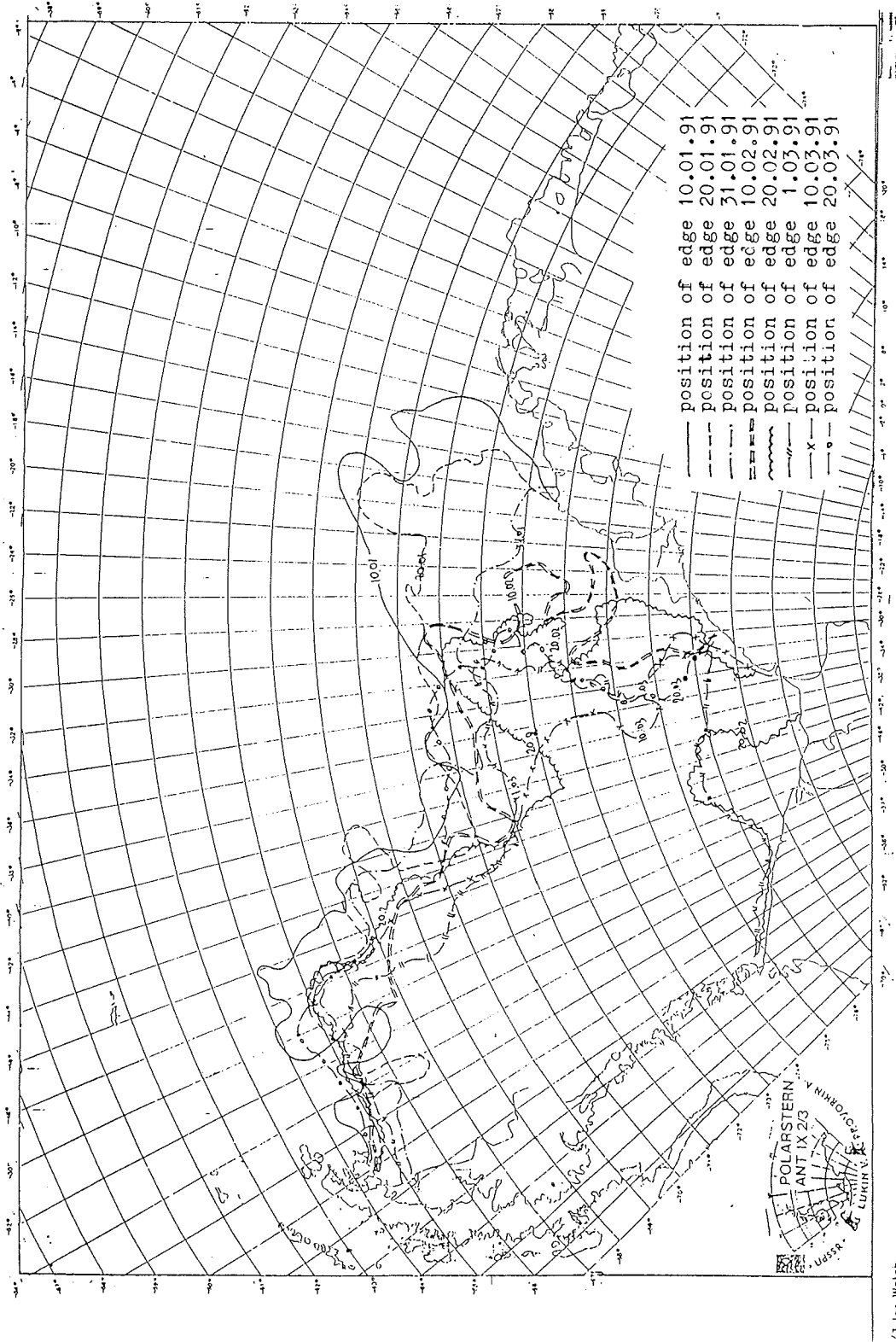


Fig. 3.5. Drift of ice at period 8 January - 7 February 1991

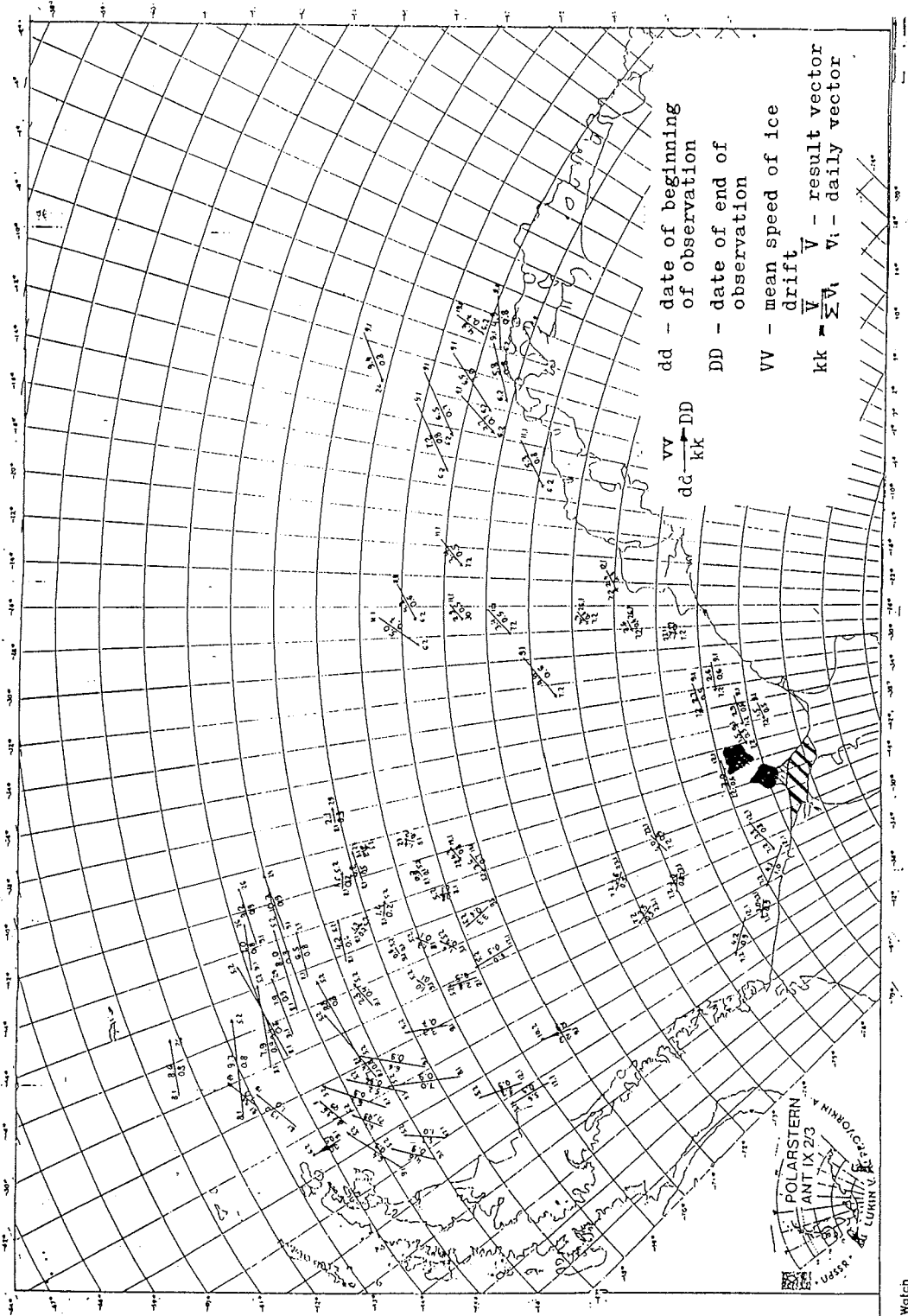
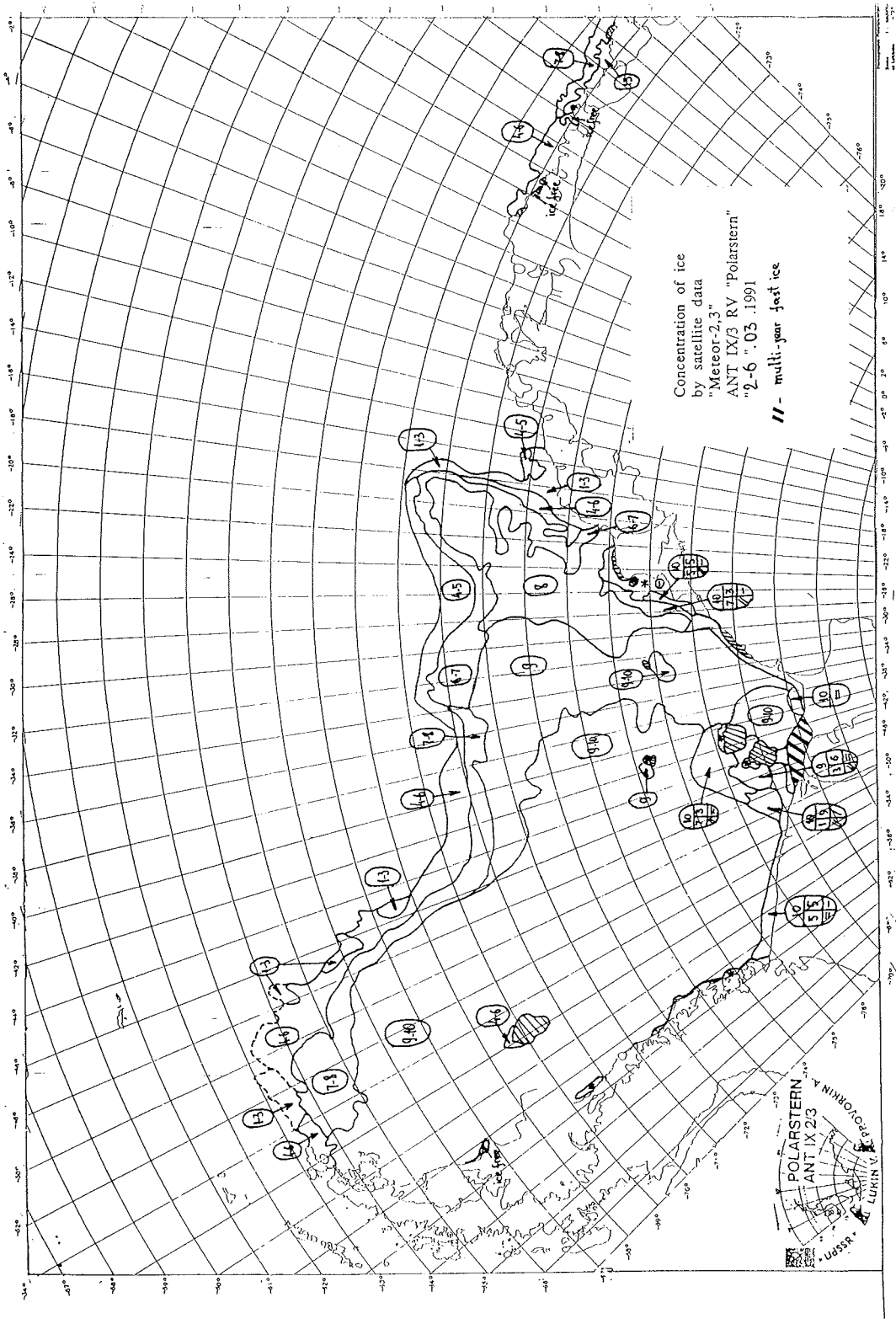


Fig. 3.6. Concentration of ice by satellite data "Meteor-2,3", 2 - 6 March 1991



4. WATER COLUMN STUDIES

4.1. Physical oceanography

M. Schroeder, A. Wisotzki, H. Witte, S. Griffith, I. Rau, (AWI)
G. Boenisch, (UH)

Instrumentation: CTD (NB Mk III B), GO-Rosette (24*12 I), XBT (T7), salinometer (Autosal) for long ice stations: CTD (SIS 500), CTD plus three component acoustic current meter (Symtronix UCM-40 Mk II)

Objectives

Due to the change of the cruise plans the objectives of the oceanographic programme focussed on the following subjects:

- Investigation of the structure and intensity of the coastal current along its path between the stations of Georg Forster (70°46'S;11°50'E) and Halley Bay (75°35'S;26°40'W) and its interaction with the interior of the Weddell Gyre. Three areas of interest were chosen: a) the region near Halley Bay where the continental shelf widens and the coastal current splits into two branches, one flowing south into the Filchner Trench, and the other following the shelf break to the west; b) the region between Vestkapp and Kapp Norvegia where a more or less even structured shelf break exists; c) the Lazarev Sea east of Georg v. Neumayer (70°37'S;08°22'W) and south of Maud Rise where the recirculation of the Weddell Gyre is a complicated system of different current branches altered especially by bottom topography.
- Description of water mass characteristics within the coastal current regime including the variability of natural and anthropogenic tracers.
- Detection of the variability of the Antarctic Circumpolar Current (ACC) via temperature profiles and calculation of seasonal changes in the heat content of the upper ocean (0 - 750 m).
- Measurement of the turbulent heat- and momentum fluxes in the oceanic boundary layer below sea-ice during summer melt.

Work at sea

For location of stations see Fig. 3.8 and Fig. 3.9

The following tasks were carried out:

- four CTD-sections with lengths of 150 - 600 km perpendicular to the slope of the continental shelf.
- different tracer samples taken and stored for later analysis at 36 stations.
- two long ice stations with a mobile system for CTD-profiles and current measurements from the sea-ice.
- repetition of XBT-sections between Cape Town and Georg v. Neumayer within a three month period.
- enroute registration of surface temperature and salinity via Thermosalinograph on board "POLARSTERN".
- measurement of deep sea current velocities in a bathymetric channel (mooring AWI 213/1 and 213/2).
- measurement of current velocities and particle fluxes with sediment traps south of the polar front (mooring AWI 400).
- deployment of meteorological ARGOS buoys.

Fig. 3.8: CTD-stations and numbers of sections (1,2) referred to in the text. In addition the location of moorings and meteorological Argos-buoys southwest of Georg v. Neumayer are marked.

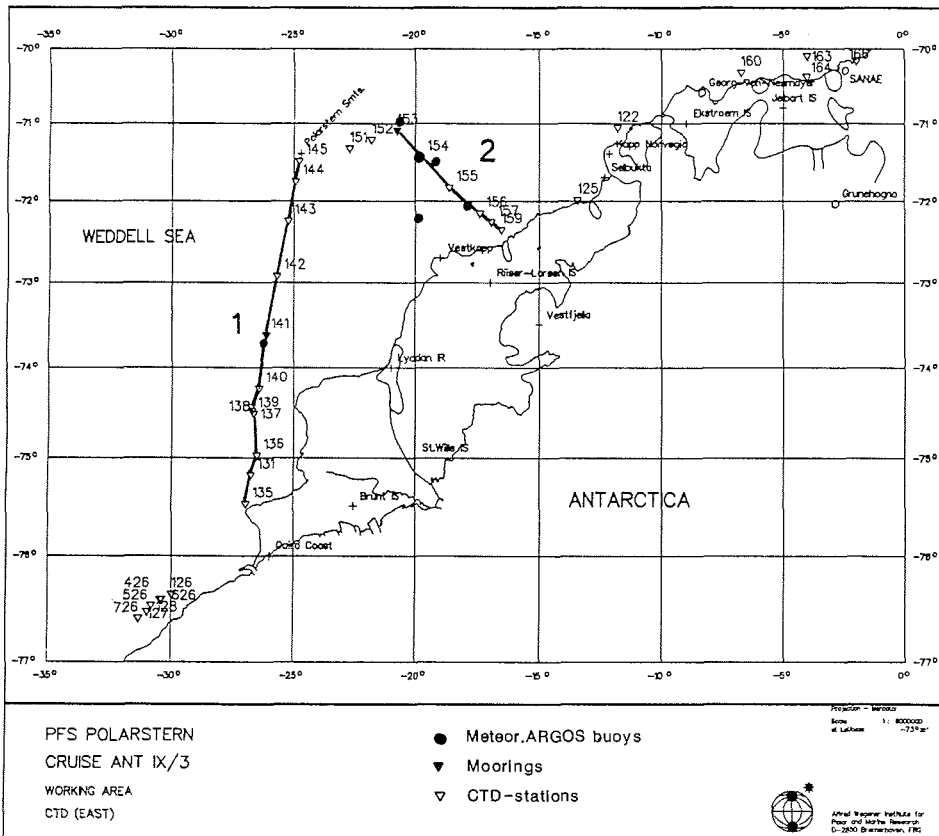
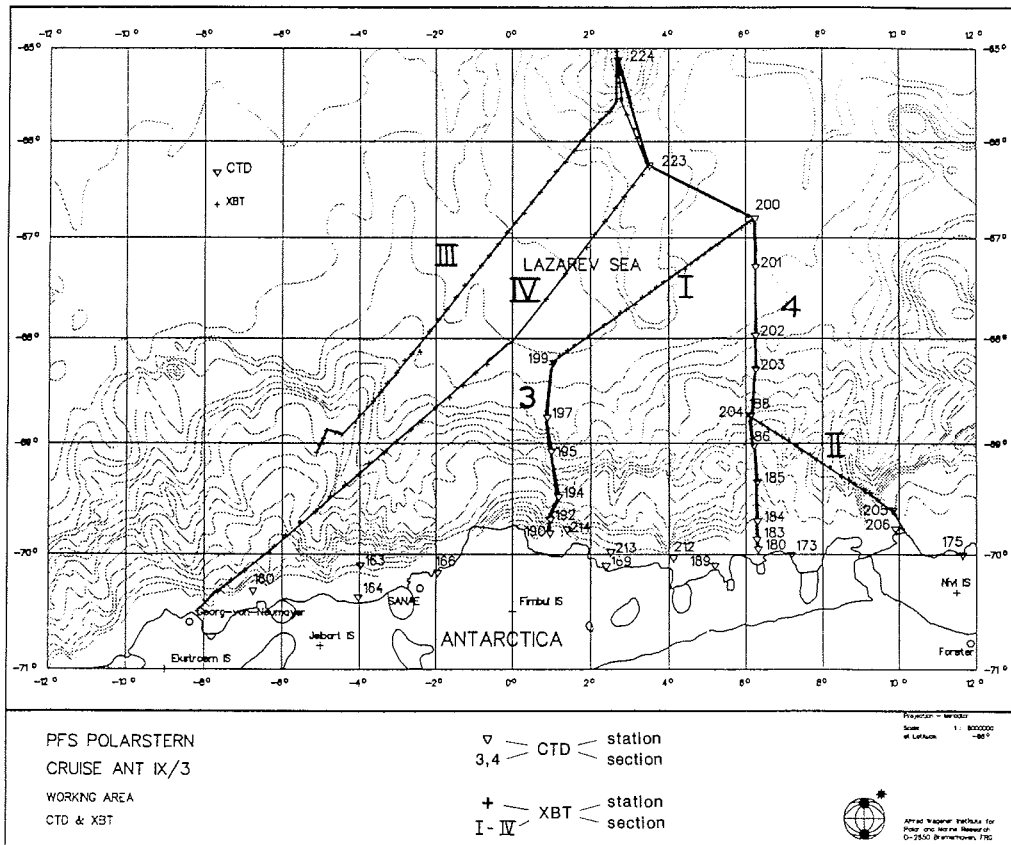


Fig. 3.9: CTD- and XBT-stations in the Lazarev Sea. (3,4 for CTD, I-IV for XBT).



Number of stations

- CTD : 63 total

0 m	<	20	<	500 m
500 m	<	11	<	1500 m
1500 m	<	22	<	4000 m
4000 m	<	10	<	5138 m

- Long ice stations : 2 (22 h, 33 h)

21 profiles

68 time series

- XBT sections: 4 total

2 between Cape Town and Georg v. Neumayer with a spacing of 25 km.

2 in the Lazarev Sea with a spacing of 15 km

- Mooring work: 4 total, 2 recovered, 2 deployed

AWI 214	recovered	Pos.: 71°03'S	11°47'W
AWI 213/2	deployed	Pos.: 73°37'S	26°07'W
AWI 213/1	recovered	Pos.: 71°06'S	20°46'W
AWI 400	deployed	Pos.: 57°35'S	04°09'E

- ARGOS buoys: 6 total

5 deployed in an area centred at Pos.: 71° 30'S 19° 50'W

Preliminary results:

Investigations of water mass characteristics and circulation and structure of the coastal current in the eastern Weddell Sea.

a) Halley Bay region.

The Weddell Sea is characterised by a large cyclonic gyre with southwestward flow off the eastern boundary. This flow is intensified at the shelf break as the coastal current has its core above the steepest part of the shelf slope. Our first CTD-section with 12 stations and a maximum spacing of 55 km was located between Halley Bay and Polarstern Seamount over a distance of 450 km (Fig.3.8). Section 2 started at mooring position AWI 213/1 running southeast towards the coast to a point 75 km north of Vestkapp. The total distance was 210 km including 6 CTD stations with a station distance of maximal 58 km. In addition, 2 CTD stations were conducted between Polarstern Seamount and AWI 213/1.

In the northeast (sec.2) the transition between Winter Water (WW) and Warm Deep Water (WDW) which is described by the $\theta = 0.0^\circ\text{C}$ isotherm and the $s = 34.60$ isohaline was found at a depth of 200 m - 250 m sloping down within 100 km towards the shelf break to a depth of 760 m (Fig. 3.10a,b). Further southwest (sec.1) this deepening of isopleths started already 320 km away from the shelf from 150 m - 200 m to a depth of 800 m near the shelf break (Fig. 3.11a, b). At both locations a cold water tongue of temperatures $\theta < -1.80$ C and salinities $s < 34.40$ extends from the shallow shelf areas to the deep ocean at a depth of 100 m - 300 m. Its length changed from 60 km at section 2 to 250 km at section 1. The remnant winter water stratum above the WDW core cooled by 0.05 - 0.1°C southward, whereas salinity did not change.

The coastal current had a horizontal extension of 100 km from the coastline with geostrophic baroclinic velocities of 0.1 - 0.2 m/s relative to the bottom and a main core above the shelf break from surface to 500 m depth. These values need to be confirmed with recalibrated CTD data and compared with moored current meter data. Water mass distribution for the drift stations (no.126-128) is dominated by 83% Eastern Shelf Water (ESW) and 12% surface water with salinities $s < 34.25$ and temperatures slightly above freezing. In the Halley Bay region the shelf stations (no.135, 131, 136) showed only 77% ESW and 12% surface water which is a slight indication for the increasing significance of ESW on the way to the south.

b) Lazarev Sea region.

The area southeast of Maud Rise is characterized by a complicated recirculating flow regime of the Weddell Gyre which is influenced by topographic structures such as Maud Rise or the Astrid Ridge further east. Due to the interference with water masses from outside the gyre and the complicated structure of different branches of the Weddell Gyre return flow, the horizontal distribution in this region, even within the same layer, is very patchy and non-uniform (Gordon & Huber 1990, Bagriantsev et al. 1989).

Therefore, two CTD-sections (1°E and $6^{\circ}15'\text{E}$) were done together with four XBT-sections to obtain information about mesoscale variability of water masses and circulation patterns. Two of these XBT-sections were part of the transects between Cape Town and Georg v. Neumayer. This transect was repeated three times within a 4 month period (one measurement during ANT IX/2) so that the seasonal variations of the ACC core and the heat content of the upper 750 m can be analysed. Some additional shelf stations were carried out to provide the physical background for an intense phytoplankton bloom detected by the biologists. The positions of these stations are also shown in Fig. 3.9. The 1°E section was 180 km long and consisted of 6 CTD-stations with a spacing of less than 60 km in a depth range of 420 m to 4500 m. The second section at $6^{\circ}15'\text{E}$ connects the Antarctic continent with Maud Rise and is 620 km long with profiles from three time segments (stat.no. 180-188, 200-204, 223-224) which was covered in two weeks. This was due to severe weather conditions and logistic constraints. The distance between the 13 CTD-stations varied from 15 km on the shelf to 120 km near Maud Rise.

At 1°E the upper core of the Circumpolar Deep Water (CDW) with temperatures $\theta > 0.8^{\circ}\text{C}$ and salinities $s > 34.68$ dominates the depth range 250 m - 600 m until 40 km to the coastline. On top of this layer the cold ($\theta < -1.5^{\circ}\text{C}$) and fresh ($s < 34.30$) coastal current deepened the isopycnals from 230 m over the deep ocean to 700 m at the continental shelf break (Fig. 3.12a, b). The westward geostrophic flow throughout the whole section is intensified in the coastal current which had a horizontal extension of 100 km from shore and is detectable to a depth of 1000 m at the transition from the shelf to the deep ocean areas. Maximum baroclinic geostrophic velocities up to 0.5 m/s relative to the bottom were calculated for the surface layer of the two southernmost stations.

To the east at station 200 the temperature in a depth from 100 m to 450 m is characterised by a core of warm water ($\theta > 1.0^{\circ}\text{C}$). This warm region was also detected on the XBT-section connecting the end point of the 1°E section (Sta. 199) with Sta. 200 at $6^{\circ}15'\text{E}$. The cold Winter Water (WW) tongue (70 - 180 m)

abruptly disappeared 60 km west of this station and was superseded by this warm water inflow from the northwest already reported by Gordon and Huber (1990) and Bagriantsev et al. (1989) (Fig. 3.13). It is a consequence of entrained waters from outside (north) the gyre into the recirculating water masses.

Depression of the $\theta = 0.0^\circ\text{C}$ isotherm and the $s = 34.60$ isohaline from 200 m depth near Maud Rise to more than 500 m at the shelf was accompanied by an upwelling of these isopleths around Sta. 200 (Fig. 3.14a,b). This is an effect which is density compensated (Fig. 3.14c) as shown by the $\text{SIG0} = 27.75$ isopycnal. The complexity of water mass composition especially near the surface and up to the underside of the Upper Circumpolar Deep Water (UCDW) is expressed by the spreading of data points in the θ - S -diagram (Fig. 3.15a). The geostrophic flow structure through this section is not as uniform as at 1°E , but shows perceptible bands of clearly different current velocities which could be interpreted by mesoscale eddies or meandering of the Weddell Gyre return flow. A final decision as to which of these processes is the most likely one could not be given yet. The coastal current was observed up to 120 km from shore to a depth of 800 m above the shelf break. At the surface baroclinic geostrophic current velocities of 0.2 m/s relative to the bottom were calculated in the vicinity of the shelf ice.

The water mass distribution was calculated following the definitions given in Hellmer et al. (1985) for the Southern Ocean. For both sections the values are the same within 1%.

Tab. 3.6: Water masses of the Lazarev Sea (percentage of total volume)

Water masses	abbreviation	total volume %
Circumpolar Deep Water	CDW	43%
Antarctic Bottom Water	AABW	47%
Winter Water	WW	2%
Low Salinity Shelf Water	LSSW	2%

Looking at the shelf stations alone (depth less than 500 m) the volumes changed to WW = 5.7% and LSSW = 6.5%. Here most of the water column belonged to surface water which had potential temperatures $-2.0 < \theta < -1.0$ C and salinities $33.10 < s < 34.27$ as a consequence of melting processes of sea-ice in the summer.

The XBT-section combining station 204 at $6^\circ 15'\text{E}$ with the coast at 10°E was not perpendicular to the coastal current. So interpretation of Fig. 3.15b that the blobs in the winter water layer ($\theta < -1.5^\circ\text{C}$) with a horizontal extension of 80 km are due to a band like structure of the current regime or due to meandering of the stream is somewhat speculative. Simultaneously, the thermocline showed variations of 150 m in the vertical at the same wavelength. But this reflects a rather complicated dynamic behaviour which has to be analysed in detail.

Fig. 3.10: a) Potential temperature and b) salinity in the top 1000 m of section 2 (see also Fig. 3.8). Heavy lines denote $\Theta=0.0^{\circ}\text{C}$ and $S=34.60$ PSU

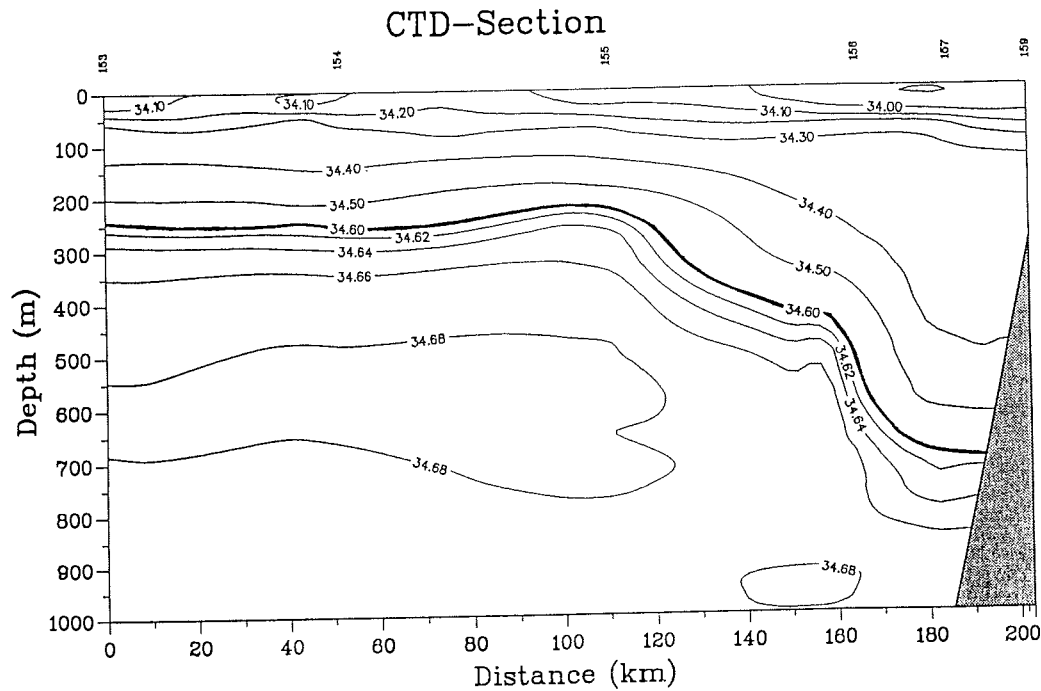
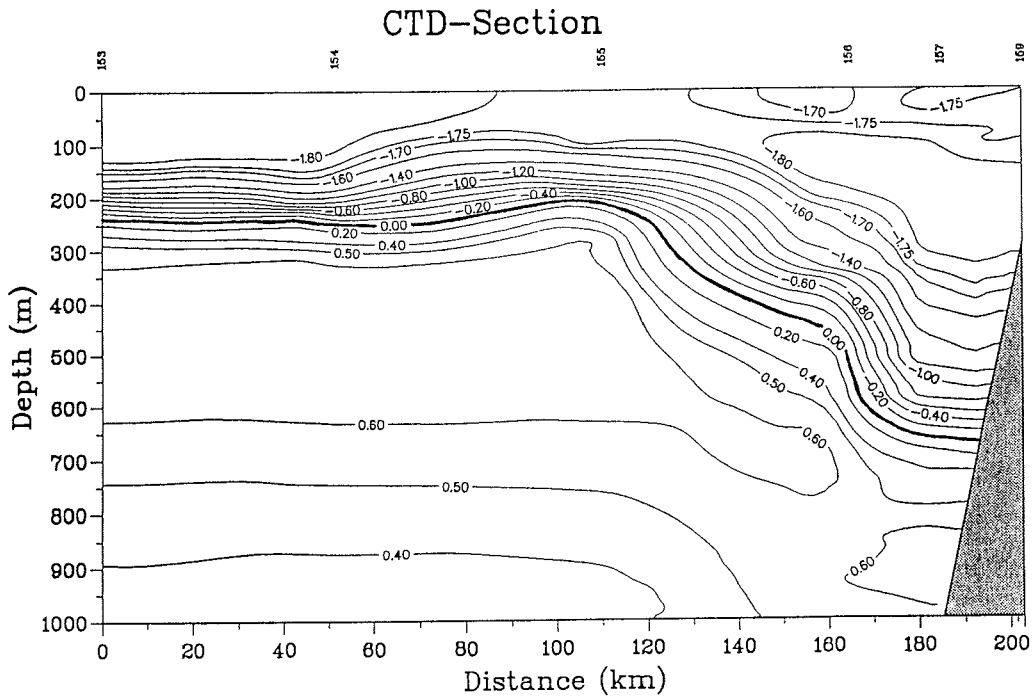


Fig. 3.11: a) Potential temperature and b) salinity in the top 1000 m of section 1 (see also Fig. 3.8). Heavy line denote $\Theta=0.0^{\circ}\text{C}$ and $S=34.60$ PSU

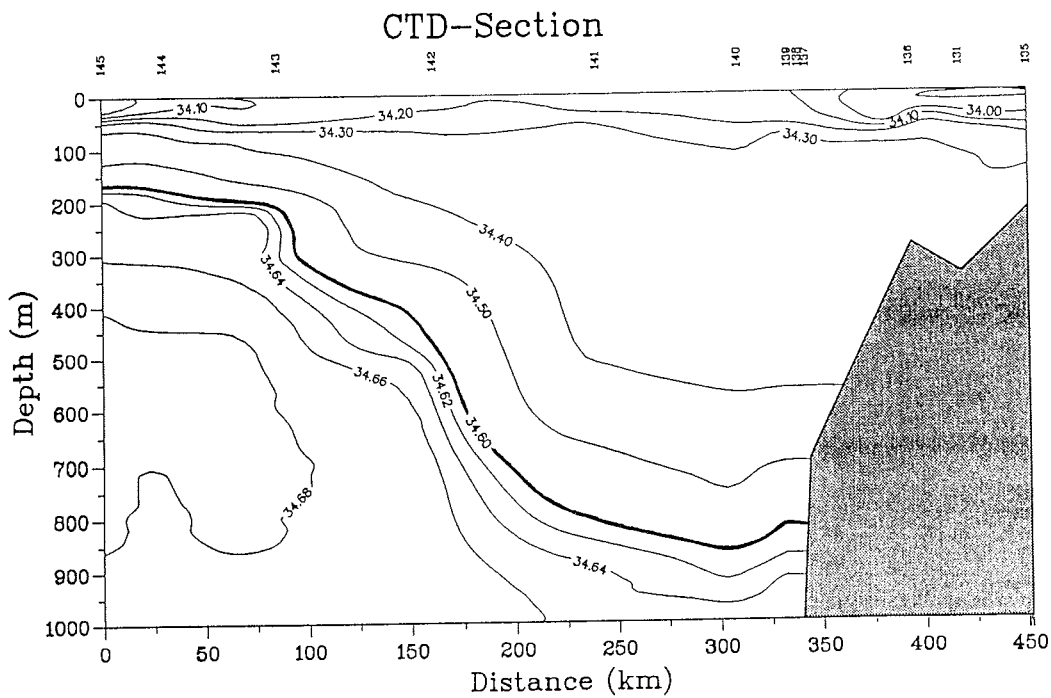
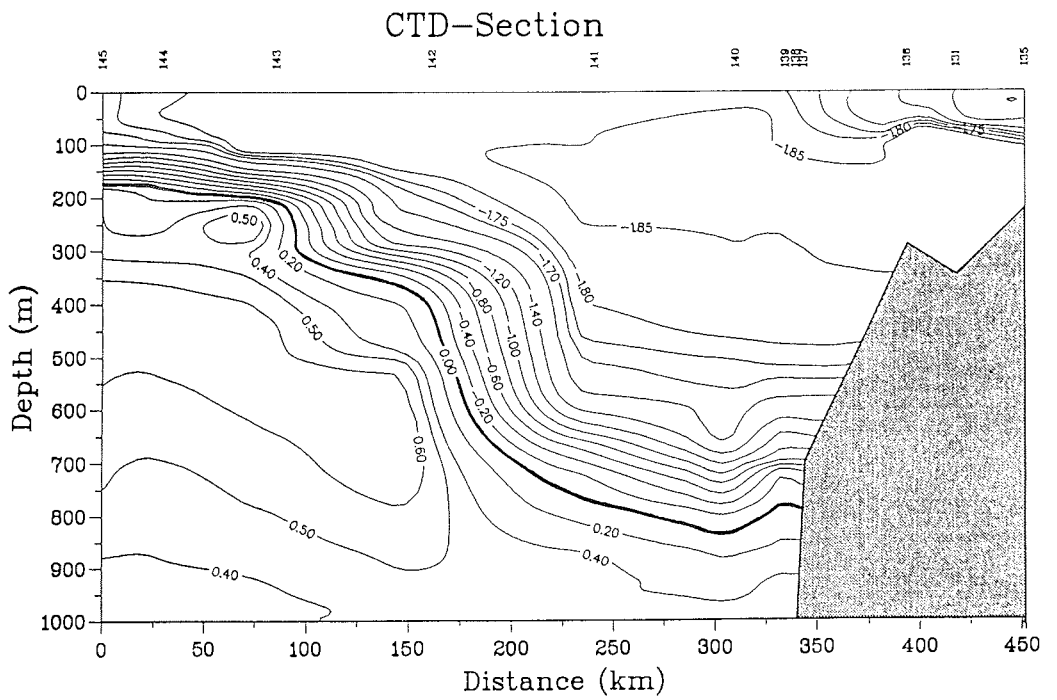


Fig. 3.12: a) Potential temperature and b) salinity of the entire water column of the 1°E transect in the Lazarev Sea (see also Fig. 3.9). Heavy lines denote $\Theta = 0.0^{\circ}\text{C}$ and $S = 34.60$ PSU

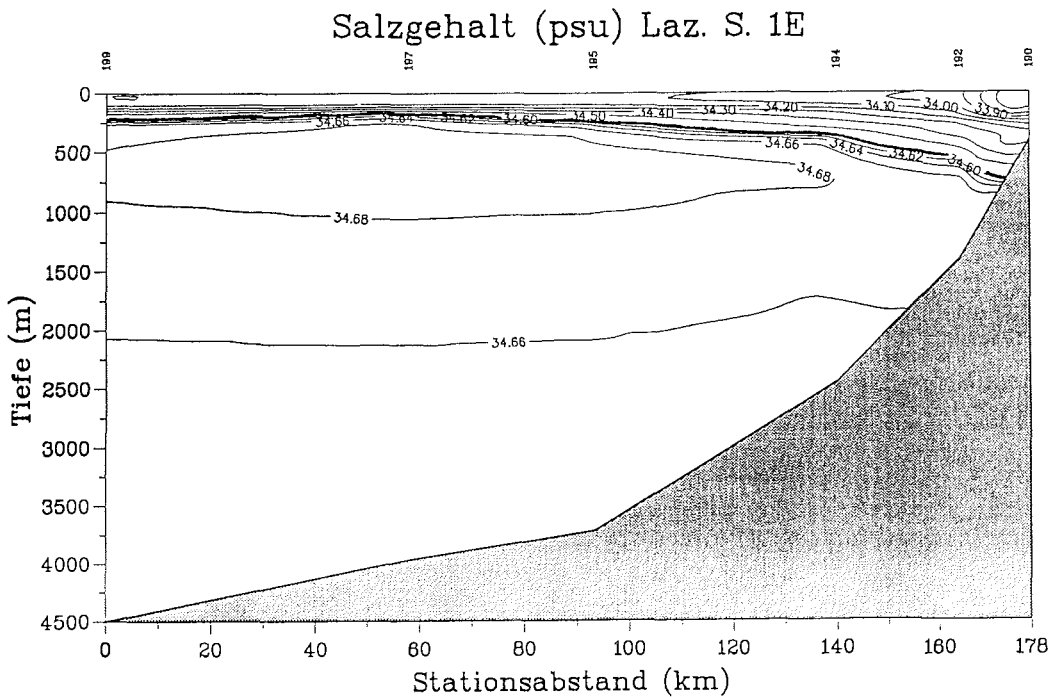
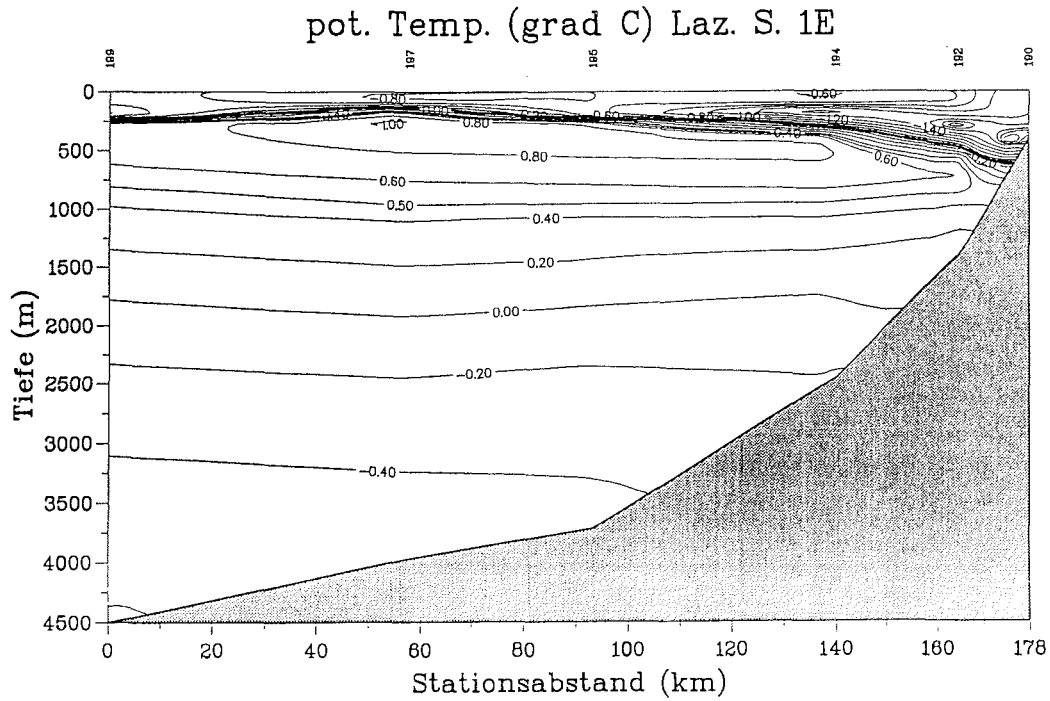


Fig. 3.13: XBT-section I connecting the CTD-sections 3 and 4 in Fig. 3.9. Heavy line marks $t=0.0^{\circ}\text{C}$, broken line delineates waters with temperatures $t > +1.0^{\circ}\text{C}$.

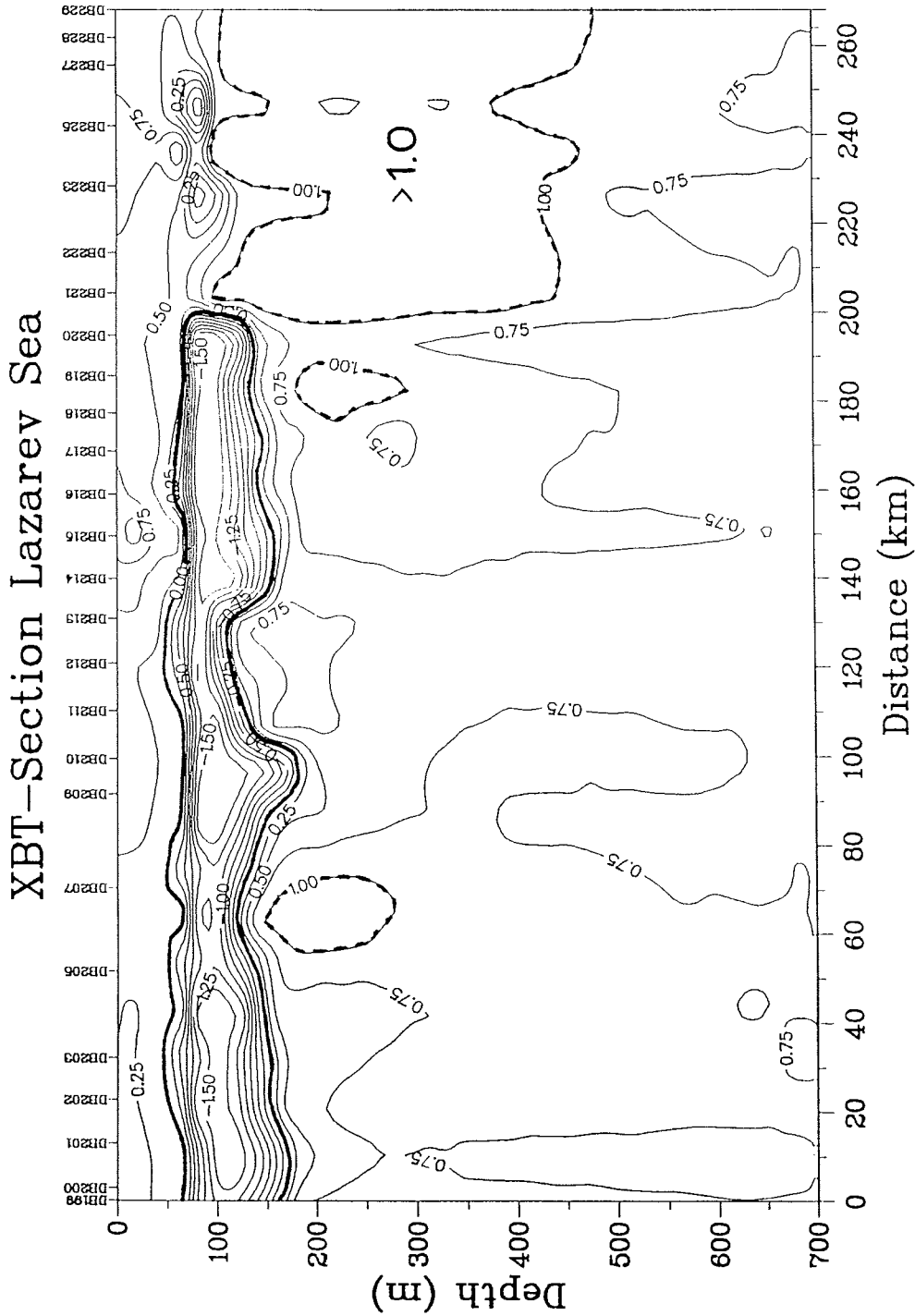


Fig. 3.14: a) Potential temperature, b) salinity and c) ζ in the top 500 m of the 6°E transect in the Lazarev Sea to Maud Rise (see also Fig. 3.9). Heavy lines denote $\Theta=0.0^{\circ}\text{C}$, $S=34.60$ PSU, and $\zeta=27.75$.

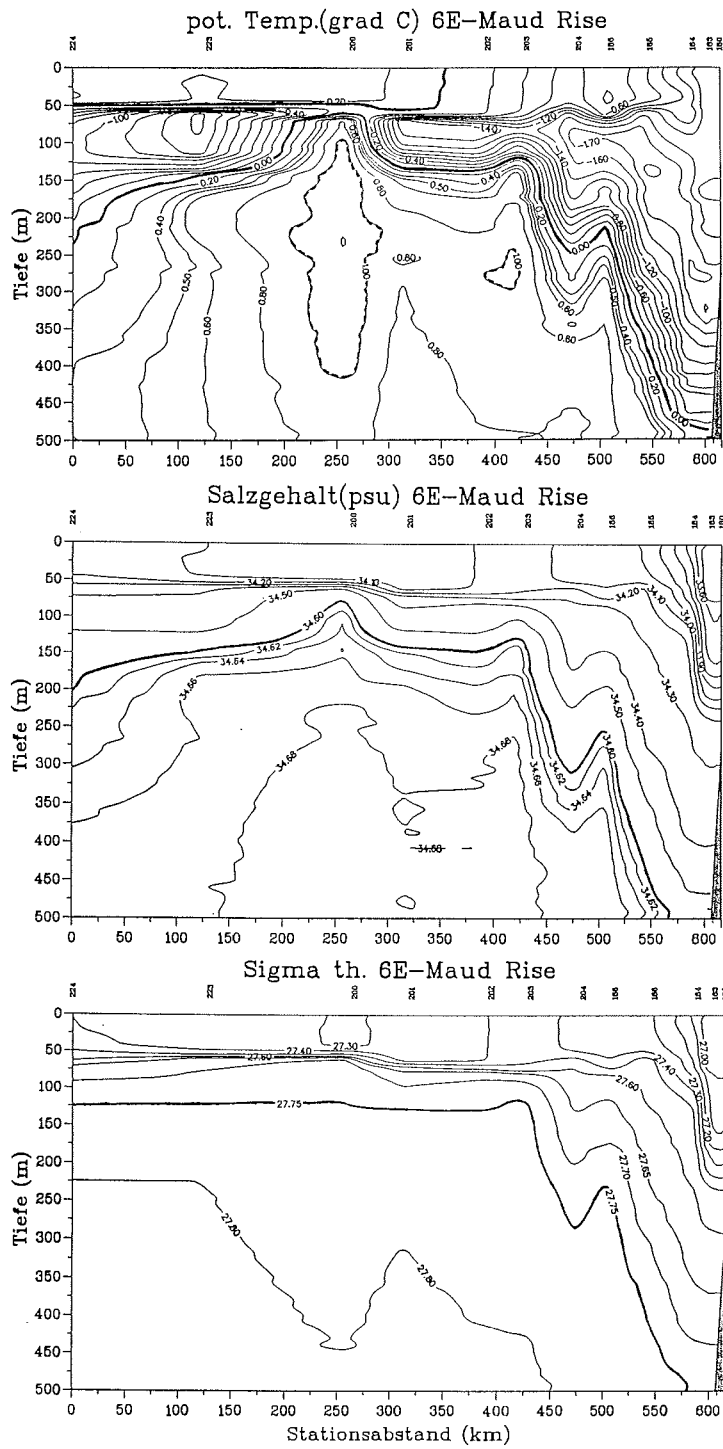


Fig. 3.15: a) θ/S -diagram for section 4 (sta. no. 180-204, 223, 224) showing large variations for surface water masses and the Upper Circumpolar Deep Water (UCDW), and b) XBT-section II connecting the CTD-section 4 (sta. no. 204) and the coastline at 10°E (see also Fig. 3.9). Areas marked with dotted lines $t < -1.5^\circ\text{C}$.

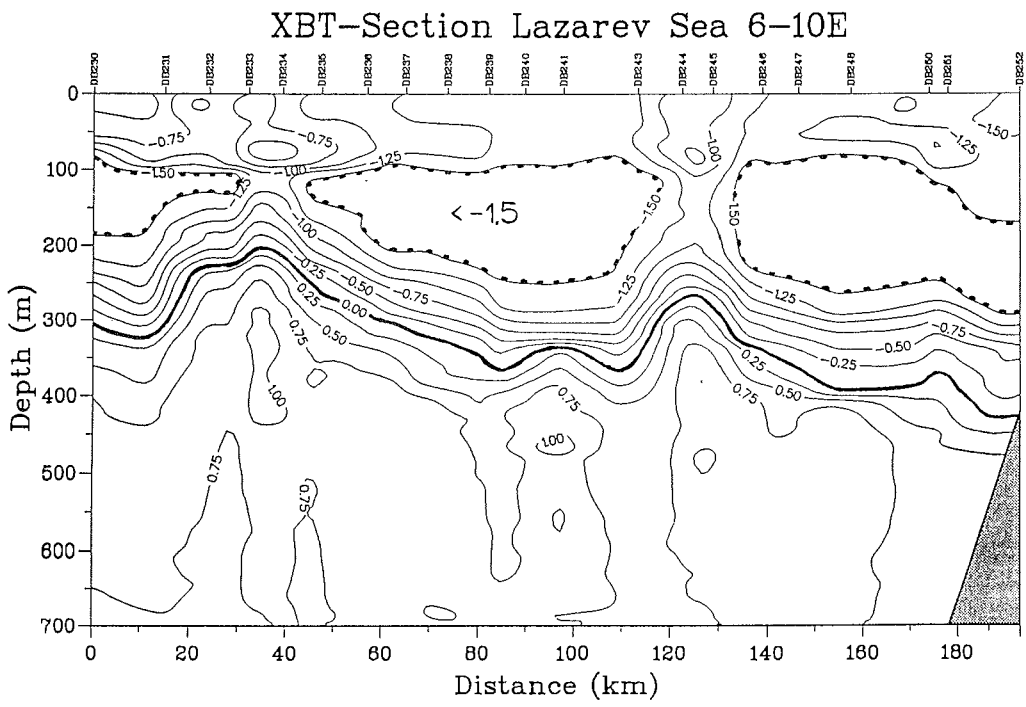
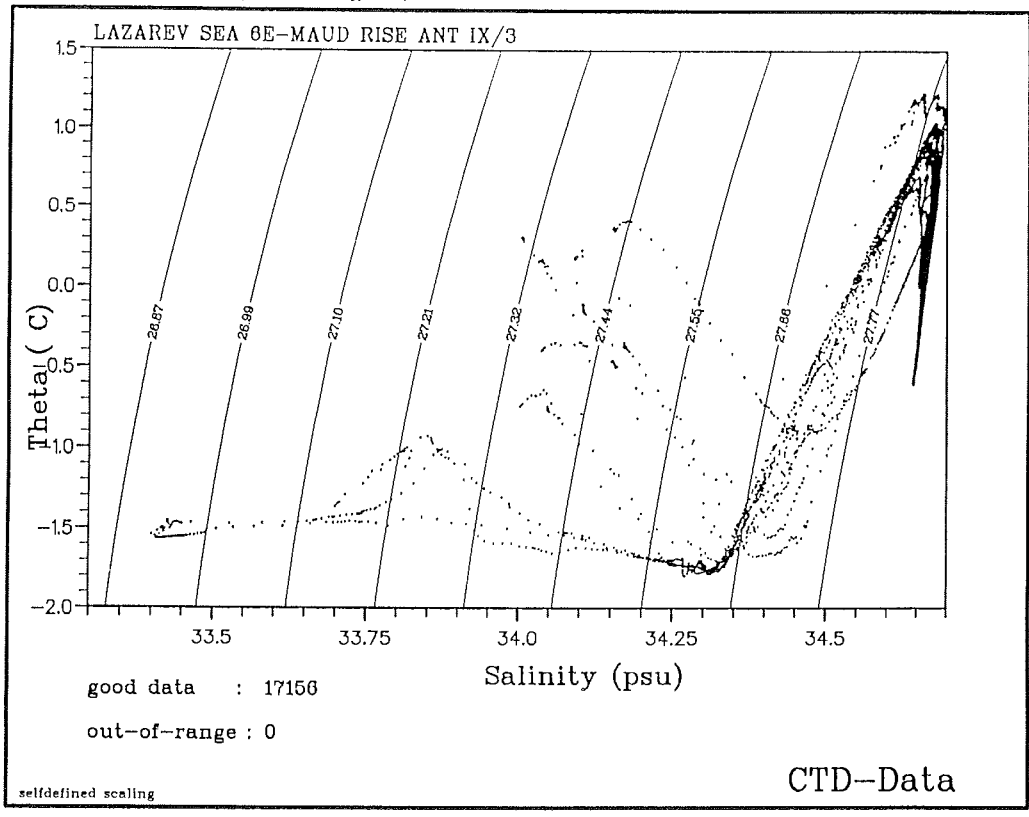


Fig. 3.16: a) XBT-section III from early January and b) XBT-section IV from the end of March between Maud Rise and the shelf break. For comparison, both sections have equal horizontal distance. Heavy lines denote $\theta=0.0^{\circ}\text{C}$ and $S=34.60$ PSU.

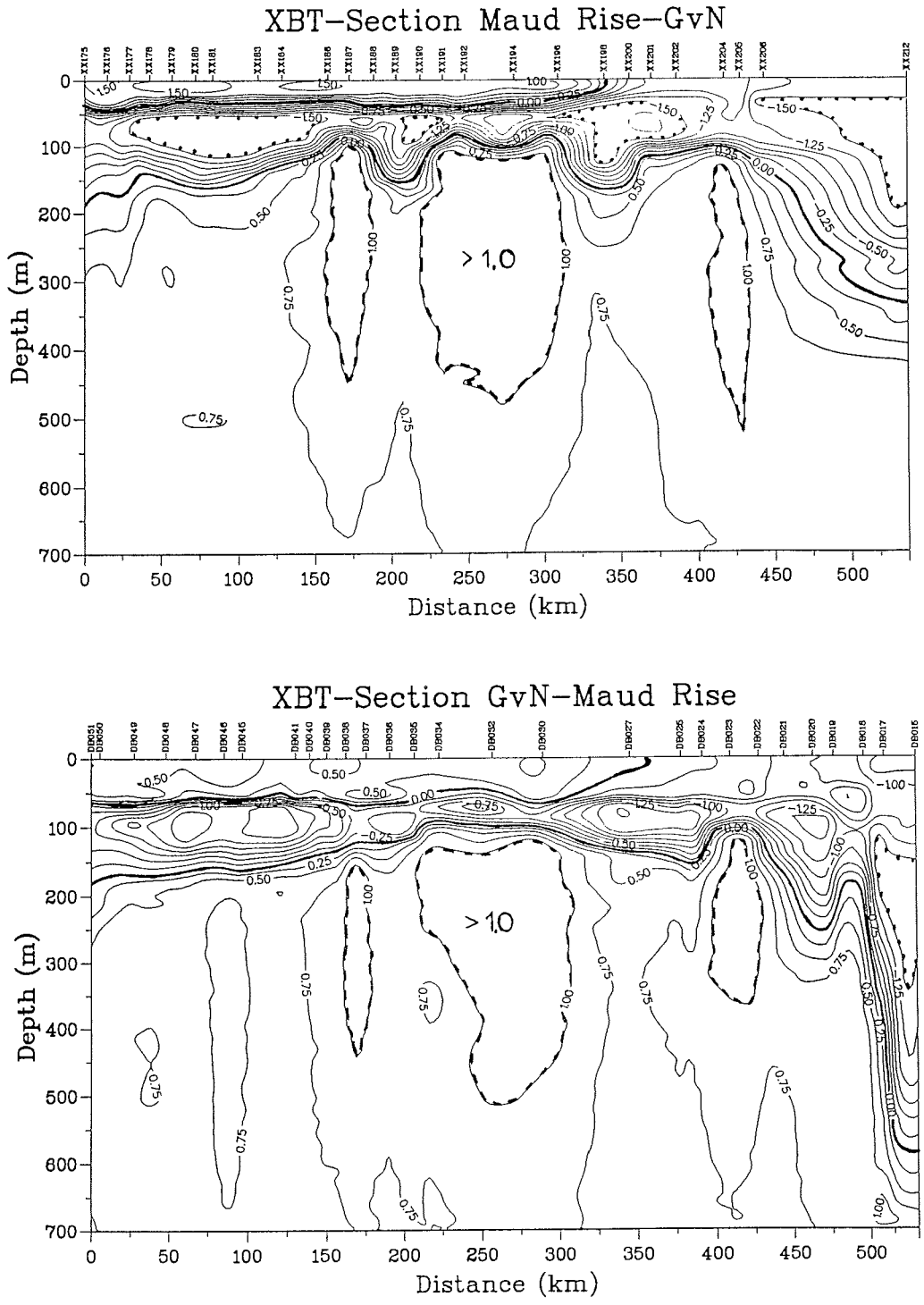


Fig.3.17: a) Bottom topography and oceanographic stations in the Lazarev Sea. The hatched areas denote locations of warm cells south of Maud Rise. Cold blobs in the coastal current are marked by cross hatching.
b) XBT-section IV in full length between Georg v. Neumayer and Maud Rise to show the temperature variations in the regime of the coastal current. Broken line marks areas with $t > +1.0^{\circ}\text{C}$, the dotted line regions with $t < -1.5^{\circ}\text{C}$.

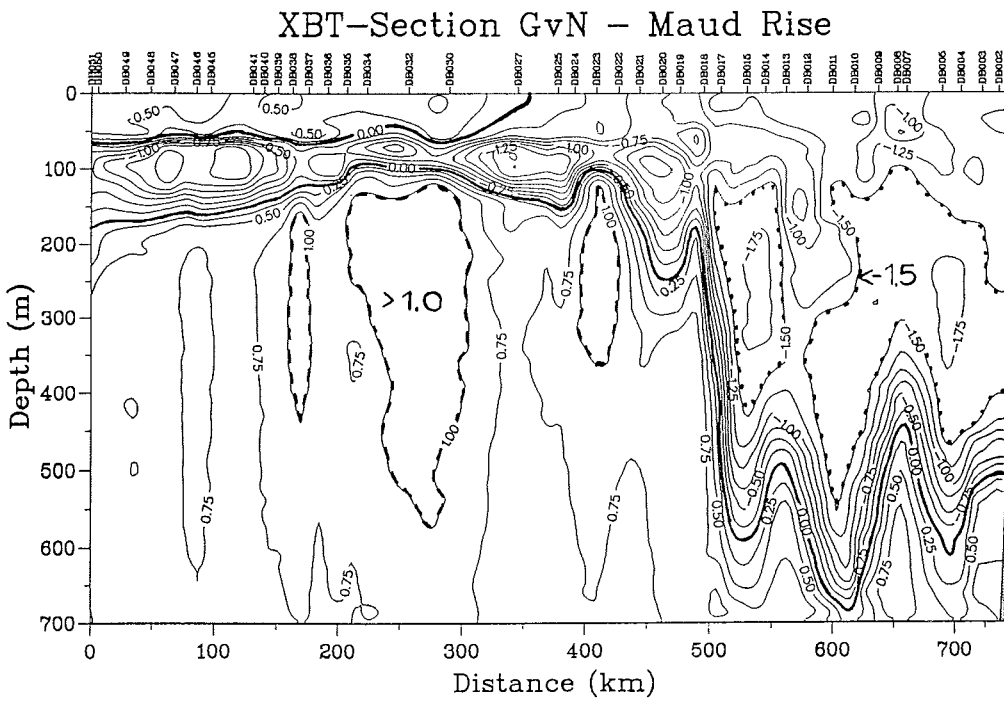
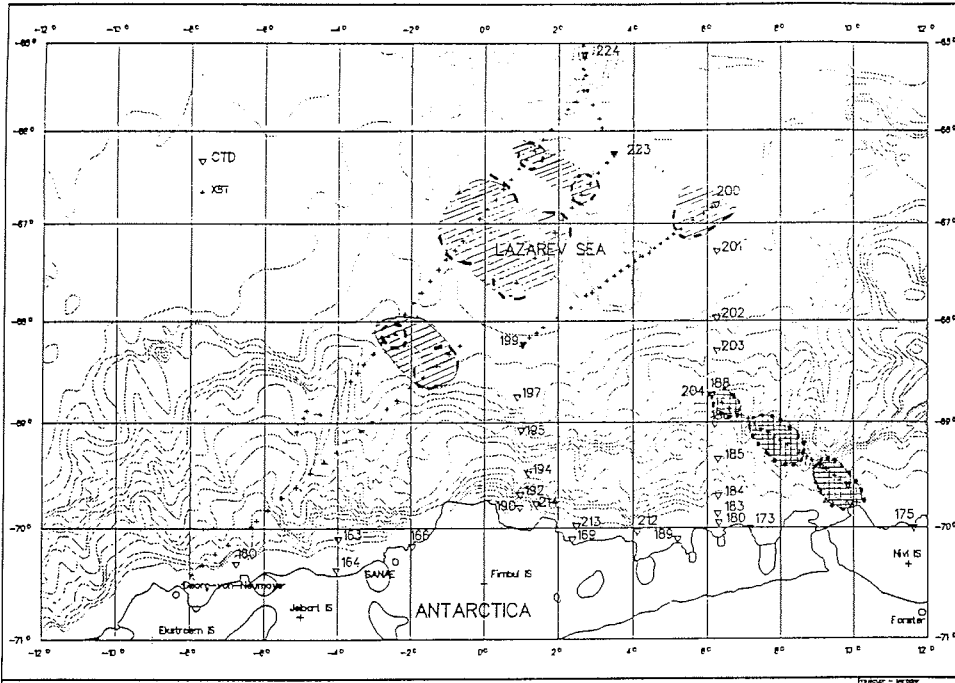


Fig.3.18: a) January transect from Cape Town to the ice edge near Georg v. Neumayer for temperature (T) and salinity (S) from the thermosalinograph on board POLAR-STEPIN (8 m depth). b) Same transect for XBT (part of which is section III). Included are the positions of the Subtropical Front (STF), Subantarctic Front (SAF), and the Polar Front (PF), which are defined by the crossing of the 10°C, 5°C, 2°C isotherm with the 200 m depth level. In addition the Continental Water Boundary (CWB) and the Maud Rise area (MR) are marked. The heavy line stands for the temperature minimum layer south of the PF, whereas the warm cells around Maud Rise are sketched by the broken line

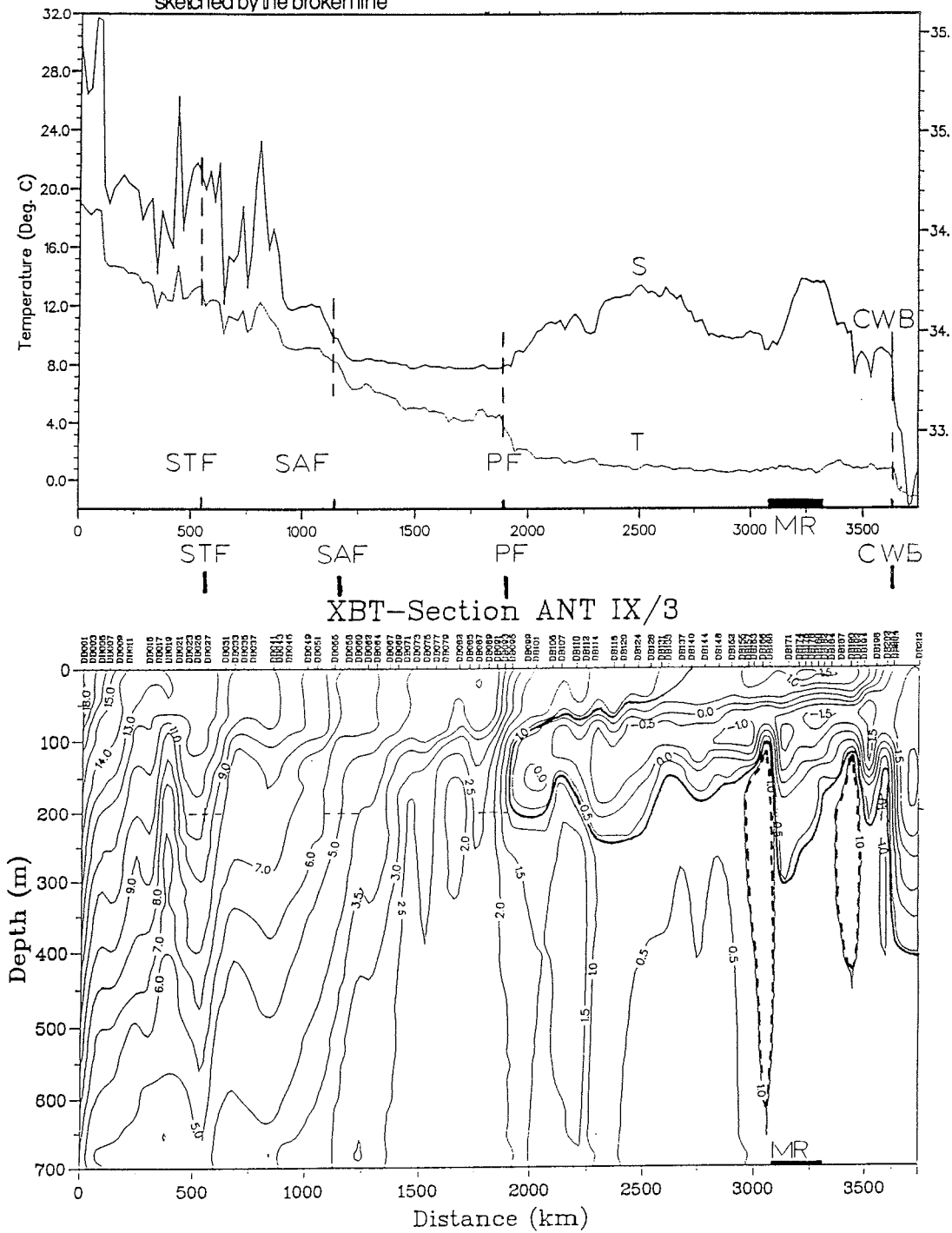
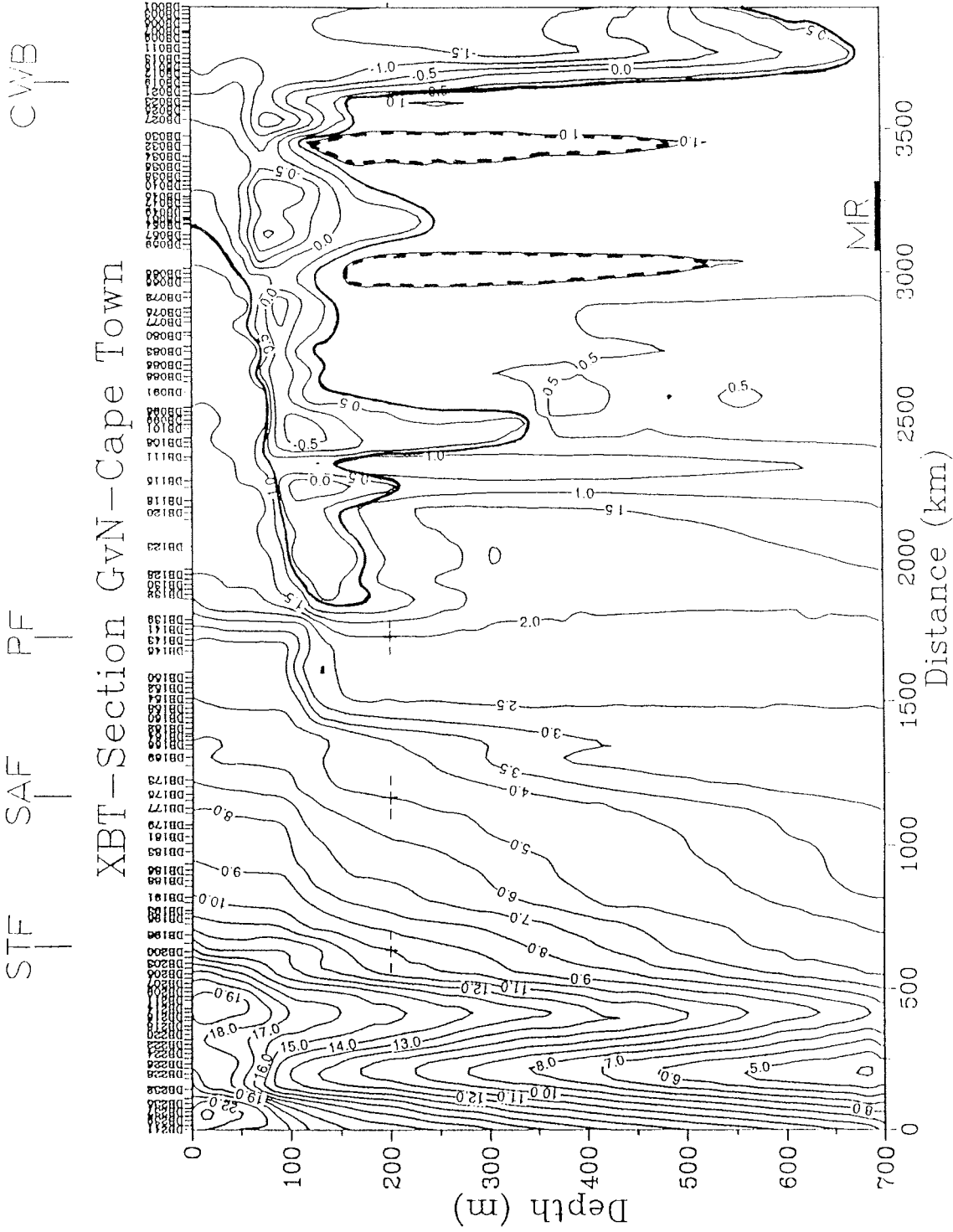


Fig.3.19: March XBT-transect from Georg v. Neumayer to Cape Town
Abbreviations as in Fig. 3.18



Comparison of both XBT-sections from and to Maud Rise yielded an excellent correspondence of the positions of warm cells southwest of the seamount (Fig. 3.16a). The stability of these cells during the whole summer season as sketched in Fig.3.17a is quite amazing. Differences in the heat content due to summer heating at the surface as well as in the winter water layer within a three month period is clearly seen in the top 150 m of Fig. 3.16b. Overall the temperature increased by more than 0.5°C in the WW-stratum but decreased in the top 50 m by 1.0°C at the end of March. This effect is explained by wind mixing by heavy storms and slight cooling due to the beginning winter season.

Looking at an expanded XBT-section from Atka-Bay to Maud Rise (Fig. 3.17b) the concentration of isotherms 250 km from the coast with a large horizontal gradient in the depth of 200 m - 550 m is evident. It marked the transition from warm water inside the gyre to the cold regime of the coastal current also known as the Continental Water Boundary (CWB). The depth variations of the pycnocline of more than 200 m could be an effect of the complicated bottom topography in this part of the shelf.

The positions of the Subantarctic Front (SAF), the Polar Front (PF), and the Continental Water Boundary (CWB) between Cape Town and Atka Bay is clearly visible both in the enroute registration of the Thermosalinograph and the hourly launched XBTs. The Subtropical Front (STF) is only detectable in the XBT-section. The crossing of the 10°C isotherm with the 200 db depth level is hard to trace, because of the complicated flow structure of the Agulhas retroflexion. As an example, the data of both instruments during the first transect in January are shown in Fig.3.18a, b. Three months later on our way back to Cape Town the general picture looked fairly similar with some specific changes. These indicate a shift of the Polar Front of about 80 km to the north and a large increase of temperatures (3-4°C) north of the Subtropical Front near the African continent (Fig. 3.19). There the dynamics of the Circumpolar Current and the Agulhas system were also intensified which can be seen by strong horizontal temperature gradients together with large vertical variations of the isotherms which are caused by eddies and meanders. Another difference is the thinner winter water layer south of the Polar Front due to summer heating from above. The $\Theta = 0.5^\circ\text{C}$ isotherm which marked the transition to the Antarctic coastal current decreased by 250 m to a depth of 680 m.

References

- Bagriantsev, N.V.; Gordon, A.L.; Huber, B.A. (1989). Weddell Gyre: temperature maximum stratum. *J. Geophys. Res.*, 94, 8331-8334
- Fahrbach, E.; Rohardt, G.; Schlosser, P.; Bayer, R. (1991). Suppression of bottom water formation in the southeastern Weddell Sea shelf due to melting of glacial ice. submitted to *Deep-Sea Res.*
- Gordon, A.L.; Huber, B.A. (1990). Southern Ocean winter mixed layer. *J. Geophys. Res.*, 95, 11.655-11.672
- Hellmer, H.H.; Bersch, M.; Augstein, E.; Grabemann, I. (1985). The Southern Ocean. *Ber. Polarforsch.*, 26, 115 pp.

4.1.1 Oceanographic tracer studies, ^3H , ^3He , ^4He , ^{18}O , AMS- ^{14}C and chlorofluoromethanes (CFM)

G. Boenisch (IUP)

Objectives

The main objectives of the tracer oceanographic program of this cruise are to

- take samples of the characteristic water masses of the Weddell Sea of time dependant tracers (tritium, CFM and ^{14}C),
- check the ^{14}C -input function of Surface Water and Winter Water as described in Schlosser et al. (1989),
- to determine the tracer content of the coastal current (tritium, CFM, ^{18}O , ^3He),
- to determine the temporal and local size of the layers of Surface Water, Winter Water and Circumpolar Deep Water (^3He , ^4He , neon),
- to determine the entrainment of Circumpolar Deep Water into the Winter Surface Layer (^3He , neon) and
- to complete a section started during the ANT V/4 cruise from the Antarctic Peninsula into the central southwestern Weddell Sea to the eastern coast (^3He , tritium).

Work at sea

A total of 418 samples were taken at 36 stations for the analysis of either ^4He , ^3He and neon or CFM. The samples have been stored in pinched-off copper tubes. The He/Ne-samples will be analysed using a special helium isotope mass spectrometer as described in Bayer et al. (1989). CFM will be measured using gas chromatography. The technique to measure CFM from copper tube samples is not yet established. On shore, analyses of CFM from copper tubes will be tried for the first time in Heidelberg.

On the same stations 385 samples have been taken for the analysis of tritium and ^{18}O . The tritium-samples have been stored in 1 l - glass bottles. They will be analysed via ^3He ingrowth with the same mass spectrometer mentioned above. ^{18}O -samples have been stored in 100 ml glass bottles and will also be measured with a commercial stable isotope mass spectrometer.

Six samples for ^{14}C measurement by AMS have been collected at 1 station. The samples are stored in pre-evacuated 1 l glass bulbs and are poisoned by addition of HgCl_2 . The procedures of CO_2 extraction and target preparation are described in Schlosser et al. (1987). Measurement will be done at the ETH/SIN AMS facility in Zürich.

Preliminary Results

As all measurements must be done on shore, preliminary results are not available.

References

- Bayer, R.; Schlosser, P.; Boenisch, G.; Rupp, H.; Zaucker, F.; Zimmek, G. (1989). Performance and blank components of a mass spectrometric system for routine measurement of helium isotopes and tritium by ^3He ingrowth method. Sitzungsberichte der Heidelberger Akademie der Wissenschaften, Mathematisch-naturwissenschaftliche Klasse, Jahrgang 1989, 5. Abhandlung: 241-279.
- Schlosser, P.; Kromer, B.; Bayer, R.; Muennich, K.O. (1989). ^{14}C -Profiles in the Central Weddell Sea. Radiocarbon, Vol 31, No. 3, 544-556.

Schlosser,P.; Pfeleiderer,C.; Kromer,B.; Levin,I.; Muennich,K.O.; Bonani,G.; Suter,M.; Woelfli,W. (1987). Measurement of small volume oceanic ^{14}C samples by accelerator mass spectrometry. Radiocarbon, v 29, No. 3, 347-352.

4.1.2. Measurements of turbulent fluctuations of temperature and current velocity at long ice stations.
M. Schröder (AWI)

Turbulence measurements during two long stations were realized which gave 22 and 33 hours of nearly continuous data sets. The large scale roughness of these ice floes with 300 * 300 m size and a mean ice thickness of 2.2 m and a snow cover of 0.26 m was measured by drilling two traverses diagonally across each floe. Measurements of the fluctuating part of current velocities and temperature should complement investigations which were done in late winter conditions 1989 to give the vertical turbulent momentum and heat fluxes in the oceanic boundary layer below the sea-ice. Together with profiles (0 - 50 m), long time series of the physical parameters in the top 10 m of the water column were performed. During the drift of the enclosed ship 7 CTD profiles with the ships CTD were done.

4.1.3. Sea ice motion and mixed layer dynamics by meteorological ARGOS buoys.

Strongly changing ice conditions led to a different form of buoy array as planned. The polygone consisted of one central buoy surrounded by four systems measuring atmospheric pressure and air temperature. Thermistor chains attached to the central buoy give the vertical temperature both in the mixed layer and in the sea-ice. The maximum distance between the buoys was restricted to 90 km of which the positions are shown in Fig. 3.8

4.2. Sea ice and plankton ecology

An interdisciplinary investigation of the physical properties of sea ice and its biota was carried out at 1 fast ice and 14 pack ice stations. Our main aim was to study both the abundance (bacteria, flagellates, diatoms, ciliates, foraminifera, metazoa) and the activity (bacteria, algae) of sea ice organisms in various habitats and to evaluate the significance of this community in the Weddell Sea ecosystem.

Plankton ecology studies were carried out on time series drifting stations in the southeast Weddell Sea in the water column under pack ice (24 under-ice profiles) and on transects perpendicular and parallel to the coast in largely ice-free waters (59 profiles). The vertical distributions of particulate matter, bacteria (biomass and production), phytoplankton (biomass, species composition and production) and zooplankton (biomass and species composition) were determined in relation to the physical and chemical characteristics of the respective water masses. In addition to these vertical hauls, continuous surface water measurements (10 - 120 min intervals) of chlorophyll *a* were obtained on all transects.

4.2.1. Sea ice physics and chemistry

R. Gradinger, J. Weissenberger (AWI)

PAR intensity (400-780 nm) was measured through the core hole down to 20 m depth using a LICOR 4π underwater sensor in conjunction with a 2π reference sensor and a L11000 data logger. In Fig. 3.20 typical light intensity distribution is shown in and below a 1.6 m thick floe. Under the ice in all cases the relative light intensity was below 1% of surface radiation.

Ice cores were taken using a 4" CRELL SIPRE ice auger. Immediately after coring, ice temperature was measured in 5 cm intervals (Fig. 3.21). The temperatures were close to the melting point (AN9302001), the profiles of the cores AN9301401 and AN9303801 indicate the heating of ice by light absorption in the upper decimetres of the floe. After the temperature measurements the cores were stored unsectioned at $-27\text{ }^{\circ}\text{C}$ for later textural analysis.

Three inch ice cores (modified SIPRE corer) were sectioned in 5 cm intervals and centrifuged in order to obtain brine samples. Salinity (Fig. 3.21), ammonia and Chl *a* concentrations were measured on board, samples for other nutrients and isotope ($^{16}\text{O}/^{18}\text{O}$) measurements were taken for later analysis. Measured brine salinities of usually less than $34 \cdot 10^{-3}$ indicate the dominance of melting processes. Melted ice core sections were used for the determination of total salt content of the ice, Chl *a*, (Gradinger, Weissenberger) particulate Si and POC, PON (Bathmann, Scharek) and lipids (Fahl).

For the measurements on pH and compartments of the carbonate system see report of Michiel v.d.Loeff.

Fig. 3.20: Light distribution below a 1.6 m thick ice floe without (HF) and with (DF) a 40 cm snow cover.

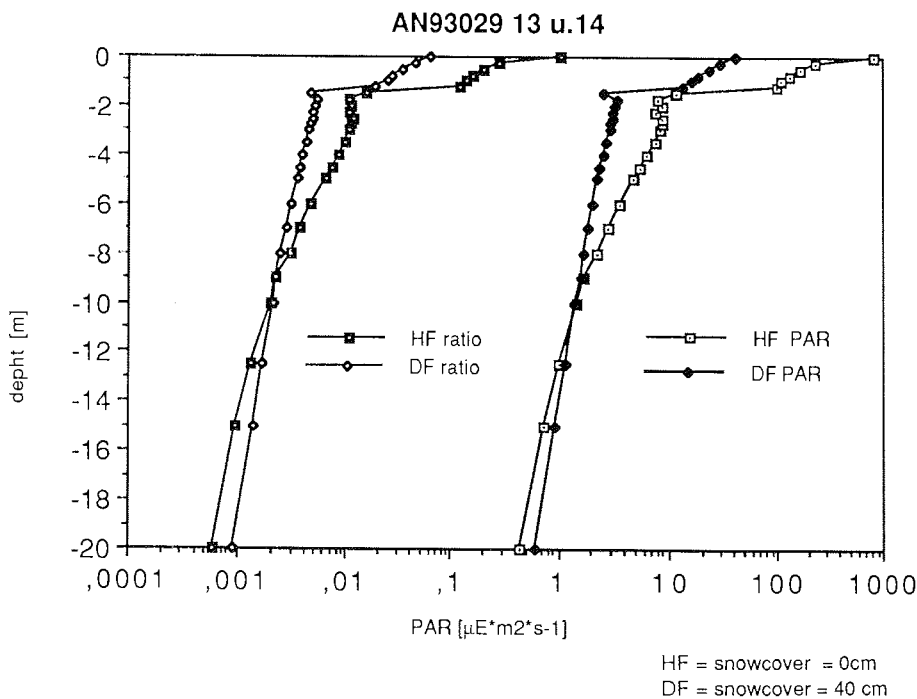
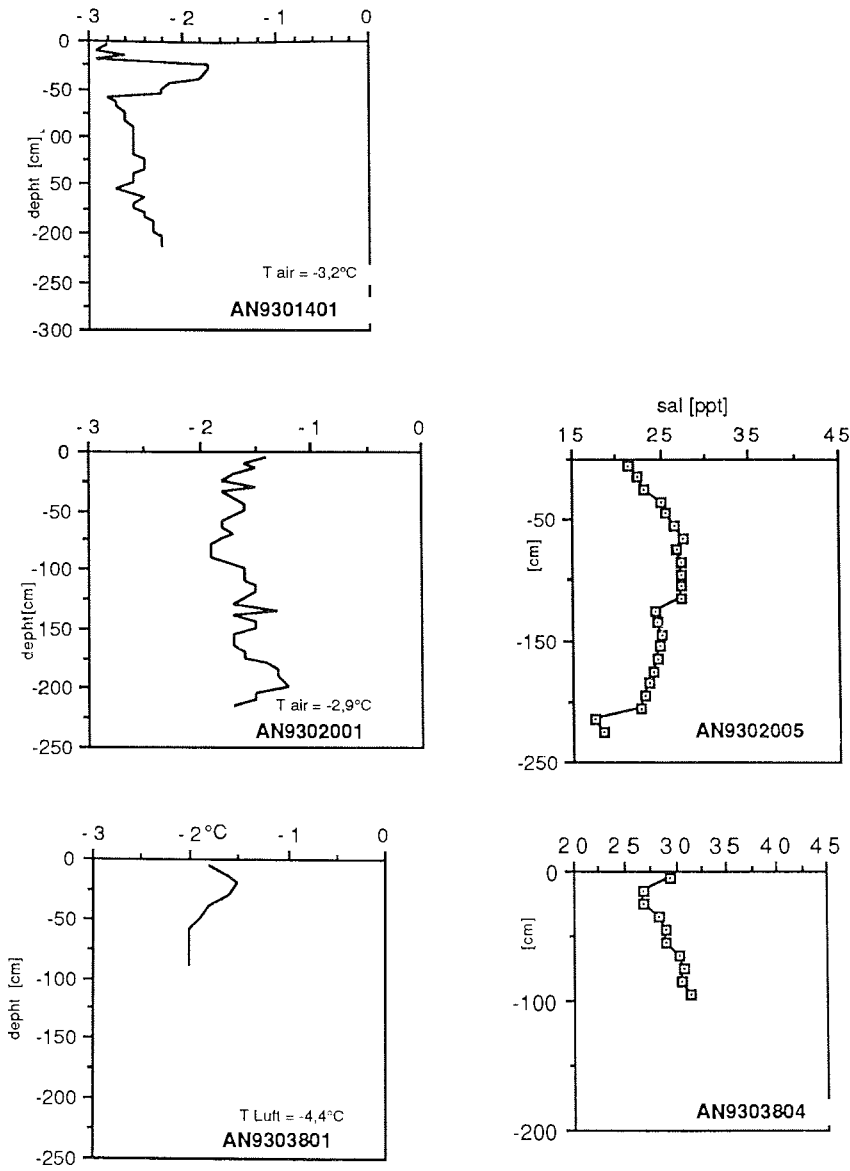


Fig. 3.21: Temperature (°C) and brine salinity ($\cdot 10^{-3}$) profiles of 3 ice cores, measured in 5 cm intervals.



4.2.2 Sea ice ecology

U. Bathmann, K. Beyer, K. Fahl, M. Gleitz, R. Gradinger, S. Grossmann, R. Scharek, S. Schröder, J. Weissenberger (AWI)

4.2.2.1. Photosynthetic capacity and carbon metabolism of different ice algal communities.

M. Gleitz (AWI)

Objectives

The biology of microalgal communities in pack ice of the south-eastern Weddell Sea in late summer and fall is influenced by ice melt and new ice formation. Accordingly, microalgae were encountered in numerous habitats within various forms of melting sea ice (at times mixed with snow in "porridge" ice), in open water trapped between floes of pressure ridges, platelet ice beneath floes in the vicinity of floating ice shelves as well as in different stages of newly formed ice. Extensive new-ice formation was observed in the first weeks of March in open water along the ice shelf between 4° - 11°E, commencing with ice crystals accumulating on the surface in long streaks reflecting Langmuir convection cells. Loosely floating pancake ice as well as larger floes of congregated pancake ice were also observed only days later.

Physical accumulation processes such as scavenging of particles by ascending ice crystals or wave induced pumping of water through newly formed ice fields as well as the physiological capacity of the organisms primarily determine the composition of microalgal communities within and beneath sea ice. Productivity and physiological status of algal species vary in response to changes in light availability, nutrient concentration and salinity, which are associated with spatial and/or temporal variations within the ice environment. For example, massive lipid accumulation was observed during this cruise in some diatom species associated with platelet ice, which was tentatively interpreted as an indication of nutrient deprived metabolism. The pattern of incorporation of radio-labelled carbon into the main end products of photosynthesis (carbohydrates, lipids, proteins and low molecular weight metabolites) may therefore provide information about such variations and may reflect physiological survival strategies of the algae.

Previous investigations have emphasized the high production potential of ice algal communities during austral spring, production data on summer and fall communities, however, are scarce. The multitude of ice algal communities encountered during this cruise provided an opportunity to fill this gap in order to gain a more comprehensive picture of the seasonal pattern of primary production and the dynamics of sea ice algae in the south-eastern Weddell Sea.

Work at sea

Sampling: Exposed sea water between floes of pressure ridges as well as ice from infiltration layers were sampled with a plastic bucket. In some cases, when only a limited volume of algal material could be collected, approx. 0,25-0,5 l of the ice-water mixture was diluted in 3-5 l of filtered seawater (FSW) to prevent a decrease in salinity when melting. On one occasion, a large, solidly frozen ice block lying on the surface of a floe (where it had been deposited during compressional break-up of the ice sheet) was sampled in order to test the capability of the enclosed algae to photosynthesis after resuspension in

sea water. Sea water adjacent to or beneath ice floes was sampled in 5 l glass bottles by means of an L-shaped plastic tube connected to a vacuum pump ("L-se"). A 10 cm section of an ice core drilled with a SIPRE ice auger (\varnothing 7,6 cm) was allowed to melt at 1°C in 5 l of FSW (inner ice sample). Additionally, several 10 cm sections of 4 ice cores taken at 50-100 cm ice depth were centrifuged at 1450 rpm for 5 min. at -2°C; the accumulated brine was diluted with FSW. New-ice samples (pancake ice or water next to pancake floes) were taken close to the ship with a wire box lowered into the water or a plastic bucket. Approx. 350-450 ml of pancake ice were thawed in 3 l of FSW at 1°C for about 12 hours. All other phytoplankton samples were taken with Niskin bottles from the upper 10 m of the water column.

Potential growth rates: Determination of photosynthetic capacity was carried out using standard ^{14}C -techniques. After taking salinity and alkalinity subsamples, 50-100 ml of sample were inoculated with approx. 5-10 μCi of $\text{NaH}^{14}\text{CO}_3$ (Amersham Buchler) and incubated for 5 hours at -1°C at 3-4 photon flux densities ranging from 50-400 $\mu\text{moles m}^{-2}\text{s}^{-1}$ (adjusted with a 4π light sensor [LICOR 193 SB] connected to a quantum meter [LICOR 185 B]) in a temperature controlled incubator in the laboratory on board. A parallel set of samples for determination of photosynthate allocation were incubated for 10 hours under identical conditions and subsequently filtered onto GF/C filters (Whatman), which were stored at -27°C awaiting further processing in the home laboratory. Samples were counted (Packard TriCarb 1900) and quench correction was performed by automatic external standardization. In all incubation series, at least two samples were exposed to high light intensities to obtain the P_{max} -value. Evaluation of the radio-labelled dissolved organic carbon content of the filtrate by means of various acidification and bubbling techniques did not result in reliable and reproducible values and was therefore omitted in later experiments. The chlorophyll *a* biomass of the samples was determined fluorometrically. Potential growth rates were calculated according to the equation of El Sayed & Taguchi (1981) under the following assumptions: Algal standing stock was determined using a carbon to chlorophyll ratio of 30 (El Sayed & Taguchi, 1981). Calculation of potential growth rates was based on daily production estimates that were normalized to a 24 hour period of saturating light levels, which clearly is an unrealistic description of the real situation.

Experiments: In order to gain a more realistic picture of primary production of ice communities exposed to direct sunlight, 3 water samples collected amongst floes were incubated under ambient conditions: A 40x60x40 cm plastic container was half filled with snow and 3 chambers with photon flux densities corresponding to 100, 50 and 25% of downwelling solar radiation (adjusted with a 4π sensor, see above) were set up using neutral density filters. The container was placed approx. 100 m away from the ship on the floe. A 4π and a 2π sensor (LICOR) were set up next to the container and connected to a LICOR datalogger in order to record the photon flux over the experimental period (approx. 22 hours). In a parallel set of samples, 100 ml of algal suspension were inoculated with 5 μCi of $\text{NaH}^{14}\text{CO}_3$. The experiment was started at 19:40 hours local time and stopped at 17:00 hours the next day. Air temperatures were in the range of -6,5° to - 8,5°C, and the sun shone for most of the time.

In a second lab experiment, the impact of salinity variation on carbon incorporation was investigated using melt pool water sampled after removing the 3 cm ice covering (initial salinity: 32,4 p.p.t.). Subsamples of 1 liter were diluted in a 2:1 or 1:2 mixture of FSW and "Milli Q" - water (Millipore), giving salinities of 24,9 and 17,1 p.p.t., respectively. Nutrients equivalent to f/2 were added to all samples in order to exclude any nutrient effects on the metabolic patterns. Samples were stored at 0°C at a continuous photon flux density of approx. 60 $\mu\text{moles m}^{-2}\text{s}^{-1}$. After 24 and 72 hours, 100 ml subsamples from the stock cultures were inoculated with 10 μCi of $\text{NaH}^{14}\text{CO}_3$ and incubated at 3 light intensities (100-400 $\mu\text{moles m}^{-2}\text{s}^{-1}$) at -1°C for 10 hours. Filtration of productivity (in-situ exp. only) and photosynthate samples was conducted as described above.

Preliminary Results and Conclusions

Potential growth rates: Estimates of production for the different ice communities are depicted in Tab. 3.7. An important result of this investigation is the low production capacity of the ice- and phytoplankton samples associated with floes in austral summer, where average P_{max} -values do not exceed 0,53 mg C (mg Chl *a*)⁻¹ h⁻¹. These values are considerably lower than data obtained for infiltration communities during austral spring (Gleitz & Kirst, in press; Lancelot & Mathot, 1989). It may be hypothesized that microalgal communities at the onset of fall are in a stagnant, post bloom situation, where nutrient depletion (in conjunction with other factors) prevents high production rates. Visual observation of melting pieces of ice or ice/water samples obtained from the infiltration layer revealed that most of the algal material is released from the ice in the form of large aggregates with relatively high sinking velocities. Interestingly, the production potential of phytoplankton in close proximity to the floes, where biomass (expressed as Chl *a*) is generally much lower, is very similar to that of microalgae within the ice. This may have been the result of ice algae being released from the ice, thus contributing to under-ice or surface-water phytoplankton between the floes. On the other hand, low P_{max} -values may also reflect shade adaptation, as some samples were obtained directly from the low light conditions beneath the floes (Weissenberger, this report). In contrast, phytoplankton from new-ice and from the polynya on the south-eastern continental shelf displayed higher production rates with average P_{max} -values above 0,86 mg C (mg Chl *a*)⁻¹ h⁻¹ and a potential doubling time of 0,75-1.0 d⁻¹.

This implies that some phytoplankton species accumulate on the sea surface during new ice formation due to physical accumulation processes. Entrapment prevents these cells from being mixed out of the euphotic zone by the destruction of the seasonally stratified upper water column. The high photosynthetic activity enables these organisms to take advantage of the stable light conditions on the sea surface without a prolonged adaptational lag period, which may enable rapid growth within the newly forming sea ice. It is, therefore, suggested that active growth contributes significantly to high microalgal standing stock in new-formed sea-ice prior to the polar winter.

Experiments: Tab. 3.8 shows the production parameters for the 3 melt pool samples for various light intensities. In all samples, P_{max} and growth rate increased several fold with decreasing photon flux density, reaching maximum values at 25% of incoming solar radiation. Due to the high albedo of snow, the flux of quanta measured with the spherical sensor presumably is a

Tab. 3.7: Standing stock, photosynthetic capacity and potential growth rate of ice- and phytoplankton communities

Sample	Date	Chl a ($\mu\text{g} / \text{l}$)	PS-Capacity ($\text{mg C}/\text{mg Chl a h}$)	Pot. Growth (divisions / d)
1) Ice floes				
under-ice com.	21.1.	16,10	0,35	0,36
brown water with platelets	23.1.	31,40	0,56	0,53
melt pool in pressure ridge	24.1.	19,55	0,29	0,30
melt pool in pressure ridge	24.1.	8,74	0,53	0,51
melt pool in pressure ridge	1.2.	3,11	0,80	0,71
ice block sample	29.1.	64,41	0,74	0,67
platelet ice	20.1.	458,64	0,07	0,08
platelet ice	22.1.	225,50	0,14	0,15
infiltration com.	6.2.	56,36	0,23	0,24
infiltration com.	11.2.	71,32	0,61	0,57
inner ice com.	10.2.	6,01	0,23	0,24
inner ice com.	10.2.	54,27	0,54	0,52
			0,42 \pm 0,24	0,41 \pm 0,21
2) Phytoplankton associated with floes				
depth profile (surface water):	25.1.			
a) 10 cm		10,81	0,73	0,66
b) 50 cm		4,81	0,61	0,57
c) 95 cm		4,51	0,49	0,48
surface water	26.1.	0,76	0,49	0,48
under-ice sample	26.1.	0,55	0,46	0,45
under-ice sample	26.1.	19,27	0,53	0,51
surface water with platelets	2.2.	10,70	0,44	0,44
surface water with platelets	2.2.	1,31	0,28	0,29
under-ice phytoplankton	21.1.	0,24	0,63	0,59
under-ice phytoplankton	28.1.	0,24	0,67	0,62
			0,53 \pm 0,13	0,51 \pm 0,11
3) New-ice				
brown-ice between pancakes	9.3.	50,61	1,30	1,03
surface water with ice crystals	10.3.	2,77	1,16	0,95
pancake ice	9.3.	63,33	0,75	0,68
pancake ice	10.3.	205,43	0,58	0,55
pancake ice	11.3.	42,22	0,60	0,57
pancake ice	11.3.	38,59	0,78	0,70
			0,86 \pm 0,30	0,75 \pm 0,20
4) Phytoplankton (coastal polynya)				
Stat. 160	16.2.	2,76	1,27	1,01
Stat. 163	17.2.	2,76	1,19	0,97
Stat. 164	17.2.	2,53	0,68	0,63
Stat. 166	18.2.	1,96	1,52	1,15
Stat. 173	20.2.	2,04	0,99	0,84
Stat. 175	21.2.	1,88	1,37	1,07
Stat. 180	23.2.	1,55	1,84	1,31
Stat. 183	23.2.	1,67	1,89	1,33
Stat. 184	24.2.	1,67	1,20	0,97
Stat. 189	26.2.	1,67	1,32	1,04
Stat. 190	27.2.	1,27	1,32	1,04
			1,33 \pm 0,34	1,03 \pm 0,20
Tab. 1: Standing stock, photosynthetic capacity and potential growth rate of ice- and phytoplankton communities.				

Tab. 3.8: Standing stock, photosynthetic- and growth rates of 3 melt pool communities incubated under natural conditions (29.-30.1.91)

Sample	Chl a ($\mu\text{g} / \text{l}$)	PS-Rate ($\text{mg C}/\text{mg Chl a h}$)	Growth (divisions / d)	Av. Photon Flux ($\mu\text{moles}/\text{m}^2 \text{ s}$)	Rel. Irradiation
melt pool I	1,90				
		0,02	0,02	1840	100%
		0,17	0,18	820	50%
		0,19	0,20	460	25%
melt pool II	0,82				
		0,06	0,07	1840	100%
		0,22	0,23	820	50%
		0,23	0,24	460	25%
melt pool III	18,86				
		0,02	0,02	1840	100%
		0,25	0,26	820	50%
		0,36	0,37	460	25%

Tab. 2: Standing stock, photosynthetic- and growth rates of 3 melt pool communities incubated under natural conditions (29.1.-30.1.91).

better estimate of the light energy the algae in their natural environment actually experience. Considering these values, the photon flux density was above $1000 \mu\text{moles m}^{-2}\text{s}^{-1}$ for most of the incubation period, reaching peak values around $3500 \mu\text{moles m}^{-2}\text{s}^{-1}$ at around noon. Obviously, strong photoinhibition (along with some ice formation in the 100% light bottles beginning after approx. 10 hours) decreased photosynthetic activity in all samples. Even the 25% light samples displayed growth and photosynthetic rates considerably lower than average values calculated from other P_{max} determinations (see Tab. 3.7). As a consequence, the production potential of phytoplankton in the ice or associated with it during summer probably is smaller by more than one order of magnitude than previously thought. However, due to the difference in ice environment and due to the decrease in downwelling irradiance this is true to a lesser extent for new-ice samples. In new-ice, potential growth rates presumably more realistically reflect actual production.

References:

- El Sayed, S.Z.; Taguchi, S. (1981). Primary production and standing crop of phytoplankton along the ice-edge in the Weddell Sea. *Deep Sea Res* 28:1017-1032.
- Gleitz, M; Kirst, G.O. (1990). Photosynthesis - irradiance relationships and carbon metabolism of different ice algal assemblages collected from Weddell Sea pack ice during austral spring (EPOS1). *Pol Biol* (subm.)
- Lancelot, C; Mathot, C. (1989). Phytoplankton: Photosynthesis, growth and respiration. *Ber. Polar Forsch.* 65: 78-86.

4.2.2.2. Microbiology of sea ice

S. Grossmann, K. Lochte (AWI)

Objectives

Biological conditions of sea areas covered with ice are different in many parameters from those of the open ocean surface. Extreme salinity and temperature ranges may affect the organisms as well as limited exchange rates of O₂, CO₂ and nutrients. On the other hand, enhanced algal concentrations can be associated with sea ice (brown ice). Microbiological investigations of ice focussed on the role of bacteria within the ice community. Bacterial numbers and biomass, bacterial growth and activity were determined. The following questions were considered:

- What differences in bacterial activity can be measured for ice, brine and water associated with ice?
- Is it possible to distinguish different ice types (pancake ice, pack ice / fast ice, platelet ice) with regard to bacterial numbers, bio-mass and activity? Are different stages of ice succession, including formation of new ice, reflected in microbiological parameters?
- How do bacteria react to high phytoplankton concentrations in ice (brown ice)?
- How applicable are microbiological "standard" methods to the investigation of sea ice?

Work at sea

In the Weddell Sea and on the eastern shelf region microbial investigations were carried out on various sea ice types and water samples associated with ice. Floes were sampled using a 3'' ice auger. The ice cores were cut in the field into 10 cm pieces. Platelet ice, slush ice and new ice was sampled by hand using a ladle or a bucket. Water samples under and between ice floes were obtained by a hand-operated, L-shaped suction tube ("L'se") or by rosette water sampler from the ship. In the lab, the ice samples were centrifuged for 15 min (450g) to separate the brine from ice crystals. After centrifugation, the remaining ice was melted. Alternatively, ice samples were just sieved or the ice core was melted without separation of brine and ice. To compensate a decreasing salinity by melting ice crystals, standard sea water salt was added during the melting process. The centrifuged or sieved brine, the melted ice and ice samples melted in total were used for the determination of the following parameters:

- Bacterial numbers and biomass by direct epifluorescence microscopy.
- Leucine turnover time and leucine incorporation rate as a measure for biomass production using ³H-labelled leucine as substrate.
- Thymidine incorporation rate as a measure of division rate using ³H-labelled thymidine.
- Percentage of actively metabolizing cells using micro-autoradiography technique with ³H-leucine as substrate (Hoppe 1976, Tabor & Neihof 1982).

The methods are described in more detail in section 4.2.3.2.

Bacterial respiration was determined in an experiment using ¹⁴C-labelled algal cells (*Anacystis*) as a substrate. To take into account the time dependent

degradation of different organic carbon-pools, subsamples were taken at various incubation times. The amount of respired ^{14}C carbon was determined using CO_2 -traps containing ethanolamin. After counting in a liquid scintillation counter, the results were corrected for the CO_2 -recovery.

A long term experiment was designed to observe the bacterial reaction to a developing or a decaying phytoplankton population. Water samples from 15m and 200m depth were incubated in two batch cultures each: the first one under light conditions ($59 \mu\text{Em}^2 \text{ s}^{-1}$) and the second one in the dark. Over a period of 21 days, bacterial numbers, biomass and activity were measured.

Preliminary results

The leucine turnover rates in ice cores are shown in Fig.3.22. Core segments of similar ice types from one core were pooled. When brine and ice were separated by centrifugation (Fig.3.22a) a high percentage of the uptake capacity for leucine was concentrated in the lower three brownish centimetres of the ice core. The clear upper part was nearly free of bacterial activity. Furthermore, the main potential for leucine uptake was located within the brine. The bacterial activity in centrifuged ice seems to be very low. The ice core which was melted as a whole (Fig.3.22b) showed similar distribution pattern of leucine turnover rates. However, the differences between brownish and clear ice regions were lower. Comparing the absolute turnover rates of these two ice cores, the first one showed a tenfold higher activity than the second one indicating a strong spatial variation (patchiness) between different locations of sampling.

Results of leucine turnover experiments of various clear and brownish platelet ice samples from two stations are shown in Fig.2. Similar to the treatment of ice cores, centrifugation of ice platelets showed that the main potential for leucine uptake was located in the water. Turnover rates of centrifuged ice platelets were very low (Fig.2, right). Alternatively, separation of ice and water by sieving revealed similar turnover rates in both (Fig.2, left). Comparing sieved and centrifuged platelet ice samples, the main potential for leucine uptake is obviously located in the water directly associated with ice (obtained only by centrifugation) more than in the water surrounding the platelets (obtained by sieving). Leucine turnover per hour varied from 0.05 to 9.5%. Because of enhanced turnover rates in brown ice zones, the bacterial activity is clearly related to the phytoplankton content of ice platelets.

References

- Hoppe, H.-G. (1976). Determination and properties of actively metabolizing heterotrophic bacteria in the sea, investigated by means of micro-autoradiography. *Mar. Biol.*, 36; 291-302.
- Tabor, P.S.; Neihof, R.A. (1982). Improved micro-autoradiographic method to determine individual microorganisms active in substrate uptake in natural waters. *Appl. Environ. Microbiol.*, 44/4; 945-953.

Fig.3.22: Leucine turnover rates of two different ice cores. Core segments of similar ice types within one core were pooled.
 - A (stat.127): before pooling, the segments were centrifuged to separate ice and brine. Brine and melted ice were incubated separately with ³H-leucine.
 - B (stat.128): before pooling, the segments were melted as a whole and were incubated with ³H-leucine.

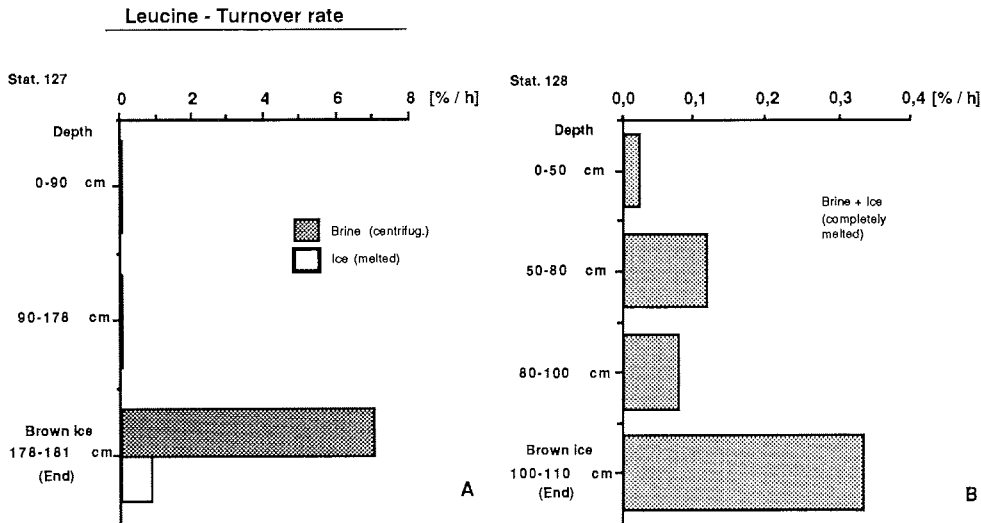


Fig.3.23: Leucine turnover rates of different platelet ice samples.
 - Right (stat.127a): platelet ice samples were centrifuged to separate ice and surrounding water. Water and melted ice were incubated separately with ³H-leucine
 - Left (stat.127b): platelet ice samples were sieved to separate ice and surrounding water. Water and melted ice were incubated separately with ³H-leucine.

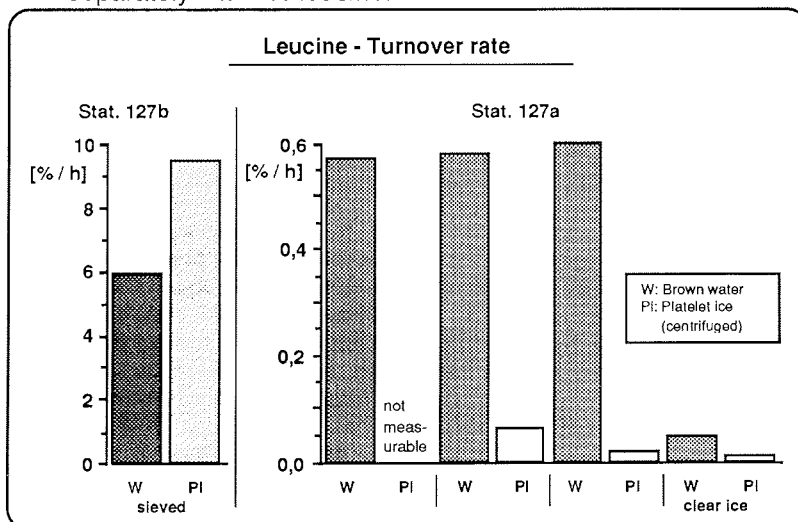
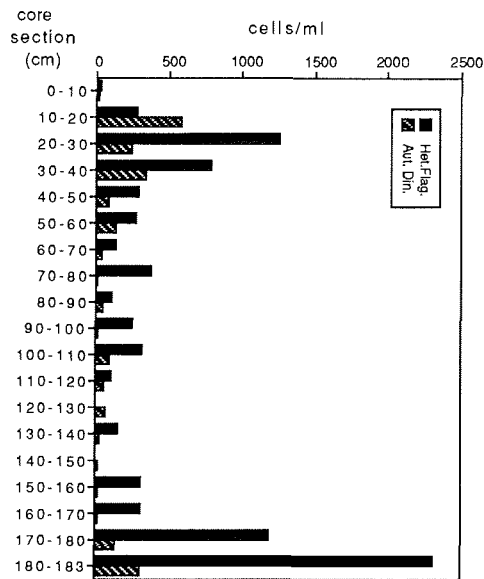
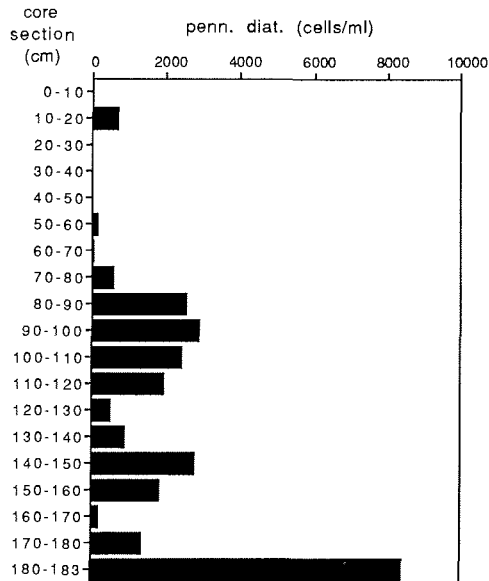


Fig. 3.24: Abundance of diatoms (b), heterotrophic flagellates (a: Het. Flag.), autotrophic dinoflagellates (a: Aut. Din.), copepods (c:Cop.), nauplii (c: Naupl.) and acol turbellaria (c: Turb.) at station AN9303201.

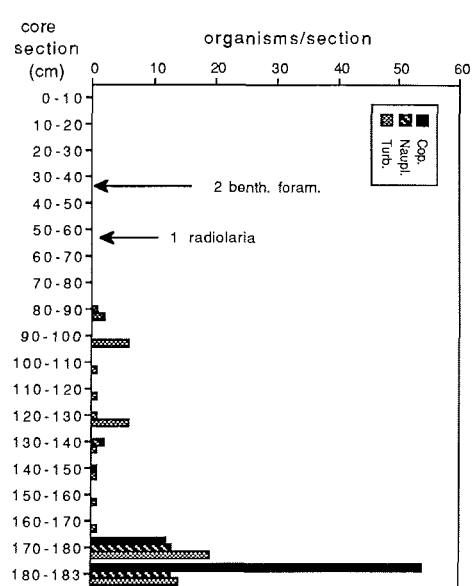
a) AN9303201: heterotrophic flagellates and autotrophic dinoflagellates



b) AN9303201: pennate diatoms



c) AN9303201: metazoa



4.2.2.3. Protozoa and metazoa living inside sea ice

K. Beyer, R. Gradinger, J. Weissenberger (AWI)

The composition of the sea ice community was studied by melting 10 cm sections of ice cores in 3 l of 0.2µm filtered sea water. Bacteria, flagellates and diatoms were counted in a subsample using epifluorescence microscopy after DAPI staining. The rest was concentrated with a 10µm gauze to determine the abundance of ciliates and metazoa. Fig. 3.24a, b demonstrates the vertical patchiness with autotrophic dinoflagellates commonly occurring in the upper part of the floes and pennate diatoms as main primary producers in the lower decimetres. Heterotrophic flagellates in the size range of 2-10µm showed maxima both in the upper and the lower horizons, while metazoa were usually concentrated in the lowermost decimetres. In other cores, foraminifera, thraustochytrids (by F. Riemann), radiolaria, ctenophores and harpacticoid copepods were observed (Fig. 3.24c). Multivariate analysis methods (factor analysis) will be applied to this data set in order to define species clusters and succession patterns of the sea ice community.

4.2.2.4. The copepod *Stephos longipes*

F. Kurbjeweit (AWI)

Objectives

Earlier investigations in the Weddell Sea showed that the calanoid copepod *Stephos longipes* seems to be associated with fast ice and particularly platelet ice (SCHIEL, SMETACEK pers. comm.). Therefore special interest was paid to its distribution and abundance in relation to sea ice in the Weddell Sea.

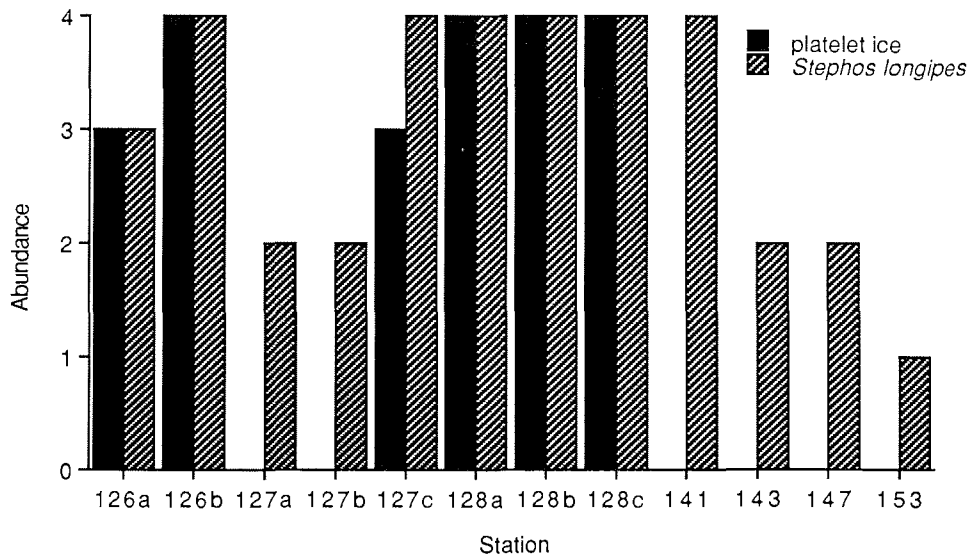
Work at sea

During the two drift stations 126 and 127/128 as well as on Sta. 141, 143, 147 and 153 water was pumped from below ice-floes by a centrifugal pump for up to two hours (24 l min⁻¹) through a 60 µm mesh size net to examine the distribution and abundance of associated zooplankton communities.

Preliminary results

First results show that the occurrence of *Stephos longipes* is associated with sea-ice, and with platelet ice in particular (Fig. 3.25). On stations where platelet ice was found in high or very high quantities (Sta. 126a/b, 127c, 128a-c) *S. longipes* was the dominant metazoan zooplankton organism. It was even more abundant than other associated organisms such as harpacticoids, foraminifers, turbellarians or ciliates that are typical for ice communities. On station 127c all metazoans were counted (Tab. 3.9) to get an overview about their abundance. Nauplii and young copepodite stages of *S. longipes* were dominant beneath the ice. It seems that *S. longipes* is significantly more abundant below platelet ice than under normal consolidated sea ice and also more abundant than in open water. This conclusion does not apply to station 141 (Fig. 3.25) where turbellarians, harpacticoids and ciliates were also abundant. The association of *S. longipes* with these three groups of organisms could also be observed on the northern shelf in open water, where ice communities may be released into the water by sea ice melting. Therefore, two conclusions seem to be valid: firstly that the life cycle of *S. longipes* is closely associated with ice, particularly platelet ice and secondly that *S. longipes* is also associated with turbellarians, foraminifers, harpacticoids and ciliates in a "platelet ice community".

Fig.: 3.25: Comparison of distribution and abundance of *Stephos longipes* with platelet ice in the southeastern Weddell Sea (0=absent; 1=very little; 2=little; 3=abundant; 4=very abundant).



Tab. 3.9: Abundance of organisms found at station 127c within 1m below the ice. Pumping time 2 hrs.

Genus	Numbers in 2.88 m ³	Numbers in 1000m ³
<i>Stephos longipes</i> :		
adults	3	1042
CV	5	1736
CIV	3	1042
CIII	11	3819
CII	15	5208
CI	31	10764
Nauplii	193	67014
turbelarians	1	347
harpacticoids	7	2431
ciliates	13	4514

4.2.2.5 The near ice water layer

U. Bathmann, K. Fahl, K. Lochte, R. Scharek, V. Smetacek (AWI)

Objectives

Physical conditions in the vicinity of ice floes can favour the development of phytoplankton and zooplankton. In particular, stabilisation of water layers in protected areas around floes as a result of melt water supply in summer or accumulation of platelet ice lead to favourable light conditions in this layer. As a consequence, rapid phytoplankton growth and biomass accumulation occurs which may be utilized by herbivorous zooplankton or can sink out and seed the water column after sea ice retreat later in the season.

Work at sea

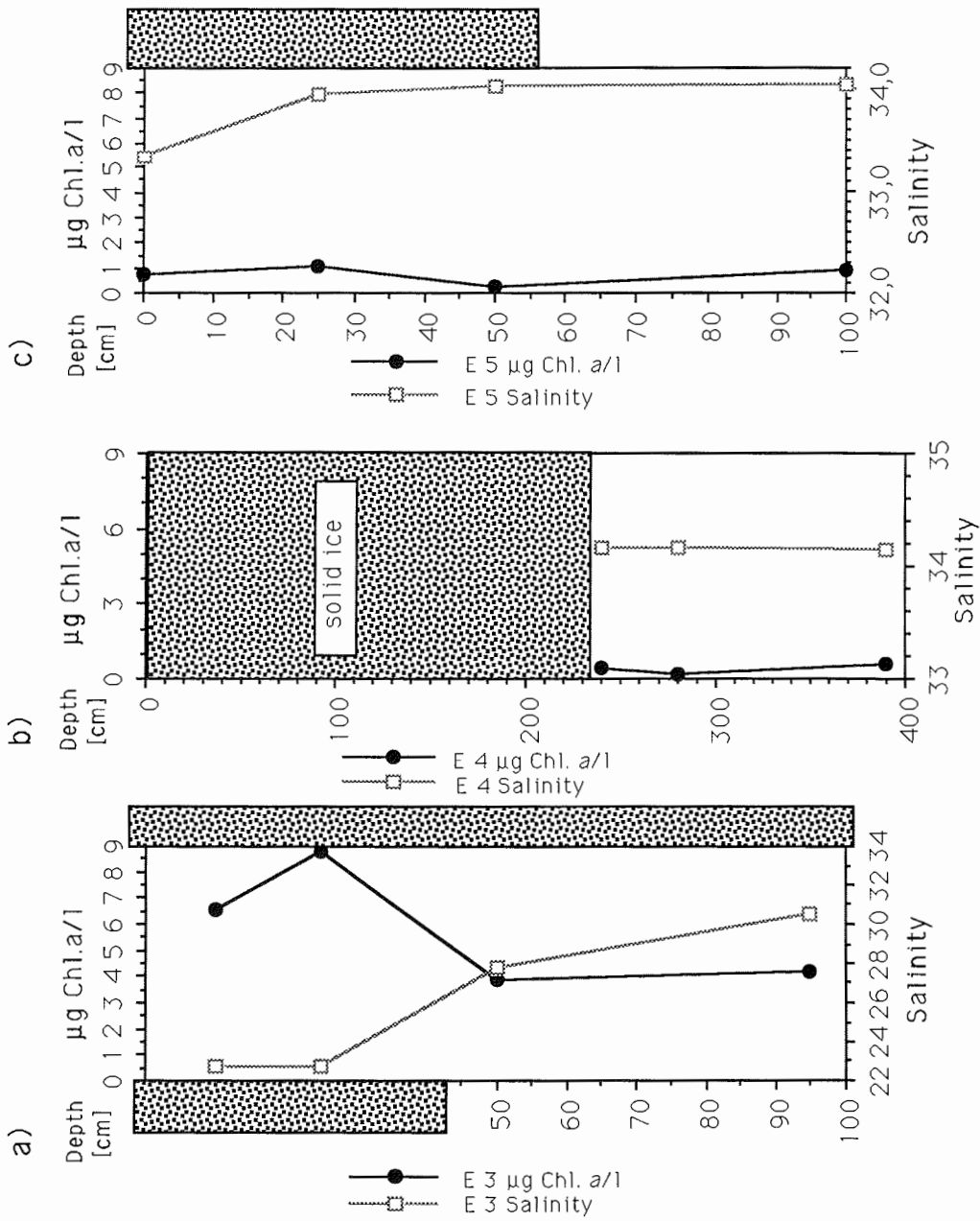
In the ice covered part of the investigation area, water under and between floes was pumped with an L-shaped plastic tube (L'se) from discrete horizons. From the sea surface next to floes, water and slush ice was carefully scooped with buckets attached to long handles. Subsamples were taken to measure salinity, nutrients, chlorophyll a, POC, PON, biogenic silica and in some cases lipid content, to investigate bacterial populations and to determine the qualitative and quantitative species composition of phytoplankton, protozooplankton and crustacean zooplankton.

First results

Salinity and chlorophyll a distributions in the near-ice water layer were very heterogeneous horizontally and vertically (Fig 3.26, see also Figs 3.27 & 3.28 in chapter 4.2.2.6). Low salinities (compared to the water column) at several locations coincided often (Fig. 3.26a) - but not always - with higher phytoplankton biomass (measured as chlorophyll a concentrations) in the respective layers. In contrast to this, elevated chlorophyll concentrations were sometimes found in layers without strong salinity gradients (Fig. 3.26b,c). As a rule, high biomass and low salinities were found in very protected near-ice areas. The heterogeneous patterns were possibly due to certain morphological features of the surrounding ice floes facilitating meltwater entrapment.

Dominant phyto- and protozooplankton species (*Thalassiosira antarctica*, *Chaetoceros* Type a Section *Hyalochaete*, *Phaeocystis* sp., *Nitzschia cylindrus*, *Polykrikos* sp.) differed from those of the underlying water column especially where ice related biomass was relatively high. In most cases, centric diatoms dominated ice associated water layers whereas pennate diatoms grew in and on floes.

Fig. 3.26: Examples of salinity and chlorophyll a profiles obtained at drifting Sta. 126 show the variability of salinity and chlorophyll patterns of a) L'se 3, b) L'se 4 and c) L'se 5. For further examples see Figs. 3.27 & 3.28.



4.2.2.6. The vertical flux under permanent sea-ice cover (Sta. 126, 127, 128)

U. Bathmann

Objectives

Amount and composition of sinking particles may be used as indicators for physical and biological processes which result in vertical mass transport under the sea ice such as ice melting, brine loss or under-ice grazing. The flux from and near sea ice was measured by means of sediment traps which were moored directly (4 m, 50 m depth) under-ice floes. The particle load (particulate organic carbon, nitrogen, carbonate, silicate) and chlorophyll *a* of the ice itself was measured from sections of ice cores which were drilled in the vicinity of the traps and sectioned according to ice texture.

First results

Particle flux under the ice floes was found to be related to ice texture, the ice biota present in a given area and the under-ice biology. During drift station I (Sta. 126, Fig. 3.27). The main components of the mass flux found in the preliminary microscopical investigations were pennate and centric diatoms (other organisms living in and directly under the ice were also frequently found). The average total flux directly (4 m) under the ice was 5 mg Chl *a* m⁻²d⁻¹ with a continuous increase from 1 to 11 mg Chl *a* m⁻²d⁻¹ during the 68 h of investigation. As the pigment concentration of the sediments was about 0.02 µg Chl *a* mg dw⁻¹ (= 0.107 mg Chl *a* m⁻² = 3 mg C m⁻²) it can be concluded that sedimentation under the sea ice was low but rather continuous during this season.

The vertical flux at drifting station II (Sta. 127/8, Fig. 3.28) differed significantly from that at station I in terms of sinking particles and biomass. As has been shown in the description of the ice cores (see 4.2.2.3), some of the ice floes from that area had bottom layers very rich in biomass (> 266 µg Chl *a* l⁻¹). This was reflected in the shallow trap and the material found in the upper trap (4 m) was dominated in the beginning by diatoms and other algae from that layer. After 14 h sampling, fecal strings were found in the traps. These strings dominated the particulate matter in the deeper trap (50m) during the entire investigation. In terms of chlorophyll biomass, this resulted in high sinking rates (> 20 mg Chl *a* m⁻²d⁻¹) directly under the floes which decreased with depth (5 mg Chl *a* m⁻²d⁻¹). In terms of carbon flux, however, this pattern should be reversed, as the optical comparison of the amount of matter collected in the two horizons showed a three to fourfold amount of total matter in the deeper trap. As a preliminary conclusion for vertical flux during drifting experiment II, it is assumed that intense grazing of euphausiids may have occurred under the ice floes while most defecation occurred in depths of more than 4 m.

Fig. 3.27: Summary view of ice, water and sediment properties at driftstation I (Sta. 126). Upper compartments present the water layer under the ice, the lower presents sedimentation at 4 m depth, the lowest the sediment, and the compartment on the right the water column.

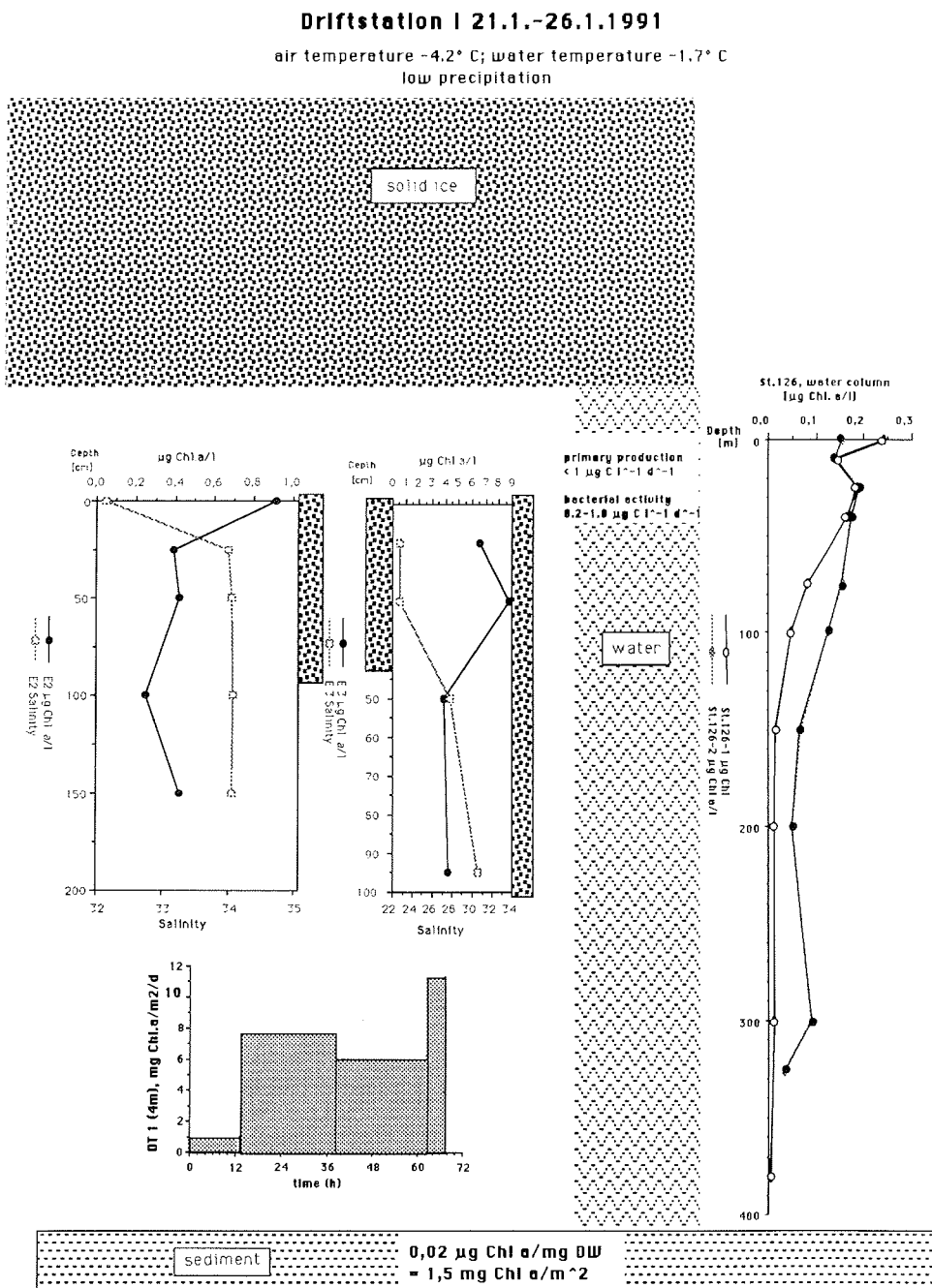
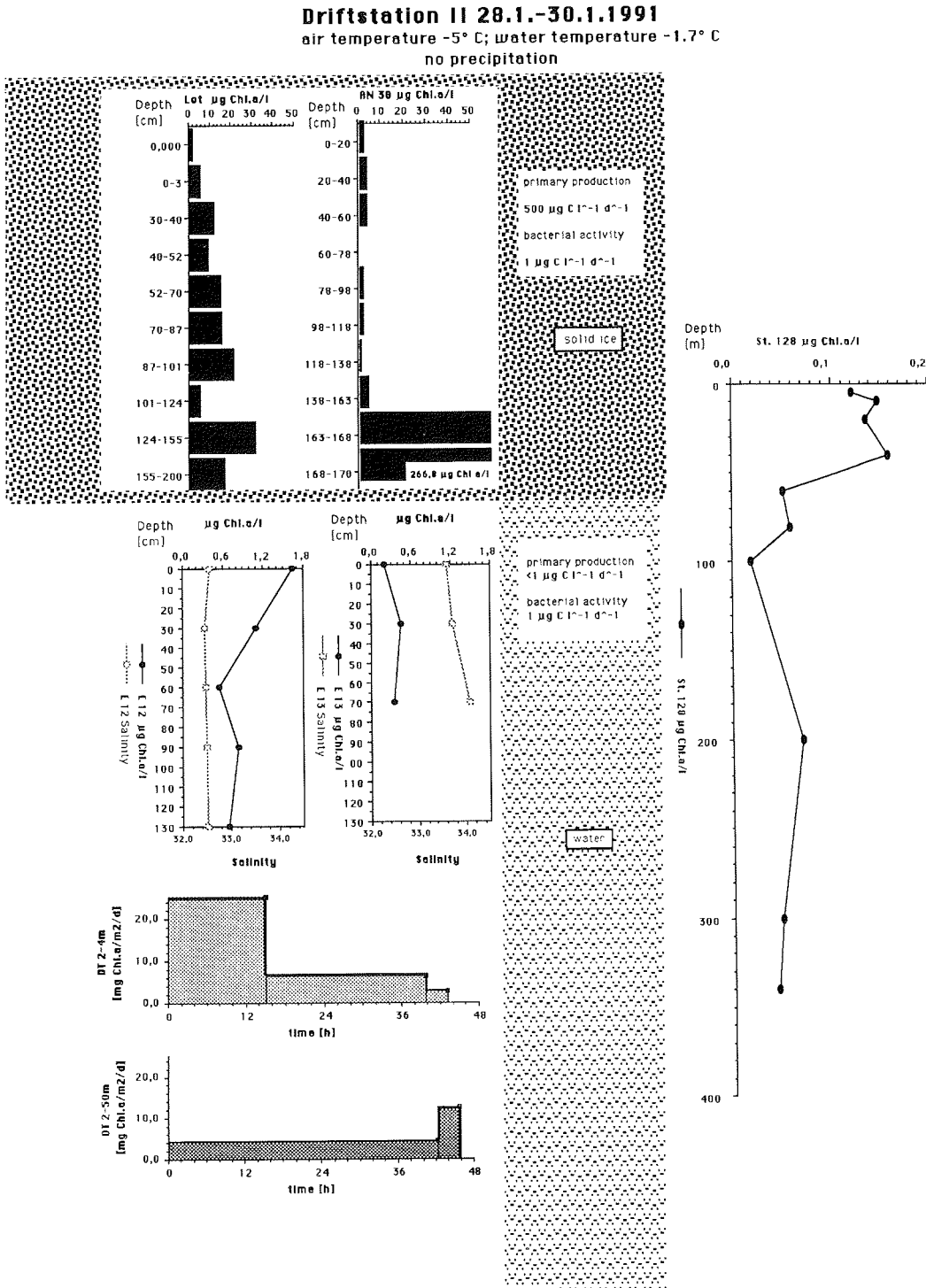


Fig. 3.28: Summary view of ice and water properties at driftstation II (Sta. 127, Sta. 128). Upper compartments present the solid ice sheet, the lower the uppermost water layer, the lowest sedimentation at 4 m and 50 m depth, and the compartment on the right presents the water column.

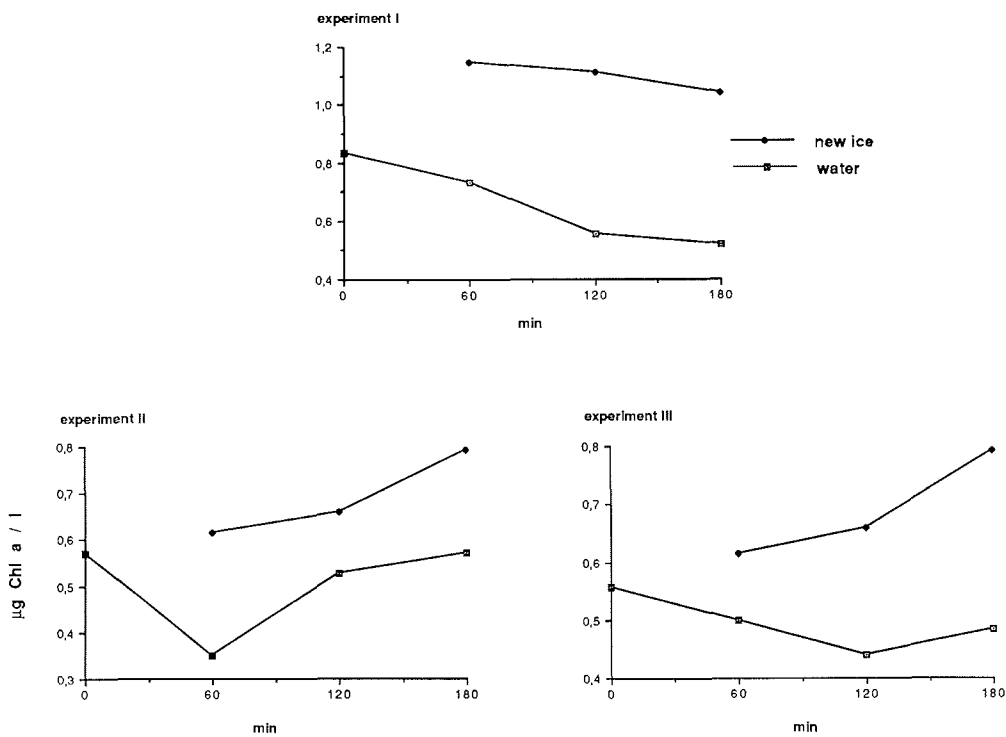


4.2.2.7. New ice formation

U. Bathmann, M. Gleitz, R. Gradinger, R. Scharek, J. Weissenberger (AWI)

At 9 stations at the end of the cruise new-formed ice (grease-ice, pancake-ice) was sampled. The Chl *a* concentrations in the new-ice showed a 3-60 fold increase in relation to the adjacent surface water. New-ice (Fig. 3.29) which was experimentally produced by freezing of sea water in small containers (60x40x40 cm) at -10°C and continuous movement showed an increase of Chl *a* within 3 h.

Fig. 3.29: Chl *a* ($\mu\text{g/l}$) increase in experimentally formed new-ice in relation to sea water content



4.2.3. Water column ecology

Bathmann U., K. Fahl, S. Grossmann, M. Gleitz, F. Kurbjeweit, K. Lochte, R. Scharek, S. Schröder, V. Smetacek, J. Weissenberger (AWI)

4.2.3.1. Primary production and light

M. Gleitz, J. Weissenberger (AWI)

Objectives

Previous investigations on distribution and primary production of phytoplankton on the south-eastern continental shelf and along the western ice edge in spring and summer have demonstrated that the Weddell Sea can be divided into a low productive northern/central domain and a high productive southern domain (El Sayed & Taguchi, 1981; v. Bröckel, 1985, v. Bodungen et al., 1988). The higher productivity and standing crop along the continental shelf was attributed primarily to water column stability which prevents the algae from being mixed out of the euphotic zone. However, reduced grazing pressure or input of essential trace elements (i.e. iron) from the sediments have also been suggested as factors controlling primary production in the Weddell Sea.

The study of primary production done during this cruise was part of an interdisciplinary programme with participation of phytoplankton ecologists, microbiologists, zoologists, geochemists and physical oceanographers. The transects parallel to the eastern shelf between 30°W to 10°E and perpendicular to the coastal current into the Weddell Gyre provided an opportunity to study the factors controlling primary production, grazing rates, bacterial consumption and hydrography in the eastern Weddell Sea and southern Lazarev Sea.

Work at sea

Light measurements: In order to relate phytoplankton primary production to the seasonal decrease in photoperiod and downwelling irradiance, photosynthetic active radiation (PAR; [$\mu\text{mol quanta m}^{-2}\text{s}^{-1}$; 400 - 700 nm]) was recorded over the experimental period. A 2- π sensor (LICOR) was installed on the ship's upper deck, where shading effects were minimal. The light sensor was connected to a LICOR data logger, which allowed continuous recordings over 24 hours. However, as the instrument was also used by other scientists, recordings are not complete. Thus, datalogger values were used to convert global radiation (W m^{-2} ; recorded continuously by the ship's INDAS system) to PAR to fill the missing gaps. The arithmetic mean of each day's readings were used to calculate the mean photon flux density ($\text{mol quanta m}^{-2}\text{d}^{-1}$) over longer time periods.

At 6 stations, the underwater light regime was measured by means of a 4- π sensor connected to a LICOR datalogger. The light probe was lowered into the water in intervals of 5 m to a final depth of 70-100 m. A 2- π sensor on deck served as a reference. The 4- π /2- π ratio was used to calculate the depths corresponding to 70, 45, 25, 10, 3 and 1% of the photon flux density directly below the water surface (=100% light depth). At all other stations, light depths were calculated using Secchi disc readings according to the equation of (Evans et al., 1987):

$$\text{sampling depth (m)} = \ln (\% \text{ light depth}/100) * (\text{Secchi depth}/-1,7)$$

Production measurements: Primary production was estimated from ^{14}C -uptake rates under simulated in situ conditions (Evans et al., 1987). The water samples were obtained by means of Niskin bottles attached to a CTD probe (General Oceanics) after light depths were determined as described above. For light depths within the upper 10 m of the water column, only one or two samples were taken, assuming a homogeneously mixed upper layer. For each light depth, two light bottles and one dark bottle (100 ml each) were filled in dim light and inoculated with approx. 7,5-10 μCi of $\text{NaH}^{14}\text{CO}_3$ (Amersham Buchler). Additionally, 3 samples were filtered immediately after adding the radiolabel and were subtracted from light and dark uptake rates. Samples were incubated in a temperature controlled incubator at -1°C for 5 or 10 hours. A photon flux density of $400 \mu\text{mol m}^{-2}\text{s}^{-1}$ (adjusted with a $4-\pi$ sensor [LICOR]) was chosen as the 100% light intensity. With decreasing light recordings due to the advancing season, simulated 100% light was reduced to $350 \mu\text{mol m}^{-2}\text{s}^{-1}$ in the experiments after February 7th. Daily production rates were calculated by multiplying ^{14}C -uptake with a factor derived from the ratio ($\text{PAR d}^{-1}/\text{PAR incubation period}^{-1}$). Daily downwelling PAR was multiplied by 0.85 in the calculations to account for reflection at the sea surface.

Samples were filtered onto cellulose nitrate filters ($0.45 \mu\text{m}$ pore size), dried at room temperature and fumed over concentrated HCl to remove any residual H^{14}CO_3 . The filters were dissolved in scintillation cocktail (Zinsser 361) for 24 hours in the dark and were subsequently counted (Packard Tri Carb 1900). Quench correction was performed by the external standardization method.

Preliminary Results and Discussion

Light measurements: The investigation period was divided into 2 periods due to the seasonal decrease in down welling irradiance with a mean daily photon flux density of $35,42 \pm 8,55 \text{ moles m}^{-2}\text{d}^{-1}$ from January 15th to February 7th and $17,28 \pm 7,86 \text{ moles m}^{-2}\text{d}^{-1}$ from February 7th to March 4th.

Production rates: Production data are depicted in Tab. 3.10. High average integrated production rates $> 400 \text{ mg C m}^{-2}\text{d}^{-1}$ were recorded over the entire investigation period in the coastal current from approx. 25°W to 6°E . Productivity decreased to approx. $200 \text{ mg C m}^{-2}\text{d}^{-1}$ for samples taken after February 7th. Despite higher phytoplankton biomass in the euphotic zone in the coastal current of the south-eastern Weddell Sea, production was higher in the Lazarev Sea (413 vs. $486 \text{ mg C m}^{-2}\text{d}^{-1}$). The relatively low growth rates (< 0.4 divisions d^{-1}) and productivity indices ($< 10 \text{ mg C [mg Chl } a]^{-1} \text{ d}^{-1}$) for both regions after February 7th together with high phytoplankton standing stock is an indication for a late bloom situation where exponential phytoplankton growth had already ceased.

In contrast to the high production in the coastal current, productivity and phytoplankton standing stock was consistently low in the Weddell Gyre. For instance, integrated production decreased by a factor of approx. 2-4 between Sta. 190-199 and 180-200 (the two Maud Rise transects). Low productivity in the Weddell Gyre ($< 160 \text{ mg C m}^{-2}\text{d}^{-1}$) can be related to low phytoplankton standing stock (and not physiological capacity), as the productivity indices as well as growth rates are not significantly different to those determined for the coastal phytoplankton. No detailed explanations for the marked contrast in primary production can be given at this point, but it is hypothesized that hydrography, the receding ice cover, zooplankton grazing and the proximity to

the Antarctic continent are major factors controlling production patterns in summer and fall in the area investigated.

Tab. 3.10: Primary production data

	Secchi- Depth (m)	1% Light Depth (m)	Production (mg C / m ² d)	Chl a (Zeu) (mg / m ²)	Prod.-Index mg C / mg Chl a d	μ (Zeu) (divisions / d)	PFD (mol Phot. / m ² d)
Coastal Current long. 27°W-12°W (15.1.-3.2.91); n=3 Stat.: 122, 125, 131	15,3 ± 3,9	55,7 ± 10,7	647,04 ± 285,70	37,20 ± 4,87	16,97 ± 5,22	0,64 ± 0,15	35,42 ± 8,55
Coastal Current long. 7°W-2°W (16.2.-18.2.91); n=4 Stat.: 160, 163, 164, 166	8,5 ± 0,4	21,5 ± 2,4	413,31 ± 83,46	56,97 ± 13,12	7,53 ± 2,27	0,32 ± 0,09	17,28 ± 7,86
Coastal Current long. 1°E-12°E Stat.: 173, 175, 180, 183, 184, 189, 190; n=7	11,3 ± 1,4	32,0 ± 3,9	486,21 ± 139,32	52,17 ± 6,22	9,35 ± 2,70	0,39 ± 0,10	17,28 ± 7,86
Weddell Gyre lat. 74°S-71°S Stat.: 141, 145, 153; n=3	24,7 ± 2,5	64,3 ± 7,5	126,77 ± 46,82	17,86 ± 1,60	7,20 ± 3,06	0,31 ± 0,12	17,28 ± 7,86
Weddell Gyre lat. 69°S-66°S Stat.: 188, 194, 197,	12,3 ± 1,9	33,4 ± 5,3	157,69 ± 74,56	25,07 ± 11,56	6,47 ± 1,83	0,28 ± 0,07	17,28 ± 7,86

References

- v. Bodungen, B.; Nöthig, E.-M.; Sui, Q. (1988). New production of phytoplankton and sedimentation during summer 1985 in the south eastern Weddell Sea. *Comp Biochem Physiol* 90:475-487.
- v. Bröckel, K. (1985) Primary production data from the south-eastern Weddell Sea. *Polar Biol* 4:75-80.
- El-Sayed, S.; Taguchi, S. (1981). Primary production and standing crop of phytoplankton along the ice-edge in the Weddell Sea. *Deep-Sea Res.* 28:1017-1032.
- Evans, C.A.; O'Reilly, J.E.; Thomas, J.P. (1987). A handbook for the measurement of chlorophyll a and primary production. *Biological Investigations of Marine Antarctic Systems and Stocks (BIOMASS)*, 8:47-109, Texas A&M University, College Station, Texas, U.S.A.

4.2.3.2. Microbiological investigations

K. Lochte, S. Grossmann (AWI)

Objectives

Organic matter generated by primary production is consumed to a large extent by microorganisms.

Bacteria can only utilize dissolved organic carbon (DOC), which is released by nearly all organisms. The largest sources in the euphotic zone are exudation of DOC by phytoplankton as part of their primary production and cell lysis during the decay phase of a phytoplankton bloom. Macromolecules can be degraded by bacterial extracellular hydrolytic enzymes thus making particulate organic carbon (POC) available for bacterial consumption.

During cruise Ant IX/3 microbiological investigations were concerned with aerobic microbial transformation of organic carbon in ice, water and sediment. These habitats represent very different types of environment in each of which the role of bacteria in the carbon cycle is likely to vary greatly. In the euphotic water column and in the ice, primary production and heterotrophic consumption are closely coupled, while in the sediment heterotrophic consumption is dependent on sedimentation rates of organic matter. Diffusion constraints within ice and sediment add further boundary conditions to the magnitude of microbial activity and create microenvironments.

The following main aspects were investigated:

1) Incorporation and remineralisation of organic substrates. ^{14}C -labelled amino acids and whole algal cells (*Anacystis sp.*) were used as dissolved and particulate model substrates. The release of $^{14}\text{CO}_2$ via respiration and the incorporation into cell material (only for amino acids) were monitored to give an indication of the rates of organic carbon breakdown and efficiency of carbon conversion.

2) Growth of bacteria. Incorporation of ^3H -thymidine into DNA and ^2H -leucine into protein were used to determine the rates of cell division and of biomass production, respectively. From these data and the efficiency of growth (from literature) the requirement for organic carbon for the bacterial population present can be estimated and related to primary production.

3) Heterogeneity and zonation of bacterial distribution. A broad base of data on the distribution patterns is required to enable a quantification of the carbon cycling via bacteria in a larger region. Particularly in ice, the small and medium scale patchiness poses a great problem.

In addition to the above main aspects, the distribution of hydrolytic enzymes (esterases) was determined. Furthermore, tests were carried out to capture water column aggregates and assess their heterotrophic activity.

Work at sea

Since the cruise plan had to be changed due to adverse weather conditions and most of the work was carried out in the Lazarev Sea in waters with little ice cover, the emphasis had to be changed from investigations of sea ice to the water column. This is exemplified by the distribution of samples summarized in Tab. 3.11

Measurements of bacterial growth in the water column and in ice cores were carried out parallel to phytoplankton sampling and primary production measurements as often as possible. In the sediment, samples were taken from the same multiple corer as the geochemical investigations. Remineralisation rates of organic carbon were determined in representative samples only.

Tab. 3.11: Microbiological investigations carried out in different habitats. The figures indicate the numbers of samples taken for each type of investigation, figures in bracket are the number of stations.

	Numbers/ Biomass	Growth or leucine uptake	Respiration activity	Esterase
Water column	286(31)	123(26)	4 (2)	35 (3)
Ice/ ice related water	65(15)	59(11)	1 (1)	23 (1)
Sediment	252(24)	17(5)	9 (3)	52 (5)
Aggregates	12(6)	8(4)	8 (4)	

Water samples were taken by CTD rosette sampler. Sediment samples were collected by multiple corer and sliced into 1 cm thick layers. Ice was sampled by ice corer and cut into sections of 10 cm length. Depending on the visual assessment, sections of similar physical or biological structure (congelation ice, grained ice, brown ice) were pooled. Loose frazil or platelet ice was sampled by bucket or sieve. The ice samples were either centrifuged to remove brine or were analysed without centrifugation. For incubation with radioactive substances ice samples were thawed and standard sea water salt was added to compensate decreasing salinity. Water column aggregates were collected by *in situ* pumps which filter the water through 1µm Nuclepore filters.

Determination of bacterial numbers and biomass is carried out by direct microscopic counting and size classification of acridine orange or DAPI stained samples (Hobbie et al. 1977). Water and ice samples were fixed in 0.4% and sediment samples in 4% formaldehyde (filtered through 0.2µm Nuclepore filter) and stored in glass bottles at 1-2°C until further analysis on land. Water column aggregates were fixed on small sections of the Nuclepore filter in 2.5% glutaraldehyde for scanning electron microscopy. All microscopic counts will be carried out on land.

Bacterial growth was measured by incorporation of ³H-thymidine into DNA according to the method of Fuhrmann & Azam (1982) and by incorporation of ³H-leucine into protein after Simon & Azam (1989). When testing different substrate concentrations to determine the saturation concentrations of thymidine and leucine, no saturation was reached at 5 nM concentrations as is usually reported in the literature. Hence, in contrast to the literature 50nM final concentration (diluted with cold thymidine or leucine) was used. All incubations were carried out at 1°C and 1 atm; sediment samples were additionally incubated at *in situ* pressure. Liquid samples for bacterial growth

determinations were already extracted and measured on board by liquid scintillation counting on a Packard TriCarb 1900. The bacterial production is reported as mol thymidine or leucine incorporated per m³ and day. This is a measure for the rate of DNA replication or for protein synthesis, respectively. The conversion to biomass production in terms of organic carbon is plagued with many assumptions and insecurities. Using literature conversion factors (Bjørnsen & Kuparinen 1991) an approximate bacterial biomass production was calculated and should be considered a preliminary estimate. Conversion factors will be checked by microscopic determination of the actual increase in bacterial biomass on separate samples incubated parallel to the radioactive ones.

Incubations of sediment samples cannot be analysed with shipboard means and have been stored frozen until they can be further processed on land.

For determination of bacterial remineralization ¹⁴C-algal cells (*Anacystis sp.*, Amersham Buchler) and ¹⁴C-amino acid mixture (Amersham Buchler) were incubated at 1°C with water, ice, sediment or aggregate samples. The CO₂ released by mineralisation of the organic substrates was trapped after acidification of the samples (Lochte 1985). The captured ¹⁴CO₂ was counted by liquid scintillation counting.

Activity of hydrolytic enzymes (esterases) was determined with fluorescein diacetate according to Holzapfel-Pschorn et al. (1987). The method was also adapted for sediments.

Long term experiments were set up to monitor the development of algae, bacteria and the changes in nutrients in large batch containers of 10 l to 20 l volume. These experiments were carried out jointly with the phytoplankton group.

Preliminary results

The preliminary results of the microbiological studies are being presented in the relevant sections:

- Microbiology of sea ice (chapter 1.2.X)
- Biological properties on the transects perpendicular to the coast (chapter 1.2.2)
- The Antarctic coastal current between the stations Georg-von-Neumayer and Georg-Forster (chapter 1.2.3)

References

- Bjørnsen, K.P.; Kuparinen, J. (1991). Determination of bacterioplankton biomass, net production and growth efficiency in the Southern Ocean. *Mar. Ecol. Prog. Ser.*, 71: 185-194.
- Fuhrmann, J.A.; Azam, F. (1982). Thymidin incorporation as a measure of heterotrophic bacterioplankton production in marine surface waters: Evaluation and field results. *Mar. Biol.*, 66: 109-120.
- Hobbie, J.E.; Daley, J.R.; Jaspas, S. (1977). Use of nucleopore filters for counting bacteria by fluorescence microscopy. *Appl. Environ. Microbiol.*, 33: 1225-
- Holzapfel-Pschorn, A.; Obst, U.; Haberer, K. (1987). Sensitive methods for the determination of microbial activities in water samples using fluoroc substrates. *Fresenius Z. Anal. Chem.*, 327: 521-523.

- Lochte, K. (1985). Biological studies in the vicinity of a shallow-sea tidal mixing front. III. Seasonal and spatial distribution of heterotrophic uptake of glucose. *Phil. Trans. R. Soc. Lond. B*, 310: 445-469.
- Simon, M.; Azam, F. (1989). Protein content and protein synthesis rates of planktonic marine bacteria. *Mar. Ecol. Prog. Ser.*, 51: 201-213.

4.2.3.3. Open ocean transects

Bathmann U., Fahl K., Gradinger R., Scharek R., Schröder S., Weissenberger J. (AWI)

Transects from Cape Town to Atka-Bay and back

During the journey to and from the investigation area in the Weddell Sea, the chlorophyll content of surface water was monitored continuously by means of a flow-through fluorometer. In addition, samples were taken from the membrane pumping system to determine phytoplankton species composition and numbers of cyanobacteria.

On the transect from Cape Town to Atka-Bay in January, in vivo fluorescence (Fig. 3.30) increased slightly from the subpolar front towards south and were highest at the polar front. Further south a steep decline in concentration was observed only increasing shortly above the Maud Rise area. In the Weddell Sea pack ice chlorophyll *a* concentrations increased further but showing high spatial variations.

A preliminary investigation of the phytoplankton species composition showed that the subpolar and not the polar front was a northern barrier for most of the Antarctic diatom species. Above Maud Rise *Phaeocystis* sp. formed the bulk of the biomass. All samples and data especially those of the transect back from Atka Bay to Cape Town at the end of March await further analysis in Bremerhaven.

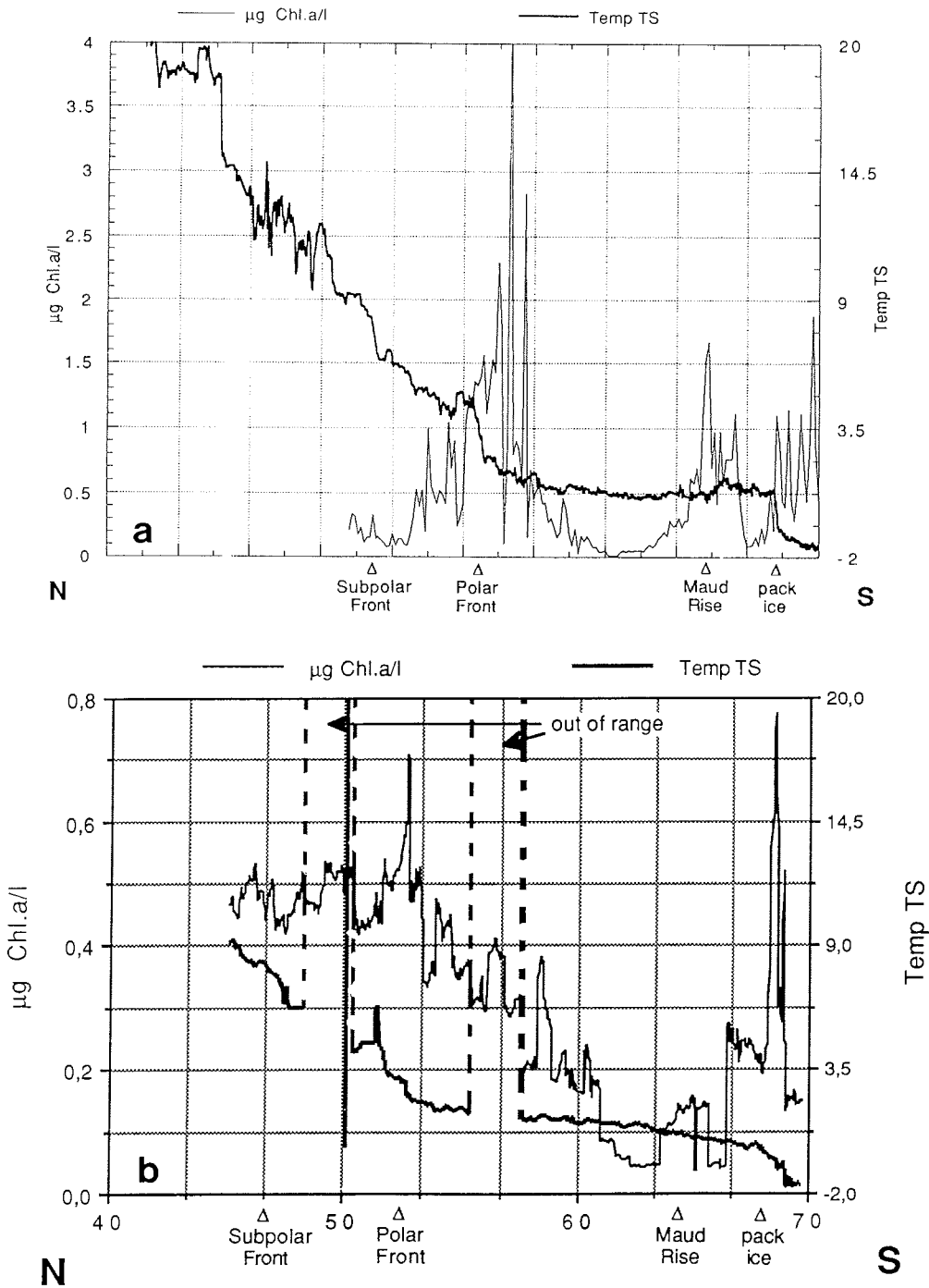
Picocyanobacteria as water mass indicators in the Southern Atlantic

Picocyanobacteria are known as main contributors to phytoplankton biomass and production in tropical and subtropical seas. Recent studies in the North Atlantic have shown that their abundance decrease with increasing latitude respectively decreasing water temperature.

Along two transects reaching from South Africa (Cape Town) to the Weddell Sea (GvN) we investigated their occurrence in relation to hydrography to find out whether picocyanobacteria can be used as water mass indicators in the Southern Atlantic as well.

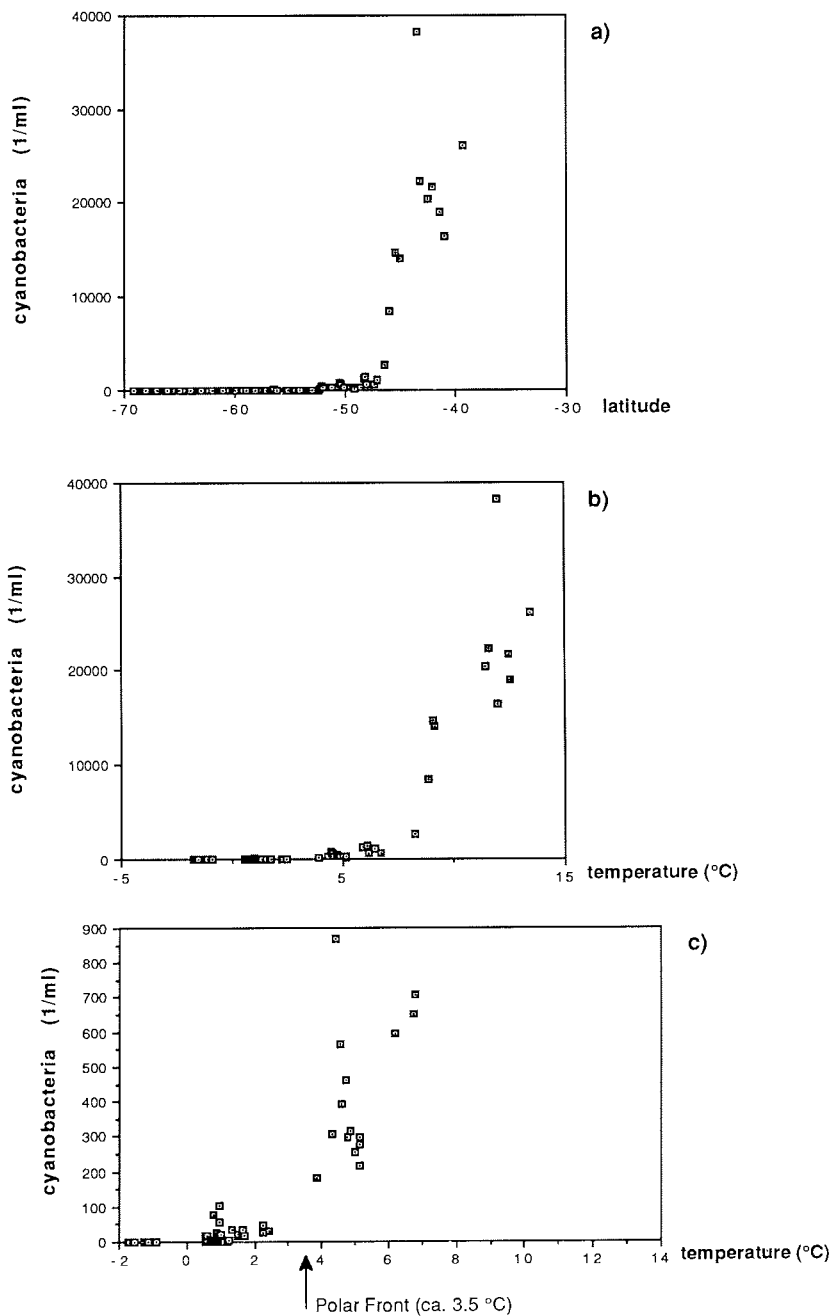
Samples were taken from a continuous membrane pumping system every 2-4 hours. After fixation with formaline (1% final concentration) and filtration of 30-40ml onto 0.8 µm Nuclepore filters, cyanobacteria were counted with a Zeiss Axiovert 35 epifluorescence microscope under blue light excitation. Temperature and salinity data were taken from the INDAS system of RV Polarstern.

Fig 3.30: Surface profiles of temperature (monitored by a Thermosalinograph) and chlorophyll a along the transect from a: Cape Town to Atka Bay beginning of January 1991 and b: along the transect from Atka Bay to Cape Town end of March 1991.



The results of the first transect clearly demonstrate the relationship between abundance of picocyanobacteria and latitude (Fig. 3.31a) respectively water temperature (Fig. 3.31b, c). The highest abundances were reached north of the Subantarctic Front (Fig. 3.31 b) with a maximum of nearly 40000 cells/ml. South of the Polar Front (Fig. 3.31c), picocyanobacteria were nearly absent.

Fig. 3.31: Distribution of pico cyanobacteria along the transect from Cape Town to Atka-Bay in January 1991. Concentration of cyanobacteria a) vs latitude, b) vs water temperature and c) extended ordinate of b) to resolve distribution pattern wouth of the Subarctic Front.



The results indicate that picocyanobacteria can be used as water mass indicators in the Southern Atlantic. Further studies on cell size and frequency of dividing cells will focus on the question if different populations exist in the various hydrographical domains of the investigation area to validate the idea of picocyanobacteria as biological tracers in the sea.

Biological properties on the transects perpendicular to the coast

On the transects to and from the Polarstern Seamount, the biological properties of the water column clearly reflected the physical oceanographic patterns. On the western transect (Fig. 3.32, see 4.1 sec 1) highest chlorophyll *a* concentrations in the surface layer ($>1.84 \mu\text{g Chl } a/l$) were measured at the coastal stations only. On the seamount itself the concentrations were as low as in the surrounding open ocean. On the transect back to the coast (Fig. 3.32, sec 2) biomass maxima were encountered over the slope ($>0.5 \mu\text{g Chl } a/l$) in the coastal current ($> 0.4 \mu\text{g Chl } a/l$) and close to the ice shelf at station 159 ($>0,7 \mu\text{g/l}$). Phytoplankton species composition at the different stations reflected the heterogeneous geostrophic current patterns encountered on section 1 (see 4.1). *Corethron criophilum* and *Phaeocystis* sp. were the dominant forms at coastal stations. These species, together with typical oceanic forms, also contributed the dominant fraction at the offshore stations. Oceanic species dominated at the slope Sta. 137 - 140 where geostrophic current patterns were reversed to the general southwest flow of the coastal current (see 4.1).

At the oceanic stations of the eastern section 2 a similar species composition as at the oceanic stations of section 1 was encountered with the exception of the two coastal stations. A community dominated by typical northern oceanic diatoms (*Coscinodiscus bouvet*, *Synedra reinboldii*, *Chaetoceros bulbosum*, *Dactyliosolen antarcticus*, *Chaetoceros neglectum*, *Chaetoceros dictyota* etc.) strongly indicated the impact of northern oceanic water. This again coincided with reversed geostrophic current patterns (see chapter 4.1).

The transect into the Lazarev Sea (at 1°E) was characterised by high chlorophyll *a* values at the shelf ice coast, over the shelf slope ($>1.2 \mu\text{g Chl } a/l$) (Fig. 3.33a) and at the offshore Sta. 197 at the bottom of the slope ($>1.49 \mu\text{g Chl } a/l$). The comparison with physical oceanography data showed that these maxima were associated with the centre and the the edge of the coastal current. The continuous surface registration of the chlorophyll fluorescence revealed rather distinct frontal barriers. Species composition of phytoplankton on the 1°E transect shifted from northern oceanic forms at the coast to southern oceanic forms and *Phaeocystis* sp. From the inshore to the offshore stations the physiological state of *Phaeocystis* sp. and its relative contribution to the dominant phytoplankton fraction varied. The offshore chlorophyll maximum (Sta. 197) was due to high numbers of this species at that station. Bacterial production as measured by incorporation of ^3H -Leucine into cell protein on the transect at 1°E is shown in Fig. 3.33b. At the coastal station 190 production rates were high in the surface waters with a peak value at 100 m depth. Particularly low bacterial production was observed at Sta. 192, but relatively high values were found down to 500 m depth at station 194 further offshore. Away from the coast, at Sta. 195 and 199, bacterial production was low, high values being found only in the surface layer, and in the deep water masses below 300 m no productivity could be detected. In the bottom water at the shelf slope, slightly increased values were observed presumably due to sediment resuspension caused by stronger bottom currents compared to the adjacent deep-sea plain.

Fig. 3.32: Chlorophyll *a* concentrations ($\mu\text{g/l}$) along the transects to and from the "Polarstern Seamount": a) stations 135 - 145 = section 1; b) stations 145 - 153 above the seamount, stations 153 - 159 = section 2 (see chapter 4.1, Fig. 3.8).

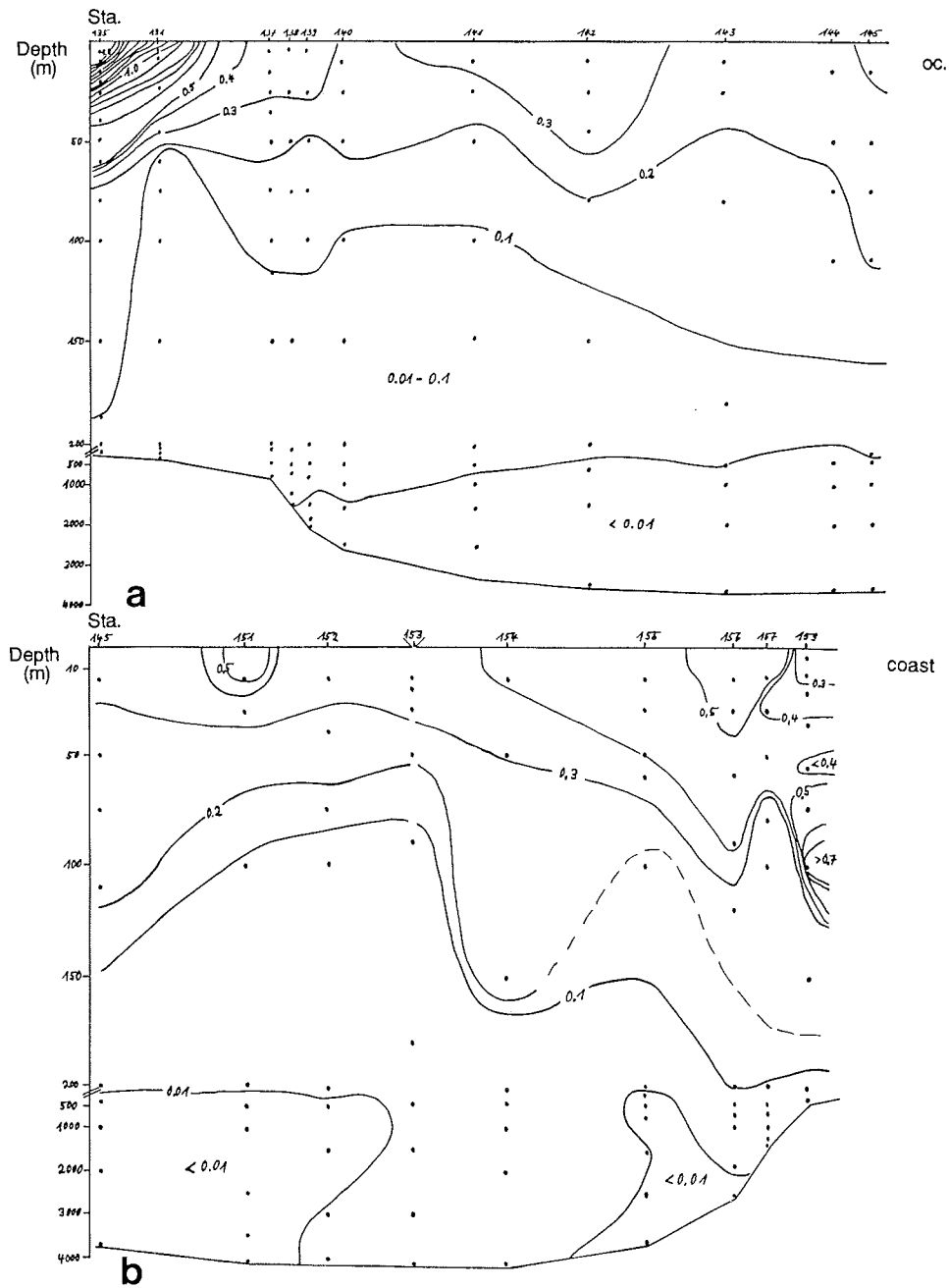


Fig. 3.33 a: Chlorophyll *a* concentrations ($\mu\text{g/l}$) along the transect at 1°E in the Lazarev Sea perpendicular to the coast. Chlorophyll distribution patterns were obtained by combination of data from Niskin bottle samples and surface registration by a flow-through fluorometer.

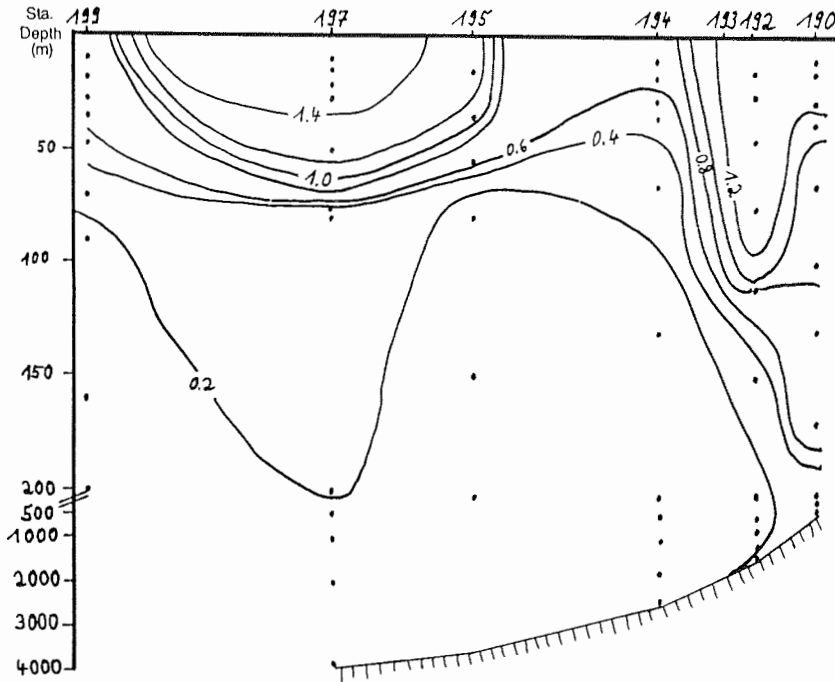
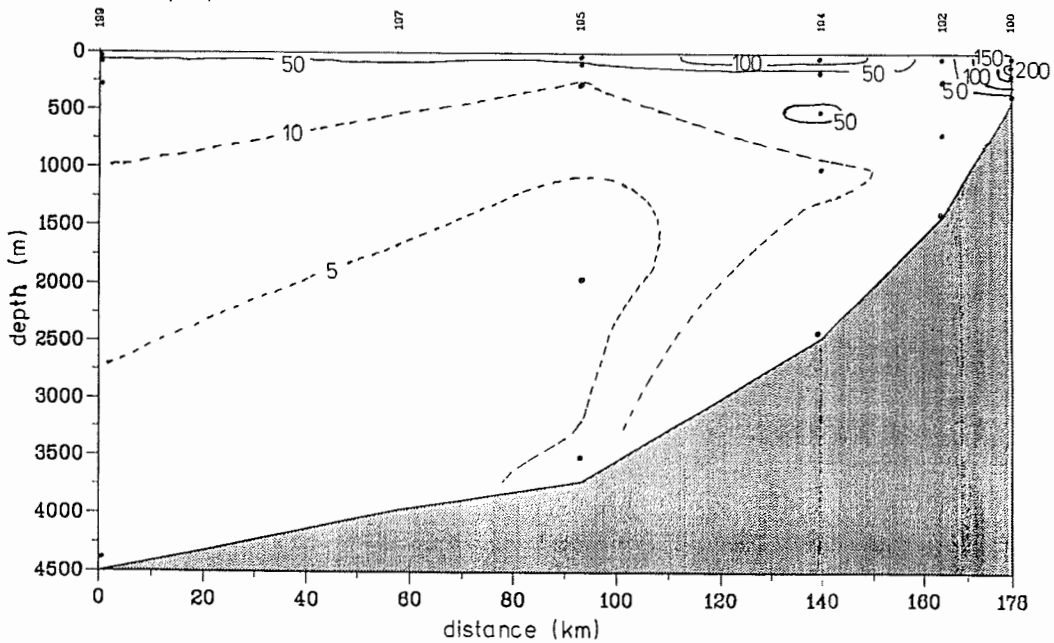


Fig. 3.33 b: Incorporation of ^3H -leucine into proteins given as $\text{pmol leucine } 1^{-1}\text{d}^{-1}$ as a measure of bacterial growth along the transect at 1°E perpendicular to the coast.



Vertical and horizontal distribution of chlorophyll values on the 6°E transect were similar to those described above. A steep gradient in salinity close to the coast was exceptional, and was associated with a chlorophyll maximum $> 1 \mu\text{g Chl } a/l$ (Fig. 3.34a). Further north biomass decreased to $< 0.5 \mu\text{g Chl } a/l$. At the Sta. 203, 204, slightly higher chlorophyll concentrations were measured. The biomass minima were found at the outermost Sta. 200. The phytoplankton species composition on this transect showed rather heterogeneous patterns with northern oceanic forms close to the coast and *Phaeocystis* sp. and southern (Weddell Gyre) oceanic species being dominant offshore. Again, from inshore to offshore stations the physiological state of *Phaeocystis* sp. and its relative contribution to the dominant phytoplankton fraction varied possibly reflecting undulation or recirculation of the Weddell Gyre. This interpretation is confirmed by the heterogeneous patterns of geostrophic currents on that transect (see chapter 4.1).

High bacterial production (incorporation of ^3H -leucine into proteins) was found at the coastal Sta. 180 & 183 decreasing further offshore along the transect 6°E (Fig. 3.34b). Extremely high values of leucine incorporation were found at Sta. 200, however, they were not reflected by thymidine incorporation into DNA, determined in parallel samples. This discrepancy can at present not be explained. From incorporation of thymidine into DNA approximate bacterial biomass production rates of $1210 \text{ mg C m}^{-2}\text{d}^{-1}$ (Sta. 180), $3270 \text{ mg C m}^{-2}\text{d}^{-1}$ (Sta. 183), $1610 \text{ mg C m}^{-2}\text{d}^{-1}$ (Sta. 184), $1895 \text{ mg C m}^{-2}\text{d}^{-1}$ (Sta. 204), $725 \text{ mg C m}^{-2}\text{d}^{-1}$ (Sta. 202) and $490 \text{ mg C m}^{-2}\text{d}^{-1}$ (Sta. 200) were calculated.

4.2.3.4. The Coastal Current between the stations Georg-von-Neumayer and Georg-Forster

U. Bathmann, S. Großmann, K. Lochte, R. Scharek, M. Schröder (AWI)

The hydrographical patterns during our investigations in the Coastal Current (CC) basically can be separated into phases of stability and mixing. At the beginning of the transect (Sta. 160-163), the upper 70 m were stabilized by warm summer surface water (-0.85°C , <33.5) under which Low Salinity Eastern Shelf Water (-1.7°C , $33.2 - 33.4$ ppm) with a thickness of about 350 m was located. Occasionally on deeper stations (Sta. 163), Warm Deep Water ($+0.65^\circ\text{C}$, >34.5) was detected above the shelf. After the 18.02.91 (Sta. 166) a strong storm from north-easterly direction caused vertical mixing down to 200 m depth. After the storm (from St. 183 on), the water column was stabilized again, but surface waters remained much cooler ($<-1.5^\circ\text{C}$, <33.45) than before. Superimposed on these patterns, recirculation and horizontal mixing of water from the Weddell Gyre and the Coastal Current in ribbon-like structures were observed (see 4.1).

Continuous chlorophyll *a* fluorescence of surface (8m) water was measured (Fig. 3.35) by means of a Turner flow-thru fluorometer attached to the membrane pump of the ship. Due to the other field programmes it was impossible to carry out semi-synoptic registrations of physical, chemical and biological parameters in the CC. In contrast, the measurements were done during intervals between 20.2 (Sta.160) and 14.3.91 (Sta.214) indicated in Fig. 3.35. The continuous surface chlorophyll registration given in that figure indicates overall high phytoplankton biomass in the CC at the end of February with patches (ribbon-like clouds) of more than $3 \mu\text{g Chl } a \text{ l}^{-1}$. The biomass

Fig. 3.34 a: Chlorophyll a concentrations ($\mu\text{g/l}$) along the transect at 6°E perpendicular to the coast. Chlorophyll distribution patterns were obtained by combination of data from Niskin bottle samples and surface registration by a flow-through fluorometer.

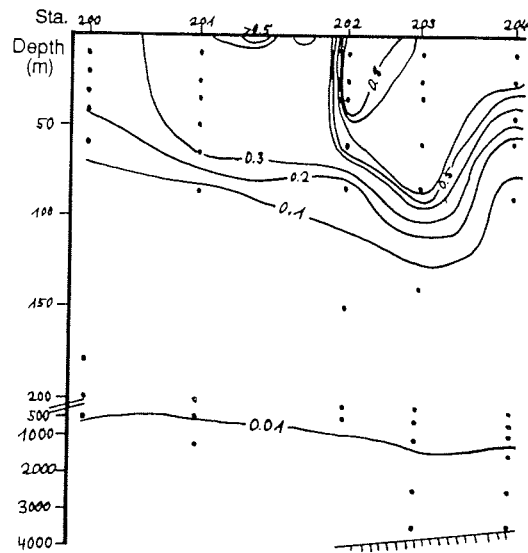
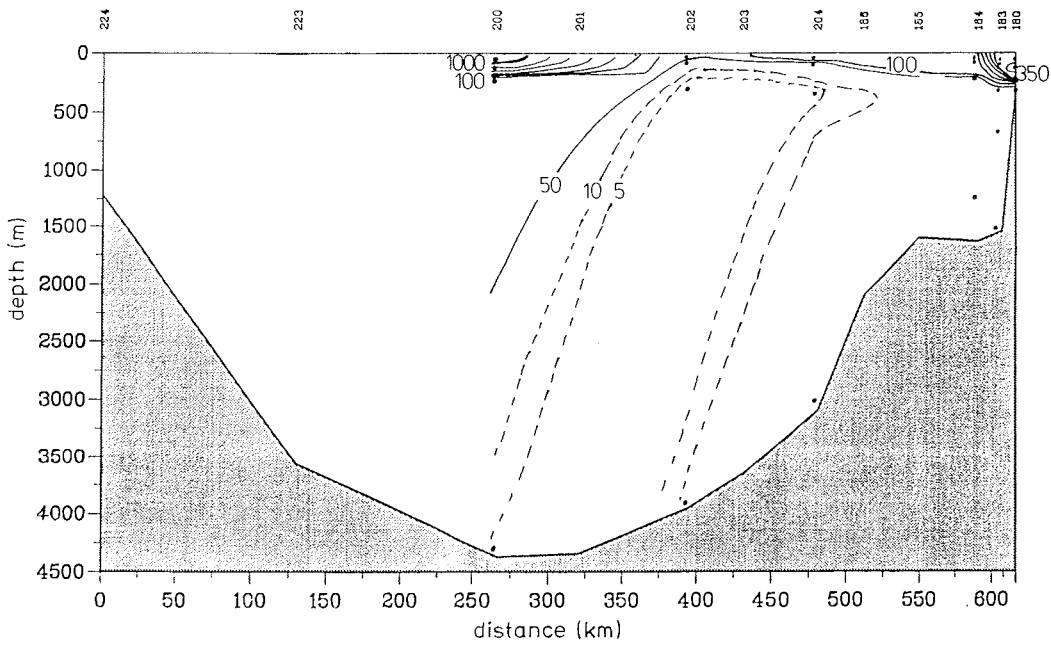


Fig. 3.34 b: Incorporation of ^3H -leucine into proteins given as $\text{pmol leucine l}^{-1}\text{d}^{-1}$ as a measure of bacterial growth along the transect at 6°E perpendicular to the coast.



decreased with time and reached levels below $0.5 \mu\text{g Chl a l}^{-1}$ after 8 March. This pattern of low biomass was detected along the entire last transect between Georg Forster and Georg von Neumayer and indicates the decline of the phytoplankton bloom in the CC with time.

Vertical distribution of the biomass as indicated by the chlorophyll *a* isolines (Fig.3.36a) also reflect the described phases. Biomass maxima ($3\text{--}6 \text{ mg Chl a m}^{-2}$) were located at about 30 m depth on stations (Sta. 160-163) within a stratified surface layer. The phytoplankton was dominated by northern oceanic, centric diatoms (*Synedra reinboldii*, *Chaetoceros bulbosum*, *Chaetoceros dictyota*, *Chaetoceros chriophilum*, *Rhizosolenia antennata f. semispina*, *Eucampia balaustium*, *Corethron criophilum*, *Dactyliosolen antarcticum*); relatively high numbers of heterotrophic dinoflagellates (mainly *Protoperidinium* spp.) and other heterotrophic protists indicated a well developed summer community.

During the storm at Sta. 166 and 169, stratification collapsed and the algae were mixed down the entire water column, but integrated biomass did not change ($500 \text{ mg Chl a m}^{-2} = 15 \text{ g C m}^{-2}$). Three days later further to the east (Sta. 175), the water column was again stratified. At this station phytoplankton species composition indicated water inflow possibly from the Riiser-Larsen-Sea. *Phaeocystis* sp. became the dominant form accompanied by *Parvicorbiccola socialis*. The colonies of both species appeared degraded and in a late state of their life. Although still present, the northern oceanic diatoms were less abundant.

Fig 3.35: Continuous measurements (10 min intervals) of fluorescence at 8 m water depth on the Lazarev Sea shelf. Various plot symbols indicate different periods of sampling. Discrete surface samples at stations are indicated by the Sta. numbers.

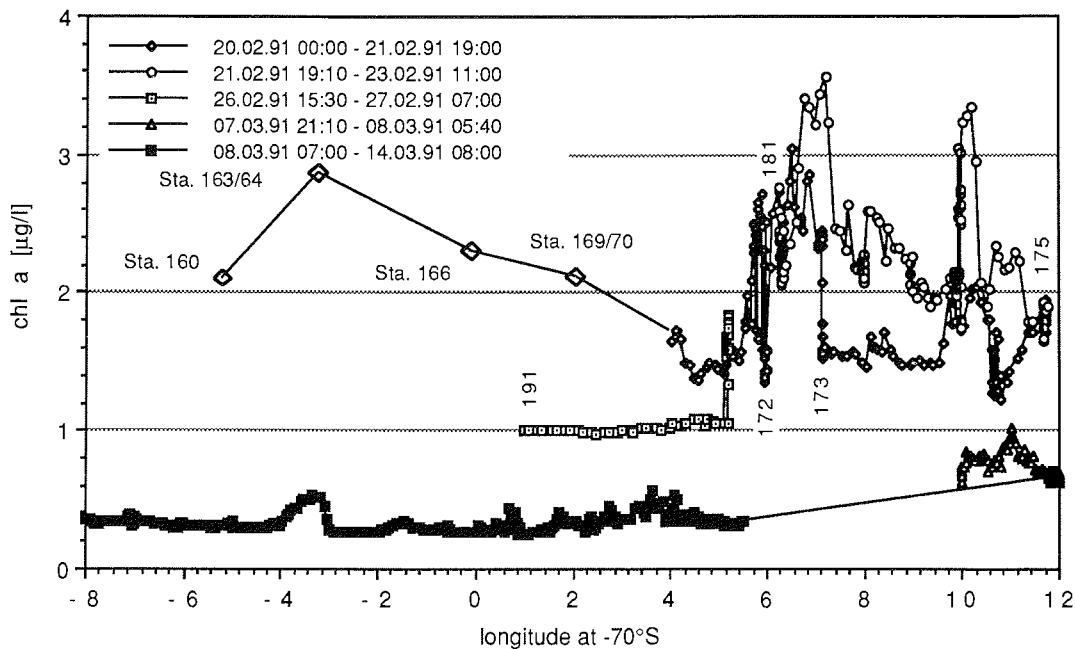


Fig. 3.36 a: Chlorophyll *a* concentrations ($\mu\text{g/l}$) in the coastal current. Chlorophyll distribution patterns were obtained by combination of data from Niskin bottle samples and surface registration by a flow-through fluorometer.

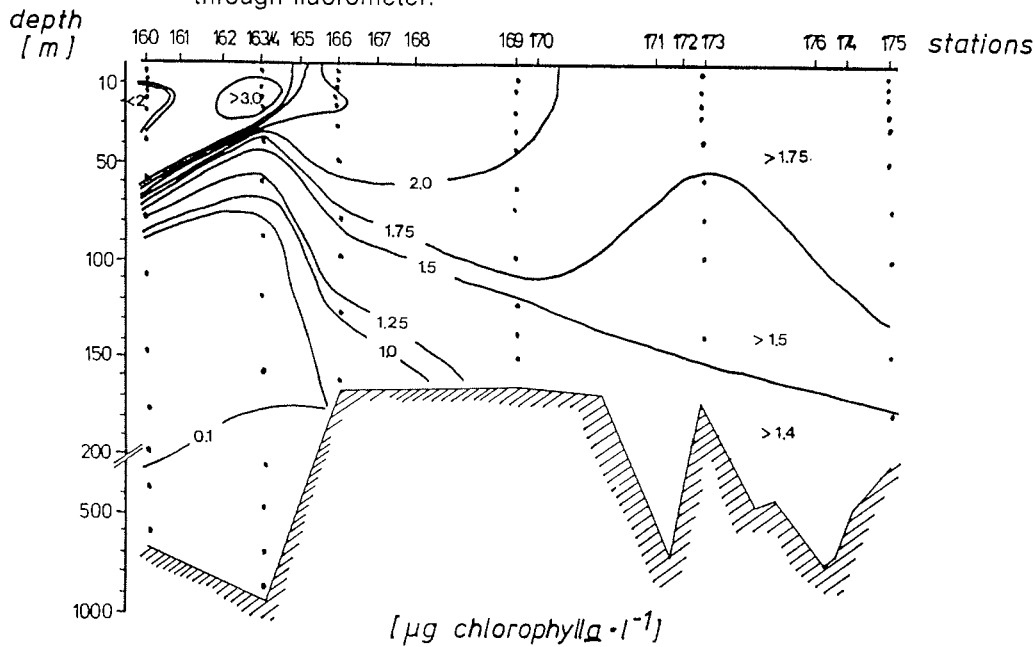
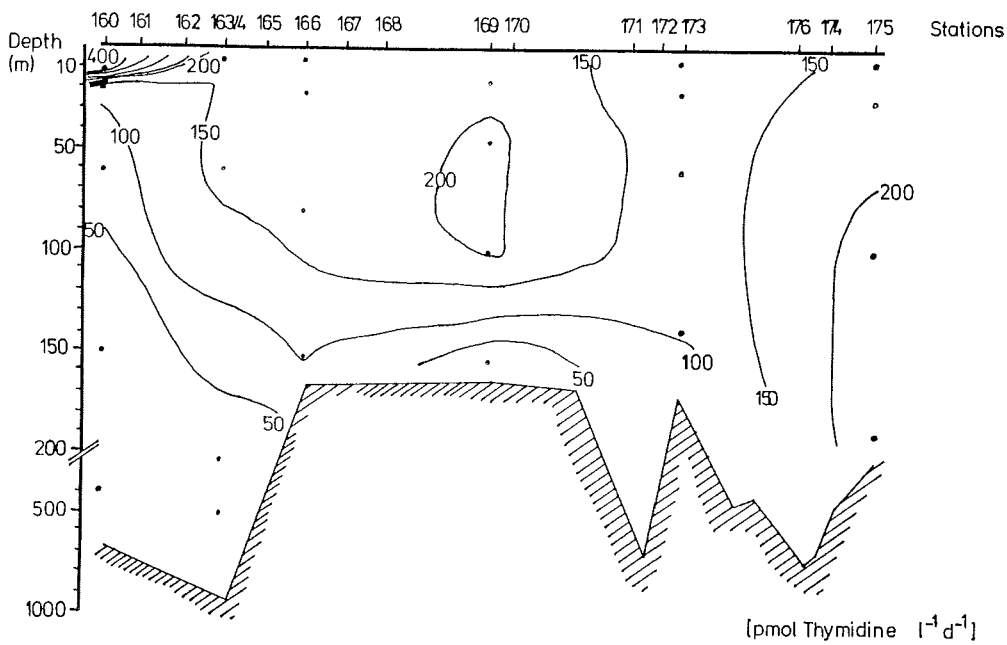


Fig. 3.36 b: Incorporation of ^3H -thymidine into DNA given as pmol thymidine $\text{l}^{-1}\text{d}^{-1}$ as a measure of bacterial cell growth in the coastal current



One week later, however, phytoplankton biomass in the CC had decreased to about 50% of initial stocks and decreased within the next 10 days to less than 1 mg Chl *a* m⁻³. During that phase, the horizontal impact of the eastern water masses could be detected by the distribution of phytoplankton species mentioned above, as far west as Sta. 181. This impact was not detected on Sta. 190 which was located at 1°E. After 13 days at nearly the same location (Sta. 214) the *Phaeocystis* sp. and *Parvicorbicola socialis* community had arrived from the east.

The bacterial production as measured by the uptake of ³H-thymidine in the coastal current (Fig. 3.36b) was clearly influenced by the storm event and the resulting mixing of phytoplankton through the entire water column. At Sta. 160 and 164, prior to the storm, high production rates were found in the stratified surface water extending down to 60 m. After the storm (Sta. 166, 169, 173 and 175) bacterial productivity was high throughout the water column. This distribution has a similar pattern to the chlorophyll *a* distribution except for the very high bacterial production values at Sta. 175. It is presumably due to the microbial degradation of moribund phytoplankton cells mixed out of the euphotic zone. Declining phytoplankton biomass and microscopic observations were indicative of a late bloom situation. This supports the assumption that the increased bacterial production thrives on accumulated phytoplankton biomass originating from a previous bloom situation. Using literature conversion factors (see 4.2.3.2) approximated integrated bacterial biomass production was estimated for the different stations (Sta. 160: 395 mg C m⁻²d⁻¹, Sta. 163/4: 1380 mg C m⁻²d⁻¹, Sta. 166: 1065 mg C m⁻²d⁻¹, Sta. 169: 1250 mg C m⁻²d⁻¹, Sta. 173: 735 mg C m⁻²d⁻¹, Sta. 175: 1620 mg C m⁻²d⁻¹).

4.2.3.5. Flux budget for the coastal current

U. Bathmann (AWI)

During our investigations between the locations of the two German Antarctic stations, a massive plankton bloom vanished out of the surface layer of the coastal current. For a budget of the vertical flux, the standing stocks of plankton material, the production and the consumption rates in the water column are compared to those of surface sediments on the shelf (only stations with depths between 450 and 750 m are presented, Fig. 3.36a, Tab. 3.12).

Tab. 3.12: Chlorophyll concentration in the upper centimetres of sediments at some stations on the Lazarev Sea shelf.

Depth/Station	Sta. 170	Sta. 172	Sta. 181	Sta. 191
0 - 0,5 cm	0,62	0,60	0,05	0,18
0,5 - 1,0 cm	0,195	0,38	0,06	0,05
1,0 - 2,0 cm	0,19	0,20	0,07	0,04
2,0 - 3,0 cm	0,05	0,15	0,10	0,05
3,0 - 4,0 cm	0,05	0,09		0,02
4,0 - 5,0 cm	0,02	0,09		
5,0 - 6,0 cm	0,01	0,01		
6,0 - 7,0 cm	0,01	0,00		

Overall losses (grazing and/or sinking) of phytoplankton biomass in the water column are based on the declining Chl *a* stocks and are about $2 \text{ g C m}^{-2}\text{d}^{-1}$ over a period of about 7 days. The fraction consumed by bacteria in the water column was higher ($700 \text{ mg C m}^{-2}\text{d}^{-1}$) than the measured total primary production ($480 \text{ mg C m}^{-2}\text{d}^{-1} \pm 180 \text{ mg}$). The material consumed by zooplankton can be calculated from the feeding rates derived from experiments. Given a number of 50 copepods m^{-3} and average daily feeding rates of about $0.02 \text{ ng Chl } a \text{ animal}^{-1} \text{ hour}^{-1}$, mesozooplankton feeding may be $240 \text{ mg C m}^{-2}\text{d}^{-1}$. The high amount of chlorophyll *a* in the first centimetres of the sediment indicate massive sedimentation of phytodetritus. Measurements of the chlorophyll inventory of the sediments were conducted by cutting subsamples from Multi-corer sediment samples into 1 cm sections. From those, wet weight, dry weight, and pigment concentrations were determined. For the latter, fluorescence readings were recorded before and after acidification with 0.1% HCl.

The transport of carbon into the sediments is calculated to be $0.5 \text{ g C m}^{-2}\text{d}^{-1}$. This material (10% of the initial phytoplankton stock of the overlying water column) was bioturbated into the sediments to 6 cm depths (Sta. 172, Tab. 3.12). 90% of this material was consumed within the first three days which we concluded by comparing the sediment load of consecutive cores. Only 10% is not consumed by the benthic infauna after one week.

The amount of carbon "missing" in these calculations of about $1 \text{ g C m}^{-2}\text{d}^{-1}$ (or 7 g C m^{-2} for the period of down-mixing of the phytoplankton bloom) thus, "left over" may have been consumed by the rich macrobenthos on the shelf or undergone downslope transport.

4.3. Plankton experiments

4.3.1. Experiments with natural algal populations from water and sea ice

Scharek, R., K. Fahl, H. H. Janssen, S. Großmann (AWI)

Objectives

1) The composition of phytoplankton populations depends on the initial species composition at the beginning of the establishment of favorable physical conditions, on the growth potential of the individual species and on the grazing pressure of herbivores. Antarctic summer phytoplankton populations can be seeded not only from the water column but also from sea ice (Garrison et al. 1987, Scharek 1991).

Experiments with natural populations from water and sea ice have been conducted during the cruise to assess the growth potential of

- a) planktonic species from different water bodies and
- b) species of ice algal populations from sea ice of different physical conditions.

2) The biochemical composition of algal cells is strongly influenced by the physical (mainly light) and chemical (mainly nutrients) environmental conditions. Light or nutrient limitation can for example lead to shifts in the pigment or storage product composition of diatoms. The biochemical composition of diatom cells under changing nutrient conditions was monitored during several weeks with special emphasis on the lipid content of the algae.

Work at sea

The algae were incubated in 10 l glass bottles at temperatures of 0°C for several weeks. The bottles were illuminated with artificial light at intensities of 60 $\mu\text{mol m}^{-2}\text{s}^{-1}$ for 20 hours and 20 $\mu\text{mol m}^{-2}\text{s}^{-1}$ for 4 hours around midnight to simulate natural light conditions at summer in the investigation area. Samples were taken at regular intervals to determine the species composition and - for approach II - also the biochemical composition of the cells and nutrient concentrations of the water. All parameters have to await analysis on land.

1) Two experiments for growth potential of phytoplankton cells were conducted:

Experiment a): Phytoplankton populations from meltwater influenced seasonal surface layers were compared with populations from underlying winter water (eastern shelf water in the coastal current, winter water in the Weddell Gyre). Water from the respective depths was taken with Niskin bottles at three stations: the coastal current Sta. 135 (229 m water depth) was located in the immediate vicinity of the shelf ice coast; Sta. 137 (700 m water depth) was located in the coastal current at the shelf break; Sta. 151 was located offshore at 4200 m water depth in the southern limb of the Weddell Gyre.

Experiment b): Pieces of sea ice were incubated in filtered surface seawater. These ice pieces originated from a ridge area located at the edge of an ice floe at Sta. 127. Three pieces of different degrees of exposition to air (air temperature was around -15°C) were chosen: one very dry piece, one dry piece, one wet piece from the water surface. All of them were coloured brown by diatoms.

2) On the drifting stations (126, 127, 128) algal populations with unusually high lipid contents (determined microscopically via staining of the cells with sudan red) had been collected from platelet and slush ice layers. Subsamples for the determination of the species composition and for measuring the biochemical composition of these populations as well as the nutrient contents of the surrounding medium were taken at the beginning of the experiment. Then the algae were incubated in nutrient rich filtered seawater. Samples were taken at regular intervals and analysed as described above to follow possible shifts in species as well as in biochemical cell composition.

Reference

- Garrison, D.L.; Buck, K.R.; Fryxell, G. A. (1987). Sea ice algal communities in Antarctica: species assemblages in pack ice and ice edge planktonic communities. *J. Phycol.* 23: 564-572.
- Scharek, R. (1991). Development of phytoplankton during the late-Winter / Spring transition in the eastern Weddell Sea (Antarctica). *Rep. Polar Res.* 94, 1-195

4.3.2. Zooplankton

4.3.2.1. Reproduction and proposed life cycles of dominant copepods in the Weddell Sea.

F. Kurbjeweit (AWI)

Objectives and Work at sea

Objectives and Work at sea apply as in the previous leg ANT IX/2 (see chapt. ANT IX/2; 4.5). Additionally, dilution series were carried out to observe the reproduction of *Metridia gerlachei* under very low phytoplankton concentrations (Verity & Smayda 1989). Also, specimens of *M. gerlachei*, *Calanus propinquus* and *Calanoides acutus* were preserved for electronmicroscopical investigations of mouth parts and the sensory apparatus (Kurbjeweit & Buchholz in press). Salps for protein analysis and chaetognaths for DNA/RNA-analysis were sampled to be processed by colleagues at home.

Preliminary results

a) Distribution and abundance

M. gerlachei was abundant on almost all stations, except on the very shallow northern continental shelf stations in the Lazarev Sea (<300m) and the drift stations in the southern Weddell Sea within the porridge ice. In the latter case, the zooplankton community in the water column was in general almost absent. The small copepod *Stephos longipes* was very abundant close to and under the ice, particularly platelet ice (see 4.2.2). Females were scarce on all stations

(< 10% of the population) and males were completely missing. *M. pygmaeus*, was rare and found only occasionally to be abundant. Adults, mainly females, were found only in very low numbers. *C. propinquus* was almost missing on stations south of GvN during the first part of the cruise (Sta. 122, 125-128). This species was abundant mainly on stations offshore where water depths exceeded 600 m. *C. acutus* showed a similar distribution as *C. propinquus*. *R. gigas* as well as *Ctenocalanus citer* were found frequently only northeast of GvN.

Besides these calanoid copepods, the cyclopoid copepods *Oithona similis*, *Oithona antarctica* and *Oncaea* ssp. were very abundant on most stations except the drift stations and therefore played an important role in the zooplankton community of the Weddell Sea. In summary, the abundance and diversity of copepods and zooplankton in general was significantly lower on stations south of G.v.N. than in the Lazarev Sea.

b) In situ egg production

On Sta. 122, 125, 126, 130, 136, 160, 198, 204 and 223 in situ egg production of *M. gerlachei* was examined in surface sea water. No clear correlation between chlorophyll *a* concentrations offered in the experiments and the egg production could be found. The egg production ranged between 0 and 9,68 eggs female⁻¹day⁻¹. On Sta. 126 (ice-drift), 136 and 223 (Maud Rise) no egg production was observed at all. *M. gerlachei* seems to sustain egg production until the end of March perhaps due to its opportunistic behaviour in using a broader food spectrum than *C. acutus* and *C. propinquus*. *C. acutus* (Sta. 153) and *C. propinquus* (Sta. 147, 153, 198 and 204) did not produce at all, probably due to their preparation for overwintering.

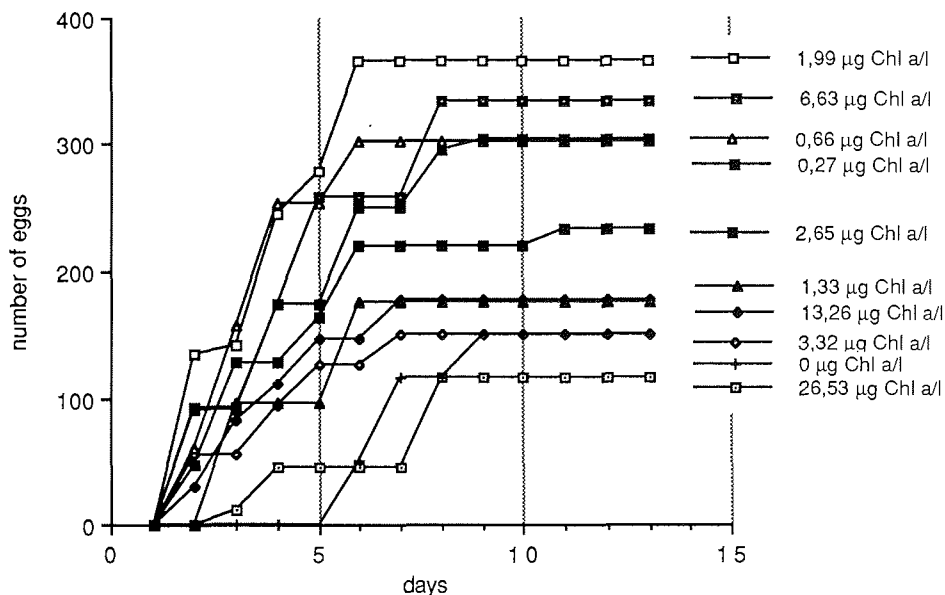
c) Egg production with superabundant food concentrations

Experiments with superabundant food concentrations were conducted only with *M. gerlachei* and *S. longipes*. In all experiments Chl *a* content exceeded $>3\mu\text{g l}^{-1}$, but egg production of *M. gerlachei* ceased in most experiments after 6 - 7 days. In contrast, egg production of *S. longipes* did not cease, but the time intervals between egg laying events were longer and the egg clutches smaller compared to *M. gerlachei*. *S. longipes* showed a significantly higher egg production when offered ice diatoms compared to *Thalassiosira* ssp. from the water column as food. This seems to be an additional proof for the association of the life cycle of *S. longipes* with ice.

d) Egg production under varying food concentrations

In two experiments the hypothesis was tested that *M. gerlachei* are food limited in the Weddell Sea. Abnormally high food concentrations seem to diminish egg production, although no clear trend could be observed (Fig. 3.37). Since *Phaeocystis* sp. was part of the food, these results have to be treated with care.

Fig. 3.37: Accumulative egg production of *Metridia gerlachei* under various food concentrations.



e) Respiration

Respiration measurements (compare with ANT IX/2) showed that small calanoid copepods as *S. longipes* respired about 0.24 $\mu\text{l O}_2/\text{animal}/\text{hour}$ and *Microcalanus pygmaeus* even less - 0,022 $\mu\text{l O}_2$, while larger animals such as *M. gerlachei* respired between 1,2 and 5,59 $\mu\text{l O}_2/\text{animal}/\text{hour}$ depending perhaps on time of the year and/or stress. *C. propinquus* showed similar respiration rates. Due to its low activity *C. acutus* had an even lower oxygen consumption than *M. gerlachei*.

f) Grazing

Additional grazing experiments were conducted with *M. gerlachei* on different stations during the cruise. Results will be given later.

References

- El-Sayed, S.; Taguchi, S. (1981). Primary production and standing crop of phytoplankton along the ice-edge in the Weddell Sea. *Deep Sea Res* 28:1017-1032.
- Evans, C.A.; O'Reilly, J.E.; Thomas, J.P. (1987). A handbook for the measurement of chlorophyll *a* and primary production. Biological Investigations of Marine Antarctic Systems and Stocks (BIOMASS), 8:47-109, Texas A&M University, College Station, Texas, U.S.A.
- Kurbjeweit, F.; Buchholz, C. (in press): Morphology and function of sensory organs in *Calanus glacialis*, *Metridia longa* and *Paraeuchaeta norvegica*.
- Smith, S.L. (1990). Egg production and feeding by copepods prior to the spring bloom of phytoplankton in Fram Strait, Greenland Sea. *Mar. Biol.* 106, 59-69.
- Strickland, J.D.H.; Parsons, T.R. (1972). A practical handbook of seawater analysis. *Fish Res Bd Canada Bull* 167:310 pp.
- v. Bodungen, B., Nöthig, E.-M.; Sui, Q. (1988). New production of phytoplankton and sedimentation during summer 1985 in the south eastern Weddell Sea. *Comp Biochem Physiol* 90:475-487.
- v. Bröckel, K. (1985). Primary production data from the south-eastern Weddell Sea. *Polar Biol* 4:75-80.
- Verity, P.G.; Smayda, J.T. (1989). Nutritional value of *Phaeocystis pouchetii* (Prymnesiophyceae) and other phytoplankton for *Acartia* spp. (Copepoda): ingestion, egg production, and growth of nauplii. *Mar. Biol.* 100, 161-171.

4.3.2.2. Feeding rates of *Calanus propinquus* and *Calanoides acutus*

U. Bathmann (AWI)

Objectives

The two species *Calanus propinquus* and *Calanoides acutus* dominate the calanoid copepods >3 mm in the Weddell Sea. Their winter feeding behaviour was shown to be quite different during a previous investigation (ANT VIII/2). While the former species was actively grazing near and directly under the ice, the latter was hibernating in the Warm Deep water (1000 m depths). During our cruise we wished to find out when and under what conditions (status of the succession of the pelagic ecosystem) *C. acutus* stopped feeding and commenced overwintering diapause.

Work at sea

Copepods of both species were collected and handled as described above (F. Kurbjeweit). The species were sorted under a stereo microscope in the experimental container (1°C) to developmental stages. Then 10 individuals of adult females and copepodite V stages were transferred into 100 ml beakers, previously filled with filtered sea water. After the water was exchanged 3 times, 10 individuals were placed in each of six 5 l glass bottles. These bottles were previously filled with a mixture of filtered sea water to which natural phytoplankton was added to an initial concentration similar to natural stocks (2 µg Chl *a/l*). Two extra bottles containing only phytoplankton served as controls. The experiments were run for 7 days under dim light conditions (< 20 µ Einst.). Every day, the concentration of Chl *a* was monitored by removing 100 ml from each bottle. Every second day, subsamples for phytoplankton cell counting were taken. After the experiment, the feeding rates were calculated.

Results

The grazing rates of the copepod *Calanus propinquus* was higher than that of *Calanoides acutus*. During February, both species fed actively. The maximum grazing rates of both species were observed at the beginning of the experiment and then decreased to levels of about 0.02 ng Chl *a/l* for *C. propinquus* and 0.008 ng Chl *a/l* for *C. acutus*. These rates were not sufficient to decrease the food concentration in the experimental bottles which remained nearly constant with time although the phytoplankton in the controls increased. At the beginning of March, however, grazing rates of *C. acutus* decreased close to detection limits, while those of *C. propinquus* remained at the level previously observed.

5. BENTHOS

5.1. Macrozoobenthos ecology

General objectives and work at sea

Faunistic-ecological investigations of Weddell Sea benthos conducted intensively during the last decade resulted in differentiation of 3 faunal categories: a) the Eastern Shelf Community which spreads out from the Atka Bay in the east down to the Vahsel Bay in the south; b) the more offshore situated Southern Shelf Community on the broad shelf near Halley Bay; c) the Southern Trench Community occurring mainly in the Filchner Depression and adjacent waters (Gutt, 1988; Voss, 1988; Hain, 1989).

During this cruise the benthic faunas of the Lazarev and Weddell Seas were compared in order to ascertain whether significant differences in benthic community composition and in the ecology of individual species exist which might be related to differences in environmental conditions (depth, topography, width of the shelf, hydrographic regime, food input etc.). Another objective was to collect as many live animals as possible for aquarium studies on reproduction, growth, physiology and behaviour.

The fauna was sampled with towed gear (Agassiz trawl, AGT, and bottom trawl, GSN), which mainly provides large amounts of material on an (at most) semi-quantitative basis, in combination with a quantitative multibox corer (MG) taking nine 240 cm² samples at a time, and imaging methods which included

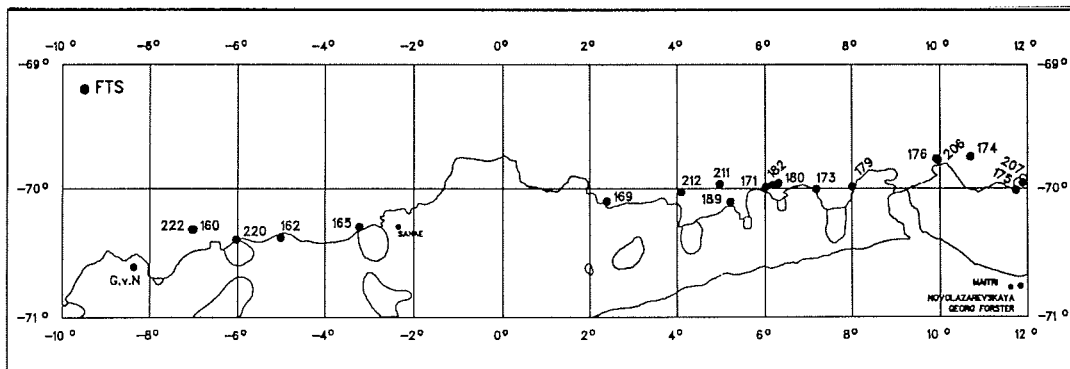
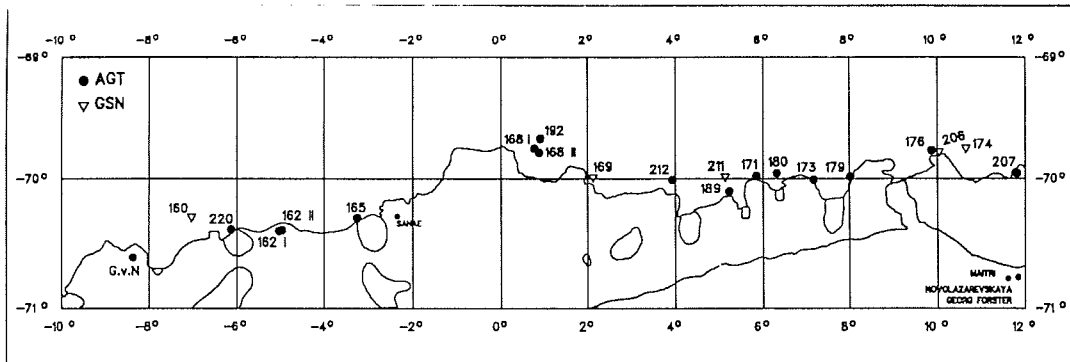
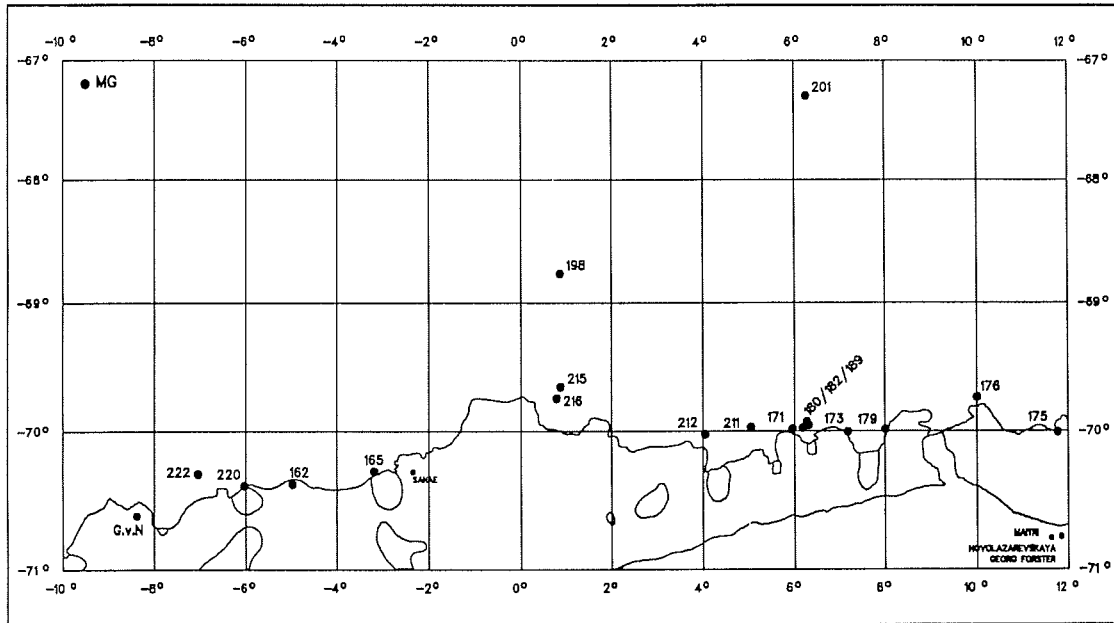
a video camera on the MG and a still underwater camera mounted on a sledge (FTS). In total, 2 such combined stations were worked in the Weddell Sea and 15 in the Lazarev Sea. Individual gear deployments were higher due to various unsuccessful attempts to achieve the full combination (time restrictions, ice cover etc.). Even where all three types of gear were deployed at one station, it was not always possible to work on the same fauna. This was especially the case in the Lazarev Sea where the slope gradient is often quite steep. The original idea of covering the 200 - 1000 m depth range in 200 m steps along the longitudinal gradient in that area could only be partly accomplished since the depth structure was not known beforehand and because of the restrictions mentioned above. Station positions are given in Figs 3.38a, b, c and the station list in the annex.

With few exceptions the samples and photos will be analysed in detail in the home laboratory. A preliminary analysis of the relative abundance of 40 taxa in 20 litre subsamples from the trawl samples was made. These data, too, will be subjected to a more detailed (cluster) analysis at the AWI that will then be compared with the multibox corer and UW camera data.

References

- Gutt, J. (1988). Zur Verbreitung und Ökologie der Seegurken (Holothuroidea, Echinodermata) im Weddellmeer (Antarktis). *Ber. Polarf.* 41: 87 pp.
- Voss, J. (1988). Zoogeographie und Gemeinschaftsanalyse des Makrozoobenthos des Weddellmeeres (Antarktis). *Ber. Polarf.* 45: 145 pp.
- Hain, S. (1989). Beiträge zur Biologie der beschalten Mollusken (Klasse Gastropoda und Bivalvia) des Weddellmeeres. PhD Thesis Bremen Univ.: 298 pp

Fig. 3.38 a, b, c: Geographic distribution of multibox corer (MG), Agassiz trawl (AGT), bottom trawl (GSN) and underwater photography (FTS) stations in the Lazarev Sea.



5.1.1. The use of Hydrosweep data for planning and realization of biological sampling activities

S. Hain & H. Hinze (AWI)

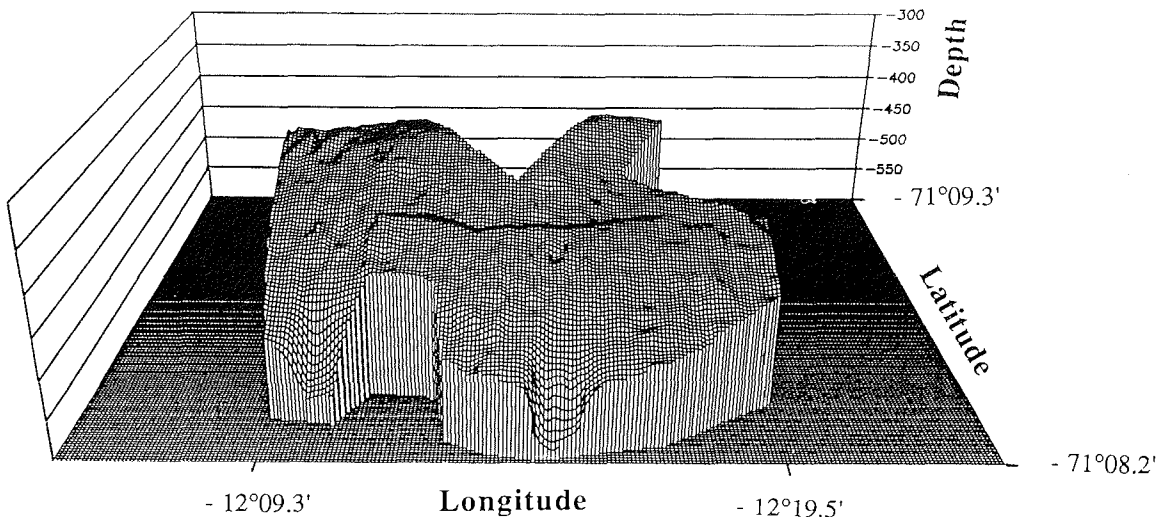
Planning of stations

During this cruise the bathymetric data produced by the swathe sounding system Hydrosweep were used for planning AGT, GSN and MG stations. For this purpose the intended sampling site was discussed with the Hydrosweep operator. The general bottom topography and the extension of the ice shelf was checked using different data sources (e.g. GEBCO). Based on these data the position for the station was determined fairly accurately and used as navigation way point for the ship. This procedure reduces the time spent searching for the required depth dramatically. Use of Hydrosweep data thus allows a careful operation of gear in the selected areas especially with regard to depth and rough bottom topography.

Postprocessing

The bathymetric data of the Hydrosweep system taken during net hauls were combined with other data to produce a computer-derived digital terrain model (DTM) of the sampling area. This model can be taken for bathymetric charting of the area and for derivation of perspective three-dimensional views. The trackline of the gear can be analyzed in relation to the bottom topography. The information whether the sampling area was within an extensive plain or on a smaller terrace surrounded by slopes, hills, or canyons is extremely valuable for scientists working at the sea floor. In many cases topographical differences and the resulting alterations of the current system may be responsible for small-scale changes in faunal distribution. Effects of this kind have been reported throughout the cruise. The procedure of post-processing all bathymetric data produced by the Hydrosweep system is very time consuming, and has therefore been done only for one location (Fig. 3.39

Fig. 3.39: AGT haul 1 & 2 (Sta. 123) off Kapp Norvegia.
Perspective view of the sampling location



5.1.2. Faunistic-ecological investigations by means of underwater photography

J. Gutt (AWI)

Objectives

Underwater photography allows a quantitative estimation of megafauna densities. It was applied within the general ecological framework to evaluate information in addition to traditional sampling gears. The dominance of different life styles (e.g. sessile - motile, colonial - solitary), different feeding types (filter feeders - deposit feeders) and substratum preference can be directly evaluated. Behavioural observations, e.g. on epizoic life, reveal interactions between different components of the ecosystem. Dispersion patterns within different spatial scales provide additional information about colonization in relation to biotic and physical environmental conditions. The scales are: 1 photography = 1 m², 1 station = 70 m². The entire area under study in the Lazarev Sea corresponds to 800 km coast line.

Preliminary results

In the Halley Bay area the underwater camera was used at 5 stations to fill up a gap in the benthos programme of the EPOS Leg 3 cruise. These casts have led to a significant increase in quality of the EPOS data. The data will be used for a comparison of two photo transects off Halley Bay and Kapp Norvegia.

East of Atka Bay, the UW camera was deployed at 18 stations: 8 on the shallower shelf down to 400 m, 7 on the deeper shelf and the shelf edge between 400 and 600 m, and 3 on the upper slope below 600 m to 1000 m, taking a total of 1260 pictures (= m²). The following trends can be formulated after a preliminary analysis of the material from the Lazarev Sea:

Stations on the shallower shelf (130-400 m) were richer in biomass and more diverse than those on the deeper shelf and on the upper slope (between 400 and 1000 m). Filter feeders such as hexactinellid sponges, bryozoans and compound ascidians became rare with increasing depth, although most of them were not totally missing even at the deepest stations. Patchiness was extreme on the shallower shelf. Stations of very high biomass (e.g. Sta. 179, Fig. 3.40a) were found close to those with an obviously poor fauna (e.g. Sta. 175). Also within single stations or even within one photograph a high degree of patchiness was observed (e.g. at Sta. 180). This patchiness concerns the entire community as well as single species; examples are the high concentrations of *Melicerita obliqua* (fusiform bryozoans) at Sta. 220 (Fig. 3.40b), of a brachiopod species at Sta. 207, or approx. 30, mostly young, specimens per m² of the sea urchin *Sterechinus neumayeri* at Sta. 165.

At Sta. 189, 211, and 212 a thick layer of green material on the seafloor indicated a recently sedimented phytoplankton bloom.

Discussion

A first analysis of underwater photos taken in the Lazarev Sea shows the presence of elements of the Eastern Shelf Community known from the Weddell Sea. At a first glance the degree of patchiness seems to be even higher than in the Weddell Sea (Gutt & Piepenburg, 1991; Gutt et al., in press). The reason for this may have to be sought in differing environmental conditions rather than in the presence of different communities in small areas. For the observed patterns a more diverse near- bottom current system fuelled by different water masses with their biological inventory or providing different

Fig. 3.40a: Sta. 179, 200 m. Dense concentration of hexactinellid sponges and bryozoans/ hydrozoans in between. Solitary coral in the center, compound ascidians in the upper left corner. Area: approx. 1 m²



Fig. 3.40b: Sta. 220, 130 m. Aggregation of fusiform bryozoans (*Melicerita obliqua*). The three crinoids indicate a strong bottom-near current corresponding well to the alignment of the bryozoans. In addition, a few small sponges and some other bryozoans can be seen. Area: approx. 1 m²



amounts of food, iceberg scouring destroying the life at the seafloor, or the inhibitory effect of the ice shelf edge on the fauna may be responsible. Biological interactions such as the influence of predators or epizoic life style may also influence the recent faunal composition.

References

- Gutt, J.; Piepenburg, D. (1991). Dense aggregations of three deep-sea holothurians in the southern Weddell Sea, Antarctica. *Mar. Ecol. Progr. Ser.* 68: 277-285.
- Gutt, J.; Gorny, M.; Arntz, W. (in press). Quantitative observations on Antarctic shrimps (Crustacea: Decapoda) in their natural environment by means of underwater photography. *Antarctic Sci.*
- Voss, J. (1988). Zoogeographie und Gemeinschaftsanalyse des Makrozoobenthos des Weddellmeeres (Antarktis). *Ber. Polarforsch.*, 45: 145 pp.

5.1.3. Quantitative macrofauna sampling and in - situ observation with the multibox corer

D. Gerdes, A. Schanz, R. Steinmetz (AWI)

In contrast to earlier investigations (ANT VI/3, EPOS 3) the multibox corer was used in combination with an attached UW video system (see Gerdes, 1990). The combination of these 2 devices in one gear allows simultaneously two different working steps: the collection of up to 9 bottom cores for analyses of distribution and abundance of benthic animals and the direct observation of faunistic structures on the sea bottom which allows a much better evaluation of the in situ situation. This equipment was used during ANT IX/3 at 9 stations in the Weddell Sea and at 18 stations in the Lazarev Sea for a quantitative analysis of the macrobenthos, covering a range from 126 m to 4294 m water depth. In total more than 13 hours of video recordings and 115 bottom cores resulted from this work. All samples were sieved over 0.5 mm mesh size and preserved in 5% formalin buffered with hexamethylene-tetraamine prior to examination in the laboratory.

Technical remarks

The multibox corer in combination with the UW video system was used for the first time on this leg. The video equipment itself was shown to be quite robust, whereas the coaxial cable of "Polarstern" turned out to be the more sensitive part of the system. Improvements of the terminal bell of the cable are necessary. The cable must be handled carefully, especially when other gear (AGT, GSN) is used parallel on the ship.

Preliminary results

The basic objective for our investigations east of Atka Bay, where no benthic work had been done prior to this cruise, was to continue the faunal inventory of the Weddell Sea further to the east. Before careful analysis of the box cores, statements about similarities or differences of the abundance and biomass of benthic organisms in the two areas are difficult. A first glance at the video recordings indicates, however, that both areas have comparable faunistic elements. Shallower shelf stations in the Lazarev Sea were richer in biomass and diversity than deeper ones, as is also known from the Weddell Sea deep-sea stations in both areas (Sta. 146 II, 198, 201; depths between 3700 and

4300 m) showed a very poor fauna. There was evidence of extreme patchiness even on very small scales. The video recordings underline that this trend, which became visible when comparing the individual box cores from several MG stations, also holds true on larger scales.

Reference

Gerdes, D. (1990). Antarctic trials of the multibox corer, a new device for benthos sampling. *Polar records* 26(156): 35-38

5.1.4. Preliminary subsample evaluation from AGT and GSN catches

W. Arntz, D. Gerdes, M. Gorny, J. Gutt, A. Schanz, R. Steinmetz (AWI)

Objectives

Using towed gear, data from the rough sample (sorted on deck) and a subsample (sorted in detail in the lab) proved to be a valuable source of information during the EPOS 3 cruise (Arnaud et al., 1990). A matrix was developed during that cruise and slightly changed for this cruise, using 40 faunal taxa and 4 categories of frequency: absent, rare, common, and very abundant. The haul on deck was searched by a number of specialists who recorded the larger and more conspicuous forms and picked out certain groups. A subsample (20 l during ANT IX/3) was sorted by experienced people also for smaller organisms. The combined rough + sub-sample data can be assumed to present a fairly precise picture of faunal composition. Thus, the first objective was to provide this kind of rapid information which may serve additionally for separating benthic communities by cluster analysis, as can be demonstrated by the EPOS data (R. Herman, pers.comm.). The next step, then, is to have the species (at least, the key species which are either very abundant or very constant) identified by specialists, and to use species instead of larger taxa for a second run of the cluster analysis.

Preliminary results

16 successful AGT and 8 successful GSN hauls taken in the Weddell and Lazarev Seas were analysed in the way described above (Tab. 3.13 & 3.14). The GSN used was a 140 ft commercial bottom trawl with 10 mm meshes in the codend; the AGT (width 3 m) also had 10 mm meshes, but a 4 mm inlet was used from the third haul to prevent the smaller fauna from being washed out, and a 30 kg weight attached to the "codend". In catches with large amounts of sponge spicules and bryozoan debris loss of small organisms is most effectively prevented by this mass which acts like a narrow-meshed sieve. This may be why catches from shallower areas or from medium water depths were usually much richer in small organisms than deep-water hauls where this mass is missing.

At first glance no other general trends are identifiable along the longitudinal or depth gradient, but clustering may produce quite a different picture. Each station seemed to have its own set of fauna and its own characteristics, thus underlining the impression of extreme patchiness derived from the video and UW camera transects. In some cases certain taxa dominated the fauna in a way which hitherto had been observed only for sponges and bryozoans. Examples are AGT 11 (Sta. 173), AGT 12 (Sta. 176) and GSN 4 (Sta. 158) with about 50% of the catch consisting of pterobranchs; AGT 17 (Sta. 207) with

Tab. 3.14: Relative abundance of benthic taxa in the bottom trawl (GSN) in the Weddell and Lazarev Seas by degree longitude

GSN No.	3	2	4	5	6	9	8	7
Station No.	133	130	158	160	169	211	206	174
Depth range (m)	424	561	623	830	560	661	343	432
°West	436	626	539	802	450	742	336	432
°East	26	25	16	6				
					2	5	9	10
Porifera	++	+	+	++	++	+	++	+
Actiniaria	++	++	++	+	++	+	++	++
Scleractinia	-	+	+++	+	+	+	-	++
Stylasteroidea	-	-	-	++	+	+	-	++
Hydroidea	+	+	++	+	+	+	++	++
Alcyonaria	-	-	-	+	-	+	+	+
Pennatularia	++	-	+	-	+	++	+	+
Gorgonaria	+	+	++	+	++	++	+	+++
Bryozoa	+	++	++	+	+	++	+++	+
Brachiopoda	+	++	+	+	+	-	+	+
Turbellaria	-	-	-	-	-	-	-	-
Nemertini	+	+	+	+	+	+	+	+
Echiurida	-	+	++	-	+	-	-	-
Priapulida	-	++	-	-	-	-	-	-
Sipunculida	-	+	+	+	+	+	+	+
Polychaeta Errant.	+	++	+++	++	+	+	++	++
Sedent.	+	++	++	+++	+	+++	++	+
Aplacophora	-	-	+	-	-	+	+	+
Polyplocophora	-	-	++	-	++	+	++	++
Prosobranchia	+	++	++	+	+++	++	+	++
Opistobranchia	+	++	++	+	+	++	+	+
Scaphopoda	-	-	-	-	-	-	-	-
Bivalvia	+	+	++	+	+++	+	+	++
Cephalopoda	+	++	++	++	++	++	+	++
Pycnogonida	+	+	+++	+++	+	+++	+	+
Decapoda	+++	+++	+++	+++	+	+++	++	+
Mysidacea	+	+++	++	+	+	++	+	+
Cumacea	-	-	++	-	++	+	+	++
Isopoda	-	+	+	+	+	+	++	++
Amphipoda	+	+	+++	+	++	+	+	+++
Cirripedia	-	-	+	-	-	+	-	+
Crinoidea	+++	+	++	+	+	+	++	+
Asteroidea	+++	+++	++	++	++	++	++	++
Ophiuroidea	++	+	++	+++	++	++	++	+++
Echinoidea Reg.	++	++	++	+++	++	+++	+	++
Irreg.	-	-	+++	+	+	++	++	+
Holothuroidea	+++	+++	++	++	+++	+	++	++
Pterobranchia	+++	+	+++	+	+	+	-	+
Ascidiae	+	+++	++	+	+	+	++	++
Pisces	+	+++	+++	+++	++	+	+	++
Stones	-	++	+	+	++	+	+++	+

about 75% dominance by brachiopods obviously growing on the level bottom, without stones; and AGT 19 (Sta. 220) with a similarly high dominance of crinoids. Other examples include unusually high amounts of regular sea urchins, pycnogonids, the red deep-water shrimp *Nematocarcinus lanceopes*, or the "Red Knight" *Epimeria rubrieques*, an amphipod species. Cumaceans were often found in large numbers, and ostracods (which are not listed in the Tables) were very common in AGT 11 (Sta. 173) and GSN 7 (Sta.174). On the other hand isopods, which had been very diverse and abundant in the Weddell Sea, mostly appeared with only 1-2 genera per haul and were nowhere really abundant. GSN 9 from about 700 m depth provided three extremely rare species which may turn out to be of special zoogeographic importance: the first living specimen of the scallop *Adamussium colbecki* from the Atlantic sector of the high Antarctic, the large deep-sea balanid *Verruca gibbosa* (so far only known from the Filchner area in the Atlantic high Antarctic), and 2 specimens of the shrimp *Eualus kinzeri*.

Reference

Arnaud, P.M.; Galeron, J.; Arntz, W.; Petersen, G.H. (1990). Semi-quantitative study of macrobenthic assemblages on the Weddell Sea shelf and slope using trawl catch subsamples. In: Arntz, W., W. Ernst & I. Hempel (eds), 1990. The expedition Antarktis VII/4 (EPOSI leg 3) and VII/5 of RV "Polarstern" in 1989. Ber. Polarforsch. 68: 214 pp.

5.1.5. Studies on the benthic molluscs (Gastropoda and Bivalvia) S. Hain (AWI)

Objectives

The principal objective of this study was to compare the molluscan fauna of the Lazarev Sea with that of the Weddell Sea where at least 150 gastropod and 50 bivalve species live (Hain, 1990). Furthermore, an attempt has been made to get additional material of selected species from the SE Weddell Sea, to focus on small (less than 4 mm shell size) gastropod and bivalve species, and to obtain living specimens for analyses of reproduction and behaviour in the cool containers on board and later on at the AWI.

Preliminary results

Two AGT hauls were taken off Kapp Norvegia to obtain additional living specimens of a left-handed gastropod species single specimens of which had been caught in this area during the expeditions ANT V/3 and VII/4 (EPOS 3). For evaluation of the systematical and evolutionary position of this species, a potential "missing link" between marine opisthobranchs and freshwater pulmonates, the soft parts of additional specimens have to be sectioned. The preliminary sorting of the samples has revealed no further individuals, but preserved material from the sample will be sorted at the AWI.

A preliminary comparison of the benthic molluscan fauna from the Lazarev Sea with that of the Weddell Sea reveals strong superficial similarities. Similar to the "Eastern Shelf Community" (Voss, 1988), the fauna of the continental shelf down to 600 m water depth was found to be dominated by sponges and/or gorgonarians and bryozoans. The molluscan species which are associated with this fauna in the Weddell Sea such as *Parmaphorella mawsoni*, *Margarella* spp., *Harpovoluta charcoti* (Gastropoda) and *Limopsis*

marionensis, *Lissarca notorcadensis*, *Philobrya sublaevis*, *Adacnarca nitens*, and *Limatula hodsoni* (Bivalvia) were regularly found. Protobranch bivalves and gastropods which are typical of soft bottom sediments ("Southern Trench Community", Voss, loc.cit.) were found only in small numbers.

One living specimen of the Antarctic scallop *Adamussium colbecki* (Fig. 3.41a) was obtained from GSN 9 (Sta.211). The recovery of the first living specimen at water depths between 568 and 644 m is exceptional because *A. colbecki* is most common in littoral areas (Dell, 1990) and was found exclusively as dead shell material on former expeditions (Hain, loc.cit.).

On the EPOS 3 expedition many small archaeogastropod taxa with shell sizes less than 4 mm were obtained by sieving subsamples. In cooperation with foreign specialists these Antarctic species are being studied for evaluation of their evolutionary and zoogeographical relationships with other groups and areas. To obtain further specimens of small-sized species and juveniles, a subsample of 50 l was taken at 11 stations. The material was sieved using a stacked column of two sieves (4 mm and 0.5 mm), and the contents of the latter were preserved in 100% alcohol. The molluscs will be sorted at the AWI or the sorting center at Stockholm University.

The epifauna on stones was carefully investigated by eye or microscope for small and rare molluscan species. The study confirms previous analyses that basically attached bivalves prefer other organisms as settling ground; only *Cyclopecten* spp. (Pectinidae) were found attached to stones. Several limpet-shaped gastropod species feed on the detritus which covers the surface of the stones. All of these species were very rare (*Fissurisepta antarctica* and *Lothia coppingeri* were found at two stations, *Puncturella enderbyensis* at one station) and occurred only with single specimens on larger boulders. Stones smaller than 20 cm in diameter were never colonized. An extraordinary finding was the recovery of two living monoplacophoran specimens. Sixteen recent species of this primitive molluscan class are known world wide from deeper water areas up to now. The first specimen from Sta.158 is conspecific to specimens from the eastern Weddell Sea which will be described as *Laevipilina antarctica* (Warén & Hain, subm.). A second specimen from Sta. 212 was photographed alive (Fig. 3.41b in the aquarium). This specimen differs in its shell dimensions (3.03/2.68/0.88 length/width/height in mm) and gill morphology from the other material. A detailed comparison of shell, radula and soft parts with other monoplacophoran species will reveal the systematic position of this specimen.

For investigations on the behaviour and reproductive biology, several hundred gastropods, bivalves and egg masses of approximately 40 species are kept alive in temperature controlled aquaria. This material will complete the collection of living Antarctic molluscs from past expeditions at the AWI. A large material of the bivalve *Limopsis marionensis* was preserved for growth studies. The soft body morphology of active and crawling specimens of 25 gastropod and bivalve species was documented macrophotographically since most of these features cannot be seen using preserved material. Many gastropods cover large parts of their shell with extensions of the mantle (e.g. *Falsimargarita gemma*, *Newnesia antarctica*, *Naticidae* spp.) and possess long epipodial tentacles (*Trochidae* spp.) which are used as tactile organs.

Fig. 3.41a: Living specimen of *Adamussium colbecki* (Smith,1902)
Shell width 23 mm

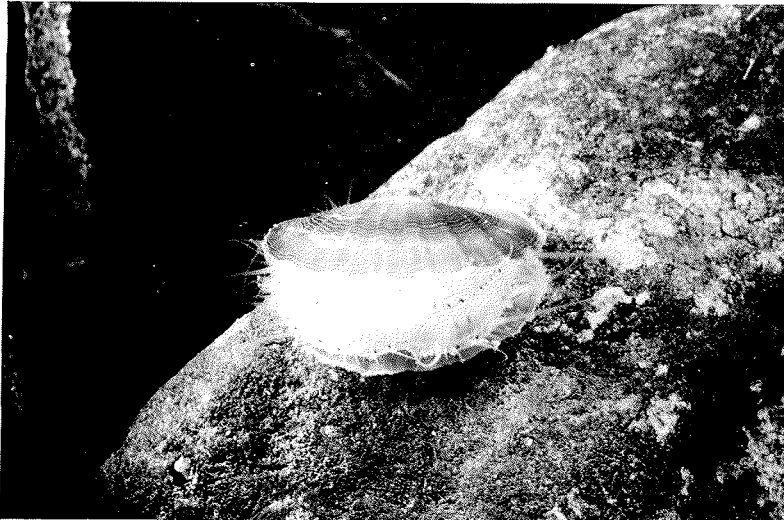
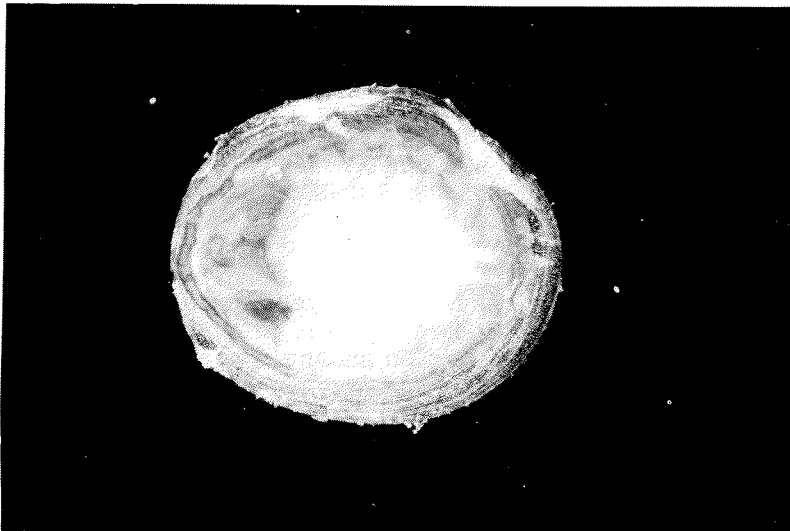


Fig. 3.41b: Living monoplacophoran specimen (*Laevipilina* sp.)
Shell length 3.0 mm



The movement of the tentacles within the water indicates that they may function as well as sensory organs for other parameters (e.g. water currents).

Substrate preference and crawling activity of several gastropod species was tested using two aquaria with hard and soft substrates. Most naticids were observed digging up to 5 cm (max. thickness of sediment layer in the aquarium) deep within 5 to 10 minutes after being transferred to the aquaria. The only exception was a specimen of *Falsilunatia* sp. which was inactive on the soft bottom for more than half an hour. Transferred to the hard substrate aquarium, the specimen started to crawl immediately which indicates that this species lives epibenthically and probably feeds on epizoic attached bivalves.

References

- Dell, R.K. (1990). Antarctic mollusca, with special reference to the fauna of the Ross Sea. Bull. R. Soc. New Zealand, 27: 311 pp.
- Hain, S. (1990). Die beschalteten benthischen Mollusken (Gastropoda und Bivalvia) des Weddellmeeres, Antarktis. Ber. Polarf., 70: 181 pp.
- Voss, J. (1988). Zoogeographie und Gemeinschaftsanalyse des Makrozoobenthos des Weddellmeeres (Antarktis). Ber. Polarforsch., 45: 145 pp.
- Waren, A.; HAIN, S. (subm.). *Laevipilina antarctica*, a new monoplacophoran from the Antarctic. Veliger.

5.1.6. Amphipod biology

A. Schanz (AWI)

Objectives

The species composition, depth zonation and spatial distribution patterns of amphipods in the Lazarev Sea was compared with that found in the southeastern Weddell Sea. This work continues ongoing zoogeographical classification of benthic amphipods. Furthermore, comparisons of reproductive patterns in epibenthic and infaunal amphipods were to be made, in which endobenthic amphipods (e.g. species living as commensals in sponges and tunicates) are included. Finally, living material for measurements of metabolic rates has been collected to identify potential differences in activity patterns and food specialisation between amphipods of both regions.

Preliminary results

Species composition

Bottom trawl and AGT hauls from the Lazarev Sea revealed a remarkable variety in species composition, abundance and biomass of amphipods. Catches per GSN haul ranged between 1 individual (Sta. 133, 424 m depth) and about 300 individuals (Sta. 158, 580 m). Before detailed analyses of the catches, statements about differences between the amphipod faunas of the Weddell and Lazarev Seas are difficult to make. It seems that no distinct differences exist between the two areas with respect to abundance and species composition; this has, however, to be verified by further examination at AWI.

Live maintenance

Approximately 600 amphipods were maintained in 25-l aquaria in a temperature controlled laboratory container at water temperatures of $-1^{\circ}\text{C} \pm 0.5^{\circ}\text{C}$. A major percentage of the specimens belong to the genus *Epimeria*

(*Paramphitoidae*), e.g. *E. robusta*, *macrodonta*, and the "Red Knight" *E. rubrieques* which was described only 5 years ago. These species are known to suffer less under artificial conditions than others and are therefore particularly suited for future growth studies at the AWI. For physiological experiments (O_2 consumption, N excretion) different *Lysianassidae* specimens, among others some individuals of *Waldeckia obesa*, are kept alive. Bottom trawl catches from water depths between 450 m and 620 m (Sta. 158 and 169) were also rich in *E. rubrieques*. More than 50% of the females were egg-bearing; in mid-February 11 juveniles hatched from one female and crept on its dorsum.

5.1.7 Distribution and reproductive biology of caridean shrimps (Decapoda: Natantia) in the Lazarev Sea, and comparisons with the Weddell Sea M. Gorny, W. Arntz (AWI)

Objectives

The distribution of benthic caridean shrimps in the southeastern Weddell Sea is well known from various "Polarstern" cruises (Arntz & Gorny, in press). The aim of this study was to document the occurrence and bathymetric distribution of shrimps along the shelf and upper slope of the Lazarev Sea, and to complement earlier data on size composition, life cycle and reproductive biology of shrimps in the high Antarctic. For this latter purpose material was used from all stations including those off Halley Bay and Kapp Norvegia (cf Fig. 3.42a).

Preliminary results

Five species of shrimps were collected on cruise ANT IX/3; these were:

Hippolytidae

Chorismus antarcticus (724 specimens; 292 were from the Lazarev Sea)

Lebbeus antarcticus (18/4)

Eualus kinzeri (2/2)

Crangonidae

Notocrangon antarcticus (1036/130)

Nematocarcinidae

Nematocarcinus lanceopes (6099/5253).

Eualus kinzeri was only recently found off Kapp Norvegia on the EPOS 3 cruise. The very high number of *Nematocarcinus* is due to two particularly large hauls in the Lazarev Sea (GSN 5, Sta.160: n=1177; GSN 9, Sta. 211: n=3540). *Notocrangon* seems to be less common in the Lazarev Sea compared to the Weddell Sea.

Bathymetric distribution of shrimps very much followed the pattern observed in the Weddell Sea (Arntz & Gorny, loc.cit.), with *Chorismus* dominating in the shallowest parts, *Notocrangon* at intermediate depths, and *Nematocarcinus* occupying the deeper bottoms below 600 m (Fig. 3.42a). There were, however, two exceptions (Sta. 173 and 207) where *Notocrangon* occurred in much shallower waters (232/210 m) than usual. *Chorismus* and *Notocrangon* co-occurred in 11 cases whereas otherwise there were only few overlaps in the depth distribution of the different species. In a single case (GSN 4 off Kapp Norvegia, 576 m) all shrimp species except *Eualus kinzeri* occurred together. Only one haul yielded no shrimps at all.

The length-frequency distributions of shrimps in the catches will be analyzed at the AWI. Of two species, larger individuals were found in the Lazarev Sea than observed hitherto in the Weddell Sea: a female of *Chorismus* had a carapace length (CL) of 22.2 mm, and a female of *Nematocarcinus* measured 42 mm CL.

Egg-bearing ("berried") females of all 5 species were encountered (95 specimens of *Chorismus*, 56 *Notocrangon*, 38 *Nematocarcinus*, 1 *Lebbeus* and 2 *Eualus*). The percentage of berried females in the catches was always below 0.3% except AGT 3 where it was 0.36%. *Nematocarcinus* females with external eggs were found most frequently at the deepest stations below 700 m. Egg numbers were counted of all berried females mainly to increase the data obtained during EPOS Leg 3 and preceding cruises. Numbers generally increase with the size of the females; however, only part of the counts can be considered to be realistic since many females, especially the larger ones, loose considerable portions of their eggs from the pleopods during the trawling procedure. Shrimps that have lost a large part of their eggs can be distinguished by eye. To be on the safe side, all values below the 95% confidence limit were discarded. Using only the "good" values (in the case of *Nematocarcinus*, only one-quarter of the original data), the following regressions of egg number vs. CL are derived for 3 dominant species (Fig. 3.42b). For *Chorismus*, where data exist both for the Weddell and Lazarev Seas, the two curves differ significantly.

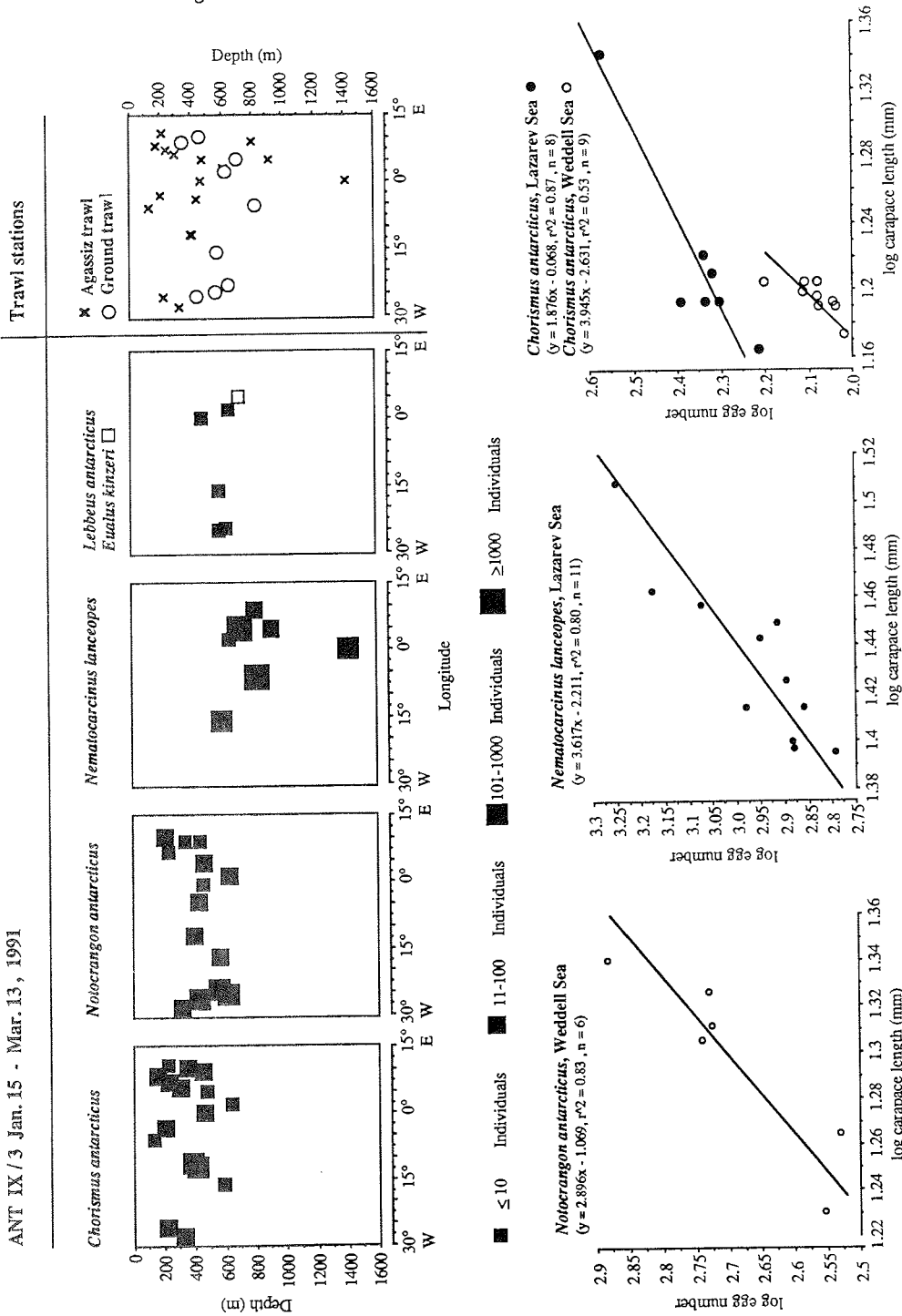
The single berried *Lebbeus* female bore 43 eggs of very large size ($2.65 + 0.13$ (SD) mm). Of the 2 *Eualus* specimens, 1 was in good condition and had 208 small eggs whereas the other one was damaged and had obviously lost a large part of its egg mass, of which only 33 (large) eggs remained. At the AWI, also the ovaries of the females with internal eggs ("headroe") will be considered for oöcyte counts and ovary weight determinations. For this purpose, part of the material was preserved in formalin.

A relatively large number of shrimps (133 *Chorismus*, 82 *Notocrangon*, and - for the first time - 10 *Nematocarcinus*), among them 50 berried females of the former two species, are kept alive in a cool container at a water temperature of -1°C . They will be used to study larval development (in coop. with BAH), oxygen consumption, growth and behaviour. Observations in the aquaria on board showed that *Chorismus* is more active and aggressive than *Notocrangon* and attacks live prey (small isopods and *Notocrangon*) whereas *Notocrangon* skims the bottom for organic material, possibly also minute prey, and scavenges e.g. on fish meat. More detailed feeding experiments are planned for the return trip.

Discussion

The shrimps caught in the Lazarev Sea confirm that natant decapods are a dominant element not only in the Weddell Sea (Arntz & Gorny, loc.cit.) but also in the part of the Southern Ocean adjacent to the east. As in the Weddell Sea, no reptant decapods were found, but all 5 benthic species occurred, and there were shrimps in all trawl hauls except one. The low number of *Notocrangon* registered in this area may be a consequence of the limited number of hauls and the uneven depth distribution of the catches.

Fig. 3.42. a) Bathymetric distribution and rough catch sizes (log scale) of caridean shrimps species during cruise ANT IX/3 in the Weddell and Lazarev Seas
 b) Egg numbers of three common caridean shrimp species in relation to carapace length



Generally, the depth zonation of the shrimps in the area between GvN and Forster strongly resembles that described for the SE Weddell Sea. However, the increased presence of *Notocrangon* in two shallow-water hauls, especially that taken off Forster at 210 m depth with hardly any *Chorismus* present at all, points to the possibility that the observed depth preferences of the two species may be a consequence of the general scarcity of shallow-water bottoms in the area and competition: *Chorismus* normally occupies the upper zone down to about 450 m depth and, by its aggressive behaviour, suppresses the upper distributional limit of *Notocrangon*. Whenever the two species occur together at depths shallower than 450 m, *Chorismus* is clearly dominant. However, if shallower areas are available (off Forster there are several inlets which could not be trawled due to time restrictions but which, according to Hydrosweep observations, are shallower than the area at the ice edge), both species extend their distribution upward. In this context it is interesting to note that in other areas (South Georgia: Maxwell 1977, Clarke and Lakhani 1979; Ellis Fjord: Kirkwood & Burton 1988) *Chorismus* is a true shallow-water species.

Compared with the EPOS Leg 3 cruise, relatively few berried females were found. Except for *Nematocarcinus*, where berried females seem to live at greater depths than immature animals or those with headroe, females with eggs attached to the pleopods do not reveal any particular depth distribution in summer whereas in spring, when the larvae are about to hatch, all species prefer shallower waters (Arntz & Gorny, loc.cit.). Due to the substantial egg losses in the trawl, only part of the material can be used, and the data have to be combined with those of former cruises. A combination of former material with that taken during ANT IX/3 will be presented at the EPOS Symposium. Among other results it will be shown that female sizes and egg numbers of high Antarctic *Chorismus* and *Notocrangon* differ significantly from those of Subantarctic specimens caught near South Georgia. In this context the observed difference in egg number between *Chorismus* caught off Halley Bay and in the Lazarev Sea is of particular interest.

References

- Arntz, W.; Gorny, M. (in press). Shrimp (Decapoda, Natantia) occurrence and distribution in the eastern Weddell Sea, Antarctica. *Polar Biol.*
- Clarke, A.; Lakhani, K.H. (1979). Measures of biomass, moulting behaviour and the pattern of early growth in *Chorismus antarcticus* (Pfeffer). *Br. Antarct. Survey Bull.* 47: 61-88.
- Kirkwood, J. M.; Burton, H.R. (1988). Macrobenthos species assemblages in Ellis Fjord, Vestfold Hills, Antarctica. *Mar. Biol.* 97: 445-457
- Maxwell, J.G.H. (1977). The breeding biology of *Chorismus antarcticus* (Pfeffer) and *Notocrangon antarcticus* (Pfeffer) (Crustacea, Decapoda) and its bearing on the problems of the impoverished Antarctic decapod fauna. In: Llano, G.A. (ed.), *Adaptations within Antarctic ecosystems*. Proc. 3rd Scar Symp. Antarctic Biol., Gulf Publ., Houston/Texas: 335-342.

5.1.8. Ecohistological studies on Antarctic benthic invertebrates

H-H. Janssen (AWI)

Objectives

The extreme conditions of the Antarctic ecosystem such as cold water and distinct seasonality are believed to be met by special adaptations of the organisms. However, comparative studies on the cellular level are scant. Hence, it was planned to obtain well-fixed tissues from selected Antarctic invertebrates, preferably molluscs, for light and electron microscopic evaluation. This will allow the study of different ecological aspects. Furthermore, simple analytical methods were to be tested on board RV "Polarstern" which could serve in future ecological studies involving more detailed analyses of invertebrate histophysiology.

Preliminary results

Sampling and cooperation

The intended comparative study on bivalve gills was postponed in favour of comparative work on gastropods, since relatively few species of bivalves were found. Additionally, non-molluscan invertebrates were preserved for histological analysis using up to six different fixations. The samples obtained allow us to continue earlier studies on digestive tracts. Their evaluation will last two years. It is intended that the work will provide further data on the feeding and breeding biology of selected invertebrates. Further material was collected for various specialists (Tab. 3.15).

Tab. 3.15 : Benthic material collected for specialists

Sample	Purpose of study	For person / institute	Observations
Octopus kidney infested by Mesozoa-Dicyemida	Dicyemid ultrastructure, taxonomy, lifecycle	Czaker Univ. Wien	50% of investigated octopus (predominately Pareledone spp.) are infested
Echinoidea (Sterechinus spp.)	population dynamics, gonad histology, parasites	Brey AWI	Sterechinus, a food item of octopods, may serve as intermediate host for parasitic leeches of octopuses
Archaeogastropoda	taxonomy, systematics	Warén, Zool. Mus. Stockholm	many small specimens (< 4mm shell size) in subsample
Actinia	faunistics, taxonomy	Riemann-Zürneck AWI	-
Sponges, hemichordates	faunistics, biochemistry	Tendal, Zool. Mus. Copenhagen	-
Various suspension feeders	biochemistry of metabolites	Proksch Braunschweig	-
Polynoid polychaetes	faunistics, taxonomy	Stiller AWI	large individuals often infested by parasitic copepods
Parasitic copepods	taxonomy	Schminke Univ. Oldenburg	-
Priapulida	ultrastructure	Storch Univ. Heidelberg	very rare, obtained only off Halley Bay

Experiments

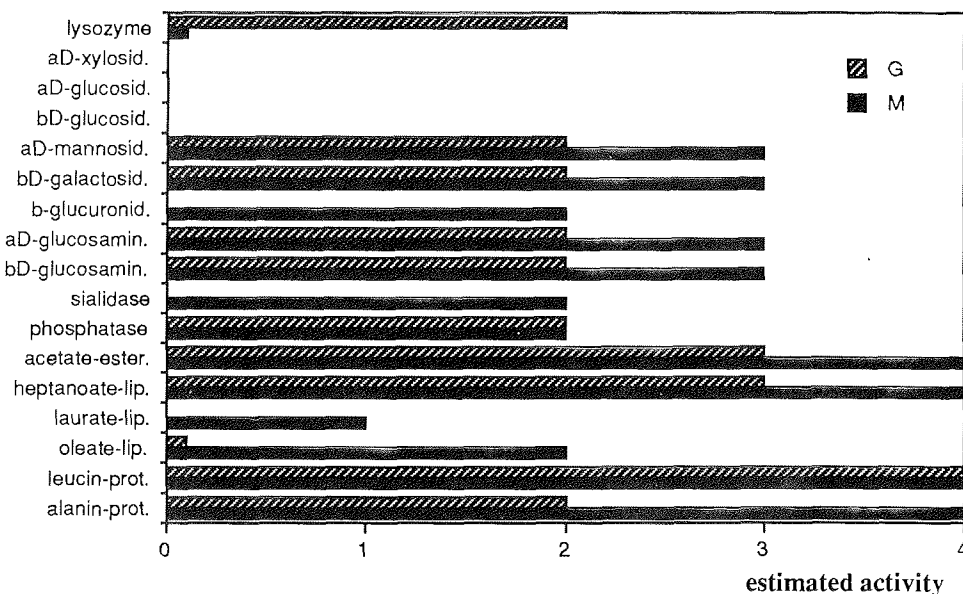
Histochemical tests delivering rapid additional information on a given organism, even under field conditions, were complemented by employing fluorogenic 4-methylumbelliferyl-substrates (MUF technique) and proved to be effective. An interdisciplinary interest in these tests developed on board, as they can easily be adapted to sediment, fluff or plankton samples. On future cruises the use of the MUF-technique is planned also for quantitative studies (fluorometry), e.g. in cooperation with microbiologists or planktologists. First fluorometric experiments proved to be promising.

The tests yielded data on the presence and distribution of enzymes and inorganic compounds both in selected organs and in small whole animals (Fig. 3.43). The following are preliminary results:

- Antarctic invertebrates, as related species in temperate waters, possess enzymes on their body surface which enable them to digest and incorporate dissolved or particulate food matter after body contact. Hydrolases are partly released to the environment.
- Esterases and lipases generally show strong activity, confirming that lipids play a significant role in nutrition. This is supported by the findings of considerable quantities of lipids in ice-algae.
- Antarctic invertebrates may accumulate iron in such amounts that it can be demonstrated by simple means, e.g. in the midgut gland and radula of some molluscs as well as in the soft tissue of some species of sponges. In view of their large biomass in Antarctic benthos communities, sponges might exercise some influence on the iron content of shelf waters.

A number of baits were deployed at about 350 m depth in the southern Weddell Sea during the ice floe station. Although the exposure time was only one night, hundreds of amphipods (*Abyssorchomene* sp.) were lured by certain baits offered to them (meat, fish, olive oil) whereas vegetable baits had no effect. Baited traps should be brought out preferably for a couple of days, so trapping can be easily combined with stations on ice floes. For this purpose traps should be fully collapsible so that they can be lowered and lifted through bore-holes in the floe using standard ice drills (diameter 15 to 25 cm). Lowering over the edge of the floe is dangerous and may lead to loss of the trap. In view of the difficulties in obtaining large amounts of intact animals by standard trawling methods, baited traps represent a reasonable alternative. However, if only a few animals can be obtained in good condition, histology represents a very suitable supplement for studies on fisheries, population dynamics or ecology, as only few well-preserved specimens are required for a whole range of different analyses, such as are under way now.

Fig. 3.43: *Limopsis marionensis*. Enzymes in midgut gland (M) and gills (G) as demonstrated by the MUF-technique. Enzyme activity estimated by eye to a random scale. Note the presence of digestive enzymes in the gills and the differences between the two organ systems tested. aD = alpha-D; bD = beta-D; most of the enzyme names are abbreviated by omitting the suffix -ase.



5.2. Meiofauna and microfauna

5.2.1. Studies of small rhizopodan protists and nematodes at the sediment surface and in sea ice

F. Riemann (AWI)

Objectives and Work at sea

Besides the long biogeographic isolation of Antarctica, it is the strong seasonality of biotic production (and sedimentation) as well as the presence of algal bearing pack ice that are expected to influence the composition and structure of the marine fauna. In order to ascertain the possible impact of these unique features on the microfauna, sediment samples of the top millimeters, preferably those covered with a recently deposited phytodetritus layer, in addition to ice samples were examined during this cruise.

Bottom samples taken at 39 stations either with the multiple corer or from the surface of undisturbed sediments retrieved with the Reineck boxcorer and 19 ice samples were investigated with particular attention directed to those fragile microorganisms which may be destroyed in the course of the usual formaldehyde bulk preservation. Stress was laid on live or subvital observations made on freshly retrieved samples. Permanent microscopical preparations of stained material were made on board ship. Rose Bengal solutions made up by dissolving the stain in alkaline formaldehyde proved to be a useful aid for

the detection of protists in sediment samples and in ice biota aggregates. Sediment subsamples (11) were taken with a small corer for later quantitative examination; whereby the top 2-mm layer was preserved separately from the remaining 28-mm layer of the sediment.

Preliminary results

Sediment samples

Several of the sediment samples taken between 140 and 4000 m depth showed patches of a flocculent brownish or grayish surface layer, 1 to 2 mm high, sometimes lumpy or with faecal strings, the latter derived from a small elaspodid holothurian species. The flocculent material was phytodetritus, often in the form of densely packed, shredded diatom frustules and was identified as crustacean faecal material, presumably derived from euphausiids. In addition, there were intact diatom frustules. Aggregates siphoned off the sediment surface from 660 m depth (Sta. 167) contained intact, chain forming centric diatoms and colonies of the prymnesiophyte *Phaeocystis*. Nematodes were comparatively abundant in this sample (13 individuals in ca 0.5 ml of surface material, *Monoposthia* sp. with 5 specimens being dominant). Rarely, however, the remains of diatom cell contents were visible in other samples. The flocculent bottom surface deposits consisting of more degraded faecal material usually contained only a few inhabitants. A small calcareous foraminifera, tentatively identified as *Epistominella* sp., occurred in 7 samples, sometimes in higher numbers. In a 1.4 mm large aggregate of shredded crustacean faecal material, 8 foraminifera were found (Sta. 167). The occurrence of *Epistominella* which appeared to be an opportunistic inhabitant of recent deposits on the sediment surface was reminiscent to seasonal phytodetritus sedimentation in the north Atlantic deep sea, where *Epistominella* and other foraminifera showed a significant response to the short term availability of freshly sedimented phytoplankton as a food source.

The nematodes in the present phytodetritus material, because of their small size, require careful sorting at the home laboratory in order to assess their ecological significance. Thick carpets of branched calcareous bryozoans which reached to a height of 10 cm over the sediment were found to be effective traps for sedimented phytodetritus aggregates which were inhabited by nematodes (Sta. 209, 210. *Araeolaimus* sp. was identified in live aliquot samples). They were preserved for a later nematode study too.

Of particular interest was a strongly degraded flocculent layer found on the sediment surface in 4300 m depth (Sta. 200). The main eucaryotic inhabitants were 10 to 18 μm large roundish, naked amoebae, which could be observed still living immediately after retrieval of the sample. They occurred at high numbers (ca 10-20) in small patches.

Though not belonging to microscopic organisms, the finding of one specimen of the enigmatic rhizopodan group Xenophyophorea should be mentioned here. At Sta. 214, on a mixture of mud and coarse sand at the surface of a boxcorer sample, one 1.5 cm large specimen was detected. Its wall consisted of a fragile, anastomosing latticework system of sand agglutinations and contained the typical chitinoid tubes filled with faecal pellets. This specimen is the third record for this organism group in Antarctic waters.

Ice samples

The eucaryotic ice biota were strongly dominated by diatoms and the prymnesiophyte *Phaeocystis*. The present special research objective was to examine whether labyrinthomorph protists belonging to the family *Thraustochytridae* would occur in sea ice. Unfortunately, because of the enormous abundance of *Phaeocystis* cell aggregates occurring in various cell forms and sizes, which stained heavily with Rose Bengal, the search for similar globular protists was difficult. Apparently, thraustochytrids were absent in the investigated samples from floating pack ice. However, large numbers could be detected in an ice core section close to the lower end of a 231 cm long core drilled in fast ice at the Halley station. Clusters of the fungus-like protists were enclosed in mucous tubes formed by aggregations of the pennate diatom *Berkeleya rutilans*. In addition, thraustochytrids were found in a sample of ice platelets taken through the drill hole at the same station. The occurrence of thraustochytrids in Antarctic waters and sediments had been shown previously, mostly with culture experiments using baits; the present material provides the first direct demonstration of the enigmatic organisms in sea ice.

Microbiota on a mooring rope

During the retrieval of a moored hydrographic gear (Sta. 122, exposition time 1 year), a dense, brownish to greenish, felted, 2 to 3 cm high epigrowth was observed on the rope sections which were exposed at water depths between 325 and 425 m. The epigrowth consisted of dense masses of 24 to 30 µm long hydrozoan cnida, in exploded condition mainly, mats of coccoid bacteria, and aggregates or clusters of globular bodies of various sizes in the range of few micrometers. The globular structures were strongly stained by Rose Bengal. Fluorescence microscopy showed the absence of chlorophyll. Since live observations revealed the presence of small, laterally flagellated cells in the epigrowth, it is possible that these were developmental stages of thraustochytrid protists, and the globular structure the sporangia. Live samples for later cultivation experiments and aliquots fixed for electron microscopy were collected.

5.3. Comparative investigations on fishes of the Weddell Sea and the Lazarev Sea

A.P.A. Wöhrmann, C. Zimmermann (IPÖ)

Introduction

The evolution of antarctic fishes and their present distribution has been strongly influenced by low temperatures, extensive areas of perennial sea ice and high oxygen concentrations. Today, antarctic fishes inhabit the world's coldest marine environment. The coastal regions of higher latitudes around Antarctica are in permanent contact with ice, and have therefore almost constant temperatures around -1.8°C with negligible variations. Within 20 Mio years of evolution, antarctic fishes have achieved various unique physiological and biochemical adaptations to their habitat.

Some major adaptations of antarctic fishes are:

- the presence of macromolecular antifreeze substances in their body fluids.
- the biochemical composition of the cell membranes, which plays an important role in cold adaptation especially of the central nervous system. Distinct correlations between the molecular ganglioside composition (a class of complex glycolipids) and the state of thermal adaptation of temperate vertebrates had been discovered with the general tendency that the lower the environmental temperature, the higher is the polarity of brain gangliosides. However, studies on samples taken during Polarstern-cruise ANT VII/3 indicate that there is no variation in ganglioside composition of most notothenioids. Only the ganglioside structure and composition of *Bathyraco marri* brains are different to those of other species.
- the blood physiology, which indicates major differences to fishes of more temperate regions. Investigating the biochemistry and physiology of antarctic fish blood will help to answer questions about the ecology, biology and evolution of these fishes. During Polarstern-cruise EPOS Leg 3 blood samples were taken from more than 10 high-antarctic fish species for the first time. Major differences to the haematologic parameters of fishes from temperate latitudes are a tendency to reduce haematocrit (Hct) and erythrocyte counts (RBC number), as well as modifications in their haemoglobins. The haemoglobins of the species *Aethotaxis mitopteryx* and *P. antarcticum*, two of the few pelagic fishes of the Antarctic ocean, differ both in function and structure from that of other species.

Originally it was planned to focus on the southwestern Weddell Sea. Due to the extraordinary ice conditions during the season 1990/91, this plan was abandoned in favour of a comparison of the shelf communities in the Weddell Sea, with fishing sites near Halley Bay, Vestkapp and the Lazarev Sea. Trawling had to be called off several times when the ice conditions became too difficult. The distribution of stations may therefore seem a little opportunistic.

Although the bathymetry of the Lazarev Sea differs in principle from that of the southwestern Weddell Sea, various points of the scientific programme could be adapted for this site: the Lazarev Sea lies in the eastern part of the Weddell Gyre. Here, the shelf is narrow and some regions are completely covered with shelf ice. The continental slope is steep. The benthos and fish fauna of the Lazarev Sea are little investigated, as is the case for the southwestern Weddell Sea. First random samples were taken by ANDRIASHEV (1965). Observations made during this cruise yielded some interesting points for discussion in comparison with the better known regions of the eastern Weddell Sea.

Objectives

One restriction of this study was to achieve the best possible integration of various biological, physiological and biochemical methods of investigation. We focussed on the following aspects:

- A general study of the composition of the demersal fish fauna of the Lazarev Sea, including taxonomy, biogeography, horizontal and vertical distribution of the species, to identify and describe fish communities inhabiting these waters and compare them to those of the Weddell Sea or other areas along the continent, in continuation of earlier studies by Ekau (1988), Kock et al. (1984) and Schwarzbach (1988).

- A study of the biological characteristics, e.g. growth and reproduction, of the most abundant channichthyids (*Chionodraco myersi*, *Cryodraco antarcticus*, *Pagetopsis maculatus* and *Dacodraco hunteri*).
- A lipid, protein and carbohydrate analysis of muscle, liver, gonad and other tissues to study the energy budget of the most abundant species (e.g. *Pleuragramma antarcticum*, *Chionodraco myersi*, *Trematomus lepidorhinus* and *Dolloidraco longedorsalis*), in combination with data on growth, reproduction, feeding and ecology.
- A food analysis (stomach contents) to study the trophic interactions with other organisms within the water column and benthic communities.
- Studies on the blood physiology of uninvestigated high-Antarctic fish species and for a completion of existing data (Kunzmann & Di Prisco 1990). Emphasis was placed on the completion of the EPOS-material with blood samples from *Aethotaxis mitopteryx* and *Pleuragramma antarcticum* and previously uninvestigated species, especially of the genus *Trematomus*.
- Biochemical, histochemical and cytological investigations of brain function. The major intention was the completion of the EPOS-material with brain samples from different species of the families *Bathydraconidae*, *Channichthyidae* and a few non-endemic species.
- Investigations of antifreeze glycoproteins (AFGP's) in deep and shallow water fishes like bathydraconids, artedidraconids, rays and others. These included tests of the presence of known and new forms of antifreeze proteins.
- Several additional investigations and collections. These included samples of sensory organs like eyes and barbels of artedidraconids in order to study the physiology of feeding. Collection of live fish for rearing experiments to investigate ontogeny, early life history, swimming and feeding behaviour and possibly daily rhythms. Collection of fish, especially of the genus *Pogonophryne*, to study phylogeny in co-operation with Hureau (Paris) and Stehman (Hamburg). Samples of maturing females and their gonads were taken for further study of the reproductive mechanism and the egg structure at AWI (Ekau) and at the University of Düsseldorf (Greven).

Work at sea

A. Sampling

Different fishing gear were deployed for the collection of demersal and pelagic fish, in order to investigate the bottom and midwater layers in the different areas "eastern shelf" (Halley Bay to Kapp Norvegia) and "northern shelf" (Atka Iceport to Astrid Ridge).

Agassiz Trawl (AGT):

An AGT with 10 mm mesh in the cod-end was deployed 19 times in water depths between 118 and 1400 m. The horizontal and vertical mouth opening was 3 by 1 m. The net was usually towed with a speed of 1 knot for 15 minutes or for one hour at the deeper stations. Three hauls were made close to Halley Bay, two near Kapp Norvegia, and fourteen on the shelf area between Atka Bay and Astrid Ridge. Catches from this net were primarily used to provide live fish. Especially in water depths (800 m and deeper), which could not be reached with the bottom trawl, catches were analysed qualitatively and quantitatively for species composition.

Bottom Trawl (GSN):

The net was a commercial-scale 140 feet (47 m) headline bottom trawl with an effective mouth opening of 22.5 by 3 m at depth. The mesh size at the cod-end was 20 mm. The net was used 9 times on bottom depths between 336 and 830 m on the shelf near Halley Bay, Vestkapp and between Atka Bay and Astrid Ridge (Lazarev Sea). Due to the difficult bottom topography, hauling times varied between 15 and 45 min at 3-5 knots. Catches from this net were analysed quantitatively and qualitatively for species and size distributions.

Traps:

Two times fish traps were lowered under the sea ice. These activities were limited to the drifting stations south of Halley Bay. No fish was caught under the sea ice, only a number of amphipods (Arntz et al. this volume). In addition, fish larvae were occasionally collected by a Bongo net (BO) and a multiple opening and closing net (Multi Net MN), used for zooplankton collections. The Bongo and Multi Net catches are reported in detail in the zooplankton section of this volume.

B. Processing

The work followed a strict routine. Live fishes were immediately transferred into buckets with cold seawater and later on into aquaria inside a cooled laboratory-container. Dead fishes were taken to the fish laboratory, where species, weight and length were determined. In most cases they were identified according to the FAO identification sheets (Fischer & Hureau 1985). For the abundant species, e.g. *P. antarcticum*, *Macrourus holotrachys*, *T. lepidorhinus* and *C. myersi*, length-frequency distributions were computed. For all species, sex and maturity stages were determined using the Everson scale (Everson 1977).

After the determination of weight and length, dead specimens were stored frozen (-27°C) for later study of the total lipid content. Gutted fish, liver and gonad were stored separately. Specimens of the unidentified species (e. g. *Zoarcidae*, *Liparididae* and *Pogonophryne* spp.) were preserved and stored in 5% formaldehyde for further taxonomic work at the Paris museum. Larvae and juveniles were identified, measured and preserved in 5% formaldehyde.

384 samples of muscle, liver and gonad of anaesthetized fishes were taken and deep-frozen at -80°C for future analysis of lipids, proteins, carbohydrates, and enzyme polymorphisms (*D. longedorsalis*). Some muscle samples of deep-water fishes (*Bathyraco macrolepis*, *M. holotrachys*, *Bathyraja maccaini*, *Muraenolepis marmoratus*) were also frozen for antifreeze glycoprotein analysis. Gonads from 14 species were removed on board and preserved in glutaraldehyde, Bouin or formaldehyde for fecundity analysis in Bremerhaven and Düsseldorf.

Special attention was paid to the species of bathydraconids and channichthyids. For a study on growth, otoliths were taken from 271 specimens of *Chionodraco myersi*, *Pagetopsis maculatus*, *Cryodraco antarcticus* and *Dacodraco hunteri*. These are the dominant channichthyids of the eastern Weddell Sea shelf water (300 to 700 m) and the Lazarev Sea. Furthermore, otoliths (n) from *Macrourus holotrachys* (21), *Dissostichus mawsoni* (3), *Aethotaxis mitopteryx* (14), und *Bathyraco macrolepis* (4) were taken. Bathydraconids occurred abundantly in the deeper water (600 to 1200 m) of

the Halley Bay and Filchner area and will be studied in detail for biochemical composition of antifreeze glycoproteins and brain lipids. For biochemical investigations, 369 brain samples from 27 species were deep-frozen at -80°C for quantitative determination of lipids, especially gangliosides and phospholipids. Brains (≥ 30 from each species) from *C. myersi*, *T. lepidorhinus*, *D. hunteri*, *B. marri* and *M. holotrachys* were frozen for studies of ganglioside structure. For histochemical and cytological investigations 59 brains from 19 species were preserved with paraform-glutaraldehyde and Bouin.

For blood physiological investigations 50 blood samples were taken for immediate determination of erythrocyte count (RBC number), haematocrit (Hct) and haemoglobin content (Hb). In most cases the fishes were immediately transferred to aquaria and allowed approximately 48 hours to recover from stress due to catching and handling. However, blood samples from delicate or injured specimens have been taken from the caudal vein of unanaesthetized fish into heparinized syringes shortly after sorting the haul. The whole sampling procedure has routinely been completed within 60 seconds after first handling of a specimen. After determination of Hct, RBC number and Hb, blood cells and plasma were separated by centrifugation and deep frozen (-80°C). The plasma will be used for analysis of total proteins, lipids and several selected enzymes and hormones. The cells were collected for purification of Hb and structural (amino acid sequence), as well as functional studies (oxygen affinity, Bohr and Root effect) by Kunzmann (IPÖ Kiel) and Di Prisco (IIGB Naples).

Live fishes, larvae and eggs were kept in cooled aquaria under controlled water temperatures (-1.0°C) and light regimes (darkness; three hours dim light per day). The behaviour and food uptake of various specimens were studied. The observations will be continued at the AWI, Bremerhaven.

A summary of all samples taken is given in Tab. 3.16.

Tab. 3.16: Samples collected for further studies

Sample type	n specimens	n species
frozen specimens (-20°C) for lipid analysis	1776	64
muscle, liver and gonad (-80°C) for lipid anal.	384	41
otoliths for growth study	313	11
muscle for AFGP analysis	82	41
brains for biochemical investigations	369	27
brains for histochem. and cytol investigations	59	19
retina for structural investigations	26	12
samples for blood physiology	50	11
gonads for fecundity analysis	14	9
fish specimens for reference collections	136	48
muscle, liver for enzyme polymorphism study	50	2
live fish in cooled aquaria	85	23

Preliminary results

With the bottom gears AGT and GSN, a total of 3582 fish specimens, weighing more than 350 kg have been identified and investigated. This number includes 742 specimens of *P. antarcticum*, which were collected during haul 130.1 and 130.2 (Tab. 3.17). 1888 specimens (45 species) of demersal fish were identified from the eastern shelf and slope of the Weddell Sea and 1694 specimens of 55 species from the Lazarev Sea (Tab. 3.17). By numbers, 85.5% of the fish belong to the suborder Notothenioidei, representing 47 species (plus several unidentified species of the genus *Pogonophryne*). Besides this suborder, fishes of the families Zoarcidae (53), Liparididae (32), Macrouridae (330), Muraenolepidae (48), Myctophidae (28) and Rajidae (13) were collected. Twelve specimens of squids were caught.

Fig. 3.44 shows the family composition of all hauls depending on latitude and water depth. One striking feature is a dominance of the channichthyids near Vestkapp and near 2°E in water depths between 500 and 600 m at the shelf break. At most stations in the Lazarev Sea, the contribution of non-notothenioid fishes was by far higher than in the Weddell Sea and even increased with depth. This is especially due to species like *Macrourus holotrachys*, *Paraliparis* sp. and *Bathyraja* sp.

In the Weddell and Lazarev Seas, Artedidraconidae and Nototheniidae are the dominating families of the shallow waters. Bathydraconidae are fairly rare at all stations. Only in the deepest Agassiz trawls (1400 m) and at the shallow sites, they showed higher abundances. When using an AGT instead of an GSN, the size of caught specimens is smaller and the size-composition different, as can be seen in Fig.3.44.

The most abundant species by numbers in the eastern Weddell Sea are *P. antarcticum*, *C. myersi*, *T. lepidorhinus* and *D. longedorsalis* (Fig. 3.45). This contrasts with the observations made in the Lazarev Sea, where *C. myersi* and *T. lepidorhinus* are also abundant. However, *P. antarcticum* and *D. longedorsalis* are not present. Instead we found *Notothenia kempi*, a characteristic species of the sub-antarctic shelf water.

With 55 species, the fauna in the Lazarev Sea is highly diverse. *C. antarcticus*, *D. hunteri*, *A. mitopteryx*, *Trematomus centronotus* and various artedidraconids are common on the shelf. Typical species or families of the continental slope are *M. holotrachys*, *B. marri*, *Muraenolepis marmoratus* and members of Rajidae, Liparididae and Zoarcidae. The plankton feeder *A. mitopteryx* and the piscivorous *D. hunteri* are common in all depths, from the shallow shelf water (300 m) to the deeper continental slope (800 m). The typical krill-feeders of the eastern Weddell-shelf area, *P. maculatus* and *P. macropterus*, are completely missing and *P. antarcticum* is rare. *D. longedorsalis*, a dominant species by number of the southeastern Weddell-shelf which feeds on polychaets, is also missing in the Lazarev Sea. The species *Trematomus eulepidotus* and *Trematomus scotti*, the dominating Nototheniids of the last expeditions (ANT VI/3 and ANT VII/4) to the eastern Weddell Sea, are very similar in their occurrence.

station	123.1	123.2	129	130.1	130.2	133	135	158	160	162.1	162.2	165	168	169	171	173	174	176	179	180	189	192	206	207	211	212	220	Total	
app. depth	400	400	320	570	610	430	220	600	800	430	440	200	500	510	880	230	430	750	170	290	470	1400	340	240	660	700	120		
species	CODI	AGT	AGT	GSN	GSN	GSN	AGT	GSN	GSN	AGT	AGT	AGT	AGT	GSN	AGT	AGT	GSN	AGT	AGT	AGT	AGT	AGT	GSN	AGT	GSN	AGT	AGT		
Nototheniidae undet.	e	0	0	0	0	0	0	1	1	0	0	0	0	0	0	2	0	0	5	0	0	0	1	1	0	0	2	13	
<i>Notothenia kemp</i>	d07	0	0	0	0	0	0	0	1	0	0	0	0	0	0	0	41	0	0	1	0	0	0	0	0	0	18	0	70
<i>Nototheniopsis larseni</i>	d08	0	0	1	0	0	0	0	0	0	0	0	0	0	0	0	0	0	0	0	0	0	0	0	0	0	0	3	4
<i>Aethiopsis miloptyx</i>	e01	0	0	0	0	0	0	0	12	0	1	0	0	10	1	0	19	1	0	0	0	0	0	0	0	10	0	54	
<i>Disostichus newsoni</i>	e05	0	0	0	1	0	0	0	1	0	0	0	0	1	0	0	2	0	0	0	0	0	0	0	0	1	0	1	7
<i>Pleuragamma antarctica</i>	e10	0	0	0	332	410	0	0	3	5	0	1	12	10	1	9	12	0	8	7	0	0	1	0	2	0	0	813	
<i>Pogothenia bernacchi</i>	e15	0	0	0	6	13	0	0	0	0	0	0	0	0	0	0	0	0	0	0	0	0	0	0	0	0	0	19	
<i>Trematomus centronotus</i>	e16	0	1	0	0	0	0	0	0	0	0	0	6	0	0	4	0	0	0	1	0	0	0	0	0	0	0	26	38
<i>Trematomus alepidotus</i>	e17	6	3	0	1	0	3	2	38	0	1	0	1	7	0	3	2	4	0	1	0	0	0	1	0	0	0	2	74
<i>Pogothenia hanson</i>	e18	0	0	0	0	3	0	0	0	1	0	1	0	3	0	0	0	0	0	0	0	0	0	0	0	0	0	0	8
<i>Trematomus lepidorhinus</i>	e19	3	5	2	0	0	0	4	194	81	0	2	30	0	50	0	105	1	6	14	2	0	14	2	46	7	9	582	
<i>Trematomus boenbergii</i>	e20	0	0	1	0	2	0	1	6	1	0	1	0	0	0	0	0	0	0	0	0	0	0	0	0	0	0	14	
<i>Trematomus nicolai</i>	e22	0	0	0	0	0	0	0	0	0	0	1	0	0	0	0	0	0	0	0	0	0	0	0	0	0	0	1	2
<i>Trematomus scotti</i>	e24	1	2	2	10	7	4	1	3	3	4	7	3	0	0	0	0	0	0	0	0	3	0	1	6	0	0	0	57
Σ, Nototheniidae		10	11	6	350	435	7	8	245	106	4	14	59	0	86	2	22	183	2	20	23	5	0	18	9	61	25	44	1755
<i>Bathyraja maccaini</i>	RAJ	0	0	0	1	0	0	0	1	9	0	0	0	0	0	0	0	0	0	0	0	0	0	0	0	0	0	0	12
<i>Bathyraja sp.1</i>	RAJ	0	0	0	0	0	0	0	1	0	0	0	0	0	0	0	0	0	0	0	0	0	0	0	0	0	0	0	1
Liparididae undet.	LJP	0	0	0	0	0	0	0	1	1	0	0	0	1	0	0	3	0	0	0	0	0	0	0	0	0	0	0	6
<i>Paraliparis sp.</i>	PAR	0	0	0	4	1	0	0	1	0	0	0	1	0	0	0	2	0	0	0	0	0	0	5	0	0	0	0	26
Zoarcidae undet.	ZOA	4	1	0	0	0	0	0	3	0	0	0	0	1	2	0	1	1	0	0	0	0	0	0	0	0	0	0	13
<i>Lycodichthys sp.</i>	LYI	0	0	0	0	0	0	0	15	0	0	0	0	2	0	0	0	0	0	0	0	0	0	1	0	2	0	0	20
<i>Lycenchelys sp.</i>	LYE	0	0	0	0	0	0	0	0	0	0	0	0	0	0	0	11	0	0	0	0	0	0	0	0	0	0	0	11
<i>Austrolychthys sp.</i>	AUS	0	0	0	0	0	0	0	0	0	0	0	0	1	0	0	1	0	0	0	0	0	0	0	0	0	0	0	2
<i>Ophthalmycterus sp.</i>	OPH	0	0	0	0	0	0	0	0	0	0	0	0	0	0	0	2	0	0	0	0	0	0	0	0	0	0	0	2
<i>Lycodapus sp.</i>	LYA	0	0	0	0	0	0	0	5	0	0	0	0	0	0	0	0	0	0	0	0	0	0	0	0	0	0	0	5
<i>Muraenolepis marmorata</i>	MUA	0	0	0	0	0	0	0	3	27	0	0	0	0	1	0	0	0	0	0	0	0	0	0	0	2	0	0	34
<i>Muraenolepis microps</i>	MUI	0	0	0	0	0	0	0	0	0	0	0	0	0	0	0	13	0	0	0	0	0	0	0	0	0	0	0	14
<i>Macrourus holotrachys</i>	MAC	0	0	0	0	0	0	0	13	280	0	0	0	0	0	1	0	0	0	0	0	0	0	0	0	35	1	0	330
<i>Myctophidae gen.sp.1</i>	MYC	0	0	0	0	0	0	0	1	1	0	0	0	0	0	0	0	0	0	0	0	0	0	0	0	0	0	0	10
<i>Myctophidae gen.sp.2</i>	MYC	0	0	0	0	0	0	0	0	0	0	0	0	0	0	0	0	0	0	0	0	0	0	0	0	0	0	0	15
<i>Myctophidae gen.sp.3</i>	MYC	0	0	0	0	0	0	0	0	0	0	0	0	0	0	0	0	0	0	0	0	0	0	0	0	0	0	0	3
Squid	SQU	0	0	0	0	0	0	0	1	0	0	0	0	0	0	0	3	0	0	0	0	0	0	0	0	0	0	0	12
Σ, no-Notothenioids		4	1	0	5	1	0	0	49	324	0	1	0	2	6	2	4	33	0	0	0	0	1	6	0	75	2	0	516
Total		32	20	12	438	608	34	18	726	476	6	18	76	2	351	5	45	303	3	36	50	7	6	39	14	158	30	69	3582
Biomass (g)		1030	1427	411	22574	28996	2486	196	70000	110078	242	689	2349	19	51797	200	1257	28996	425	561	3075	209	280	1346	109	21215	1980	3732	
Biomass (g/m²)		0.5	0.6	0.4	0.4	0.7	0.1	0.1	1.4	1.3	0.2	0.5	1.4	0.0	0.8	0.1	0.4	0.8	0.2	0.3	1.5	0.1	0.0	0.1	0.0	0.2	0.1	0.4	

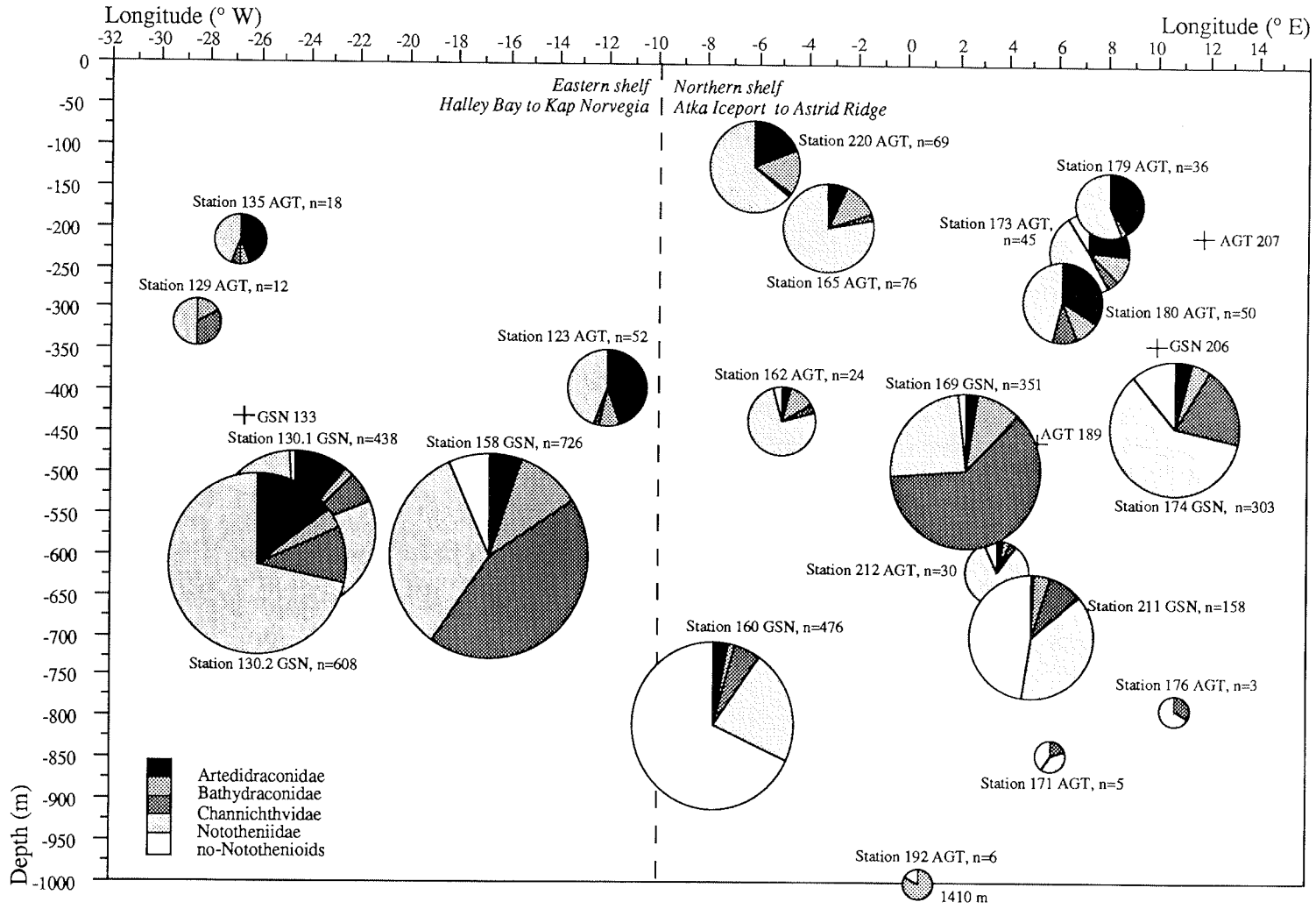


Fig. 3.44: Catch-size and -composition (families) with depth and longitude of the station. The circle diameter is correlated with number of specimens in the haul (n). Circle centre: Station position. AGT & GSN: used net; + stations without haul or with untypical events

Fig. 3.45: Composition of the total catch concerning the species of the Weddell Sea (eastern shelf area) and the Lazarev Sea (northern shelf area), listed separately

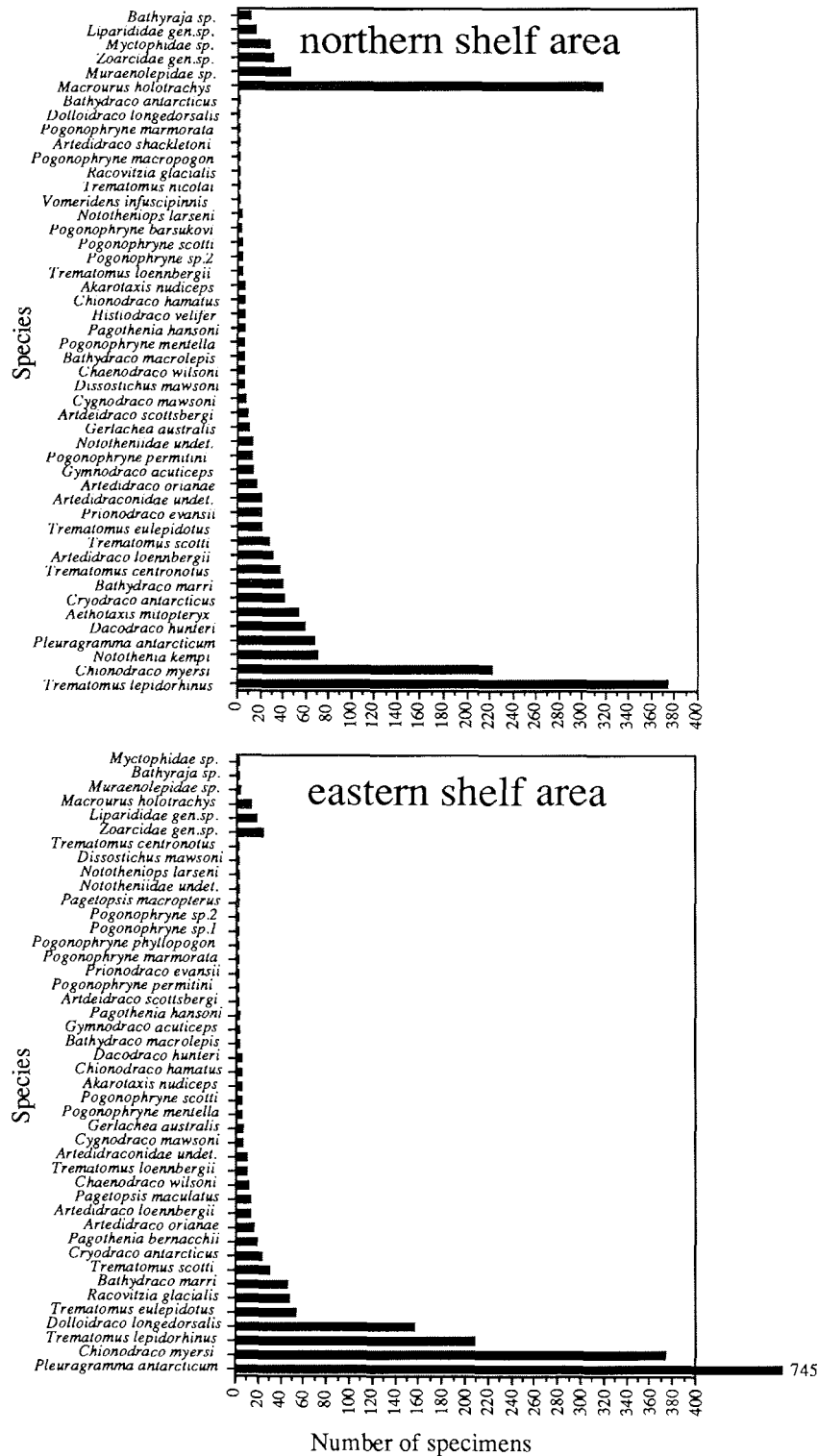
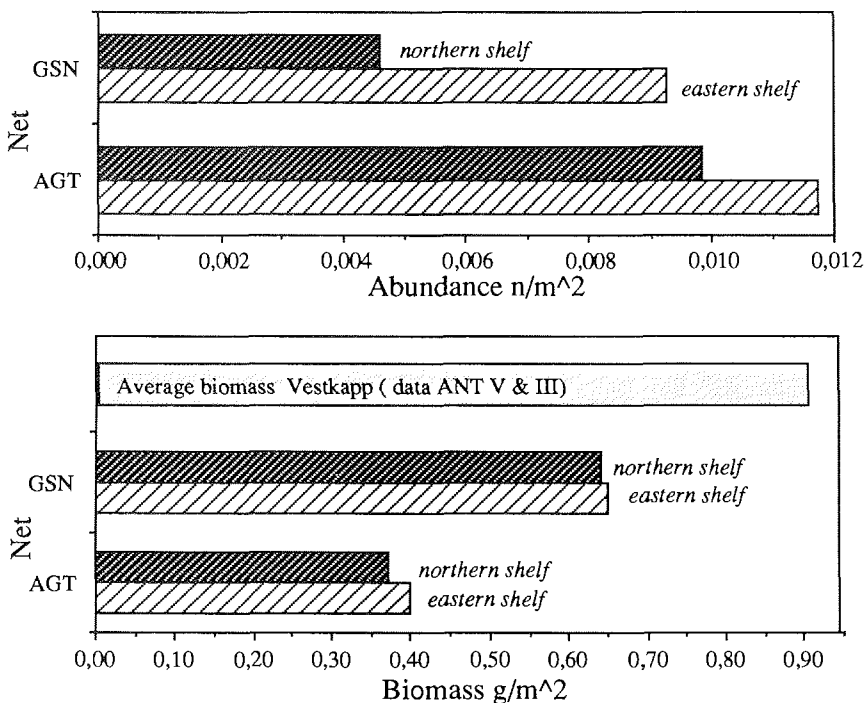


Fig.3.46 shows abundance and biomass for all catches and fishing-sites. The number of specimens per m² is obviously lower with bottom trawling than with the Agassiz trawl. Another striking feature is the higher mean fish density in the eastern Weddell Sea compared to the shelf regions of the Lazarev Sea. After a careful estimate, the total biomass of both locations is, however, assumed to be equal. Biomass estimates based on the nine GSN hauls were 0.74-1.54 t/km² for the shelf near Halley Bay, 1.49 t/km² for the Vestkapp area, and 0.13-1.49 t/km² for the Lazarev Sea. In comparison to this, the estimate for the Vestkapp area was 0.6-1.8 t/km² based on 7 GSN hauls (EKAU 1990) during the Winter-Weddell-Sea-Project (WWSP) 1986. The species composition found in WWSP differs significantly from that found here. The biomass and diversity are relatively low for the eastern shelf, *P. antarcticum* and *C. myersi* were the most abundant representatives.

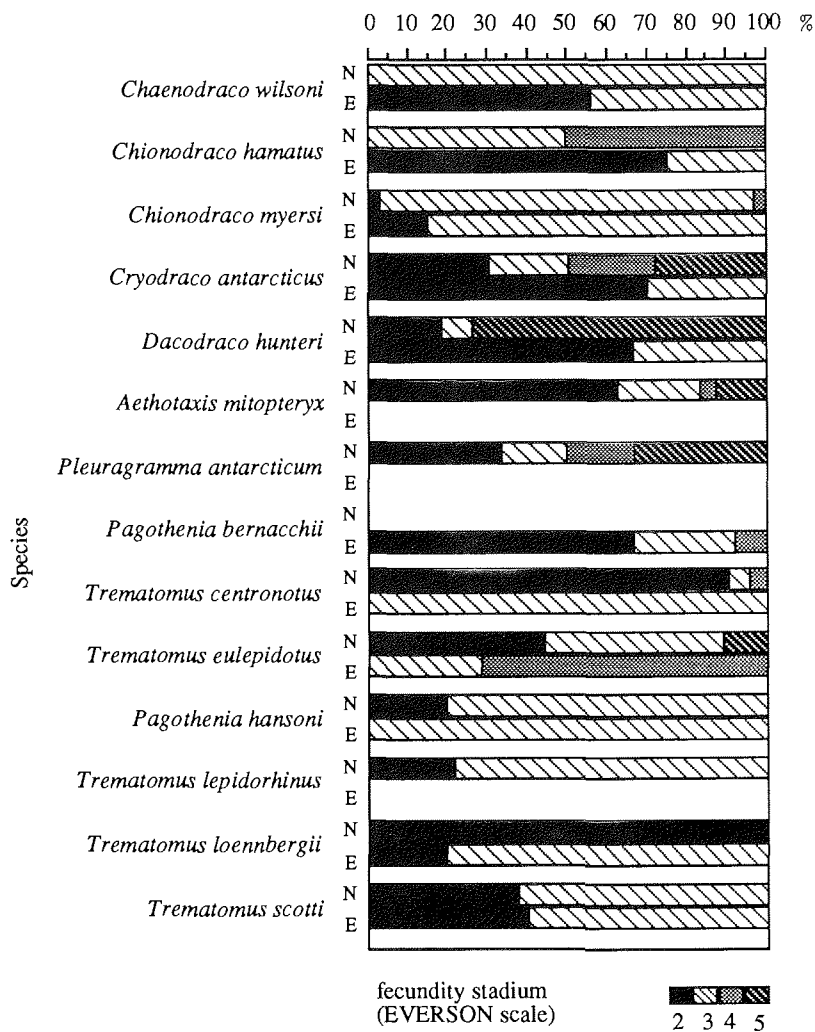
First results of a stomach content analysis from 12 species are shown in Tab. 3.18. The number of empty stomachs was relatively high in channichthyids. These species tend to feed on pelagic fish (*Pleuragramma antarcticum*) and euphausiids. Most of the benthos feeders, e.g. *Trematomus* sp., had filled stomachs. These findings agree well with stomach analyses made for fish collected during ANT I and II (Schwarzbach, 1988) and ANT V/3 (Wöhrmann, 1988). It is striking that in contrast to the Weddell Sea the typical krill-feeders are rare or missing in the Lazarev Sea. Here, *T. lepidorhinus*, known from the Weddell Sea for being a generalist, is the most abundant notothenioid. It feeds mainly on benthic organisms, such as amphipods, crinoids, anemones and polychaetes. *C. myersi*, the dominant species off Vestkapp, feeds on the fully pelagic *P. antarcticum*. Its stomach contained a lot of euphausiids besides fish. The two common channichthyids of the Lazarev Sea, *D. hunteri* and *C. antarcticus* also feed on fish, but mainly on demersal notothenioids.

Fig. 3.46: First abundances and biomass estimation for Weddell Sea (eastern shelf area) and Lazarev Sea (northern shelf area) listed separately for bottom trawl (GSN) and Agassiz trawl (AGT). Data comparison from ANT III/3 and ANT V/3 for the Vestkapp area (Ekau, 1990)



Maturity stages of all species were investigated. Fig. 3.47 shows some of them. When investigating fishes from the eastern Weddell Sea (January/February), ripe gonads close to spawning were only found in *T. eulepidotus*. One female *T. eulepidotus* spawned in the aquarium. Females of all *Pogonophryne* spp., *C. antarcticus* and *T. centronotus* investigated in the Weddell Sea were in an advanced maturity stage, indicating late summer spawning. The gonads of *T. lepidorhinus* were less developed. Spawning of these species is more likely to occur in autumn or early winter. In contrast, *C. antarcticus*, *T. centronotus* und *Pogonophryne* ssp. were caught at the end of February and in the beginning of March in the Lazarev Sea and were in a state of spawning soon. Most *D. hunteri* had already spawned. The gonads of *T. lepidorhinus* were still developing, like in the month before.

Fig. 3.47: Analysis of gonads from 14 species of the Lazarev Sea in comparison with the same species of the Weddell Sea. Results in % of investigated gonads



The blood physiological data gained on board agree with those from the EPOS Leg 3 cruise: There were no obvious differences in haematology of artedidraconids, bathydraconids and nototheniids. Thus, *A. mitopteryx* and *P. antarcticum* seem to have a comparatively low haematocrit and haemoglobin content. Specimens of the strictly benthic genus *Pogonophryne* had little blood in relation to their body weight. The blood was congested with phlegm despite the extraordinary extraction from the atrium and it coagulated quickly, although increasing amounts of heparin were given.

Finally, we would like to mention some peculiarities we observed during the cruise through the Lazarev Sea:

- many species seem to spawn in March, at the end of the austral summer.
- the majority of fishes have fed (except the piscivorous species). Large fat resources could be found underneath the first dorsal fin and in the innards. This is in clear contrast to observations made during ANT III/3 (January/February) and ANT V/3 (October/November) in the eastern Weddell Sea.
- species of the genus *Pogonophryne* were especially attractive for various reasons. For instance, 10 different species were identified, but not all could be determined. This genus inhabits the continental slope and shows a high diversity in a small area. Furthermore, two extremely large specimens of *P. macropogon* (standard length 28 cm, fresh weight approx. 900 g) were caught. The liver and stomach of all *Pogonophryne* spp. were heavily infested with parasites.
- the channichthyid *Cryodraco antarcticus* was caught in all depths. The large number of very large specimens (> 50 cm), caught on the shallow continental shelf even with the slow Agassiz trawl is astonishing. These were mainly gravid females and males that may have come to shallower waters for spawning.
- *Dissostichus mawsoni* was found in all the bottom trawls. Specimens of *Notothenia kempfi*, usually known from the sub-antarctic regions, were far below the observed maximal length of 35 cm (HUREAU & FISCHER 1985). At the deeper stations, *M. holotrachys* was dominant. It was present in all hauls, with lengths from 5 to more than 80 cm and a weight reaching over 3 kg. Unusual was the frequent presence of *A. mitopteryx* at shallow and deep stations. One large specimen with 425 mm SL exceeded the calculated theoretical endlength for the Weddell Sea (SL 409 mm; Ekau, 1988).

The length-weight relationship of 4 species is illustrated in Fig. 3.48.

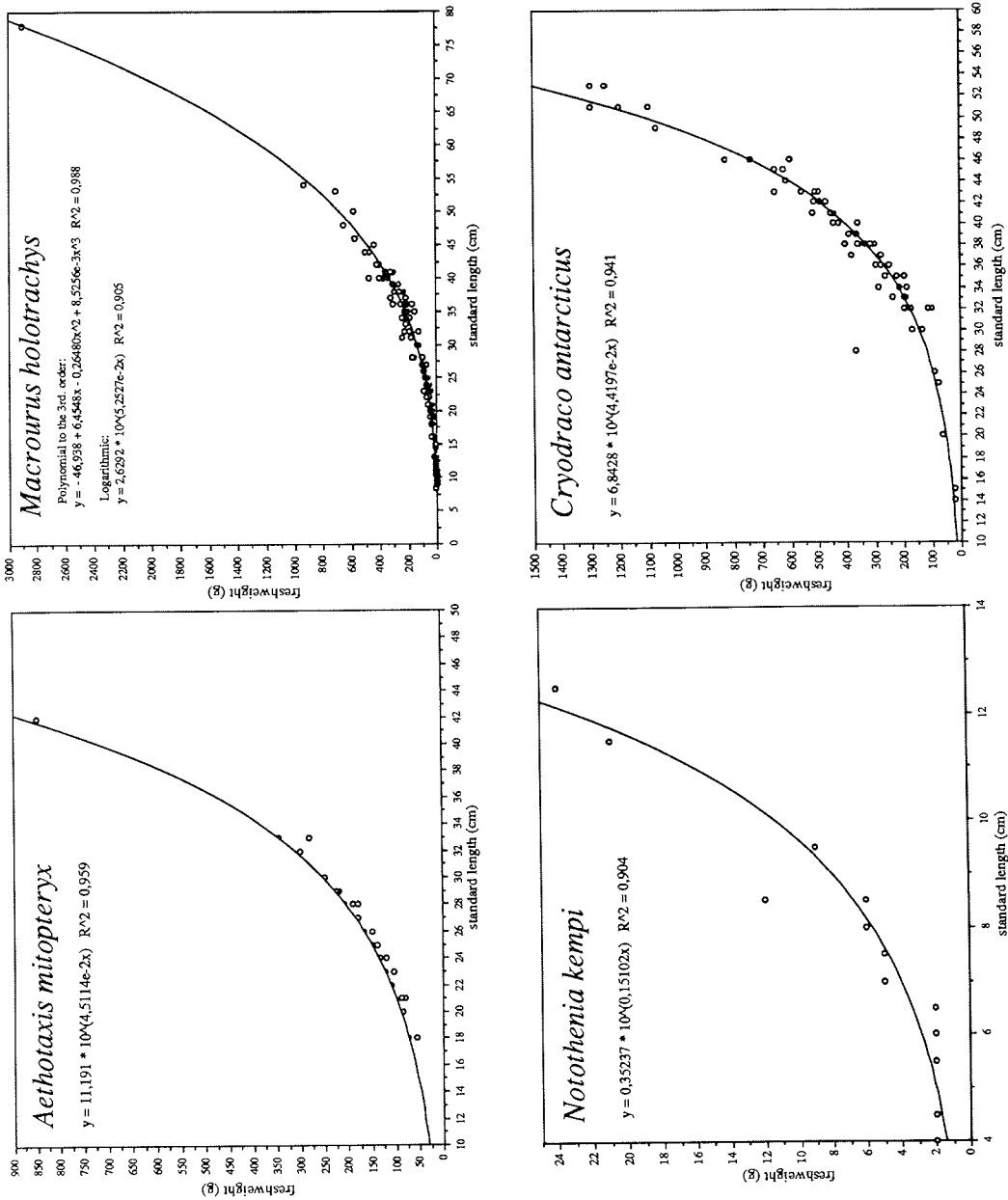
Perspectives for the future

Our major intention was the collection of samples to be analyzed during the coming year. From earlier investigations we guess that lipid-chemical analyses will provide promising results. Brain and tissue samples will be analysed this year for their gangliosides and their antifreezing substances. Furthermore, the samples may elucidate the growth of channichthyids and the zoogeography of the Lazarev Sea fishes. The following questions may be answered:

1. Are there differences in the fish fauna of the two investigated regions ?
2. Why are fishes from more moderate latitudes so abundant in the deep waters of the Lazarev Sea ? (Was this a unique event?)
3. Is the food supply on the northern shelf really better than in the Weddell Sea, as the catch of extraordinarily large specimens may indicate?
4. Does the lack of the main predators, seals and penguins play a role?

For the future, it would be interesting to collect data from the eastern and western side of the Astrid ridge. Depths similar to those from EPOS Leg 3 should be sampled to gain comparable data. For a complete faunistic analysis, sampling with the benthic-pelagic trawl (BPN) would be desirable. Special interest should be paid to the shallow and the deeper regions on the continental slope. Investigations of biochemistry, physiology and metabolism should follow, because in this respect the southwestern Weddell Sea still remains in the focus of scientific interest.

Fig. 3.48: Length-weight-relations of four important species of the Lazarev Sea, *Aethotaxis mitopteryx*, *Notothenia kempii*, *Cryodraco antarcticus* and *Macrourus holotrachys*



Tab. 3.18: Analysis of stomach contents from 12 species of the Lazarev Sea, in comparison to other summer data from fishes of the eastern Weddell Sea (Schwarzbach 1988; Wöhrmann 1988). Results in % of investigated stomachs. 0 = empty stomach, 1 = little, 2 = 33%, 3 = 66%, 4 = full stomach; F = fish, Pa = *P. antarcticum*, E = euphausiids, B = benthic invertebrates, P = polychaets, undet = undetermined.

Species	n	0	1	2	3	4	F	Pa	E	B	P	undet
<i>Chaenodraco wilsoni</i>	5	100.0	-	-	-	-	-	-	-	-	-	-
<i>Chionodraco hamatus</i>	3	66.7	-	33.3	-	-	00.0	-	-	-	-	-
<i>Chionodraco myersi</i>	150	77.3	8.7	10.7	4.7	3.3	2.9	26.5	29.4	-	-	41.2
<i>Cryodraco antarcticus</i>	49	65.3	6.1	2.0	16.3	10.2	41.2	23.6	5.9	-	-	29.4
<i>Dacodraco hunteri</i>	52	75.0	5.8	5.8	5.8	7.7	38.5	46.1	7.7	-	-	7.7
<i>Aethotaxis mitopteryx</i>	22	86.4	13.6	-	-	-	-	-	-	-	-	100.0
<i>Pagothenia bernacchii</i>	21	-	61.9	9.5	9.5	19.1	23.8	-	-	-	-	-76.2
<i>Trematomus centronotus</i>	29	13.8	-	6.9	31.0	48.3	-	-	-	100.0	-	-
<i>Trematomus eulepidotus</i>	7	42.9	-	-	28.6	28.6	-	-	25.0	25.0	-	50.0
<i>Pagothenia hansonii</i>	8	50.0	37.5	-	-	12.5	-	-	-	-	-	100.0
<i>Trematomus lepidionus</i>	32	45.8	21.9	9.4	15.6	7.3	3.8	-	3.8	21.2	7.7	63.5
<i>Trematomus scotti</i>	14	-14.3	23.8	28.6	14.3	19.0	-	-	-	22.2	-	77.8

Acknowledgement

We gratefully acknowledge the invaluable help of Sabina Griffith, Kiel, for translating this script and Andreas Kunzmann, Kiel, for editing.

References

- Andriashev, A.P. (1965). A general review of the antarctic fish fauna. - In: van Mieghem, J. & van Oye, P. (eds.) Biogeography and ecology in Antarctica. Junk Publishers, The Hague, 491-550
- Ekau, W. (1988). Ökomorphologie nototheniider Fische aus dem Weddellmeer, Antarktis. - Ber. Polarforsch. 51: 1-112
- Ekau, W. (1990). Demersal fish fauna of the Weddell Sea, Antarctica. Antarctic Science 2(2): 129-137
- Everson, I. (1977). The living resources of the Southern Ocean. - FAO GLO/SO/77/1: 1-156
- Fischer, W.; Hureau, J.C. (1985). FAO species identification sheets for fishery purposes, Southern Ocean. - Food and agriculture organization of the United Nations, FAO, Rome, 1-400
- Kock, K.-H.; Schneppenheim, R.; Siegel, V. (1984). A contribution to the fish fauna of the Weddell Sea. - Arch. Fisch. Wiss. 34 (2/3): 103-120
- Kunzmann, A.; Di Prisco, G. (1990). On the blood physiology of high-Antarctic fishes. - II Int. Conf. Biol. Ant. Fishes, Ravello 30.05.-01.06.90
- Schwarzenbach, W. (1988). Die Fischfauna des östlichen und südlichen Weddellmeeres: geographische Verbreitung, Nahrung und trophische Stellung der Fischarten. - Ber. Polarforsch. 54: 1-94
- Wöhrmann, A. (1988). Jahreszeitliche Unterschiede in der Ernährung antarktischer Fische (Notothenioidei: *Trematomus eulepidotus*, *T. scotti* und *Chionodraco myersi*). - Diplomarbeit, math.-naturwiss. Fak. Univ. Kiel, 1-111

6. GEOLOGY

6.1. Marine-geological and geophysical investigations

6.1.1. Glaciomarine sedimentary processes in the Weddell Sea and Lazarev Sea

G. Kuhn, W. U. Ehrmann, M. Melles, G. Schmiedl (AWI), M. J. Hambrey (SPRI)

Introduction

The main objective of the sedimentological programme was to obtain information concerning the factors which have influenced the deposition of sediments on the seafloor in the past. In order to obtain this information, it was necessary to study recent glaciomarine sedimentary processes and interpret them with regard to their topographic, oceanographic and glaciological environments. By sampling and dating older sediments and interpreting them in the light of glaciomarine sedimentary processes, we would like to build up a model of the sedimentation history of a region influenced by the East Antarctic Ice Sheet.

Sampling areas

One of our goals was to investigate proximal glaciomarine sedimentary processes on the continental shelf close to the ice shelf margins. Because the original intention to sample these environments in the southwestern part of the Weddell Sea was thwarted by severe ice conditions, a comprehensive programme was initiated in the eastern Weddell Sea (Fig. 3.49), and more particularly in the Lazarev Sea along the ice-covered coasts of Dronning Maud Land (Fig. 3.50).

In addition to the continental shelf programme, samples were taken along two profiles down the continental slope in order to obtain information concerning facies changes from proximal to more distal glaciomarine settings, and to determine climatic changes over a time scale that embraces both glacial and interglacial periods.

On the previous Polarstern cruise ANT-VIII/5 (1989/90), a deep-sea area in the central Weddell Sea was investigated along geophysical and bathymetrical transects. As a result, a seamount-like structure, the informally named "Polarstern Seamount", was detected (Fig. 3.49). This seamount was one of the sampling areas during the ANT-IX/3 cruise. Attempts were made to retrieve glaciomarine and hemipelagic sediments, which in this area were expected not to be so strongly affected by bottom currents as are the sediments in the deeper surrounding seas.

In order to study the bottom currents, a current-meter mooring was deployed near an erosional structure on the sea floor at 73°37.6'S 26°07.0'W (Fig. 3.49) in cooperation with the oceanographic group. Another current-meter mooring deployed one year earlier at 71°05.8'S 20°47.1'W was successfully recovered. The data will be processed after returning to Bremerhaven, and it is hoped that it will be possible to determine, whether continuous contour currents or turbidity currents have formed this structure.

Fig. 3.49: Geological sampling locations (heavy dots) in the eastern Weddell Sea. The triangles mark the positions of the current meter moorings, the inset shows a detailed map of the Polarstern Seamount

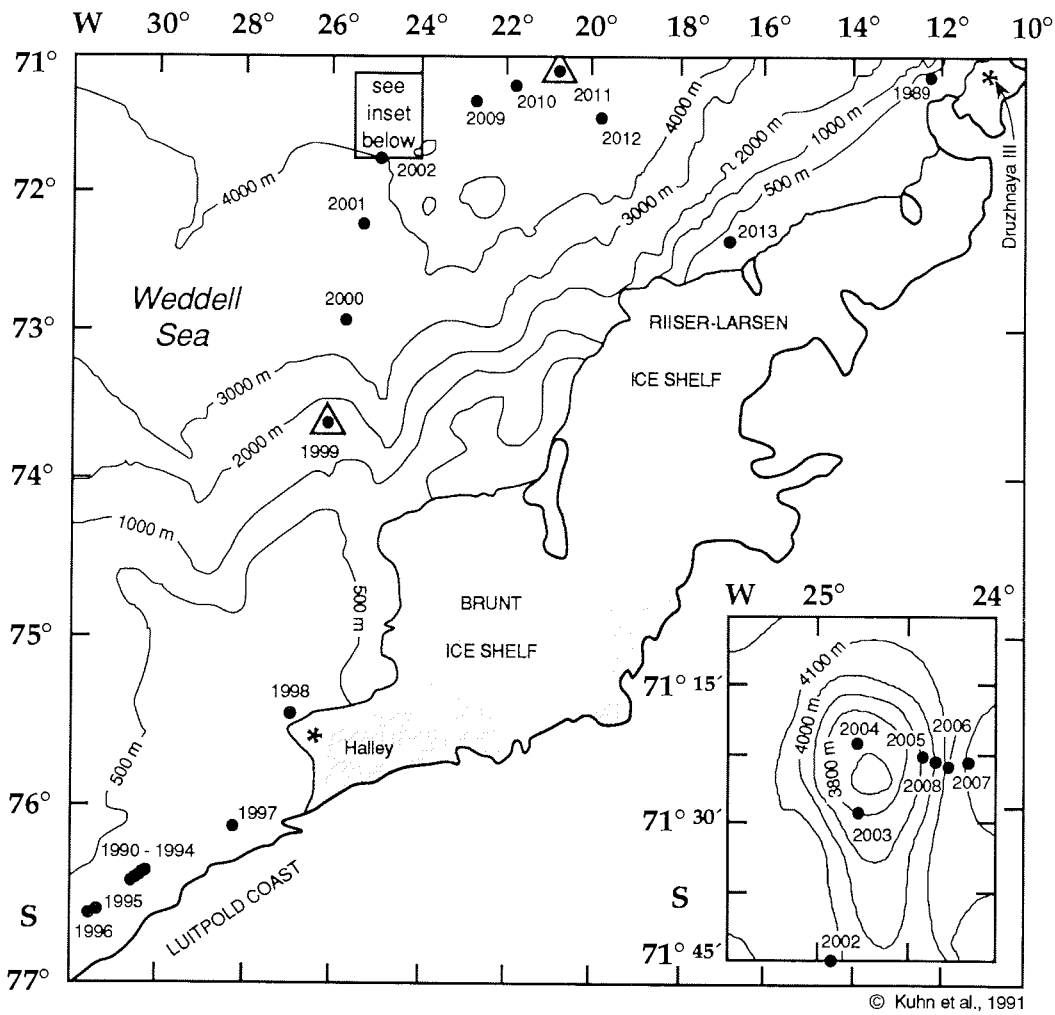


Fig. 3.50: Geological sampling locations in the Lazarev Sea

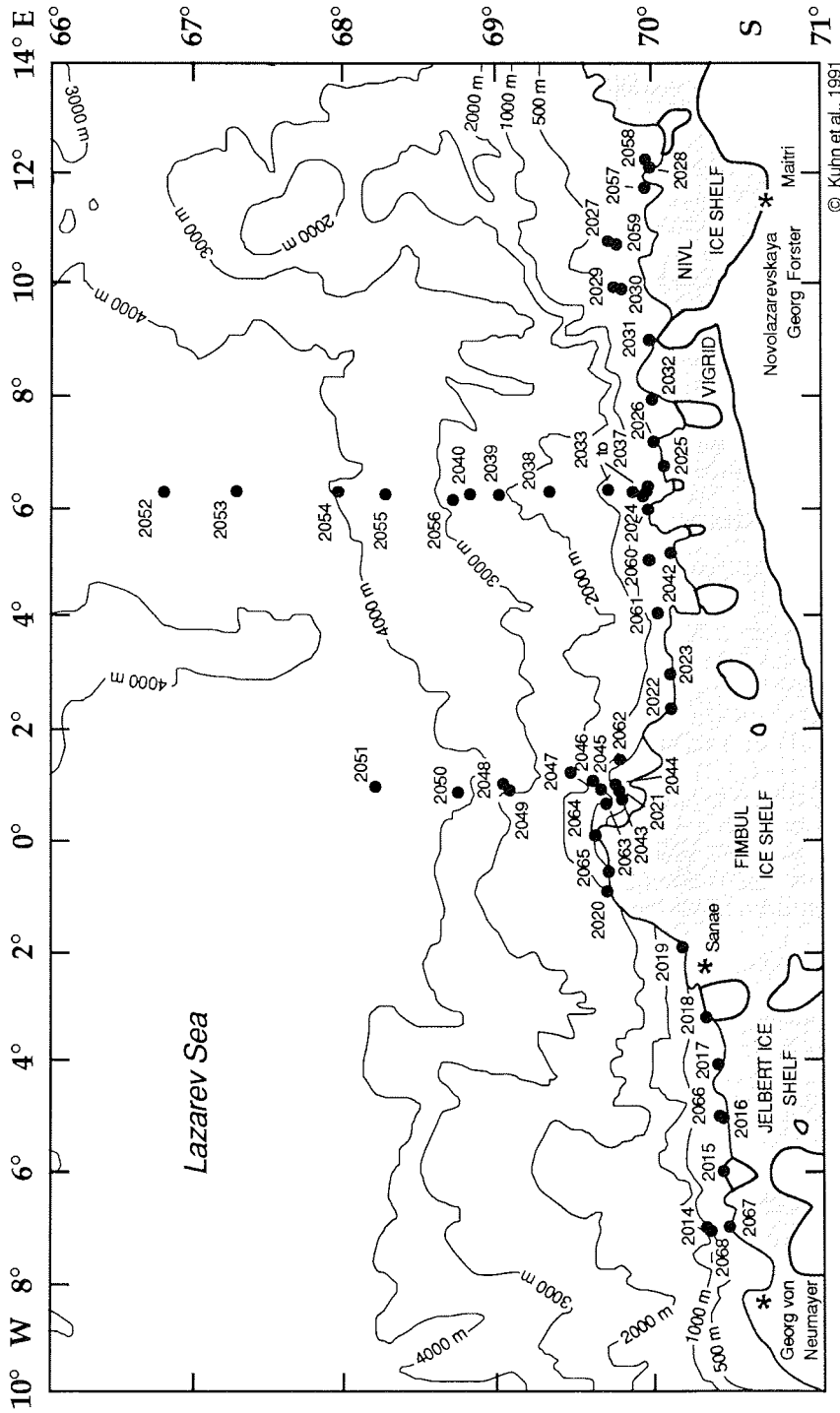


Fig. 2: Geological sampling locations in the Lazarev Sea.

On the transit back to Cape Town one site was sampled on the top of Maud Rise, and another site sampled a prominent acoustic sub-bottom reflector of uncertain origin on the flank of Maud Rise.

During the cruise ANT-IX/3 sediment echo-sounding with the Parasound system was run throughout on a routine base and provided important information concerning the physical properties of the sediments. The system was also helpful in the selection of the geological sampling sites.

Methods

Undisturbed samples were recovered from the upper sediment layers of the seafloor by means of a large box corer (GKG, 50 x 50 cm, penetration up to 60 cm), a multi box corer (MG, 12 boxes, Gerdes 1990), a multicorer (MUC, 12 cores, Ø 6 cm, penetration up to 35 cm) and a minicorer (MIC, 2 cores, Ø 6 cm, penetration up to 35 cm, developed at the AWI, cf. cruise report ANT-IX/2). The MIC was installed beneath the CTD equipment and therefore did not require additional sampling time. After description and photographic documentation of the sediments, the following samples were taken from the sediment surface:

sedimentology (ca. 250 ml, 1-1.5 cm deep, or two MUC cores: 0-1, 1-3, 3-5, ...)
organic carbon and carbonate (ca. 20 ml, 0.5 cm deep)
benthic foraminifera (412 cm², thickness 1-1.5 cm, a 12 cm Ø subcore, or five MUC cores)
radiolaria and diatoms (412 cm², thickness 0.3-0.5 cm, or 2 MUC cores)

For laboratory analysis of the upper sediment layer, an archive core was taken with a PVC-Liner (Ø 12.5 cm) out of the box corer. Sediment slices measuring 1 cm x 15 cm x 27.5 cm were taken for X-radiography in order to carry out textural investigations. After all the above samples had been taken, the residual sediment of the box corer was sieved over a 2 or 6.3 mm mesh for collection of gravel clasts. Many clasts were also collected using the Agassiz trawl (AGT) or a bottom trawl (GSN).

Older sediments were sampled with a gravity corer (SL, Ø 12.5 cm, 1.5 t, up to 15 m long) or a piston corer (KOL, Ø 8.5 cm, 1 t, 10 m long). The sediment cores in the liner tubings were cut into 1 m long sections. Sediment samples were taken from the cut surfaces of the sediment cores and from the core-catcher for an immediate smear slide analysis.

The sediment core 2003-2 from the Polarstern Seamount was opened on board, described and sampled. After preparing sediment slices for X-radiography (27.5 x 10 x 1 cm), samples for sedimentological analyses were taken at an average interval of 5 cm. Smear slides were made at varying intervals and used in the resulting sediment description. For sedimentological and palaeomagnetic analyses, four subsamples 1.5 to 2 cm thick were obtained from each sampled horizon:

5 cm³ for water content, density, organic and inorganic carbon
7 cm³ orientated sample for palaeomagnetic investigations
5 cm³ for grain size distribution and clay mineralogy and
70 cm³ for coarse fraction analyses.

The last-mentioned samples were wet-sieved through a 63 μm mesh. The remaining sand fraction was dried at 60°C. The distribution of foraminifera, radiolaria and terrigenous sand grains was estimated.

Continental shelf

One of the main objectives of the sedimentological research programme during ANT-IX/3 was to link the proximal glacial marine sediments in front of ice shelves, glacier tongues and ice rises with the dynamics of the ice masses. A thorough knowledge of the sedimentary facies typical of these specific depositional environments is crucial for interpreting transport mechanisms and for more precise palaeoenvironmental interpretation of sediment cores, not only here but also in other regions. This work will contribute towards a more detailed reconstruction of the glacial history of Antarctica. Another long-term aim is to develop sedimentary models for heavily glacially influenced continental margins.

It was planned to carry out this project in the southwestern Weddell Sea, much of which is permanently ice-covered. Because the ice conditions too heavy this year, the research programme had to be transferred to the continental margins of the eastern Weddell Sea and especially the Lazarev Sea. In the eastern Weddell Sea, our samples cover the areas off Luitpold Coast, Brunt Ice Shelf and Riiser-Larsen Ice Shelf (Fig. 3.49) and supplement our data-set from previous cruises. In the Lazarev Sea, geological sampling by the Alfred Wegener Institute was carried out for the first time in the areas off Jelbert Ice Shelf, Fimbul Ice Shelf, Vigrid Ice Shelf, Nivl Ice Shelf and some small ice rises (Fig. 3.50). The samples were taken in a systematic way, as close as possible to the ice shelf or grounded ice edge, and at more-or-less constant distances of about 1° longitude (ca. 35 km).

The investigations of the sedimentary facies and mapping of the different facies types will improve our knowledge about source areas and transport mechanisms in this part of Antarctica. This knowledge may then be used to decipher the geological past using long sediment cores. Temporal variations in the source areas and the nature of ice movement, ice coverage and sediment transport will thus be revealed.

Preliminary results from investigations of the gravel fraction of the sediments are presented separately in one of the following sections. It appears from the sediment descriptions and radiograph evaluations of the box cores, and from the smear slide analyses of the sediment cores that the sediment composition on the eastern Weddell Sea continental shelf (Fig. 3.49) is more homogeneous than on the Lazarev Sea shelf (Fig. 3.50).

On the southeastern Weddell Sea continental shelf, the surface sediments consist mostly of terrigenous gravelly and muddy sands with a relatively low biogenic content. On the upper eastern flank of the Crary Trough, adjacent to the Luitpold Coast, six sampling attempts with the large gravity corer (GSL) failed and only a few coarse-grained sediments were recovered with the core catcher. This may indicate that, in the eastern Crary Trough, the basement crops out and is only partly covered by a very thin sediment layer a few centimetres thick. This interpretation is also compatible with video-recordings made with a camera installed on the multi box corer (MG). The video showed a regular fracture pattern and cracks in the rock outcrops. Our interpretation is

also supported by shallow seismic data (Maisey, 1980). The soft glaciomarine sediments may have been deposited following the retreat of the ice sheet, which probably covered the southern Weddell Sea continental shelf during the late Weichselian glaciation and may have created the Cray Trough by deep glacial erosion (Elverhøi, 1981).

On the Lazarev Sea continental shelf, at least four sites yielded a highly consolidated, texturally homogeneous pebbly mud, using a gravity corer. At two of these sites the sediment contains very little biogenic material, whereas at the other two sites no biogenic components at all were observed in smear slides. Measurements were made of the grain fabric in these undisturbed samples. Three out of four showed a strong preferred orientation, the other a random fabric. This diamict, at least in part, is possibly a lodgement till, deposited during the northward advance of the continental ice sheet during the Weichselian glaciation. A continuously high carbonate content in the overlying soft sediments, arising from the skeletons of bryozoa, promises detailed stratigraphic information by means of ^{14}C -dating. Of special interest is the date of the onset of Holocene ice retreat, which so far has only been poorly dated in different continental shelf areas around Antarctica. The Holocene sediments often show distinct down-core changes in composition, indicating changes in the environmental conditions during the retreat of the Holocene ice masses. The surface sediments may be divided into two major sediment types. One type consists almost totally of calcareous biogenic components, mainly bryozoa; the other type is characterised by well sorted terrigenous sands or gravelly sands, which contain relatively few biogenic components. Both sediment types show an irregular distribution pattern. The coarse grain-sizes indicate especially that high current velocities prevail along the ice margin, probably related to the Antarctic Coastal Current. To the north, with increasing water depths and distance from the ice edge, a distinct increase in the fine fraction occurs, indicating a decrease in current velocities near the sea bottom.

South-north profiles

Geological profiles from the continental shelf area via the continental slope to the adjacent deep-sea basin document the transition from proximal to distal glaciomarine facies. This part of the project is a continuation of previous studies in the eastern Weddell Sea. Its main aim is the investigation and quantification of glaciomarine sedimentation processes and the oscillations of the ice shelves in response to Quaternary climatic changes.

During ANT-IX/3, sampling was undertaken on two south to north profiles in the Lazarev Sea (Figs. 3.50 & 3.51). On both profiles, near-surface sediments were sampled by means of a large box corer, multicorer, minicorer or multi box corer. Where possible, deeper sediments were sampled by means of a gravity corer. The first profile is situated in ca. longitude 1°E , comprises Sites PS2044 to PS2051, and thereby extends through water depths from 825 m to 4444 m. The second profile is situated in c. longitude 6°E , where Sites PS2033 to PS2040 and PS2052 to PS2056 were established in water depths ranging from 310 m to 4300 m (Figs. 3.50 & 3.51).

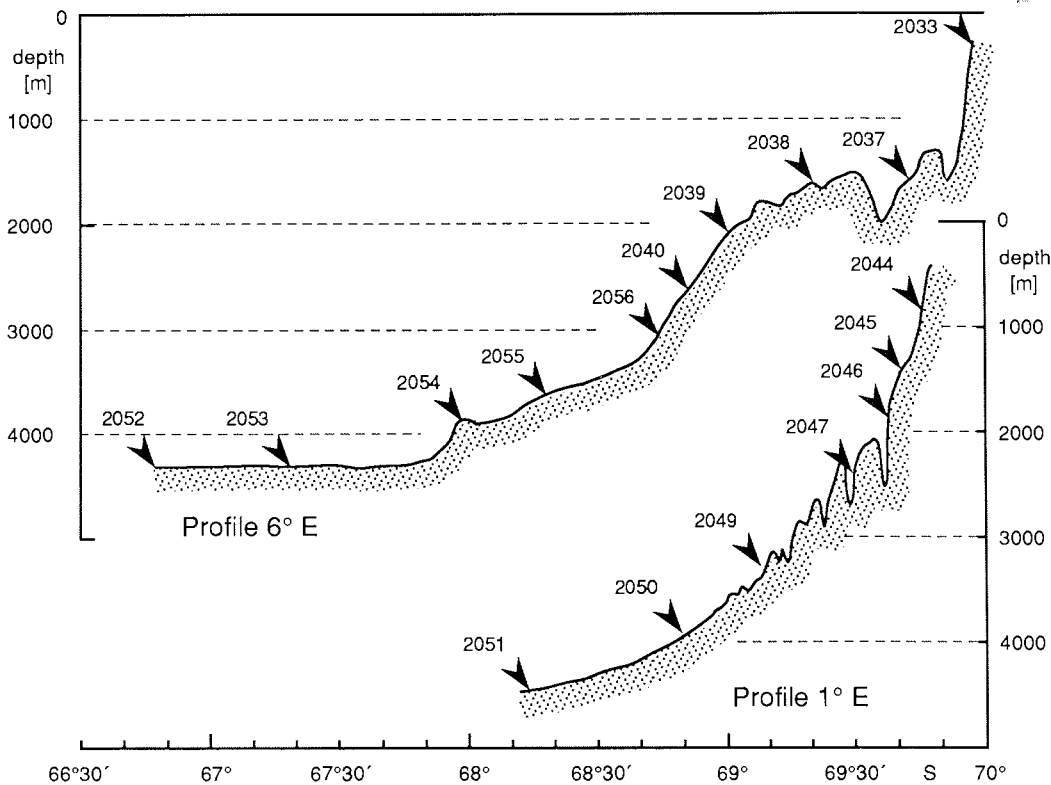
Smear slide analyses of the cut surfaces of the sediment cores were undertaken as summarised in the Appendix. The sediments recovered from the Antarctic continental margin of the Lazarev Sea are composed mainly of

terrigenous material, such as quartz, feldspar and clay minerals, with the main lithology being mud. The terrigenous material was transported by icebergs, currents and downslope gravity processes. Biogenic components, notably foraminifera, diatoms, radiolaria and sponge spicules were also detected. Most of the sediment samples, even those from a great water depth, contain foraminifera in trace amounts up to a few percent. This may open the possibility of building up a stable isotope stratigraphy for these cores. Diatoms normally exceed foraminifera in abundance and may allow a biostratigraphic age to be determined.

Polarstern seamount

The deep-sea area of the southern Weddell Sea has been investigated during previous Polarstern cruises. A seamount-like structure with an elevated seismic basement and positive gravity anomaly, was detected during the cruise ANT-VIII/5. This seamount rises from 4200 m to 3600 m water depth. The sediments on the surrounding deep abyssal plain have been sampled in some places on former Polarstern cruises. The sediments are laminated with some laminae showing fining-upwards gradation and an erosive base. These sediments were deposited under the influence of currents. On the top of the seamount two surface samples and two sediment cores were taken. Four additional sites were sampled on the seamount's eastern flank (Fig. 3.49).

Fig. 3.51: Geological sampling sites along two S-N sections across the continental margin off Dronning Maud Land (for location cf. Fig. 3.45)



Core PS2003-2 from the top of the seamount was opened and described during this cruise (Appendix). This core is 920 cm long and shows a homogeneous structural pattern. Bedding is very rare and lamination invisible. The sediments are moderately bioturbated. The amount of ice-rafted debris and terrigenous sand is more or less constant (Fig. 3.52). No signs of current activity or hiatuses in the cored section have been detected so far. The upper 230 cm of the core contains planktonic foraminifera as a common constituent of the sediment. The foraminifera content decreases downcore and the sediment contains only traces of biogenic components between 230 and 610 cm. In the lower part of the core (620 to 920 cm) siliceous microfossils are common. Stratigraphical investigations of the biogenic sediment components, including stable isotope studies in the upper part of the core, and palaeomagnetic studies, will allow the sediments to be dated. Therefore the data from this site will probably play an important role in correlating the relatively poorly dated sediments in the southern Weddell Sea.

The seafloor on top of the Polarstern Seamount is densely covered with Mn-encrusted dropstones, as observed by the underwater video-recording obtained from a camera installed at the multi box corer (MG), as well as in the retrieved sediments. The average size of the dropstones was less than 7 cm. The sediments just below the dropstone layer also contain dropstones, but they are dispersed. The dropstone layer was probably not caused by current activity, because that would have also resulted in enrichment of coarse sand, and this is not in evidence.

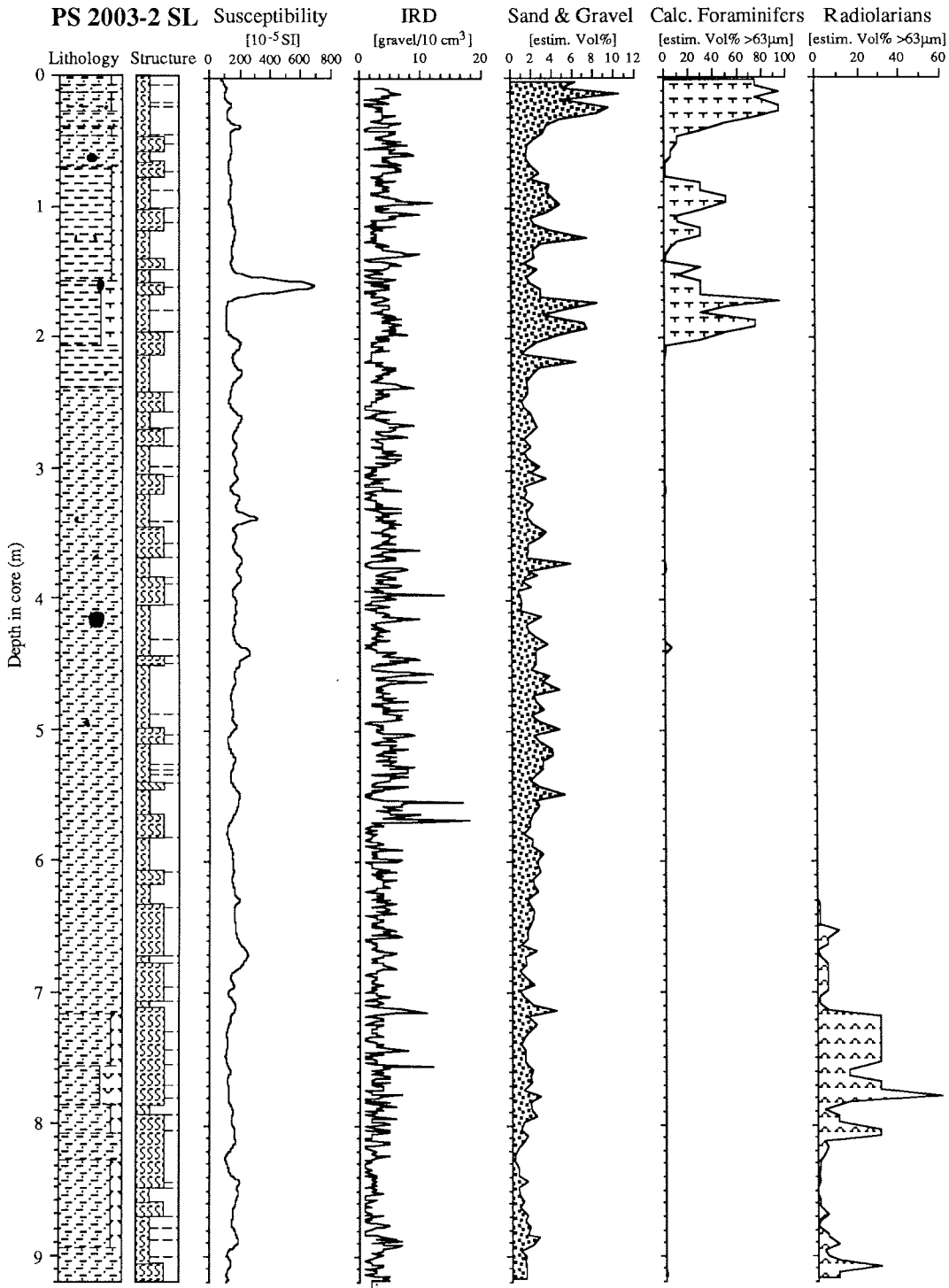
Maud Rise

Maud Rise is an aseismic elevation situated in the southernmost Atlantic Ocean and rises from the deep-sea basin at a depth of some 4500 m to c. 1200 m, which is well above the calcite compensation depth (CCD). Its isolated position prevents the Maud Rise from coming under any direct continental influence, such as from slumping and turbidity processes. The sediments deposited under such conditions are therefore suitable for a wide range of geological studies. Sedimentological investigations based on previous Polarstern cruises and on Ocean Drilling Program (ODP) Leg 113 had the aim of reconstructing the paleoceanography of the Southern Ocean, the Cenozoic paleoclimate and the glacial history of Antarctica. Sampling during ANT-IX/3 was intended to address two special questions.

At Site PS2069 in 1221 m water depth, the top of the Maud Rise was sampled in order to study the composition of the sediment layer overlying the hard acoustic basement, and to obtain information concerning the nature and age of the basement. The sediment cover was only a few centimetres thick and consisted of foraminiferal ooze. Beneath, ca. 30 cm of highly altered basalt was recovered.

Site PS2070 was chosen in order to sample an acoustically hard sub-surface reflector, which was recorded on earlier cruises at several locations on Maud Rise with the Parasound-system and the 3.5kHz sediment echosounder. The nature of this reflector is not yet clear, but it is assumed to be caused by porcellanite nodules. Porcellanite is a diagenetic alteration product of biogenic opal which normally forms in much older and more deeply buried sediments. Isolated pieces of porcellanite were previously recovered by ODP Leg 113, but were not in contact with the sediment. Therefore previous age

Fig. 3.52: Sediment parameters of core PS2003-2. (for legend see Appendix)



determinations and diagenetic studies were of limited value. At the sampling site, the corresponding reflector was at a depth of c. 5 m. The piston corer penetrated the reflector and recovered 7.18 m of highly biogenic sediment. No statement about the nature of the reflector can be made so far, because the core remained unopened, and only 8 cut surfaces of the core were investigated by smear slides aboard ship (Appendix). Approximately the upper 3.5 m consisted of a light brownish grey diatom-bearing foraminiferal ooze, and the deeper sediments a light grey radiolaria-bearing diatom ooze.

Shape, surface features and lithology of clasts

The gravel component in marine sediments of the continental shelf, continental slope and ocean basins around Antarctica is almost totally the result of transport by glacier ice, in particular by grounded ice, ice shelves, ice tongues and icebergs. Yet, few systematic observations have previously been made of the gravel component of Antarctic glaciomarine sediments (Oskierski, 1988).

A large number of clasts was sampled in both shallow and deep water around more than 1500 km of the Antarctic margin of Coats Land and Dronning Maud Land, East Antarctica (Figs. 3.49, 3.50). The gravel fraction was taken from sediments obtained by the geological sampling equipment (GKG, SL, GSL), a biological multi box corer (MG), a bottom trawl (GSN) and an Agassiz trawl (AGT) (Tab. 3.19.). Onshore investigations were undertaken during a half-day visit to Georg Foster station in Schirmacher Oasis (Fig. 3.50). In the vicinity of Georg Forster Station samples were taken from basal ice in a detached, dead remnant of the ice sheet; from sediment deposited directly by ice on the top of a roche moutonnée; and from debris immediately in front of the stagnant ice.

Often, the stones in the marine sediments include large boulders up to 1.5 m across. Shape data from these samples are thus representative of cobbles and boulders, as well as pebbles, although no significant differences in shape could be detected between the different size classes. In most cases, the number of clasts analysed was around fifty, representing the largest clasts from a recovered sample for ease of measurement. Some sites yielded fewer gravel clasts, and at others up to 100 were measured to compare the shapes of different lithologies. The long (a), intermediate (b) and short (c) axes were measured using a millimetre rule. The ratios b/a and c/b were calculated for each clast and the sphericity estimated using the chart of Krumbein (1941). This chart also characterises Zingg shape: discs, spheres, blades and rods (Tab. 3.20). The roundness of all clasts was recorded from a visual comparison chart for assessment of Powers' roundness index (Tab. 3.20). Following Boulton (1978), Powers' Roundness was plotted versus Krumbein Sphericity for a full representation of clast shape (Figs. 3.53 & 3.54).

Clast lithology was recorded in a rough-and-ready manner. The dominant types are basalt and dolerite, metabasic volcanic rocks, granite, and high grade metamorphic rocks, including granite-gneiss, gneiss, schist, quartzite. Discrimination between metamorphic and non-metamorphic rocks was sometimes difficult in hand specimen, and thin-section work will be necessary to check the validity of the data. Sedimentary rocks were poorly represented, except for diamict clasts at some localities (Tab. 3.21). At most localities, shapes and surface markings associated with glacially transported clasts were recorded, especially faceted surfaces (one or more), flat-iron shapes, bullet-nosed shapes and striations (Tab. 3.22).

Tab. 3.19: List of geological sampling sites with surface samples, core recovery data and clast samples.

Station-No.	Latitude	Longitude	Water	Sed. surf. samples				Sediment-	Clasts	
Geology	Ship 18/		depth	S.	C.	F.	R.	cores [cm]	from	
1989	123/4	71°08,5'S	12°12,8'W	443	x	x		x	GKG 26	AGT, AGT, GKG
1990	126	76°23,2'S	30°12,0'W	368	x	x	x	x	GKG 16, SL 119	GKG
1991	126	76°24,8'S	30°21,2'W	325						MG
1992	126	76°25,5'S	30°25,8'W	319					GSL cc	
1993	126	76°25,5'S	30°25,8'W	319					GSL cc	
1994	126	76°26,1'S	30°30,1'W	309					GSL cc	
1995	127	76°36,1'S	31°19,4'W	394	x	x			MG 32	MG, GSL
1996	127	76°37,3'S	31°27,9'W	305					SL cc	SL
1997	129	76°07,2'S	28°15,4'W	369	x	x				AGT, MG
1998	135	75°28,5'S	26°57,5'W	237	x	x				
1999	141	73°37,1'S	26°06,8'W	3350	x	x			MIC 4	
2000	142	72°55,0'S	25°41,4'W	3572	x	x			MIC 25	
2001	143	72°14,3'S	25°15,6'W	3785	x	x			MIC 20	
2002	144	71°45,1'S	24°55,1'W	4100	x	x			MIC 25	
2003	145	71°29,1'S	24°46,4'W	3718	x	x	x		MUC 20, SL 920	
2004	146	71°21,3'S	24°46,7'W	3684	x	x			MG 38, SL 500	
2005	147	71°22,8'S	24°25,1'W	3806	x	x	x	x	GKG 44, SL 898	GKG
2006	148	71°23,9'S	24°16,3'W	4230	x	x	x	x	GKG 43, SL 546	
2007	149	71°23,4'S	24°09,5'W	4217	x	x	x	x	GKG 43, SL 473	GKG
2008	150	71°23,3'S	24°20,8'W	3927	x	x	x	x	MUC 25, SL 672	
2009	151	71°19,7'S	22°41,9'W	4192	x	x			MIC 25	
2010	152	71°12,7'S	21°47,5'W	4271	x	x			MIC 13	
2011	153	71°05,7'S	20°46,8'W	4453		x	x		MUC 15	
2012	154	71°26,7'S	19°48,4'W	4350	x	x			MIC 24	
2013	158	72°21,8'S	16°52,1'W	623						GSN
2014	160	70°18,6'S	6°52,2'W	830						GSN
2015	161	70°24,2'S	6°00,4'W	125	x	x			SL 37	GSL
2016	162	70°23,1'S	4°59,0'W	428						AGT, AGT, MG
2017	164	70°21,9'S	4°02,3'W	508	x	x	x		GKG 15, SL 43	GKG
2018	165	70°18,0'S	3°12,9'W	148	x	x				AGT
2019	166	70°09,9'S	1°56,6'W	161	x	x	x	x	GKG 14, SL cc	GKG
2020	167	69°42,6'S	0°56,8'W	2046	x	x	x	x	GKG 43, SL 934	no gravel
2021	168	69°47,2'S	0°52,2'E	465						AGT
2022	169	70°06,2'S	2°22,9'E	163	x	x				GSN
2023	170	70°06,3'S	3°00,5'E	414	x	x	x	x	GKG 53	GKG
2024	171	69°58,6'S	5°56,7'E	551	x	x	x	x	GKG 30, SL 59	GKG
2025	172	70°02,6'S	6°44,9'E	638	x	x	x	x	GKG 21, SL 224	GKG
2026	173	70°00,3'S	7°11,1'E	176	x	x			MG 31	
2027	174	69°43,4'S	10°45,3'E	420						GSN
2028	175	70°00,7'S	11°44,9'E	203	x	x	x	x	GKG 60, SL 181	GKG
2029	176	69°45,0'S	9°57,8'E	895						MG
2030	177	69°47,9'S	9°55,5'E	259	x	x				
2031	178	69°59,4'S	8°58,5'E	450	x	x	x	x	GKG 28, SL 58	GKG
2032	179	69°58,1'S	8°01,5'E	191	x	x	x	x	GKG 22	GKG
2033	180	69°58,3'S	6°20,6'E	311	x	x	x		SL cc	AGT
2034	181	69°57,0'S	6°14,5'E	734	x	x	x			GKG
2035	182	69°56,1'S	6°12,0'E	1143	x	x	x			

Station-No. Geology	Ship 18/	Latitude	Longitude	Water depth	Sed. surf. samples				Sediment- cores [cm]	Clasts from
					S.	C.	F.	R.		
2036	183	69°52,1'S	6°15,8'E	1541		x			MIC 23	
2037	184	69°42,9'S	6°16,3'E	1586	x	x	x	x	MUC 23, SL 358	
2038	185	69°21,2'S	6°17,1'E	1603	x	x	x	x	MUC 21, SL 1269	
2039	186	69°01,4'S	6°13,7'E	2073	x	x	x		MUC 31, SL 1150	
2040	187	68°50,5'S	6°14,1'E	2625	x	x	x	x	MUC 29, SL 1267	
2041	188	68°44,4'S	6°07,8'E	3062					CTD only (Station 2056)	
2042	189	70°05,9'S	5°11,9'E	470	x	x	x		SL 82	GKG
2043	190	69°47,6'S	0°44,4'E	380	x	x	x		GKG 13, SL 36	GKG
2044	191	69°46,4'S	0°59,9'E	825	x	x	x	x	GKG 33, SL 408	GKG
2045	192	69°41,0'S	0°55,6'E	1392	x	x	x		SL 1084	AGT
2046	193	69°37,2'S	1°02,6'E	1798	x	x	x	x	MUC 17, SL 709	
2047	194	69°29,4'S	1°12,7'E	2375	x	x	x	x	MUC 31, SL 324	
2048	195	69°04,0'S	0°58,9'E	3587					MIC cc	
2049	196	69°05,2'S	0°53,4'E	3264		x	x	x	MUC 35, SL 219	
2050	198	68°46,1'S	0°52,3'E	3903	x	x	x	x	MUC 33, MG 41, SL 180	
2051	199	68°13,9'S	0°59,9'E	4444	x	x	x	x	MUC 7, SL cc	
2052	200	66°48,3'S	6°15,8'E	4299	x	x	x	x	MUC 31	
2053	201	67°17,9'S	6°15,5'E	4305	x	x			MG 45, SL cc	
2054	202	67°57,7'S	6°14,7'E	3882	x	x			MUC 34	
2055	203	68°17,4'S	6°14,9'E	3606	x	x	x	x	MUC 33, SL 1079	
2056	204	68°44,6'S	6°08,1'E	3060	x	x	x	x	MUC 31, SL 474	
2057	208	69°57,3'S	11°48,6'E	210	x	x	x		GKG 14	GKG
2058	209	69°58,3'S	12°10,7'E	155	x	x	x		GKG 44, SL 44	GKG
2059	210	69°45,3'S	10°42,4'E	348	x	x	x	x	GKG 20, SL cc	GKG
2060	211	69°58,2'S	5°01,5'E	551	x	x				MG
2061	212	70°01,2'S	4°05,5'E	905	x	x	x	x	GKG 25	GKG, AGT
2062	214	69°47,2'S	1°26,7'E	1602	x	x	x	x	GKG 52, SL 457	GKG
2063	216	69°44,9'S	0°46,2'E	530	x	x			MG 15	
2064	217	69°38,5'S	0°03,3'E	1501	x	x	x	x	GKG 30, SL 82	GKG
2065	218	69°42,9'S	0°33,6'W	2060	x	x	x	x	GKG 49	
2066	219	70°23,6'E	5°00,4'W	430	x	x	x	x	GKG 26, SL 200	GKG
2067	221	70°26,1'S	7°00,1'W	610	x	x	x	x	GKG 43	GKG
2068	222	70°18,9'S	7°03,0'W	550	x	x			MG 30	
2069	224	65°08,6'S	2°41,5'E	1222					KOL 33	
2070	225	65°06,3'S	3°37,0'E	2611					KOL 718	
2071	226	65°07,1'S	3°40,2'E	2624					Piston corer lost	
2072	227	60°33,9'S	3°57,6'E	5373	x	x	x		MUC 33	

Sediment surface samples for: S. = Sedimentology
 C. = Carbonate and organic carbon
 F. = Foraminifera
 R. = Radiolaria and Diatoms

GKG = Großkastengreifer (large box corer)
 SL = Schwerelet (gravity corer)
 GSL = Großschwerelet (large gravity corer)
 KOL = Kolbenlot (piston corer)
 MG = Mehrfachgreifer (multi box corer)
 MUC = Multicorer (multicorer, with 12 cores)
 MIC = Minicorer (minicorer, with 2 cores)
 AGT = Agassiz Trawl
 GSN = Grundschleppnetz (bottom trawl)
 cc = Core Catcher

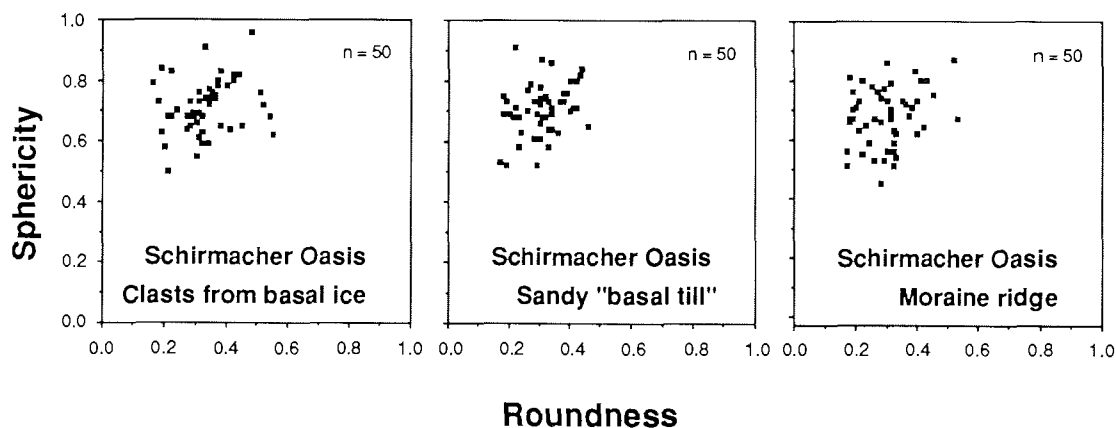
Tab. 3.20: Power's Roundness and Zingg Shape of clasts.

Station- of No.	Powers' Roundness [%]						Zingg Shape [%]				No. clasts
	VA	A	SA	SR	R	WR	Discs	Spheres	Blades	Rods	
1989-3 lower L.	6	38	44	12	0	0	27	48	6	18	50
1989-3 upper L.	4	20	52	24	0	0	28	28	14	30	50
1990-3	6	30	40	18	6	0	30	38	10	22	50
1991-2	2	32	48	18	0	0	28	40	8	24	100
1995-1	16	36	48	0	0	0	16	48	8	28	25
1995-2	24	40	30	6	0	0	40	33	13	14	100
1996-1	18	52	26	4	0	0	38	30	10	22	50
1997-1	0	8	52	36	4	0	28	40	8	24	25
1997-2	2	24	46	28	0	0	32	42	6	20	50
2005-2	2	16	38	28	16	0	46	18	12	24	50
2007-2	2	8	61	29	0	0	27	39	6	29	49
2013-1	6	16	39	27	12	0	29	33	12	25	51
2014-1	0	10	32	46	12	0	22	34	4	40	50
2015-4	0	32	38	24	6	0	30	48	8	14	50
2016-1	0	6	22	44	28	0	22	44	0	33	18
2016-2	0	14	32	39	14	0	29	54	0	18	28
2016-3	0	18	32	38	12	0	32	38	10	20	50
2016-3 *	4	38	38	15	4	0	46	23	12	19	26
2017-2	2	17	33	33	15	0	29	47	8	16	49
2018-2	0	2	27	44	27	0	31	51	2	16	45
2019-2	0	16	36	32	16	0	34	42	4	20	50
2021-1	3	16	50	28	3	0	38	44	0	19	32
2022-1	0	10	24	42	24	0	16	66	2	16	50
2023-1	2	18	38	42	0	0	30	36	8	26	50
2024-3	2	16	42	34	6	0	18	64	6	12	50
2025-1	0	21	42	32	6	0	28	28	8	36	72
2027-1	0	14	42	44	0	0	14	76	2	8	50
2028-1	0	4	42	48	6	0	26	50	4	20	50
2029-1	0	4	54	42	0	0	26	40	14	20	50
2031-1	0	2	51	45	2	0	35	37	6	22	49
2032-2	0	12	58	22	6	2	26	54	0	20	50
2033-2	0	10	32	50	8	0	32	50	2	16	50
2034-3	0	11	39	46	4	0	24	39	11	26	54
2042-3	0	4	41	55	0	0	24	53	6	16	49
2043-2	0	12	39	41	8	0	29	57	2	12	49
2043-3**	2	24	42	30	2	0	24	52	6	18	50
2044-2 upper L.	0	14	40	38	8	0	40	34	10	16	50
2044-2 lower L.	0	9	44	45	2	0	35	38	9	18	55
2045-4	0	16	36	40	8	0	56	24	8	12	50
2057-2	0	6	32	52	10	0	24	40	4	32	50
2061-2	0	0	26	56	16	2	40	26	4	30	50
2064-2	0	16	52	28	4	0	30	44	4	22	50

* = Fine gravel clasts from a diamict intraclast

** = Clasts from compacted diamict

Fig. 3.53: Roundness versus sphericity of clasts collected near Georg Forster station in Schirmacher Oasis



The following observations may be made concerning the different types of glaciological-oceanographic setting:

Ice sheet margin, Schirmacher Oasis: A sample was obtained from the basal debris zone exposed at the surface of a stagnating, detached remnant of the ice sheet between Forster and Novolazarevskaya stations. Clast shapes of all classes occur, though there are few blades, and roundness values indicate a predominance of subangular and (to a lesser extent subrounded) clasts. These characteristics reflect varying degrees of working at the ice-bedrock interface. Fig. 3.53 shows low-medium roundness and medium-high sphericity. This falls within the basal ice transport zone of Boulton (1978), but with a marked shift to the angular end of the field.

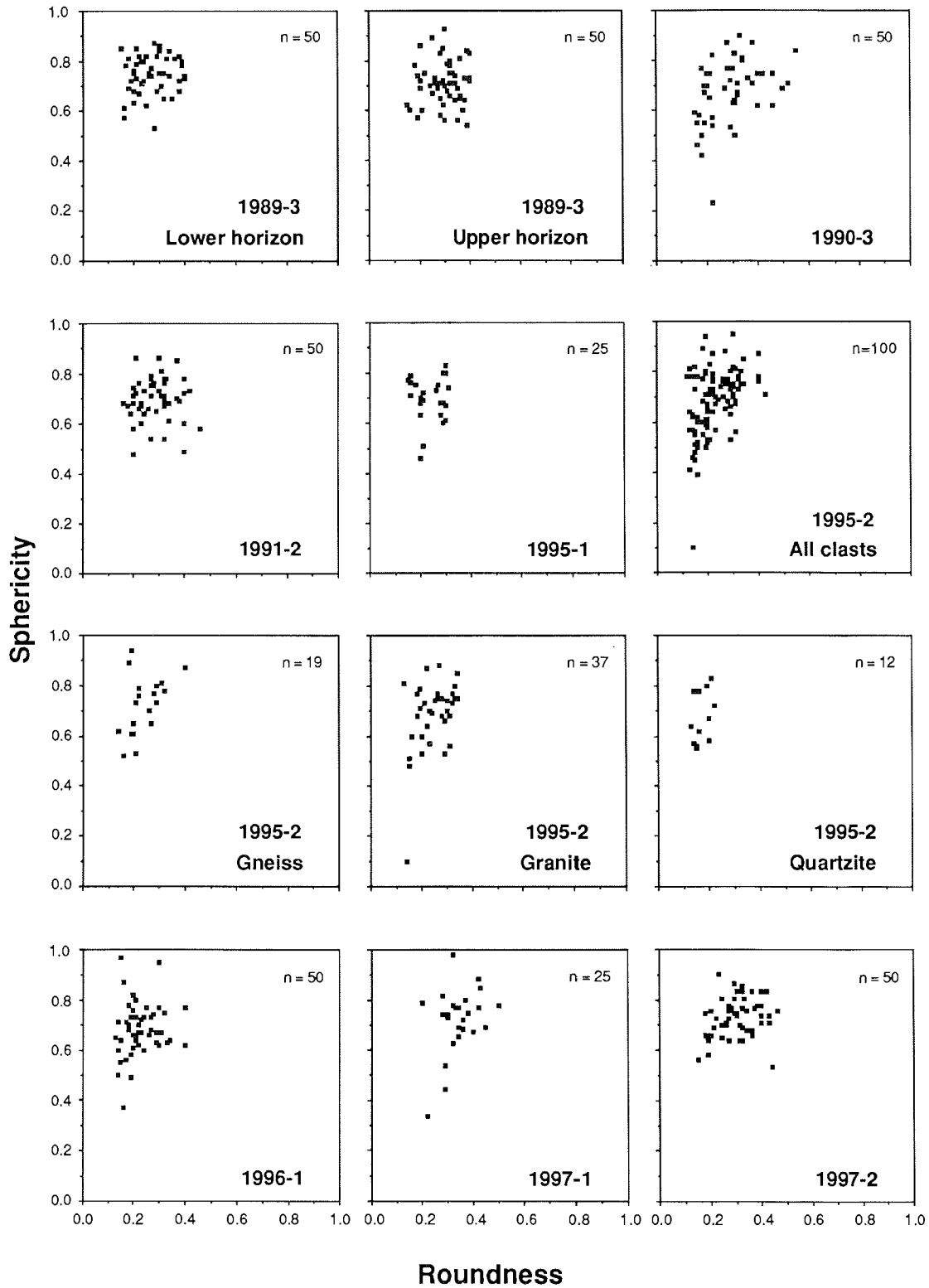
Ice Shelves: Data from most ice shelf settings illustrate a broad similarity to the basal ice of Schirmacher Oasis (Figs. 3.53 and 3.54).

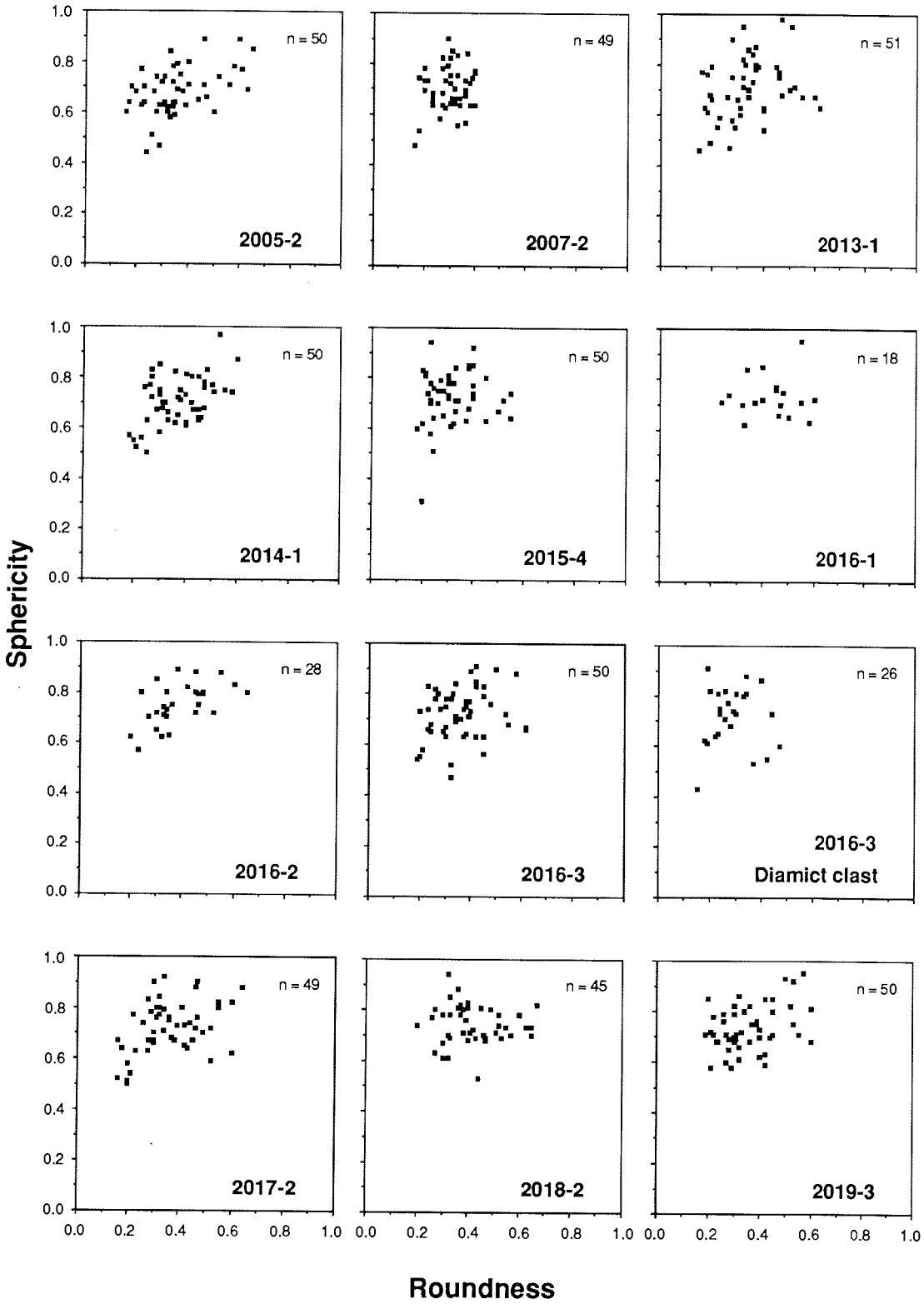
Grounded Ice Margin: A broadly similar pattern of shapes is recorded as in the basal ice sample, but with a slight tendency towards greater angularity. Samples from the southern limit of ANT-IX/3 in the Weddell Sea yielded distinctly more angular clasts than elsewhere (Fig. 3.54).

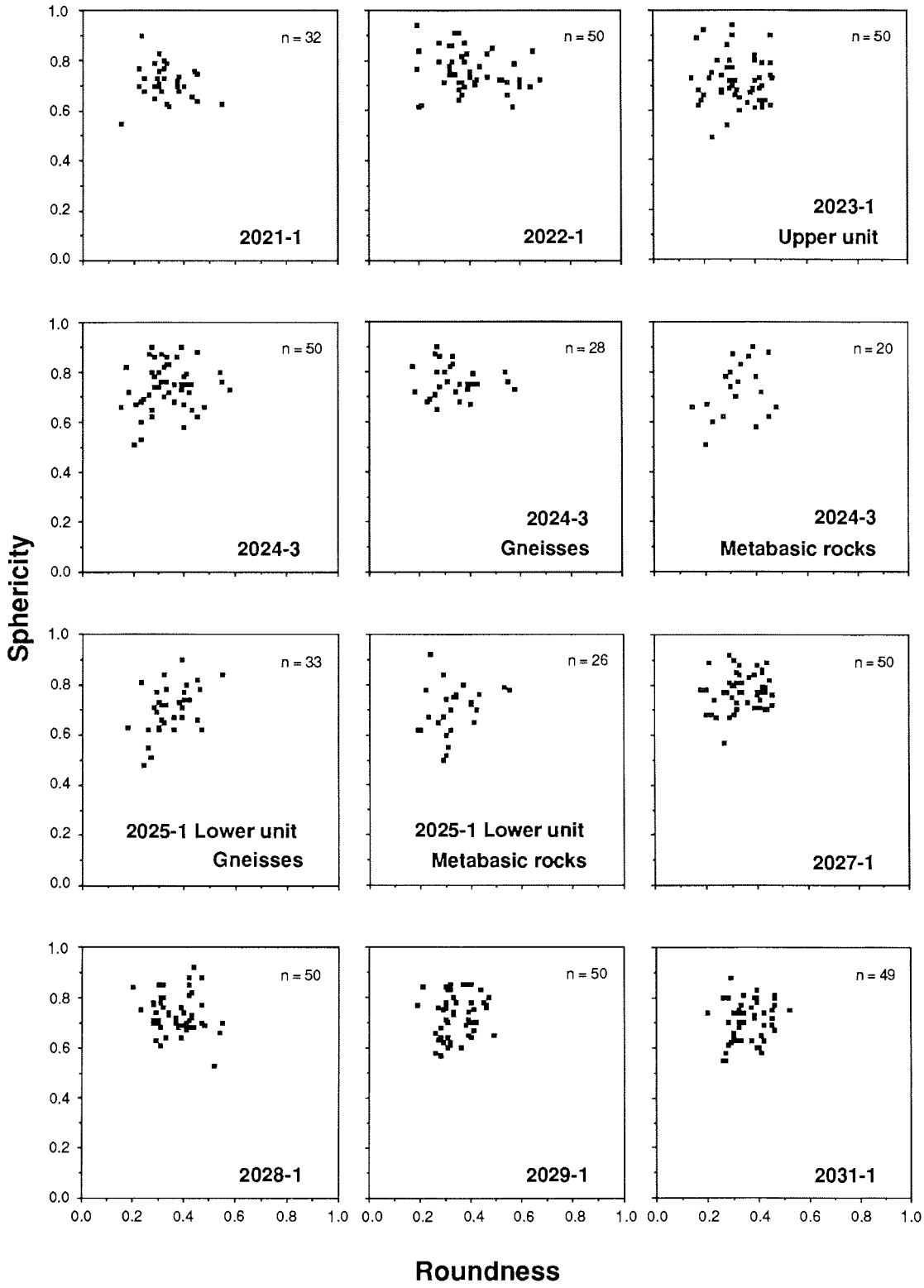
Deep Ocean Basin: Most deep water sites (>1000 m) yielded too few clasts for shape analysis. However, abundant clasts occur as lag deposits in and around the Polarstern Seamount in the northeastern Weddell Sea. The roundness-sphericity plot indicates a strong cluster of points at the more angular limit of Boulton's basal ice zone, and slightly more angular than the basal ice zone at Schirmacher Oasis (Fig. 3.54).

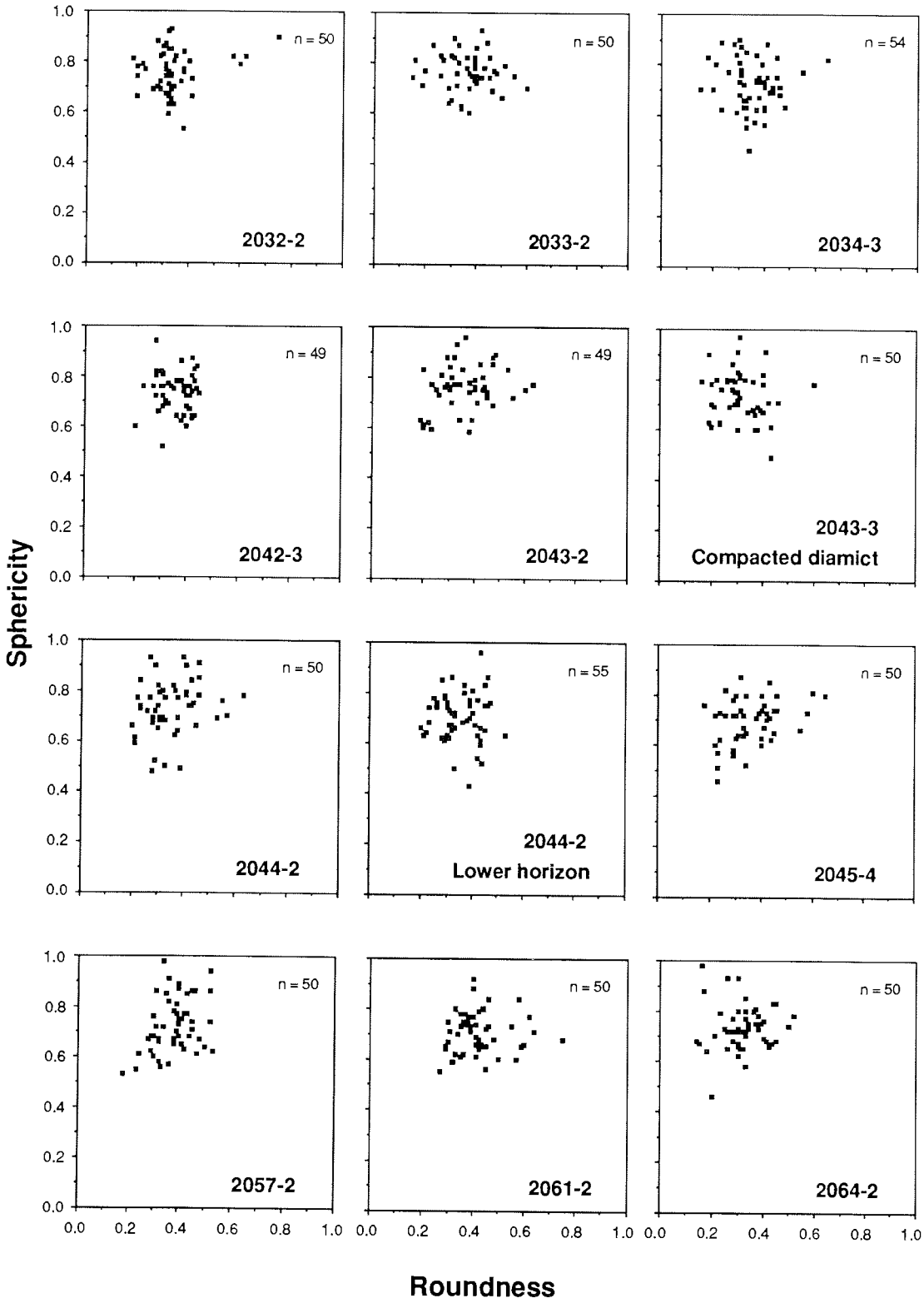
Shapes and surface features typical of glacial environments, resulting from processes at the ice-bedrock interface are common; wide variations in these different properties occur (Tab. 3.22).

Fig. 3.54: Roundness versus sphericity of clasts from glaciomarine sediments of the Weddell Sea and Lazarev Sea









Tab. 3.21: Lithology of clasts (a) in the NE Weddell Sea (continental shelf sites arranged from north to south); and (b) bordering the coast of the Dronning Maud Land (sites arranged from west to east).

a										
Locality	Station No.	Water Depth	No. of clasts	Diamict	Sedi-ments	Vol- canics	Granite	Schist	Gneiss	Meta-sedim.
Coats Land	1990-3	368	101	0	0	11	31	46	5	7
	1991-2	325	50	0	0	0	30	42	18	10
	1995-1	394	25	0	0	0	48	16	20	16
	1996-1	305	50	0	0	0	6	86	8	0
	1997-1&2	369	75	0	0	0	16	35	47	2
Riiser-Larsen Ice S.	2013-1	623	51	2	2	66	2	18	4	6
Kapp Norvegia	1989-1&2	443	64	1	1	90	1	1	4	1
	1989-3 upper L.		100	7	5	75	7	0	2	4
	1989-3 lower L.		102	1	2	92	1	0	2	2
"Polarstern Seamount"	2005-2	3806	52	0	2	0	14	25	45	14
	2007-2	4217	49	0	4	2	59	12	21	2

b											
Locality	Station No.	Water Depth	No. of clasts	Diamict	Sedi-ments	Meta- volc.	Gra- nite	Gra- nitoid	Schist	Gneiss	Meta-sedim.
Ekstroem Ice Shelf	2014-1	830	50	0	0	72	0	6	6	4	12
	2067-1	610	100	0	0	83	0	2	1	7	7
Unneruskollen	2015-4	125	50	12	0	8	4	2	12	0	62
	2066-1	430	50	0	8	78	0	4	0	4	6
Jelbert Ice Shelf	2016-1,2,3	428	96	1	8	35	7	12	2	6	31
	2017-2	508	49	0	0	26	0	31	0	4	39
	2018-2	148	45	0	0	34	2	13	0	4	47
Fimbul Ice Shelf	2019-2	161	50	0	2	58	0	2	14	0	24
	2020-1	2046	no gravel								
	2022-1	530	50	8	2	46	2	2	4	36	0
	2023-1	414	50	0	0	56	0	0	0	40	4
	2024-3	551	50	0	0	42	0	0	0	58	0
	2033-2	311	50	0	0	60	0	0	0	36	4
	2034-3	734	54	6	0	36	0	0	0	54	4
	2042-3	470	49	0	0	45	0	0	6	45	4
	2043-2	414	49	2	0	49	0	4	4	33	8
	2043-3	414	50	0	0	64	0	2	0	24	10
	2044-2	800	105	0	0	24	1	0	10	61	4
	2045-4	1392	50	0	2	20	0	0	8	60	10
	2060-1	551	117	0	0	62	0	0	0	36	2
	2061-2	876	50	0	2	80	0	0	18	0	0
	2064-2	1580	50	0	4	36	0	2	10	46	2
Ice rise	2025-1	638	72	0	0	48	0	0	0	46	6
Vigrid Ice Shelf	2031-1	450	49	0	0	20	0	0	0	80	0
	2032-2	191	50	0	8	24	0	0	10	58	0
Nivl Ice Shelf	2027-1	420	50	0	0	32	0	4	0	64	0
	2028-1	203	50	0	8	6	0	0	6	80	0
	2029-1	895	50	0	0	34	0	0	0	66	0
	2057-2	210	50	0	0	4	0	0	24	72	0
	2058-1	155	41	0	0	12	2	0	17	69	0
	2059-1	348	50	0	0	42	4	0	0	54	0

Tab. 3.22: Data concerning typical glacial shapes and surface features of clasts from sample sites in the eastern Weddell Sea, off the coast of Dronning Maud Land and from Schirmacher Oasis, 100 km inland from the Dronning Maud Land coast.

Location	Station No.		Facets	Striae	Bullet-nosed	Flatiron	Sample size	
			[%]	[%]	[%]	[%]		
Kapp Norvegia	1989-1	AGT	84	24	16	0	25	
Coats Land	1990-3	GKG	n/d	2	n/d	n/d	100	
	1991-2	MG	54	3	0	0	50	
	1995-2	GSL	n/d	2	1	0	100	
	1996-1	SL	n/d	10	0	2	50	
	1997-1	AGT	76	4	0	0	25	
	1997-2	MG	68	2	0	0	50	
"Polarstern Seamount"	2005-2	GKG	76	(all clasts with surface coating of MnO ₂)			50	
	2007-2	GKG	0	(some clasts with surface coating of MnO ₂)			50	
Riiser Larsen Ice Shelf	2013-1	GSN	80	38	14	8	50	
Ekstroem Ice Shelf	2014-1	GSN	96	28	28	4	50	
Unneruskollen	2015-4	GSL	76	4	10	0	50	
Jelbert Ice Shelf	2016-1& 2	AGT	95	18	29	0	46	
	2016-3	MG	90	10	10	0	50	
	2017-2	GKG	84	8	10	2	49	
	2018-2	AGT	86	4	20	8	45	
	2019-2	GKG	88	14	24	0	50	
Ice rise, Sanae	2021-1	AGT	87	3	18	3	32	
Fimbul Ice Shelf	2022-1	GSN	90	20	22	0	50	
	2023-1	GKG	68	26	2	0	50	
	2024-3	GKG	80	18	10	0	51	
	2025-1	GKG	86	25	16	5	72	
	2027-1	GSN	90	18	8	0	50	
Nivl Ice Shelf	2028-1	GKG	80	4	16	2	50	
	2029-1	MG	82	26	10	0	50	
	2031-1	GKG	84	22	10	2	49	
Ice rise, west of Nivl	2032-2	GKG	82	6 *	20	0	50	
Vigrid Ice Shelf	2033-2	AGT	96	28	6	2	50	
	2034-3	GKG	90	28	22	2	54	
	2042-3	GKG	90	24	12	2	49	
	2043-2	GKG	78	20	12	2	49	
	2043-3	SL #	80	"some"	6	0	50	
	2044-2	GKG upper L.	86	14	12	0	50	
	2044-2	GKG lower L.	92	16	12	0	55	
	2045-4	AGT	80	28	10	0	50	
	Nivl Ice Shelf	2057-2	GKG	90	4	20	2	50
		2058-1	GKG	n/d	7	n/d	n/d	41
2059-1		GKG	n/d	24	n/d	n/d	50	
Fimbul Ice Shelf	2060-1	MG	69	23	4	4	117	
	2061-2	GKG	96	52	30	2	50	
	2064-2	GKG	74	14	12	2	50	
Ekstroem Ice Shelf.	2067-1	GKG	n/d	42	n/d	n/d	100	
	Schirmacher Oasis	Basal ice	76	10	20	0	50	
		Sandy" basal till"	78	0	8	0	50	
Moraine ridge		68	0	12	0	50		

* = Bryozoa may obliterate many striae

= Compacted diamictite, beneath unconsolidated surface layer

n/d = no data

The aims of further investigations are as follows:

- (1) To determine the character of clasts in glaciomarine sediments in a variety of glaciological settings with a view to establishing transport and depositional mechanisms.
- (2) To define, from the lithology of the clasts, the "average" geology of source areas which are, except for nunataks, largely inundated by the East Antarctic ice sheet.
- (3) To consider whether there are variations in clast character with distance of transport from the continental shelf to the deep ocean basins.
- (4) To examine the influence of lithology on clast shape and surface texture.
- (5) To establish the relative importance of adjacent land ice as opposed to iceberg transport from more distal locations in the composition of the sediments.
- (6) To compare clast shape in different sedimentary facies, e.g. glaciomarine sediment and lodgement till on the continental shelf.

Benthic foraminiferal assemblages and stable isotopes

On the eastern continental margin of the Weddell Sea, the distribution and community structure of recent benthic foraminiferal assemblages is correlated with particulate organic matter flux, sediment conditions and the distribution of bottom water masses (Mackensen et al., 1990). As part of the marine geological activities, surface sediment samples were collected at 45 locations (Tab. 3.19) in the eastern Weddell Sea and the Lazarev Sea by either a large box corer (50 x 50 cm surface) or a multicorer (12 cores, each 6 cm Ø). Areas of particular interest were the two S-N profiles at longitudes 1°E and 6°E, which extended from the shelf to the deep-sea floor of the Lazarev Sea. Samples were taken from water depths of 250, 400, 600, 800, 1000, 1400, 1600, 1800, 2100, 2400, 2700, 3000, 3300, 3600, 3900, 4300 and 4400 m.

Undisturbed surface sediment samples were taken and preserved in Rose Bengal methanol in order to stain and analyse their benthic foraminiferal fauna:

- Large box corer: - defined area 412 cm², thickness 1.0-1.5 cm and
- subcore 12 cm Ø, intervals 0-1, 1-2, 2-3, 3-4, 4-5, 7-8,
10-11, 14-15 cm depth in core.
- Multicorer: - 5 cores, each 6 cm Ø, intervals 0-1, 1-2, 2-3, 3-4, 4-5,
7-8, 10-11, 14-15 cm depth in core.

At several locations organic fluff was observed and stained separately to investigate its influence on the community structure. Studies of the benthic foraminifera on this leg, in addition those from Leg ANT-VIII/6, will focus on the following main investigations:

- (1) The distribution of recent benthic foraminiferal assemblages and the environmental factors limiting their distribution off Dronning Maud Land in comparison with previous results from the eastern Weddell Sea;
- (2) Down-core changes in the benthic foraminiferal assemblages resulting from early diagenetic processes (i.e. examining the contrast between live and fossil assemblages);

- (3) Comparisons with long sediment cores to reconstruct palaeoenvironmental conditions, such as changes in the bottom water masses around the eastern boundary of the Weddell Gyre; and
- (4) Stable oxygen and carbon isotope composition of the bottom water and calcareous foraminiferal tests will be measured in order to estimate vital effects and palaeoproductivity, to infer bottom water characteristics and finally to derive a $\delta^{18}\text{O}$ stratigraphy.

Siliceous microorganisms

Additional surface samples were collected at 34 locations (Tab. 3.19) in the eastern Weddell and Lazarev Seas, also using the large box corer and the multicorer, with a view to improving the data-sets on the distribution and preservation of siliceous microfossils (diatoms, silicoflagellates, radiolaria) in the surface sediments of the Southern Ocean.

Undisturbed samples from the sediment surface were taken and preserved in methanol in order to analyse their siliceous microfossils:

Large box corer: - defined area 412 cm², thickness 0.3-0.5 cm and
Multicorer: - 2 cores, each 6 cm Ø, intervals 0-0.5 and 0.5-1.5 cm depth in core.

Using statistical methods, these data-sets will serve as reference data in palaeoceanographic reconstructions of the past.

References:

- Boulton, G. S. (1978). Boulder shapes and grain size distributions of debris as indicators of transport paths through a glacier and till genesis. - *Sedimentology*, 25: 773-799.
- Elverhøi, A. (1981). Evidence for a late Wisconsin glaciation of the Weddell Sea. - *Nature*, 293: 641-642.
- Gerdes, D. (1990). Antarctic trials of the multi-box corer, a new device for benthos sampling. - *Polar Record*, 26(156): 35-38.
- Krumbein, W. C. (1941). Measurement and geological significance of shape and roundness of sedimentary particles. - *J. Sedim. Petrol.*, 11: 64-72.
- Mackensen, A.; Grobe, H.; Kuhn, G.; Fütterer, D. K. (1990). Benthic foraminiferal assemblages from the eastern Weddell Sea between 68° and 73°S: Distribution, ecology and fossilization potential. *Mar. Micropaleontol.*, 16: 1-43.
- Maisey, G. H. (1980). Shallow seismic profiling on the south eastern Weddell Sea continental margin. - *Pap. Meet. Norwegian Petroleum Directorate*, Feb. 21-22.
- Oskierski, W. (1988). Verteilung und Herkunft glazial-mariner Gerölle am Antarktischen Kontinentalrand des östlichen Weddellmeeres. - *Ber. Polarforsch.*, 47: 1-167

6.1.2. Physical properties of the sediments and other geophysical investigations

S. Gerland, G. Kuhn, F. Gingele, R. Kringel, B. Maus (AWI)

Physical Properties of Seafloor Sediments

Physical properties of the sediments were measured on all the cores, that were taken during the cruise ANT-IX/3. Altogether, 25 cores with a length of more than one metre (total length: 153.81 m) were taken with a gravity corer and a piston corer. Shorter archive cores from a large box corer were also measured in the same manner as for the longer cores.

Magnetic susceptibility is a physical property connected to the sediment that contain magnetic minerals (magnetite etc.). By measuring the magnetic susceptibility it is possible to distinguish between those parts of cores with a high concentration of magnetic minerals and those with a low concentration. As an example, the magnetic susceptibility values of core PS 2003-2 are plotted versus core depth (Fig. 3.52). Over the whole depth the core shows susceptibility variations of different wave lengths. The maximum peak at a depth of about 1.70 m results from a dropstone. At a later date, an exact interpretation of the measurements will be possible by comparing all measured physical properties and geological parameters.

Another physical property which was measured during the cruise is electrical resistivity of the sediments. The electrical resistivity is connected directly with the porosity and water content of the sediment. After the data have been processed, they will be used for geological interpretation, together with other parameters.

The cores taken during the cruise ANT-IX/3 are characterised by different patterns of the physical properties, for example the low magnetic susceptibility on Maud Rise where biogenic components are dominant and high values on the continental shelf regions where the components are predominantly terrigenous.

Another interesting aspect, which will be undertaken after the data processing, is the comparison of the physical properties with the sediment echo-sounding data, measured by the Parasound System.

Sediment Echo-Sounding

Throughout the entire cruise of ANT-IX/3 sediment echo-soundings were registered on a routine basis with the sediment echo-sounding system Parasound. The data were stored in analogue form and digitally. It will be possible with the digital data to process these high resolution seismogrammes using same methods as in reflection seismics.

During the cruise, the echo-sounding profiles were used for pre-site surveys of geological sampling stations. These surveys provide additional data for the geological sampling programmes; they contain information concerning the nature of the ocean floor as well as about reworking of sediments by bottom currents, gravitational sediment transport or grounded ice processes.

At the sites where sediment cores were taken, registrations were made with different frequencies and pulse lengths. These data will be interesting for a

comparison of the echo-soundings with the physical and sedimentological parameters of the sediment cores.

Over the whole cruise, about 90 magnetic tapes were used for recording the digital data. When measurements are being made in continental shelf regions, it must be considered that the tape use is about three tapes per day, whereas over deep sea regions it is about one tape per day. The exact tape use depends on the registration parameters. Further information about the Parasound System are given in the Polarstern ANT-VIII/6 cruise report.

Gravity Measurements

During the Polarstern cruise ANT-IX/3 gravity measurements at sea were undertaken with a KSS 31 Marine Gravity Meter (Bodenseewerke), which is installed inside the ship. With this instrument it is possible to register relative gravity values. The data were stored in both analogue and digital form (1 Hz). In order to compare the measured data with other geophysical and geological investigations, special mention should be made of the measurements in the regions of Maud Rise and Polarstern Seamount. In addition, gravity measurements were also undertaken on land, using a Lacoste-Romberg Gravity Meter (G-744) with a feedback-system:

At the beginning and end of the cruise the connections between the Sea Gravity Meter and a point of known absolute gravity in Capetown, South Africa were measured. This is necessary for recalculating the relative gravity data and obtaining absolute values.

In the area of the Schirmacher Oasis on the Antarctic continent, near the Georg-Forster-Station, gravity values on rock were measured. The values can be used later for calibrating and comparing Sea- and Land Gravity Meter data.

6.2. Bathymetry and Seafloor Mapping by Hydrosweep J. Dreyer, H. Hinze, I. Munsch (AWI)

6.2.1. Depth and Navigation Data Evaluation, Processing and Seafloor Mapping

During the cruise bathymetric survey of the seafloor was carried out continuously by the swath sounding system Hydrosweep. Hydrosweep (= HYDROgraphic multibeam SWEEPing survey echosounder) is a sonar system with a 90° coverage angle of 59 single beams, which then covers a swath's width of about twice the water depth. Also advantageous is the cross-fan calibration method to compensate for sound velocity variations. The Hydrosweep system is introduced by Schreiber and Schenke (1989) for its scientific efforts on polar marine research. The integration of cross-profiles perpendicular to the ship's axis over the ship's track then gives the topography of the seafloor. The spatial coverage of depth data follows the ship's track which then yield a stripe of isobaths ("Streifenplot"), see Fig.3.55.

New profiles partially were arranged parallel to existing survey lines to cover an entire area for mapping. Sometimes the tracks were spreaded widely to yield a more rough estimation of the topography within a larger area. Often there are areas in shallow water as well as in deep sea regions, in which the results of the survey of topography and morphology are different from the

mapped features within the available bathymetric GEBCO charts. Mainly, this is caused by poor and widely spread original sounding data off Antarctica. The ship's tracks were not those of an ideal boxed survey. So only few examples can be given to describe detailed the seafloor topography of the recent leg.

The AWI Bathymetric Group developed software components to allow a pre-processing of the Hydrosweep data aboard. The Hydrosweep data are transmitted in real-time to a program for graphic display and interactive editing. All accepted data then are used to calculate a grid for isoline interpolation. The isobaths can be displayed on screen or can be plotted on a plotter within their true geographic orientation. The online-mapping is not only used for first documentation of measurements but also for online-navigation and for control of sounding data and navigation. In sciences it can be used for a pre-site survey e.g. for biological sampling (see Fig. 3.39) or geological coring.

About 120 online plots with 20 m isobath increment have been produced during this leg. On deep sea the scale varied between 1:250000 and 1:150000, close to the Antarctic continent and above the shallow shelf region the scaling 1:100000 was applied. Between the ports and 60°S more than 46000 km² were surveyed within the South Atlantic. The surveyed area south of 60°S covers about 28000 km² in the deep sea area and 3600 km² upon the continental shelf area.

The compilation of large-scaled bathymetric charts requires high accuracy for both, the sound velocity and the ship's position. The latter depend on the available navigation mode. If the coverage of Global Positioning System (GPS) satellites results in a poor dilution of precision or if no GPS or NNSS-Transit satellites are visible at all, navigation will be done by dead-reckoning. Precise ship position data are necessary for the post-processing of Hydrosweep data aboard. Therefore, correction of all navigation data was done on board. The ship's INDAS data were analyzed, eg. for outlayers and data gaps. The GPS satellite coverage allowed a quite continuously tracking during the cruise. This gave accuracies of better than 100 m for this period as long as no offset appears. The ship's position then was corrected for position drift offsets. The Hydrosweep data and an extracted set of INDAS navigation data then were corrected for precise positioning. However, occasionally some periods with gross and non-correctable data appeared, and data of these periods can not be used for precise post-processing.

The sound velocity is derived within the Hydrosweep system by its self-calibrating mode in sufficient quality. However, the operator has to check the results, because rough topography and severe ice conditions may introduce systematic errors to the sound velocity estimation. Thus, the Hydrosweep results were compared to sound velocity values from actual CTD measurements (both sensors) and tabularized data. Sometimes updates had to be done and results of CTD profiles were used for reduction.

Isoline maps and three-dimensional perspective views of the seafloor topography and selected features are necessary to observe and to decipher interrelationships e.g. in marine geology and geophysics, sea bottom life or oceanographic currents. To produce previous maps and perspectives aboard

the vessel, a digital terrain model (DTM) of the sea bottom was determined and used for hardcopy outputs (printer, plotter). Also initial attempts were made to animate a "DTM fly-by". This was done aboard on an improvised video amateur level. The movies recorded showed the animation of a horizontal rotation ("fly around") and an increase of view angle ("fly across") for DTMs. Even at this level of DTM animation it was evident, how steady changes in the view of a DTM might increase the knowledge of interrelationships.

6.2.2. Sea Floor Topography in Selected Areas (Examples)

Various results of tectonic effects, erosion and sedimentation are observed within the region between the SW Weddell Sea off Coats Land and Astrid Ridge off Dronning Maud Land. Features of regional extend as well as features of local importance like ice plough marks could be studied. Thus correlations between seafloor topography and geophysics and geology and between seafloor morphology and sea bottom life can be studied.

6.2.2.1. Maud Rise

The Maud Rise is a marginal plateau in the eastern Weddell Sea. In general it can be characterized as a block-shaped feature of about 400 by 280 km² in extension with its longer sides striking NW-SE. The slopes and scarps are interspersed by sections of minor slopes or larded with pinnacles (which are any high tower or spire-shaped pillar of rock, or coral, alone or cresting a summit, IHO 1989). Details on Maud Rise topography and geology are presented by Bohrmann et al. (1991).

Up today, the top of the rise was not reached by bathymetric survey. However, based upon a recent map (Bohrmann et al. 1991), Polarstern's track were scheduled to survey the central part. The N-S going Hydrosweep profile (Fig.3.55) was crossing the approximate top of Maud Rise (Jan 11, 1991). Thus, a relatively flat guyot-type feature was surveyed and later cored (see 6.1.1.).

The geographic region also includes an extremity limb of about 300 km length south of Maud Rise trending N-S at about between 66°30'S,3°E and 68°S,4°E. The limb was reached by one Hydrosweep profile.

6.2.2.2. Explora Escarpment

The existing Explora Escarpment survey box was prolonged in its NE part. The previous ANTVIII/5 survey box consisted in a strip about 10 nm wide and following the escarpment for about 350 km. It shows a nearly linear about 1500 m steep slope. The northern part of the escarpment seems to be broken off by tectonic events and thus was surveyed by chance by three parallel Hydrosweep-tracks, see Fig.3.56. The prolonged survey box of about 46 km length and 20 km wideness showed chaotic fracturing within this area. Geophysical research is scheduled for the surveyed area in 1991/92 to study tectonics and geodynamics of the Weddell Sea region.

Fig. 3.55: Online "Streifenplot": strip of isobaths following the ship's track. Informations plotted are: track plot and time marks. The isobath increment is 20 m. Location: Central N-S section of Maud Rise

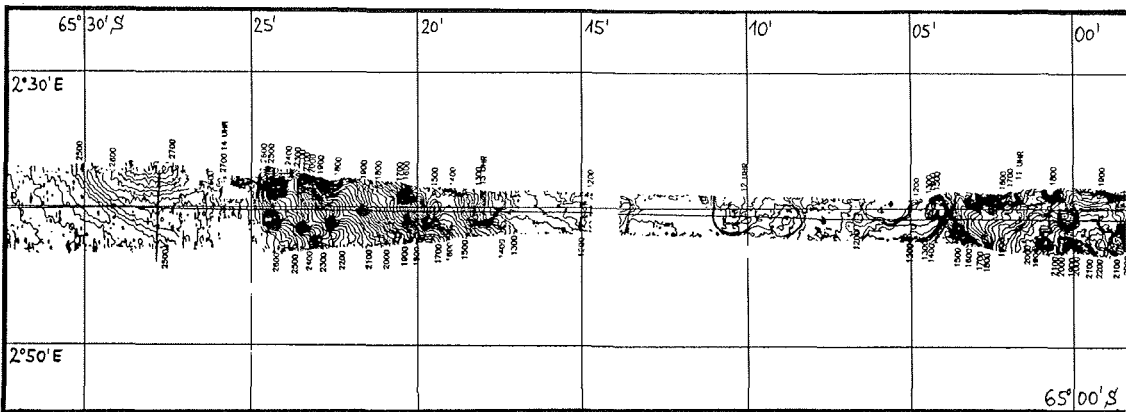
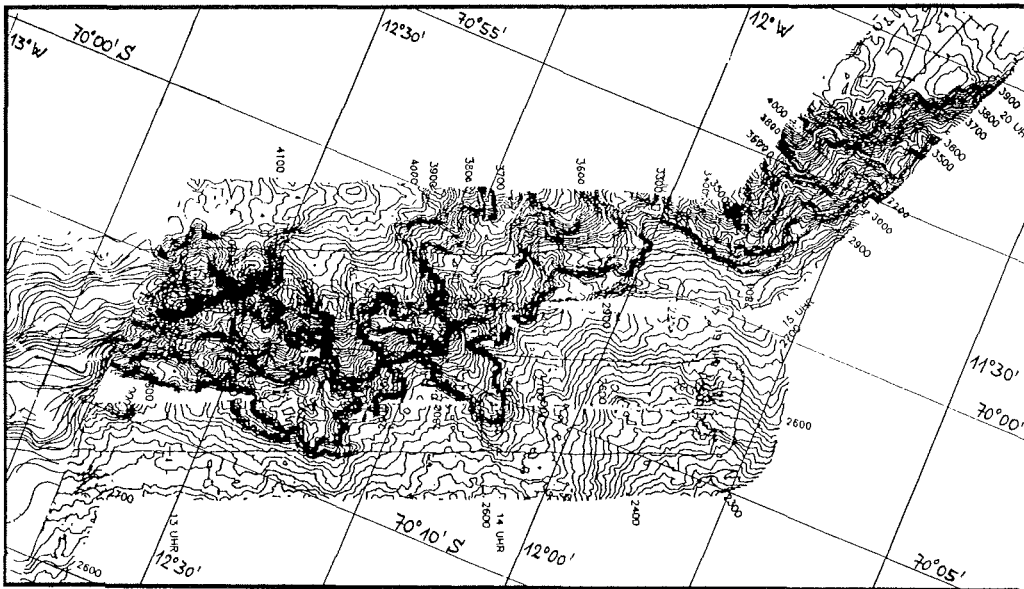


Fig. 3.56: Explora Escarpment: online isobath plot and previously (during ANT VIII/5) determined contours (northeastern part of DTM). Online plot (Feb. 14, 1991) with 20 m and scabrous DTM result with 100 m contouring interval.

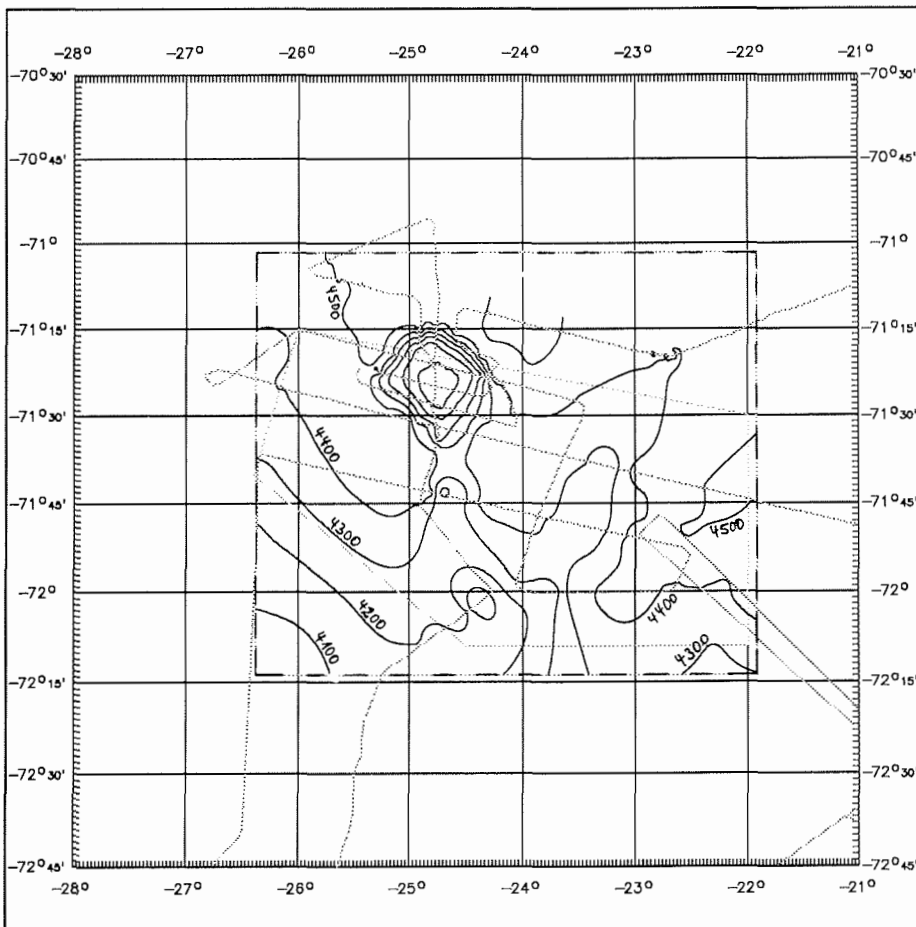


6.2.2.3. Schwerehoch Knoll

A seahill or knoll was found to be associated with a positive gravity anomaly high within the NE Weddell Sea by ANT VIII/5. Fig.3.57 gives an idea of this area mapped by Hydrosweep, for the compilation some soundings from a nautical chart were added. The knoll has a gentle smooth surface for a depth range of 2500 to 1500 meter. Its upper layer predominantly consists of foraminifera sands.

Following international definitions, a knoll is a relatively small isolated elevation of a rounded shape (IHO 1989) and is rising more than 500 meters and less than 1000 meters and is of limited extent across the summit (DMA 1990). Thus, the surveyed topographic features within this area are not seamounts or rises but knolls.

Fig. 3.57: "Schwerehoch" knoll: recently calculated isobaths from "Polarstern" and other data. Dotted lines are Polarstern track lines of expeditions ANT viii/5 and ANT ix/3.



6.2.2.4. Continental Slopes and Shallow Waters

Various results of tectonic effects, erosion and sedimentation are observed within the coastal region between the SW Weddell Sea and Astrid Ridge. Also local features like ice plough marks could be studied and correlations between seafloor morphology and sea bottom life. Many morphological features and structures are arranged parallel to tectonic fractures, e.g. scarps, terraces, aligned seahills, slopes, erosion gullies.

Off Fimbulisen (Fimbul Ice Shelf), the continental slope, erosion gullies and a new canyon were mapped at the 1°E longitudinal section. Fig.3.58 gives an impression of the canyon's southern part. This canyon is not identical with the Sanae Canyon, which is located between 4° and 1°W. The recently found canyon shows all the characteristics of a canyon, which are a relatively narrow, deep depression with steep sides, the bottom of which has a continuous slope, and developed on the continental slope (IHO 1989). It is collecting bottom waters between about 0°30'E and 2°00'E. The main canyon originates at about 69°42'S, 1°30'E and strikes SE-NW. Probably its design is linked to the eastern graben fault of the Jutulstraumen system. Minor distributary channels are clearly visible at the continental slope in depths between 600 and 2000 mbsl by the survey. At 69°29'S, 1°03'E the canyon strikes S-N. The canyon has steep margins of 500 to 700 m.

At the 6°E-section scarps are within a depth region of the continental slope of about 1700 to 2600 m. The terrain has two clearly separable terraces with two scarps of about 120 m each (Fig.3.59). The eastern margin of the feature is vaulted, a western margin was not covered. The curvating of the scarps indicates a rounded feature, it then may have a diameter of about 22 km and its center at 69°07'S, 5°58'E. Small pinnacles close to the presumable center of the caldera-like feature may indicate a volcanic origin. Because only the eastern part of the feature could be mapped, it is not clear whether the scarps indicate a graben or a caldera. Note that in the central region of Astrid Ridge (at about 67°48'S, 11°30'E, depth ranging from 1600 to 2000 m) a similar feature might exist (ANT VIII/6) which could be a caldera or a graben.

6.2.2.5. Ice Plough Marks and Sea Bottom Life

Passing the SW ice front of Ekströmsen, first icebergs plough tracks were visible at the Hydrosweep bottom map (BOMA) online-display. Icebergs scores of the ocean floor since that during all our journey close to the Antarctic continent were observed (e.g. see Fig.3.60). Mainly the plough marks are found in areas of stony (morainic?) material as later seen by video camera in water depths between 200 and 400 mbsl. The width of their track varies between 20 and 200 m, and parallel plough scores were visible even by 500 m wide Hydrosweep swath profiles. Parallel plough tracks seemed to be correlated for the observer, because at least in some distinguished furrows they show simultaneous depth variations (tide or ocean gauge?) along the track and also perpendicular to the asymmetric cross-profiles.

In general the ploughs strike dominantly parallel to the recent ice front or to a generalized ice front line. The furrows can be followed for up to several kilometers, and in several places some generations of crossing plough are observed. Several times the scour berm is clearly distinguishable by the

Fig. 3.58: Canyon off central Filbulisen: online isobath plot (Feb. 18/19, 1991) joined by hand-drawn contours of previous and following Hydro-sweep surveys. Online plot with 20 m and other contours with 100 m isoline interval.

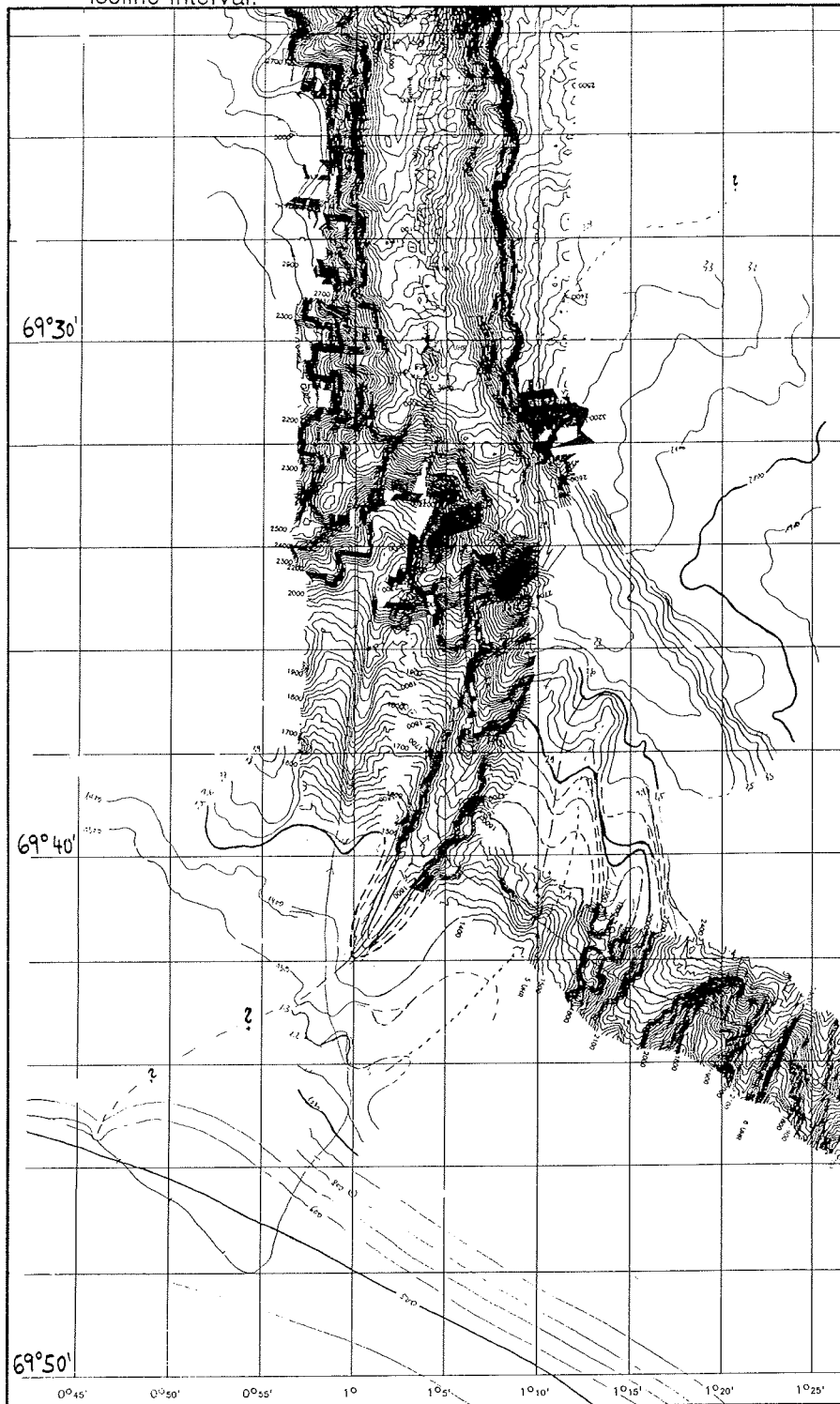
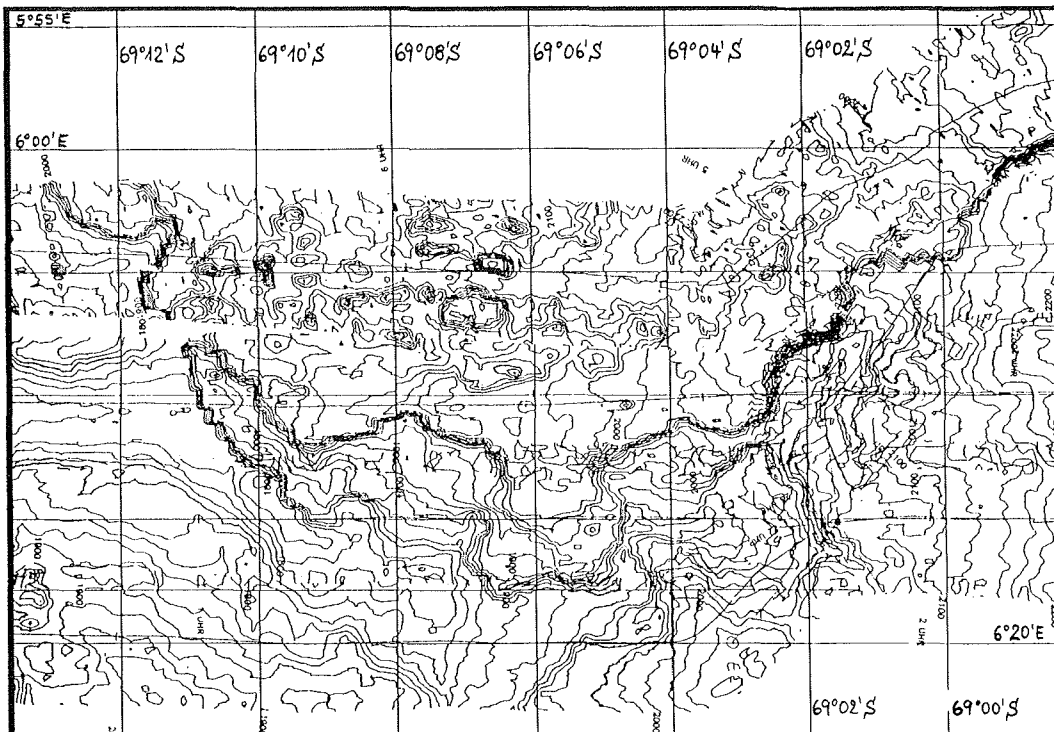


Fig. 3.59: Caldera-like feature off eastern Fimbulisen: Online plots of all tracks (Feb. 1991), 20 m contour interval.



asymetry of the features cross profile. Because the larger scour berm mainly is located towards the ice front line side, it suggests a drift of solely and isolated icebergs parallel to the ice front, and thus within the coastal current, and slightly towards the ice front or coast line.

This also suggests evidence for a coastal current close to the ice front or a balanced current regime of sub-iceshelf upwelling of fresh water and the coastal current system. Swithinbank (1957), as a result of examination of the morphology of the ice shelves near Maudheim, Quarisen, concluded that their seaward limits were dependent on the existence of shoals which could ground the ice. Thus, analysis of present-day sea depths could establish the probable seaward limits of an ice shelf under conditions of more intensive glacerization (Thomas 1973).

Off Ekströmisen (Ekström Ice Shelf) two different scores are found at 70°33'S, 9°20'W. Iceberg plough marks are running in 62° direction (SSW-NNE). Perpendicular various scores in -28° (332°) direction (SSE-NNW) are found. The latter direction corresponds with the recent ice shelf motion of Ekströmisen, which is extrapolated from flow lines at this site for about -31° (Hinze 1990). Fig.3.61 places the site below an ice shelf part (situation of November 1975, IfAG 1989) and indicates the observed ice plough marks and the modelled ice shelf flow line. The ice shelf portion off the actual ice front

obviously was existing until 1985 and gone before March 1986. However, the ice shelf plough marks are not very recent. Ekströmsisen today has an ice thickness of about 200 m at its front part but the scores can be found in 420 mbsl today. This phenomena requires hypothesis of thicker ice shelves and/or sea level change, both linked to glacial climate conditions.

The influence of tsunamis and the effects of sea currents on ice tongues is discussed by Thomas (1973) and generally can be transferred onto the Stancomb-Will Ice Stream (N of Halley Station) and Trolltunga (E of Sanae station). However, regular tidal effects should not be excluded since they can vary locally and their amount is not studied in situ. Up to today, no gauge recording system was implemented at the eastern Weddell Sea coast. Ice shelves, which were broken off, probably could be suitable for the study of sea life behaviour. Areas within the Weddell sea region are the western Ronne Ice Shelf, the Filchner-Schelfeis, the two ice tongues and the Ekströmsisen part mentioned above. The re-settlement of sea bottom life in hazarded areas probably could help in absolute time scaling of the hazards relicts, e.g. plough marks and berms.

Iceberg ploughing impinges on bottom life. This clearly was confirmed by the video camera fixed at the multicorer (see 5.1.3.). Hydrosweep mapping of shallow waters may help for pre-site survey of intensive biological observations and sampling, e.g. see also Hain and Hinze (see 5.1.1.), which was carried out for some locations. However, sometimes no mapping was possible because the direction of the Hydrosweep swath was the same than the one of the vessels motion (drifting in the sea ice).

Occasionally notes on few sites:

Some tracks and sampling was carried out north of Halley Station. The surveys were off the Brunt Ice Shelf with ice motion upstream of Halley Station between 300 and 500 m/a and off the Stancomb-Wills Ice Stream with velocities of 1300 to 1500 m/a (Thomas 1973). Plough marks of various orientation are found in depths between 300 and 400 mbsl.

Site 173, AGT 11: Distinct location at the presumed ending of a fjord, covered by the NE part of Fimbulisen. Depth sampled by AGT ranged between 228 and 225 mbsl.

Site 207, AGT 17: Relatively flat ground at shallow water (208 to 210 mbsl), sampling location is probably located at a tiny (morphologically ?) ridge, which strikes from NW to the deeper area in SE. The ridge rises about 5 meters above the surrounding bottom, which falls towards the SE, suggesting fjordic conditions below the NE shelf ice tip of Nivlisen, where the "Thuleland" port is located. However, no depth data south of site 207 are known for further interpolations.

6.2.3. Future Research and Development Work

The "digital terrain model fly-by" animation shall be continued at AWI with direct linkage of the host computer and a digital data video recorder. The animated three-dimensional perspective fly-by across and around the sea bottom and additional informations will allow us to observe and to decipher interrelationships in marine geology and geophysics or sea bottom life (fauna

et flora) or oceanographic currents and will improve our knowledge of the seafloor.

The seafloor and the sea bottom topography of areas covered by sea ice, shelf ice, glaciers and ice tongues are not that easy to get. Seismic shot data and oversnow traverses e.g. give sporadic depth data. Within the glaciological community, the use of submersibles was discussed within the Filcher-Ronne Ice Shelf (FRIS) Programme Workshops (Bremerhaven 1989, Cambridge 1990). E.g. bathymetric and oceanographic data could be recorded and samples could be taken, from the water as well as from the sea bottom.

Manned submarines will not be suitable for the time being below the ice shelves. Unmanned submersibles could serve in different ways. Programm and feasibility studies in UK covered two different types of launchers, DOGGIEs (Deep Ocean Geological and Geophysical Investigation Equipment) and DOLPHINs (Deep Ocean Long Path Hydrographic Investigation Nautil). One type of sensors could be used for multiple data recording and in situ sampling activities. Thus, its field of operation is limited to a certain distance (e.g. within the Weddell Sea or below the FRIS). Longer ranges could be realized with the other type of sensor, but thus probably the data types recorded during the profiling will be limited and sampling shall not be possible.

Also the bedrock topography will be included to describe and map the seafloor and its ice-covered areas as well as the dried heights of Antarctica. Thus all data on unbedded and bedrock surface are necessary for mapping the submarine and subglacial topography of Antarctica.

References:

- IHO 1989: Standardization of Undersea Feature Names. International Hydrographic Organization, Intergovernmental Oceanographic Commission, 2nd edition, BP-0006, July 1989.
- Hinze, H. (1990). Zum Einsatz von Satelliten-Positionierungsverfahren für glaziologische Aufgaben in der Antarktis. Wiss.Arb d.Fachr.Verm.wes. d.Univ.Hannover Nr.163, 1990.
- Bohrmann,G.; Hinze,H.; Spiess, ; Kuhn,T. (1991). Reflector "Pc" - a prominent feature in the Maud Rise sediment sequence (Eastern Weddell Sea): occurrence, regional distribution and implication to silicia diagenesis. Submitted to: Marine Geology.
- Schreiber,R.; Schenke,H.W. (1989). Atlas Hydrosweep: Efficient Hydrographic Surveying of EEZ with New Multibeam Echosounder Technology for Shallow and Deep Water. Proc. EEZ Resources: Technology Accessment Conference, Jan 22-26, 1989, Honolulu, p.3-16..3-30, 1989.
- Thomas, R.H. (1973). The dynamics of the Brunt Ice Shelf, Coats Land, Antarctica. BAS Scient.Report No.79, 1973.
- Swithinbank, C. (1957). Glaciology I: The morphology of the ice shelves of western Dronning Maud Land. Norw.-Brit.-Swed. Antarct.Exped., Scient.Results, 3A, 1-37.

Fig. 3.60: Ice plough off Quarisen at $70^{\circ}52'S, 11^{\circ}03'W$. Post-mission streifenplot with 2 m contour interval and perspective view. Vessel is going SW, looking on both is from north (top = S)

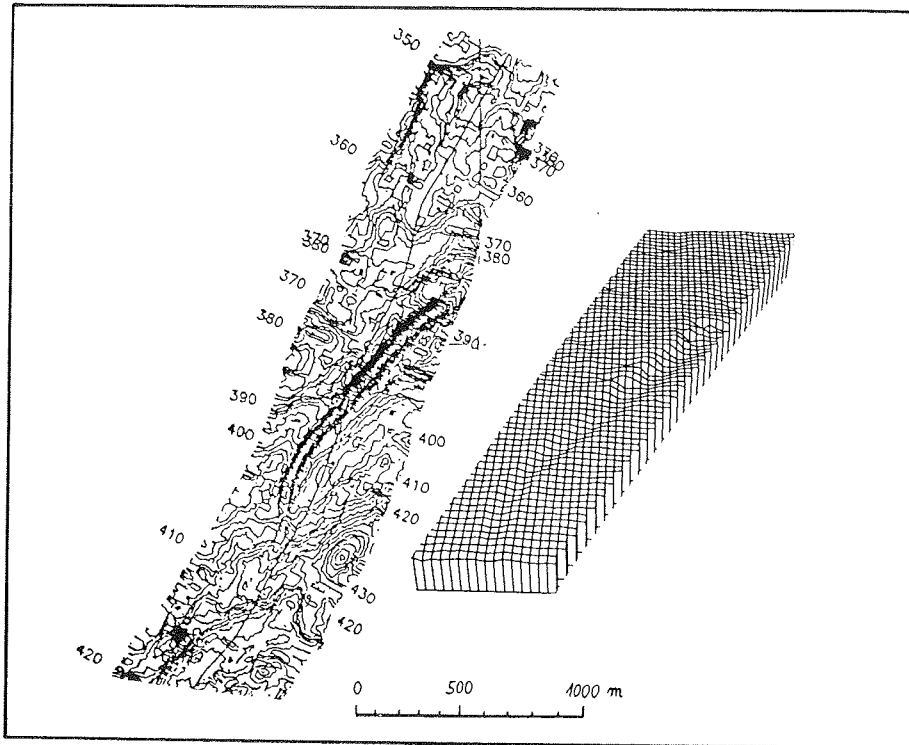


Fig. 3.61: Iceberg and ice shelf ploughs off Ekströmisen. Landsat mosaic and flow lines from: Hinze 1990.



6.3. Geochemistry

M. Rutgers v. d. Loeff, H. Hölzen, A. Michel (AWI)

6.3.1. Uranium-series radionuclides in the water column.

Purpose of the studies

Sea water contains Uranium in constant and well-known amounts. Many of the decay products of Uranium are radioactive isotopes themselves of highly particle-reactive elements like lead, Thorium, Protactinium. Consequently, they are removed from the water column by settling particles. The resulting disequilibria in the decay series are therefore useful indicators of particle fluxes in the water column. Moreover, they give us information on the history of specific water masses and of ventilation of ocean basins.

The distributions of the shorter lived isotopes ^{234}Th (24 days half-life) and ^{210}Po (138 days half-life) can be directly related to recent particle fluxes and to the development stage of a plankton bloom. They were studied in coordination with the planktologists. During the ANT VIII/3 expedition we observed a strong southward increase of the long-lived isotopes ^{230}Th and ^{231}Pa on a transect across the southern polar front. This was attributed to upwelling of Lower Circumpolar Deep Water, which forms the main source of water for the ventilation of the Weddell Sea. This isotope signal can be used as a tracer for ventilation and vertical particle flux in the Weddell Sea. To this purpose we needed profiles of ^{230}Th in the Weddell Sea proper, covering the water masses at various stages of their residence in the Weddell Basin.

Sampling and methods

For the analysis of the short-lived isotopes we sampled the water column with 270-Liter Gerard bottles. The analysis of the long-lived isotopes requires larger volumes. Around 1 m³ of water was filtered in-situ with autonomous filtration units. The particles are retained on a large filter; the dissolved radionuclides are absorbed on MnO₂-coated cartridges. Each pump was deployed together with a Gerard bottle for an accurate calibration of the efficiency of these absorbers. All analytical separations and purifications were performed on board; Since the counting will only be performed after return at AWI, no results became available during the expedition.

The various drifting stations gave ample opportunity to sample Shelf waters and the Coastal Current. (Sta. 125, 126, 127, 128, 135, 163 with pumps; Sta. 189,190,192 only with Gerard bottles for short-lived nuclides.)

Our inability to reach the South and Southwest precluded the measurement of the isotopic composition of newly formed bottom waters. However, apart from Ice Shelf Water, the major water masses of the Weddell Sea could be sampled on the transects to the Polarstern Seamount (Sta. 141 and 153) and to Maud Rise (Sta. 196,199,200 and 202). At Sta. 200 we reached a lobe of Warm Deep Water with a potential temperature of 1.2°C. This high temperature indicates a recent origin in the Circumpolar Deep Water, and makes this station an important link with the data obtained during ANT VIII/3 in the Antarctic Circumpolar Current. Sta. 227, on the return to Cape Town, was scheduled in the centre of the eastern Weddell Gyre to study the isotopic signature of water that has been for a long time in the Gyre. The low oxygen and high pCO₂ in the warm deep water at this station indicated in-situ

mineralisation. This station was the only one that yielded us samples of Weddell Sea Bottom Water (potential temperature: -0.85°C).

6.3.2. The carbonate system

6.3.2.1. Carbon Dioxide and Oxygen

Circumpolar Deep Water, and its Weddell Sea descendant Warm Deep Water, is enriched in total carbonate and over-saturated in carbon dioxide. The upwelling of CDW could lead to CO_2 emanation to the atmosphere. On the other hand, primary production consumes CO_2 and carries it down to deep waters. The balance between upwelling and export production determines whether the Weddell Gyre is a source or a sink for atmospheric CO_2 .

Oxygen was determined with an automated Winkler titration. Measurements of the carbonate system had not been scheduled, and a pH meter was the only equipment available. We have calculated the carbonate system from measurements of pH and alkalinity, which is not the most precise way possible, but gave very useful results.

6.3.2.2. Water column.

In agreement with earlier studies with more accurate equipment we did not observe any differences in alkalinity (normalized to 35.00. salinity) in the water column, and used the literature value of $A_{\text{T}}=2.384 \text{ mM}_w$.

The behaviour of the CO_2 system is best illustrated in a plot of the components CO_2 partial pressure ($p\text{CO}_2$), Carbonate ion (CO_3^{2-}), and total CO_2 (Ct_T) against oxygen concentration. (Fig. 3.62) $p\text{CO}_2$ reaches a maximum of around 600ppm in the Warm Deep Water, well correlated with a minimum in oxygen of 200 μM at a potential temperature of 1.2 C. This water forms a potential source for CO_2 to the atmosphere ($p\text{CO}_2$ approaching 350 ppm). There is a gradual transition towards equilibrium with the atmosphere of both oxygen (341 μM at 2.5°C) and CO_2 in the surface water. The intense plankton bloom in the coastal current stands out in the figures with an over-saturation of oxygen and an under-saturation of CO_2 in a DCt/DO_2 molar ratio of 2.5. The expected DCt/DO_2 ratio for primary production in a closed system is only about 0.7. (As changes in alkalinity were not observed, calcite production must have been negligible). The low ratio observed must result from the time needed for re-equilibration with the atmosphere which is more than 10 times slower for CO_2 than for O_2 . Thus, most of the O_2 production has been lost to the atmosphere, whereas part of the CO_2 depletion may persist until the winter ice is formed.

The depletion of Ct in the shelf waters during the bloom reached a maximum at Sta. 173 of about 60 μM over a depth range of 150m (Fig. 3.63), corresponding to a nitrate depletion of 9 μM and an integrated carbon deficit in the order of 100g C/m². When comparing this high number with the standing stock of 15g C/m² as derived from Chl *a* data (4.2.3.5), it should be realized that the depletion in Ct has been built up gradually during the summer, due to the slow exchange of CO_2 with the atmosphere. These predictions can be verified and quantified as nitrate and ^{234}Th data become available.

Fig.3.62: Total carbonate (normalized to a salinity of 35%) against oxygen concentration for all samples of the Maud Rise transects and Coastal Current. The high gradient of DC_{T_N}/DO_2 shows that much of the oxygen produced has been lost to the atmosphere, whereas the uptake of CO_2 from the atmosphere cannot keep up with its consumption in the surface water.

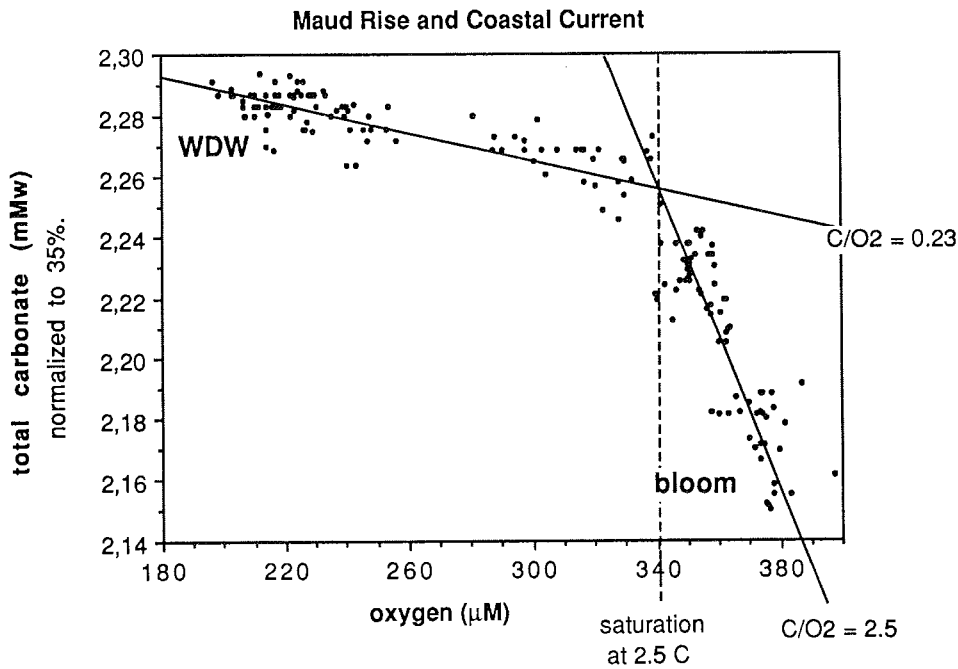
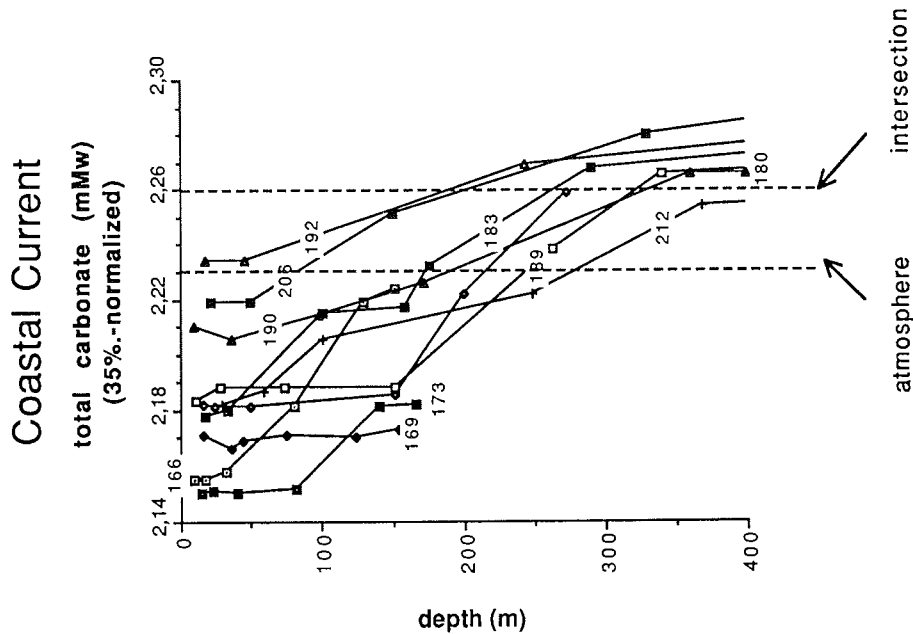


Fig. 3.63: Profiles of total carbonate (C_{T_N}) in the Coastal Current. The vertical broken lines represent equilibrium with the atmosphere (left) and the intersection point in Fig.3.62 (right)

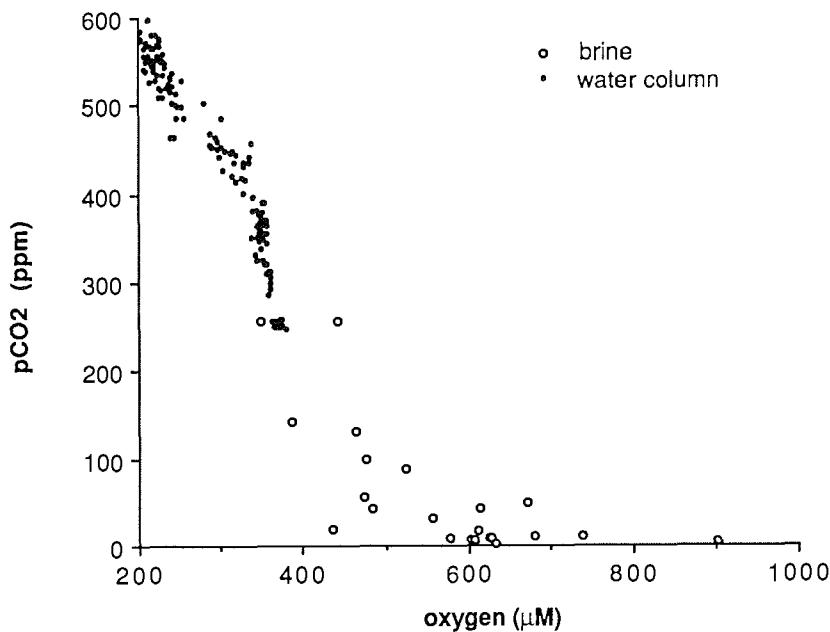


6.3.2.3. CO₂ and oxygen in ice.

It is to be expected that gas contents in brines are far from equilibrium with the atmosphere. First, when seawater freezes, the dissolved gases become strongly over-saturated. Gas bubbles form, and part of the gases escape. Second, the primary production will rapidly change the gas content in the enclosed channels in the ice.

The "ice team" supplied us with brine by drilling wells in the ice to various depths. The wells filled rapidly with brine, and could be sampled with minimum atmospheric contamination. The brines were always strongly super-saturated in oxygen. We observed gas bubbling up in fresh ice cracks, and presume they consisted mainly of oxygen. The relationship with pCO₂ (Fig.3.64) shows that the main reason was not the physical freezing, but rather primary production. CO₂ becomes depleted down to 0.3 μM, and can very well be growth limiting. (Nutrient data are not yet available on-board). In this respect the sea-ice environment resembles semi-enclosed systems like water sheets on rock or on a sand flat. Under these circumstances phytoplankton cannot afford to isotopically discriminate the available inorganic carbon, a result that supports the explanation given by Fischer for his δ¹³C values of ice algae. Although CO₂ gets strongly depleted by the high pH (up to pH 10), inorganic carbonate remains available (total carbonate did not fall below 1mM), and the brines are strongly supersaturated with respect to calcite.

Fig. 3.64: Partial pressure of CO₂ against oxygen concentration in samples from the water column (filled circles) and in brines (open circles). pCO₂ in the atmosphere is about 350 ppm

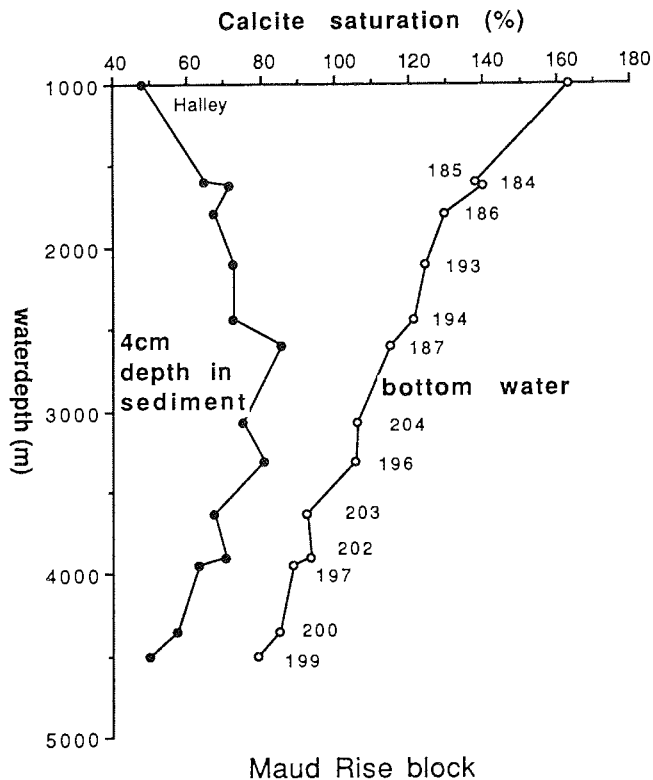


6.3.2.4. Calcite saturation and mineralization in the sediment

The uptake of CO_2 in the coastal surface water leads here to an over-saturation of calcite of over 280%, thus favouring organisms that produce calcite shells. The degree of saturation of the deep water in the Weddell Sea with respect to calcite can be derived from data available in the literature. Our measurements of pH in deep waters agree with these literature data, and resulted for the Lasarev Sea in a depth of 3200m below which calcite is undersaturated (Fig. 3.65).

The actual dissolution of calcite at the seafloor is determined both by the degree of under-saturation of the bottom water and by the release of CO_2 resulting from mineralization of organic material in the upper few cm of the sediment. From pH and oxygen measurements in cores from the transects to Maud Rise, we estimated the degree of calcite saturation in the pore water. It turns out that slope sediments are strongly undersaturated with respect to calcite at a depth of a few cm in the sediment, as a result of the high input and mineralization rate of organic material. According to these preliminary data the calcite preservation should be best at a water depth around 3000m. This optimum is not related to differences between water masses, but results entirely from the opposite depth-dependences of the input of organic matter and of calcite solubility.

Fig. 3.65: Calcite saturation in bottom water and at 4 cm depth in the pore water on the transect south of Maud Rise



FAHRTABSCHNITT ANT IX/4**Kapstadt - Bremerhaven - 30.03.91 - 13.05.90****1. ZUSAMMENFASSUNG UND FAHRTVERLAUF**
H.-W. HUBBERTEN (AWI)

Im Mittelpunkt der Expedition ANT-IX/4 stand die marin-geologische Probenahme im Bereich der antarktischen und subantarktischen ozeanographischen Frontensysteme zwischen 35° und 55° südlicher Breite. Ziel dieser Beprobung war es, Sedimentmaterial zu gewinnen, mit dessen Untersuchung Informationen zur paläozeanographischen Entwicklung des Gebietes südlich und nördlich der Polarfrontzone erhalten werden können. In diesem Gebiet treffen die antarktischen Kaltwassermassen mit den nördlichen subantarktischen und subtropischen Warmwassermassen zusammen. In mittleren und grösseren Tiefen werden die Wassermassen überwiegend vom nordatlantischen Tiefenwasser (NADW), dem Circumpolaren Tiefenwasser (CDW) und dem Antarktischen Bodenwasser (AABW) gebildet. Diese Wassermassen sowie deren Veränderungen in Lage und Bedeutung während der quartären Glazial-Interglazialzyklen, sind eng verknüpft mit Parametern wie Produktivität, Wärmetransport, atmosphärische Zirkulation und klimatischen Veränderungen und steuern in ihrer Wechselwirkung den CO₂-Haushalt im System Ozean-Atmosphäre.

Die durchgeführten Arbeiten stehen in einem engen Zusammenhang mit dem Sonderforschungsbereich 261 des Alfred-Wegener-Instituts für Polar- und Meeresforschung und der Universität Bremen. Unter dem Thema: "Der Südatlantik im Spätquartär: Rekonstruktion von Stoffhaushalt und Stromsystemen", lassen sich die wissenschaftlichen Zielsetzungen wie folgt zusammenfassen:

- die Rekonstruktion der Temperaturen des Oberflächenwassers sowie der Zirkulation der Oberflächen-Stromsysteme, besonders die Nord-Süd-Verschiebung der hydrographischen Frontensysteme und der Meereisgrenze;
- die Rekonstruktion charakteristischer Wassermassenparameter der Zwischen- und Bodenwassermassen sowie deren Ausbreitung und Zirkulationsmuster, insbesondere die Verteilung und Mächtigkeit des Antarktischen Bodenwassers (AABW).

Nach vorliegenden Ergebnissen der Expedition ANT-VIII/3, bei der im November 1989 auf einem ähnlichen Kurs das Profil Kapstadt - Bouvet Island beprobt wurde, wurden die geologischen Stationen für ANT-IX/4 so ausgewählt, dass das damals gewonnene Material ergänzt wurde. Dabei konzentrierten sich die Stationsarbeiten auf submarine morphologische Erhebungen wie den Agulhas Rücken, den Meteor Rücken und den Mittelatlantischen Rücken (Fig. 4.1 bis 4.4). Grössere Lücken, die während ANT-VIII/3 aus Wettergründen und wegen gerätetechnischer Probleme entstanden waren, wurden gefüllt. Der Gewinnung von Porzellanit, einem verfestigten Gestein aus umkristallisiertem biogenen Opal, galt das Interesse nordöstlich Bouvet Island. Auf einem Profil mit 10 Stationen wurden die Oberflächensedimente nördlich und südwestlich von Bouvet Island in unterschiedlichen Wassertiefen beprobt. Ein weitgestecktes Süd-Nord-Profil, ausgehend vom Mittelatlantischen-Rücken bis hin zu 35°N, soll zusätzliche Informationen über die hydrographischen Frontensysteme liefern (Fig.4.4).

Fig.4.1: Fahrtroute von FS "Polarstern" während des Fahrtabschnittes ANT-IX/4. (Cruise track of RV "Polarstern" during Leg ANT-IX/4)

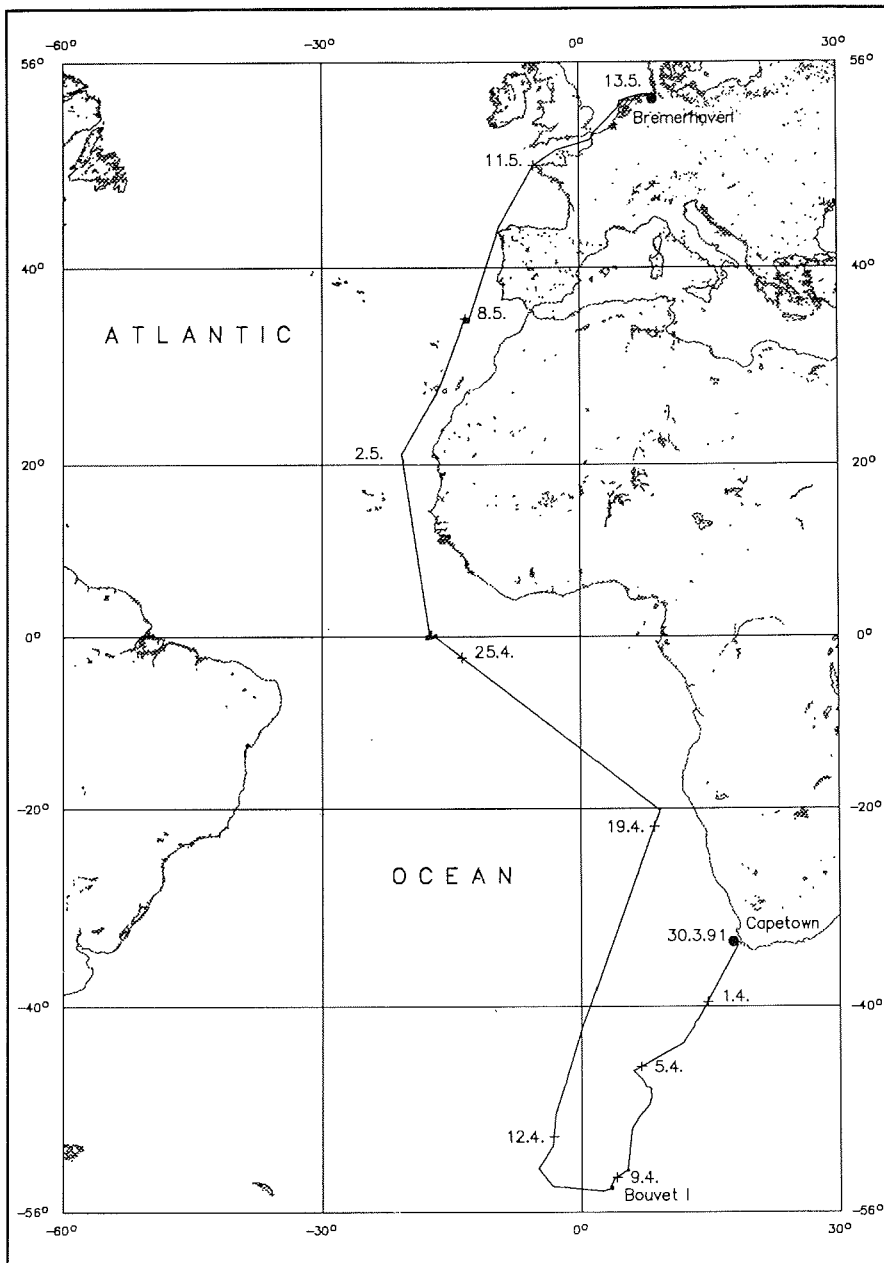


Fig.4.2.: Stationskarte von ANT-IX/4. (Site localities of ANT-IX/4)

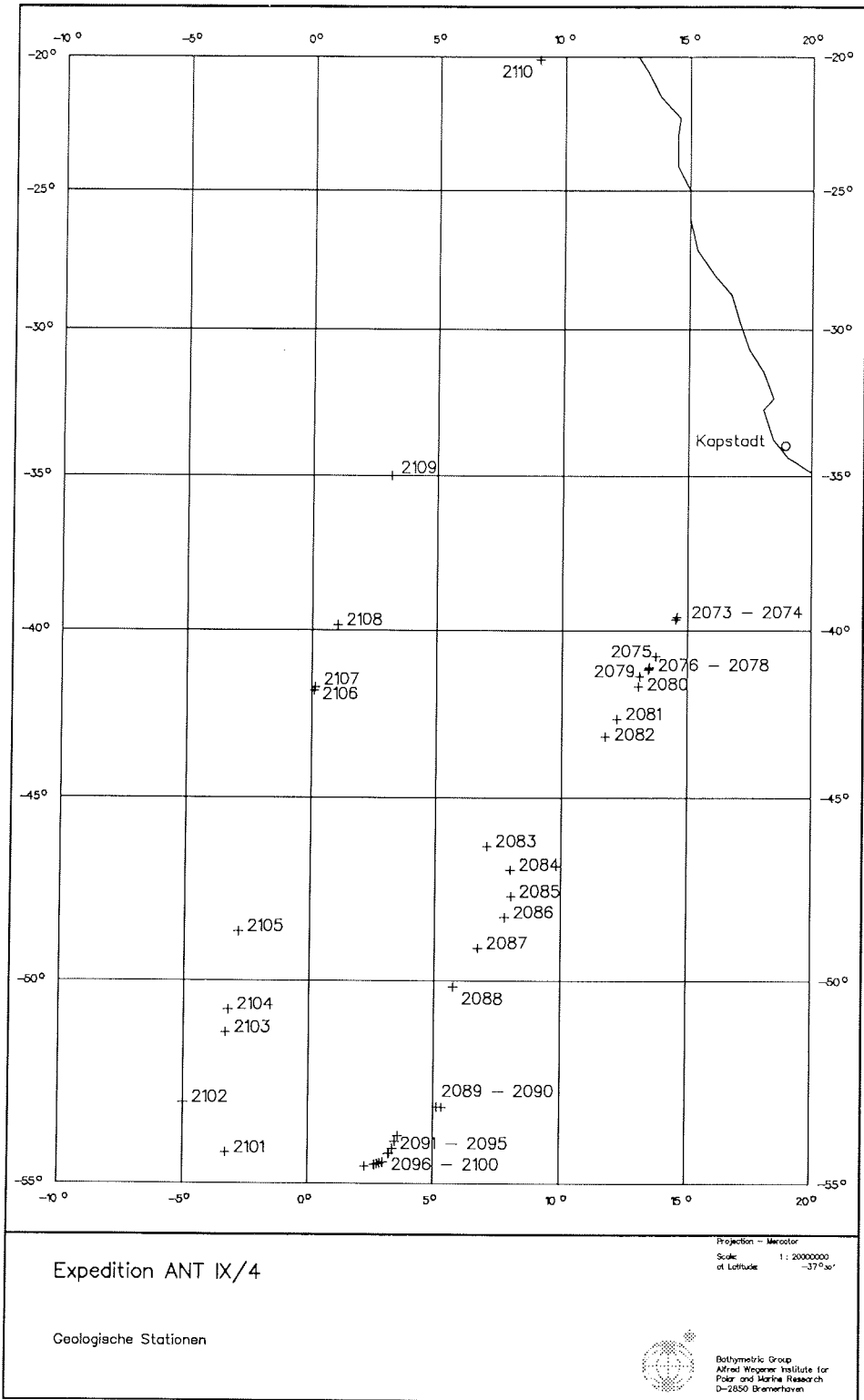


Fig.4.3:
Lage der Stationen und Bathymetrie
auf dem Profil Kapstadt - Bouvet
Island. (Site localities and bathymetry
on transect Capetown - Bouvet Islan

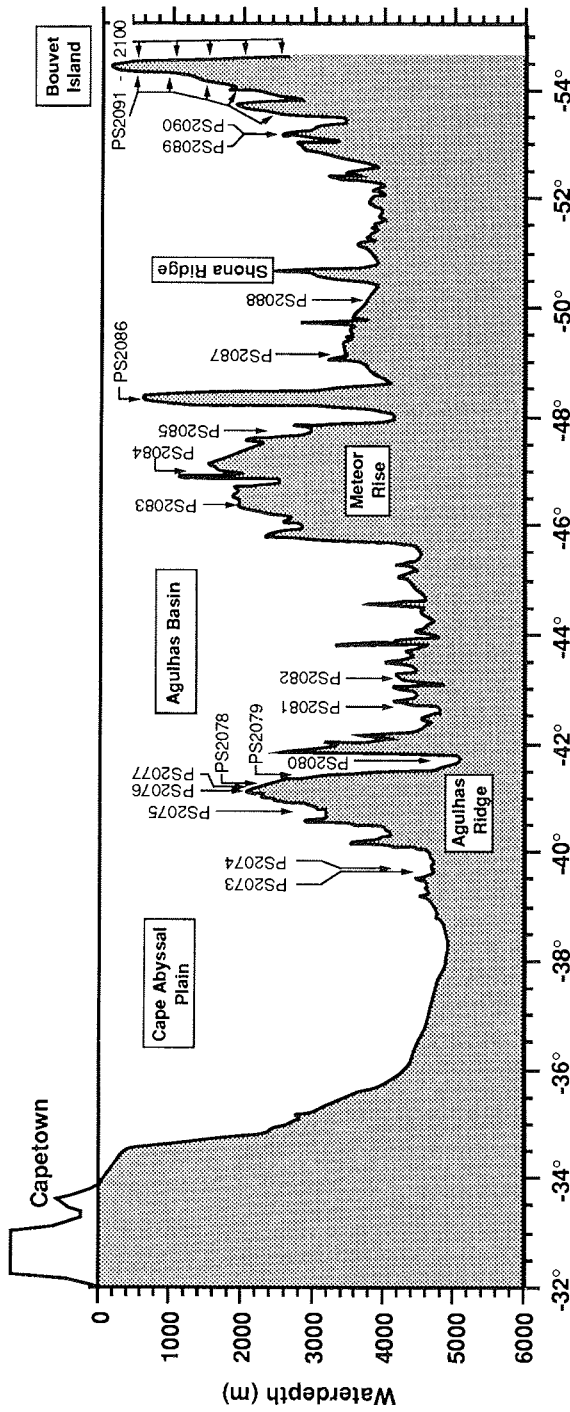
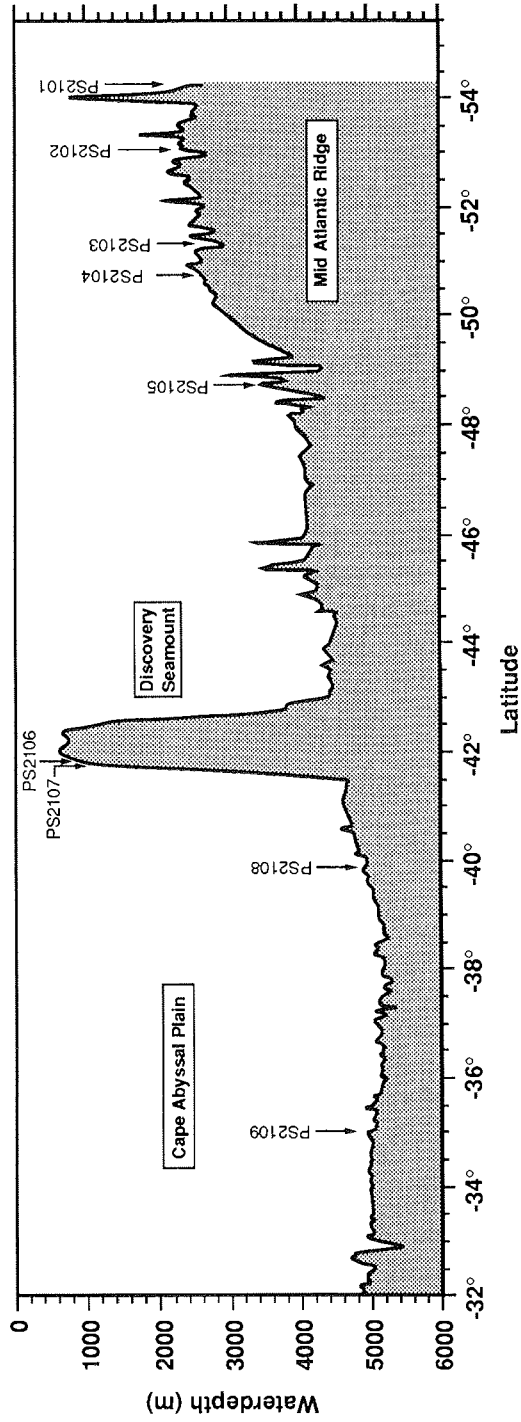


Fig.4.4:
Lage der Stationen und Bathymetrie
auf dem Profil Mittel-Atlantischer-
Rücken - Kap Becken. (Site localities and bathymetry
on transect Mid Atlantic Ridge - Cape
Abyssal Plain)



Parallel zu den Stationsarbeiten mit den geologischen Geräten wurden Beprobungen im Rahmen von aktuopaläontologischen Untersuchungen durchgeführt. Dazu wurden an allen Stationen Planktonnetze eingesetzt. An 11 Stationen kam das Multinetz zum Einsatz und an vier Stationen wurden die oberen 200 m der Wassersäule mit einer Wasserschöpferrosette beprobt. Zur Erfassung der hydrographischen Daten wurde bei jedem Multicorer-Einsatz eine Festspeicher-CTD ca. 20 m über dem Gerät am Draht mitgeführt. Mit dem Bordthermosalinographen wurden während der gesamten Fahrt Temperatur und Salinität gemessen und aufgezeichnet.

Von mehreren Gruppen wurden zum Teil während der ganzen Fahrt Oberflächenwasserproben mit Hilfe der Bordpumpe genommen. An diesen Proben werden Untersuchungen des Planktons, der kieseligen und kalkigen Mikroorganismen sowie einiger umweltrelevanter Organohalogenverbindungen vorgenommen. Zur Untersuchung der Organohalogenverbindungen in der Atmosphäre und ihrer Wechselwirkung mit dem Meerwasser wurden ebenfalls über die gesamte Dampfstrecke Luftproben gesammelt.

Als Unterstützung der marin-geologischen Arbeiten wurden fast auf dem ganzen Fahrtabschnitt bathymetrische Vermessungen mit einem Fächerecholot (Hydrosweep) und sedimentechographische Untersuchungen mit dem hochauflösenden Parasound-System durchgeführt. In zwei Hydrosweep-Profilfahrten von jeweils 48 Stunden wurden Teile der Romanche Bruchzone und der Ampère Seamount vermessen. Ziel dieser Arbeiten sind die Erstellung von bathymetrischen Karten der beiden Gebiete.

Zur Erfassung der Partikelsedimentation durch die Wassersäule wurden auf dem Walfisch-Rücken und vor Cap Blanc Jahresverankerungen der Universität Bremen aufgenommen und an den selben Orten neue Verankerungen ausgebracht. Die Verankerungssysteme waren jeweils mit zwei zeitgesteuerten Sedimentfallen und automatisch registrierenden Strömungsmessern ausgestattet.

Am 30. März 1991 um 15 Uhr Ortszeit verließ FS "Polarstern" den Hafen von Kapstadt und lief mit südlichem Kurs in Richtung Arbeitsgebiet. An Bord befanden sich 42 Besatzungsmitglieder und 23 wissenschaftliche Fahrtteilnehmer. Wegen der marin-geologischen Ausrichtung der Expedition stellten die Geowissenschaftler den Hauptteil der wissenschaftlichen Fahrtteilnehmer. Daneben waren noch einige Chemiker an der Fahrt beteiligt. Noch am selben Abend wurde mit dem Routinebetrieb des Fächersonarsystems Hydrosweep und des Sedimentecholots Parasound begonnen. Die Hydrosweep Aufzeichnungen wurden dann die ganze Fahrt bis zum Ablaufen vom Ampère Seamount am 8.5.91 kontinuierlich fortgeführt. Der Betrieb des Parasound-Systems erfolgte bis zum Ablaufen von der Romanche Bruchzone am 27.4.91.

Durch unerwartet gutes Wetter begünstigt, waren die Laborräume bald komplett eingerichtet, so dass an Bord alles bereit war, um am 31.3.91 gegen 20 Uhr mit den ersten Stationsarbeiten zu beginnen. Diese, sowie die etwas südlicher gelegene zweite Station (PS2073 und PS2074), beide nördlich der subtropischen Front im Kap Becken gelegen, wurden ausgewählt, um Material zu gewinnen, das eine Rekonstruktion des vom Indischen Ozean in den Süd-Atlantik strömenden Agulhas Stroms erlaubt. Der Einsatz von Schwerelot, Multicorer mit Festspeicher-CTD, Planktonnetzen und Multinetz

verlief an der ersten Station erfolgreich. Lediglich eine Niskin-Flasche, die zum Sammeln einer grösseren Menge Bodenwassers am Multicorer angebracht worden war, kam nicht mehr an Deck zurück.

Am 1.4.91 wurde mit der Beprobung des ersten zentralen Arbeitsgebietes, des Agulhas Rückens und des südlich davon gelegenen Agulhas Beckens begonnen. Auf dem Agulhas Rücken wurden vier Stationen (PS2075 - PS2079) abgearbeitet, wobei es mit Hilfe der Parasound Beobachtungen gelungen ist, ausstreichende ältere Sedimente, die voraussichtlich bis ins Miozän reichen, zu beproben. In der Nacht vom 2. zum 3. April wurde bei $41^{\circ}50'S$ die Subtropische Front überfahren, die durch einen charakteristischen Temperaturabfall des Oberflächenwassers von 18 auf $12^{\circ}C$ gekennzeichnet war. Bei auffrischendem Wind wurden am 3.4.91 zwei Stationen in Wassertiefen über 4500 m bearbeitet (PS2081 und 2082). Bei Sturmböen bis Windstärke 10 musste der Einsatz des Multinetzes wie auch noch mehrere Male auf der weiteren Fahrt gestrichen werden. Nachdem die subantarktische Front bei ca. $46^{\circ}S$ überquert worden war, erreichte FS "Polarstern" am 5.4.91 das zweite zentrale Arbeitsgebiet dieser Fahrt, den Meteor Rücken. Der Meteor Rücken, eine sich von NW nach SE über ca. 400 Meilen erstreckende submarine Erhebung, wurde bei ANT-IX/4 in der Streichrichtung abgefahren um erste sedimentechographische Informationen dieses Gebietes zu erlangen. An drei Stationen in Wassertiefen zwischen 1600 und 3000 m wurde eine geologische Beprobung vorgenommen (PS2083-PS2085). Von einem, bis auf ca. 600 m Wassertiefe aufragenden, bislang namenlosen Seamount, konnte die komplette Sedimentauflage bis ins Anstehende beprobt werden (PS2086).

Am 7.4.91 überquerte FS "Polarstern" die Polarfront und trat in das Gebiet der Antarktischen Zone ein. Auf der Position der Polarfrontverankerung PF3, die am 8.11.1989 ausgebracht und bei der Expedition ANT-IX/2 wieder aufgenommen worden war, wurden zur erneuten Kontrolle des Partikelflusses Planktonnetze und ein Multinetz eingesetzt. Der 8.4.91 war für die gezielte Beprobung eines Porzellanit-Horizontes vorgesehen. Dieser Horizont, der als markanter sedimentechographischer Reflektor in einem Gebiet um $53^{\circ}10'S$; $5^{\circ}20'E$ auftritt, wird von umkristallisiertem biogenen Opal gebildet, der sich in jungen Sedimenten normalerweise nur unter dem Einfluss erhöhter Temperatur bilden soll. Mit einer sechsstündigen Parasound-Hydrosweep-Profilfahrt wurden zwei geeignete Positionen ausgewählt, an denen die Sedimentabfolge mit drei Kolbenlot-Einsätzen erfolgreich beprobt wurde. Wie sich später beim Öffnen eines Kernes herausstellte, ist es tatsächlich gelungen, diese Lage zum ersten Mal innerhalb ihres Sedimentverbandes zu bekommen. Am 9.4.91 erfolgte die Beprobung von Oberflächensedimenten nördlich und südlich des Südwest-Indischen-Rückens (PS2091-PS2099). Im Norden bei 2500 m Wassertiefe beginnend, wurden in 500 m Tiefenabständen fünf Stationen bis in eine Tiefe von 500 m westlich von Bouvet Island durchgeführt. Auf der südlichen Seite des Rückens wurde die Beprobung dann in umgekehrter Reihenfolge zu grösseren Wassertiefen hin vorgenommen.

Am Mittel-Atlantischen-Rücken beginnend, war ein zweites Stationsprofil geplant worden, das nach Norden bis $35^{\circ}N$ reichend, einen weiteren Probensatz aus den verschiedenen hydrographischen Fronten bringen sollte.

Da für den aus zeitlichen Gründen vorgesehenen Nordkurs keinerlei sedimentechographische Aufzeichnungen früherer Fahrten zur Verfügung standen, mussten die Stationspositionen bei kontinuierlicher Parasound-Beobachtung ausgewählt werden. Leider ist es jedoch nicht immer gelungen, in den gewünschten Wassertiefen geeignete Positionen zu finden, die den Einsatz langer Lote zuließen. Zwischen dem 10. und dem 12.4.91 wurden am Nordhang des Mittel-Atlantischen Rückes fünf geologische Stationen durchgeführt, die aber nur zum Teil gutes Material brachten (PS2102 - PS2105). Am 13.4. musste zum ersten Mal bei dieser Fahrt eine Station komplett gestrichen werden. Ein schwerer Sturm, der in Böen Orkanstärke erreichte, liess keine Decksarbeit zu. Am 14.4.91 stand die Beprobung des Discovery Seamounts auf dem Programm. Geplant war bei diesem, bis in eine Wassertiefe von ca. 500 m aufragenden Seamount, eine Probenahme die von der Tiefsee ausgehend unterschiedliche Tiefenniveaus erfassen sollte. Die topographischen Bedingungen, im Süden sehr steil ansteigend, im Norden steil abtauchend, liessen den Einsatz von Probenahmegeräten jedoch erst ab 1500 m Wassertiefe zu. Da die auftretenden Sedimente aus reinen Foraminiferensanden bestehen, war es nur bei einem Multicorer-Einsatz möglich, etwas Material an Deck zu bringen (PS2106). Bei einem Schwerlot und einem weiteren Multicorer wurde das Sediment vermutlich beim Hieven durch die Wassersäule ausgespült. Am 15. und 16.4.91 wurden die zwei letzten Stationen in ca. 5000 m Tiefe im Kapbecken durchgeführt. Dabei wurden neben den geologischen Geräten und den Netzen auch die Wasserrosette eingesetzt. Damit war die geologische Probennahme der Expedition ANT-IX/4 abgeschlossen und FS "Polarstern" nahm nördlichem Kurs in Richtung Bremerhaven. Gleich nach Abschluss der Stationsarbeiten wurde damit begonnen, Sedimentkerne zu öffnen, zu beproben und zu bearbeiten. Diese Arbeiten wurden bis zum 30.4.91 fortgeführt.

Am 19.4.91 erreichte FS "Polarstern" die Position der Verankerung WR-3 am Walfischrücken. Die ausgelöste Verankerung wurde schnell entdeckt und über die Steuerbordseite geborgen. Um die Beobachtungen fortzusetzen, wurde an gleicher Stelle erneut eine ähnliche Verankerung über die Heckslippe ausgebracht. Vom 25. bis 27.4.91 erfolgte eine bathymetrische Vermessung eines Teiles der Romanche Bruchzone. Mit insgesamt 570 Seemeilen Profilfahrt konnte eine grössere Lücke geschlossen werden, die nach vorherigen Vermessungen noch offen geblieben war. Eine weitere Verankerung wurde am 2.5.91 vor Cap Blanc aufgenommen und an selber Stelle durch eine neue ersetzt (CB-3 und CB-4). Vom 6.5. bis 8.5.91 stand eine weitere Hydrosweep Vermessung auf dem Programm. Während 48 Stunden wurden Profilfahrten über dem bei ca. 35°N gelegenen Ampère Seamount durchgeführt. Parallel dazu wurde für diese Zeit auch das Parasound System wieder in Betrieb genommen. Diese Vermessung dient als Vorstudie für ein anlaufendes Projekt im Rahmen des europäischen MAST-Programms. Am 8.5.91 um 8 Uhr waren damit die wissenschaftlichen Aktivitäten der Expedition ANT-IX/4 beendet. Die weitere Heimreise erfolgte problemlos und am 13.5.91 machte FS "Polarstern" um 13 Uhr in Bremerhaven fest.

In den ersten 16 Tagen der Expedition ANT-IX/4 wurde ein intensives marin-geologisches Beprobungsprogramm durchgeführt. Dieses Programm, das zum Teil unter schlechten Wetterbedingungen in Tag und Nachtarbeit

durchgeführt werden musste, konnte nur durch hohen Einsatz von Wissenschaft und Besatzung realisiert werden.

Herrn Kapitän Jonas und seiner Besatzung gilt höchstes Lob und Dank für ihren Einsatz und die Unterstützung bei der Durchführung der Stationsarbeiten, sowie für die immer freundliche Atmosphäre an Bord von FS "Polarstern".

2. SUMMARY AND ITINERARY

H.-W. Hubberten (AWI)

The main purpose of the expedition ANT-IX/4 was to conduct a marine geological sampling program in the area of the Antarctic and Subantarctic oceanographic frontal systems between latitudes 35° and 55° south. The aim of this program was to obtain sediment samples from which information about the paleoceanographic evolution of the area north and south of the Antarctic polar front can be deduced. At that area cold Antarctic water masses meet warm subtropical waters. The water masses occurring in intermediate and extreme depths consist mainly of North Atlantic Deep Water (NADW), Circumpolar Deep Water (CDW) and Antarctic Bottom Water (AABW). These water masses as well as their significance and position during the Quaternary glacial and interglacial cycles are strongly connected to parameters such as productivity, heat transport, atmospheric circulation and climate changes. Due to these interrelations they are responsible for the CO₂ budget of the atmosphere-ocean system.

The program conducted during ANT-IX/4 is related to the Sonderforschungsbereich 261, a joint project between the Alfred-Wegener-Institute and the University of Bremen. Under the topic "The South Atlantic during the late Quaternary: Reconstruction of mass balance and heat transport" the scientific goals of the cruise ANT-IX/4 can be summarized as follows:

- the reconstruction of the surface water temperatures as well as the circulation of the surface water current systems with the main focus on north-south variations of the hydrographic frontal systems and the sea ice boundary.
- the reconstruction of characteristic water mass parameters of the intermediate and deep water masses as well as their propagation and circulation with special interest on the distribution of the Antarctic Bottom Water (AABW).

The geological stations of the expedition ANT-IX/4 were selected using the preliminary results of the expedition ANT-VIII/3 during which a profile between Capetown and Bouvet Island was sampled in November 1989. The investigations were concentrated on submarine morphological elevations such as the Agulhas Ridge, the Meteor Rise and the Mid-Atlantic-Ridge (Figs. 4.1 to 4.4). Gaps left by ANT VIII/3 due to bad weather conditions and problems with the sampling equipment, could be closed. In the area northeast of Bouvet Island the main focus was to find samples of porcellanite, a material which forms through the recrystallization of biogenic opal. Surface sediments were sampled at 10 stations located in different water depths on a profile north and southwest of Bouvet Island. Starting at the Mid-Atlantic Ridge a widely spaced south-north profile was sampled up to 35°N with the aim to get additional informations about the hydrographic frontal systems (Fig. 4.4).

Beside the sampling of sediment material a program was carried out to sample siliceous and calcareous microorganisms within the water column using plankton nets and vertical nets. To obtain hydrographic data a solid-state

memory-CTD was connected about 20 m above the multicorer at all MUC stations. Salinity and temperature were continuously recorded using the thermosalinographic system of RV "Polarstern". Surface water samples were collected by various groups during almost the entire cruise utilizing the ship's pumping system. They will be used to study calcareous and siliceous microorganisms as well as some organohalogenic compounds. Air samples also taken during the entire cruise allow to study the content of organohalogenic compounds within the atmosphere as well as their air-sea exchange properties.

Complementary to the marine-geological program a bathymetric survey with the Hydrosweep-system and sedimentary seismic profiling with the high-resolution Parasound-system were carried out throughout the trip. During two Hydrosweep surveys of 48 hours each, parts of the Romanche Fracture Zone and the Ampere Seamount were studied with the aim to get data for producing bathymetric maps of that areas.

To monitor the particle flux through the water column annual moorings of the University of Bremen were recovered at the Walvis Ridge and off Cap Blanc and new moorings were deployed at the same positions. These moorings were equipped with two sediment traps and automatic registering current meters.

RV "Polarstern" left Capetown on March 30 at 3 pm with a southern course towards the working area, with 42 crew members and 23 scientists. The scientific party consisted of mainly geologists and some chemists. On the evening of March 30, the continuous recording of the ocean-bottom bathymetry with the Hydrosweep system and the seismic profiling with the Parasound system was begun. The Hydrosweep survey was continued until May 8, Parasound profiling was carried on until April 27. Favourable weather conditions allowed to have all laboratories completely equipped when the scientific program was started on March 31 at 8 pm. The first two stations (PS2073 and PS2074) are both located north of the Subtropical Front within the Cape Basin. They were selected in order to obtain material allowing the reconstruction of the Agulhas Current which flows from the Indian Ocean into the South-Atlantic. Gravity corer, multicorer with solid-state memory-CTD, plankton nets and a vertical net were successfully employed at this station.

On April 1 the station work on the first central working area, the Agulhas Ridge and the Agulhas Basin began. Four stations (PS2075-PS2079) were successfully sampled at the Agulhas Ridge. With help of Parasound observations it was possible to sample older sediments, which could be tentatively dated to a Miocene age. The Subtropical Front, characterized by a decrease in the water temperature from 18 to 12°C, was crossed during the night of April 2 to 3 at 41°50'S. Two stations (PS2081 and PS2082) were sampled at water depths of more than 4500 m on April 3. Because of increasing wind velocities of up to 10 it was not possible to deploy the vertical net.

After having passed the Sub-Antarctic Front at 46°S RV "Polarstern" arrived on April 5 at the second main working area of this cruise, the Meteor Rise. During ANT IX/4 the Meteor Rise has been crossed parallel to its NW-SE axes to obtain some first sediment seismic informations of this area. Sampling was

carried out at four stations at water depth between 1600 and 3000 m (PS2083 - PS2085). On the top of a nameless seamount, the complete sediment cover was successfully cored down to the badrock at a water depth of 600 m (PS2086).

On April 7 RV "Polarstern" crossed the Polar Front and entered the area of the Antarctic Zone. The sampling of a specific sedimentary horizon, assumed to consist of porcellanite, was planned on April 8. This horizon, which appears as a prominent seismic reflector in an area around 53°10'S; 5°20'E, consists of recrystallized biogenic opal which normally forms only in young sediments under the influence of higher temperatures. With help of six hours parasound profiling, two positions were selected on which three piston corer successfully cored the sediment column. When opening one of these cores later, it was found that for the first time, this porcellanite has been sampled within its sedimentary sequence. Sampling of surface sediments north and south of the Southwest-Indian-Ridge followed on April 9 (PS2091-PS2099). Starting in the north at a water depth of 2500 m, surface sediments and bottom water were successfully sampled at five stations in steps of 500 m to a depth of 500 m west of Bouvet Island. At the southern flank of the ridge, sampling was carried out from shallow to deeper water. It was planned to sample a second south-north profile over the oceanographic frontal systems further west beginning at the Mid-Atlantic-Ridge and reaching 35°N.

There was no sedimentary echographic information from earlier cruises available for the planned route. For this reason sampling positions had to be selected by continuous observation of the Parasound registrations. Unfortunately it was not always possible to find proper positions in the desired water depth which allowed sampling with longer coring equipment.

Between April 10 and 12 five geological stations were sampled at the northern flank of the Mid-Atlantic-Ridge but only partially good material was recovered (PS2102-2105). For the first time on the cruise one complete station had to be cancelled on April 13 due to bad weather conditions. Sampling at the Discovery Seamount was planned on April 14. The aim of this sampling was to obtain sediment material from different water depths from the deep sea up to about 500 m. Due to the topographic conditions, i.e. very steep slopes at the southern and northern flank, only two stations above 1500 m water depth were selected. The occurring sediments consisted of almost pure foraminiferal sands which could be brought on deck with one multicorer only (PS2106).

The two last geological stations of cruise ANT IX/4 were sampled within the Cape Basin on April 15 and 16. Immediately after finishing the geological sampling, sediment cores were opened, sampled and investigated. These activities continued until April 30.

On April 19 RV "Polarstern" was at the position of mooring WR-3 on the Walvis Ridge. The mooring was recovered without any problem and a similar mooring was deployed at the same position for continuous observation.

Between April 25 and 27 a bathymetric survey of a part of the Romanche Fracture Zone was carried out. Covering a distance of about 570 nm made it possible to close a large gap which remained open from earlier Hydrosweep profiling. On May 2 a further mooring was recovered off Cap Blanc and substituted by a new one (CB-3 and CB-4). Another bathymetric survey was carried out between May 6 and 8 at the Ampere Seamount at 35°N. During 48

hours this seamount could be completely covered by ship tracks. Parallel to the Hydrosweep survey, sediment seismic investigations were undertaken using the Parasound system. These studies are related to a future project within the European MAST program. The scientific activities of ANT-IX/4 ended on May 8 at 8 am. The cruise ended on May 13 at 3 pm at Bremerhaven.

An intensive marine-geologic sampling program was carried out during the first 16 days of the expedition ANT-IX/4. With partly bad weather conditions this program could only be realized due to the great engagement of crew and scientists. Thanks are due to Captain Jonas and his crew for the enthusiastic help during the station work as well as for the good atmosphere on board of RV "Polarstern".

3. DAS WETTER WÄHREND ANT-IX/4 E. Röd (DWD)

Aus dem südafrikanischen Frühherbst - gerade war hier eine für die Jahreszeit ungewöhnliche Hitzeperiode mit Temperaturen nahe 40°C gewittrig zu Ende gegangen - führte die Route zunächst in die subantarktischen Breiten bei der Bouvet Insel. Schon bald nach dem Auslaufen gelangte das Schiff in ein westnordwestliches Starkwindfeld, das sich zwischen dem Subtropenhoch und der südatlantischen, von Gough Island über Bouvet verlaufenden Tiefdruckrinne gebildet hatte. Die anfangs noch ziemlich weit entfernt ost-südostwärts ziehenden Tiefzentren brachten bereits auf 37°S Windstärke 7. Nach kurzer Wetterberuhigung folgte als Abschluß einer Serie ein 980 hPa-Tief, das auf 43°S die Brise bis zum schweren Nordweststurm zunehmen ließ, der aber schon vom 3. zum 4. April durch die Passage einer markanten Kaltfront beendet wurde. Die postfrontal von Südwesten her einströmende Kaltluft war um 14 Grad empfindlich kälter und wesentlich trockener als die vorher wetterbestimmende Subtropikluft.

Kräftiger Druckanstieg leitete anschließend eine antizyklonale Phase ein, die am 4./5.4. mit 1018 hPa ihren Höhepunkt erreichte. Ein weiteres, wieder über die Bouvet Insel hinwegziehendes Tief war im Satellitenbild sehr eindrucksvoll ausgebildet und ließ schweren Sturm befürchten. Ein zweites Tief, dem sich das erste nach einem unübersichtlichen Kurs um Bouvet angliederte, verhinderte jedoch das Entstehen scharfer Druckgradienten, weshalb der Wind mit NE 6-7 überraschend schwach blieb. Eine zugehörige, über dem Fahrtgebiet fast stationäre Warmfront brachte am 8.4. den einzigen Tag mit beständigem Nebel.

Am 10.4. war "Polarstern" bereits am südlichsten Punkt des Fahrtabschnittes angelangt und dementsprechend einer neuen, auf 65°E ostwärts ziehenden Zyklone gefährlich nahe. Im Satellitenbild war sie viel undeutlicher ausgeprägt als ihre Vorgängerin, baute aber trotzdem ein umfangreiches Starkwindfeld und hohe See auf. In der labilen Kaltluft, die in der Höhe Temperaturrückgang um 15°C verursachte, kam es wiederholt zu intensiven Graupelschauern mit schweren Sturmböen.

Der nächste, bei South Georgia aufgetauchte Wirbel zog mit seinem Frontensystem und einem Kerndruck von 980 hPa unter Vertiefung am 12.4. über das Einsatzgebiet hinweg, vereinigte sich mit dem vorhergehenden und bildete ein spektakuläres Tiefdrucksystem. Ungewöhnlich hoher Luftdruck bei

den South Orkneys (in Grytviken 1023 hPa) löste einen neuerlichen Polarluftvorstoß aus. Der stürmische Südwestwind nahm in Nähe der wiederholten und intensiven Graupelschauer Orkanstärke an, baute eine zehn Meter hohe See auf und flaute erst im Verlauf des 13.4. allmählich wieder ab. Eine kräftige, abgeschlossene Hochzelle mit 1024 hPa beendete am 15.4. auf der Position Walfischrücken diese letzte südhemisphäre Sturmlage. Dem Starkwindfeld eines neuen, von Gough Island heranziehenden Tiefs konnte "Polarstern" mit Nordostkurs davonfahren und wurde nur von seinem Regengebiet erfasst.

Am 18.4. kündigte sich auf 25°S der Südostpassat an und begleitete die Fahrt bis zur intertropischen Konvergenzzone (ITCZ). Trotz sehr hoher relativer Luftfeuchtigkeit blieb die Sicht durchweg gut, Nebelfelder waren nur weitab von der Schiffsroute über den küstennahen Auftriebsgebieten zu sehen. Dem mit 1015 hPa bis auf 12°S ausgedehnten Subtropenhoch stand ein gut ausgebildetes Hitzetief über Niger-Obervolta gegenüber und verstärkte die Strömung zeitweise bis auf 6Bft.

Die ITCZ lag über dem afrikanischen Kontinent zwischen 10 und 15°N, über dem Seegebiet vor Westafrika zwischen 4 und 8°N. Deutlich nach Süden davon abgesetzt zeigten sich im Satellitenbild hochreichende Wolkencluster in Äquatornähe, die wiederholt wolkenbruchartige Schauer, kurze Böen um 7Bft, aber keine Gewitter auslösten. Am 28.4. querte die Route bei 5°N die Achse der ITCZ und gelangte dabei aus der drückend schwülen Südströmung in die merklich kühlere und trockenere des beginnenden nordhemisphärischen Passates, der zunächst rein nördliche Richtung hatte. Die Konvergenz hatte wieder einzelne, zum Teil sehr starke Regenfälle produziert, trotz hoher Labilität - ein Indiz dafür war ein deutlich ausgebildeter Tornado-Rüssel (funnel cloud) - auch hier keine elektrischen Entladungen. Die Schauerböen gingen kurzzeitig bis in Windstärke 8.

Nach Norden hin nahm die Passatströmung allmählich auf 5-6, strichweise bis 7 Bft zu und drehte ab 22°N auf Nordost. Diese Strömung wurde angetrieben durch ein von den Azoren weit nach Norden verschobenes, mit 1040 hPa westlich von Irland blockierendes Hoch, das sich erst in der letzten Fahrtwoche unter allmählicher Abschwächung zu seinem angestammten Platz bei den Azoren verlagerte. Die Trajektorie der herangeführten Luft ließ sich auf direktem Weg bis in den skandinavischen Raum verfolgen, wodurch auch die erfrischende Kühle in den Tropen und Subtropen zu erklären war. So war die deutlich unternormale Lufttemperatur durchwegs niedriger als die Wassertemperatur. Die Passatinversion war daher besonders scharf ausgeprägt (bis 12°C) mit relativ tiefer Basis zwischen 300 und 500 m.

Am 1. Mai konnte nahe Cap Blanc eine auffällige Schwingung der Inversion beobachtet werden, die offenbar durch das Umströmen des Kaps ausgelöst war: mit einer Periode von 20 Minuten pendelte der Wind von 350°/18 Knoten auf 70°/10 Knoten und mit gedämpfter Amplitude wieder zurück. Nach neun solcher Zyklen klang die Schwingung ganz ab. Die gleichzeitig registrierte Druckwelle hatte eine Amplitude von 1,5 hPa. Im Satellitenbild war über dem Fahrtgebiet ein Muster von strömungsparallelen Wolkenstreifen zu erkennen. In diesem Zusammenhang sind auch Karmannsche Wirbelstraßen zu erwähnen, die in den Satellitenaufnahmen der östlichen Subtropen mehrmals auftraten. Der widrige Nordnordostwind mit durchschnittlich 7 Bft und die

dadurch aufgebaute Dünung von 3-4 m hielten zunächst an. Erst der 9.5. brachte in Höhe von Kap Finisterre deutliches Abflauen auf N 5, der 10.5. auf N 4-5 und das Wochenende weiteres Rückdrehen auf West vor dem Ausgang des Ärmelkanals.

Die Route von Polarstern hatte somit entlang einem Meridionalschnitt von der Subantarktis bis in die nördliche Westwindzone zwei vollständige Hadley-Zirkulationen mit den zugeordneten Klimagebieten durchquert und konnte bei relativ ruhigem Wetter in die Nordsee einlaufen.

4. BATHYMETRISCHE UND SEDIMENTECHOGRAPHISCHE PROFILMESSUNGEN

4.1 Bathymetrie und Meeresbodenkartierung mit Hydrosweep

T. Kuhn, (AWI); F. Niederjasper, M. Schacht, T. Schöne

Die Hydrosweep-Vermessung während ANT-IX/4 erfolgte in den Abschnitten:

- Einzelprofilmessung zwischen geologischen Verankerungs- und Probenstationen
- Detailvermessung im Bereich der Romanche Bruchzone
- Detailvermessung des Ampère Seamount

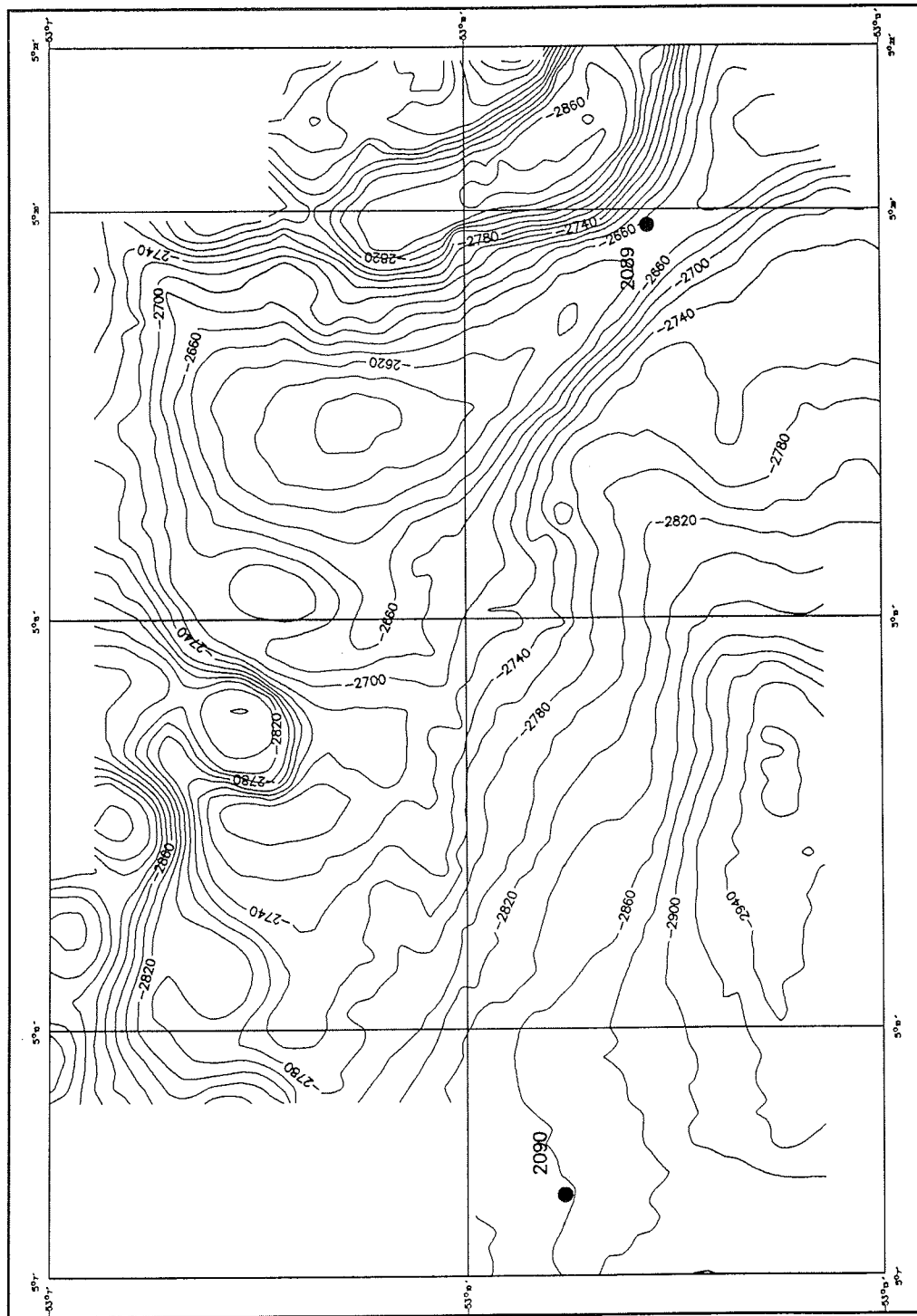
Einzelprofilmessung zwischen geologischen Verankerungs- und Probenstationen

Vier Stunden nach Ablegen in Kapstadt wurde das Fächerecholot Hydrosweep in Betrieb genommen. Ein hauptsächlich in südwestlicher Richtung verlaufendes Hydrosweep-Profil führte über den südafrikanischen Kontinentaltang, den Agulhas Rücken, den Meteor Rücken, den Shona Rücken zum Südwest-Indischen-Rücken. Der in Richtung NW - SO verlaufende Meteor Rücken wurde in südöstlicher, später in südlicher Richtung überlaufen. Südwestlich vom Meteor Rücken überstreicht das Aufnahmeprofil einen in den Karten bisher unbenannten Seamount, der aus einer Tiefe von 4000 m bis auf ca. 600 m ansteigt.

Nördlich des Südwest-Indischen-Rückens wurde für die Erkundung der Porzellanit-Stationen PS2089 und PS2090 ein kleines Gebiet von ca. 17 x 11 km mit Parasound und Hydrosweep vermessen. Die Isolinienkarte zeigt die lokale Morphologie im Bereich der beiden Stationen. PS2089 liegt an der tiefsten Stelle eines schmalen Sattels, PS2090 ca. 200 m tiefer an einem flach auslaufenden Hang (Fig. 4.5).

Ab Bouvet Island setzte sich das Hydrosweep-Profil in westlicher, später nordwestlicher Richtung über die Bouvet Bruchzone zum Mittel-Atlantischen-Rücken fort. Ab hier führte es dann in Richtung NNO über den Discovery Seamount, das Kap Becken, die Namibia Tiefsee-Ebene zum nordöstlichen Teil des Walfisch Rücken und weiter in Richtung NW zur Romanche Bruchzone.

Fig. 4.5: Bathymetrie im Bereich der Stationen PS2089 und PS2090
Fig. 4.5: Bathymetric chart of the area of Sites PS2089 and PS2090



Die während der Profilmfahrt mit Hydrosweep in quasi Echtzeit erstellten Tiefenlinienkarten dienten neben den Parasound-Informationen häufig als Grundlage für die Festlegung der geologischen Probenstationen. Während der Stationen wurde Hydrosweep, besonders bei stark strukturiertem Meeresboden, zur genauen Positionierung des Schiffes benutzt. Die Hydrosweep-Daten der Einzelprofilmessungen können zusammen mit den Daten früherer Expeditionen zur Herstellung von Planungskarten für zukünftige Expeditionen genutzt werden. Außerdem sollen sie zur Ergänzung und Vervollständigung von kleinmaßstäbigen bathymetrischen Karten, wie z.B. der GEBCO, dienen.

Detailvermessung im Bereich der Romanche Bruchzone

Die Romanche Bruchzone ist mit bis zu 7800 m Wassertiefe die tiefste Bruchzone des Atlantischen Ozeans. Sie ist damit von großer Bedeutung für die Ausbreitung der kalten Bodenwassermassen zwischen den west- und ostatlantischen Tiefseebecken. An ihr versetzt der von Norden kommende Mittel-Atlantische-Rücken um ca. 800 km nach Osten. Um detaillierte Kenntnisse über die tatsächliche Morphologie der Romanche Bruchzone und den angrenzenden Bereich des Mittel-Atlantischen-Rückens zu bekommen, soll sie in einem Langzeitprojekt etappenweise vollständig vermessen werden.

Im Rahmen der Erprobung des Hydrosweep-Systems der "Polarstern" wurde während der Reise ANT-VIII/1 bereits der zentrale Grabenbereich und zwei westlich und östlich anschließende Gebiete vermessen. Daran schließt sich im Nordosten ein von dem französischen Forschungsschiff "Jean Charcot" vermessenes Gebiet an. Während ANT-IX/4 konnte eine große Lücke zwischen den französischen Messungen geschlossen werden. Um den südöstlichen Anschluß der Bruchzone an den Mittelatlantischen Rücken zu finden, wurden die Messungen der "Jean Charcot" im Süden und Osten ergänzt. Insgesamt wurden in 48 Stunden rund 570 nm zurückgelegt und dabei eine Fläche von 5300 km² vermessen (Fig. 4.6). Erste Auswertungen zusammen mit den französischen Messungen zeigen den sich nach Osten verengenden Graben, dessen Sohle Undulationen bis zu 600 m aufweist. Der nördliche Hang der Bruchzone wird durch ein nach Westen steil ansteigendes Zwischenplateau unterbrochen, das im Osten fast in der Grabensohle ausläuft. Oberhalb dieses Plateaus geht der Hang in einen nach Westen fallenden Rücken über, der im Osten bis zu einer Wassertiefe von 1000 m ansteigt. Der südliche Hang der Bruchzone wird im Osten von den ersten Verwerfungen des nach Süden weiter verlaufenden Mittelatlantischen Rückens unterbrochen.

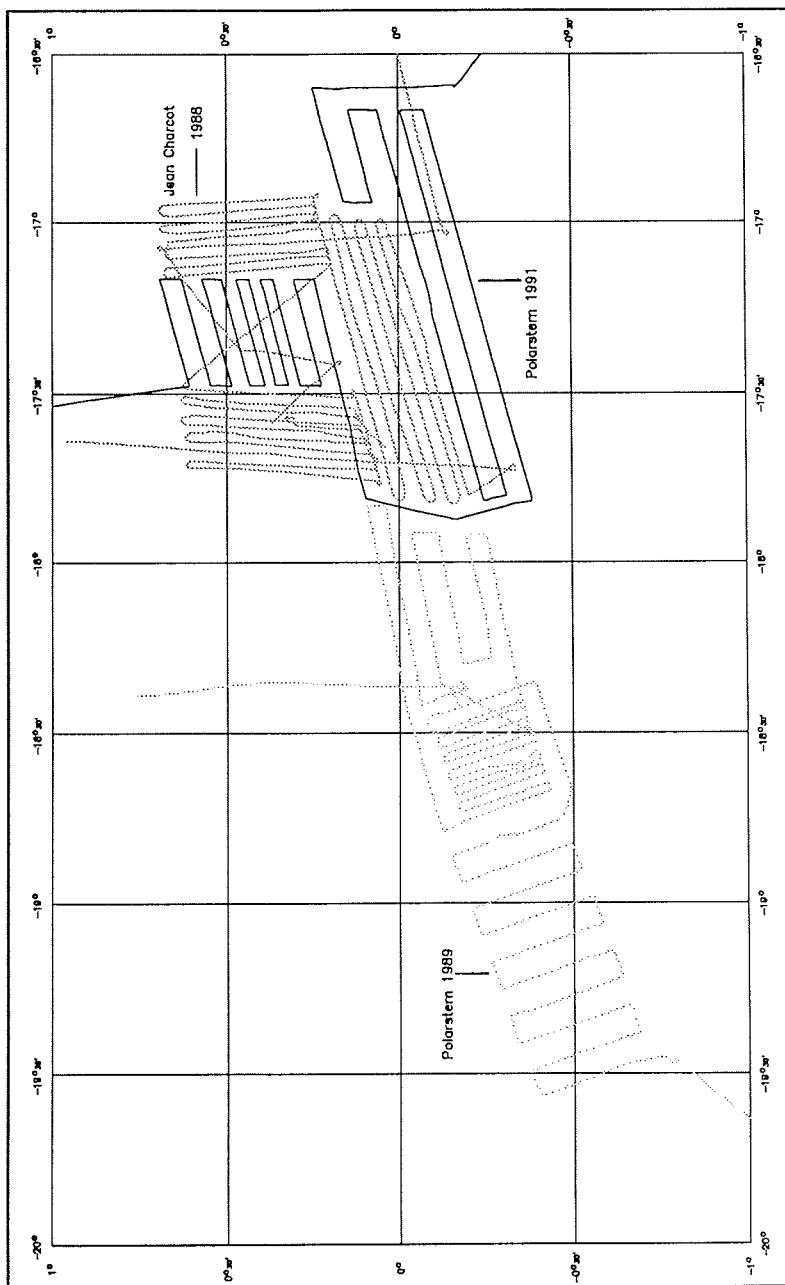
Detailvermessung des Ampère Seamount

Im Seegebiet vor Portugal sollen vom Zentrum für Rohstofforientierte Meeresforschung der TU Clausthal, in Zusammenarbeit mit anderen europäischen Universitäten und Forschungsinstituten, Untersuchungen zu geochemischen Flüssen im System Wassersäule/Meeresboden durchgeführt werden. Die Untersuchungen finden im Rahmen des von der EG-Kommision genehmigten Forschungsvorhabens MARFLUX (MARine FLUXes), das im Zuge des ebenfalls von der EG-Kommission aufgelegten MAST-Programmes (MARine Science & Technology) durchgeführt wird, statt. Untersucht werden soll das Gebiet des Ampère Seamounts, der etwa in der Mitte zwischen Madeira und Lissabon liegt.

Da es keine exakten bathymetrischen Karten dieses Gebietes gibt und die für die Untersuchung zur Verfügung stehenden Forschungsschiffe "Tyro" oder "Charles Darwin" keine Fächerecholotsysteme besitzen, stellte das AWI die "Polarstern" für eine detaillierte Hydrosweep-Vermessung zur Verfügung. In ca. 50 Stunden Profilfahrt wurden rund 600 nm zurückgelegt und dabei eine Fläche von 3600 km² vermessen. Die bereits an Bord angefertigten Arbeitskarten zeigen einen von 4800 m auf weniger als 60m Wassertiefe ansteigenden Vulkankegel mit eiförmigen Grundriß. Auf seiner östlichen Seite erfolgt

Fig. 4.6: Hydrosweep- und Seabeamprofile im Bereich der Romanche Bruchzone.

(Hydrosweep and Seabeam profiles at the Romanche Fracture Zone)



der Anstieg kontinuierlich, während er auf der westlichen Seite von großen, sich in Ost-West-Richtung erstreckenden Plateaus unterbrochen wird. Seine Spitze wird ebenfalls von zwei Plateaus gebildet, das östliche liegt in rund 100 m Wassertiefe, das westliche in etwa 400 m Tiefe (Fig. 4.7 & 4.8).

Fig. 4.7: Bathymetrische Karte des Ampère Seamount
Fig. 4.7: Bathymetric chart of the Ampère Seamount

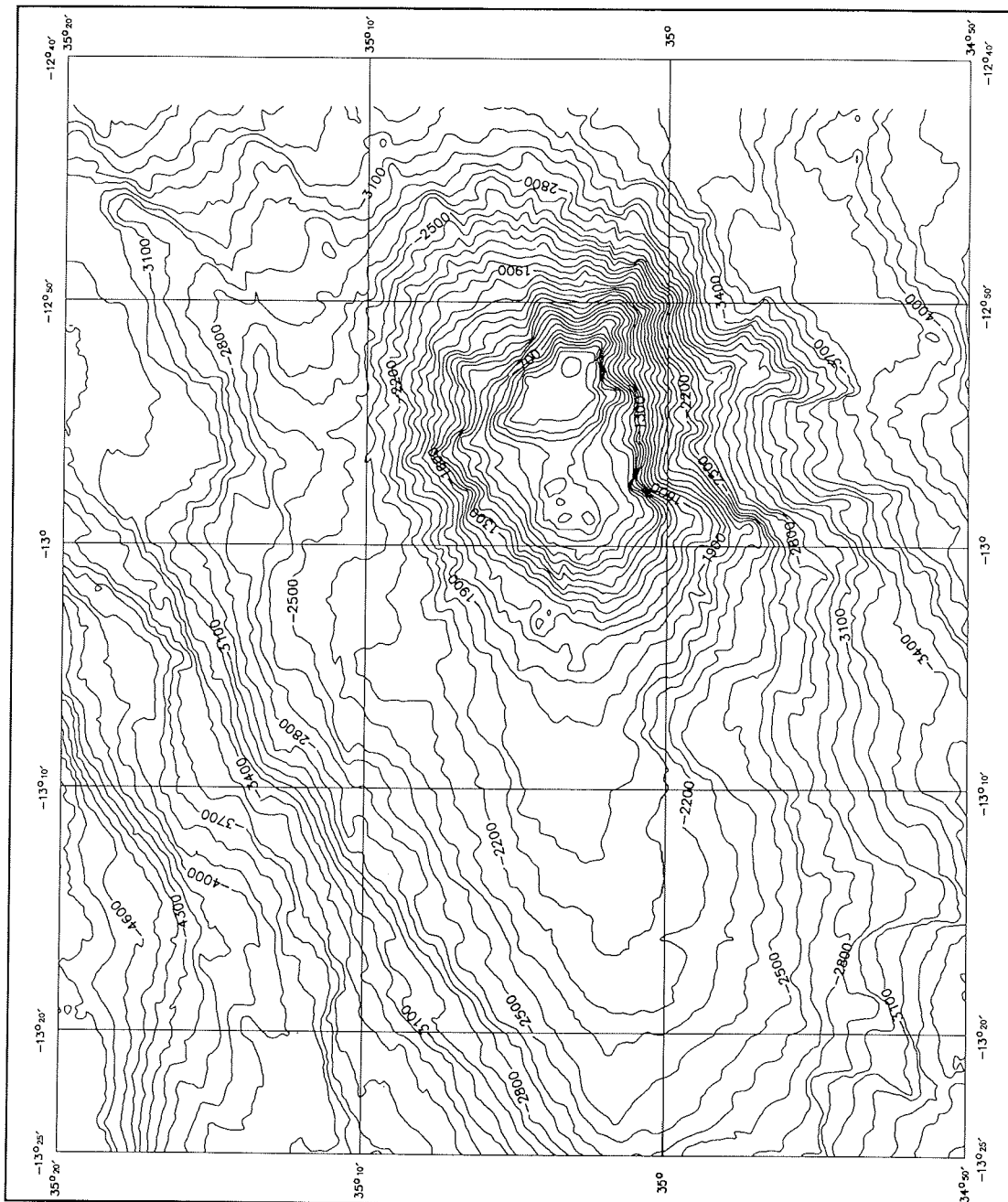
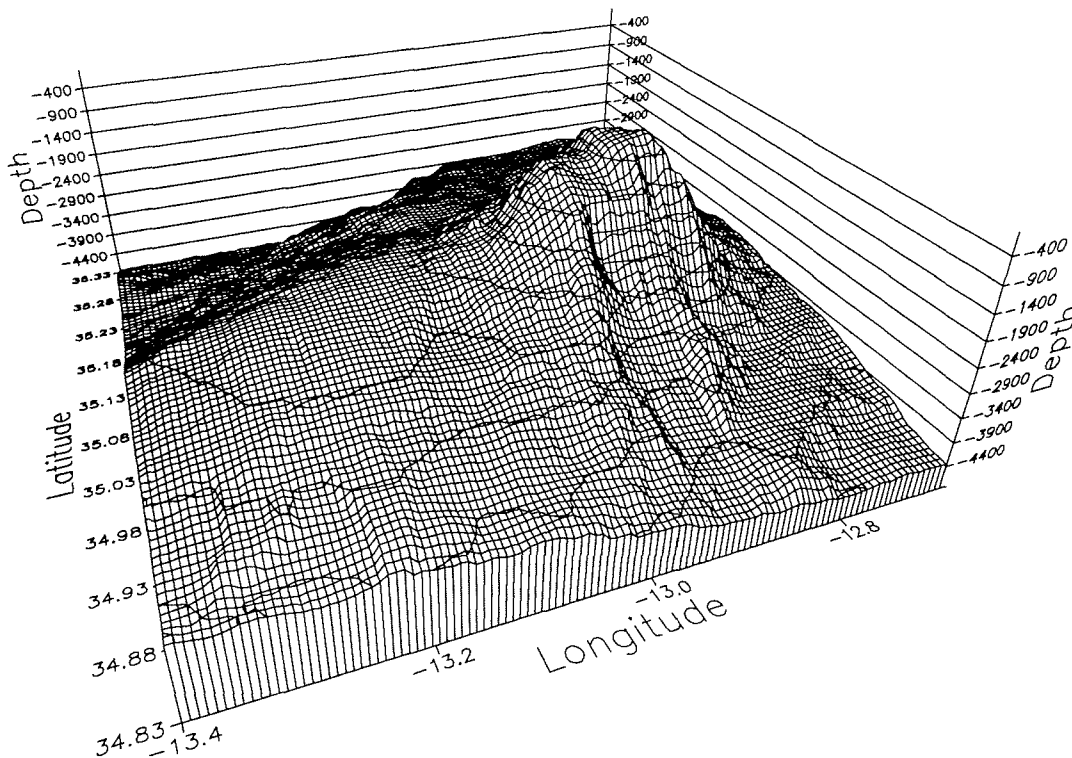


Fig. 4.8: Perspektivansicht des Ampère Seamount. (Aspect of the Ampère Seamount)



4.2. Sedimentechographie M. Rehfeldt

Seit der Installation des Parasound Systems im Frühjahr 1989 und der komplexen Inbetriebnahme im Rahmen der Expeditionen ANT-VIII/1, ANT-VIII/3 und ANT-VIII/6 steht auf FS "Polarstern" ein leistungsfähiges, hochauflösendes Sedimentecholot einschließlich einer digitalen Datenerfassung zur Verfügung. Im folgenden Abschnitt soll die Anlage zunächst kurz vorgestellt werden. Anschließend werden ausgewählte Ergebnisse diskutiert und Betriebserfahrungen sowie aufgetretene Probleme dargestellt.

Die Parasound-Anlage auf FS "Polarstern"

Das auf FS "Polarstern" installierte Sedimentecholot besteht aus folgenden Systemkomponenten:

- Echolot Atlas Parasound (PARAMetric sediment survey echoSOUNDer)
- Registriereinheit Atlas DESO 25
- Datenerfassungseinheit Hewlett-Packard HP3852A
- Steuerrechner Hewlett-Packard HP Vectra RS/25C
- Drucker Hewlett-Packard HP PaintJet
- Magnetbandlaufwerk 1/2 "

Das Parasound-Echolot ist ein niederfrequentes (2.5-5.5 kHz), hochauflösendes Sedimentecholot. Es werden gleichzeitig zwei hochfrequente Schallimpulse ($f_1=18$ kHz, $f_2=20.5 \dots 23.5$ kHz) hoher Leistung abgestrahlt. Aufgrund von Nichtlinearitäten in der Wassersäule kommt es zur Mischung dieser beiden Frequenzen (parametrischer Effekt); es entsteht die niederfrequente Differenzfrequenz (f_2-f_1) sowie die hochfrequente Summenfrequenz (f_1+f_2). Die Differenzfrequenz erlaubt eine gute Eindringung in die Sedimente, da die Dämpfung im Sediment mit steigender Frequenz zunimmt. Der Vorteil gegenüber herkömmlichen 3.5 kHz-Systemen besteht darin, daß die Differenzfrequenz mit dem gleichen Öffnungswinkel von ca. 4° abgestrahlt wird wie die beiden Primärfrequenzen. Dadurch wird eine wesentlich bessere horizontale Auflösung erreicht. Der Durchmesser der beschallten Fläche auf dem Meeresboden beträgt ca. 7% der Wassertiefe im Vergleich zu ca. 36% bei 3.5 kHz-Loten.

Während des Betriebes der Anlage ist durch geeignete Wahl der Parameter eine Optimierung der Ergebnisse in Hinblick auf erreichbare Eindringung in das Sediment (tiefster dargestellter Reflektor) sowie erzielbare vertikale Auflösung (Trennung dicht benachbarter Reflektoren) möglich. Je kleiner die Frequenz, desto kleiner ist die Dämpfung im Sediment und desto größer wird die mögliche Eindringung. Gleichzeitig besitzen niederfrequenter Schallimpulse eine größere Wellenlänge ($f = 2.5$ kHz - $\lambda = 0.60$ m; $f = 5.5$ kHz - $\lambda = 0.27$ m), was zu einer Verschlechterung der vertikalen Auflösung führt. Zwischen beiden Kriterien ist ein Kompromiß zu finden.

Ein weiteres Kriterium für die Frequenzoptimierung ist das Frequenzspektrum der Störsignale. Eine wesentliche akustische Störung während des Stationsbetriebes stellt das Bugstrahlrudern dar (Spieß et al., 1990). Ein Großteil der Störleistungen liegt dabei im Bereich um 2.8 kHz, sodaß es günstig ist, auf höhere Frequenzen auszuweichen. Desweiteren ist der erreichbare Störabstand wesentlich von den Nutzsignalamplituden abhängig. Bei Sedimenten mit geringen Reflexionskoeffizienten, wie sie im Bereich der Polarfront anzutreffen sind, machen sich diese Störungen recht deutlich bemerkbar. Deshalb wurden Stationsregistrierungen soweit wie möglich bei abgeschalteten Querstrahlrudern vorgenommen. Durch die Veränderung der Impulsdauer lassen sich ebenfalls Eindringung und Auflösungsvermögen beeinflussen. Eine höhere Pulszahl vergrößert die abgestrahlte Energie und bewirkt eine tiefere Eindringung in das Sediment. Durch das längere Signal verschlechtert sich zwangsläufig die mögliche vertikale Auflösung (und umgekehrt).

Die Registriereinheit DESO 25 dient der kontinuierlichen Aufzeichnung der empfangenen Echosignale. Dabei werden die Signalamplituden durch unterschiedliche Graustufen dargestellt. Zusätzlich werden regelmäßig Zeitmarken eingeblendet und in größeren Abständen Datum, Uhrzeit, Position und alle wesentlichen Systemparameter (Frequenz, Pulse, TVC, Mode) ausgegeben.

Mit Hilfe der Datenerfassungseinheit HP3852A werden das parametrische Echo, die Einhüllende des Echos sowie das NBS-Echo mit 40 kHz abgetastet, digitalisiert und stehen dann einer weiteren digitalen Verarbeitung zur Verfügung. Die Synchronisierung der Datenerfassung erfolgt mit ausgewählten Parasound-Triggersignalen. Über eine HP-Interface-Bus Schnittstelle

gelangen die digitalen Daten an den Steuerrechner. Über ein serielles Interface stehen auch die wichtigsten Einstellungen der Parasound-Anlage (Frequenz, Pulszahl, Tiefenfenster,...) sowie die Positions-, Kurs- und Wassertiefendaten aus dem INDAS-Schiffsdatennetz zur Verfügung. Das Programm "PARADIGMA" realisiert die Weiterverarbeitung der o.g. Daten. Dabei laufen im Wesentlichen die folgenden Prozesse ab:

- Einlesen der digitalen Seismogramme
- Decodieren, Plotten und Speichern der Seismogramme
- Einlesen und Darstellen der Parasound- und INDAS-Daten
- Plotten und Speichern des Schiffskurses
- Druckerprotokoll mit Uhrzeit, Kursdaten, Wassertiefen und Parasound
- Daten

Bei allen Einzelprozessen lassen sich eine Vielzahl von Parametern variieren bzw. sie lassen sich an- und abschalten. Nähere Informationen sind im Handbuch zum Programmsystem zu finden.

Die Datenspeicherung erfolgt im SEGY-Format zunächst auf der Festplatte des Steuerrechners. Aufgrund der geringen Zugriffszeit lassen sich Registrierabstände von minimal 1 s erzielen, was einem horizontalen Lotabstand von ca. 5 m entspricht. Günstige Werte liegen bei 5-10 s (entsprechend 25-50 m). Die registrierte Seismogrammlänge läßt sich von 10 bis 100% des eingestellten Tiefenfensters (i.a. 200 m) variieren. Bei einem Registrierabstand von 10 s und 200 m Fensterlänge werden pro Tag etwa 100 MByte Daten aufgezeichnet. Dementsprechend ist täglich ein Backup der Festplatte auf ein Magnetband vorzunehmen, was ca. 25 - 30 min in Anspruch nimmt und zu einer Unterbrechung der Aufzeichnung führt.

Ergebnisse der Sedimentechographie

Parasound wurde unmittelbar nach dem Auslaufen aus Kapstadt in Betrieb genommen und im gesamten Arbeitsgebiet dank der Unterstützung vieler freiwilliger Wachgänger kontinuierlich betrieben. Aufgrund der unterschiedlichen Morphologie sind auch die Ergebnisse von unterschiedlicher Qualität. In Gebieten mit geringer Bodentopographie, wie z.B. am Kontinentalhang oder im Kap- und Angolabecken, waren kontinuierlich gute Registrierungen möglich. Bei Hangneigungen, die größer als der Öffnungswinkel der Schallkeule waren, besteht das empfangene Signal nur noch aus dem an geometrisch kleinen Unebenheiten zurückgestreuten Signal mit sehr kleinen Amplituden. In Gebieten mit solcher Morphologie, wie z.B. in der Romanche Fracture Zone, sind nur noch abschnittsweise Registrierungen möglich. Auch eine korrekte digitale Tiefenbestimmung mit Parasound gelang dann nicht mehr, es mußte zur Nachführung des Tiefenfensters auf die Hydrosweep-Tiefen zurückgegriffen werden. Insgesamt wurde in sehr unterschiedlichen Wassertiefen gearbeitet, die von einer geringsten Tiefe von ca. 65 m auf der Spitze des Ampere-Seamounts bis zu über 5000 m im Kao Becken reichten. Fig.9 zeigt ein ausgewähltes Ergebnis der Parasound-Analogaufzeichnungen sowie ein digitales Amplitudenplot.

Porzellanit-Reflektor auf dem Südwest-Indischen Rücken.

Im nördlichen Hangbereich des Südwest-Indischen Rückens nördlich der Insel Bouvet war schon mehrfach in den sedimentechographischen Aufzeichnungen von Polarstern ein sehr intensiver akustischer Reflektor in den dort dominierenden Diatomeenschlämmen festgestellt worden. Nachdem vor allem bei den Bohraktivitäten des Ocean Drilling Programs in der Antarktis

mehrfach Funde von Porzellanit in Diatomeenschlammern bekannt wurden, lag die Vermutung nahe, daß der Reflektor eine Porzellanitschicht darstellt. Porzellanite in unverfestigten Diatomeen-Schlammern bilden aufgrund ihrer hohen Dichte hervorragende akustische Reflektoren in den sedimentechographischen Aufzeichnungen (Kap. 5.3.3). Nach 3.5 kHz-Aufzeichnungen von ANT-IV/4 wurde schon für eine Kernbeprobung während der Expedition ANT-VIII/3 eine Position ausgewählt, wo dieser Reflektor bis ca. 10 m an die Sedimentoberfläche heranreichte. Der auf der Sta. PS1770-1 gewonnene Schwerelotkern (ANT-VIII/3) konnte diesen Reflektor nicht beproben, da nur eine Eindringung von 7,40 m erreicht wurde.

Während ANT-IX/4 sollte im Umfeld der ANT-VIII/3-Sta. PS1770 mittels PARASOUND-Matratzenfahrt eine Position gefunden werden, an der eine Beprobung des Reflektors in geringerer Sedimenttiefe möglich erschien. Die Suchfahrt, deren Kursroute nach den vorhandenen sedimentechographischen Aufzeichnungen und den bathymetrischen Informationen gewählt wurde, erbrachte lediglich eine Position in einer leichten morphologischen Depression, wo der Reflektor in ca. 8 m Sedimenttiefe lag (Fig. 4.10). Die Sta. PS2089 wurde ausgewählt und der Kolbenlotkern PS2089-2 enthielt eine Porzellanitschicht (siehe Kap. 5.3.3).

Frequenz-Variationen

Auf 4 ausgewählten Stationen (PS 2076, PS 2081, ODP 704, PS2102) wurden Frequenzvariationen durchgeführt. Dazu wurden bei Frequenzen von 2.5 - 5.5 kHz und Pulslängen von 1 und 4 Schwingungen jeweils 2 Minuten registriert. Um die bereits diskutierten Störungen möglichst gering zu halten, erfolgten die Messungen bei abgeschalteten Querstrahlrudern. Ein erstes Ergebnis in Form der Parasound-Analogregistrierung und der zugehörigen Amplitudenplots zeigt Fig.4.11. Deutlich erkennbar ist das unterschiedliche Hintergrundrauschen (Maschinengeräusche), welches bei höheren Frequenzen kleiner wird. Dies deutet auf ein Störspektrum, das ein Maximum bei kleineren Frequenzen besitzt. Die erzielte Auflösung, besonders im oberflächennahen Bereich, ist bei kurzen Signalen (1 Puls) wesentlich besser gegenüber einer Pulslänge von 4, allerdings auf Kosten der erreichbaren Eindringtiefe. In weiteren Auswertungen sollte eine Korrelation zwischen den Seismogrammen und sedimentphysikalischen Parametern der Kerne vorgenommen werden.

Fig.4.9: Parasound-Beispiel für extrem große Eindringtiefe (bis 200 m)
49°44'S; 3°5'W (Parasound record with high penetration depth (up
to 200 m) 49°44'S; 3°5'W)

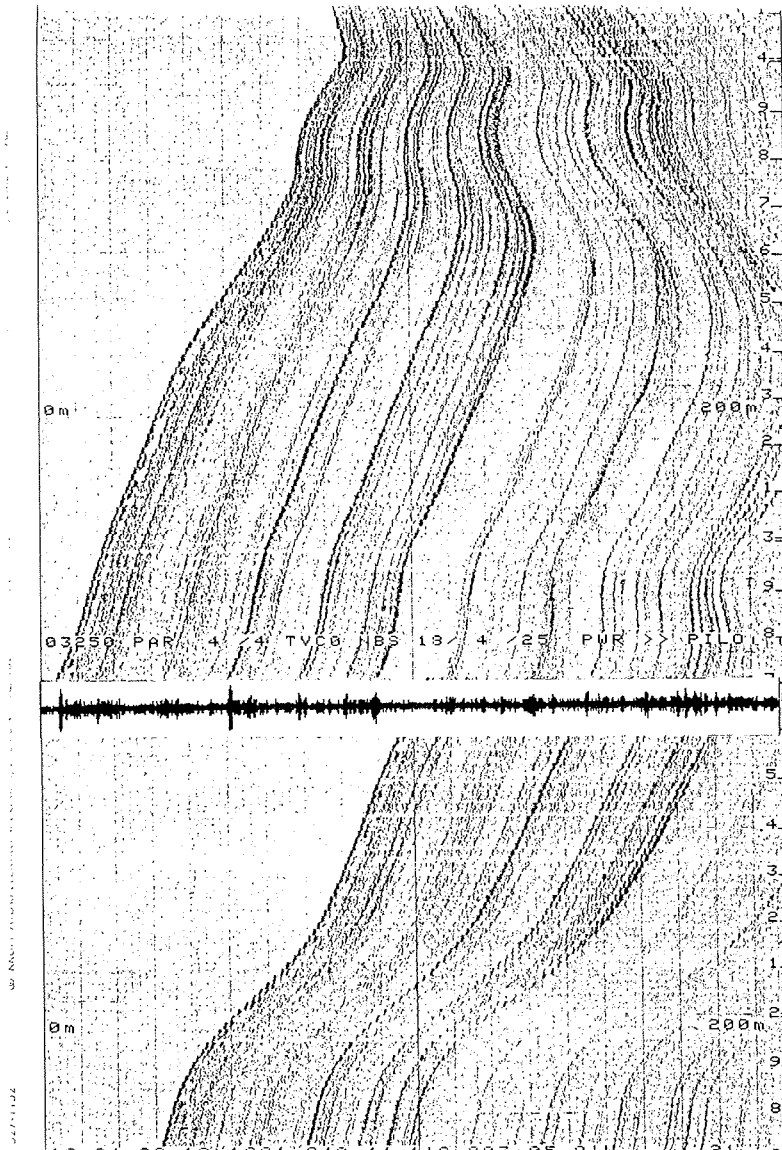


Fig. 4.10: Parasound-Aufzeichnung im Bereich der Sta. PS2089 (Parasound record close to Sta. PS2089)

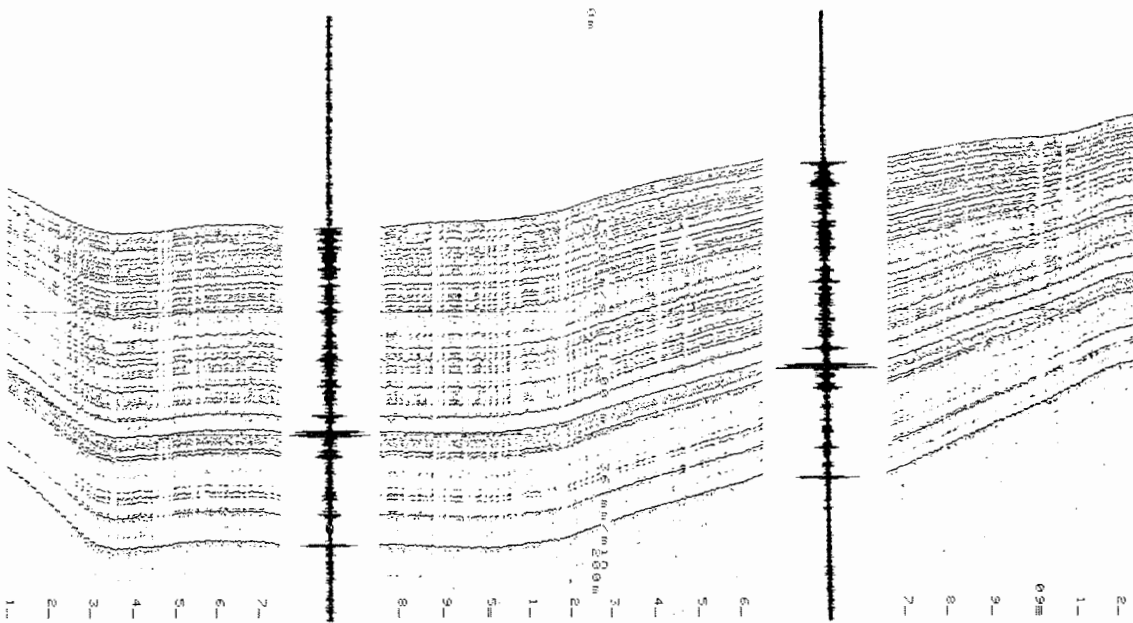
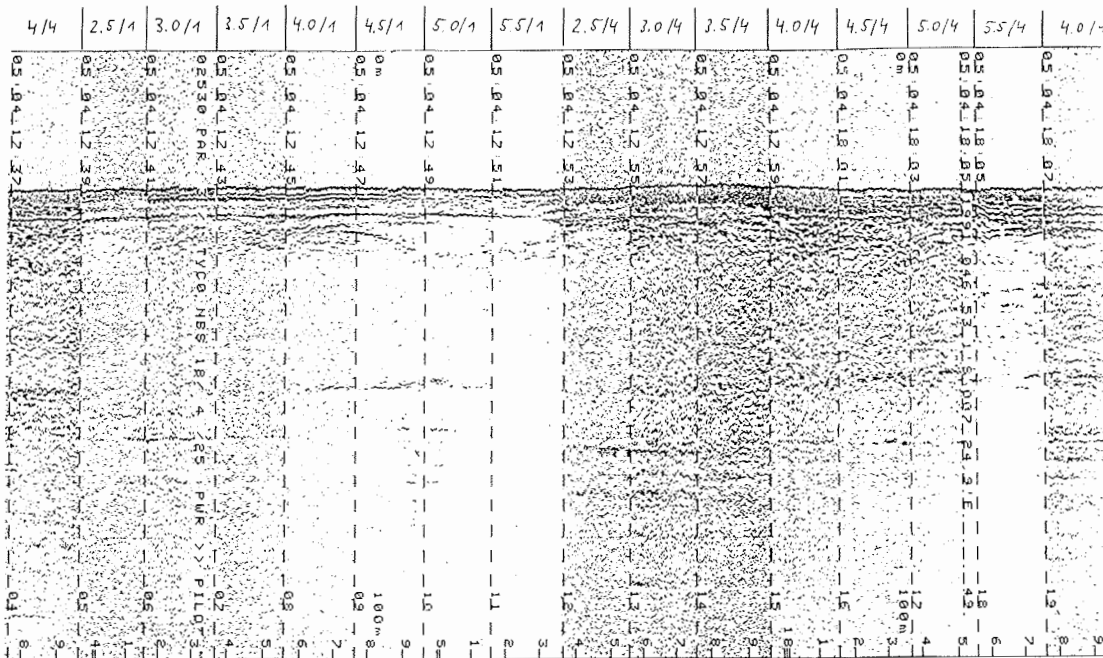


Fig.4.11: Frequenzvariation auf Sta. ODP 704 (46°53'S; 7°25'E) (Frequency variation at Sta. ODP 704 (46°53'S; 7°25'E))



Betriebserfahrungen und Probleme

Insgesamt kann eingeschätzt werden, daß das Parasound-System zufriedenstellend gearbeitet hat und keine größeren Störungen aufgetreten sind. Kleinere Probleme werden im Folgenden kurz aufgelistet:

1. Totalausfall des DESO 25; Getriebe blockiert aufgrund von eingeklemmten Papierresten, Gerät wurde komplett gewechselt und repariert
2. DESO 25 zeigt fast ständig Error 66 an; es konnte keine Funktionsbeeinträchtigung festgestellt werden
3. DESO 25 zeigt wiederholt Error 64 an; Blockieren der seriellen Schnittstelle und keine Tiefenwerte an Echoscope und INDAS; Fehler konnte durch Aus- und Einschalten behoben werden
4. INDAS zeigt keine PS- und HS-Tiefen mehr an; Fehler wurde durch kurzzeitiges Ziehen eines Steckers an der DEV-Anlage behoben
5. Parasound zeigt falsche digitale Tiefen; die Tiefen lagen meist unmittelbar hinter dem Beginn des Tiefenfensters und stimmten nicht mit der Lage der Echosignale überein; Fehler trat wiederholt und über längere Zeiträume auf und konnte weder durch manuelles Nachführen des Tiefen-Suchfensters noch durch handgeregelt Verstärkung des entsprechenden Kanals zufriedenstellend beseitigt werden
6. Es treten asynchrone Störungen durch ein Fremdlot (Navigationslot) auf; Störsignale sind auf dem Echoscope deutlich, aber auf der DESO-Registrierung kaum zu erkennen
7. Nicht reproduzierbare Abstürze des Paradigma-Programmes; insbesondere bei Manipulation des Kursplots brach das Programm mit einem Laufzeitfehler ("psplot.for, run-time error F6099 Integer overflow" bzw. "Filename missing or blank UNIT 101") ab

5. **MARIN-GEOLOGISCHE UND SEDIMENTPHYSIKALISCHE ARBEITEN**

5.1. **Geräteinsatz und Probennahme**

G. Bohrmann, C. Klindworth, T. Kuhn, N. Lensch, A. Mackensen,
R. Petschick, (AWI) G. Ruhland (FGB)

Multicorer, Kastengreifer

Zur Beprobung von ungestörten Sedimentoberflächen nebst überstehendem Bodenwasser wurde der Multicorer (MUC) mit 12 Rohren von je 6 cm Durchmesser auf 32 Stationen eingesetzt. Nur einmal wurde zusätzlich auf Sta. 2079 ein Großkastengreifer gefahren, da hier vermutlich sandige, nicht bindige Sedimente eine erfolgreiche Beprobung mit dem MUC nicht zugelassen hatten. Jedoch auch der Einsatz des GKG brachte nicht den erhofften Erfolg. Von 32 Einsätzen des MUC blieben vier erfolglos, zwei davon vermutlich wegen stark sandigen, nicht-bindigen Sediments, einmal (PS 2100-1) wegen extremer topographischer Bedingungen (Fig.4.12). Auf allen Stationen wurde zusammen mit dem MUC eine Festspeicher-CTD eingesetzt, so daß vollständige potentielle Temperatur und Salinitätsprofile vorliegen (vgl.Kap. 6.1.).

In der Regel wurden auf jeder Sta. 4-5 der gewonnenen MUC-Kerne sofort nach Bergung der Kerne für die Bearbeitung der Foraminiferenfaunen beprobt und konserviert (vgl. Kap. 5.4.2.). Zusätzlich wurden 2 Kerne für die Untersuchung der Radiolarien und Diatomeen beprobt (vgl. Kap. 5.4.1.). 1-2 Kerne wurden bei -28°C tiefgefroren und für sedimentologische Unter-

suchungen archiviert. Desgleichen wurde ein Kern zur weiteren geochemischen Bearbeitung tiefgekühlt (vgl. Kap. 4.2.). Auch das überstehende Bodenwasser wurde zur Bestimmung der stabilen Isotopenzusammensetzung des gelösten CO₂ unmittelbar nach Bergung des MUC beprobt, konserviert und versiegelt (vgl. Kap.5.4.2.).

Schwerelot, Kolbenlot

Während ANT-IX/4 wurden 23 Sedimentlote eingesetzt, wobei 21 Einsätze erfolgreich waren und eine Gesamtkernlänge von ca. 190 m erbrachten (Stationsliste, Anhang, 10.1.). Die Kerne wurden auf dem Arbeitsdeck von Polarstern in Segmente von einem Meter und weniger zerteilt und danach vorwiegend bei 4°C gelagert und transportiert. Von den Schnittstellen der Kernsegmente wurde vor dem Verschließen mit Endkappen ein Smearslide für die sedimentpetrographische Bearbeitung angefertigt. Eine mikropaläontologische Beprobung des Kernfängers wurde zur stratigraphischen Einstufung der Sedimentkernbasis eines jeden Lotes durchgeführt (siehe Kap. 5.5.). Während das Schwerelot vorwiegend zur Kernung von Beckensedimenten benutzt wurde, kam das Kolbenlot meist auf den submarinen Rücken, bei karbonatischen Ablagerungen zum Einsatz. Je nach zu erwartender Eindringtiefe des Lotes wurden 1-3 Kernrohre von je 5 m Länge (entsprechend 5, 10 und 15 m Gesamtkernrohrlänge) gewählt. Eine Übersicht der benutzten Kernrohrängen und der Kerngewinne der einzelnen Sedimentlote vermittelt die Fig. 4.13.

Schwerelot (SL)

Bei 13 Schwereloteinsätzen wurden 9 mal 15 m, 2 mal 10 m und 2 mal 5 m Rohrlänge benutzt (Fig. 4.13). An 11 erfolgreichen Schwerelotstationen konnten insgesamt ca. 100 Sedimentkernmeter gewonnen werden (= 60% Kerngewinn). Lediglich auf 2 Stationen war der Schwereloteinsatz erfolglos. Auf Sta. PS2105-1 war das Kernrohr zwar ins Sediment eingedrungen, allerdings hatte sich beim Herausziehen des Lotes die Apfelsine im Kernfänger nach außen verbogen, so daß beim Hieven das bereits gekerntete Sediment nicht gehalten werden konnte. Ebenfalls keinen Kerngewinn erbrachte die Sta. PS2106-3 auf dem Discovery Seamount. Geringe Restsedimente im Kernfänger belegen einen ehemals gekernteten Foraminiferensand, der wohl aufgrund seiner geringen Bindigkeit während des Hievens ausgewaschen wurde. Auf der Sta. PS2086-1 wurde das Kernrohr wegen zu geringer Eindringung vom Gewichtsträger (1,5 t) abgeknickt.

Kolbenlot

Der Einsatz des Kolbenlotes war auf allen 10 Stationen erfolgreich, wobei 9 mal 15 m Kernlänge benutzt wurde (Fig. 4.13; Stationsliste Anhang, 10.1.). Auf dem Seamount südlich des Meteor Rückens auf der Sta. PS2109-1 wurde das Kolbenlot mit nur 10 m Rohrlänge eingesetzt. Die zu geringe Eindringung des Lotes (ca. 4 m) führte allerdings dort zu einer Verbiegung des Kernrohres. Insgesamt konnten ca. 90 Sedimentkernmeter (= 61% der eingesetzten Rohrlänge) geborgen werden. Der Pilotcorer hat bei den wenigsten Einsätzen einen zufriedenstellenden Kerngewinn erbracht (siehe Stationsliste, Anhang, 10.1). Häufig hat der Verschlußmechanismus nicht funktioniert und ein Großteil des Sedimentes wurde beim Hieven ausgespült.

Fig. 4.12: Übersicht der Kerngewinne (cm) der Multicorer- und Kastengreifereinsätze (Core recovery (cm) of multicorer and boxcorer)

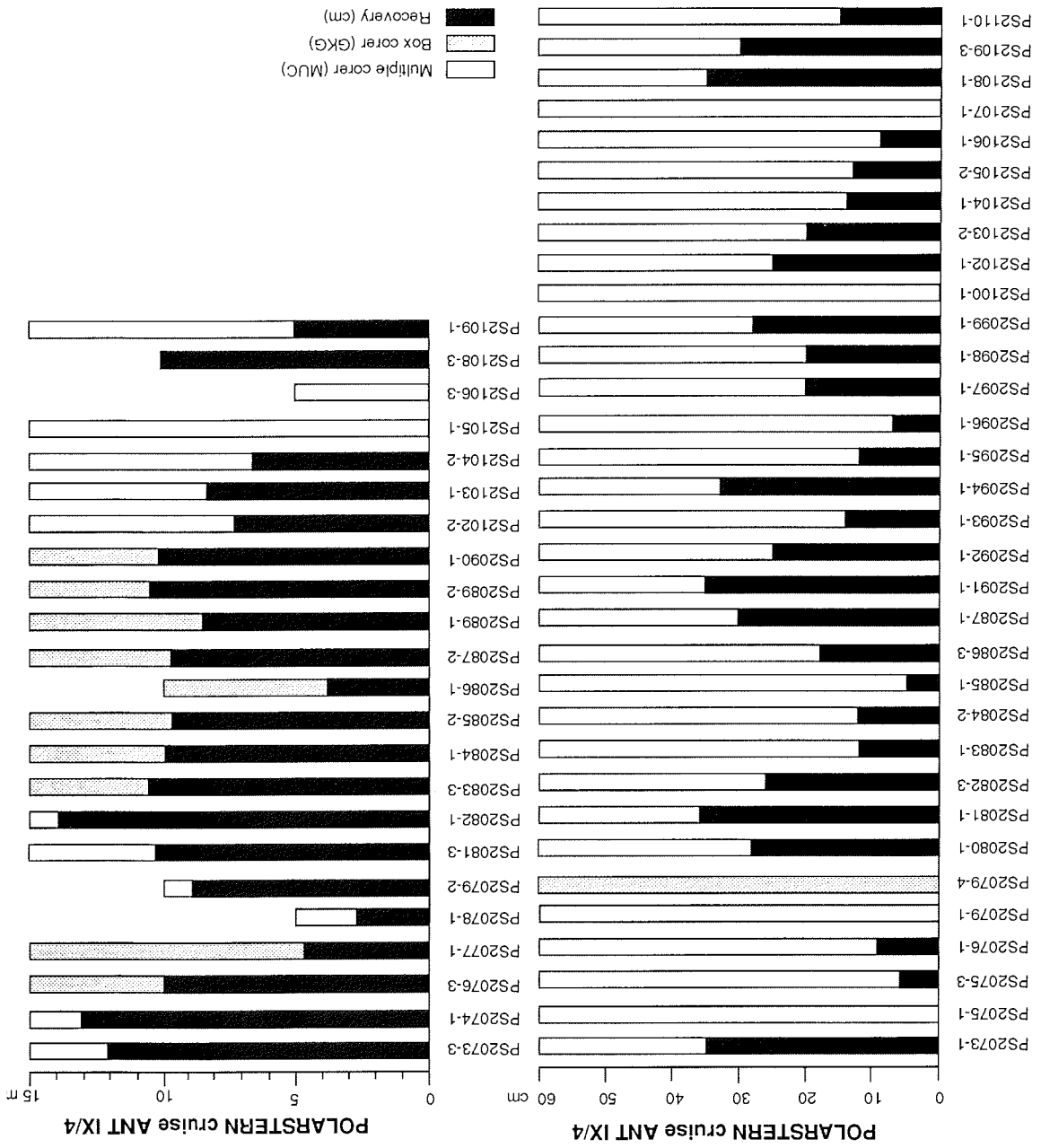


Fig. 4.13: Übersicht der benutzten Kernohrlängen und erzielten Kerngewinne in m bei Scherlot- und Kolbenlot-Einsätzen. (Length of core barrel and core recovery (m) of gravity corer and piston corer.)

5.2. Sedimentphysikalische Untersuchungen

T. Krüger, R. Petschick (AWI)

5.2.1. Messung der magnetischen Suszeptibilität

Die magnetische Suszeptibilität ist ein Maß für die Magnetisierbarkeit einer Materie. Sie ist eine stoffspezifische Größe und direkt abhängig von dem Anteil magnetisierbarer Komponenten in einer Substanz. Damit kann die Messung der Suszeptibilität an ungeöffneten Sedimentkernen Aufschluß über wechselnde Anteile an magnetischen Mineralen (z.B. Magnetit, Maghemit) geben, wie sie z.B. durch einen Eintrag von vulkanischen Aschen, durch terrigene Komponenten z.B. durch IRD (eistransportiertes Material = "ice rafted debris") gegeben ist.

Sedimentkerne innerhalb des subpolaren Südatlantik können charakteristische Suszeptibilitätsschwankungen aufweisen, die durch wechselnde Sedimentationsverhältnisse zwischen Glazial und Interglazial hervorgerufen werden. In den Glazialen ist von einer verstärkten Anlieferung an basischen Vulkanitgeröllen auszugehen. Dagegen sind in den Interglazialen bevorzugt biogene Sedimente mit nur geringen Anteilen an magnetisierbaren Substanzen abgelagert worden. Somit können Suszeptibilitätskurven als ein stratigraphisches Hilfsmittel als auch für die lithostratigraphische Korrelation der Kerne untereinander eingesetzt werden.

Methodik

Die Messung der Volumensuszeptibilität (im folgenden Suszeptibilität genannt) erfolgte an den ungeöffneten Kernsegmenten mit Hilfe eines Magnetic Susceptibility Meter MS2 der Fa. Bartington und einem dazugehörigen Core Logging Sensor. Der Sensor produziert bei einer Frequenz von 0.565 kHz ein magnetisches Wechselfeld, welches beim Einbringen einer Probe gestört wird. Die resultierende Frequenz wird von dem Magnetic Susceptibility Meter auf die magnetische Suszeptibilität umgerechnet und digital angezeigt.

Die Segmente wurden auf einem Schlitten durch die Meßspule geschoben, wobei in einem Abstand von jeweils 1 cm eine Messung durchgeführt wurde. Die Steuerung der Schlittenbewegung sowie die anschließende Meßdatenerfassung erfolgte mit Hilfe eines PC's. Die erreichte Auflösung betrug 10⁻⁵ SI-Einheiten. Auf Grund des hohen Störpegels durch das Schiff konnte die Meßempfindlichkeit nicht höher gewählt werden.

An Bord wurde noch keine detaillierte Datenbearbeitung vorgenommen. Die durch die Meßanordnung bedingte gleitende Mittelwertbildung führt zu einer "Verwischung" der scharfen Schichtgrenzen; diese können erst bei einer späteren Datenaufarbeitung teilweise wieder rückgängig gemacht werden.

Ergebnisse und Diskussion

Die Kerne aus dem Kap-Becken, dem Agulhas-Rücken und dem Agulhas-Becken sowie aus dem Bereich des Meteor-Rückens (PS2073-3 bis PS2087-2) lieferten nur sehr geringe Suszeptibilitätswerte. Sie liegen zum Teil unterhalb der Nachweisgrenze, sodaß hierfür eine Nachmessung im Labor bei einer höheren Empfindlichkeit erforderlich ist. Die an Bord erzielten Ergebnisse lassen die Aussage zu, daß es sich um feinterrigene und biogenreiche

Sedimente handelt, in denen sich nur selten episodisch verstärkte Einträge von magnetisierbaren Material nachweisen lassen.

Die Suszeptibilitätsprofile der Kerne aus dem Gebiet nördlich von Bouvet Island (PS2089-1, -2, PS2090-1) und dem Bereich des Mittelatlantischen Rückens (PS2102-2, PS2103-1 und PS2104-2) zeigen dagegen charakteristische Intensitätsmuster, die auf Schwankungen in der Sedimentation von magnetisierbaren Komponenten hinweisen.

Ein gutes Beispiel hierfür liefert der an Bord geöffnete Schwerelotkern PS2102-2 (Fig. 4.14). Für diesen Kern ist ein vorläufiges Alter von maximal 200.000 a festgelegt worden (vgl. Kap. 5.5.), was eine gute Auflösung der letzten Klimazyklen erwarten läßt. Die Kurve weist tatsächlich jeweils zwei Abschnitte mit erhöhten Suszeptibilitätswerten auf. Die Bereiche mit niedrigen Werten korrelieren dabei mit den Diatomeenschlämmen der Warmzeiten. Die hier periodisch auftretenden Schwankungen sind apparativ bedingt. Die Abschnitte mit hohen Suszeptibilitäten decken sich mit Terrigen- und vulkanogenen IRD-reichen und Diatomeen-ärmeren Sedimenten der Kaltzeiten. Einzelne hierin auftretende Maxima stellen sandige Lagen mit besonders hohen IRD-Anteilen dar.

Unter Berücksichtigung, daß innerhalb des Kernes keine Schichtlücken auftreten, wurde bei PS2102-2 danach wahrscheinlich eine Abfolge vom Holozän bis zur vorletzten Kaltzeit erfaßt (= Sauerstoffisotopen-Stadium VI). Das Holozän liegt dabei in einer besonders großen Mächtigkeit von über 3 Metern vor.

Ein Beispiel für die Möglichkeit der Korrelation von geographisch benachbarten Kernen zeigt der Vergleich der Suszeptibilitätskurven der beiden Kolbenlotkerne PS2089-1 und PS2089-2 (Fig. 4.15), die an gleicher Station beprobt wurden. Von PS2089-2, welcher bereits an Bord geöffnet wurde, liegt eine Kernlogbeschreibung vor. Die Wechsel in der Lithologie und Suszeptibilität dieses Kernes sind ebenfalls auf Klimaschwankungen zurückzuführen, wobei sich hierin offenbar mindestens drei Glaziale und zwei Interglaziale zeigen. Die vorläufige Korrelation der Intensitätsmaxima beider Kerne zeigt dabei eine sehr gute Übereinstimmung, wenn davon ausgegangen wird, daß PS2089-1 in den oberen drei Metern eine jüngere Sedimentfolge enthält, die im Parallelkern fehlt. Dies wird bestätigt durch die mit Hilfe der Parasound-Echographie für den harten Reflektor des Porzellanites erwartete Kerntiefe von ca. 8 m, welcher in PS2089-2 jedoch bereits in einer Tiefe von 6 m auftrat. Falls der Kern PS2089-1 ebenfalls einen Porzellanit in gleicher Position enthält, ist dieser bei ca. 7,6 m zu erwarten.

Es fällt weiterhin auf, daß die warmzeitlichen Abschnitte beider Kerne trotz ihrer kurzen Distanz unterschiedlich mächtig sind.

5.2.2. Messung des elektrischen Widerstandes

An Bord wurde neben der Suszeptibilität auch die elektrische Leitfähigkeit aller Kerne gemessen. Diese ist abhängig von der Porosität und dem Wassergehalt der Proben. Eine Auswertung der Daten wird erst später erfolgen; auch hiervon werden Beiträge zur sedimentphysikalischen und lithologischen Interpretation der Kerne erwartet.

Fig. 4.14: Die magnetische Volumenssuszeptibilität im Profil von Kern PS2102-2.
(Magnetic susceptibility profile of core PS2102-2.)

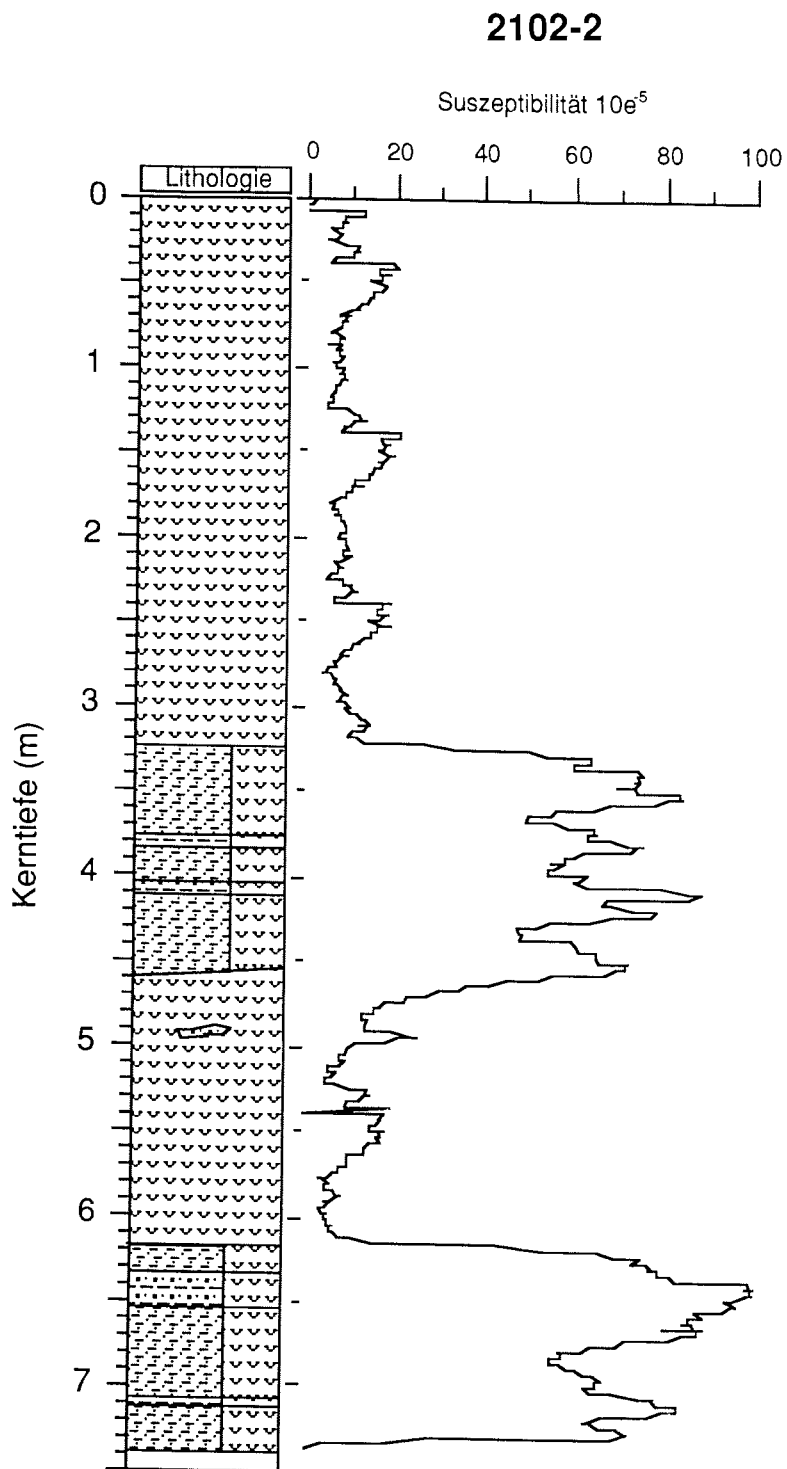
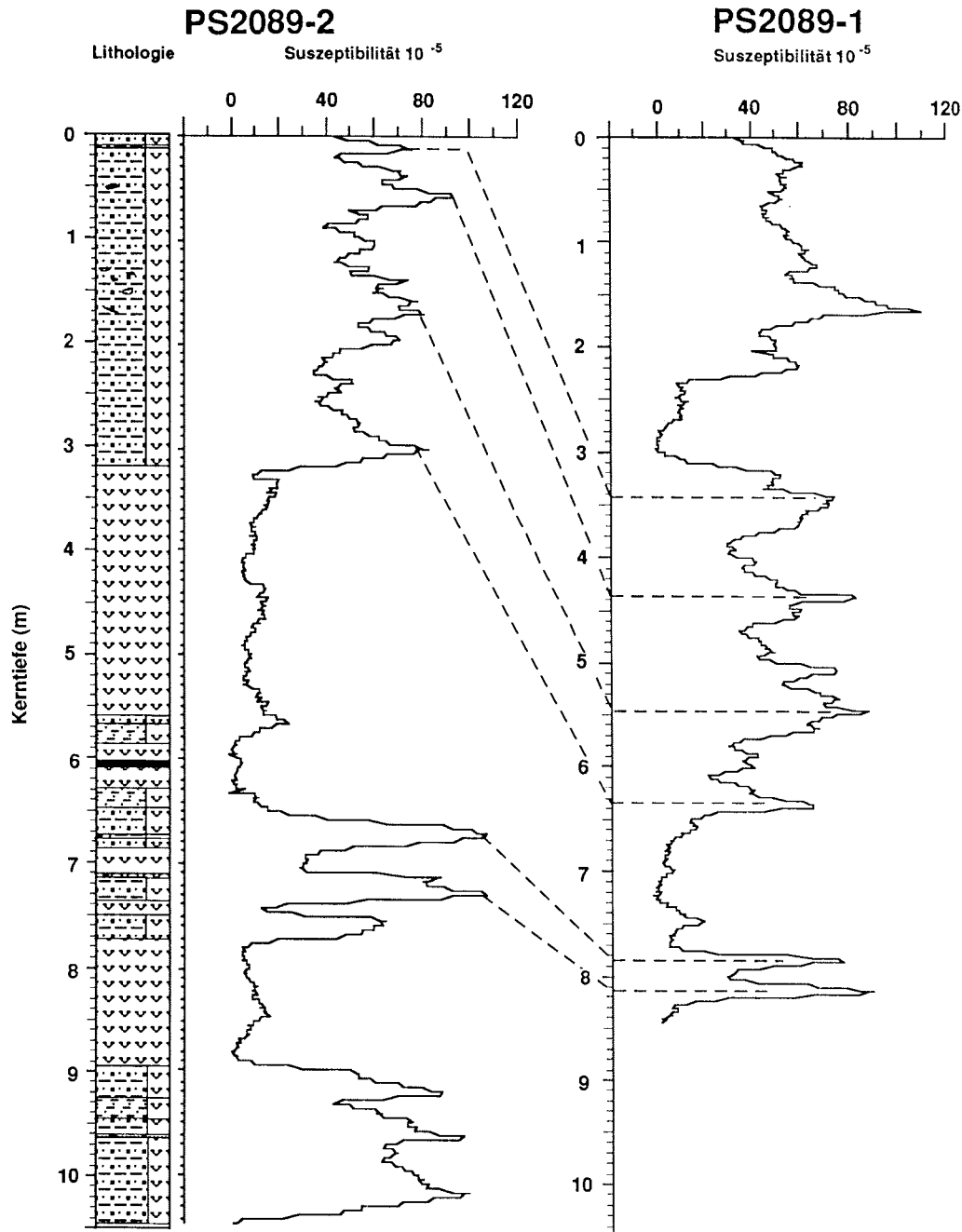


Fig. 4.15: Die magnetische Volumenssuszeptibilität der Kerne PS2089-1 und PS2089-2 und Korrelation korrespondierender Suszeptibilitätsmaxima. (Magnetic susceptibility of PS2089-1 and PS2089-2 and correlation of corresponding susceptibility maxima.)



5.3. Sedimentologische Untersuchungen

Die sedimentologischen Analysen an dem gewonnenen Kern- und Oberflächensediment-Material dienen zusammen mit den mikropaläontologischen und isotopegeochemischen Untersuchungen der Rekonstruktion paläozeanographischer Parameter, wie Paläoströmung, Paläotemperatur und Paläoproduktivität im Wechsel von Glazial-/Interglazial-Zeiten. Neben der Bestimmung der Korngrößen (Kies/Sand/Silt/Ton), der Karbonat- und Corg-Gehalte werden sedimentphysikalische Parameter wie Porosität und Feuchtraumdichte gemessen. Mittels Röntgendiffraktometrie werden Tonmineralzusammensetzung, Quarz-, Feldspat- und Opalgehalte bestimmt.

5.3.1 Beprobung von Sedimentkernen

G. Bohrmann, A. Abelmann, H.-W. Hubberten, C. Klindworth, T. Kuhn, N. Lensch, A. Mackensen, R. Petschick, U. Zielinski (AWI)

Während des Fahrtabschnittes ANT-IX/4 konnten 3 Schwerelotkerne (PS2074-1, PS2082-1, PS2102-2) und 6 Kolbenlotkerne (PS2070-1, PS2076-3, PS2082-1, PS2083-3, PS2084-1, PS2086-1, 2089-2) geöffnet und entsprechend den Bearbeitungsschwerpunkten beprobt werden (insgesamt ca. 87 Kernmeter). Mit Ausnahme von PS2070-1 (Maudkuppe, ANT-IX/3) waren alle Sedimentkerne während ANT-IX/4 gekernt worden. Nach dem Öffnen der Kernliner und der Säuberung der Sedimentoberfläche wurde das Kernprofil photographisch dokumentiert. Sedimentscheiben von ca. 0,5 cm Dicke wurden für Röntgenpräparate entnommen, um an Bord von allen 87 Kernmetern kontinuierlich Radiographien herzustellen. Die Radiographien dienen zur Untersuchung von Mikrogefügen sowie zur Quantifizierung von eistransportierten Detrituskomponenten (IRD) nach der Methode von Grobe (1987).

Von jedem Kern wurde eine makroskopische Sedimentbeschreibung angefertigt, (siehe Anhang, 10.2.). Dabei wurden neben der Farbeinstufung mittels der "Munsell Soil Color Chart" auch mikroskopische Smearslide-Analysen zur sedimentpetrographischen Einstufung benutzt. Die Einteilung in Sedimenttypen wurde nach einem am AWI gebräuchlichen Klassifizierungsschema für Tiefseesedimente durchgeführt (siehe Legende im Anhang, 10.2.). Alle geöffneten Kerne wurden meist in 10 cm oder 5 cm Abständen beprobt, entsprechend den vorher abschätzbaren Sedimentationsraten. Tab. 4.1 vermittelt einen Überblick über die Art der Proben und ihre Anzahl pro Kern. Proben für die paläomagnetische Alterseinstufung (Kunststoffboxen: 2.5 x 2.5 x 1.5 cm) wurden von 5 Kernen genommen. Die Proben für die Radiolarien- und Diatomeenbearbeitung (2 x 10 ml Spritzen in 50 ml Polystyrolbecher) wurden im Kern in gleicher Sedimenttiefe mit den Paläomagnetikproben genommen. Versetzt dazu wurde die sedimentologische Beprobung durchgeführt, bei der folgende 3 Subproben anfielen:

- 1.) Probe zur Bestimmung des Wassergehaltes, der Feuchtraumdichte, des Karbonat- und Corg-Gehaltes (5 ml Spritze in vorgewogenes Schnappdeckelglas),
- 2.) Probe (5 ml Spritze) für röntgendiffraktometrische Untersuchungen der Gesamtmineralogie (Opal-, Quarz-Gehalt, usw.),
- 3.) Korngrößenprobe (2 x 5 ml Spritze) zur Bestimmung des Kies/Sand/Silt/Ton-Verhältnisses und zur röntgendiffraktometrischen Tonmineralanalyse.

Zusätzlich wurde eine Grobfraktionsprobe genommen, die bei Schwerelotkernen aus der Kerntiefe der Sedimentologieprobe oder bei Kolbenlotkernen 1 cm versetzt dazu stammt. Die Grobfraktionsprobe wurde gleich an Bord über einem Sieb mit 63 mm Maschenweite geschlämmt und getrocknet, sodaß hieraus erste Foraminiferen für Isotopenmessungen bereits ausgelesen werden konnten.

Tab. 4.1: Liste von Probenart und -anzahl der an Bord geöffneten Sedimentkerne.

Proben	PS 2070-1	PS 2074-1	PS 2076-3	PS 2082-1	PS 2083-3	PS 2084-1	PS 2086 -1	PS 2089-2	PS 2102-2
Radiographien	X	X	X	X	X	X	X	X	X
Paläomagnetik	-	133	101	141	107	-	-	102	-
Radiolarien/ Diatomeen	87	133	101	142	108	122	75	104	73
Wassergehalt	88	139	111	159	107	122	75	108	73
Dichte/Kohlenstoff									
Gesamtmineralogie	88	139	111	159	107	122	75	108	73
Opalgehalt									
Korngrößen	-	139	111	159	107	122	75	108	73
Tonmineralogie									
Grobfraktion	88	139	111	159	105	122	75	108	72
Foraminiferen									
Isotope									

5.3.2 Sedimentbeschreibung

G. Bohrmann, R. Petschick (AWI)

Entsprechend der wissenschaftlichen Fragestellung wurden von den 21, während ANT-IX/4 gewonnenen Sedimentkernen, 8 ausgewählt und bereits an Bord geöffnet und beprobt. Die Karte in Fig. 4.16 gibt einen Überblick der Schwerelot- und Kolbenlot-Positionen. Eine Übersicht über die Hauptlithologien der geöffneten Kerne vermittelt Fig. 4.17. Entsprechend ihrer ozeanographischen Lage und ihrer Wassertiefe variieren die Hauptsedimenttypen erheblich.

Der nördlichste Sedimentkern **PS2074-1** stammt aus dem Kap-Becken ca. 30 Seemeilen nördlich der Steilstufe des Agulhas Rückens aus einer Wassertiefe von 4644 m (Fig. 16, 17 und 18). Der vorwiegend aus terrigenem Mud bestehende Kern enthält nur untergeordnet kalkige Biogene. Coccolithen und Foraminiferen zu wechselnden Anteilen sind häufiger in Kernabschnitten vorhanden, welche einheitlich als Calcareous Mud klassifiziert wurden. Calcareous Mud, welche sich gegenüber dem vorwiegend grauen bis dunkelgrauen Mud durch hellgraue Farbtöne auszeichnet, dominiert die oberen 3,5 m des Schwerelotkerns, während er darunter seltener und geringmächtiger wird (Fig. 4.17). Im tieferen Teil des Kernes sind solche Calcareous Mud-Lagen anhand ihrer Sedimentstrukturen in den Radiographien als Turbidite zu erkennen (Lamination, schwache Gradierung, scharfe Basis usw.; Fig. 4.17). Die Faunenanalyse einer relativ reinen Foraminiferen-Lage eines solchen Turbidites (Foraminiferal Ooze in 878-881 cm Tiefe), zeigte, daß ein Großteil der benthischen Foraminiferen aus einer Wassertiefe zwischen 1000-2000 m stammt (Mackensen, persönl. Mitteilung). Die Smearslide-Analysen dieses Kernes zeigen neben den durchweg vorhandenen Schwammnadeln kaum kieselige Biogene. Weitere Hinweise für Umlagerung von Komponenten bilden die gut gerundeten Glaukonite und

Echinodermenbruchstücke oder ältere Fossilien wie Actiniscidien. Die karbonatischen Biogene sind z.T. schlecht erhalten. Authigene Karbonat-Rhomboeder konnten ebenfalls beobachtet werden.

Der Kolbenlotkern **PS2076-3** wurde beim Überqueren des aseismischen submarinen Agulhas Rückens, nördlich der Agulhas Fracture Zone im Bereich der höchsten Erhebung in 2109 m Wassertiefe gekernt (Fig. 4.18). Entsprechend seiner Lage oberhalb der Calcitkompensationstiefe (CCD) handelt es sich um karbonatische Biogenschlämme, wobei vorwiegend weißer Foraminiferal Ooze mit hellgrauem Foraminiferal Mud wechsellagert (Fig. 4.17, Anhang, 10.2.). Opaline Gerüstbildner sind selten und werden nicht gesteinsbildend. Der Foraminiferal Ooze zeigt in den Smearslides signifikant höhere Gehalte an kalkigen Nannofossilien als der Foraminiferal Mud. Ein weißer, markanter Coccolithenschlamm (Nannofossil Ooze) ist zwischen 260-301 cm zu finden. Dropstones sind meist relativ klein (vorwiegend in der Sand- bis Feinkies-Fraktion) und nur vereinzelt zu finden. Sie dominieren meist in dem Foraminiferal Mud.

Deutlich höhere Anteile an kieseligen Skeletten enthalten die Sedimente von Kern **PS2082-1**, die über weite Bereiche als Diatomaceous Mud zu klassifizieren sind. Der fast 14 m lange Schwerelotkern stammt aus dem Agulhas Becken aus 4610 m Wassertiefe (Fig. 4.18). Die kieseligen Sedimente haben geringmächtige Einschaltungen von Calcareous Mud, die aufgrund der Coccolithenvorherrschaft meist als Nannofossil Mud bezeichnet werden können (Fig. 4.17, Anhang, 10.2.). Ein reiner Foraminiferen-Schlamm ist nur zwischen 6-19 cm zu finden. Oberhalb der Redox-Grenze, bei ca. 56 cm, sind in der oxischen Zone schwach braune Sedimentfarben zu finden, während darunter graue, häufig olivgraue Farben vorherrschen. Ein 5 cm mächtiger, gelblich brauner Fe/Mn-reicher Terrigenschlamm, dessen Obergrenze sehr stark bioturbant ist, bildet einen makroskopisch sehr auffälligen Horizont zwischen 33-38 cm. Auffällig sind auch die zahlreichen Farblaminationen und Bioturbationsspuren mit dunklen Reduktionshöfen unterhalb der suboxischen Zone.

Die Kolbenlotkerne **PS2083-3** und **PS2084-1** stammen beide vom Meteor Rücken, aus 1936 m und 1667 m Wassertiefe (Fig. 4.19). PS2083-3 liegt auf dem Plateau-artigen, zentralen Teil des Meteor Rückens, während PS2084-1 im südöstlichen Rückenbereich in der Nähe der ODP-Bohrung 703 gekernt wurde (Fig. 4.19). Beide Kernabfolgen befinden sich oberhalb der CCD und sind durch karbonatische Biogenschlämme (weißer Foraminiferal Ooze und hellgrauer Foraminiferal Mud) gekennzeichnet. Entsprechend ihrer ozeanographischen Lage innerhalb der nördlichen Polarfront-Zone, südlich der Subtropischen Front, sind sie durch recht hohe Anteile an opalinen Skeletten, vorwiegend an Diatomeen und Radiolarien gekennzeichnet, die in geringerem Umfang auch gesteinsbildend sind (Diatomaceous Ooze; Anhang, 10.2.). Eine ca. 65 cm mächtige Nannofossil Ooze-Lage tritt in den Kernen in etwa dem gleichen Tiefenniveau auf (169-236 cm; 162-225 cm). In beiden Kernen ist darin eine ca. 16-18 cm lange und 3-4 cm breite Bioturbationsspur zu finden, die in ähnlicher Gestalt im gleichen Tiefenniveau aus dem ANT-VIII/3-Kern PS1754-1 bekannt ist. Aufgrund des charakteristischen Auftretens in einem Horizont in weit auseinanderliegenden Sedimentprofilen muß dieser Bioturbation eine überlokale Bedeutung beigemessen werden. Im Kern PS2083-3 ist die Grabröhre, welche in der Radiographie eine typische

Spreitenfeinstruktur zeigt, mit einem Sand-reichen Sediment gefüllt. Smearslide-Untersuchungen dieses Sedimentes zeigen eine frische Glaukonitbildung die in Radiolarien-Skeletten und teilweise in Foraminiferenschalen zu beobachten ist. Nach Odin & Matter (1981) ist eine Glaukonitbildung in dieser Wassertiefe nur während sehr geringen Sedimentationsraten oder Sedimentations-Unterbrechungen möglich. Die Glaukonitbildung könnte also Hinweis auf einen möglichen Hiatus in diesem Niveau oder etwas darüber geben. Im Gegensatz zu den weiter nördlich gelegenen Kernen sind beide Kerne vom Meteor Rücken durch einen erheblich höheren Anteil an eistransportiertem Detritus (IRD) gekennzeichnet. Einzelne Dropstones mit bis ca. 1 cm Durchmesser sind zu finden. Dropstone-reiche Lagen wurden teilweise als Foraminiferal Sandy Mud klassifiziert. Einige sind durch eine Fining Upward Sequence charakterisiert, wobei nach oben sowohl der mittlere Korndurchmesser als auch der Gehalt an IRD abnimmt.

Der Kolbenlotkern **PS2086-1** wurde auf einem Seamount südlich des Meteor Rückens in 649 m Wassertiefe gekernt. Entsprechend seiner Hochlage weit oberhalb der CCD besteht er aus schwach olivem bis leicht gelblichem Foraminiferal Ooze, der aufgrund der sehr schnellen Entwässerung bei der Kernbearbeitung und seinem makroskopischen Erscheinungsbild fast ausschließlich aus sandkorngroßen Foraminiferen besteht. Die Smearlide-Mikroskopie zeigte ebenfalls kaum feinkörnige Komponenten, wie kalkiges Nannoplankton. Sehr auffällig ist sowohl der hohe Gehalt an Dropstones als auch ihre Größe. Ein gabbroider Dropstone (120 cm) erreichte mit 6 cm Durchmesser fast den Durchmesser des Liners (Anhang, 10.2.). Die makroskopische Betrachtung einzelner Dropstones zeigte, daß in Sedimentkern PS2086-1 nicht nur basaltisches Material als IRD vertreten ist, sondern auch granitoides.

Vom Südwest-Indischen Rücken (Fig. 4.16) stammt der Kolbenlotkern **PS2089-2**, welcher nördlich der Insel Bouvet in 2615 m Wassertiefe zur Beprobung einer Porzellanit-Schicht gezogen wurde (siehe Kap. 4.2. und 5.3.3). Die Lithologie dieses Kerns zeigt neben der Besonderheit des Porzellanit-Gesteines (Kap. 5.3.3) signifikante Wechsel zwischen Diatomaceous Ooze und Diatomaceous Mud bzw. Diatomaceous Sandy Mud, welche sich in dem Muster der magnetischen Suszeptibilität widerspiegeln (siehe Kap. 5.2). Ein Vergleich der magnetischen Suszeptibilität mit dem Kolbenlotkern 2089-1 deutet möglicherweise auf eine Nichtbeprobung der obersten Sedimentschichten im Kern 2089-2 (Kap. 5.2). Kernabschnitte von hellgrauem, weißen oder leicht gelblichen reinen Diatomaceous Ooze werden von deutlich dunkleren (grauen, dunkelgrauen und olivgrauen) terrigenreichem Diatomaceous Mud getrennt (Fig. 4.17). Aufgrund ihrer hohen Dropstone-Führung wurde er häufig als Sandy Mud eingestuft. Der eistransportierte Detritus wird in hohem Maße von basaltischen Gesteinen und Gläsern dominiert. Eine reine Lage vulkanischen Aschematerials wurde in 660-662 cm Sedimenttiefe gefunden.

Vom südwestlichsten Expeditionspunkt stammt der Schwerelotkern **PS2102-2**, dessen Sedimente in 2390 m Wassertiefe von Diatomeen dominiert werden (Fig. 4.17). Sehr reiner und heller Diatomaceous Ooze tritt über weite Kernabschnitte auf und wird von zwei Horizonten von grauem Diatomaceous Mud unterbrochen, welcher nur untergeordnet aufgrund der geringen Dropstone-Führung als Diatomaceous Sandy Mud einzustufen ist. Der

Fig. 4.16: Positionen der Kolbenlot- und Schwerelotkerne von ANT-IX/4. Die an Bord geöffneten Kerne sind unterstrichen.

Fig. 4.16: Positions of gravity and piston corer stations from ANT-IX/4. Cores opened on board are underlined.

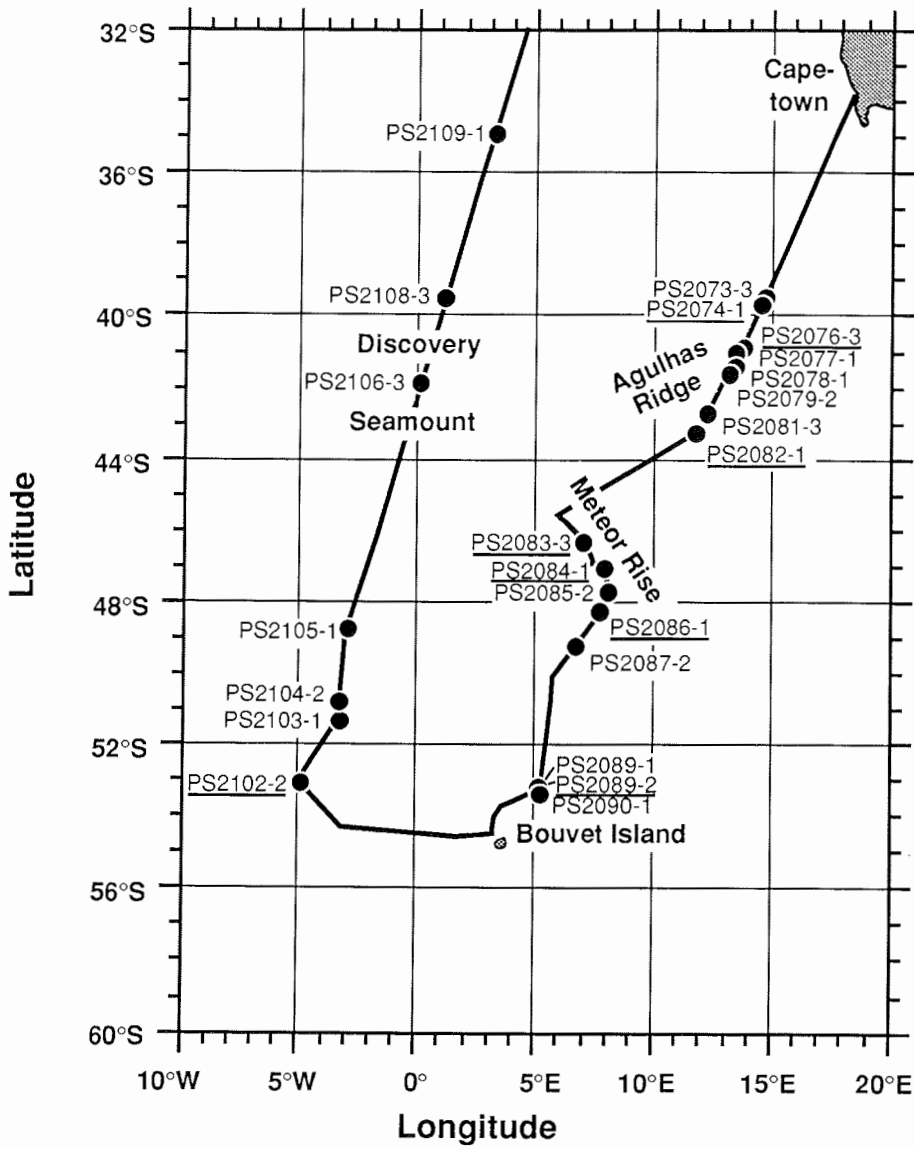
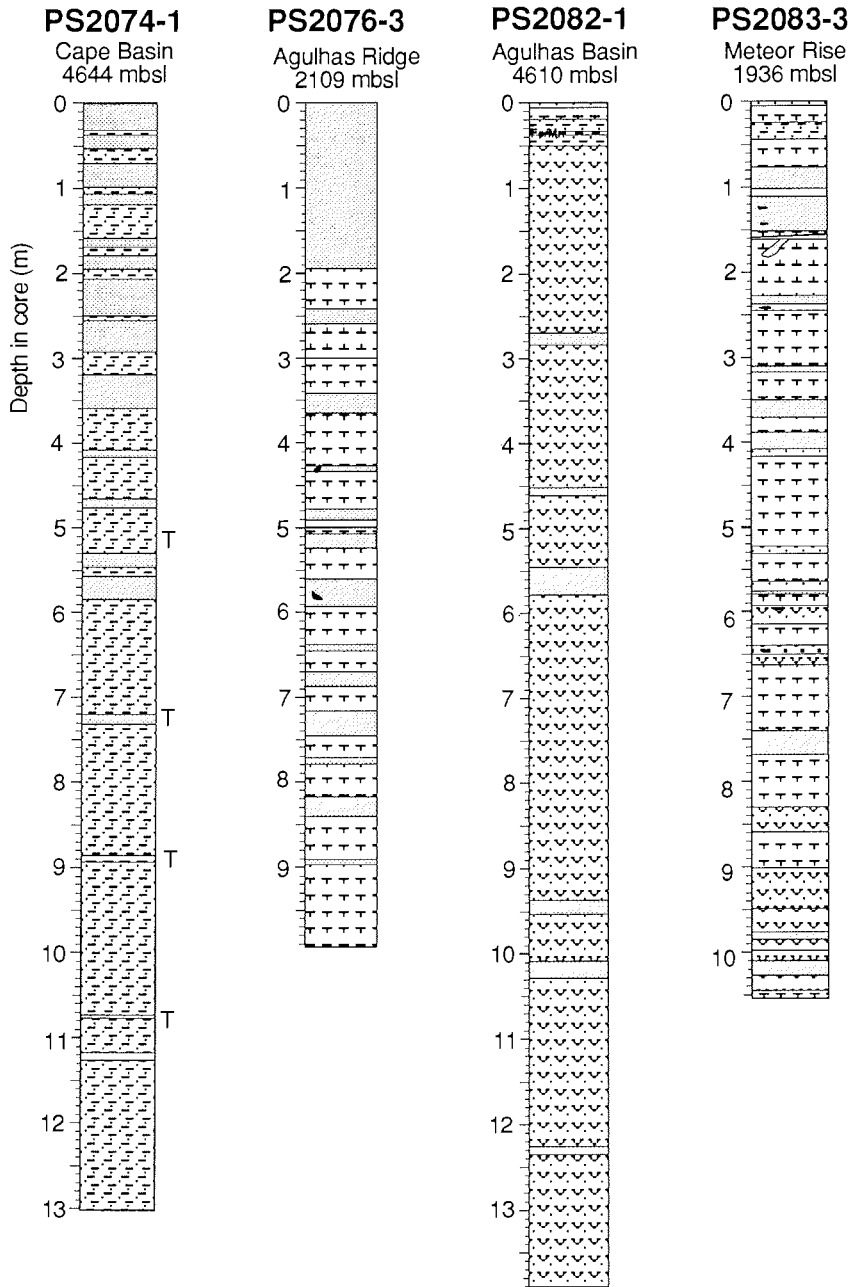
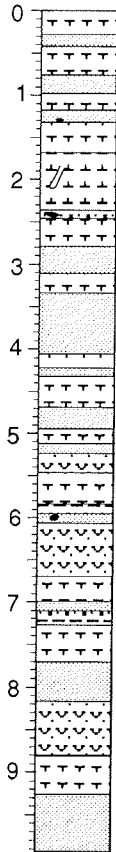


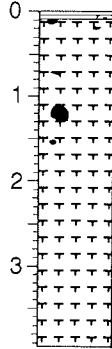
Fig. 4.17 a, b: Sedimentkernprofile der während ANT-IX/4 bearbeiteten Kerne.
 Fig. 4.17a, b: Core logs of the cores opened during ANT-IX/4



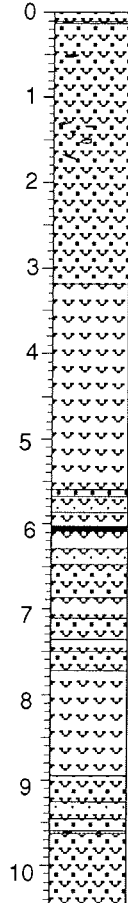
PS2084-1
Meteor Rise
1667 mbsl



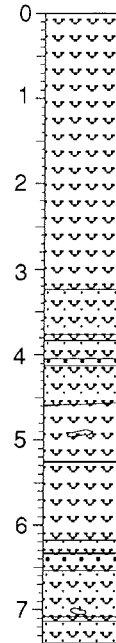
PS2086-1
S. of Meteor R.
649 mbsl


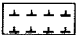




PS2089-2
SW Mid-Atl. Ridge
2618 mbsl



PS2102-2
W Mid-Atl. Ridge
2390 mbsl



-  foraminiferal ooze
-  nannofossil ooze
-  calcareous mud
-  diatomaceous ooze



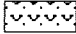

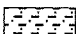

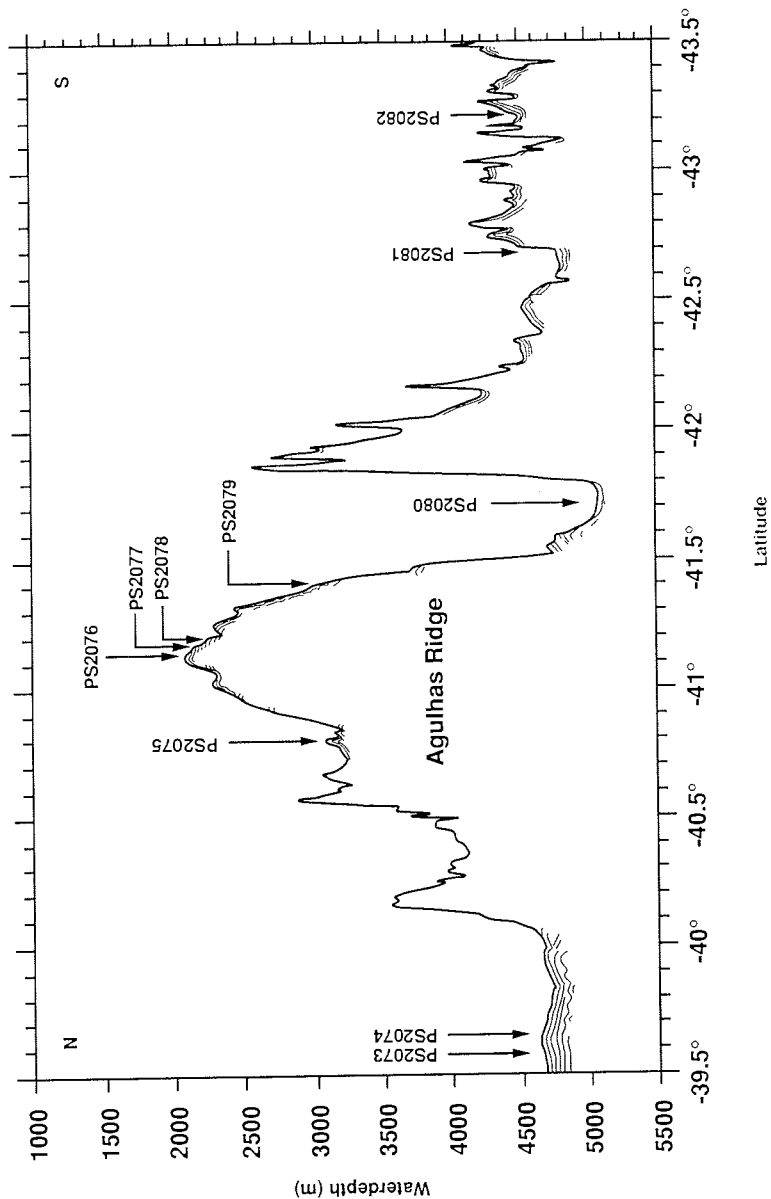
-  pebbles, dropstones
-  T Turbidite
-  diatomaceous mud
-  diatomaceous sandy mud
-  mud
-  porcellanite

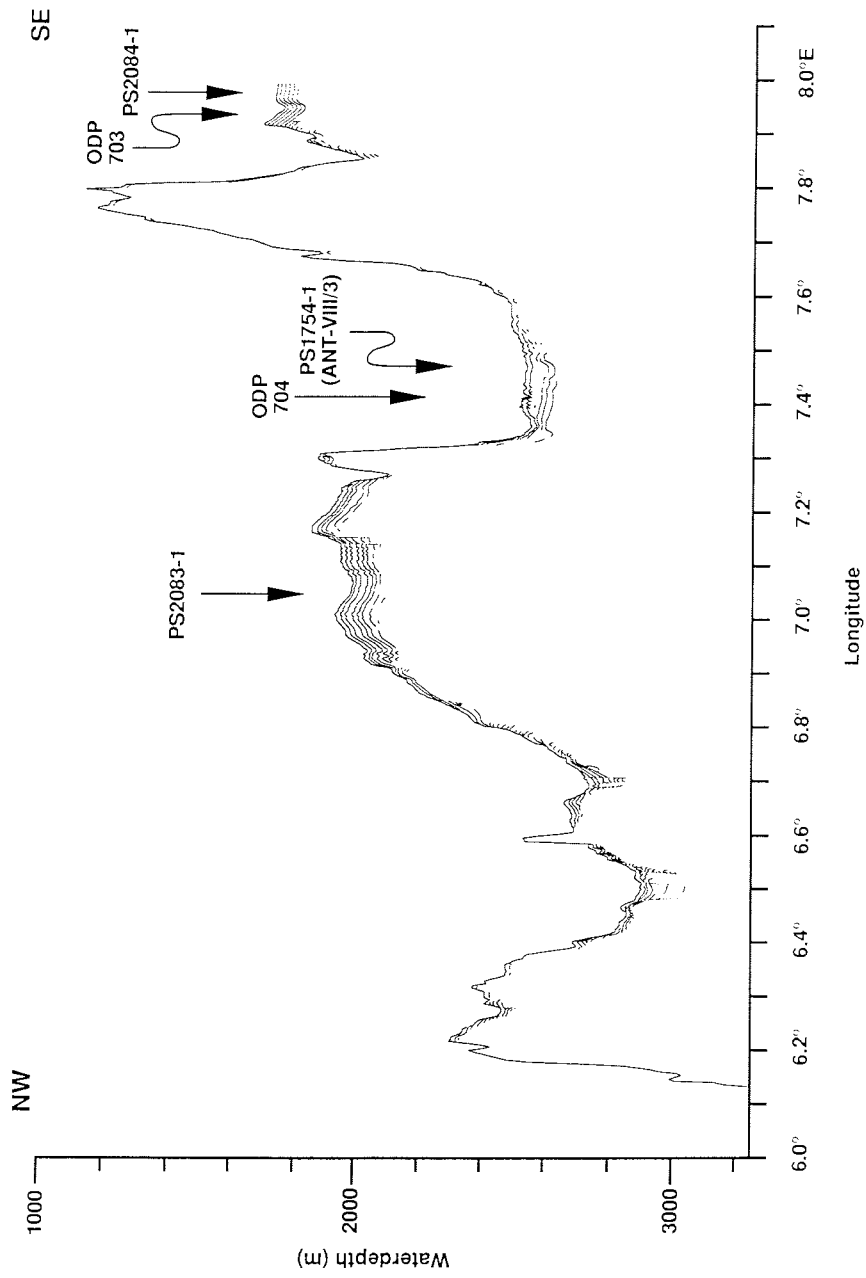
Fig. 4.18: Nord-Süd-Profil über der Agulhas Rücken mit Lage der ANT-IX/4 Stationen. Sedimentverteilung schematisch nach Parasound-Auswertung.

Fig. 4.18: North-south profile of the Agulhas Ridge showing the positions of the core stations. Schematic sediment distribution after Parasound recording.



Opalreichtum dokumentiert die Nähe des Ablagerungsmilieus zur Polarfront, einem Hochproduktionsgebiet für Phytoplankton. Nach sedimentologischem Vergleich mit anderen Kernen aus dem Gebiet repräsentieren die oberen 324 cm von Kern 2102-2 sehr wahrscheinlich das Holozän, wo es zu sehr hohen Opalakkumulationsraten kam.

Fig. 4.19: Stationen auf dem Meteor Rücken.
Fig. 4.19: Geologic stations on the Meteor Rise



5.3.3 Porzellanitbeprobung G. Bohrmann (AWI)

Porzellanite sind monomineralische Gesteine aus Opal-CT, die während der Sedimentdiagenese als knollige oder schichtgebundene Lagen aus Festgestein gebildet werden. Als Ausgangsmaterial wird heute allgemein der biogene Opal (Opal-A) kieseliger Skelette angesehen. Dabei kommt es im Sediment zur Auflösung des instabilen Skelettopals von Diatomeen, Radiolarien oder anderen Kieselschalern, wodurch die SiO_2 -Konzentration im Porenwasser erhöht wird. Bei SiO_2 -Übersättigung im Porenwasser wird Silikat in Form von Opal-CT wieder ausgefällt, wobei durch die Zementation ein Festgestein geringer Porosität entsteht. Porzellanite sind die diagenetischen Vorläufer der aus Quarz bestehenden Cherts (Feuersteine), denen sie im makroskopischen Erscheinungsbild sehr ähnlich sind. Porzellanite sind in allen Ozeanen in älteren Sedimenten (meist älter als 15 Ma) größerer Versenkungstiefe (meist >200 m) vertreten und werden allgemein durch die dort herrschenden erhöhten Temperaturen erklärt. In jüngster Zeit wurden vier sehr junge Porzellanitvorkommen in geringer Sedimenttiefe (5-20 m) bekannt, die alle in der Antarktis liegen (Bohrmann et al. 1990). Die Sauerstoffisotopen-Untersuchungen der Opal-CT-Mineralphasen (Botz und Bohrmann, in Druck) zeigten, daß die Porzellanite nicht unter erhöhten Temperaturen entstanden sind, wie dies allgemein für die Transformation von Opal-A in Opal-CT angenommen wird. Damit muß nach prinzipiell neuen Gesetzmäßigkeiten der Genese wie geochemischen Parametern gesucht werden.

Alle vier Vorkommen von jungem Porzellanit waren Zufallsbeprobungen, wobei der Porzellanit selbst gestört und nicht im Sedimentverband geborgen wurde. Während ANT-IX/4 sollte eine gezielte Probenahme von ungestörtem Porzellanit im Sedimentverband durchgeführt werden. Ähnliche Beprobungen waren während ANT-VIII/3 und ANT-VIII/6 (Gersonde & Hempel, 1990; Fütterer, 1991) erfolglos geblieben. Die Stationspunkte für die Kernentnahme wurden mit Hilfe der PARASOUND-Echogramme ausgesucht (siehe Kap. 4.2.). Zwei Kolbenloteinsätze erbrachten einen 8,5 m (PS2089-1) und einen 10,5 m (PS2089-2) langen Sedimentkern, welche über die beiden Kurven der magnetischen Suszeptibilität miteinander korreliert werden können (siehe Kap. 5.2.1.). Kern PS2089-2 wurde an Bord geöffnet und erbrachte eine 5 cm mächtige, lagig aufgebaute Porzellanitschicht (602-607 cm), welche in schwach gelbliche bis weiße, sehr reine Diatomeenschlämme eingeschaltet ist (siehe Anhang, 10.2.). Damit ist es gelungen, einen jungen Porzellanit-Horizont im Sedimentverband zu beproben, welcher nun für geochemische Untersuchungen zur Verfügung steht. Eine erfolgreiche Porzellanitbeprobung war ebenfalls während ANT-IX/3 auf der Maudkuppe gelungen, wie erst beim Öffnen von Sedimentkern PS2070-1 während ANT-IX/4 festgestellt werden konnte.

5.3.4 Tonmineralogie R. Petschick (AWI)

Tonminerale, die in fast allen Tiefseeablagerungen verbreitet sind und oft den Hauptteil der Tonfraktion in diesen Sedimenten bilden (d.h. im Korngrößenbereich < 2 μm), sind im subpolaren Südatlantik bisher kaum untersucht worden.

An den Multicorer-Oberflächensedimenten soll erstmals das rezente Verteilungsmuster der Tonmineralassoziationen im subpolaren Südatlantik in engräumiger Form erfaßt werden. Hierdurch sollen Zusammenhänge zwischen der Schichtsilikat-Zusammensetzung und den großräumigen Zirkulationssystemen, sowohl der Oberflächen- wie der Tiefenströmungen erarbeitet werden. Erste Ergebnisse aus Oberflächenproben der Polarstern-Expedition ANT-VIII/3 erlauben dabei den Schluß, daß die Verbreitung einzelner Tonmineral-Vergesellschaftungen deutliche Beziehungen zu den Hauptwassermassen erkennen lassen. Danach zeichnen sich Sedimente, die im Einflußbereich von kaltem Tiefenwasser (Unteres Zirkumpolares Wasser, Antarktisches Bodenwasser) abgelagert wurden, durch eine Chlorit- und Illit-Betonung aus. Sedimente aus intermediären Wassertiefen, welche sich im Einzugsgebiet des Nordatlantischen Tiefenwassers befinden, haben dagegen eine stärkere Beteiligung an Kandit- und Smektit-Mineralen. Dadurch ist es u.U. möglich, durch Kartierung einzelner Tonmineral-Komponenten die Transportwege der feinkörnigen Terrigene und damit die vorherrschenden Stromsysteme aufzuzeigen. Die während der Expedition ANT-IX/4 bevorzugt aus flachen Stationen gekerntes Sedimente des Agulhas- und Meteor-Rückens sind dabei von besonderer Wichtigkeit. Diese sind teilweise völlig unbeeinflusst vom Tiefenwasser und offenbaren somit die Tonmineral-Vergesellschaftungen, welche über oberflächennahe Wasserschichten akkumuliert werden.

Anhand der Tonmineral-Assoziationen in den Sedimentkernen sollen mögliche Fluktuationen im Strömungsmuster und in der Wassermassenverteilung erkannt werden, welche in den Glazialen und Interglazialen innerhalb der letzten 300.000 Jahre stattgefunden haben. Erste Ergebnisse an Schwerelotkernen von der Expedition ANT-VIII/3 zeigen für den östlichen Südatlantik innerhalb der Kaltzeiten eine sehr deutliche Nordverschiebung des Chlorit- und Illit-reichen Tonmineraldetritus, teilweise bis weit über die heutige Polarfront. Anhand der aus unterschiedlichen Wassertiefen stammenden Sedimentkerne von ANT-IX/4 soll dabei aufgezeigt werden, ob in den Kalt- und Warmzeiten Änderungen der Transportmechanismen stattgefunden haben. Eine wichtige Frage ist hierbei, inwieweit in den Glazialen ein direkter Eintrag des Tonmineraldetritus über Eisberge erfolgt ist oder ob dieser wie in den Interglazialen mehr durch Strömungstransport stattgefunden hat.

5.3.5 Barytakkumulation im Oberflächensediment G. Bohrmann (AWI)

Die Untersuchungen der GEOSECS-Kampagne zeigen im Atlantischen Ozean eine positive Korrelation zwischen der Primärproduktion und partikulärem Barium in Form von Baryt. Obwohl die genauen Mechanismen der Baryt-Bildung innerhalb der Wassersäule kontrovers diskutiert werden, scheint der Bariumflux zum Meeresboden von der biologischen Produktivität gesteuert. Damit läßt sich möglicherweise das Bariumsignal im Sediment als ein Produktivitätsindikator nutzen. Um dies im Bereich der Antarktis zu testen, werden Untersuchungen zum biogeochemischen Kreislauf von Barium mittels Sedimentfallenmaterial, Oberflächensedimenten und längeren Sedimentkernen durchgeführt. Während der "Polarstern"-Fahrt ANT-IX/4 wurden dazu von den Multicorer-Stationen Oberflächensedimente beprobt. Es werden daran neben elektronenmikroskopischen Untersuchungen zur Barytkristallisation, die Bariumgehalte naßchemisch gemessen, die mit Hilfe der

Sedimentationsrate in Barytakkumulationsraten umgerechnet werden. Zusammen mit dem Oberflächenprobensatz von ANT-VIII/3 sollen damit Gebiete unterschiedlichen Bariumfluxes erkannt werden und mit den wichtigsten Sedimentparametern und den rezenten ozeanographischen Systemen korreliert werden.

5.3.6 Rekonstruktion von Oberflächenwassertemperaturen mit Hilfe von Ketonen G. Ruhland (FGB)

Zur Erforschung der Paläoklimatologie ist es notwendig, die Verteilung der Wassermassen und Strömungssysteme der Ozeane zu kennen. Hilfe dabei bietet die Rekonstruktion der Oberflächentemperaturen der Ozeane. Um Kenntnisse darüber zu erhalten, können Biomarker zur herangezogen werden, die bestimmte Umweltbedingungen widerspiegeln. Solche Biomarker sind z.B. langkettige, mehrfach untersättigte Ketone (C 37), die von Coccolithophoriden (*Emiliana huxleyi*) produziert und in die Zellmembran eingebaut werden. Dabei ist die Untersättigung der Ketone ein Maß für die Temperatur, in der die Coccolithophoriden gelebt haben. Man kann für das Verhältnis von zwei- und dreifach untersättigten Ketonen einen Index (Uk 37') aufstellen, der sich nach Laborexperimenten in Beziehung zur Wassertemperatur setzen läßt: $Uk37' = 0.034 \cdot T + 0.039$.

Ein Vorteil dieser Messung ist, daß sich die Ketone u.U. auch dann noch im Sediment nachweisen lassen, wenn die kalkigen Coccolithen schon weggelöst sind.

Mit Hilfe der MUC-Proben, die auf dieser Reise genommen wurden, sollen Erkenntnisse darüber gewonnen werden, wie weit nach Süden eine Temperaturrekonstruktion mit dieser Methode möglich ist und ob sich Aussagen darüber machen lassen, ob die südliche Polarfront ihre Lage in Glazialzeiten gegenüber Interglazialzeiten verändert hat.

5.4. Paläontologische Bearbeitung von Sedimentproben

5.4.1. Diatomeen und Radiolarien A. Abelmann, U. Zielinski (AWI)

Kieselige Mikrofossilien (Diatomeen, Radiolarien und Silikoflagellaten) sind wichtige Bestandteile der Sedimente des zirkumantarktischen Ozeans und lassen sich zur Datierung der Sedimentabfolgen und zur Rekonstruktionen der paläozeanographischen und -klimatologischen Bedingungen in der geologischen Vorzeit nutzen. Mit dem auf der Expedition ANT-IX/4 gewonnenen Probenmaterial soll im Rahmen des SFB 261 ("Der Südatlantik im Spätquartär: Rekonstruktion von Stoffhaushalt und Stromsystemen") die paläozeanographische und paläoklimatische Entwicklung des subpolaren und polaren Südatlantiks im Jungquartär behandelt werden. Schwerpunktmäßig sollen mit den kieseligen Mikrofossilien untersucht werden:

- die Lageveränderung der ozeanographischen Frontsysteme und der Meereisgrenze
- die Paläo-Oberflächenwassertemperaturen

Das bereits bestehende Probenetz, das während der Polarstern-Expedition ANT-VIII/3 gewonnen wurde, ist auf der Expedition ANT-IX/4 besonders im nördlichen Teil des Untersuchungsgebietes, im Bereich der subtropischen Front, ergänzt und verdichtet worden. Das aus diesem Bereich gewonnene Probenmaterial soll unter anderem zur Rekonstruktion des Agulhas Stromes benutzt werden, der warmes Oberflächenwasser aus dem Indischen Ozean in den Süd-Atlantik transportiert. Es soll hierbei der Fragestellung nachgegangen werden, ob der Wärmetransport aus dem Indischen Ozean sich im Wechsel von Warm- und Kaltzeiten verändert hat. Ein weiterer wichtiger Untersuchungspunkt ist die Kartierung der nördlichen Verbreitung der Polarfrontzone und der Meereisgrenze während der jungpleistozänen Vereisungsmaxima. Dazu wurde Probenmaterial auf zwei NS-Profilen über die antarktischen Fronten von ca. 42° bis 54°S gewonnen.

Bereits an Bord wurden Schwerelot- und Kolbenlotkerne (PS2074-1, PS2076-3, PS2082-1, PS2083-3, PS2084-1, PS2086-1, PS2089-2, PS2102-2) in Probenabständen von 5-10 cm detailliert beprobt. Am Kolbenlotkern PS2083-3 (Meteor-Rücken) wurde schon an Bord eine Gesamtanalyse der Radiolarienfauna durchgeführt. Hierzu wurde das Probenmaterial chemisch aufbereitet und anschließend über 41 µm gesiebt. Die mikroskopischen Präparate wurden in Kanadabalsam eingebettet. Es wurden pro Präparat zwischen 350 und 450 Radiolarien ausgezählt. Die erste Auswertung der Zählungen zeigt einen deutlichen Wechsel in der Zusammensetzung der Radiolarienfauna an, der bestimmten Warm- und Kaltzeiten zugeordnet werden kann (s. Kap. 5.5.).

Grundlage für quantitative und semi-quantitative paläozeanographische Rekonstruktionen ist eine Erfassung der biogeographischen Verteilung kieseligler Mikrofossilvergesellschaftungen in den Oberflächensedimenten und deren ozeanographische Parameter (z.B. Wassertemperatur, Salzgehalt, Nährstoffverteilung, Meereisbedeckung). Zur Erweiterung des bereits auf vorangehenden Polarstern-Expeditionen erstellten Referenzdatensatzes wurden auf der Expedition ANT-IX/4 insgesamt 28 Oberflächenproben mit dem Multicorer gewonnen. Pro Station wurden die obersten 2,5 cm von zwei Multicorerkernen detailliert beprobt, wobei neben einer Oberflächenprobe (0-0,5 cm Kerntiefe) je eine Probe von 0,5-1,5 cm und 1,5-2,5 cm entnommen worden ist. Jeweils ein Multicorerkern wurde durchgehend in 1 cm-Abständen beprobt.

An Bord wurde bereits die Radiolarienfauna in den Oberflächenproben semi-quantitativ untersucht. Die Aufbereitung und Zählung des Probenmaterials wurde wie bei den Sedimentkernen durchgeführt (s. oben). Die Untersuchungen der Oberflächenproben der ANT-VIII/3 und ANT-IX/4 Expeditionen ergeben eine Untergliederung des Gebietes zwischen 39°S und 55°S in vier biogeographische Radiolarienzonen.

Der deutlichste Wechsel in der Artenzusammensetzung wurde an der subtropischen Front und im Bereich der subantarktischen Front beobachtet, der auf die hier ausgeprägten Temperatur- und Salzgehaltsgradienten zurückzuführen ist. Im Bereich der Polarfront dagegen ist lediglich eine Veränderung der prozentualen Häufigkeit bestimmter Arten zu beobachten. Eine weitere Veränderung in der Artenzusammensetzung kommt im Bereich

um 55°S vor, die allerdings nicht so signifikant ist wie an den nördlichen Fronten.

5.4.2 Benthische Foraminiferen und stabile Isotope

A. Mackensen, H.W. Hubberten, C. Klindworth (AWI)

Benthische Foraminiferen leben in jeweils bestimmten Artengemeinschaften angepaßt an spezifische Umweltbedingungen. Die Bodenwassermasse ist als das die benthische Foraminifere direkt umgebende physikochemische Milieu ist entscheidend für die Verbreitung epibenthisch lebender Arten; für die Infauna ist jedoch besonders die Höhe der Exportproduktion bedeutend, die letztlich Nahrungszufuhr und Sauerstoffgehalt im Porenwasser kontrolliert. Folglich ist die Zusammensetzung der Gesamtfaua prinzipiell in erster Linie abhängig von der jeweiligen Bodenwassermasse, aber in zweiter Hinsicht von der Höhe der Exportproduktion. Somit lassen sich jeder gegebenen Bodenwassermasse mindestens zwei charakteristische Faunen zuordnen, wobei bei erhöhter Produktion der Anteil der Infauna größer wird. Eine bestimmte benthische Foraminiferenfaua spiegelt also sowohl eine überregionale (Alter und Herkunft der Bodenwassermasse) als auch eine lokale Komponente (Exportproduktion am Ort der Probennahme) wider. Welcher Anteil überwiegt wird durch die jeweiligen regionalen ozeanographischen, klimatischen und morphologischen Verhältnisse im Untersuchungsgebiet bestimmt (vgl. Mackensen et al., 1990). Deshalb ist es für jede paläozeanographische Interpretation unabdingbar, das rezente Beziehungsgeflecht so aufzuschlüsseln, daß der Einfluß der sich gegenseitig beeinflussenden Endglieder Bodenwassermasse auf der einen Seite und Produktivität auf der anderen Seite auf die Zusammensetzung der Fauna, abschätzbar wird.

Zu diesem Zwecke wurde ein 1989 auf ANT-VIII/3 geborgener und sich in der abschließenden Auswertung befindender Oberflächenprobensatz während dieser Reise gezielt durch ausgewählte Stationen komplettiert (vgl. Kap. 5.3.1., Anhang, 10.1.). So wurden insbesondere Stationen auf den untermeerischen Rücken, möglichst in Wassertiefen oberhalb ca. 2000 m mit dem Multi-Corer (MUC) beprobt. Von den Sedimentkernen, die mit dem Multi-Corer entnommen wurden, wurden in der Regel mindestens 4 Rohre (Ø 6 cm) bis zu einer Teufe von 5 cm zentimeterweise in Scheiben beprobt. Desgleichen wurden die Intervalle zwischen 7-8 cm, 10-11 cm und 14-15 cm beprobt. Alle Proben wurden sofort in mit Bengal Rosa gefärbtem Methanol konserviert.

Bei der Interpretation des stabilen Kohlenstoffisotopensignals, das im Gehäuse kalkschaliger benthischer Foraminiferen gespeichert wird, muß, genau wie bei der Auswertung fossiler Artenvergesellschaftungen, versucht werden, den Einfluß der Bodenwassermasse von dem der Produktivität zu unterscheiden und zu quantifizieren (vgl. Mackensen und Douglas, 1989): Welches Signal überwiegt, das überregionale, das Auskunft gibt über Alter und Nährstoffe der Bodenwassermasse, oder das lokale, das die Intensität der "Biologischen-Pumpe" widerspiegelt, läßt sich nur im Verbund mit unabhängig gewonnenen Daten entscheiden. Wir versuchen daher, die Faunenanalyse mit einer Auswertung der am selben Material gemessenen $\delta^{13}\text{C}$ -Daten zu verbinden. Von vielen Tiefwasserarten ist der sogenannte "Vital-Effekt", die arteigene isotopische Fraktionierung des Organismus beim

Einbau des Sauerstoffs und des Kohlenstoffs in das karbonatische Gehäuse, nicht oder nicht sicher bestimmt. Deshalb wurden, auch zur Charakterisierung der Bodenwassermassen, von jeder Multi-Corer Station jeweils 100 ml des überstehenden Bodenwassers zur $\delta^{18}\text{O}$ - und 250 ml zur $\delta^{13}\text{C}$ -Bestimmung entnommen. Die Proben zur $\delta^{13}\text{C}$ -Bestimmung wurden mit HgCl_2 vergiftet. Anschließend wurden alle Proben mit Wachs unter Luftabschluß versiegelt.

Bereits an Bord wurde begonnen, die geöffneten Schwerelot- und Kolbenlotkerne (PS2082-1, PS2083-3, PS2089-2) überblicksmäßig auf ihren Gehalt an planktischen und benthischen Foraminiferen zu untersuchen. Die über 63mm naß gesiebten Proben wurden über 125 mm trocken getrennt, und die Fraktion >125 mm wurde bearbeitet. Aus dem Kolbenlotkern PS2089-3 wurde die planktische Foraminifer *N. pachyderma* sin. für die isotopengeochemische Analyse ausgelesen. Es konnten jedoch nur aus den vermutlich warmzeitlichen Intervallen genügend Individuen für die Analyse mit dem Massenspektrometer gewonnen werden. Es sollte sich aber auch damit zumindest eine erste isotopenstratigraphische Einstufung vornehmen lassen.

Erste Ergebnisse

Die Kerne PS2082-1 und PS2083-3 wurden zunächst nur zum Zwecke einer isotopenstratigraphischen Einstufung untersucht. Es konnten sowohl benthische als auch planktische Foraminiferen in ausreichender Anzahl ausgelesen werden. Dabei wurde versucht, endobenthische und epibenthische Arten, sowie flach und tiefer lebende planktische Arten für die Labormessungen auszulesen (z.B. in PS2082-1: *Melonis sphaeroides*, *M. pompilioides*, *Pullenia bulloides*, *Cibicidoides wüllerstorfi*, *Globigerina bulloides*, *N. pachyderma*, *Globorotalia inflata*), um einerseits die glazial-interglazialen Zyklen mit sich in den Übergangsbereichen überlappenden Arten abdecken zu können, und andererseits bereits Basismaterial für eine weitergehende paläozoanographische Interpretation des Kohlenstoffsignals zur Verfügung zu haben. Besonders PS2082-1 aus dem Agulhas Becken von $43^{\circ}13.2'\text{S}$ und $11^{\circ}44.3'\text{E}$, zeichnet sich aufgrund einer ersten ökostratigraphischen Einschätzung der Wechsel in den benthischen Foraminiferenvergesellschaftungen durch eine vermutlich lückenlose Sedimentation, bei einer hohen Sedimentationsrate von ca. 5 cm/1000 a, über die letzten drei Klimazyklen aus. Bis auf kurze völlig karbonatfreie Abschnitte in den Glazialzeiten ist zumindest mit Hilfe von planktischen Foraminiferen eine genaue stratigraphische Einstufung der Sauerstoffisotopenstadien 1 bis 9 möglich (vgl. Abelmann et al.). *Cibicidoides* spp., eine Gattung, die Kohlenstoff beim Einbau ins Gehäuse im isotopischen Gleichgewicht mit dem Meerwasser fraktioniert, ist kontinuierlich, mit Ausnahme der Isotopenstadien 2, 6 und 8 vertreten, so daß die Interpretation des $\delta^{13}\text{C}$ -Signals in direktem Vergleich mit den nördlichen Meteor-Kernen vom Walfisch-Rücken und aus dem Angola-Becken, sowie aus dem äquatorialen Bereich möglich ist. Der direkte Anschluß an unsere Untersuchungen vom antarktischen Kontinentalhang (Mackensen et al., 1989; Grobe et al., 1990) ist über die ebenfalls zahlreich vertretene *Epistominella exigua* möglich.

5.5. Stratigraphische Ergebnisse

A. Abelmann, H.-W. Hubberten, M. Knappertsbusch, A. Mackensen, U. Zielinski (AWI)

Wesentliche Grundlage für paläozeanographische Rekonstruktionen ist eine möglichst detaillierte Alterseinstufung der Sedimentkerne. Eine vorläufige Datierung mit Hilfe von Radiolarien, Diatomeen, Coccolithen wurde bereits an Bord vorgenommen. Die Basisalter der Kerne wurden bei allen nicht an Bord geöffneten Kernen lediglich mit Hilfe der Kernfängerproben bestimmt (Tab. 4.2). Diese Datierungen haben ausdrücklich vorläufigen Charakter, da sie lediglich auf der Analyse einer Probe beruhen, bei der Verunreinigungen nicht ausgeschlossen werden können. Für die bereits an Bord geöffneten Kerne wurden neben den Kernfängerproben Sedimentkernproben im Abstand von 20 bis 100 cm untersucht. Am Kern PS2083-3 erfolgte im Probenabstand von 10-20 cm eine detaillierte Alterseinstufung der jungpleistozänen Abfolgen mit der *Cycladophora davisiana* Stratigraphie (Hays et al., 1976; Morley & Hays, 1981; Martinson et al., 1987) (Fig. 4.20). Nachträglich wurden an dem bereits an Bord präparierten Probenmaterial der Kerne 2082-1, 2083-3 und 2089-2 Isotopenmessungen an planktischen Foraminiferen vorgenommen.

Für die biostratigraphische Bearbeitung wurde das Probenmaterial, wie unter Kapitel 5.4.1. beschrieben, aufbereitet. Die Diatomeen- und Coccolithenuntersuchungen wurden an "smear-slides" durchgeführt. Grundlage der biostratigraphischen Alterseinstufung sind die Radiolarienzonierung von Hays und Opdyke (1967), die Diatomeenzonierungen von Gersonde und Burckle (1990) und Baldauf und Barron (1991) sowie die Coccolithenzonierung von Martini (1971). Zusätzlich konnte mit Einschränkung das FAAD und LAAD der Diatomeenart *Hemidiscus karstenii* (Burckle, 1982, Burckle et al., 1978) als weitere Zeitmarken für die pleistozänen Sedimentabfolgen benutzt werden.

Erste Ergebnisse können für folgende Regionen dargestellt werden (siehe Übersichtskarte Kernstationen, Fig. 4.16):

Kap-Becken

Die stratigraphische Einstufung der beiden nördlichsten Kerne aus dem Kap-Becken zeigen Diskrepanzen zwischen den Altersangaben der kieseligen Mikrofossilien (Radiolarien und Diatomeen) und der Coccolithenstratigraphie, bislang nur vorläufig vorgenommen werden, da ein Teil der antarktischen, stratigraphisch nutzbaren Diatomeen- und Radiolarienarten in diesen Kernen nicht vorkommen. Das Basisalter des Kerns PS2073-3 wurde mit Hilfe von Coccolithen auf ein Alter jünger 0,27 Ma (NN21) eingeschätzt, die Diatomeen weisen dagegen auf ein Alter von mehr als 0,6 Ma hin. Die Basis des Kerns PS2074-1 wurde Radiolarien und Diatomeen auf ein Alter von ca. 2,2 Ma eingestuft, die Coccolithen zeigen ein vorläufiges Alter von jünger 1,9 Ma (NN19) an (Tab. 4.2).

Agulhas-Rücken

Miozäne und pliozäne Alter wurden an der Basis der Kerne PS2078-1 und PS2077-1 ermittelt (Tab. 4.2). Sie stellen damit die ältesten Sedimente dar, die auf diesem Fahrtabschnitt gewonnen wurden.

Agulhas-Becken

Die Sedimentkerne aus dem Agulhas Becken (PS2081-1, PS2082-1) wurden auf ein Alter zwischen 0,2 und 0,7 Ma datiert (Tab. 4.2). Die am Kern PS2089-2 ermittelten Sedimentationsraten liegen bei 4-7 cm/1000 Jahre.

Meteor Rücken

Zwei der fünf auf dem Meteor-Rücken am südlichen Rand erteuften Kerne (PS2083-2087) wurden bereits an Bord detailliert beprobt und haben ein Basisalter von 0,8-0,9 Ma (Tab. 4.2). Am Kern PS2083-3 konnten zusammen mit der Isotopenkurve an planktischen Foraminiferen, den *C. davisiana* Fluktuationen und ergänzend mit den biostratigraphischen Zeitmarken der Radiolarienart *Stylatractus universus* und der Diatomeenart *Hemidiscus karstenii* (bei 0,2 und 0,4 Ma), die Isotopenstadien 1 bis 11 abgegrenzt werden. Aus dem Verlauf der *C. davisiana* Kurve, und mit den biostratigraphischen Zeitmarken ergibt sich eine Schichtlücke, die das Isotopenstadium 7 und möglicherweise 8 umfaßt (Fig. 4.20). Die Sedimentationsraten im Kern PS2083-3 liegen zwischen 0,5 - 1 cm /1000 (Fig. 4.21).

Tab. 4.2: Basisalter der Sedimentkerne, ermittelt mit Diatomeen-, Radiolarien- und Coccolithen-Biostratigraphien. * Altersbestimmungen mit Vorbehalt, da nur die Datierung von Kernfängerproben vorliegt.

Tab. 4.2: Basic ages of the sediment cores dated with diatom, radiolarian and coccolith biostratigraphic zonations. * Age determinations are preliminary because only core catcher samples have been dated.

Kern-Nr. PS -	Breite S	Länge	Wassertiefe (m)	Gerät	Gewinn-tiefe (cm)	Gebiet	Diatomeen-Zone	Radiolarien-Zonen	Coccolithen-Zonen	Vorläufiges Alter der Kernbasis
2073-3	39°36,3	14°33,7E	4625	SL	1205	K.B.	Ai	Su?	NN21	0.27(Nannos)->0.6Ma* > 0.7 Ma
2074-1	39°40,0	14°30,7E	4644	SL	1303	K.B.	Tv	Ec?	NN19	ca. 0.4-0.7 Ma *
2076-3	41°08,8	13°27,8E	2109	KOL	993	Ag.B.	leer	Su ?	NN19	Plio. od. > (Nannos)*
2077-1	41°09,9	13°27,9E	2163	KOL	470	Ag.B.	leer	leer		Miozän*
2078-1	41°12,2	13°26,4E	2254	SL	272	Ag.B.	leer	?(Miozän)	?(Miozän)	
2079-2	41°25,3	13°06,4E	3012	SL	897	Ag.B.	leer	leer	?NN20?	0.27-0.47 Ma *
2081-1	42°41,7	12°11,3E	4801	SL	1236	Ag.B.	Ai	Ad ?	leer	ca. 0.7 Ma *
2082-1	43°13,2	11°44,3E	4610	SL	1391	Ag.B.	Tl	Ad	NN21	0.2 - 0.4 Ma
2083-3	46°21,8	07°02,3E	1936	KOL	1061	MR	Ai	Ss	NN19	ca. 0.9 Ma
2084-1	47°01,3	07°57,9E	1667	KOL	994	MR.	Ai	Ss ?	NN19	ca. 0.7-0.8 Ma
2085-2	47°44,9	07°59,9E	2977	KOL	972	MR.	Ai	Ad	NN21	ca. 0.6 -0.7 Ma
2086-1	48°19,1	07°45,4E	649	KOL	387	S'MR.	Ai	Su	?	ca. 0.6-0.7 Ma
2087-2	49°08,1	06°42,3E	3452	KOL	978	S'MR.	Tl	Ad	NN21	< 0.2 Ma*
2089-1	53°11,3	05°19,7E	2615	KOL	846	NB	Ai	Su	leer	ca. 0.6 Ma*
2089-2	53°11,3	05°19,8E	2618	KOL	1046	NB	Ai	Su	leer	0.6-0.7 Ma
2090-1	53°10,7	05°07,9E	2819	KOL	1190	NB	Tl	Ad	leer	< 0.2 Ma*
2102-2	53°04,4	04°59,1W	2390	SL	729	W'NS	Tl	Ad	leer	< 0.2 Ma
2103-1	51°19,7	03°19,4W	2947	SL	830	W'NS	Tl	Ad	leer	< 0.2 Ma*
2104-2	50°44,5	03°13,7W	2611	SL	664	W'NS	Tl	Ad	leer	< 0.2 Ma*
2108-3	39°50,2	01°02,1E	4920	SL	1016	W'NS	leer	leer	leer	kein Alter*
2109-1	34°59,9	03°10,0E	5041	SL	501	W'NS	leer	leer	leer	kein Alter*

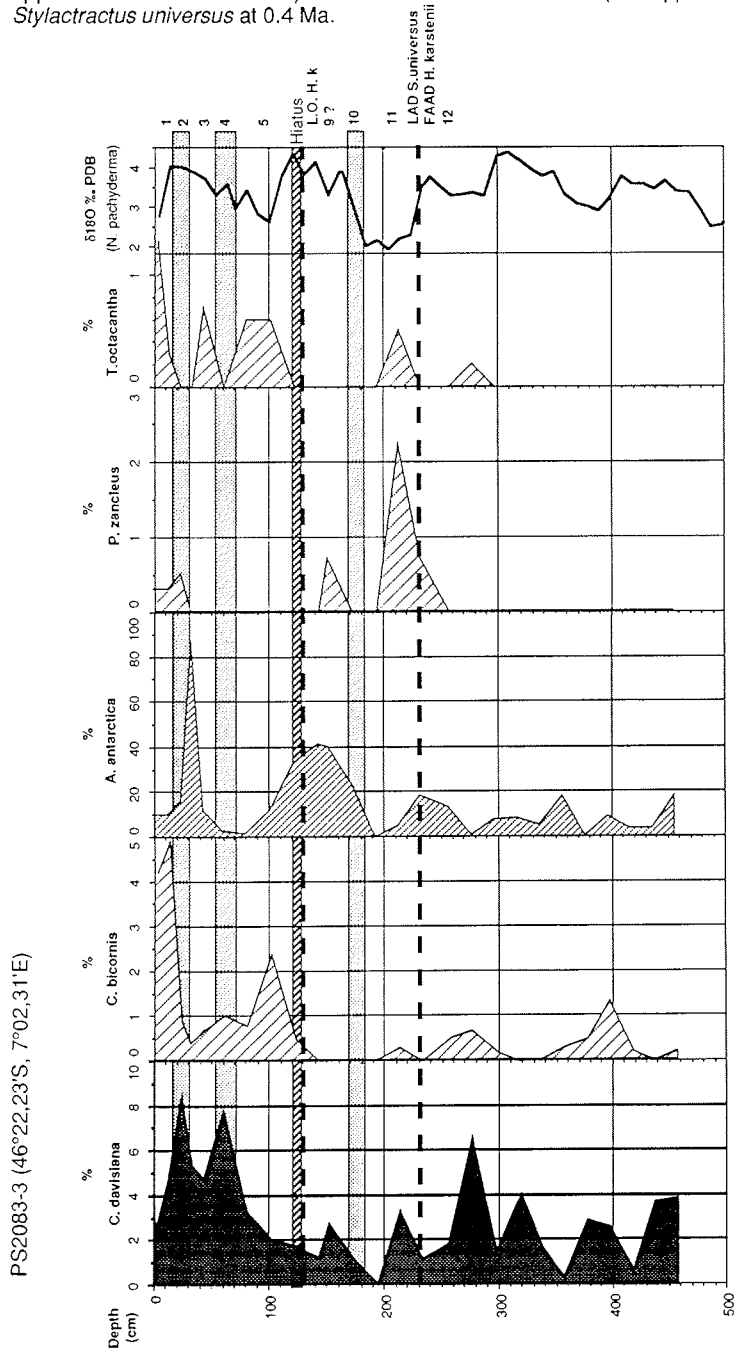
Gebiet: K.B.: Kappbereich; Ag.B.: Agulhas-Bereich; SMR: südl. Meteorbereich; NB: nördl. Bouvet; WNS: WNS Profil

Diatomeenzonen: Ai: *A. ingens*; Tv: *T. vulnificus*; Tl: *T. lentigenosa*

Radiolarienzonen: Su: *S. universus*; Ec: *E. calvertense*; Ad: *A. denticulata*; Ss: *S. saturnalis*

Fig. 4.20: Kolbenlotkern PS2083-3. Detaillierte Alterseinstufung mit der *Cycladophora davisiana*-Stratigraphie und der Sauerstoff-Isotopenstratigraphie an planktischen Foraminiferen. Daneben ist das letzte Auftreten (L.O.= last occurrence) von *Hemidiscus karstenii* bei 0.2 sowie der FAAD (= first abundance appearance date) von *H. karstenii* und der L.A.D. (last appearance date) von *Stylactractus universus* bei 0.4 Ma gekennzeichnet.

Fig. 4.20: Piston core PS2083-3. Detailed dating was done with the *Cycladophora davisiana* stratigraphy and the oxygen isotopes on planktonic foraminifera. Also indicated are the L.O. (=last occurrence) of *Hemidiscus karstenii* at 0.2 Ma, as well as the F.A.A.D. (= first appearance abundance date) of *H. karstenii* and the L.A.D. (last appearance date) of *Stylactractus universus* at 0.4 Ma.



Nördlich Bouvet

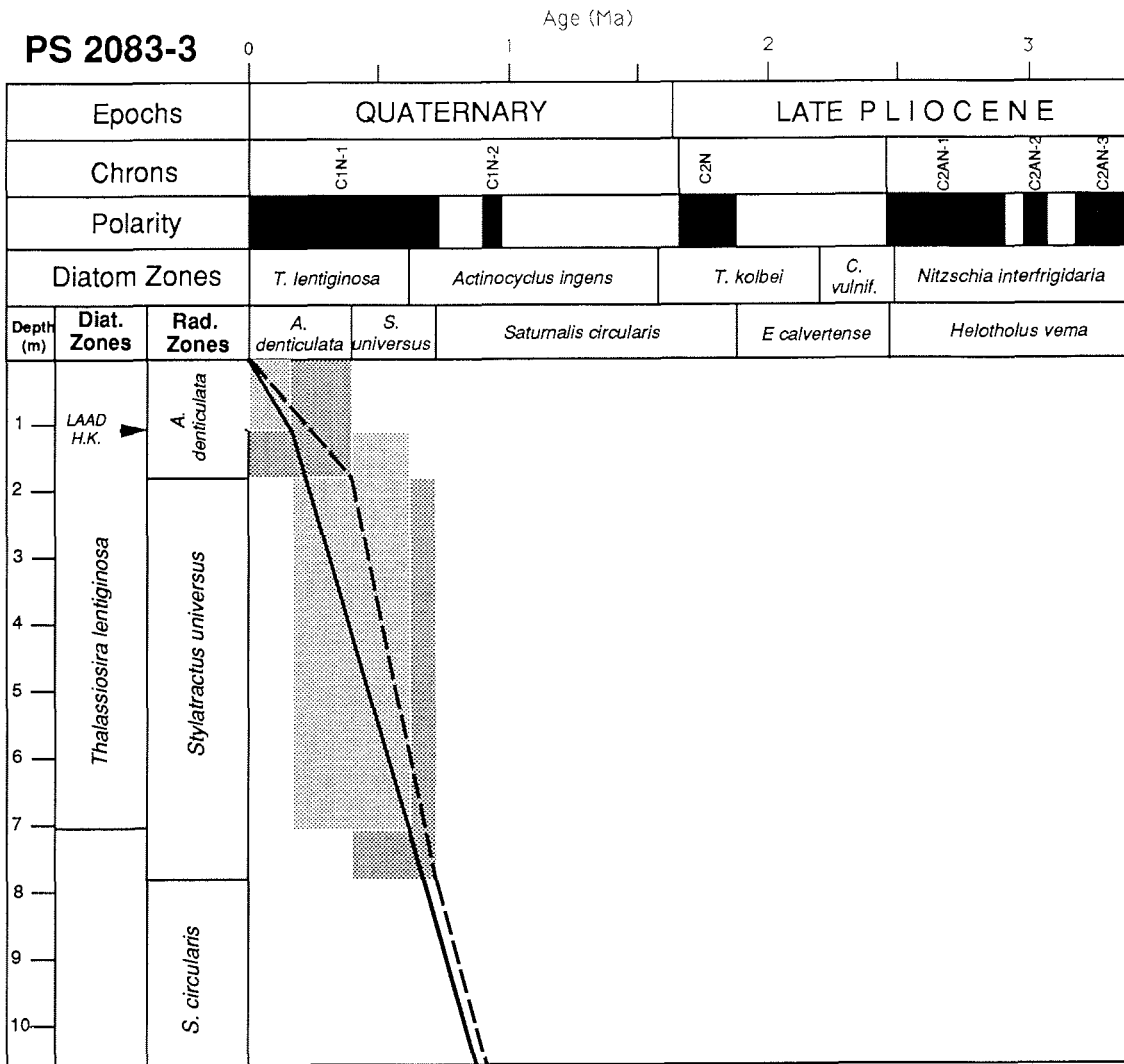
Die Kerne PS2089-1 und PS2089-2 (Porzellanitstation) haben ein Basisalter von ca. 0,6 Ma , während der Kern PS2090-1 lediglich die letzten 0,2 Ma umfaßt (Tab.4.2).

Westliches NS-Profil

Auf dem westlichen NS-Profil wurden drei Kerne gewonnen (PS2102-2, PS2103-1, PS2104-2), die alle ein Basisalter jünger 0,2 Ma aufweisen. Die abgeschätzten Sedimentationsraten liegen in diesem Bereich bei 3-4 cm /1000 Jahre (Tab. 4.2). Die beiden nördlichsten Kerne (PS2108-3, 2109-1) konnten nicht datiert werden, da in den Kernfängern keine Mikrofossilien vorhanden waren.

Fig. 4.21. Alter/Tiefen-Diagramm für Kern PS2083-3 gestützt auf Radiolarien- und Diatomeen- Biostratigraphien.

Fig. 4.21: Age - depth interpretation of Core PS2083-3 based on radiolarian and diatom biostratigraphic zonations.



6. **UNTERSUCHUNGEN IN DER WASSERSÄULE**

6.1 **CTD-Messungen** R. Petschick (AWI)

Die Festspeicher-CTD wurde an 31 geologischen Stationen eingesetzt. Das Gerät wurde turnusmäßig ca. 50 m Seillänge über dem Multicorer befestigt. Die Messung und digitale Aufzeichnung von Temperatur, elektrischen Widerstand und Druck erfolgte alle 1,5 Sekunden, wobei nur die Werte beim Fieren für die Auswertung herangezogen wurden. Beim Hieven streuten die Daten wegen offensichtlicher Turbulenzen deutlich stärker. Die Datenauslesung erfolgte ohne Ausfälle, sodaß von jeder CTD-Station ein Tiefenprofil der Salinität und der potentiellen Temperatur vorliegt.

Ziel der Messungen war es, die aktuelle hydrographische Situation, insbesondere die thermohaline Schichtung in der Wassersäule über der jeweiligen Station zu erfassen und zu interpretieren. Die Daten liefern damit Aussagen über die maßgeblichen ozeanographischen Umweltparameter, welche zur Charakterisierung von Faunen- und Florenvergesellschaftungen benötigt werden.

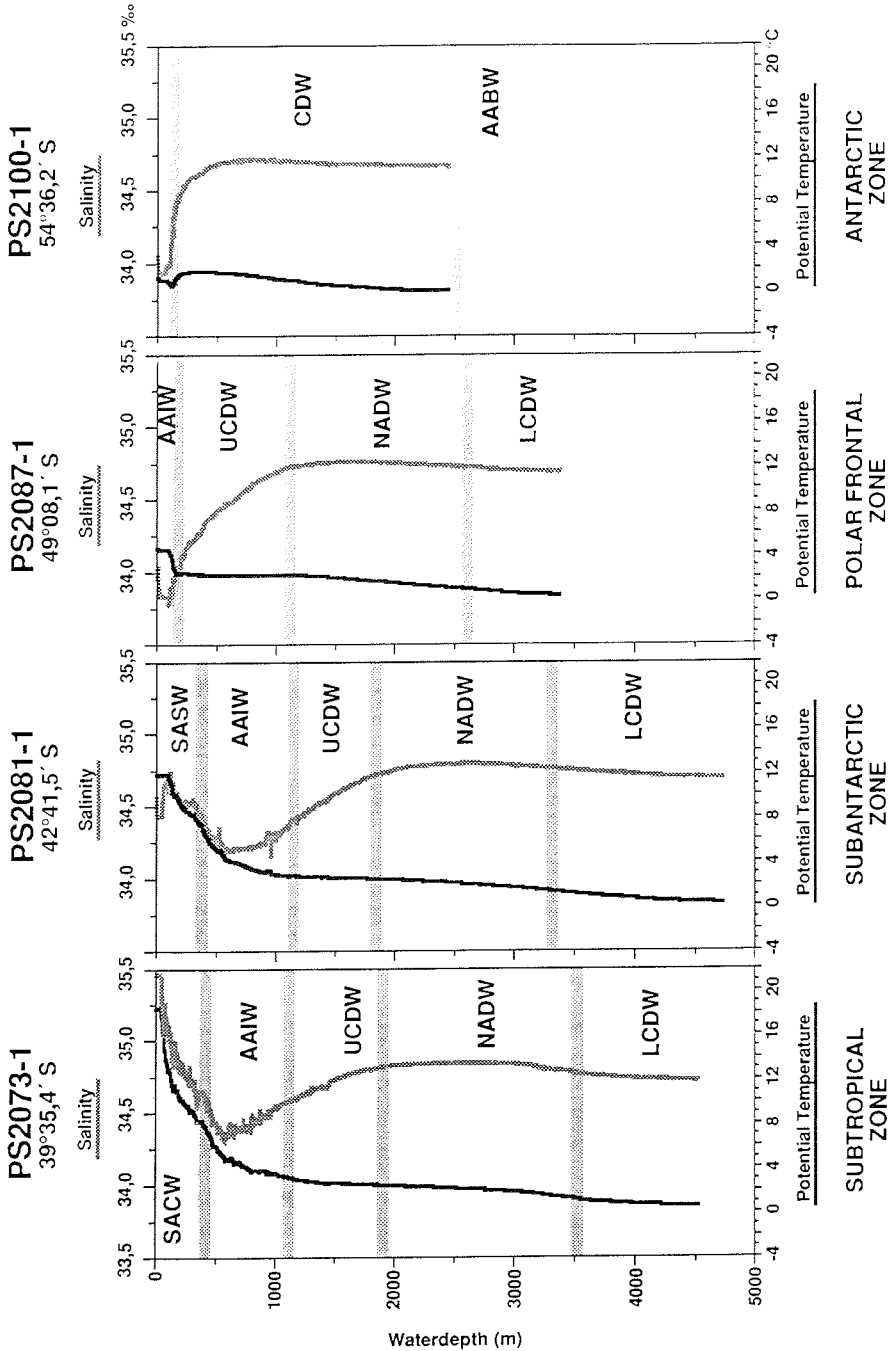
Weiterhin wurde die Festspeicher-CTD routinemäßig eingesetzt, um die Wasserschallgeschwindigkeit aus den vorhandenen Meßgrößen zu berechnen. Damit war bei der HYDROSWEEP-Vermessung eine wesentlich genauere Wassertiefenbestimmung möglich. Aus diesem Grund wurde die CTD auch im Bereich der Vermessungsstrecken an der Romanche Fracture Zone und am Ampere Seamount zur Korrektur der Wasserschallgeschwindigkeit in den obersten 1500 m gefahren. Weiterhin konnten mit Hilfe der CTD Beprobungsstrategien für den sinnvollen Einsatz des Multinetzes in unterschiedlichen Wassertiefen gezogen werden.

Ergebnisse:

Fig. 4.22 zeigt exemplarisch vier typische CTD-Kurven aus dem Gebiet der Subtropischen Zone, der Subantarktischen Zone, der Polarfrontzone und der Antarktischen Zone. Die Daten erlauben eine vorläufige Charakterisierung der Wassermassen. Für eine gesicherte Einstufung sollten aber noch geochemische Daten (z.B. Sauerstoff- und Nitratwerte) mit einfließen. Das Salinitätsminimum bei ca. 500 - 1000 m Wassertiefe beschreibt in den drei nördlichen Stationen PS 2073-1, PS2081-1 und PS2087-1 die Verbreitung von Antarktischem Zwischenwasser (AAIW), welches im Fall der ersten beiden Profile von wärmeren oberflächennahen Wasserschichten (Southatlantic Central Water = SACW und Subantarctic Surface Water = SASW) überdeckt wird. Die Sta. PS2087-1 liegt im Bereich der Polarfrontzone in welchem das Antarktische Zwischenwasser an der Oberfläche gebildet wird. Die unterhalb etwa 1000 m Wassertiefe wieder ansteigende Salinität bei weitgehend gleichbleibenden potentiellen Temperaturen bildet das Obere Zirkumpolare Tiefenwasser (UCDW) ab. Der Bereich maximaler Salinität bei weitgehend gleichbleibenden Temperaturen wird durch das keilartig von Norden nach Süden vordringende Nordatlantische Tiefenwasser (NADW) hervorgerufen. Dieses Maximum ist in der südlichsten dargestellten Sta. PS2100-1 innerhalb der Antarktischen Zone nicht mehr zu erkennen, was auf deren Vermischung mit dem Zirkumpolaren Tiefenwasser hinweist. Das Untere bis zum Boden reichende Zirkumpolare Tiefenwasser (LCDW) ist

Fig. 4.22: Vier charakteristische CTD-Tiefenprofile der Salinität und der potentiellen Temperatur, kennzeichnend für die Subtropische, Subantarktische, Polarfront- und Antarktische Zone und vorläufige Interpretation der thermohalinen Schichtung. SACW - South Atlantic Central Water, SASW - Subantarctic Surface Water, AAIW - Antarctic Intermediate Water, UCDW - Upper Circumpolar Deep Water, NADW - North Atlantic Deep Water, LCDW - Lower Circumpolar Deep Water, AABW - Antarctic Bottom Water.

Fig. 4.22: Four characteristic vertical CTD profiles of salinity and potential temperature typically for the Subtropical, the Subantarctic, the Polar Frontal and the Antarctic Zone and preliminary interpretation of thermohaline layering.



schließlich durch die wieder zurückgehende Salinität und die erneut abnehmenden Temperaturen ab einer Wassertiefe von etwa 3500 - 4000 m dokumentiert. Antarktisches Bodenwasser (AABW), gekennzeichnet durch Temperaturen unter 0°C, wurde in der Sta. PS2100-1 nicht direkt angetroffen, doch ist aus dem sehr niedrigen Wert von 0,03°C bei 2500 m Wassertiefe seine unmittelbare Nachbarschaft zu erwarten.

Die Stationsauswahl beschränkte sich auf dem ersten Fahrtabschnitt von Kapstadt nach Bouvet Island im wesentlichen auf die Gebiete des Agulhas Rückens, des Meteor Rückens und Bouvet Island selbst. Deshalb kann für dieses erste Untersuchungsprofil nur eine lückenhafte Isoliniendarstellung von Salinität (Fig. 4.23) und Potentieller Temperatur (Fig. 4.24) erstellt werden. Ein Vergleich mit den Ergebnissen von der Expedition ANT-VIII/3 (Wisotzki et al. 1990) sowie mit Literaturdaten (Withworth & Nowlin, 1987, Reid 1990) zeigt keine wesentlichen Abweichungen der im südlichen Südatlantik bekannten ozeanographischen Verhältnissen.

Im Profil vom Mittelatlantischen Rücken zum Discovery Seamount ist das vorhandene CTD-Stationsmuster zu lückenhaft, um eine vergleichbare Isoliniendarstellung zu erarbeiten. Hier ergaben sich im wesentlichen die gleichen in umgekehrter Weise zum ersten Profil folgenden CTD-Kurven.

6.2. Plankton

6.2.1. Planktonuntersuchungen

A. Abelmann & U. Zielinski (AWI)

Planktonische Organismen (Radiolarien und Diatomeen) wurden mittels Wasserpumpenproben und Netzfängen auf beiden Profilen während des Fahrtabschnittes der ANT IX/4 - Expedition beprobt. Ziel dieser Untersuchungen ist die horizontale und vertikale Verbreitung des kieseligen Planktons in Verbindung mit hydrographischen Daten zu ermitteln. Die damit gewonnenen Informationen zur Aktuöökologie stellen wichtige Daten dar, die auf die fossile Artengemeinschaft übertragen werden kann und für paläozeanographische Fragestellungen von wichtiger Bedeutung sind. Hierzu wurde der Bereich zwischen 38°S und 54°S mit Netzfängen und Wasserpumpenproben in engen Abständen beprobt. Das Probenprofil reicht von der subtropischen Zone über den subantarktischen Bereich bis zu dem südlich angrenzenden Kaltwassergürtel. Die ozeanischen Fronten wurden hierbei zweimal überquert. Nördlich der Subtropischen Front wurde die Beprobung der obersten Wasserschicht mit Hilfe von Wasserpumpenproben auf ein SN-Profil über den Äquator bis kurz vor die Kanarischen Inseln (23°46,7'N; 19°01,4'W) ausgedehnt.

Insgesamt wurden 202 Wasserproben über die schiffseigene Membranpumpe aus einer Tiefe von ca. 7 m entnommen. Pro Entnahme wurden jeweils zwei Wasserproben über 40 µm und über 10 µm Gaze gefiltert. Zusätzlich wurden insgesamt 32 Planktonnetzfüge an 16 Stationen über eine Wassertiefe von 0-100 m durchgeführt (Fig. 4.25). Pro Station wurde jeweils ein Netz mit einer

Fig. 4.23: Vertikale Verteilung der Salinität auf dem Untersuchungsprofil von Kapstadt nach Bouvet Island, basierend auf CTD-Daten.
(Vertical distribution of salinity along the transect from Cape Town to Bouvet Island, based on CTD data.)

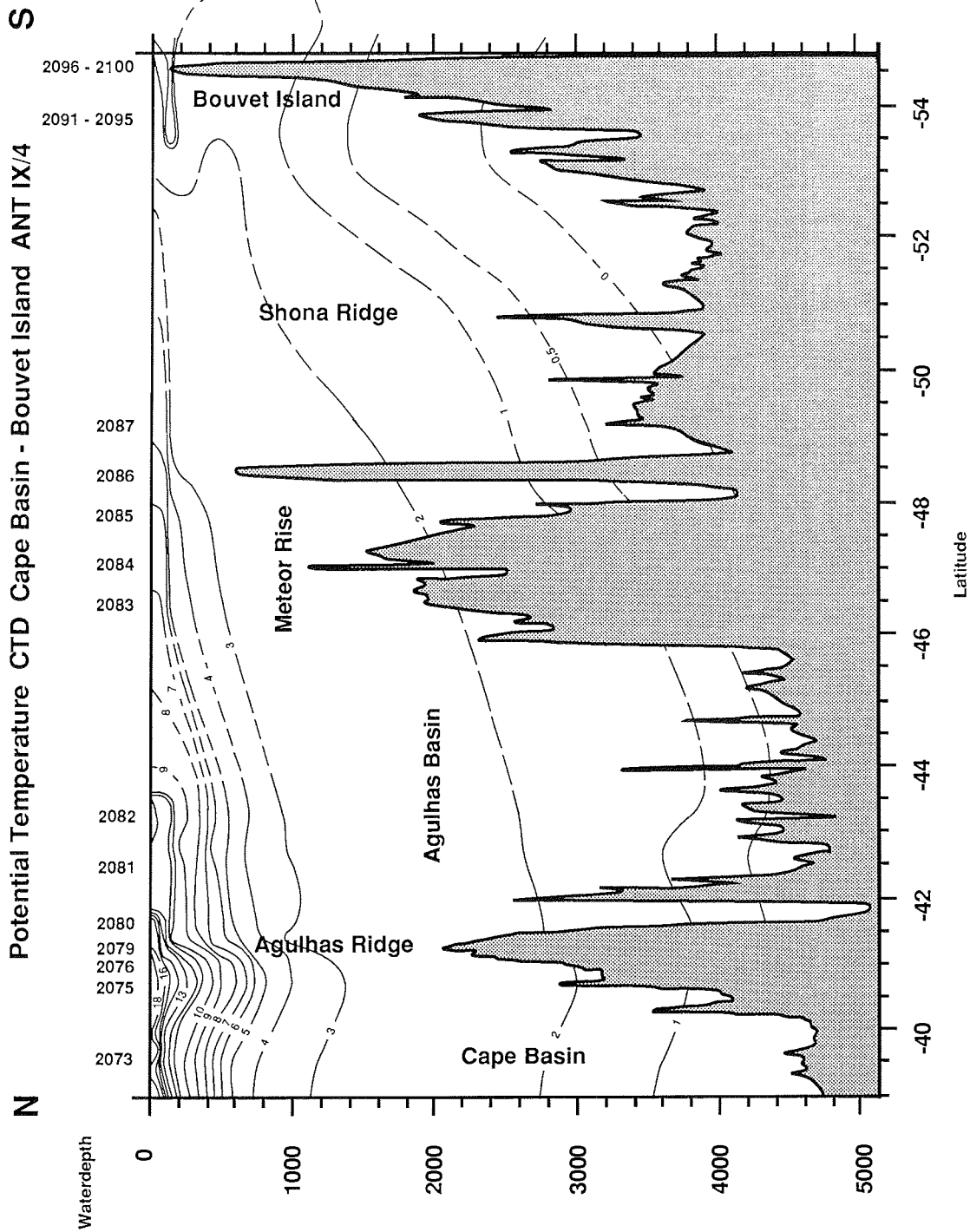


Fig. 4.24: Vertikale Verteilung der potentiellen Temperatur auf dem Untersuchungsprofil von Kapstadt nach Bouvet Island, basierend auf CTD-Daten. (Vertical distribution of potential temperature along the transect from Capetown to Bouvet Island, based on CTD data.)

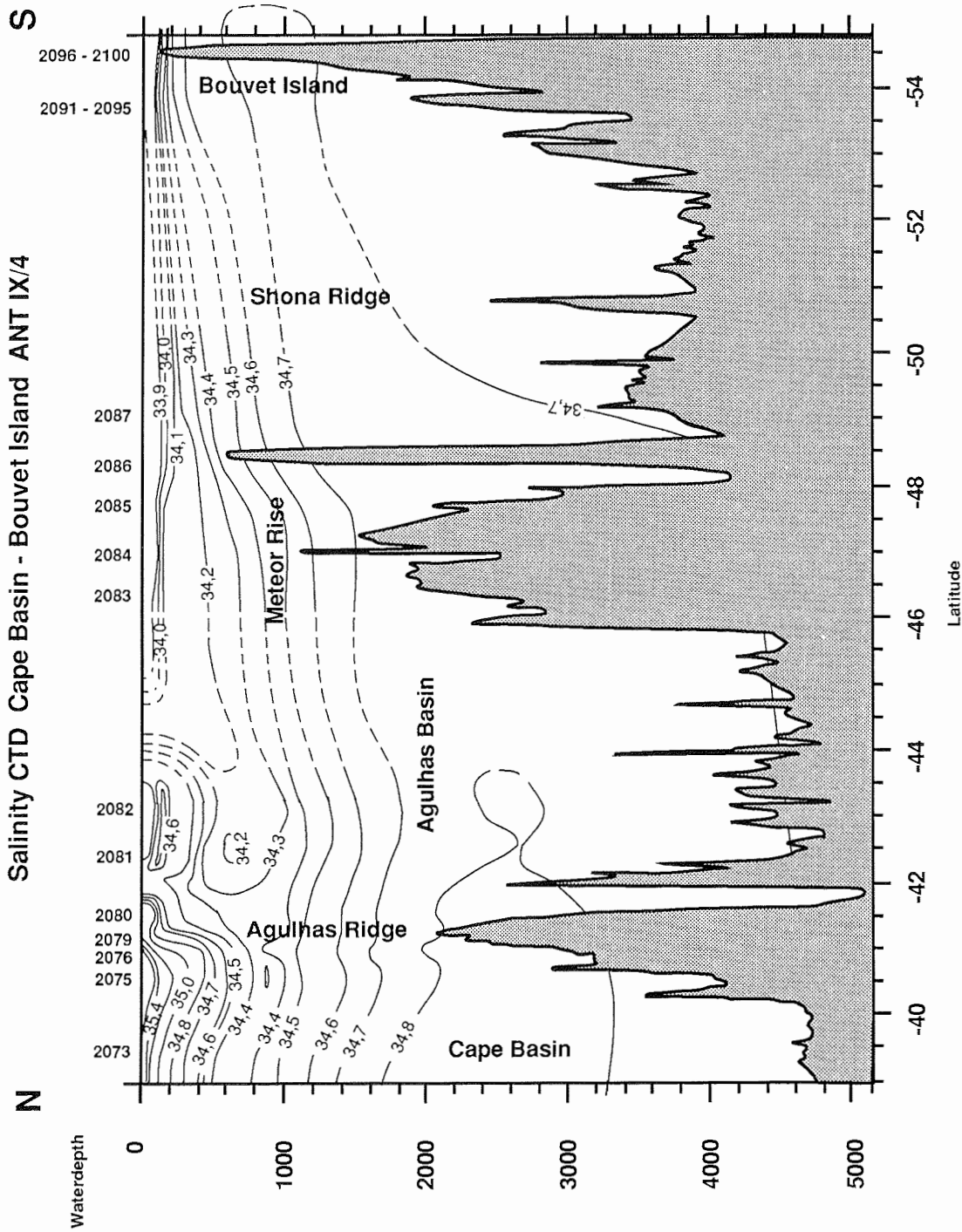
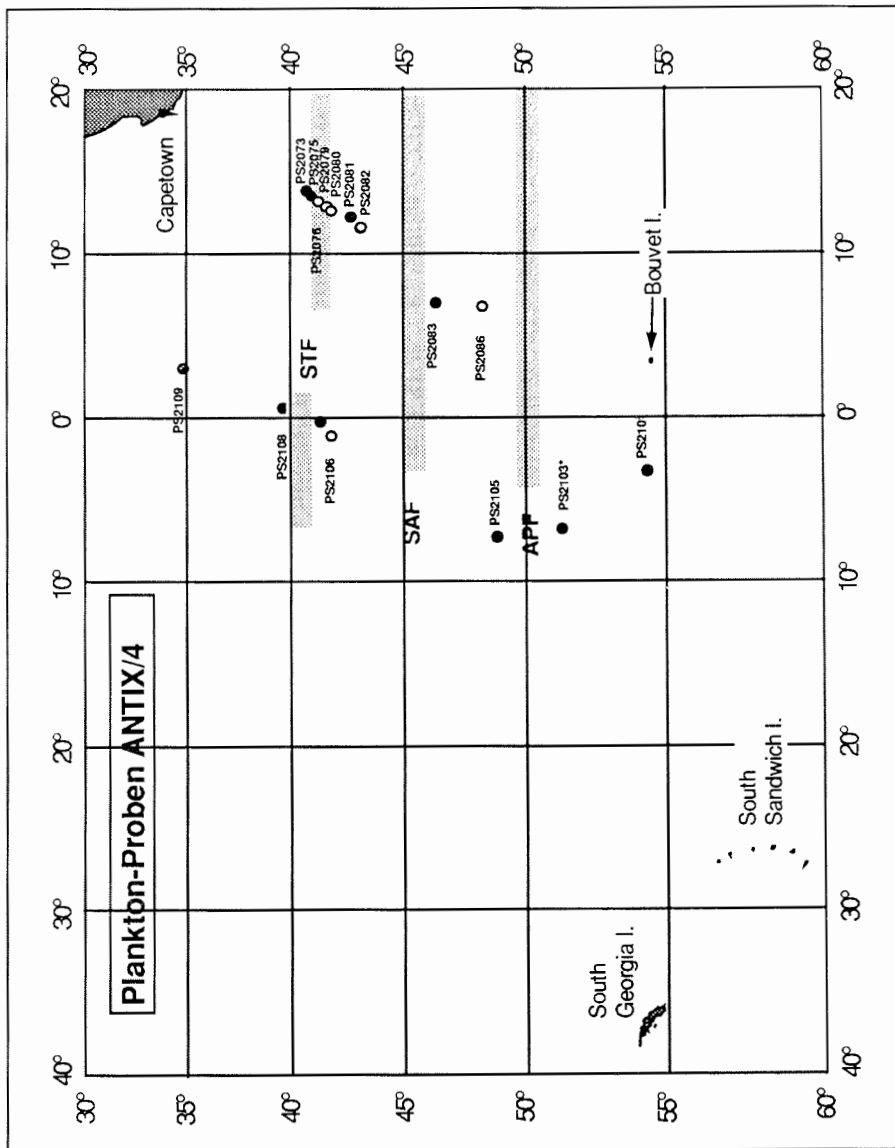


Fig. 4.25: Stationen mit Einsatz von Planktonnetz und Multinetz (schwarze Kreise). Stationen, wo nur Planktonnetze eingesetzt wurden, sind als offene Kreise, Stationen, wo nur Multinetze gefahren wurden, mit Dreieck markiert. Eingetragen ist die Lage der ozeanischen Frontensysteme, wie sie während ANT IX/4 angetroffen wurden (STF = Subtropische Front, SAF = Subantarktische Front, APF = Antarktische Polarfront).

Fig. 4.25: Site localities of plankton net hauls and multinet hauls (marked by black circles). Site localities with only plankton net hauls are marked by open circles. Site localities with only multinet hauls are marked by triangle. Stippled lines indicate location of the oceanic frontal systems as measured during ANT-IX/4 (STF = Subtropical Front, SAF = Subantarctic Front, APF = Antarctic Polar Front).



Maschenweite von 41 μm für Radiolarien und ein Netz mit 20 μm für Diatomeen gefahren.

Die vertikale Verbreitung des kieseligen Zooplanktons (Radiolarien) wurde auf dem NS-Profil mit Hilfe von 12 Multinetzeinsätzen über eine Wassertiefe von 1000 m untersucht. Hierzu wurden die Tiefenstufen anhand von hydrographischen Daten der zuvor eingesetzten Festspeicher CTD festgelegt. Die Beprobung des antarktischen Zwischenwassers war hierbei von besonderer Bedeutung. Es hierbei geprüft werden, ob bestimmte Arten mit dem antarktischen Zwischenwasser nach Norden abtauchen und in den Auftriebsgebieten des Südatlantiks wieder erscheinen.

Erste Ansprachen der Oberflächenwasserproben zeigen eine erhöhte Produktivität im Bereich der antarktischen Fronten sowie in den Auftriebsgebieten vor SW-Afrika und im Bereich des nördlichen äquatorialen Atlantik an. Aus den vertikalen Netzfängen ergibt sich eine deutliche Zunahme des Planktons in den obersten 100-200 m. Unterschiede in der Zusammensetzung konnten im Bereich unterhalb von 200 m beobachtet werden, wo im wesentlichen größeres Zooplankton dominiert, während in den obersten 200 m Phytoplankter und Protozooplankter vorherrschen.

6.2.2. Mikrozooplankton und Nannoplankton M. Knappertsbusch, H. Vonhof (VUA)

Während der Heimreise der "Polarstern" von Kapstadt über Bouvet Island nach Bremerhaven (30.3.91 bis 15.5.91), sammelten wir aus dem Oberflächenwasser kontinuierlich 136 Netzproben für Mikrozooplankton, 137 Proben für stabile Isotopen, 274 Nährstoffproben und 135 Filterproben für kalkiges Nannoplankton aus dem Oberflächenwasser. An 4 Tiefenstationen im Bereich der Polarfrontzone bis zur Subtropischen Front wurden die obersten 200 Meter der Wassersäule detailliert auf kalkiges Nannoplankton beprobt (43 Proben) und ebenfalls Proben für Nährstoffanalysen (gelöstes Silikat, Phosphat und Nitrat) eingeholt. Gleichzeitig wurden standardmäßig Temperatur- und Salinitätsprofile gemessen. Weiterhin erhielten wir von den Geologen Multicorer Oberflächen-Sedimentproben, welche zu Hause quantitativ auf kalkiges Nannoplankton untersucht und mit den zugehörigen Planktonproben verglichen werden sollen.

Mit unserem Material aus dem Oberflächenwasser möchten wir die latitudinalen Diversitätsgradienten planktonischer Foraminiferen und Coccolithophoriden in Abhängigkeit der durchfahrenen Wassermassen auskartieren. Unsere Fragestellung ist, inwieweit sich Wassermassen und Frontsysteme über faunistische und floristische Planktonzusammensetzungen erkennen lassen und wie sie sich auf die Sedimentoberfläche durchpausen. Unser spezielles Augenmerk galt dem Abschnitt zwischen Bouvet Island und der geographischen Breite von Kapstadt, wo wir aufgrund der hydrologischen Verhältnisse von der Subtropischen Konvergenzzone über die Polarfrontzone bis ins Antarktische Oberflächenwasser starke Gradienten in Diversität und Produktion der Planktonforaminiferenfauna und der Coccolithenflora zu erwarten haben. Mit den Foraminiferenproben möchten wir z.B. auch statistisch feststellen, zu welchem Ausmass die Windungsrichtungen von *Neogloboquadrina pachyderma* und *Globigerina bulloides* zur Abtrennung von Wassermassen dienen können. Dies soll uns Hinweise geben, wie diese

Parameter aus Holozänen Sedimenten interpretiert werden müssen. Die vier Tiefenstationen in der euphotischen Zone sind die südliche Ergänzung einer Serie von Vertikalprofilen im Atlantik, reichend von 59°N bis 55°S, welche dazu dienen soll die vertikale und horizontale Verteilung von Coccolithophoriden zu untersuchen (dieses Transect beinhaltet nebst ANT-IX-4 auch Material der Polarstern Expedition ANT-IX-1 und der Niederländischen JGOFS Expedition 4 von Reykjavik nach Galway im Juni 1990, siehe Fig. 4.26). Aufgrund dieser Daten soll versucht werden, die Coccolithen-Karbonatproduktion in der photischen Zone an verschiedenen geographischen Breiten quantitativ abzuschätzen.

Oberflächenwasserproben

Mikrozooplankton

Oberflächenwasser aus einer Tiefe von 10 m wurde via Planktonpumpe des Schiffes (Kreiselpumpe) und einer Schlauchleitung kontinuierlich durch ein 75 µm Netz geleitet. Um das Netz vor mechanischer Beschädigung durch Schlingerbewegungen zu schützen, wurde es in einer auf dem Heck plazierten, meerwassergefüllten Wanne (Inhalt ca. 1m³) aufgehängt, mit dem Kunststoffbecher nach oben festgebunden. Dies gewährte auch Schutz vor Austrocknen von Teilen des Netzes. Um den Wasserspiegel in der Wanne konstant zu halten, wurde eine Überlaufleitung installiert. Die durchflossene Wassermenge wurde mit einer Wasseruhr gemessen. Der mittlere Wasserfluß war 64,3 Liter pro Minute. Zeitweilig war ein maximaler Fluss von 67 Liter pro Minute vorhanden (in der Wasseruhr war ein grobes Filternetz eingebaut, welches jedoch von Zeit zu Zeit verstopfte und die Fließrate gelegentlich herabsetzte). Während der ganzen Fahrt wechselten wir die Netze etwa alle sechs Stunden aus (07.30 Uhr, 12.30 Uhr, 18.30 Uhr und 00.30 Uhr). Bei jedem Wechsel der Netze wurden Zeit, Position, Wassertemperatur (Temperatur an beiden Seiten des Schiffes sowie Temperatur des Bord-Thermosalinometers, THS), Salinität (Bord-Thermosalinometer), durchflossene Wassermenge und Schiffsgeschwindigkeit registriert, eine Probe für stabile Isotopen und zwei Nährstoffproben (200 ml für Nitrate und Phosphate und 200 ml für Silikate) gezogen. Leider erlitt am 29.4. das Bordsalinometer einen irreparablen Schaden. Für den Rest der Reise versuchten wir Näherungswerte der Salzgehalte in unserer mit Meerwasser gefüllten Wanne mit der CTD zu erhalten. Temperaturwerte liessen sich über die Direktmessung (steuerbord und backbord) errechnen (die Regressionsgerade für THS- und Direktwerte der Temperatur ist in Fig. 4.27 dargestellt, die Gleichung ist $T_{ths} = 1.01 \cdot T_{direkt} - 0.13$). Die gewonnen Planktonproben wurden in 250 ml PVC-Flaschen abgefüllt, mit gepufferter (Borax-Puffer, pH 8.2-8.5) Formaldehyd-Lösung fixiert, und dann bei +4°C im Kühlraum aufbewahrt. Die Isotopenproben (50 ml) wurden in Glasflaschen aufbewahrt und mit 3 Tropfen einer gesättigten KJ-Lösung versetzt. Die Nährstoffproben wurden ohne Vergiften sofort bei -27°C (Phosphat und Nitrat) in PVC Flaschen eingefroren. Die Silikat-Proben, ebenfalls unvergiftet, wurden bei +4°C in PVC Flaschen aufbewahrt.

Fig. 4.26: Tiefenwasserstationen der Expeditionen ANT-IX/1 und ANT-IX/4 von FS "Polarstern" sowie der Niederländischen JGOFS-4 Expedition.
Fig. 4.26: Deepwater stations of RV "Polarstern" expeditions ANT-IX/1 and ANT-IX/4 as well as those of the Netherlands JGOFS-4 expedition.

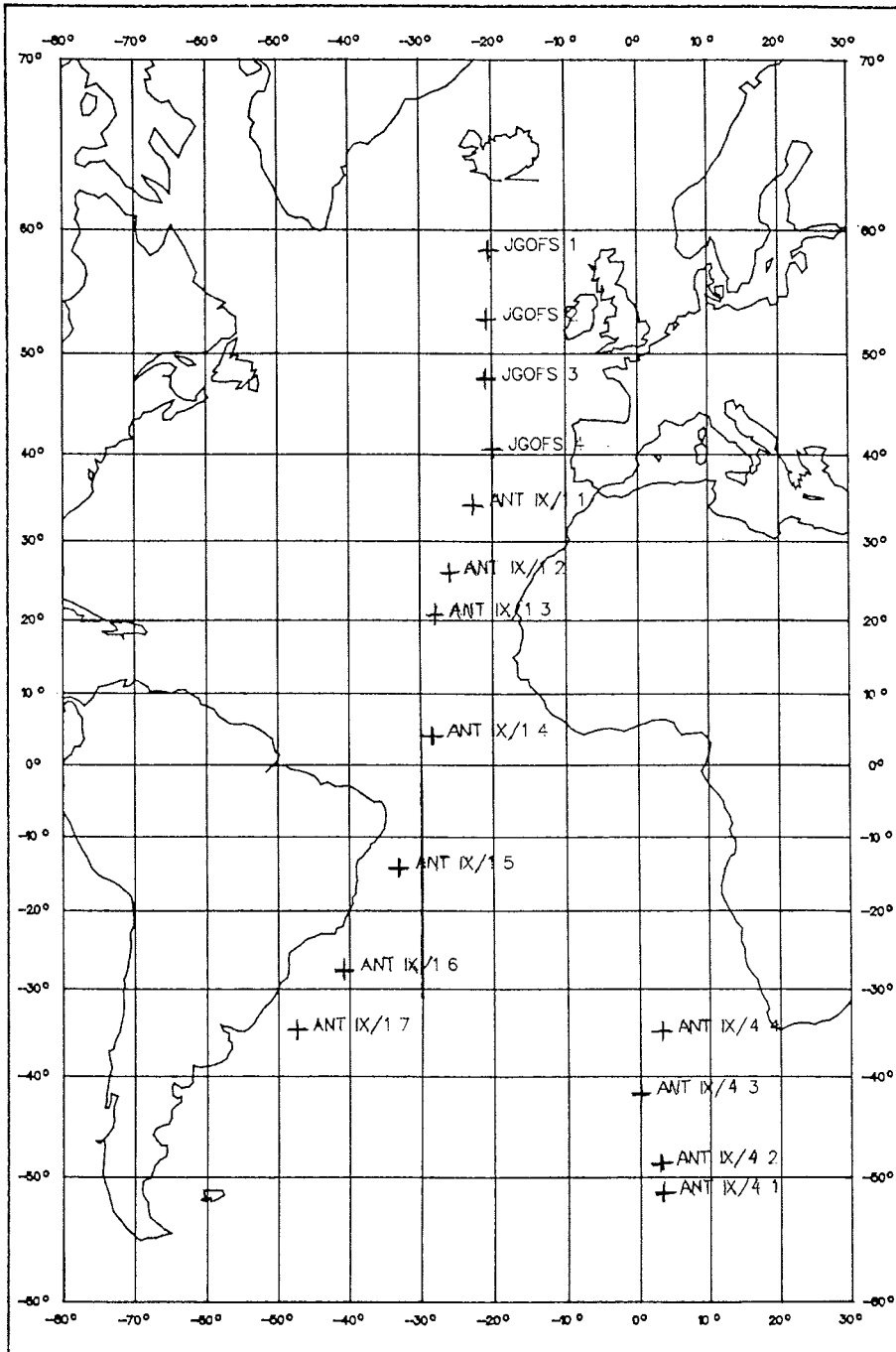
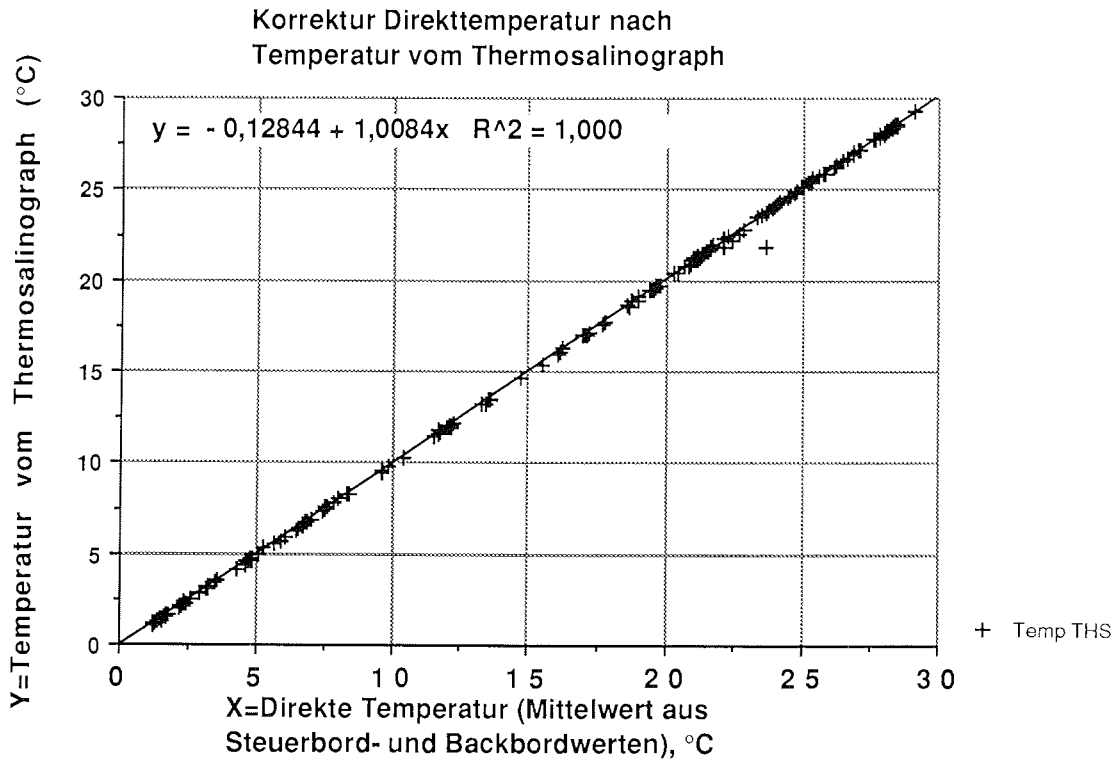


Fig. 4.27: Temperaturkorrektur des Thermosalinograph.

Fig. 4.27: Correction of the temperature measured with the thermosalinograph.



Kalkiges Nannoplankton

Die Oberflächenwasserproben für Coccolithophoriden stammen aus 10 m Wassertiefe und wurden von der Seewasserleitung im Chemie Trockenlabor (Membranpumpe) gesammelt. Die Probenahme geschah ca. alle 6 Stunden (meistens um 07.30, 12.30, 18.30 und 00.30 Uhr Schiffszeit), parallel zu den Zooplanktonproben. Für jede Probe wurden 10 Liter Seewasser in Plastikkanister abgefüllt und gleich anschliessend über ein Vakuum Millipore System filtriert (Vakuum ca. 30 cm Hg-Säule). Die Wasserproben wurden in unversehrtem Zustand filtriert. Die Filter waren Zellulose-Azetat Membran Filter (Typ HA) von Millipore, Porengrösse 0.45 μm , der Filterdurchmesser war 47 mm. Alle Filter waren vorgewogen, um später die Trockengewichte der Phytoplankton-Biomasse bestimmen zu können. Die filtrierte Wassermenge war zwischen 5 und 10 Litern, meistens 7 Liter. Um das Meersalz auszuwaschen verwendeten wir deionisiertes Wasser aus der Millipore-Wasserreinigungs Anlage. Einige Tropfen zugesetzter NH_3 -Lösung (der pH des Spülwassers war zwischen 9 und 10) verhinderten Karbonatlösung auf den Filtern. Nach der Filtration wurden alle Filter luftgetrocknet und dann in Polystrol Dosen aufbewahrt.

Tiefenstationen

Für die Untersuchung der vertikalen Verteilung des kalkigen Nannoplanktons wurden an vier Tiefenstationen (siehe Fig. 4.26) mit der Bio-Rosi (12 x 12 Liter Niskinflaschen) Wasserproben aus den folgenden Tiefen gewonnen: 3 m, 10 m, 20 m, 30 m, 40 m, 50 m, 60 m, 75 m, 100 m, 125 m, 150 m und 200 m. Diese Tiefen stimmen mit jenen des im Juni 1990 durchgeführten Niederländischen JGOFS-Leg 4 Programmes und mit den Proben von ANT-IX/1 überein. Die Wasserproben wurden in Plastik Behältern zwischengespeichert und dann sofort mit der unter oben beschriebenen Methode abfiltriert. Von jeder Probe wurden auch Nährstoffproben (200 ml für Phosphat und Nitrat, 200 ml für Silikat) abgezweigt (Aufbewahrung siehe oben). Temperatur- und Salinitätsprofile über die durchfahrenen Tiefen stammen von einer Festspeicher CTD (Seabird Electronics, Modell SBE, Messrate: Alle 1.5 Sekunde 1 Scan) gemessen, welche am Multicorer befestigt war.

Oberflächensedimentproben

Zur Bestimmung des kalkigen Nannoplanktons an der Sedimentoberfläche erhielten wir von den Multicorer Rohren ca. 1-2 mm³ Sediment vom obersten Millimeter, sowie je eine Probe des überstehenden Flokulates.

Vorläufige Beobachtungen und Ergebnisse

Hinreise: Fig. 4.28a zeigt die latitudinalen Fluktuationen der Oberflächenwassertemperatur- und Salinität an unseren Probenahmestellen während der Hinfahrt (Kapstadt-Bouvet Island). Die Salinitätswerte des Bordsalinometers während der Hinfahrt waren zu hoch im Vergleich mit entsprechenden Werten von der CTD und wurden nach folgender Formel korrigiert

$$S_{ctd} = 1,03 * S_{ths} - 4,24 \quad (\text{in } \text{‰})$$

wobei S_{ctd} : =Salinitätswerte mit der CTD, und

S_{ths} : =Ablesung am Bordsalinometer

Die stufenweise Abnahme der Temperatur (Salinität) von 19°C auf ca. 11°C und dann von 11°C auf 9°C (Salinität von 35.5 ‰ nach ca. 34 ‰) zwischen 40°S und 42°S zeigt die Subtropische Konvergenzzone an. Auf der Hinfahrt fiel diese Zone mit einer deutlichen Reduktion in der Planktonmenge zusammen (um eine grobe Vorstellung der Fluktuationen der Zooplanktonmenge in unseren 75 µm Netzfängen zu erhalten wurde die Höhe der Planktonmasse nach absedimentieren in den PVC-Flaschen gemessen (in cm), und auf 100 m³ der durchflossenen Wassermenge umgerechnet). In der Subtropischen Zone bestand das Zooplankton zu grossen Mengen aus Copepoden, planktonischen Foraminiferen, Pteropoden, Tintinniden, zahlreichen Larven und Dinoflagellaten. Die Coccolithophoridenflora waren reichhaltig, die Coccosphaeren gut erhalten und die Artzusammensetzung hochdivers (*Emiliania huxleyi*, *Helicopontosphaera carteri*, *Calcidiscus leptoporus*, *Syracosphaera pulchra*, einige wenige *Umbellosphaera tenuis*, *Syracosphaera mediterranea*, *Umbilicosphaera sibogae*, *Anthosphaera robusta*, *Oolithotus fragilis*, *Calyptrosphaera oblonga*, *Rhabdosphaera clavigera*, *Ceratolithus cristatus*, *Anoplosolenia brasiliensis*). Nach Süden hin verringerte sich die Coccolithophoridendiversität, am stärksten zwischen 43°S und 45°S. In der südlich anschliessenden Subantarktischen Zone waren unter den Coccolithophoriden lediglich noch *E. huxleyi* und gelegentlich *C. leptoporus* vorhanden. Die Subantarktische Front war in den Oberflächenwassertemperaturen und Salinitätswerten nicht identifizierbar. Auffällig ist jedoch ein gewaltiger Anstieg in der Planktonproduktion zwischen 48°S und 49°S. Gleichzeitig stellten wir

in diesem Intervall eine deutliche Änderung der Farbe der gefangenen Zooplanktonmasse von rotbraun nach oliv- oder dunkelgrün fest. Der grösste Anteil des Phytoplanktons machten Diatomeen aus. Erwähnenswert sind riesige Exemplare von *Rhizosolenia curvata*, die besonders zwischen 46° 21' S und 50° 25' S aufgetreten waren und bei 48° 22' S (Probe PL 20) in gigantischen Mengen aufgetreten waren. Andere Diatomeenarten in unseren 75 mm Netzen waren *Chaetoceros dichaeete*, *Chaetoceros sp.*, *Asteromphalus hookeri*, neben planktonischen Foraminiferen wie *Globigerina bulloides* und *Neogloboquadrina pachyderma*. Dinoflagellaten waren ebenfalls vorhanden. Zu unserem Erstaunen fanden wir in diesen hohen Breiten auch *Emiliania huxleyi* in relativ grosser Zahl. Andere Coccolithen waren jedoch in den vorläufig gesichteten Filterproben nicht vorhanden. Möglicherweise bildet diese erhöhte Oberflächenwasserproduktion die Polarfront ab. Südlich von 50°S reduzierte sich die Planktonproduktion bis an die 2°C Isotherme um mehr als das dreifache. Zwischen ca. 53°S und Bouvet Island beobachteten wir jedoch noch einmal eine sehr rasch ansteigende Planktonmenge mit vielen Diatomeen und Silicoflagellaten. Bei Bouvet Island (54°30.37' S/3°00.91' E) fanden sich grosse Mengen der Diatomee *Nitschia kergeulensis* und der Silicoflagellate *Distephanus speculum* in unseren Oberflächenwasserproben. Auch *E. huxleyi* war immer noch in relativ grosser Zahl vorhanden.

Rückreise: Auch während der Rückreise zeigte das Bordsalinometer stärkere Abweichungen in der Salinität von denen der Festspeicher CTD auf. Die Oberflächenwassersalinitätswerte des Bordsalinometers wurden daher nach den Werten der CTD folgendermassen korrigiert:

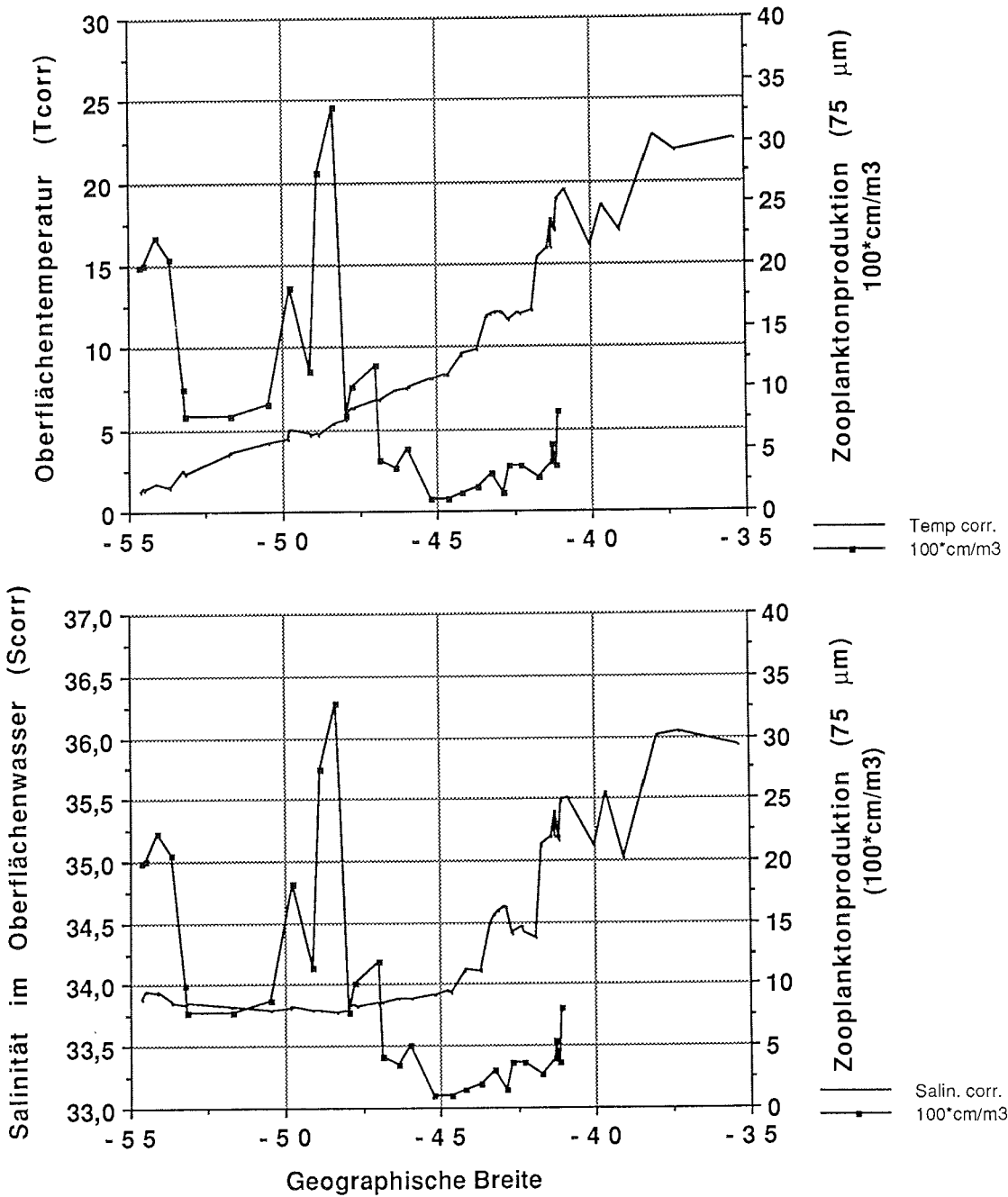
$$S_{ths} = 0,85 * S_{ctd} + 2,31$$

Fig. 4.28b zeigt den Kurvenverlauf der Oberflächenwassertemperatur und der korrigierten Salinität auf der Rückreise Bouvet Island-Bremerhaven. Temperatur- und Salinitätsverlauf erlauben keine eindeutigen Rückschlüsse zur Lokalisierung der Subantarktischen Front oder Polarfront. Auch die Lage der Subtropischen Front kommt durch den Temperaturverlauf nicht als plötzlicher Anstieg zum Ausdruck. Interessant hingegen ist, dass wie bei der Hinfahrt bei ca. 54°S und bei ca. 50°S eine deutlich erhöhte Planktonproduktion zu verzeichnen war. Zwischen 35°S und 20°S bildete sich ein Temperatur- und Salinitätsplateau aus und könnte durch den Benguelastrom verursacht sein. In diesem Abschnitt und innerhalb des Süd- resp. Nordäquatorialstromes war die Planktonproduktion vergleichsweise niedrig. Ab ca. 19°S finden wir *Globigerinoides ruber*. Im Bereich des Äquators traten auffällige, lange, schlanke Algefäden auf, die wir in denselben Breiten bereits während ANT-IX-1 beobachtet hatten. Nördlich des Äquators fanden wir in Stichproben *Globigerinoides ruber*, *Globigerinoides sacculifer*, *Globorotalia menardii* und *Globigerina falconensis*. Die deutlich erhöhte Planktonproduktion zwischen 12°N und 14°N deutet wahrscheinlich auf Küstenauftrieb hin. In diesem Bereich waren Radiolarien am häufigsten. Das Meerwasser war zeitweise braun gefärbt, sämtliche Nannoplanktonfilter verstopften augenblicklich und das Filtergut war orange gefärbt (normalerweise gelb-grün). Die hohe Trübung mag zum Teil auch durch Einmünden grosser Flüsse (Gambia, Senegal ?) verursacht worden sein. Leider standen uns zu diesem Zeitpunkt keine verlässlichen Salinitätsmessungen mehr zur Verfügung, sodass wir auf weniger genaue Messungen mit der CTD in unserem Auffangbecken angewiesen waren. Trotzdem zeigen diese Werte einen deutlich erniedrigten Salzgehalt im Oberflächenwasser an. In der Biscaya beobachteten wir noch einmal eine deutlich erhöhte Planktonproduktion.

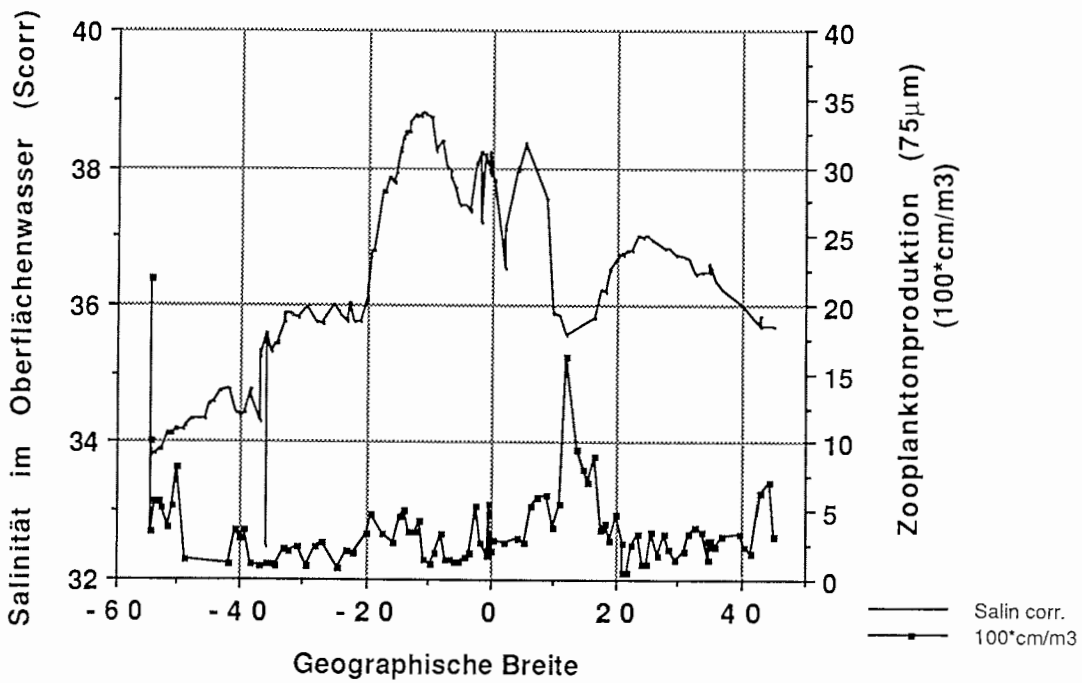
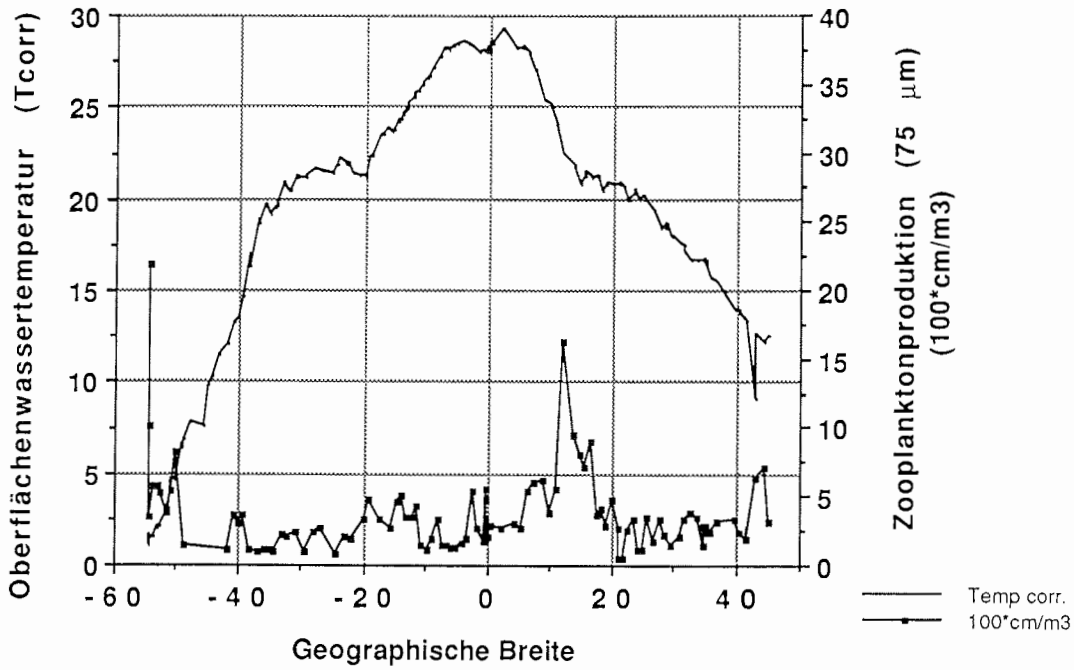
Fig. 4.28a und b: Temperatur und Salinität im Oberflächenwasser während der Hinreise (Kapstadt - Bouvet Island) und der Rückreise (Bouvet Island - Bremerhaven)

Fig. 4.28a and b: Temperature and salinity of the surface water at the transects Capetown - Bouvet Island and Bouvet Island - Bremerhaven.

**Hinreise: Kapstadt-Bouvet Island
(30.3.91-9.4.91)**



Rückreise: Bouvet Island-Bremerhaven
(9.4.91-10.5.91)



6.3. Verankerungsarbeiten und Sedimentfallen G. Ruhland (FGB)

Im Verlauf der Reise ANT IX/4 wurden zwei Jahresverankerungen am Walfischrücken und vor Cap Blanc bedient, die unter geologischen und ozeanographischen Fragestellungen ausgebracht wurden. Um Sedimentationsvorgänge besser verstehen zu können, ist es notwendig, den Weg der partikulären Substanzen durch die Wassersäule bis ins Sediment zu verfolgen. Die Verankerungen dienen der Langzeitbeobachtung dieses Partikelflusses. Hierzu werden Sedimentfallen mit zeitgeschalteten Probenwechslern in der Wassersäule verankert. Sie erlauben einen Wechsel von bis zu zwanzig Probenbechern in frei wählbaren Zeitintervallen. Die gewonnenen Probenserien sollen Untersuchungen über die Entwicklung des Planktons und der damit verbundenen Sedimentation ermöglichen. Mit Hilfe der gleichzeitig verankerten Strömungsmesser, die Parameter wie Strömungsrichtung und -geschwindigkeit, Leitfähigkeit und Temperatur registrieren, sollen Aussagen über die Dynamik des Wasserkörpers sowie über die Herkunft des Probenmaterials gewonnen werden. Eine schon erfolgte Beprobung des Sediments mit Schwereloten und Multicorern an den Verankerungspositionen vervollständigt das Bild der Sedimentationsvorgänge.

In den Verankerungen wurden Sedimentfallen des Typs Salzgitter SMT 230 sowie Strömungsmesser der Typen Aanderaa RCM 8 mit Festspeicher und RCM 5 mit Bandaufzeichnung verwendet (Fig. 4.29). Vier hydroakustische Auslöser der Typen Oceano RT 161 und AR 261, die jeweils in Parallelanordnung angebracht waren, dienten der Freigabe der Verankerungen.

WR-3 und WR-4 (20° 01'S; 9° 10'E)

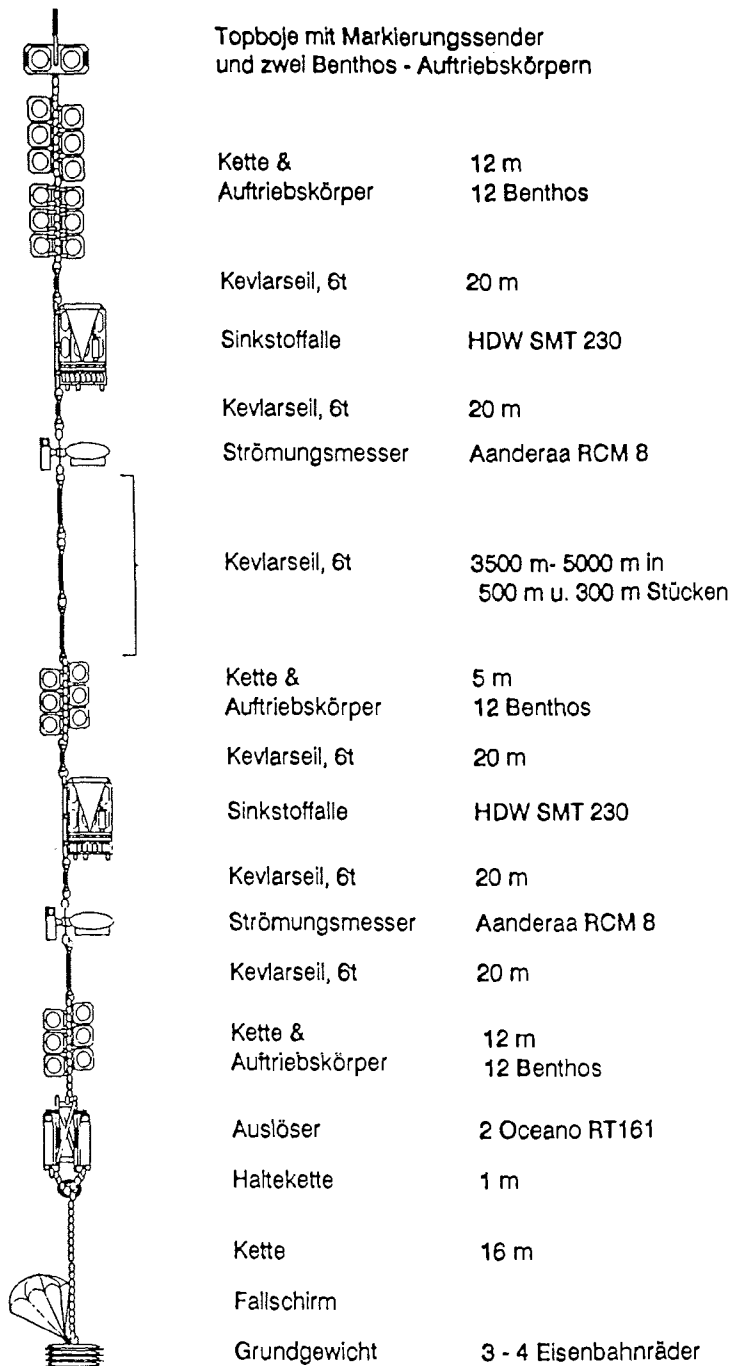
Am 19.4.91 wurde bei ruhigem Wetter die 1600 m lange WR 3-Verankerung angesprochen. Die Auslöser antworteten und wurden dann beide ausgelöst. Nach 10 Minuten konnte der angebrachte Peilsender klar empfangen werden und die Verankerung wurde in eineinhalb Stunden geborgen. Alle Geräte funktionierten fehlerfrei. Es konnten zwei komplette Probensätze aus den Sedimentfallen gewonnen werden, deren Sammelintervall jeweils 19 Tage betrug. Die Proben zeigen saisonale Schwankungen in der Sedimentation, die im September/Oktober ihr Maximum erreichten. Die Probenmengen sind in der unteren Falle in fast allen Proben höher als in der oberen Falle. Die beiden Strömungsmesser registrierten alle 120 Minuten und die Festspeicher liessen sich ohne Probleme auslesen. Um die Beobachtungen fortzusetzen wurde am Walfischrücken erneut eine vergleichbare Verankerung (WR 4) über die Heckslippe ausgebracht.

CB-3 und CB-4 (21° 07'N; 20° 40'W)

Vor Cap Blanc konnte am 2.5.91 die Jahresverankerung CB 3 ausgelöst und nach kurzer Suche aufgenommen werden. Der installierte Peilsender war nicht zu empfangen, weil das ausgesandte Signal zu schwach war. Die verankerten Sedimentfallen in 600 und 3500 Meter Tiefe waren auf ein Sammelintervall von 21.5 Tagen pro Probe programmiert. Die Fallen funktionierten beide, jedoch zeigte die obere Falle starke Korrosionserscheinungen am Druckgehäuse, die untere Falle stand nicht in Endposition und enthielt mehrere leere Probenbecher, die auf einen Fehler beim Probenwechsel zurückgeführt wurden, der bei der Abfrage der Steuerelektronik der Falle auch bestätigt wurde. Der verwendete Strömungsmesser RCM 5 war mit

einem Trübungsmesser ausgerüstet, um Aussagen über die Partikelkonzentration und damit indirekt über den Partikeltransport treffen zu können. Anschließend wurde auf der gleichen Position CB 4 als neue Jahresverankerung mit zwei Sedimentfallen und zwei Strömungsmessern ausgebracht.

Fig. 4.29: Aufbau einer Verankerung mit Sedimentfallen und Strommessern
Fig. 4.29: Mooring with sediment traps and current meters



7. SPURENSTOFFE IN DER MARITIMEN ATMOSPHERE UND HYDROSPHERE

7.1. Schwerflüchtige Organochlorverbindungen in der troposphärischen Grundschicht und im Oberflächenwasser J. Schreitmüller (UU)

Zielsetzung

Die globale Verteilung von Umweltchemikalien ist seit mehreren Jahren ein Forschungsschwerpunkt unserer Arbeitsgruppe. Während des Fahrtabschnittes ANT-IX/4 wurden mittels Luft- und Wasserproben Süd-Nord-Profile für folgende schwerflüchtige Organochlorverbindungen aufgenommen:

- Hexachlorbenzol
- Hexachlorcyclohexan (HCH)- Gruppe
- Polychlorbiphenyle (PCB)
- DDT-Gruppe
- Chlordan-Gruppe

Diese Untersuchungen schließen thematisch an den Fahrtabschnitt ANT-IX/1 von Bremerhaven nach Punta Arenas (Chile) an, wo ebenfalls für obige Verbindungen Probenahmen zur Erstellung eines meridionalen Profils durchgeführt wurden. Somit dient dieser Fahrtabschnitt hauptsächlich dazu, einen größeren Datensatz zu erhalten und bisherige Trends und Ergebnisse zu überprüfen. Zusätzlich soll zum erstenmal die Belastung von Atmosphäre und Hydrosphäre mit diesen Umweltchemikalien in küstenfernen Gebieten im Südatlantik ermittelt werden.

Die Bewertung der Analysenergebnisse soll hinsichtlich folgender Fragestellung durchgeführt werden: Wie hängt der atmosphärische Ferntransport, der Transport in der Wasserphase sowie die Gas-Wasser-Verteilung von Umweltchemikalien von deren physikalisch-chemischen Eigenschaften (Dampfdruck, Wasserlöslichkeit, Henry-Konstante, Octanol-Wasser-Verteilungskoeffizient) ab? Dabei müssen die globalen Massenkreisläufe berücksichtigt werden. Insbesondere soll die Frage geklärt werden, ob und wie stark die intertropische Konvergenzzone (ITCZ) den Austausch zwischen Nord- und Südhemisphäre einschränkt.

Durchführung der Probenahmen

Bedingt durch die für die verschiedenen Proben nötigen aufwendigen Analyseverfahren wurde auf dem Schiff nur die Probenahme durchgeführt. Die Luftprobenahme wurde zwei Tage nach dem Auslaufen aus Kapstadt aufgenommen. Dabei wurden die zu untersuchenden Verbindungen adsorptiv auf Kieselgel angereichert, wobei ein davor angebrachter Glasfaserfilter den partikelgebundenen Anteil abtrennen sollte. Eine zweite Kieselgelschicht diente zur Bestimmung des Durchbruchs. Um die Nachweisgrenze der Organohalogene deutlich zu überschreiten wurden zwischen 500 und 800 m³ Luft mittels einem High-Volume-Sampler durch die Sammeleinrichtung gesaugt. Zur Verringerung möglicher Kontaminationen durch das Schiff wurde die Probenahme auf dem Peildeck durchgeführt. Bei ungünstiger Windlage wurde der High-Volume-Sampler abgestellt. Ansonsten wurde die Probenahme kontinuierlich bis zum Ende der Reise durchgeführt. Nach

beendeter Probenahme wurde das Adsorptionsmittel in Glaskolben eingeschmolzen.

Die Beprobung des Oberflächenwassers erfolgte mittels einer schiffseigenen Rotationspumpe. Dabei wurde das Wasser durch eine XAD-Kartusche (Divinylbenzol-Polystyrol-Copolymer) gepumpt, wobei eine adsorptive Anreicherung der hydrophoben Organohalogenverbindungen erfolgte. Die Partikelphase wurde durch einen davor angebrachten Glasfaserfilter abgetrennt. Die beprobten Wasservolumina betragen zwischen 60 und 100 l, was bei einem Fluß von ca. 150 ml/min zu einer Probungsdauer von etwa 10 Stunden führte. Während Stationsbetrieb wurde aufgrund der möglichen Kontamination des Wasserkörpers durch das Schiff keine Probenahme durchgeführt. Die Glaskartusche wurde mit vorher in Hexan ausgekochten Teflondichtungen verschlossen. Die Bereiche, in denen die Wasserproben genommen wurden, sind in bei-liegender Fig. eingezeichnet. Zusätzlich wurden diskontinuierlich einige Planktonproben genommen. Dazu wurde das über eine Rotationspumpe geförderte Wasser über ein Stahlsieb mit einer Maschenweite von 250 µm filtriert. Nach beendeter Probenahme wurde das filtrierte Plankton sofort eingefroren.

Ausblick auf durchzuführende Messungen am Heimatinstitut

Die Desorption der Organohalogenverbindungen von Kieselgel, XAD sowie vom Zooplankton erfolgt mittels organischer Lösungsmittel. Nach verschiedenen Aufarbeitungsschritten (clean-up) mit adsorptionschromatographischen Methoden und einer zusätzlichen Anreicherung erfolgt die Bestimmung über die Gaschromatographie und einem für Halogenverbindungen sehr empfindlichen Elektroneneinfangdetektor (ECD). Zusätzlich sollen einige Proben mit einem massenspektrometrischen Detektor ausgewertet werden.

7.2. Organobromverbindungen in der marinen Troposphäre und im atlantischen Oberflächenwasser

T. Oertel, H. Lorenzen-Schmidt (AWI)

Das angestrebte Ziel ist auf dem Fahrtabschnitt ANT-IX/4 in Ergänzung zu vorangegangenen Fahrtabschnitten horizontale Verteilungsprofile von verschiedenen leichtflüchtigen Bromverbindungen zu messen. Ein großer Teil des atmosphärischen Broms stammt aus natürlichen Quellen (Methylbromid u. Bromoform z.B. aus Ozeanen). Insbesondere aber tragen anthropogene Emissionen u.a. der Halone 1301 (CF_3Br) und 1211 (CF_2BrCl) zum Anstieg der Bromkonzentration in der Stratosphäre bei. Aufgrund ihrer sehr großen katalytischen Effizienz können Bromatome in größerem Ausmaß als Chloratome Ozon in der Stratosphäre zerstören. Aus den ermittelten Konzentrationsprofilen werden Aussagen über die globale Verteilung dieser Stoffe sowie den biogenen und anthropogenen Beitrag auf den bromkatalysierten Ozonabbau erwartet. Zur Untersuchung des Austausches mit der Hydrosphäre wird die Konzentration der gelösten Organobromverbindungen im Oberflächenwasser ermittelt.

Die Luftprobennahme erfolgte 20m über dem Meeresspiegel im Luftchemiecontainer auf der vorderen Steuerbordseite des Peildecks. Die Windrichtung wurde ständig kontrolliert und die Probennahme bei ungünstigen Verhältnissen eingestellt, um eine Kontaminierung durch das Schiff zu vermeiden. Die Spurengase der Luft wurden durch Ausfrieren in flüssigem Argon

angereichert. Dabei wurde die Luft mit einer Membranpumpe bei konstantem Fluß durch ein mit silylierter Glaswolle gepacktes Glas-U-Rohr gesaugt, welches in flüssiges Argon eintaucht. Der Wassergehalt der Luft wurde mit einer auf -20°C gehaltenen Kühlfalle entfernt. Mit dieser Methode wurden ca. 60 Luftproben zwischen 32°S und 35°N gesammelt, die U-Rohre an beiden Enden zugeschmolzen und mit Alufolie gegen Licht geschützt bei -28°C gelagert. Diese Proben werden im AWI mittels Gaschromatographie mit EC-, MS- und FTIR-Detektion analysiert. Die geplanten "in situ" Messungen von Luftproben mit einem im Luftchemiecontainer befindlichen Gaschromatographen konnten leider aufgrund meßtechnischer Probleme nicht durchgeführt werden.

Für die Untersuchung des Austausches der leichtflüchtigen Bromverbindungen im System Ozean/Atmosphäre wurden bei ca. 50 Positionen Wasserproben aus der Seewasserleitung entnommen, in Glasampullen eingeschmolzen und bei -28°C gelagert. Diese Proben werden ebenfalls im AWI analysiert.

8. **UNTERSUCHUNGEN ZUM NAHRUNGSVERHALTEN UND ZUR AKTIVITÄT HOCHANTARKTISCHER GARNELEN (DECAPODA, NATANTIA)**

M. Gorny (AWI)

An lebenden Exemplaren von 2 benthische Garnelenarten, die im Weddellmeer und der Lazarevsee gefangen wurden, *Chorismus antarcticus* und *Notocrangon antarcticus*, konnten während des IV. Fahrtabschnittes Fütterungsexperimente und Verhaltensstudien durchgeführt werden, die später durch Mageninhaltsuntersuchungen, bzw. Experimente zum Sauerstoffverbrauch der Tiere ergänzt werden sollen. Nachdem die Tiefenzonierung und geographische Verbreitung dieser Arten im Weddellmeer bekannt ist (Arntz & Gorny, 1991) soll durch Versuche und Beobachtungen aus der Lebendhaltung, bereits vorliegenden Daten und laufenden Studien zur Reproduktionsbiologie, Populationsdynamik und zum Wachstum untersucht werden, wie sich die Garnelen den Bedingungen der Hochantarktis angepaßt haben.

Versuchsbedingungen

Auf dem III. Fahrtabschnitt wurden insgesamt 133 *Chorismus antarcticus* und 88 *Notocrangon antarcticus* gefangen und in einem Kühlcontainer bei Wassertemperaturen von -1°C ($\pm 0,5^\circ\text{C}$) lebend gehältert. In 25 l Aquarien befanden sich je nach Größe bis zu 8 Tiere, wobei nicht nach Arten getrennt wurde. Allen Tieren wurde über einen Zeitraum von 6 Wochen jeden 3. Tag abwechselnd Fisch- und Garnelenfleisch als Nahrung angeboten sowie zusätzlich lebende Isopoden (*Aega gracilis*). Verhaltensstudien wurden teilweise mit einer Farbvideokamera aufgezeichnet (Sony U-matic). Um die Tiere dabei in ihrer Reaktion so wenig wie möglich zu beeinflussen, erfolgten die Aufnahmen bei geringer Beleuchtung (mit roter Scheinwerferfolie abgeklebte Leuchtstoffröhre).

Vorläufige Ergebnisse

Wurden Stücke von Fisch- oder Garnelenfleisch in die Aquarien gegeben, so bewegten sich die *Chorismus antarcticus* nach kurzer Zeit darauf zu, ergriffen die Brocken mit ihren Scheren und begannen zu fressen. *Notocrangon*

antarcticus reagierte dagegen nur, wenn das Futter in unmittelbare Nähe der Tiere gebracht wurde. Sie fraßen dann nur solche Nahrungsbrocken, die die sie mit ihren Scheren ergreifen und in einem Stück hinunterschlingen konnten. Dieser Vorgang konnte bis zu 5 mal hintereinander wiederholt werden. Große Fischstücke und tote Garnelen wurden dagegen von *C. antarcticus* im Laufe mehrerer Tage, oft von mehreren Tieren gleichzeitig, bis auf den Panzer ausgefressen. Lebende Garnelen, insbesondere frisch gehäutete Tiere oder solche, die möglicherweise durch Verletzungen aus dem Fang geschwächt waren sowie die lebenden Isopoden wurden nur von *C. antarcticus* angegriffen und ebenfalls gefressen.

Chorismus antarcticus zeigte gegenüber *Notocrangon antarcticus* ein wesentlich agileres Verhalten. Die Tiere saßen auf den zur Belüftung dienenden Schaumstoffluftfiltern, bewegten sich aber von Zeit zu Zeit langsam durch die Aquarien. An *N. antarcticus* konnten Verhaltensstudien zum Aktivitätsrhythmus aufgezeichnet werden, wobei alle beobachteten Tiere das gleiche Verhaltensmuster zeigten. Lange Phasen der Reglosigkeit, in denen nur die Antennen bewegt wurden wechselten stetig mit kurzen Aktivitätsphasen ab. Die Tiere gruben dann entweder mit ihren Scheren im Sediment oder bewegten sich von der Stelle. Nachdem die Tiere ihren Standort verändert hatten, wurde meist durch Schlagen mit den Pleopoden eine Kuhle erzeugt, in der sich die Tiere dann niederließen. Anschließend wurde mit den Scheren das Sediment durchgegraben. Das typische Verhaltensmuster dieser Art ist in Fig.4.30. exemplarisch anhand der Aktivitäten eines Versuchstieres dargestellt.

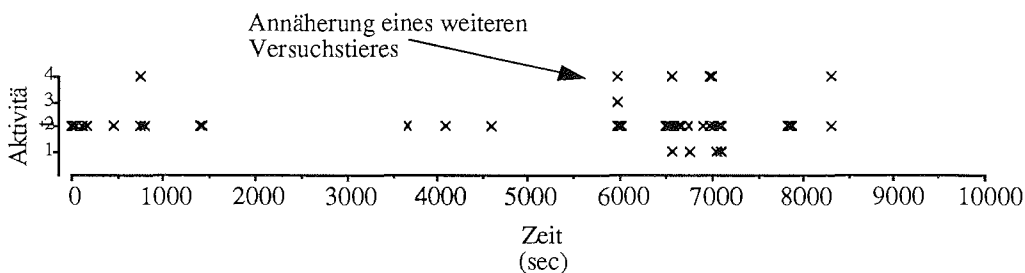


Fig. 4.30: Aktivität von *Notocrangon antarcticus* (Versuchstier 3, Beobachtungszeitraum 10000 sec = 2 Std 47 min).

Aktivitätsskala:

1 Bewegung der Pleopoden, 2 Bewegung der Zangen, 3 Bewegung von Pleopoden und Zangen, 4 Veränderung des Standortes

Fig. 4.30: Activity of *Notocrangon antarcticus* (3 animals, observation period 10000 sec = 2 hrs 47 min.)

Activities

1 movement of pleopods, 2 movement of claws, 3 movement of both 1 + 2, 4 change of animal's location

Diskussion

Die Verhaltensweisen beider Arten dürften ihren natürlichen Gewohnheiten weitgehend entsprechen. So zeigten Unterwasseraufnahmen, daß *Chorismus antarcticus* meist auf Schwämmen sitzt, während *Notocrangon antarcticus* eher ein Substrat mit geringer Epifauna zu bevorzugen scheint und sich dort, wie auch in der Lebendhaltung beobachtet, ins Sediment eingegräbt. (Gutt et al., im Druck). Die Reaktion auf die angebotene Nahrung muß daher in Zusammenhang mit der unterschiedlichen Lebensweise der Arten betrachtet werden. *N. antarcticus* ist auf Beute angewiesen, die sich im oder direkt auf dem Sediment befindet, *C. antarcticus* dagegen in erster Linie auf solche Tiere, die auf und in den Schwämmen leben, wie z.B. Amphipoden oder Isopoden, was das räuberische Verhalten dieser Art erklären würde. Die Selektion der in den Experimenten angebotenen Nahrungsbrocken sowie die Bewegungen der Zangen läßt vermuten, daß *N. antarcticus* Beutetiere einer bestimmten Größe, wie z. B. junge Muscheln aus dem Sediment ausgräbt. Genauere Aufschlüsse über Qualität und Quantität der Nahrung beider Arten werden daher von den Mageninhaltsuntersuchungen erwartet.

Das bei *Notocrangon antarcticus* beobachtete Verhalten, nur von Zeit zu Zeit und dann relativ kurz aktiv zu werden sowie die deutlich gesteigerte Aktivität von *Chorismus antarcticus* bei Zugabe von Futter dürfte auf einer möglichst rationalen Einteilung der Energiereserven beruhen. Die Aktivität wird nur dann gesteigert, wenn sich Beute in der Nähe befindet oder wie die Reaktion von *N. antarcticus* auf die Annäherung eines weiteren Tieres interpretiert werden könnte, eine Gefahr droht (Fig. 4.30.). Denkbar wäre darüber hinaus, daß in Phasen der Bewegungslosigkeit Stoffwechselprozesse reduziert werden, um Energie zu sparen. Um diese Theorie zu überprüfen, sollen daher Messungen des Sauerstoffverbrauchs durchgeführt werden.

Reference

- Arntz, W.; Gorny, M. (1991). Shrimp (Decapoda, Natantia) occurrence and distribution in the eastern Weddell Sea, Antarctica. Polar Biol. (in press)
- Baldauf, J.G.; Barron, J.A. (1991). Diatom biostratigraphy: Kerguelen-Plateau and Prydz Bay regions of the Southern Ocean. In: Barron, J. A., Larsen, B., et al., Proc. ODP, 119, Vol. B: College Station, TX (Ocean Drilling Program).
- Bohrmann, G.; Kuhn, G.; Abelmann, A.; Gersonde, R.; Fütterer, D.K. (1990). A young porcellanite occurrence from the Southwest Indian Ridge. Mar. Geol. 92, 155-163.
- Bohrmann, G.; Spieß, V.; Hinze, H.; Kuhn, G. (eingereicht). Reflector "Pc" a prominent feature in the Maud Rise sediment sequence (Eastern Weddell Sea). occurrence, regional distribution and implications to silica diagenesis. Mar. Geol.
- Botz, R.; Bohrmann, G. (eingereicht). Low temperature opal-CT precipitation in antarctic deep sea sediments: evidence from oxygen isotopes. Earth Planet. Sci. Let.
- Burckle, L.H. (1982). First appearance datum of *Hemidiscus karstenii* in late pleistocene of the subantarctic region. Antarctic J. 17, 142-143.
- Burckle, L.H.; Clarke, D.B.; Shackleton, N.J. (1978). Isochronous last-abundance-appearance datum (LAAD) of the diatom *Hemidiscus karstenii* in the sub-Antarctic. Geology 6, 243-246.

- Fütterer, D.K. (1991). Fahrabschnitt ANT-VIII/6 (Kapstadt - Kapstadt). In: Fütterer, D.K. & Schrems, O. (Hrsg.). Die Expedition ANTARKTIS-VIII mit FS "Polarstern" 1989/90. Bericht von den Fahrabschnitten ANT-VIII/6-7. Ber. Polarforsch., 90, 3-195.
- Gersonde, R.; Burckle, L.H. (1990). Neogene diatom biostratigraphy (ODP Leg 113).- In: Barker, P. F., Kennett, J. P., et al., Proc. ODP, 113, Vol. B: College Station, TX (Ocean Drilling Program)
- Gersonde, R.; Hempel, G. (Eds.) (1990). Die Expeditionen ANTARKTIS VIII/3 und VIII/4 mit FS "Polarstern". Ber. Polarforsch. 74, 173 S.
- Grobe, H. (1987). A simple method for the determination of ice-rafted debris in sediment cores. Polarforsch. 57, 123-126.
- Grobe, H.; Mackensen, A.; Hubberten, H.-W.; Spieß, V.; Fütterer, D.K. (1990). Stable isotope record and late Quaternary sedimentation rates at the Antarctic continental margin.- Bleil, U. & Thiede, J. (Hrsg.) Geologic history of the polar oceans: Arctic versus Antarctic. (D. Reidel, Holland), 539-572.
- Gutt, J.; Gorny, M.; Arntz, W., (1991). Quantitative observations on Antarctic shrimps (Crustacea: Decapoda) in their natural environment analyzed by means of underwater photography.- Antarctic Sci. (in press)
- Hays, J. D.; Opdyke, N.D. (1967). Antarctic Radiolaria, magnetic reversals and climatic changes.- Science 158, 1001 - 1011.
- Hays, J. D.; Imbrie, J.; Shackleton, N.J. (1976). Variations in the earth's orbit: pacemaker of the ice ages. Science 194, 1121 - 1132.
- Mackensen, A.; Douglas, R.G. (1989). Down-core distribution of live and dead deep-water benthic Foraminifera in box cores from the Weddell Sea and the California continental borderland. Deep-Sea Res. 36, 879-900.
- Mackensen, A.; Grobe, H.; Hubberten, H.-W.; Spieß, V.; Fütterer, D.K. (1989). Stable isotope stratigraphy from the Antarctic continental margin during the last one million years.- Mar. Geol. 87, 315-321.
- Mackensen, A.; Grobe, H.; Kuhn, G.; Fütterer, D.K. (1990). Benthic foraminiferal assemblages from the eastern Weddell Sea between 68 and 73°S: distribution, ecology and fossilization potential. Mar. Micropaleontol. 16, 241-283.
- Martini, E. (1971). Standard Tertiary and Quaternary calcareous nannoplankton zonation. In: A. Farinacci (Ed.) Proceedings II Planktonic Conference, Roma 1970, 2, 739-85.
- Martinson, D.G.; Pisias, N.G.; Hays, J.D.; Imbrie, J.; Moore, T.C.; Shackleton, N.J. (1987). Age dating and the orbital theory of ice ages: development of a high-resolution 0 - 300000 year chronostratigraphy. Quater. Res. 27, 1-29.
- Morley, J.J.; Hays, J.D. (1981). Towards a high-resolution, global, deep-sea chronology for the last 750,000 years. Earth Planet. Sci. Let. 53, 279-295.
- Odin, G.S.; Matter, A. (1981). De glauconiarium origine. Sedimentol. 28, 611-641.
- Reid, J.L. (1990). On the total geostrophic circulation in the South Atlantic Ocean: Flow patterns, tracers, and transports. Prog. Oceanog. 23, 149-244.
- Spieß, V.; Villinger, H.; Pototzki, F.; Zöllner, T. (1990). Sedimentechographie. In: Gersonde, R. & Hempel, G. (Eds.). Die Expeditionen ANTARKTIS-VIII/3 und VIII/4 mit FS "Polarstern". Ber. Polarforsch. 74, 58-71.
- Wisotzki, A.; Schäfer, H.; Rutgers v.d. Loeff, M.; Michel, A. (1990). Untersuchungen in der Wassersäule. in: Gersonde, R. & Hempel, G. (Eds.). Die Expeditionen ANTARKTIS-VIII/3 und VIII/4 mit FS "Polarstern" 1989. Ber. Polarforsch. 74: 20-38.
- Withworth, T.; Nowlin, W.D. (1987). Water Masses and Currents of the Southern Ocean at the Greenwich Meridian. J.Geoph.Res. 92, C6, 6462-6276.

LANDGESTÜTZTE BIOLOGISCHE ARBEITEN AUF DER KÖNIG-GEORG-INSEL (SÜDSHETLANDINSELN, ANTARKTIS)

1. EINLEITUNG

Vom 19.11.1990 bis 16.3.1991 arbeiteten zwei deutsche Biologenteams auf der sowjetischen Station "Bellingshausen". Es war die erste Kooperation des AWI mit einem ostdeutschen Institut, der Forschungsstelle für Wirbeltierforschung (FiW) in Berlin. Hydrobiologisch arbeiteten M. Rauschert (FiW) und M. Stiller (AWI) zusammen, ornithologisch B. Simon (Jessen) und A. Ulbricht (Vogelwarte Hiddensee). Die Forschungsstation liegt auf der Fildeshalbinsel der König-Georg-Insel. Als Untersuchungsgebiet ist etwa der Bereich von 58°58' - 58°46'W und 62°09' - 62°14'S anzusehen (Fig. 5.1). Stützpunkt für die populationsdynamischen Arbeiten der Ornithologen war das deutsche Refugium auf der Ardley-Insel. Die faunistisch/ökologischen Untersuchungen im Benthal der Maxwellbucht und der Fildesstraße gingen von "Bellingshausen" aus und wurde mit Hilfe eines Kunststoffbootes durchgeführt.

Das Verhältnis zu den Gastgebern war freundschaftlich. Unsere Arbeiten wurden durch den Leiter und die Mannschaft der Station gut unterstützt, wofür unser besonderer Dank gilt. Desgleichen danken wir dem Kapitän der "Polarstern" und seiner Crew sowie den Wissenschaftlern, die den Umweg über die König-Georg-Insel machten und den Zeitverlust in der Maxwellbucht auf sich nahmen.

2. SUMMARY

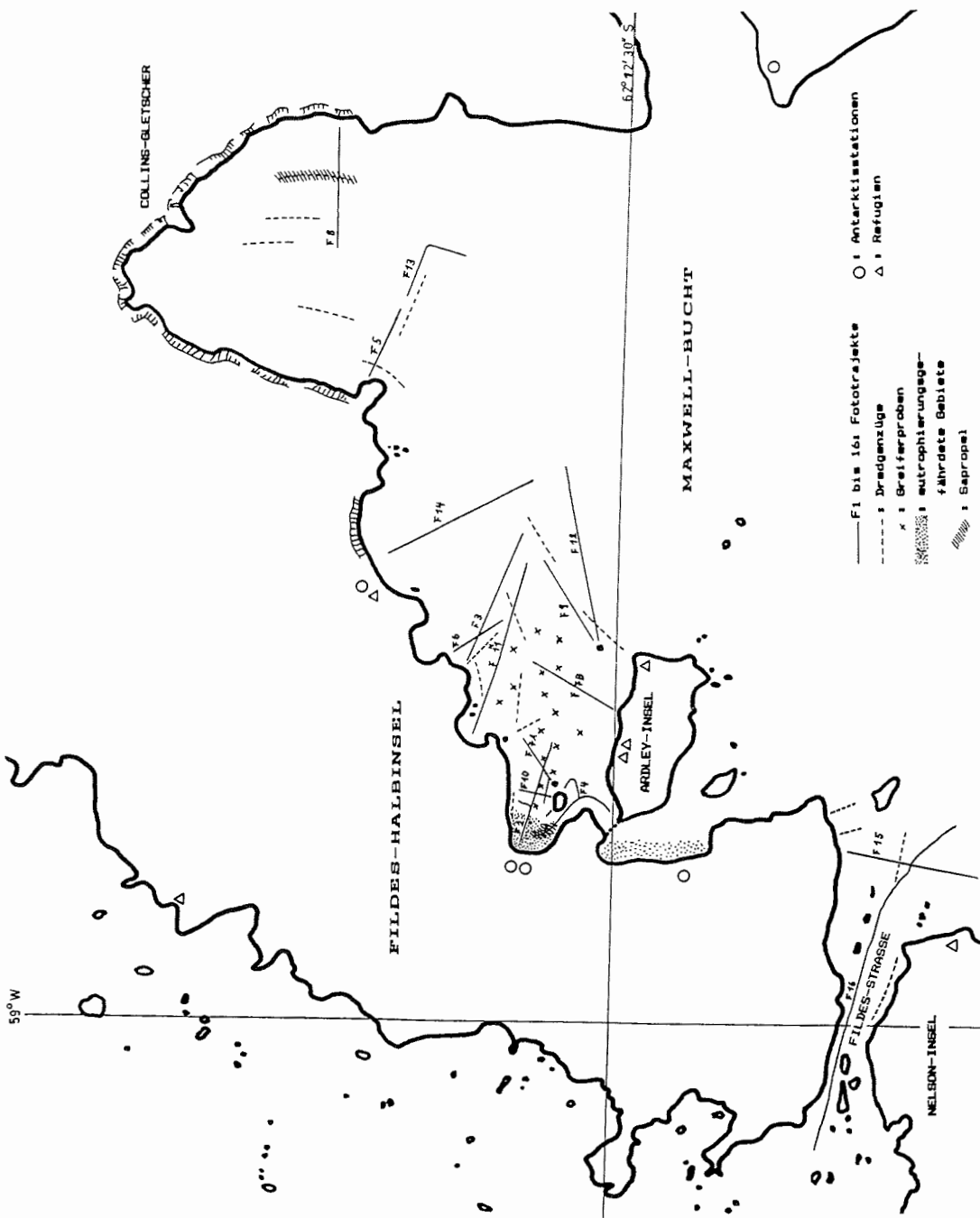
Investigations on marine benthos have been carried out during a stay at the Soviet Antarctic station "Bellingshausen" (King-George-I., South Shetland Is.) from November 19, 1990 to March 16, 1991. 12 dredge samples and 45 grab samples were taken from different depths between 15 and 100 m. Furthermore, fotos from the sea-bottom have been made in depths between 5 and 150 m by means of an underwater camera.

According to first systematic analyses of samples, more than 120 amphipod species were collected, 17 species more than found during earlier expeditions in this area. Some of the species of the family *Stenothoidae* have been newly described. For one species a new genus had to be created.

The exceedingly large abundance of the lysianassid amphipod *Cheirimedon femoratus* in sediments enriched with organic material and hydrogen sulphide suggests that this species is an indicator for saprobic bottom environments.

Polychaetes are represented by species of 27 families, making up 53% of the polychaete families found in the Antarctic Ocean. The grab samples show that polychaetes are the dominant taxon in the soft sediments, representing 80 - 90% of the individuals of the endobenthos. In lower depths, their abundance amounts up to 28000 Ind. * m⁻². In greater depths, their abundance decreases to 3000 - 4000 Ind. * m⁻². Especially the families *Orbinidae*, *Apisthobranchidae* and *Cirratulidae* contribute to these high abundances. Underwater photography was used to describe the environment in more detail.

Fig. 5.1: Die Fildeshalbinsel (König-Georg-Insel, Südshetlandinseln) mit den Untersuchungsgebieten in der Maxwellbucht und der Fildes-Straße
 Fig. 5.1: Investigation areas in the Maxwell Bight and Fildes Strait, Fildes Peninsula (Ging-Georg-Island, South Shetlands)



3. FAUNISTISCH/ÖKOLOGISCHE ARBEITEN IM BENTHAL DER MAXWELLBUCHT UND DER FILDES-STRASSE

M. Rauschert, (FiW); M. Stiller (AWI)

3.1 Technik, Methodik

Bei unserer Ankunft fanden wir noch winterliche Verhältnisse vor. Der Zugang zum Meer blieb dem Boot durch eine starke Barriere und immer wieder andriftendes Packeis versperrt. Dadurch konnte erst am 13. Dezember mit den Untersuchungen begonnen werden. Vorher kam es nur zu Probennahmen im Eulitoral und in einem Fall wurde ein Dredgenzug von Bord des sowjetischen Forschungsschiffes "Akademik Fedorov" durchgeführt.

Für die quantitative Probennahmen wurde ein Van-Veen-Greifer eingesetzt, der eine Fläche von 0,05 m² erfaßte. Qualitative Proben wurden mit einer Schlittendredge genommen. Sie besaß eine Öffnung von 15 x 50 cm, war innen mit 2 Netztüchern bestückt und außen mit einem Schutz aus Sacktuch versehen. Das erste Netz in Fangrichtung besaß eine Maschenweite von 15 mm und hielt die größeren Arten zurück. Kleinere Arten sammelten sich dahinter in einem feineren Netztuch (Maschenweite 0,5 mm). Um zu verhindern, daß sich das Zoobenthos gegenseitig beschädigte, wurden die Dredgenproben bald mit Formalin vorfixiert und später in Konservierungsflüssigkeit (3% Formalin oder 75% Alkohol) für die weitere Bearbeitung aufbewahrt.

Die Unterwasser-Fotokamera bestand aus einer Kleinbildkamera "Nikon" F 300 mit einem Flektogon 2,8/20 mm in einem bis in 160 m Tiefe druckfesten Gehäuse aus glasfaserverstärktem Polyester, das eine gewölbte Frontscheibe aus Piadryl besaß. Sie war in einen Rahmen montiert und in einem Winkel von etwa 60° auf den Boden gerichtet. Dabei erfaßte sie einen Ausschnitt von etwa 65 x 145 cm. Ausgelöst wurde sie über Voreilgewicht und Magnetschalter. Ein ebenfalls druckfest und wasserdicht gekapselter, über die Kamera synchron gezündeter Elektronenblitz leuchtete das Bild aus. Ein jeweils im Foto mit abgebildeter Tiefenmesser dokumentierte die Aufnahmetiefe. Die Wassertiefen wurden auf allen Stationen mit einem Echolot gemessen.

3.2 Quantitative Probennahmen

In Tiefen von 15, 20, 30, 40, 60, 80 und 100 m wurden auf insgesamt 45 Stationen Proben mit dem Van-Veen-Greifer genommen (aus jeder Tiefenzone 6 Proben). In einer auf 23 m Tiefe abfallenden Bodensenke vor der chilenischen Station wurden an verschiedenen Stellen insgesamt 3 Greiferproben gezogen, die durch starken Schwefelwasserstoff-Geruch auffielen und keinerlei lebende Infauna aufwiesen. Neben der in Massen gefangenen Indikatorart für Sapropel, dem Amphipoden *Cheirimedon femoratus* (Lysianassidae) befanden sich in diesen Fängen nur vereinzelt phytophage Amphipodenarten (Eusiridae), die mit eingedrifteten Makroalgenresten dorthin verfrachtet wurden. Wellen und Dünung erschwerten die Probennahmen erheblich. Die gewonnenen Proben wurden mit gepuffertem Formalin fixiert und während der Expedition schon teilausgewertet. Die verschiedenen Sedimente sollen Korngrößenanalysen unterzogen werden.

3.3. Qualitative Probennahmen

Zur Komplettierung der Faunenliste des Untersuchungsgebietes wurden zahlreiche Dredgenzüge durchgeführt und dabei speziell die in den Jahren vorher kaum untersuchten Tiefen von 50 bis 100 m erfaßt. Ein großer Teil dieser Fänge konnte bereits während der Expedition nach unterschiedlichen systematischen Einheiten sortiert werden. Amphipoden und Polychaeten wurden intensiver durchgesehen.

3.4. Bodenmorphologie und Bodenbesiedlung

Um einen Eindruck der unterschiedlichen Biotope des Bearbeitungsgebietes zu erhalten, wurde vom Gezeitenbereich bis in 150 m Tiefe an verschiedenen Transekten der Boden fotografiert. Er vermittelte ein gutes Bild der epibenthischen Arten und kann zur Feststellung der Abundanzen typischer und auffälliger Arten herangezogen werden.

Der Meeresboden flacherer Regionen besteht aus Felsen und Geröll, in flach auslaufenden Buchten (z. B. vor der Station "Bellingshausen") kommt auch sandiger oder kiesiger Grund vor. Während dem offenen Meer zugewandte, wellenexponierte oder strömungsbegünstigte, steil abfallende Küsten noch in mehr als 50 m Tiefe viele Hartgrundelemente aufweisen, zwischen die mehr oder weniger Schlick gelagert ist, zeigen ruhige Buchten ein anderes Bild. Hier ist schon ab 10 m Tiefe mit Schlick zu rechnen (z. B. vor "Bellingshausen") und in etwa 30 m Tiefe finden sich bereits Vertreter der Makrofauna, die sonst erst unterhalb von 60 m das Bild bestimmen. Als typisch und besonders auffällig ist dafür der Ophiuroide *Ophionotus victoriae* zu nennen, der oft in bemerkenswerter Abundanz in Schlickgründen vorkommt. Die meist große Homogenität und relative Artenarmut der Weichbodenfauna ändert sich an Stellen mit "Dropstones". Dort tritt ein reiches Epibenthos auf. Zum Siedeln wird nicht nur harter anorganischer Untergrund benutzt, sekundär dienen auch andere sessile Arten als Siedlungssubstrat.

Endobenthische Arten sind durch die Photographie kaum zu erfassen. Als Ausnahmen wären z. B. Terebelliden zu nennen, deren weit auf dem Boden ausgestreckte Tentakeln sich gut erkennen lassen und auch die deutlich sichtbaren Siphonen der klammuschelähnlichen *Laternula elliptica*.

In krassem Gegensatz zu den Stillwassergebieten finden sich im Verlauf der Hauptströmungsrichtung der Fildes-Straße noch in 100 m Tiefe keine dichteren Schlicklagen. Das Wasser ist hier durch heftige Gezeitenströmungen (bis zu 5 Knoten) in wechselnder Richtung ständig in Bewegung und läßt Schlickablagerungen nur an strömungsabgewandten Stellen zu. Das auffälligste Epibenthos mit dem größten Artenspektrum findet man an Stellen, die nicht der direkten Strömung ausgesetzt sind. Bis in über 30 m Tiefe sind die steil abfallenden Felswände von üppig entwickelten Makroalgen bestanden (*Himantothallus grandifolius*, *Cystosphaera jacquinotii* u.a.). Dazwischen siedelt in einem dichten und dicken "Teppich" eine Vielzahl von Schwämmen auf dem Gestein. Unterhalb 30 m Tiefe herrschen zunächst Bryozoen vor (hauptsächlich Flustridae). Auffällig häufig werden mit zunehmender Tiefe Gorgonaria (Primnoidae). Die stark strömungsexponierte Sohle der Fildes-Straße ist etwas dünner besiedelt. Hier bestimmen ab etwa 30 m Tiefe Schwämme, Bryozoen und Ascidien das Bild. Je weniger anfällig

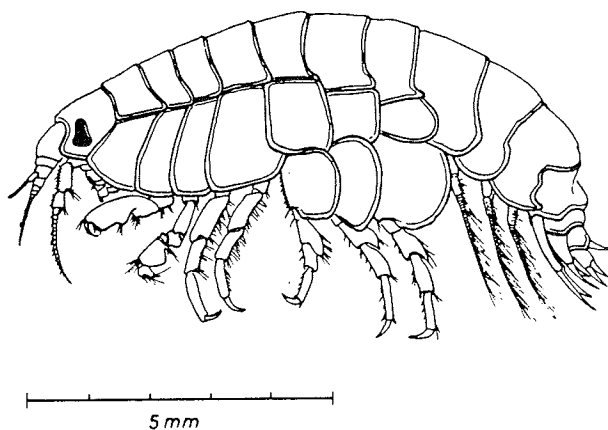
das Substrat auf strömungsbedingte Umschichtungen ist, desto reicher kann sich dort die Epifauna entwickeln.

3.5 Sapropel-Indikator

In die stationsvorgelagerten Teile der Maxwellbucht werden ständig erhebliche Abwassermengen geleitet, die zu einer starken Wassertrübung führen. Schon während der 1980 - 1982 und 1984 - 1986 in diesem Gebiet durchgeführten Benthosuntersuchungen wurde im Amphipoden *Cheirimedon femoratus* (Pfeffer, 1888) - Familie Lysianassidae - eine Indikatorart für Eutrophierung vermutet (Rauschert, 1991, p. 61, Fig. 17). Diese Vermutung konnte jetzt bestätigt werden. *Cheirimedon femoratus* ist eine indirekte Indikatorart, die Sauerstoffdefizit (Schwefelwasserstoff-Anreicherung) im Bodengrund anzeigt. Er kommt als einzige Art in Massen auf Faulschlick (Sapropel) vor. Sapropel kann durch Eutrophierung, z. B. Einleitung von Fäkalien aus den Polarstationen in vorgelagerte Meeresteile entstehen, die durch stagnierende Wassermassen gekennzeichnet sind (Fig. 5.1). Auf die leeseitig der Insel Albatros, vor der chilenischen Station, angetroffenen Verhältnisse in einer bis 23 m tiefen Bodensenke wurde in diesem Zusammenhang schon unter 3.2 hingewiesen.

Neben dem hier in Massen lebenden *Cheirimedon femoratus* kommen nur sporadisch wenige mit Makroalgenresten eingedrifteten phytophage Amphipodenarten vor. Das an dieser Stelle vorgefundene Sapropel zeichnet sich durch starken Schwefelwasserstoff-Geruch aus, ist mit abgestorbenen Algenresten durchsetzt. Infauna und Epifauna wurde nicht gefunden. Als Ursachen können die eingeleiteten Fäkalien der Stationen Tte. Marsh und Bellingshausen vermutet werden.

Fig. 5.2: Indikator auf Sapropel: *Cheirimedon femoratus* (Lysianassidae, Amphipoda)



Ein ähnlicher ausschließlich durch *Cheirimedon* besiedelter Bereich findet sich im Untersuchungsgebiet auch vor dem Collins-Gletscher - weit vom Einflußgebiet jeglicher Stationen entfernt (Fig. 5.1). Dort lagert vor einer in etwa 50 m Tiefe beginnenden Stufe fauliger Schlick mit gut erhaltenem Schill einiger Mollusken. Die Molluskenreste (hauptsächlich *Neobuccinum eatoni*, *Yoldia eightsii* und *Laternula elliptica*) deuten auf ehemals normal besiedelten Boden. In einem engeren Gebiet wurden 2 Dredgenzüge in einer Tiefe von 50 bis 60 m durchgeführt, die starkes Sapropel mit z. T. schon teilweise zersetztem Molluskenschill und massenhaft die Indikatorart *Cheirimedon femoratus* erbrachten. Nach der photographischen Untersuchung (nicht gezeigt) besteht der Boden sowohl im ersten Fall (Fäkalieneinfluß) als auch hier aus Schlick, an dessen Oberfläche die amphipoden sitzen. Epifauna war in beiden Gebieten nirgends anzutreffen. Möglicherweise waren an der in 50 - 60 m Tiefe beginnenden Bodenschwelle Eisberge gestrandet und hatten die gesamte Makrofauna vernichtet. Die vor dem Gletscher zu jeder Jahreszeit dicht in Gefrierpunktnähe liegenden Temperaturen lassen wahrscheinlich eine schnelle Mineralisierung der abgestorbenen organischen Reste nicht zu. Die Bakterienrasen werden von *Cheirimedon* beweidet. Daß es sich bei diesem auffälligen Befund um die Folge einer regional begrenzten Katastrophe handeln muß wird dadurch erhärtet, daß sich an das Gebiet mit der vermutlich durch Eisberge zerstörten Makrofauna Areale mit äußerst reich entwickeltem Zoobenthos in offensichtlich ungestörten Biotopen anschließen.

3.6 Bemerkungen zur Polychaetenfauna

In den 31 ausgewerteten Dredgen- und Greiferproben sind Arten aus 27 Polychaetenfamilien gefunden worden. Damit zeichnet sich das Untersuchungsgebiet durch Präsenz von etwa 53% der bisher aus der Antarktis bekannten Familien aus. Obwohl mit der Artbestimmung erst begonnen wurde, kann schon jetzt festgestellt werden, daß der Großteil der Familien durch mehrere Arten repräsentiert ist.

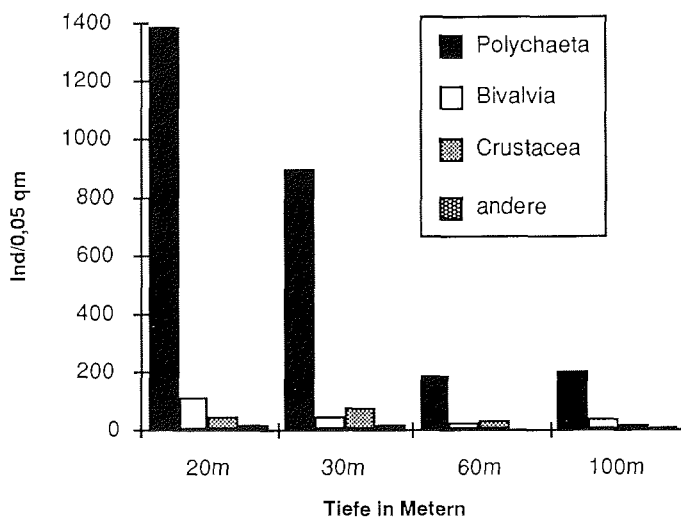
Aus den Ergebnissen der Sortierung ausgewählter Greiferproben (je 4 Proben aus den Tiefen 20, 30, 60 und 100 m sowie je einer Probe aus 15, 40 und 80 m) wird deutlich, daß der Anteil der Polychaeten an der Besiedlung des Endobenthos zwischen 78 und 90% der Gesamtabundanz ausmacht. Die Abundanz der Polychaeten nimmt mit der Tiefe ab (Fig. 5.3). In 20 m Tiefe ergab sich eine Besiedlungsdichte von 27720 Ind./m². In 60 und 100 m Tiefe betrug sie nur noch 3715 bzw. 3910 Ind./m².

An den hohen Individuenzahlen in geringen Wassertiefen sind hauptsächlich die Familien Orbinidae, Apisthobranchidae und Cirratulidae beteiligt. In 20 bis 30 m Tiefe erreichten die Orbinidae bis zu 7344 Ind./m², die Apisthobranchidae 7820 Ind./m², während sie im Bereich von 60 bis 100 m nur noch mit weniger als 400 Ind./m² oder gar nicht vertreten waren. Auch die Cirratulidae kommen bei 20 bis 30 m auf Abundanzen von 45800 Ind./m². Allerdings sind sie auch in größeren Tiefen des Untersuchungsgebietes noch sehr häufig und stellen dort mit bis zu 2000 Ind./m² die dominante Familie dar.

Weitere Familien, die häufiger in den flacheren Bereichen gefunden wurden, sind die Dorvillidae, Nephtyidae, Polynoidae und Capitellidae. Typische Vertreter der größeren Tiefen sind Terebellidae, Ampharetidae und Hesionidae. Bei allen anderen Familien weisen die Ergebnisse keine

deutliche Präferenz für bestimmte Tiefen im untersuchten Bereich auf oder ihr Vorkommen ist so sporadisch, daß sich aus den bisher vorliegenden Daten noch kein eindeutiges Bild ergibt.

Fig. 5.3: Ergebnisse der Sortierung der Greiferproben aus der Maxwellbucht. Angegeben sind die Individuenzahlen der Taxa pro 0,05 m² aus unterschiedlichen Tiefen.



3.7 Bemerkungen zur Amphipodenfauna

Die aus den Probennahmen der vorausgegangenen Expeditionen erarbeitete Liste von 103 Arten konnte auf mehr als 120 Arten erhöht werden. Besonderes Augenmerk richtete sich auf die Stenothoidae. Nach den Eusiridae stellen sie mit bisher 20 voneinander differenzierten Arten die artenreichste Familie im Gebiet dar, deren Vertreter sich normalerweise habituell stark ähneln. Drei relativ seltene, morphologisch stark abgewandelte *Stenothoidae* könnten in einer neuen Gattung oder Untergattung zusammengefaßt werden. An einer Revision der Familie wird z. Zt. gemeinsam mit H.-G. Andres (Hamburg) gearbeitet.

References

- Piepenburg, D. (1988). Zur Zusammensetzung der Bodenfauna in der westlichen Fram-Straße. Ber. Polarforsch. 52: 1-118
- Rauschert, M. (1991). Ergebnisse der faunistischen Arbeiten im Benthal von King George Island (Südshetlandinseln, Antarktis). Ber. Polarforsch. 76: 1-75
- Voss, J. (1988). Zoogeographie und Gemeinschaftsanalyse des Makrozoobenthos des Weddellmeeres (Antarktis). Ber. Polarforsch. 45: 1-145

Tab. 5.1: Liste der gefundenen Amphipodenarten

- Acanthonotozomatidae
1. Acanthonotozomoides oatesi (BARNARD, 1930)
 2. Gnathiphimedia fuchsi THURSTON, 1974
 3. G. cf. fuchsi
 4. G. cf. incerta BELLAN-SANTINI, 1972
 5. G.sexdentata (SCHELLENBERG, 1926)
 6. Panoploea joubini CHEVREUX, 1912
 7. P. cf. joubini
 8. Pariphimedia integricauda CHEVREUX, 1906
 9. P. normani (CHUNNINGHAM, 1871)
 10. u.l. spp. aff.
- Ampeliscidae
12. Ampelisca bouvieri CHEVREUX, 1912
 13. sp. aff.
- Amphilochidae
14. Gitanopsis cf. simplex SCHELLENBERG, 1926
 15. G. squamosa (THOMSON, 1880)
 16. G. cf. squamosa
- Aoridae
17. Lembos fuegiensis (DANA, 1853-1855)
- Colomastigidae
18. Colomastix fissilingua SCHELLENBERG, 1926
- Corophiidae
19. Gammaropsis cf. georgianus SCHELLENBERG, 1931
 20. G. longicornis WALKER, 1906
 21. G. sublitoralis SCHELLENBERG, 1931
 22. Haplocheira barbimana (THOMSON, 1879)
- Dexaminidae
23. Paradexamine fissicauda CHEVREUX, 1906
 24. P. pacifica (THOMSON, 1879)
 25. Polycheria antarctica (STEBBING, 1875)
- Eophliantidae
26. Wandelia crassipes CHEVREUX, 1906
- Eusiridae
27. Atyloella magellanica (STEBBING, 1888)
 28. A. quadridens (BARNARD, 1930)
 29. Atylopsis megalops NICHOLLS, 1938
 30. A. fragilis RAUSCHERT, 1989
 31. Bovallia gigantea PFEFFER, 1888
 32. Djerboa furcipes CHEVREUX, 1906
 33. Eurymera monticulosa PFEFFER, 1888
 34. Eusiroides georgianus BARNARD, 1932
 35. Eusirus antarcticus THOMSON, 1880
 36. E. perdentatus CHEVREUX, 1912
 37. E. spec.

38. Gondogoneia antarctica (CHEVREUX, 1906)
 39. G. cf. bidentata (STEPHENSEN, 1927)
 40. G. redfearni THURSTON, 1974
 41. G. cf. spinicoxa BELLAN-SANTINI & LEDDYER, 1974 (?)
 42. Liouvillea oculata CHEVREUX, 1912
 43. Metaleptamphopus pectinatus CHEVREUX, 1912
 44. Oradarea bidentata BARNARD, 1932
 45. O. edentata BARNARD, 1932
 46. O. ocellata THURSTON, 1974
 47. O. tridentata BARNARD, 1932
 48. O. unidentata THURSTON, 1974
 49. Paramoera fissicauda (DANA, 1852)
 50. P. hurlevi THURSTON, 1974
 51. P. walkeri (STEBBING, 1906)
 52. Pontogeneiella brevicornis (CHEVREUX, 1906)
 53. P. longicornis (CHEVREUX, 1906)
 54. Prostebbingia gracilis (CHEVREUX, 1912)
 55. Schraderia acuticauda BELLAN-SANTINI & LEDDYER, 1974
 56. S. barnardi THURSTON, 1974
 57. S. dubia THURSTON, 1974
 58. S. gracilis PFEFFER, 1888
 59. - 61. spp. aff.
- Gammaridae**
62. Paraceradocus gibber ANDRES, 1984
 63. P. miersii (PFEFFER, 1888)
 64. P. spec.
- Haustoriidae**
65. Urothoides oniscoides BARNARD, 1932
- Ischyroceridae**
66. Ischyrocerus camptonyx THURSTON, 1974
 67. Jassa falcata (MONTAGU, 1808)
 68. J. ingens (PFEFFER, 1888)
 69. Ventojassa georgiana (SCHELLENBERG, 1931)
- Leucothoidae**
70. Leucothoe spinicarpa (ABILDGAARD, 1789)
- Liljeborgidae**
71. Liljeborgia octodentata SCHELLENBERG, 1931
 72. L. macrodon SCHELLENBERG, 1931
- Lysianassidae**
73. Cheirimedon femoratus Pfeffer, 1888
 74. Eurythenes gryllus (LICHTENSTEIN, 1822)
 75. Hippomedon kerquelensis (MIERS, 1875)
 76. Lysianassa cf. subantarctica (SCHELLENBERG, 1931)
 77. u.78. Orchomene spp. 1 u. 2
 79. Pachychelium antarcticum SCHELLENBERG, 1926
 80. Tryphosella cf. sarsi BONNIER, 1893
- Melphidippidae**
81. Melphidippa antarctica SCHELLENBERG, 1926

Dediceratidae

82. Methalimedon nordenskjöldi SCHELLENBERG, 1931
83. Monoculodes antarcticus BARNARD, 1932
84. M. scabriculosus BARNARD, 1932
85. Dediceroidea cf. macrodactylus SCHELLENBERG, 1931 (?)
86. Parhalimedon turqueti CHEVREUX, 1906

Pagetinidae

87. Pagetina genarum BARNARD, 1932

Paramphitoidae

88. Epimeria monodon STEPHENSEN, 1947
89. Parepimeria cf. crenulata CHEVREUX, 1913

Phoxocephalidae

90. Pseudharpinia dentata SCHELLENBERG, 1931
91. Heterophoxus cf. trichosus BARNARD, 1932
92. H. videns BARNARD, 1932
93. Paraphoxus rotundifrons (BARNARD, 1932)

Podoceridae

94. Podocerus capillimanus NICHOLLS, 1938
95. Pseudodulichia antarctica (RAUSCHERT, 1988)

Sebidae

96. Seba antarctica WALKER, 1906
97. S. cf. dubia SCHELLENBERG, 1926
98. S. cf. stoningtonensis THURSTON, 1974

Stegocephalidae

99. Stegophippsiella cf. pacis BELLAN-SANTINI & LEDOYER, 1974

Stenothoidae

100. Antatelson antennatum BELLAN-SANTINI & LEDOYER, 1974
101. A. walkeri (CHILTON, 1912)
102. Metopoides angustus RAUSCHERT, 1990
103. M. cf. crassus SCHELLENBERG, 1931
104. M. lanceolatus RAUSCHERT, 1990
105. M. latus RAUSCHERT, 1990
106. M. leptomanus RAUSCHERT, 1990
107. M. cf. macrocheir SCHELLENBERG, 1926
108. M. sarsi (PFEFFER, 1888)
109. Probolisca ovata (STEBBING, 1888)
110. Prometopa edentata RAUSCHERT, 1990
111. Prothamatelson nasutum (CHEVREUX, 1912)
112. Thamatelson herdmani WALKER, 1906
113. Thamatelsonella kingelepha RAUSCHERT & Andres
114. Torometopa andresi (RAUSCHERT, 1990)
115. T. antarctica (WALKER, 1906)
116. T. foliodactyla (RAUSCHERT, 1990)
117. T. macromana (RAUSCHERT, 1990)
118. T. serrata (RAUSCHERT, 1990)
119. gen. et sp. n.

Caprellidae

120. Dodecasella elegans BARNARD, 1932
121. u. 122 . spp. aff.

**4. UNTERSUCHUNGEN AM ADELIEPINGUIN
(*PYGOSCELIS ADELIAE*) UND AM ESELSPINGUIN
(*PYGOSCELIS PAPUA*) AUF ARDLEY ISLAND (KING
GEORGE ISLAND, ANTARKTIS) IM SÜDSOMMER
1990/91.**

J. Ulbricht, B. Simon (FiW)

Den Rahmen für die Adeliepinguin-Untersuchungen von Oktober 1990 bis Februar 1991 bildete das "Ecosystem Monitoring Programm" vom Committee for the Conservation of Antarctic Marine Living Resources (CCAMLR). Auf der Insel Ardley nisteten in dieser Saison etwa 1000 Adeliempaare. Ziel des Programms ist die Erfassung verschiedener - in erster Linie brutbiologischer und demographischer - Parameter, die einen möglichen Monitoringwert für die Größe und Verteilung von Krillbeständen besitzen. Dazu wurden von CCAMLR folgende Standardmethoden vorgegeben:

- Bestimmung der Gewichte der Altvögel bei der Ankunft.
Der Ernährungszustand der Pinguine zum Zeitpunkt ihrer Ankunft in den Brutkolonien gibt Auskunft über die Menge und Erreichbarkeit ihrer Hauptnahrung (Krill) im Winter bzw. zeitigen Frühjahr. Nach ihrer Ankunft beginnt für die Vögel eine mehrwöchige Fastenzeit, während der sie von ihren Fettreserven zehren müssen. Der Programmpunkt beinhaltet den Fang einer Stichprobe der Erstankömmlinge und deren Wägung.
- Ermittlung der Länge des ersten Bebrütungsabschnittes
Nach der Eiablage übernimmt in der Mehrzahl der Fälle das Männchen die Bebrütung. Nach 1 - 2 Wochen (mitunter sogar mehr) wird es vom Weibchen abgelöst. Bei einem Teil der Paare ist dieser Modus jedoch umgekehrt. Die Länge des ersten und zweiten Bebrütungsabschnittes zusammengerechnet soll Rückschlüsse sowohl auf die vorhandenen Fettreserven als auch auf die bestehende Nahrungssituation (und damit die Möglichkeit zur Regenerierung der Energiereserven) während dieser Zeit ermöglichen. Die Bestimmung der Länge des ersten bzw. zweiten Bebrütungsabschnittes erfolgte durch tägliche Kontrollen markierter Individuen.
- Größe des Brutbestandes
Die Ermittlung der jährlichen Brutbestandsgröße wurde wie folgt standardisiert: Zählung der Brutpaare in einer Stichprobe von etwa 10% des Gesamtbestandes und zwar eine Woche nach dem Höhepunkt der Eiablage (d.h., 2/3 der Paare in den ausgewählten Brutgruppen haben ein Gelege).
- Demographische Parameter
Dieser Punkt zielt langfristig auf die Feststellung der Rückkehr- bzw. Überlebensrate von als Jungvögel markierten Pinguinen. Dazu versahen wir - z. T. gemeinsam mit chilenischen Ornithologen - 750 fast flügge Adelies mit Flügelringen.
- Dauer der Nahrungsausflüge
Mangels anderer Möglichkeiten, wie z. B. Telemetrie, bestimmten wir durch Beobachtung die Länge der Nahrungsausflüge der Altvögel während der Nestlingsphase der Jungen (Alter 1-2 Wochen). Die Kontrollen individuell markierter Paare erfolgten über mehrere Tage stündlich. Die Dauer der

Nahrungsausflüge gibt einen Hinweis auf die Verfügbarkeit der Hauptnahrung Krill in der Umgebung der Kolonien.

- Der Bruterfolg wurde registriert
 - a) bei einer Stichprobe von 100 Paaren, deren Nester auf einer Linie durch verschiedene Brutgruppen innerhalb einer Kolonie lagen;
 - b) in 5 ausgewählten kleineren Kolonien.Auch der Bruterfolg soll einen Indikatorwert besitzen für die Nahrungssituation in der entsprechenden Saison.
- Gewicht der Jungvögel zum Zeitpunkt des Flüggegerdens
 - Bei 460 Adelpinguinen wurde das Gewicht zum Zeitpunkt des Flüggegerdens oder kurz davor bestimmt. Die Mittelwerte geben langfristig einen Hinweis auf die Nahrungssituation in der jeweiligen Saison. Außerdem läßt sich aus den Einzelgewichten eine Winter-Überlebenswahrscheinlichkeit abschätzen.
- Kükennahrung
 - Der Programmpunkt konnte nicht untersucht werden.

Ein weiterer Schwerpunkt unserer Arbeiten bestand darin zu prüfen, inwieweit das CCAMLR Pinguinprogramm auch auf den Eselspinguin (Brutbestand 1990/91 auf Ardley ca. 3700 Paare) anwendbar ist. Dabei wurden vor allem folgende Fragen untersucht: Brutbiologie, Brutablöserhythmus, Dauer der Nahrungsausflüge, Bruterfolg, Gewicht der Jungvögel zum Zeitpunkt des Flüggegerdens.

ANHANG 1: STATION LISTS

Abkürzungen für die Geräte:

Abbreviations for scientific instruments:

AGT	Agassiztrawl
AN	Apsteinnetz
AWI	Verankerungen
Bio-Rosi	Rosette mit 12 Schöpfern a 12 Liter
BO	Bongonetz
CTD	Conductivity Temperature Depth Sonde mit Wasserschöpfer-Rosette,
FS-CTD	Festspeicher-CTD-Sonde
FTS	Photoschlitten
GKG	Großkastengreifer
GS	Gerard-Großwasserschöpfer
GSL	Großschwerelot
GSN	Grundschieppnetz
HS	Hydrosweep
ISP	In-situ-Pumpe
KOL	Kolbenlot
LS	Lichtsonde
MG	Mehrfachgreifer
MIC	Mini multicorer
MIC	mit Sediment-Minicorer
MN	Multinetz
MUC	Multicorer
PL	Planktonnetz
PS	Parasound
QM	Quantameter
SED	Secchi-Scheibe
SL	Schwerelot
UNIB	Mooring University of Bremen

Stationsliste ANT IX/1

siehe Tabellen im Text.

Stationsliste ANT IX/2

Station No.	Date	Time (GMT)	Latitude (S)	Longitude (W)	Depth (m) (uncorr.)	Operation
18/035	20.11.90	19:09	62°12.2'	58°53.3'	220	CTD,MN
		21:40	62°12.2'	58°53.8'	188	
18/036	21.11.90	00:10	62°22.9'	57°59.9'	1970	CTD
		02:21	62°23.6'	58°00.3'	1966	
18/037		07:37	62°34.9'	55°25.7'	140	AGT,ADCP
		12:08	62°32.5'	55°14.0'	199	
18/038		14:55	62°53.9'	54°23.7'	202	AGT
		16:10	62°54.9'	54°22.2'	198	
18/039		19:45	63°20.1'	52°59.9'	448	CTD,QM, AWI 215
		22:15	63°20.1'	52°57.8'	438	
18/040	22.11.90	23:42	63°16.0'	53°20.1'	403	CTD,SED,QM, AN,MN,BO, BIO-ROSI
		03:27	63°15.5'	53°22.3'	403	
18/041		06:22	63°25.1'	52°33.3'	509	CTD
		07:07	63°25.5'	52°32.9'	512	

Station No.	Date	Time (GMT)	Latitude (S)	Longitude (W)	Depth (m) (uncorr.)	Operation
18/042		08:50	63°29.7'	52°06.9'	954	CTD,MIC,
		16:06	63°29.9'	52°04.4'	978	AWI 206/2
18/043		19:34	63°37.7'	51°22.0'	2147	CTD,AN
		20:55	63°37.7'	51°21.7'	2189	
18/044	23.11.90	00:18	63°45.8'	50°54.4'	2500	CTD,MIC,AN,
		10:18	63°44.3'	50°55.5'	2492	AWI 207/2
18/045		15:21	63°51.9'	50°01.1'	2929	CTD,SED,QM,
		19:04	63°51.2'	50°02.3'	2917	AN,MN,BO, BIO-ROSI
18/046		23:16	63°57.0'	49°09.1'	3478	CTD,AN,
	24.11.90	03:00	63°56.9'	49°08.7'	3482	AWI 216
18/047		09:34	64°14.0'	47°34.1'	4003	CTD
		11:45	64°13.9'	47°33.8'	4180	
18/048		18:29	64°25.6'	45°51.7'	4434	CTD,MIC,SED,
	25.11.90	03:14	64°24.2'	45°48.1'	4434	AN,MN,BO, QM,BIO-ROSI, AWI 217
18/049		09:55	64°37.2'	44°13.2'	4599	CTD,SED,AN
		12:19	64°37.1'	44°11.5'	4577	
18/050		19:01	64°48.9'	42°29.5'	4686	CTD,MIC,AN,
	26.11.90	00:15	64°49.1'	42°30.5'	4673	AWI 218
18/051		07:44	65°02.6'	40°45.4'	4747	CTD
		10:11	65°02.6'	40°45.0'	4758	
18/052		20:00	65°42.5'	38°59.9'	4636	HS,PS
	27.11.90	09:41	65°48.2'	40°20.3'	4520	
18/053		13:42	65°54.3'	40°16.1'	4625	CTD,MIC,AN
		16:32	65°54.2'	40°16.0'	4642	
18/054		16:35	65°54.2'	40°16.0'	4642	HS,PS
	28.11.90	08:00	65°44.1'	37°46.1'	4704	
18/055		08:38	65°40.3'	37°44.6'	4732	CTD,MIC,AN,
		14:14	65°39.7'	37°42.1'	4733	AWI 219
18/056		19:50	65°12.2'	39°22.4'	4757	CTD,MIC,BIO-ROSI,
	29.11.90	00:11	65°11.8'	39°17.6'	4760	AN,BO,MN, QM,SED
18/057		05:35	65°24.8'	37°55.2'	4715	CTD,MIC
		07:55	65°24.6'	37°54.6'	4714	
18/058		12:57	65°36.3'	36°30.3'	4763	CTD,MIC,
		22:07	65°38.4'	36°28.7'	4736	AN,MN, AWI 208/2
18/059	30.11.90	01:32	65°43.4'	35°26.8'	4777	CTD,MIC
		03:50	65°43.4'	35°27.4'	4784	
18/060		07:15	65°49.8'	34°21.0'	4796	CTD
		09:39	65°50.5'	34°21.8'	4795	
18/061		13:41	65°57.3'	33°18.9'	4799	CTD,MIC,MN,
	01.12.90	05:01	65°55.4'	33°35.8'	4763	AWI 220
18/062		11:32	66°03.3'	32°32.7'	4769	CTD
		14:08	66°03.5'	32°33.5'	4771	
18/063		16:44	66°07.3'	31°46.8'	4766	CTD,MIC,BIO-ROSI,
		21:12	66°07.3'	31°48.2'	4797	AN,BO,MN, QM,SED
18/064	02.12.90	00:08	66°11.1'	31°08.6'	4823	CTD
		02:21	66°10.7'	31°06.6'	4823	
18/065		05:19	66°16.8'	30°17.6'	4789	CTD,MIC,
		10:49	66°16.6'	30°17.8'	4784	AWI 221
18/066		12:59	66°21.7'	29°32.1'	4790	CTD,SED,AN
		15:13	66°21.4'	29°32.3'	4790	
18/067		17:46	66°27.9'	28°43.9'	4823	CTD,MIC,MN
		21:00	66°28.2'	28°46.0'	4847	
18/068		23:32	66°31.2'	27°59.0'	4833	CTD
	03.12.90	01:38	66°31.0'	28°00.4'	4855	

Station No.	Date	Time (GMT)	Latitude (S)	Longitude (W)	Depth (m) (uncorr.)	Operation
18/069		05:21	66°37.2'	27°07.2'	4871	CTD,MIC,
		20:50	66°37.4'	27°07.1'	4851	AWI 209/2
18/070	04.12.90	00:07	66°13.8'	27°43.6'	4864	CTD
		02:22	66°13.7'	27°44.0'	4865	
18/071		06:07	65°49.7'	28°22.9'	4881	CTD
		08:38	65°47.9'	28°23.3'	4902	
18/072		11:23	65°27.3'	28°58.0'	4902	CTD
		13:49	65°25.3'	28°59.3'	4924	
18/073		17:57	65°05.2'	29°30.7'	4922	CTD,SED
		20:09	65°03.9'	29°30.3'	4922	
18/074	05.12.90	01:34	65°28.1'	29°50.6'	4876	CTD,SED
		03:44	65°28.3'	29°50.1'	4877	
18/075		09:03	65°57.2'	30°04.4'	4836	CTD,MIC,SED,
		14:09	65°57.8'	30°03.2'	4836	AN,BO,MN, QM,BIO-ROSI
18/076		16:53	66°17.4'	30°17.8'	4789	CTD
		18:57	66°17.9'	30°19.1'	4799	
18/077		22:19	66°41.5'	30°35.6'	4726	CTD
	06.12.90	00:17	66°41.9'	30°37.1'	4726	
18/078		03:22	67°04.9'	30°51.7'	4673	CTD
		05:28	67°04.9'	30°54.1'	4673	
18/079		08:34	67°28.5'	31°05.5'	4608	CTD,MIC,SED,
		09:49	67°28.7'	31°07.0'	4608	QM,AN
18/080		14:45	67°19.1'	29°57.3'	4664	CTD,MIC
		16:49	67°18.7'	29°58.3'	4663	
18/081		21:15	67°08.6'	28°47.1'	4747	CTD,MIC
		23:20	67°08.7'	28°48.4'	4747	
18/082	07.12.90	03:47	66°57.5'	27°36.8'	4813	CTD,MIC
		05:59	66°56.9'	27°36.6'	4813	
18/083		10:12	66°45.5'	26°23.7'	4841	CTD,MIC
		13:01	66°45.4'	26°23.0'	4841	
18/084		16:09	66°53.4'	25°33.5'	4828	CTD,MIC
		18:47	66°53.2'	25°31.9'	4827	
18/085		21:16	67°03.6'	24°51.4'	4828	CTD,
	08.12.90	02:03	67°03.1'	24°54.2'	4836	AWI 222
18/086		05:50	67°13.5'	24°09.2'	4843	CTD,MIC
		08.08	67°13.2'	24°08.9'	4851	
18/087		12:09	67°21.9'	23°19.4'	4861	CTD,SED,QM,
		16:09	67°21.9'	23°17.2'	4861	AN,BO,MN
18/088		19:55	67°30.7'	22°31.7'	4878	CTD,MIC
		22:11	67°30.3'	22°31.5'	4879	
18/089	09.12.90	02:36	67°39.9'	21°39.8'	4892	CTD
		04:49	67°40.3'	21°38.1'	4892	
18/090		08:36	67°50.6'	20°51.2'	4910	CTD,MIC
		10:57	67°50.2'	20°50.0'	4910	
18/091		15:42	67°59.7'	19°58.9'	4906	CTD,
		20:04	67°59.3'	19°56.6'	4907	AWI 223
18/092		23:38	68°16.8'	19°20.4'	4840	CTD,MIC
	10.12.90	01:49	68°17.3'	19°20.4'	4839	
18/093		05:05	68°33.2'	18°37.1'	4763	CTD
		07:20	68°34.1'	18°35.6'	4763	
18/094		12:04	68°49.1'	17°55.5'	4769	CTD,MIC,SED,
		19:42	68°52.5'	17°50.4'	4770	AN,BO,MN, QM,BIO-ROSI, AWI 224
18/095		22:04	69°04.5'	17°16.0'	4750	CTD
	11.12.90	00:18	69°05.1'	17°13.4'	4773	
18/096		03:20	69°21.8'	16°29.8'	4720	CTD,MIC
		05:40	69°22.4'	16°29.8'	4720	

Station No.	Date	Time (GMT)	Latitude (S)	Longitude (W)	Depth (m) (uncorr.)	Operation
18/097		09:17	69°39.4'	15°43.8'	4742	CTD,SED,
		22:46	69°39.6'	15°42.9'	4745	AWI 210/2
18/098	12.12.90	01:20	69°48.2'	15°14.7'	4764	CTD,MIC
		03:40	69°48.7'	15°13.5'	4766	
18/099		05:50	69°58.0'	14°42.3'	4719	CTD
		08:16	69°58.5'	14°42.3'	4719	
18/100		10:40	70°07.5'	14°15.3'	4530	CTD,MIC
		12:43	70°08.4'	14°14.6'	4514	
18/101		16:48	70°18.7'	13°39.8'	4328	CTD,MIC,
		20:50	70°18.8'	13°42.4'	4366	AWI 225
18/102	13.12.90	23:30	70°22.6'	13°32.5'	2943	CTD,MIC,
		03:26	70°23.5'	13°32.3'	2941	AWI 226
18/103		04:35	70°25.2'	13°17.7'	2745	CTD
		05:56	70°25.4'	13°18.4'	2731	
18/104		07:30	70°29.7'	13°08.1'	2374	CTD,MIC
		09:37	70°29.8'	13°08.6'	2419	
18/105		12:20	70°38.2'	12°44.1'	2209	CTD,SED
		13:38	70°38.5'	12°45.0'	2267	
18/106		16:10	70°47.6'	12°21.8'	1996	CTD,MIC
		17:17	70°47.9'	12°22.9'	1996	
18/107		18:21	70°51.4'	12°15.0'	1907	HS,PS
		21:01	70°58.9'	11°58.9'	1450	
18/108	14.12.90	22:50	70°59.1'	11°49.7'	1114	CTD,MIC,SED,
		03:34	70°59.8'	11°53.4'	1247	AN,BO,MN, QM,BIO-ROSI
18/109		05:10	70°54.5'	11°56.5'	1584	CTD,
		07:34	70°54.7'	11°57.8'	1598	AWI 212/2
18/110		14:23	70°29.4'	13°07.0'	2416	AWI 211/2
		22:17	70°29.7'	13°08.9'	2381	
18/111	15.12.90	22:34	70°29.4'	13°06.8'	2376	HS,PS
		01:36	70°35.6'	12°28.6'	2067	
18/112		07:34	70°59.6'	11°45.0'	777	CTD,SED,
		10:00	70°59.5'	11°46.9'	893	AWI KN4
18/113		11:14	71°02.9'	11°42.8'	384	CTD,SED,
		12:58	71°02.9'	11°41.2'	384	AWI 214/2
18/114		14:07	71°05.0'	11°34.0'	257	CTD,MIC,
		16:29	71°05.5'	11°32.0'	276	AGT
18/115		17:50	71°06.8'	11°23.2'	491	CTD,SED,BIO-ROSI,
		20:39	71°06.8'	11°23.2'	490	AN,BO,MN
18/116	16.12.90	21:22	71°05.3'	11°34.0'	232	HS,PS
		22:20	70°25.9'	09°00.0'	350	
18/117	20.12.90	06:06	68°00.5'	03°57.8'	4233	BIO-ROSI,SED,AN
		07:01	68°00.4'	03°58.1'	4262	
18/118	23.12.90	14:44	54°21.1'	03°20.6'	2732	CTD,MIC,
		18:27	54°19.7'	03°24.4'	2677	AN,BIO-ROSI, UNIB BO1
18/119	25.12.90	04:04	50°07.7'	05°50.0'	3781	UNIB PF3/PF4
		10:31	50°07.0'	05°52.3'	3807	

Stationsliste ANT IX/3

Stat. No.18/	Date	Position	Echo depth (m)	Gear	Start (GMT)	Haul dur. (min)	Comment and Geological Station No.
121	14/01/91	70°34,2'S/08°08,6'W	142	-	08:30	105	Eisarbeiten
122	15/01/91	71°03,2'S/11°45,9'W	429	AWI	08:45	047	Bergung
				LS ; AN	09:32	006	
		71°03,4'S/11°46,4'W	425	CTD	09:44	044	
		71°03,7'S/11°47,2'W	422	BO	10:31	036	
123	15/01/91	71°08,8'S/12°12,2'W	400	AGT	12:26	098	30 Min. Schleppzeit 1989-1
		71°08,8'S/12°14,4'W	404				
		71°08,8'S/12°13,4'W	400	AGT	14:47	071	30 Min. Schleppzeit 1989-2
		71°08,8'S/12°16,0'W	405				1989-3
124	15/01/91	71°08,6'S/12°12,8'W	436	GKG	16:23	020	
125	17/01/91	71°58,9'S/13°25,6'W	346	CTD	15:08	045	
				LS	15:58	017	
				SED	16:16	006	
				BO	16:17	036	
		71°58,7'S/13°25,4'W	342	CTD	17:08	020	
126	21/01/91	76°22,3'S/30°07,7'W	394	CTD	14:12	040	
				SED	14:21	003	
				-	15:02		Eisarbeiten
				BO	15:26	043	
				AN	15:30	002	
				MN	16:27	031	
		76°22,4'S/30°08,1'W	388	FTS	17:01	041	
		76°22,6'S/30°08,9'W	391	GS	18:14	208	
				Reusen	19:20	900	
		76°23,1'S/30°11,6'W	358	GKG	22:32	016	1990-1
				SL	23:09	011	1990-2
		76°23,2'S/30°12,5'W	373	GKG	23:43	017	1990-3
	22/01/91	76°24,0'S/30°17,4'W	341	MN	06:27	030	
				-	09:15	120	Eisarbeiten
		76°24,7'S/30°20,7'W	333	MG	09:55	035	1991-2
		76°24,9'S/30°21,9'W	326	GKG	10:47	018	1991-1
		76°25,1'S/30°22,8'W	335	CTD	11:39	033	
				MN	12:15	153	im Eis verhakt
				-	15:05	145	Eisarbeiten
		76°25,5'S/30°25,8'W	320	GSL	15:44	011	1992-1
		76°25,5'S/30°25,8'W	330	GSL	16:05	011	1992-2
		76°25,5'S/30°25,8'W	330	CTD	17:03	033	
	23/01/91	76°25,5'S/30°25,9'W	320	MN	08:05	023	
		76°25,5'S/30°25,9'W	320	CTD	08:58	034	
				FTS	09:42	074	
				-	09:00	125	Eisarbeiten
				BO	11:10	035	
				Helicopter	12:23	693	Eisarbeiten
		76°25,5'S/30°25,9'W	321	FTS	12:36	048	
				GSL	13:40	018	1993-1
				MN	14:04	027	
		76°25,5'S/30°25,8'W	322	GSL	14:37	015	1993-2
				MG	15:09	029	
				MN	20:02	020	
	24/01/91	76°25,5'S/30°25,8'W		MN	01:59	024	
		76°25,7'S/30°28,0'W		GS	08:30	236	
				-	10:35	070	Eisarbeiten
		76°26,1'S/30°30,1'W		GSL	12:37	010	1994-1
		76°26,1'S/30°30,5'W	312	FTS	13:22	478	
				-	15:25	101	Eisarbeiten
		76°27,2'S/30°37,9'W	313	MG	21:32	475	
	25/01/91	76°28,0'S/30°44,3'W		-	08:50	650	Eisarbeiten

Stat. No.18/	Date	Position	Echo depth (m)	Gear	Start (GMT)	Haul dur. (min)	Comment and Geological Station No.
	26/01/91	76°28,5'S/30°47,8'W	336	CTD	10:55	037	
		76°28,0'S/30°48,1'W		-	08:30		Eisarbeiten
127	28/01/91	76°28,5'S/30°47,6'W	336	BO	11:36	039	
		76°36,0'S/31°18,8'W	367	CTD	10:02	039	
				SED	10:37	008	
				BO	10:45	045	
				-	13:19		Eisarbeiten
		76°36,1'S/31°19,4'W	384	MG	13:29	044	1995-1
		76°36,1'S/31°19,4'W	377	GSL	14:35	013	1995-2
		76°36,1'S/31°19,4'W	365	GKG	15:01	014	1995-3
		76°36,1'S/31°19,7'W	346	MG	16:16	028	
	29/01/91	76°37,0'S/31°25,7'W	307	GS	08:30	240	
		76°37,5'S/31°28,1'W	306	SL	12:40	013	1996-1
128	01/02/91	76°33,7'S/31°02,3'W	374	-	09:55	139	Eisarbeiten
				GSL	12:34	004	GSL ins Eis
				-	16:14	081	Eisarbeiten
	02/02/91	76°32,2'S/30°02,5'W	371	-	08:20	185	Eisarbeiten
		76°33,5'S/31°58,0'W	344	CTD	10:47	038	
129	02/02/91	76°07,6'S/28°22,8'W	315	AGT	20:06	049	15 Min. Schleppzeit
		76°07,3'S/28°23,0'W	324				1997-1
		76°07,0'S/28°18,7'W	339	FTS	21:28	042	
		76°07,0'S/28°15,3'W	375	MG	22:37	040	1997-2
130	03/02/91	75°15,0'S/25°50,1'W	561	GSN	08:42	095	20 Min. Schleppzeit
		75°16,1'S/25°57,7'W	586				
		75°16,8'S/25°53,9'W	604	GSN	12:03	140	15 Min. Schleppzeit
		75°17,4'S/25°57,0'W	626				
		75°18,3'S/25°57,9'W	652	BO	14:40	033	
131		75°10,7'S/26°45,2'W	356	FTS	16:58	043	
		75°10,7'S/26°45,9'W	357	LS	17:54	021	
				CTD	18:20	041	
		75°10,7'S/26°45,5'W	356	SED	18:38	003	
			357	AN	18:44	003	
132	03/02/91	75°11,0'S/26°45,0'W	367	-	20:05	650	Profilfahrt
133	04/02/91	75°15,9'S/26°38,9'W	424	GSN	08:05	080	16 Min. Schleppzeit
		75°16,8'S/26°35,7'W	436				
134	04/02/91	75°16,0'S/25°58,6'W	575	FTS	10:45	056	
135	04/02/91	75°28,6'S/26°56,6'W	226	FTS	14:00	042	
		75°28,5'S/26°57,2'W	229	MG	14:50	033	1998-1
		75°28,5'S/26°57,5'W	229	CTD	15:37	043	
		75°28,5'S/26°57,8'W	229	AN	15:54	021	
		75°28,5'S/26°57,6'W	229	GS	16:30	044	
		75°28,6'S/26°57,6'W	228	-	16:57	031	Eisbergbesuch 1998-2
		75°27,9'S/26°54,4'W	221	AGT	18:15	044	15 Min. Schleppzeit
		75°27,7'S/26°53,9'W	221				1998-3
136	05/02/91	74°58,4'S/26°31,0'W	296	CTD	00:06	035	
		74°58,4'S/26°30,8'W	295	BO	00:45	034	
		74°58,3'S/26°30,5'W	295	MN	01:26	027	
		74°58,1'S/26°30,4'W	295	FTS	01:58	042	
137	05/02/91	74°31,2'S/26°39,5'W	719	CTD	12:22	053	
		74°31,1'S/26°39,5'W	713	AN	12:41	014	
		74°31,3'S/26°39,5'W	703	SED	12:57	006	
		74°31,3'S/26°39,2'W	690	MN	13:20	049	
138	05/02/91	74°29,4'S/26°43,5'W	1536	CTD	14:38	072	
		74°29,4'S/26°43,4'W	1506	SED	14:49	011	
139	05/02/91	74°26,4'S/26°44,9'W	2215	MN	16:54	069	
		74°26,4'S/26°45,0'W	2205	AN	17:21	004	
		74°26,4'S/26°45,0'W	2206	SED	17:26	009	
		74°26,6'S/26°44,0'W	2201	CTD	18:11	075	
140	05/02/91	74°14,3'S/26°26,7'W	2687	MN	21:41	078	
		74°14,4'S/26°26,0'W	2655	GTD	23:06	087	

Stat. No.18/	Date	Position	Echo depth (m)	Gear	Start (GMT)	Haul dur. (min)	Comment and Geological Station No.		
141	06/02/91	73°37,6'S/26°07,0'W	3360	AWI	10:18	066	Verank. ausgelegt		
		73°37,4'S/26°07,1'W	3353	-	13:00	198	Eisarbeiten		
		73°37,3'S/26°07,0'W	3356	CTD+MIC	13:37	105	1999-1		
		73°37,0'S/26°06,9'W	3361	SED	14:34	011			
		73°36,7'S/26°06,7'W	3377	MN	15:57	066			
		73°36,4'S/26°06,5'W	3379	GS	17:12	664			
		73°36,3'S/26°07,1'W	3157	AN	17:27	006			
142	07/02/91	73°36,1'S/26°06,0'W	3385	-	18:41	081	Eisarbeiten		
		72°55,1'S/25°41,3'W	3587	CTD+MIC	07:01	129	2000-1		
		72°55,0'S/25°41,5'W	3591	AN	07:57	003			
143	07/02/91	72°55,0'S/25°41,9'W	3591	SED	08:02	005			
		72°14,5'S/25°15,1'W	3830	CTD+MIC	16:22	129	2001-1		
		72°14,5'S/25°15,1'W	3830	-	16:23	235	Eisarbeiten		
144	08/02/91	72°14,1'S/25°16,3'W	3826	MN	18:41	060			
		72°45,0'S/24°55,0'W	4128	CTD+MIC	01:13	134	2002-1		
145	08/02/91	71°29,4'S/24°46,9'W	3763	CTD	06:05	129	2003-1		
		71°29,3'S/24°46,4'W	3762	SL	08:28	082	2003-2		
		71°29,1'S/24°46,4'W	3757	SED	09:05	003			
		71°28,9'S/24°47,3'W	3748	-	10:10	095	Eisarbeiten		
		71°28,9'S/24°47,3'W	3748	GKG	10:11	109	2003-3		
		71°28,3'S/24°49,9'W	3722	MUC	12:12	080	2003-4		
		71°28,0'S/24°50,6'W	3723	AN	13:27	002			
		71°21,3'S/24°46,3'W	3712	SL	15:54	081	2004-1		
146	08/02/91	71°21,1'S/24°47,0'W	3745	MG	17:25	159	2004-2		
		71°21,2'S/24°46,1'W	3729	-	20:45	085	Frequenztest		
		71°21,2'S/24°46,1'W	3729	-	21:30	172	Profilfahrt		
		70°55,0'S/24°46,0'W	3706	-	00:22	483	Profilfahrt		
		71°21,6'S/24°46,9'W	3720	MG	08:25	135	2004-3		
147	09/02/91	71°22,7'S/24°25,2'W	3741	SL	11:40	080	2005-1		
		71°22,7'S/24°24,2'W	3849	GKG	13:18	095	2005-2		
		71°22,8'S/24°25,1'W	3831	-	15:06	032	Frequenztest		
148	09/02/91	71°23,6'S/24°19,6'W	3998	GKG	16:02	122	2006-1		
		71°23,9'S/24°17,1'W	4145	SL	18:24	080	2006-2		
		71°25,5'S/24°16,9'W	4191	-	20:38	667	Profilfahrt		
149	10/02/91	71°23,3'S/24°10,2'W	4251	SL	08:07	083	2007-1		
		71°23,5'S/24°08,3'W	4256	-	10:00	204	Eisarbeiten		
		71°23,3'S/24°08,2'W	4257	GKG	10:15	105	2007-2		
		71°23,4'S/24°09,8'W	4240	-	12:12	032	Frequenztest		
150	10/02/91	71°23,3'S/24°20,7'W	3951	SL	14:07	077	2008-1		
		71°23,3'S/24°20,8'W	3947	MUC	15:35	079	2008-2		
		71°23,4'S/24°20,6'W	3930	AN	16:36	009			
		71°23,3'S/24°20,6'W	3932	-	16:58	032	Frequenztest		
		71°23,4'S/24°20,6'W	3929	-	17:30	150	Profilfahrt		
151	11/02/91	71°19,8'S/22°41,5'W	4233	CTD+MIC	01:29	139	2009-1		
152	11/02/91	71°13,0'S/22°47,5'W	4242	CTD+MIC	06:40	138	2010-1		
153	11/02/91	71°05,8'S/20°46,8'W	4428	AWI	14:30	270	Verank. geborgen		
		71°05,6'S/20°45,3'W	4450	-	19:40	205	Eisarbeiten		
		71°05,6'S/20°45,3'W	4450	BO	19:46	034			
		71°05,6'S/20°45,3'W	4450	SED	19:48	003			
		71°05,4'S/20°45,0'W	4450	CTD	20:24	146			
		71°05,3'S/20°46,5'W	4450	AN	22:07	018			
		71°05,3'S/20°46,9'W	4450	MN	22:56	086			
		12/02/91	71°05,4'S/20°47,4'W	4416	GS	00:28	366		
		154	12/02/91	71°05,7'S/20°46,6'W	4442	MUC	06:51	089	2011-1
				71°26,6'S/19°48,3'W	4313	CTD+MIC	13:21	135	2012-1
155	12/02/91	71°26,7'S/19°48,4'W	4373	-	14.11	149	Eisarb., Zent.boje plaz		
		71°49,3'S/18°38,3'W	3676	CTD	22:00	120			
156	13/02/91	71°49,3'S/18°38,2'W	3675	AN	23:20	005			
		72°08,6'S/17°26,1'W	2038	CTD	06:02	087			
		72°11,3'S/17°13,1'W	1851	-	08:42	033			

Stat. No.18/	Date	Position	Echo depth (m)	Gear	Start (GMT)	Haul dur. (min)	Comment and Geological Station No.
157	13/02/91	72°15,3'S/16°58,5'W	1367	CTD	10:45	059	
		72°15,3'S/16°58,7'W	1354	AN	11:12	007	
		72°15,3'S/16°58,7'W	1354	SED	11:20	002	
158	13/02/91	72°21,8'S/16°52,1'W	623	GSN	13:35	120	20 Min. Schleppzeit 2013-1
		72°21,0'S/16°48,6'W	539				
159	13/02/91	72°21,1'S/16°33,4'W	304	CTD	16:13	031	
		72°21,1'S/16°33,5'W	304	SED	16:22	003	
		72°21,1'S/16°33,7'W	303	AN	16:30	009	
160	14/02/91	70°14,0'S/12°40,0'W	2723	-	12:26	791	Profilfahrt
	16/02/91	70°28,0'S/07°33,0'W	588	-	00:50	230	Profilfahrt
160	16/02/91	70°19,4'S/07°00,5'W	496	FTS	06:03	050	
		70°19,6'S/07°02,5'W	476	BO	07:01	035	
		70°18,6'S/07°03,1'W	830	GSN	08:35	130	30 Min. Schleppzeit 2014-1
		70°19,0'S/06°47,7'W	802				
		70°19,3'S/06°43,3'W	758	LS	11:02	014	
		70°19,2'S/06°43,5'W	764	SED	11:05	004	
		70°19,2'S/06°43,7'W	780	AN	11:09	011	
		70°19,3'S/06°43,9'W	703	CTD	11:21	054	
		70°24,2'S/06°00,5'W	120	GKG	14:08	008	2015-1
		70°24,2'S/06°00,4'W	117	AN	14:15	001	
161	16/02/91	70°24,2'S/06°00,4'W	118	SL	14:35	015	2015-2
		70°24,2'S/06°00,4'W	122	SED	14:38	001	
161	16/02/91	70°24,2'S/06°00,6'W	116	GSL	14:54	007	2015-3
		70°24,1'S/06°00,9'W	119	GSL	15:04	007	2015-4
		70°24,8'S/05°00,1'W	429	AGT	17:34	065	kein Fang
		70°24,7'S/04°59,9'W	434				2016-1
		70°24,3'S/04°56,9'W	437	AGT	18:54	065	15 Min. Schleppzeit 2016-2
162	16/02/91	70°24,2'S/04°56,4'W	437				2016-2
		70°23,3'S/04°58,2'W	431	MG	21:52	038	2016-3
		70°23,2'S/05°00,5'W	430	FTS	21:44	071	
		70°22,7'S/05°04,8'W	434	-	23:04	274	
		70°05,8'S/03°58,9'W	1026	CTD	06:05	059	
163	17/02/91	70°05,8'S/03°58,9'W	1026	SED	06:00	001	
		70°05,7'S/03°59,7'W	1077	AN	06:56	005	
		70°05,6'S/04°00,1'W	1139	GS; ISP	07:18	250	
		70°22,6'S/04°01,4'W	528	CTD	13:30	038	2017-1
164	17/02/91	70°22,6'S/04°01,5'W	527	SED	13:33	002	
		70°22,7'S/04°01,7'W	529	AN	13:40	004	
		70°22,2'S/04°02,7'W	524	GKG	14:17	017	2017-2
		70°21,9'S/04°02,4'W	517	SL	14:49	017	2017-3
		70°17,7'S/03°11,5'W	150	MG	17:40	039	2018-1
165	17/02/91	70°17,7'S/03°11,5'W	151	AN	17:42	004	
		70°18,1'S/03°13,2'W	155	FTS	18:31	049	
		70°19,1'S/03°16,5'W	206	AGT	19:38	039	7,5 Min. Schleppzeit
		70°19,2'S/03°16,8'W	204				2018-2
		69°47,9'S/03°08,5'W	2780	-	24:00	330	Profilfahrt
		70°09,8'S/01°57,1'W	162	CTD	06:01	031	2019-1
		70°09,8'S/01°57,1'W	162	SED	06:05	004	
166	18/02/91	70°09,7'S/01°57,2'W	157	AN	06:25	005	
		70°09,7'S/01°57,1'W	157	GKG	06:42	010	2019-2
		70°09,8'S/01°56,8'W	171	SL	07:10	010	2019-3
		69°42,8'S/00°59,4'W	2108	AN	11:14	004	
		69°42,6'S/01°00,1'W	2209	GKG	11:22	058	2020-1
167	18/02/91	69°42,7'S/01°00,4'W	2229	SED	11:26	004	
		69°42,5'S/00°57,0'W	2083	SL	12:50	047	2020-2
		69°45,8'S/00°47,3'E	498	AGT	19:24	080	kein Fang
168	18/02/91	69°46,1'S/00°47,8'E	508				
		69°47,2'S/00°52,5'E	447	AGT	21:00	078	15 Min. Schleppzeit
		69°47,4'S/00°52,9'E	455				2021-1
		69°44,9'S/01°00,0'E	1147	-	23:10	650	Profilfahrt

Stat. No.18/	Date	Position	Echo depth (m)	Gear	Start (GMT)	Haul dur. (min)	Comment and Geological Station No.
169	19/02/91	69°58,9'S/02°06,3'E	560	GSN	12:21	116	24 Min. Schleppzeit
		70°03,1'S/02°19,9'E	450				2022-1
		70°06,0'S/02°22,6'E	170	GKG	15:57	007	2022-2
		70°06,1'S/02°23,4'E	175	FTS	16:23	043	
		70°06,2'S/02°23,3'E	162	CTD	17:12	032	2022-3
		70°06,2'S/02°23,1'E	166	SED	17:36	004	
170	19/02/91	70°06,3'S/03°01,0'E	417	GKG	19:55	012	2023-1
		69°59,2'S/06°00,9'E	516	FTS	06:54	031	
171	20/02/91	69°58,9'S/05°56,9'E	465	MG	09:00	037	2024-1
		69°56,6'S/05°56,9'E	566	SL	09:56	014	2024-2
		69°58,3'S/05°55,1'E	596	GKG	10:25	016	2024-3
		69°58,2'S/05°46,5'E	813	AGT	11:40	077	15 Min. Schleppzeit
		69°58,1'S/05°45,2'E	965				
172	20/02/91	70°02,6'S/06°44,8'E	659	GKG	16:21	018	2025-1
		70°02,6'S/06°44,8'E	659	SED	16:22	003	
		70°02,6'S/06°44,8'E	656	AN	16:26	005	
		70°02,6'S/06°44,6'E	656	SL	16:55	025	2025-2
173	20/02/91	70°00,5'S/07°08,9'E	228	AGT	18:20	038	15 Min. Schleppzeit
		70°00,4'S/07°07,4'E	224				2026-1
		70°00,2'S/07°11,2'E	167	MG	19:38	045	2026-2
		70°00,3'S/07°11,1'E	171	AN	20:28	007	
		70°00,3'S/07°10,9'E	175	FTS	20:37	048	
		70°00,2'S/07°11,0'E	179	CTD	21:30	028	
174	21/02/91	70°00,2'S/07°11,3'E	181	BO	22:00	017	
		69°43,7'S/10°44,7'E	432	GSN	08:38	091	15 Min. Schleppzeit
		69°42,6'S/10°47,5'E	432				2027-1
		69°44,7'S/10°41,7'E	410	FTS	11:46	057	
		69°44,7'S/10°41,7'E	413	SED	11:50	002	
175	21/02/91	69°44,6'S/10°40,9'E	430	AN	12:02	007	
		70°00,8'S/11°45,3'E	207	GKG	15:22	010	2028-1
		70°00,7'S/11°45,0'E	199	SL	15:47	009	2028-2
		70°00,7'S/11°44,4'E	202	GSL	16:23	008	2028-3
		70°00,7'S/11°44,4'E	202	SED	16:26	004	
		70°00,7'S/11°44,2'E	198	GKG	16:46	011	2028-4
		70°00,7'S/11°44,1'E	200	FTS	17:03	038	
		70°00,7'S/11°44,5'E	202	CTD	17:46	024	2028-5
		70°00,5'S/11°45,1'E	201	MG	18:46	028	
		70°00,4'S/11°45,3'E	203	MN	19:24	014	
		22/02/91	69°39,0'S/10°00,0'E	2234	-	02:30	132
176	22/02/91	69°44,7'S/10°00,0'E	948	MG	06:07	053	2029-1
		69°45,4'S/09°55,9'E	866	FTS	07:12	046	
		69°46,2'S/09°52,1'E	746	AN	08:12	002	
		69°46,2'S/09°52,4'E	734	AGT	08:24	131	30 Min. Schleppzeit
177	22/02/91	69°45,9'S/09°53,8'E	774				
		69°47,9'S/09°55,6'E	256	GKG	11:14	011	2030-1
178	22/02/91	69°47,9'S/09°55,3'E	257	SED	11:16	008	
		69°59,9'S/08°58,4'E	469	GKG	14:26	022	2031-1
		69°59,8'S/08°58,3'E	470	SED	14:34	002	
179	22/02/91	69°59,5'S/08°58,8'E	462	SL	15:02	015	2031-2
		69°57,9'S/08°01,3'E	185	SL	18:01	010	2032-1
		69°58,1'S/08°01,6'E	192	GKG	18:24	008	2032-2
		69°59,1'S/08°00,4'E	181	AGT	18:54	044	15 Min. Schleppzeit
		69°59,3'S/07°59,9'E	161				
		69°58,1'S/08°00,8'E	200	MG	21:06	005	
		69°59,1'S/08°00,5'E	192	AN	21:22	008	
		69°59,1'S/08°00,4'E	191	FTS	21:32	050	
23/02/91	69°38,0'S/06°17,0'E	1956	-	02:57	102	Profilmfahrt	

Stat. No.18/	Date	Position	Echo depth (m)	Gear	Start (GMT)	Haul dur. (min)	Comment and Geological Station No.
180	23/02/91	69°57,3'S/06°18,9'E	286	CTD	06:03	032	2033-1
		69°57,3'S/06°18,9'E	286	SED	06:04	004	
		69°57,3'S/06°19,0'E	281	MN	06:39	018	
		69°57,3'S/06°19,0'E	281	AN	06:40	004	
		69°57,3'S/06°18,7'E	288	MG	07:12	035	
		69°57,4'S/06°18,3'E	293	FTS	07:56	042	
		69°57,5'S/06°19,8'E	282	AGT	09:20	109	15 Min. Schleppzeit
		69°57,7'S/06°21,0'E	298				2033-2
		69°58,3'S/06°20,7'E	313	GKG	10:35	011	2033-3
		69°58,5'S/06°20,1'E	312	SL	11:00	010	2033-4
181	23/02/91	69°56,1'S/06°17,7'E	698	SL	12:00	020	2034-1
		69°56,2'S/06°16,6'E	738	GKG	12:28	028	2034-2
		69°56,4'S/06°16,2'E	727	SED	12:38	004	
182	23/02/91	69°56,9'S/06°14,8'E	723	GKG	13:15	027	2034-3
		69°55,6'S/06°15,7'E	1007	MG	14:09	123	
		69°55,7'S/06°15,4'E	1024	AN	14:22	003	
183	23/02/91	69°56,1'S/06°14,0'E	1011	GKG	15:37	034	leer 2035-1
		69°55,9'S/06°12,5'E	1131	GKG	16:23	028	2035-2
		69°58,3'S/06°10,7'E	909	FTS	17:18	066	
		69°51,9'S/06°16,9'E	1549	CTD+MIC	19:31	071	2036-1
		69°51,9'S/06°16,9'E	1561	AN	19:38	014	
184	24/02/91	69°51,9'S/06°16,9'E	1561	SED	19:39	002	
		69°50,0'S/06°13,0'E	1374	-	21:11	635	Profilfahrt
		69°43,0'S/06°17,6'E	1667	CTD	08:06	075	2037-1
		69°43,0'S/06°17,5'E	1659	SED	08:09	015	
		69°43,0'S/06°17,2'E	1641	AN	08:30	005	
		69°42,9'S/06°16,7'E	1624	MN	09:28	071	
		69°42,5'S/06°16,0'E	1637	MUC	10:40	040	2037-2
		69°42,9'S/06°16,4'E	1613	SL	11:40	037	2037-3
		69°42,9'S/06°16,3'E	1612	-	12:19	034	Frequenztest
		69°40,4'S/06°18,9'E	1829	-	13:30	085	Profilfahrt
185	24/02/91	69°21,0'S/06°17,2'E	1621	CTD	15:27	060	2038-1
		69°20,9'S/06°17,4'E	1621	SED	15:50	001	
		69°20,9'S/06°17,4'E	1621	AN	16:00	005	
		69°20,9'S/06°17,6'E	1612	SL	16:31	040	2038-2
		69°21,2'S/06°17,5'E	1620	MUC	17:25	042	2038-3
		69°21,0'S/06°17,2'E	1601	-	18:22	033	Frequenztest
		69°19,7'S/06°14,8'E	1591	- -	19:14	090	Profilfahrt
		69°01,4'S/06°14,6'E	2113	SL	21:10	045	2039-1
186	24/02/91	69°01,2'S/06°13,1'E	2123	MUC	22:11	041	2039-2
		69°01,0'S/06°11,5'E	2086	CTD	23:15	083	2039-3
		69°01,2'S/06°10,2'E	2083	AN	23:50	002	
		69°01,3'S/06°13,8'E	2104	-	00:59	028	Frequenztest
		69°00,0'S/06°04,0'E	2156	-	01:52	261	Profilfahrt
187	25/02/91	68°50,4'S/06°14,6'E	2674	MUC	06:15	055	2040-1
		68°50,6'S/06°14,9'E	2671	SL	07:40	053	2040-2
		68°50,5'S/06°14,3'E	2620	- -	09:02	038	Frequenztest
188	25/02/91	68°44,1'S/06°07,9'E	3122	CTD	10:38	122	2041-1
		68°44,1'S/06°07,6'E	3119	SED	10:44	002	
		68°44,5'S/06°07,8'E	3096	MN	12:46	074	
		68°44,6'S/06°11,0'E	3098	GS	14:28	013	Abbruch: Sturm
		26/02/91	68°39,5'S/06°01,0'E	3238	-	01:30	862

Stat. No.18/	Date	Position	Echo depth (m)	Gear	Start (GMT)	Haul dur. (min)	Comment and Geological Station No.
189	26/02/91	70°06,1'S/05°12,2'E	476	LS	15:15	015	
		70°06,1'S/05°11,7'E	480	CTD	15:34	041	2042-1
		70°06,0'S/05°11,6'E	480	SED	15:49	004	
		70°06,1'S/05°11,1'E	489	GS	16:23	044	
		70°06,2'S/05°10,1'E	494	MG	17:17	034	2042-2
		70°06,3'S/05°12,4'E	484	FTS	18:06	047	
		70°06,1'S/05°12,2'E	477	AGT	19:14	068	15 Min. Schleppzeit
		70°06,0'S/05°13,2'E	467				
		70°05,8'S/05°13,4'E	464	MN	20:46	034	
		70°05,9'S/05°12,3'E	479	GKG	21:29	016	2042-3
		70°05,9'S/05°11,9'E	4683	SL	21:56	018	2042-4
190	27/02/91	69°49,0'S/00°58,7'E	418	LS	07:01	012	
		69°48,5'S/00°57,4'E	426	CTD	07:19	039	2043-1
		69°47,9'S/00°56,2'E	451	SED	07:40	002	
		69°46,9'S/00°50,0'E	448	GS	08:44	042	
		69°46,3'S/00°48,5'E	473	MN	09:35	027	
		69°47,2'S/00°45,8'E	414	GKG	10:28	013	2043-2
		69°47,7'S/00°45,2'E	391	SL	11:00	017	2043-3
		69°46,5'S/00°59,5'E	778	SL	12:34	024	2044-1
191	27/02/91	69°46,2'S/00°58,7'E	814	GKG	13:16	020	2044-2
		69°41,2'S/00°57,9'E	1418	CTD	14:42	062	2045-1
192	27/02/91	69°41,1'S/00°57,3'E	1425	SED	15:17	001	
		69°40,9'S/00°56,3'E	1430	GS	15:56	097	
		69°40,2'S/00°54,6'E	1359	MN	17:40	064	
		69°40,9'S/00°57,3'E	1441	MUC	19:33	033	2045-2
		69°41,1'S/00°55,9'E	1390	SL	20:32	034	2045-3
		69°40,3'S/00°51,1'E	1398	AGT	21:44	186	60 Min. Schleppzeit
		69°40,5'S/00°54,8'E	1393				2045-4
		69°41,1'S/00°54,7'E	1429	-	01:35	031	Frequenztest
193	28/02/91	69°37,3'S/01°03,3'E	1837	-	02:54	186	Profiffahrt
		69°37,2'S/01°02,1'E	1818	SL	06:19	043	2046-1
		69°37,3'S/01°02,6'E	1820	MUC	07:13	043	2046-2
194	28/02/91	69°37,2'S/01°02,4'E	1793	-	08:09	031	Frequenztest
		69°29,1'S/01°10,7'E	2421	CTD	10:26	089	2047-1
		69°29,1'S/01°10,6'E	2425	SED	10:28	005	
		69°29,0'S/01°10,4'E	2434	AN	11:02	011	
		69°28,9'S/01°09,6'E	2495	MN	12:00	073	
		69°29,5'S/01°12,0'E	2407	MUC	13:36	054	2047-2
		69°29,4'S/01°12,4'E	2298	SL	14:47	052	2047-3
		69°29,4'S/01°11,7'E	2422	-	15:40	034	Frequenztest
		69°28,0'S/00°55,0'E	2268	-	16:46	152	Profiffahrt
		69°04,1'S/00°59,4'E	3683	CTD+MIC	19:25	116	2048-1
		69°04,1'S/00°59,4'E	3648	SED	19:50	001	
195	28/02/91	69°04,1'S/00°59,4'E	3648	AN	19:52	005	
		69°03,7'S/00°59,9'E	3431	MN	21:31	088	
		68°37,0'S/00°57,0'E	4243	-	01:46	236	Profiffahrt
		69°04,9'S/00°53,3'E	3324	GS+CTD	06:08	352	2049-1
		69°04,9'S/00°53,1'E	3320	MUC	12:09	069	2049-2
196	01/03/91	69°04,9'S/00°53,1'E	3313	MUC	13:33	071	2049-3
		69°05,2'S/00°52,7'E	3289	SL	15:01	070	2049-4
		69°05,1'S/00°53,4'E	3237	-	16:23	030	Frequenztest
		68°45,2'S/00°53,3'E	3920	CTD	19:03	124	2050-3
		68°45,2'S/00°53,3'E	3920	SED	19:06	005	
197	01/03/91	68°45,0'S/00°53,6'E	3913	AN	20:21	007	
		68°40,0'S/00°59,0'E	4215	-	21:50	474	Profiffahrt

Stat. No.18/	Date	Position	Echo depth (m)	Gear	Start (GMT)	Haul dur. (min)	Comment and Geological Station No.
198	02/03/91	68°46,1'S/00°52,2'E	3929	SL	06:08	078	2050-1
		68°46,0'S/00°52,3'E	3909	MUC	07:36	082	2050-2
		68°46,0'S/00°52,2'E	3882	MG	09:25	143	2050-4
		68°46,0'S/00°52,6'E	3899	BO	12:00	031	
		68°45,9'S/00°52,6'E	3901	-	12:37	035	Frequenztest
199	02/03/91	68°40,0'S/01°08,0'E	4207	-	14:11	168	Profilfahrt
		68°13,9'S/00°58,8'E	4466	SED	17:04	006	
		68°13,9'S/00°58,9'E	4465	CTD	17:09	162	2051-1
		68°14,1'S/00°59,0'E	4464	AN	18:50	007	
		68°14,0'S/00°58,8'E	4464	MN	19:58	138	
	03/03/91	68°14,0'S/00°59,1'E	4465	GS	21:22	598	
		68°14,4'S/01°01,8'E	4468	MUC	07:33	126	2051-2
		68°13,8'S/00°58,9'E	4464	MUC	12:52	100	2051-3
		68°14,2'S/00°58,7'E	4461	SL	14:45	088	2051-3
		68°14,0'S/01°01,1'E	4462	-	16:14	036	Frequenztest
200	04/03/91	66°48,2'S/06°14,5'E	4095	CTD	07:30	139	2052-1
		66°48,2'S/06°14,5'E	4095	SED	07:32	005	
		66°48,2'S/06°14,7'E	4296	AN	09:38	012	
		66°48,1'S/06°14,8'E	4298	MN	09:51	080	
		66°48,2'S/06°15,3'E	4321	GS	11:15	380	
		66°48,1'S/06°16,0'E	4322	MUC	17:42	086	2052-2
		66°48,1'S/06°15,9'E	4321	MUC	19:23	082	2052-3
		67°17,7'S/06°15,2'E	4294	CTD	03:00	137	
201	05/03/91	67°17,7'S/06°16,3'E	4293	AN	04:38	006	
		67°17,7'S/06°16,3'E	4293	SED	04:46	003	
		67°18,0'S/06°14,9'E	4294	MG	06:12	161	2053-1
		67°18,0'S/06°15,1'E	4271	SL	09:05	086	2053-2
		67°18,0'S/06°16,6'E	4271	-	10:35	030	Frequenztest
		67°58,1'S/06°15,0'E	3965	CTD	15:35	127	2054-1
		67°58,2'S/06°15,2'E	3913	SED	16:00	003	
202	05/03/91	67°58,2'S/06°15,2'E	3913	AN	16:04	004	
		67°58,0'S/06°15,2'E	3907	MN	17:46	081	
		67°57,8'S/06°14,5'E	3906	MUC	19:10	081	2054-2
		67°59,9'S/06°16,0'E	3896	GS	21:02	622	
		68°17,7'S/06°15,0'E	3606	CTD	09:28	113	2055-1
		68°17,8'S/06°14,8'E	3603	SED	10:06	008	
		68°17,7'S/06°14,8'E	3603	AN	10:14	008	
		68°17,7'S/06°15,0'E	3605	SL	11:30	078	2055-2
203	06/03/91	68°17,6'S/06°15,3'E	3609	MUC	12:57	076	2055-3
		68°17,4'S/06°14,8'E	3609	-	14:23	036	Frequenztest
		68°19,0'S/06°20,0'E	3584	-	15:24	138	Profilfahrt
		68°44,4'S/06°08,0'E	3097	SL	18:22	064	2056-1
		68°44,6'S/06°07,9'E	3088	SED	19:14	002	
		68°44,6'S/06°07,7'E	3088	MUC	19:39	061	2056-2
		68°44,5'S/06°08,0'E	3056	-	21:05	030	
		68°44,4'S/06°07,3'E	3055	CTD	21:41	105	2056-3
204	06/03/91	68°44,3'S/06°06,3'E	3050	AN	22:35	002	
		68°44,3'S/06°05,2'E	3046	BO	23:30	030	
		69°36,0'S/09°49,8'E	2468	CTD	10:38	090	
		69°35,9'S/09°49,7'E	2478	SED	11:29	001	
205	07/03/91	69°35,9'S/09°49,7'E	2478	AN	11:30	007	
		69°46,9'S/10°01,0'E	343	GSN	14:27	079	15 Min. Schleppzeit, schwerer Haker
206	07/03/91	69°46,8'S/10°01,6'E	338	-			
		69°46,2'S/09°57,4'E	601	FTS	16:18	055	
		69°46,2'S/09°53,6'E	689	CTD	17:20	044	
		69°46,1'S/09°50,3'E	867	SED	18:06	003	
		69°46,1'S/09°50,1'E	893	MN	18:08	066	
		69°46,1'S/09°45,8'E	911	AN	18:20	014	

Stat. No.18/	Date	Position	Echo depth (m)	Gear	Start (GMT)	Haul dur. (min)	Comment and Geological Station No.
207	08/03/91	69°57,2'S/11°53,6'E	217	FTS	10:32	043	
		69°57,4'S/11°48,0'E	208	AGT	12:36	045	15 Min. Schleppzeit
		69°57,5'S/11°48,9'E	210				2057-3
208	09/03/91	69°57,3'S/11°48,5'E	218	GKG	09:28	007	2057-1, leer
		69°57,3'S/11°48,6'E	210	GKG	09:38	017	2057-2
209	09/03/91	69°58,3'S/12°10,7'E	150	GKG	11:38	018	2058-1
		69°58,4'S/12°10,4'E	158	SL	12:11	008	2058-2
210	09/03/91	69°45,3'S/10°42,7'E	350	GKG	16:45	023	2059-1
		69°45,4'S/10°41,8'E	359	SL	17:25	019	2059-2
211	10/03/91	69°58,9'S/05°08,4'E	661	GSN	11:14	151	47 Min. Schleppzeit
		69°57,9'S/05°00,4'E	742				
		69°57,8'S/04°57,3'E	695	FTS	14:29	059	
		69°58,3'S/04°57,3'E	408	BO	15:52	033	
		69°58,7'S/04°57,5'E	346	-	16:32	002	Eiscollektion
		69°58,1'S/05°02,1'E	750	MG	17:05	039	2060-1
		69°55,0'S/04°30,0'E	1670	-	19:15	525	Profilfahrt
		70°01,9'S/04°06,7'E	881	CTD	05:56	047	2061-1
		70°01,6'S/04°06,4'E	930	MN	06:58	067	
		70°01,7'S/04°05,1'E	838	AN	07:25	003	
212	11/03/91	70°01,7'S/04°06,0'E	901	FTS	08:14	064	
		70°01,2'S/04°07,4'E	963	GKG	09:49	026	2061-2
		70°01,2'S/04°04,6'E	920	GKG	10:30	025	2061-3
		70°01,3'S/04°04,3'E	830	-	11:05	020	Eiscollektion
		70°01,4'S/04°03,4'E	796	MG	11:28	030	
		70°00,5'S/03°56,4'E	607	AGT	13:07	090	30 Min. Schleppzeit
		70°00,4'S/03°57,3'E	644				2061-4
		69°58,8'S/02°29,3'E	645	CTD	19:46	042	
		69°58,7'S/02°27,8'E	649	MN	20:34	046	
		69°50,0'S/02°15,0'E	1375	-	22:38	322	Profilfahrt
214	12/03/91	69°46,5'S/01°23,7'E	1871	CTD	06:10	072	2062-1
		69°46,5'S/01°27,7'E	1594	MN	07:41	070	
		69°46,5'S/01°27,7'E	1594	AN	07:43	007	
		69°46,5'S/01°27,6'E	1594	SED	07:47	002	
		69°47,0'S/01°28,8'E	1449	GKG	09:10	039	2062-2
215	12/03/91	69°46,9'S/01°27,1'E	1617	SL	10:09	036	2062-3
		69°39,8'S/00°52,4'E	1628	MG	12:17	058	
		69°45,1'S/01°47,0'E	516	MG	15:16	022	2063-1
		69°38,9'S/00°03,1'E	1521	SL	18:25	035	2064-1
		69°39,0'S/00°02,0'E	1573	GKG	19:14	040	2064-2
		69°39,0'S/00°02,3'E	1648	-	20:10	005	Eiscollektion
		69°43,2'S/00°33,0'W	2052	GKG	21:43	057	2065-1
		70°24,3'S/05°00,0'W	435	GKG	11:46	017	2066-1
		70°23,9'S/05°00,2'W	435	SL	12:20	014	2066-2
		220	13/03/91	70°24,1'S/06°01,2'W	126	MG	15:20
70°24,1'S/06°01,7'W	126			MG	15:32	008	
70°24,1'S/06°02,1'W	124			FTS	15:51	037	
70°24,0'S/06°02,7'W	124			AN	15:57	013	
70°24,1'S/06°07,8'W	119			AGT	16:48	035	15 Min. Schleppzeit
221	13/03/91	70°24,3'S/06°08,6'W	126				
		70°26,0'S/07°00,0'W	625	GKG	19:10	018	2067-1
222	13/03/91	70°19,0'S/07°02,5'W	584	MG	20:24	024	2068-1
		70°19,1'S/07°02,3'W	509	FTS	20:58	048	
223	18/03/91	66°14,8'S/03°30,3'E	3597	CTD	06:08	118	
		66°14,5'S/03°29,3'E	3539	BO	08:12	036	
		66°14,1'S/03°29,2'E	3523	SED	08:28	003	
		66°14,1'S/03°29,2'E	3520	AN	08:36	010	
		65°34,2'S/02°46,8'E	2705	-	12:52	140	Profilfahrt

Stat. No.18/	Date	Position	Echo depth (m)	Gear	Start (GMT)	Haul dur. (min)	Comment and Geological Station No.
224	18/03/91	65°07,7'S/02°41,5'E	1245	CTD	15:25	053	2069-1
		65°08,1'S/02°41,4'E	1246	SED	15:53	002	
		65°08,2'S/02°41,5'E	1247	AN	16:10	008	
		65°08,2'S/02°41,6'E	1245	BO	16:23	039	
		65°08,4'S/02°42,0'E	1240	GKG	17:05	035	2069-2, umgekippt
		65°08,7'S/02°41,8'E	1231	GKG	17:49	039	2069-3
		65°08,9'S/02°41,8'E	1217	KOL	18:59	051	2069-4
		65°07,1'S/03°36,8'E	2599	KOL	22:28	102	2070-1
225	18/03/91	65°06,4'S/03°36,6'E	2650	-	00:29	029	Frequenztest
		65°06,7'S/03°39,3'E	2639	KOL	01:24	106	2071-1, KOL verloren
226	19/03/91	65°05,5'S/03°35,8'E	2619	-	03:41	859	Profilfahrt
		60°40,0'S/03°57,5'E	5068	CTD	06:05	147	2072-1
227	20/03/91	60°34,2'S/03°57,8'E	5373	GS; ISP	09:35	426	
		60°33,5'S/03°58,0'E	5376	SED	12:45	005	
		60°34,3'S/03°56,2'E	5372	MUC	16:48	110	2072-2
		57°37,6'S/04°03,16'E	4467	AWI	12:30	221	ausgelegt AWI 400
228	21/03/91	57°35,8'S/04°06,5'E	4436	CTD	17:15	147	

Ende der Stationsarbeit.

Stationsliste ANT IX/4

In der Stationsliste sind alle Geräteeinsätze aufgeführt, die auf den jeweiligen Stationen durchgeführt wurden. Die Entnahmepositionen von Planktonproben, die über das schiffseigene Pumpsystem genommen wurden, sowie die Positionen der genommenen Luftproben, sind in der Liste nicht mit aufgeführt (Vgl. Kap. 6.2.1., 6.2.2., 7.1, 7.2). Die mit PL (=Planktonnetz) gekennzeichneten Geräte, stehen für den Einsatz von zwei Planktonnetzen mit 20 und 41mm Maschenweite.

Stations-Nr. Reise 18/	AWIGEO Nr.	Datum	Uhrzeit	geographische		Wasser-	Gerät
				Breite	Länge	tiefe (m)	(Gewinn in m)
229	PS 2073-1	31.3.91	22:11	39°35.40'S	14°33.95'E	4692	MUC, FS-CTD, (0.35)
229	PS 2073-2	31.3.91	23:15	39°35.41'S	14°34.37'E	4691	PL, 100m
229	PS 2073-3	1.4.91	0:30	39°36.33'S	14°33.68'E	4625	SL (12.05)
229	PS 2073-4	1.4.91	1:45	39°35.79'S	14°34.05'E	4693	MN, 1000m
230	PS 2074-1	1.4.91	4:24	39°40.00'S	14°30.70'E	4644	SL, (13.03)
231	PS 2075-1	1.4.91	13:05	40°48.42'S	13°44.26'E	3113	MUC, FS-CTD, (0.00)
231	PS 2075-2	1.4.91	14:15	40°48.44'S	13°44.28'E	3126	PL, 100m
231	PS 2075-3	1.4.91	15:24	40°48.46'S	13°43.51'E	3129	MUC (0.06)
231	PS 2075-4	1.4.91	16:15	40°48.84'S	13°42.97'E	3188	MN, 1000m
232	PS 2076-1	1.4.91	20:14	41°08.12'S	13°28.87'E	2086	MUC, FS-CTD, (0.09)
232	PS 2076-2	1.4.91	20:57	41°08.47'S	13°29.15'E	2091	PL, 100m
232	PS 2076-3	1.4.91	22:13	41°08.94'S	13°28.24'E	2109	KOL (9.93), PC (0.18)
233	PS 2077-1	2.4.91	1:51	41°09.95'S	13°27.74'E	2163	KOL (4.70), verbogen
234	PS 2078-1	2.4.91	4:13	41°12.33'S	13°26.91'E	2254	SL, (2.72)
235	PS 2079-1	2.4.91	8:44	41°24.49'S	13°05.44'E	2995	MUC, FS-CTD (0.00)
235	PS 2079-2	2.4.91	10:32	41°24.26'S	13°06.34'E	3012	SL (8.97)
235	PS 2079-3	2.4.91	11:10	41°24.02'S	13°06.25'E	3045	PL, 100m
235	PS 2079-4	2.4.91	12:18	41°24.19'S	13°06.62'E	3009	GKG (0.00)
236	PS 2080-1	2.4.91	17:20	41°43.02'S	13°02.82'E	5078	MUC, FS-CTD, (0.28)
236	PS 2080-2	2.4.91	18:35	41°42.98'S	13°02.18'E	5082	PL, 100m
237	PS 2081-1	3.4.91	5:31	42°41.53'S	12°11.48'E	4794	MUC, FS-CTD, (0.36)

Stations -Nr. Reise 18/	AWIGEO Nr.	Datum	Uhrzeit	geographische		Wasser- tiefe (m)	Gerät (Gewinn in m)
				Breite	Länge		
237	PS 2081-2	3.4.91	6:30	42°41.58'S	12°11.51'E	4795	PL, 100m
237	PS 2081-3	3.4.91	7:50	42°41.68'S	12°11.29'E	4801	SL (12.36)
237	PS 2081-4	3.4.91	8:45	42°41.68'S	12°11.11'E	4802	MN, 1000m
238	PS 2082-1	3.4.91	16:03	43°13.21'S	11°44.30'E	4610	SL (13.91)
238	PS 2082-2	3.4.91	17:00	43°13.20'S	11°45.01'E	4610	PL, 100m
238	PS 2082-3	3.4.91	18:40	43°13.09'S	11°45.54'E	4661	MUC, FS-CTD, (0.26)
239	PS 2083-1	5.4.91	10:08	46°22.23'S	07°02.17'E	1955	MUC, FS-CTD, (0.12)
239	PS 2083-2	5.4.91	10:45	46°22.26'S	07°02.72'E	1954	MN, 1000m
239	PS 2083-3	5.4.91	12:52	46°21.90'S	07°02.31'E	1936	KOL (10.61)
239	PS 2083-4	5.4.91	13:33	46°21.51'S	07°02.47'E	1927	PL, 100m
241	PS 2084-1	5.4.91	21:56	47°01.37'S	07°57.94'E	1667	KOL (9.94)
241	PS 2084-2	5.4.91	23:40	47°01.47'S	07°57.55'E	1664	MUC, FS-CTD, (0.12)
242	PS 2085-1	6.4.91	6:56	47°44.97'S	07°59.83'E	2982	MUC, FS-CTD, (0.05)
242	PS 2085-2	6.4.91	9:11	47°44.95'S	07°59.98'E	2977	KOL (9.72)
243	PS 2086-1	6.4.91	16:40	48°19.10'S	07°45.43'E	649	KOL (3.87)
243	PS 2086-2	6.4.91	17:00	48°19.15'S	07°45.52'E	648	PL, 100m
243	PS 2086-3	6.4.91	17:44	48°19.16'S	07°45.40'E	649	MUC, FS-CTD, (0.18)
244	PS 2087-1	7.4.91	4:35	49°08.06'S	06°42.36'E	3451	MUC, FS-CTD, (0.30)
244	PS 2087-2	7.4.91	6:54	49°08.04'S	06°42.24'E	3452	KOL (9.78), PC (0.80)
245	PS 2088-1	7.4.91	15:23	50°09.41'S	05°44.52'E	3767	PL, 100m
245	PS 2088-2	7.4.91	15:39	50°09.51'S	05°44.49'E	3769	MN, 1000m
247	PS 2089-1	8.4.91	12:49	53°11.32'S	05°19.81'E	2615	KOL (8.46)
247	PS 2089-2	8.4.91	14:59	53°11.30'S	05°19.82'E	2618	KOL (10.46), PC (0.36)
248	Ps 2090-1	8.4.91	17:35	53°10.70'S	05°07.98'E	2819	KOL (11.90), PC (0.55)
249	PS 2091-1	9.4.91	2:54	53°52.33'S	03°35.89'E	2490	MUC, FS-CTD (0.35)
250	PS 2092-1	9.4.91	5:30	54°00.58'S	03°28.74'E	1897	MUC, FS-CTD (0.25)
251	PS 2093-1	9.4.91	7:02	54°10.30'S	03°22.76'E	1441	MUC, FS-CTD (0.14)
252	PS 2094-1	9.4.91	9:15	54°17.27'S	03°16.06'E	937	MUC, FS-CTD (0.33)
253	PS 2095-1	9.4.91	10:19	54°18.54'S	03°13.94'E	486	MUC, FS-CTD (0.12)
254	PS 2096-1	9.4.91	12:54	54°30.42'S	03°00.96'E	502	MUC, FS-CTD (0.07)
255	PS 2097-1	9.4.91	14:08	54°31.51'S	02°53.94'E	1020	MUC, FS-CTD (0.20)
256	PS 2098-1	9.4.91	15:20	54°32.40'S	02°48.00'E	1500	MUC, FS-CTD (0.20)
257	PS 2099-1	9.4.91	16:51	54°33.60'S	02°40.53'E	2006	MUC, FS-CTD (0.28)
258	PS 2100-1	9.4.91	19:45	54°36.18'S	02°17.88'E	2558	MUC, FS-CTD (0.00)
259	PS 2101-1	10.4.91	13:18	54°17.07'S	03°20.43'W	2525	PL, 100m
259	PS 2101-2	10.4.91	13:35	54°17.11'S	03°20.48'W	2549	MN, 1000m
260	PS 2102-1	11.4.91	1:10	53°04.55'S	04°59.82'W	2388	MUC, FS-CTD (0.25)
260	PS 2102-2	11.4.91	2:33	53°04.38'S	04°59.14'W	2390	SL, (7.29)
261	PS 2103-1	11.4.91	15:03	51°19.75'S	03°19.53'W	2946	SL, (8.30)
261	PS 2103-2	11.4.91	16:42	51°19.82'S	03°19.41'W	2947	MUC, FS-CTD (0.20)
261	PS 2103-3	11.4.91	17:27	51°19.90'S	03°19.48'W	2950	MN, 1000 m
261	PS 2103-4	11.4.91	17:39	51°19.94'S	03°19.40'W	2935	Bio-Rosi, 200 m
262	PS 2104-1	12.4.91	0:15	50°44.55'S	03°12.71'W	2592	MUC, FS-CTD (0.14)
262	PS 2104-2	12.4.91	2:29	50°44.53'S	03°13.73'W	2611	SL, (6.64)
263	PS 2105-1	12.4.91	15:36	48°41.74'S	02°51.00'W	3574	SL, (0.00)
263	PS 2105-2	12.4.91	17:10	48°41.64'S	02°50.85'W	3618	MUC, FS-CTD (0.13)
263	PS 2105-3	12.4.91	17:57	48°41.58'S	02°51.02'W	3611	PL, 100 m
263	PS 2105-4	12.4.91	18:18	48°41.70'S	02°50.91'W	3598	MN, 1000 m
263	PS 2105-5	12.4.91	19:43	48°42.19'S	02°51.01'W	3566	Bio-Rosi, 200 m
264	PS 2106-1	14.4.91	8:13	41°51.24'S	00°05.64'E	912	MUC, FS-CTD (0.09)
264	PS 2106-2	14.4.91	8:40	41°51.24'S	00°05.87'E	911	PL, 100 m
264	PS 2106-3	14.4.91	9:07	41°51.12'S	00°05.94'E	911	SL, (0.00)
265	PS 2107-1	14.4.91	11:09	41°44.99'S	00°08.05'E	1298	MUC, FS-CTD (0.00)

Stations -Nr. Reise 18/	AWIGEO Nr.	Datum	Uhrzeit	geographische		Wasser- tiefe (m)	Gerät (Gewinn in m)
				Breite	Länge		
265	PS 2107-2	14.4.91	11:39	41°44.89'S	00°08.00'E	1300	MN, 1000 m
265	PS 2107-3	14.4.91	12:50	41°44.76'S	00°07.76'E	1298	Bio-Rosi, 200 m
266	PS 2108-1	14.4.91	23:40	39°50.21'S	01°02.03'E	4920	MUC, FS-CTD (0.35)
266	PS 2108-2	15.4.91	0:47	39°50.26'S	01°01.95'E	4923	PL, 100 m
266	PS 2108-3	15.4.91	1:51	39°50.23'S	01°02.09'E	4920	SL, (10.16)
266	PS 2108-4	15.4.91	2:44	39°50.47'S	01°02.09'E	4918	MN, 1000 m
267	PS 2109-1	16.4.91	4:47	34°59.99'S	03°10.01'E	5041	SL, (5.01), verbogen
267	PS 2109-2	16.4.91	5:40	35°00.00'S	03°10.08'E	5037	PL, 100 m
267	PS 2109-3	16.4.91	7:10	34°59.93'S	03°10.09'E	5035	MUC, FS-CTD (0.30)
267	PS 2109-4	16.4.91	8:15	34°59.75'S	03°10.16'E	5033	MN, 500 m
267	PS 2109-5	16.4.91	8:50	34°59.66'S	03°10.02'E	5033	Bio-Rosi, 200
269	PS 2110-1	19.4.91	13:43	20°07.13'S	08°58.21'E	2262	MUC, FS-CTD (0.15)
269	PS 2110-2	19.4.91	14:15	20°07.17'S	08°58.13'E	2256	PL, 100 m
269	PS 2110-3	19.4.91	14:35	20°07.15'S	08°58.11'E	2252	MN, 1000 m

ANHANG 2: CORE DESCRIPTIONS

Kernbeschreibungen: In folgenden Abbildungen sind die an Bord geöffneten Schwerelot- und Kolbenlot-Kerne beschrieben. Für die Beschreibungen wurden die nachfolgend dargestellten Symbole verwendet.

CORE DESCRIPTIONS

Lithology

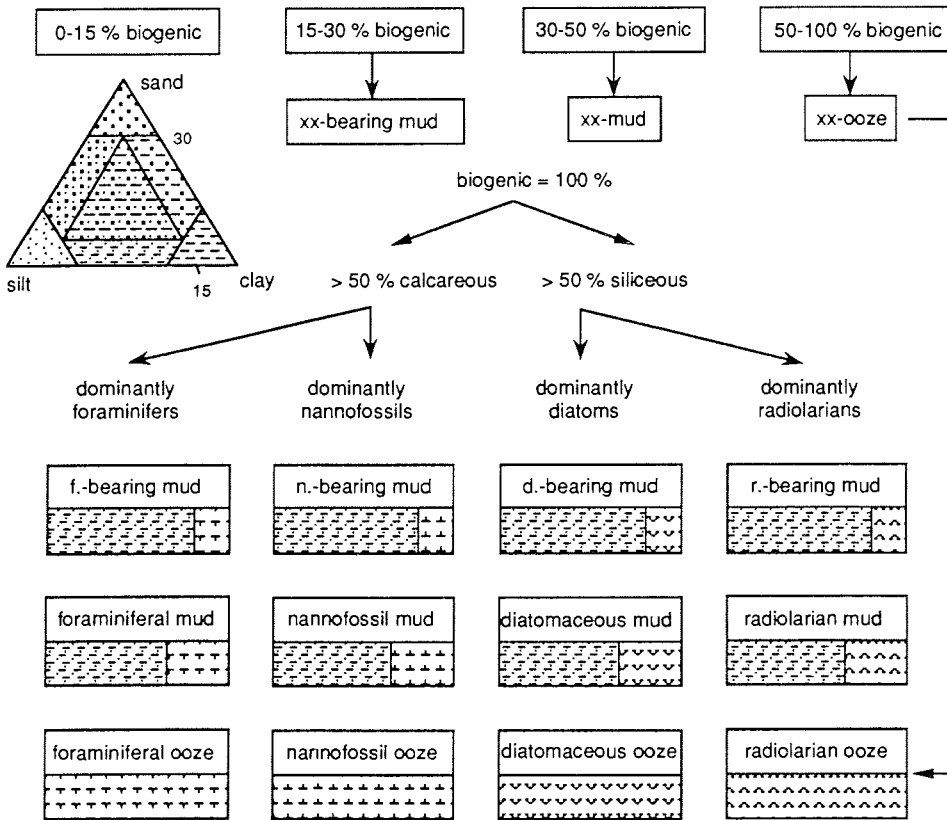
- sand
- sandy silt
- sandy clay
- sandy mud
- silt
- mud
- clay

- foraminiferal ooze
- nannofossil ooze
- diatomaceous ooze
- radiolarian ooze
- volcanic ash
- chert / porcellanite
- pebbles, dropstones
- sediment clasts

Structure

- bioturbation
- stratification
- lamination
- coarsening upward sequence
- fining upwards sequence
- sharp boundary
- gradational boundary
- transition zone

Nomenclature



< 2%: traces ca. 5%: some ca. 10%: minor

PS2003-2 (SL)

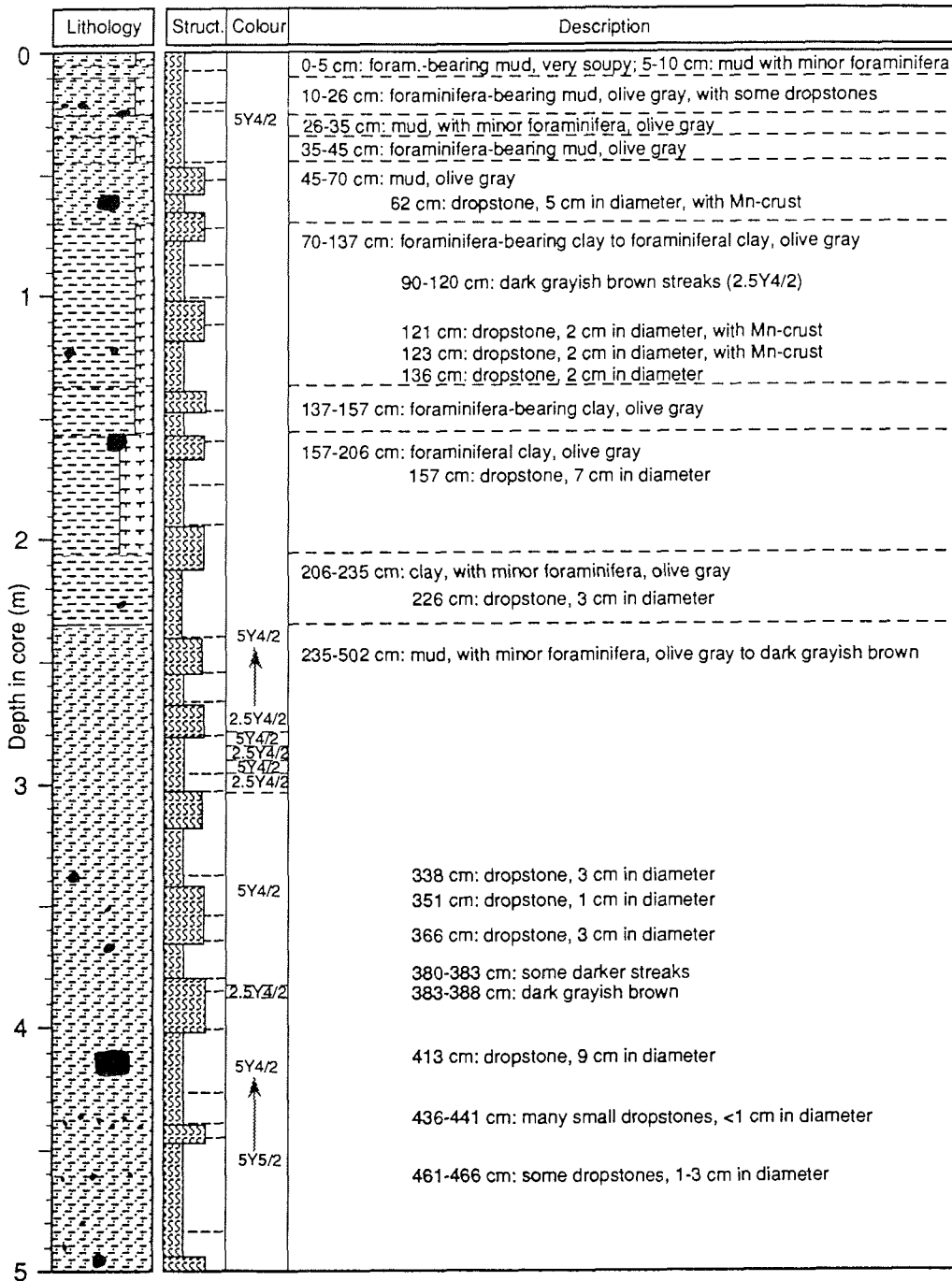
Polarstern Seamount

ANT IX/3

Recovery: 9.20 m

71° 29.1'S, 24° 46.4'W

Water depth: 3718 m



PS2003-2 (SL)

Polarstern Seamount

ANT IX/3

Recovery: 9.20 m

71° 29.1'S, 24° 46.4'W

Water depth: 3718 m

	Lithology	Struct.	Colour	Description
5				502-715 cm: mud, olive gray to grayish brown
				525 cm: 2 dropstones, 1-2 cm in diameter
				545-567 cm: olive gray with brown streaks, some small dropstones
6				599 cm: dropstone, 2cm in diameter
				620-631 cm: some small dropstones, <1 cm in diameter
				657-678 cm: mud, with traces of diatoms and radiolaria, some small dropstones (<2 cm in diameter), grayish brown with brown streaks
				678-715 cm: mud, with some diatoms and radiolaria, olive gray
7				715-755 cm: diatom-bearing mud, with minor radiolaria and some dropstones, grayish brown to olive gray
				755-785 cm: diatomaceous mud, with minor radiolaria, olive gray
8				785-807 cm: diatom-bearing mud, grayish brown
	807-827 cm: mud, with minor diatoms and radiolaria, olive gray			
	815 cm: dropstone, 2 cm in diameter			
	827-894 cm: diatom-bearing mud, with some radiolaria and sponge spicules, grayish brown			
	842 cm: dropstone, 3 cm in diameter			
	891 cm: dropstone, 2 cm in diameter			
9	894-901 cm: diatom-bearing mud, light brownish gray			
	901-920 cm: mud, with minor diatoms, grayish brown			
	920 cm: end of core			
10	smear slides: 0, 35, 53, 81, 114, 135, 149, 188, 215, 235, 293, 300, 335, 363, 386, 435, 472, 520, 558, 583, 620, 699, 720, 745, 776, 776, 820, 840, 870, 897, 920 cm			

PS1990-2 (SL)

Eastern Crary Trough

ANT IX/3

Recovery: 1.19 m

76° 23.2'S, 30° 12.0'W

Water depth: 368 m

Lithology	Description
0	0 cm: silt, with minor sponge spicules and some diatoms, dark gray (5Y4/1)
1	69 cm: silt, with traces of sponge spicules, very dark gray (5Y3/1)
	119 cm: sandy mud, with traces of sponge spicules, very dark gray (5Y3/1)

PS2004-1 (SL)

Polarstern Seamount

ANT IX/3

Recovery: 5.00 m

71° 21.3'S, 24° 46.7'W

Water depth: 3684 m

Lithology	Description
0	7 cm: mud, with minor foraminifera and traces of diatoms and sponge spicules, olive (5Y5/3)
1	100 cm: mud, with minor foraminifera, olive (5Y4/3)
2	200 cm: foraminifera-bearing mud, olive (5Y5/3)
3	300 cm: mud, with traces of foraminifera, olive (5Y5/3)
4	400 cm: mud, olive (5Y5/3)
5	500 cm: mud, olive (5Y5/3)

PS2006-2 (SL)

Polarstern Seamount

ANT IX/3

Recovery: 5.46 m + CC

71° 23.9'S, 24° 16.3'W

Water depth: 4230 m

Lithology	Description
0	0 cm: mud, with some diatoms, some sponge spicules and traces of foraminifera, dark grayish brown (2.5Y4/2)
1	49 cm: mud, dark grayish brown (2.5Y4/2)
2	146 cm: mud, grayish brown (2.5Y5/2)
3	246 cm: mud, grayish brown (2.5Y5/2)
4	346 cm: mud, grayish brown (2.5Y5/2)
5	446 cm: mud, with traces of sponge spicules, grayish brown (2.5Y5/2)
	546 cm: mud, with traces of sponge spicules, grayish brown (2.5Y5/2)

PS2005-1 (SL)

Polarstern Seamount

ANT IX/3

Recovery: 8.98 m + CC

71° 22.8'S, 24° 25.1'W

Water depth: 3806 m

Lithology	Description	
0	0 cm: foraminiferal clay, olive gray (5Y5/2)	occasional pebbles and granules occur throughout, coated in Mn, some "welded" together
1	98 cm: foraminiferal mud, olive gray (5Y5/2)	
2	198 cm: mud, olive gray (5Y5/2)	
3	298 cm: mud, olive gray (5Y5/2); horizon of pebbles coated in Mn	
4	398 cm: mud, olive gray (5Y5/2)	
5	499 cm: mud, with traces of sponge spicules, olive gray (5Y5/2)	
6	598 cm: mud, with traces of sponge spicules, diatoms and radiolaria, olive gray (5Y5/2)	
7	698 cm: mud, with traces of radiolaria and sponge spicules, olive gray (5Y5/2)	
8	798 cm: mud, with some diatoms and traces of radiolaria, silicoflagellates and sponge spicules; olive gray (5Y5/2).	
9	898 cm: diatom-bearing mud, with traces of radiolaria, silicoflagellates and sponge spicules; olive gray (5Y5/2)	

PS2007-1 (SL)

Polarstern Seamount

ANT IX/3

Recovery: 4.73 m

71° 23.4'S, 24° 09.5'W

Water depth: 4217 m

Lithology	Description	
0	0 cm: mud, with some diatoms and traces of radiolaria and sponge spicules, grayish brown (2.5Y5/2)	
1	73 cm: sandy silt, well sorted and with angular grains, contains some diatoms and traces of radiolaria and sponge spicules, dark grayish brown (2.5Y4/2)	
2	173 cm: mud, with traces of sponge spicules, grayish brown (2.5Y5/2)	
3	273 cm: mud, with traces of diatoms, grayish brown (2.5Y5/2)	
4	373 cm: mud, with traces of diatoms, grayish brown (2.5Y5/2)	
4	473 cm: sandy mud, olive (5Y4/3)	

PS2008-1 (SL)

Polarstern Seamount

ANT IX/3

Recovery: 6.72 m + CC

71° 23.3'S, 24° 20.8'W

Water depth: 3927 m

Lithology	Description
0	0 cm: foraminiferal clay, with traces of diatoms, dark grayish brown (2.5Y4/2)
1	73 cm: mud, dark grayish brown (2.5Y4/2)
2	173 cm: mud, grayish brown (2.5Y5/2)
3	272 cm: mud, grayish brown (2.5Y5/2)
4	372 cm: mud, grayish brown (2.5Y5/2)
5	472 cm: mud, grayish brown (2.5Y5/2)
6	572 cm: mud, grayish brown (2.5Y5/2)
	672 cm: mud, with traces of foraminifera, grayish brown (2.5Y5/2)

PS2015-2 (SL)

Lazarev Sea

ANT IX/3

Recovery: 0.37 m + CC

70° 24.2'S, 06° 00.4'W

Water depth: 125 m

Lithology	Description
0	0 cm (GKG): sandy silt, with some diatoms and traces of sponge spicules, black (5Y2.5/1)
	37 cm: sandy mud, with some diatoms, traces of sponge spicules, very dark gray (5Y3/1)

PS2017-3 (SL)

Lazarev Sea

ANT IX/3

Recovery: 0.43 m

70° 21.9'S, 04° 02.3'W

Water depth: 508 m

Lithology	Description
0	10 cm (GKG): sandy mud, with traces of diatoms and sponge spicules
	43 cm: sandy mud, dark gray (5Y4/1)

PS2031-2 (SL)

Lazarev Sea

ANT IX/3

Recovery: 0.58 m

69° 59.4'S, 08° 58.5'E

Water depth: 450 m

Lithology	Description
0	58 cm: sandy mud, with traces of sponge spicules, dark gray (5Y4/1)

PS2020-2 (SL)

Lazarev Sea

ANT IX/3

Recovery: 9.34 m

69° 42.6'S, 00° 56.8'W

Water depth: 2046 m

Lithology	Description
0	0 cm: diatom-bearing sandy silt, with minor foraminifera and sponge spicules and some radiolaria, dark grayish brown (2.5Y4/2)
1	42 cm: diatom-bearing mud, with traces some sponge spicules, dark gray (5Y4/1)
2	142 cm: diatom-bearing mud, with some sponge spicules and traces of foraminifera and radiolaria, dark gray (2.5Y4/0)
3	243 cm: diatom-bearing sandy mud, with some sponge spicules and traces of foraminifera and radiolaria, dark gray (5Y4/1)
4	343 cm: diatom-bearing sandy mud, with traces of foraminifera, radiolaria, and sponge spicules, dark gray (5Y4/1)
5	443 cm: diatom-bearing silt, with traces and foraminifera and radiolaria, dark gray (5Y4/1)
6	533 cm: sandy mud, with minor diatoms and traces of radiolaria and sponge spicules, dark gray (5Y4/1)
7	633 cm: mud, with some diatoms and traces of sponge spicules, dark gray (5Y4/1)
8	733 cm: sandy mud, with some diatoms and traces of sponge spicules, dark gray (5Y4/1)
9	834 cm: sandy silt, with traces of diatoms, foraminifera and sponge spicules, dark gray (5Y4/1)
9	934 cm: sandy silt, with traces of foraminifera, diatoms and sponge spicules, dark gray (5Y4/1)

PS2025-2 (SL)

Lazarev Sea

ANT IX/3

Recovery: 2.24 m

70° 02.6'S, 06° 44.9'E

Water depth: 638 m

Lithology	Description
0	0 cm (GKG): diatom-bearing sandy silt, with minor sponge spicules and traces of radiolaria and foraminifera
1	78 cm: sandy mud, with some diatoms and traces of sponge spicules, dark gray (5Y4/1)
2	170 cm: sandy mud, with traces of sponge spicules, very dark gray (5Y3/1)
2	224 cm: sandy mud, with traces of diatoms and sponge spicules, very dark gray (5Y3/1)

PS2028-2 (SL)

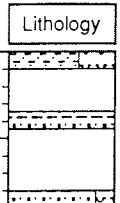
Lazarev Sea

ANT IX/3

Recovery: 1.81 m

70° 00.7'S, 11° 44.9'E

Water depth: 203 m

Lithology	Description
Depth in core (m) 0 	0 cm: diatomaceous mud, with minor sponge spicules, some radiolaria, some foraminifera and traces of bryozoa (large fragments), olive gray (5Y4/2) 81 cm: sandy mud, with minor diatoms and some sponge spicules, very dark gray (5Y3/1) 181 cm: diatom-bearing sandy mud, with some sponge spicules, very dark gray (5Y3/1)

PS2037-3 (SL)

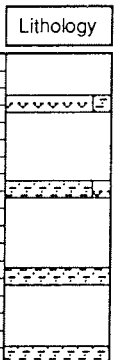
Lazarev Sea

ANT IX/3

Recovery: 3.58 m + CC

69° 42.9'S, 06° 16.3'E

Water depth: 1586 m

Lithology	Description
Depth in core (m) 0 1 2 3 	58 cm: mud-bearing diatom ooze, with minor sponge spicules and traces of radiolaria, dark gray (5Y4/1) 158 cm: diatom-bearing mud, with some sponge spicules and traces of radiolaria, dark gray (5Y4/1) 258 cm: mud, with traces of diatoms and sponge spicules, gray (5Y5/1) 358 cm: mud, with traces of diatoms and sponge spicules, gray (5Y5/1)

PS2042 (SL)

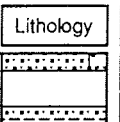
Lazarev Sea

ANT IX/3

Recovery: 0.82 m + CC

70° 05.9'S, 05° 11.9'E

Water depth: 470 m

Lithology	Description
0 	0 cm: diatom-bearing sandy silt, with some sponge spicules and traces of foraminifera and radiolaria, dark gray (5Y4/1) 82 cm: sandy mud, dark gray (5Y4/1)

PS2043-3 (SL)

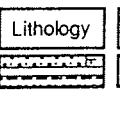
Lazarev Sea

ANT IX/3

Recovery: 0.36 m + CC

69° 47.6'S, 00° 44.4'E

Water depth: 380 m

Lithology	Description
0 	0, 8 cm (GKG): foraminifera-bearing sandy silt, with minor diatoms and some sponge spicules, dark gray (5Y4/1) 36 cm: sandy mud containing gravel, compacted, dark gray (2.5Y4/0)

PS2038-2 (SL)

Lazarev Sea

ANT IX/3

Recovery: 12.69 m

69° 21.2'S, 06° 17.1'E

Water depth: 1603 m

Lithology	Description
0	0 cm: diatomaceous ooze, with some sponge spicules and radiolaria, olive gray (5Y4/2)
1	79 cm: mud, with traces of diatoms and sponge spicules, dark gray (5Y4/1)
2	179 cm: mud, dark gray (5Y4/1)
3	279 cm: foraminifera-bearing sandy silt, with some sponge spicules and traces of diatoms, dark gray (5Y4/1)
4	379 cm: silt, with some diatoms, some sponge spicules and traces of foraminifera, dark gray (5Y4/1)
5	479 cm: diatomaceous mud, with minor sponge spicules and traces of radiolaria, dark gray (5Y4/1)
6	579 cm: mud, with some foraminifera and traces of diatoms and sponge spicules, dark gray (5Y4/1)
7	679 cm: mud, with some foraminifera, some sponge spicules and traces of diatoms, dark gray (5Y4/1)
8	779 cm: mud, with some foraminifera and traces of diatoms and sponge spicules, dark gray (5Y4/1)
9	869 cm: mud, with traces of foraminifera, diatoms and sponge spicules, gray (5Y5/1)
10	969 cm: mud, with some foraminifera, some diatoms and traces of sponge spicules, dark gray (5Y4/1)
11	1069 cm: muddy diatomaceous ooze, with some sponge spicules and traces of radiolaria, dark gray (5Y4/1)
12	1169 cm: foraminifera-bearing mud, with some diatoms and some sponge spicules, dark gray (5Y4/1)
12.69	1269 cm: mud, with some foraminifera, some sponge spicules and traces of diatoms, dark gray (5Y4/1)

PS2039-1 (SL)

Lazarev Sea

ANT IX/3

Recovery: 11.50 m + CC

69° 01.4'S, 06° 13.7'E

Water depth: 2073 m

Lithology	Description
0	0 cm: diatomaceous mud, with minor sponge spicules, some foraminifera and some radiolaria, olive gray (5Y4/2)
1	53 cm: mud, with minor foraminifera and traces of diatoms and sponge spicules, olive gray (5Y4/2)
2	153 cm: foraminifera-bearing mud, with some diatoms, some sponge spicules and traces of radiolaria, dark gray (5Y4/1)
3	253 cm: mud, with some diatoms and traces of sponge spicules, olive gray (5Y4/2)
4	353 cm: mud, with minor foraminifera and traces of diatoms and sponge spicules, gray (5Y5/1)
5	453 cm: diatomaceous mud, with minor foraminifera, some radiolaria and some sponge spicules, gray (5Y5/1)
6	553 cm: diatomaceous mud, with minor sponge spicules, some radiolaria and traces of foraminifera, olive gray (5Y5/2)
7	653 cm: diatomaceous clay, with some radiolaria and traces of sponge spicules, olive gray (5Y5/2)
8	750 cm: mud, with minor diatoms and traces of sponge spicules and radiolaria, olive gray (5Y5/2)
9	850 cm: foraminifera-bearing mud, with some sponge spicules and traces of diatoms, olive gray (5Y5/2)
10	950 cm: foraminifera-bearing mud, with traces of diatoms and sponge spicules, olive gray (5Y5/2)
11	1050 cm: sandy mud, with some foraminifera, some sponge spicules and traces of diatoms, olive gray (5Y5/2)
11	1150 cm: mud, with traces of foraminifera, diatoms and sponge spicules, olive gray (5Y5/2)

PS2040-2 (SL)

Lazarev Sea

ANT IX/3

Recovery: 12.67 m + CC

68° 50.5'S, 06° 14.1'E

Water depth: 2625 m

Lithology	Description
0	0 cm: diatomaceous mud, with minor foraminifera and traces of sponge spicules and radiolaria, olive gray (5Y5/2)
1	83 cm: mud, with traces of sponge spicules and diatoms, olive gray (5Y4/2)
2	182 cm: foraminifera-bearing mud, with traces of diatoms and sponge spicules, olive gray (5Y4/2)
3	281 cm: mud, with some foraminifera and traces of diatoms and sponge spicules, olive gray (5Y4/2)
4	381 cm: clay, with minor foraminifera and traces of diatoms and sponge spicules, dark gray (5Y4/1)
5	481 cm: mud, with minor foraminifera and traces of sponge spicules, dark gray (5Y4/1)
6	581 cm: mud, with traces of foraminifera and sponge spicules, olive gray (5Y4/2)
7	681 cm: muddy foraminiferal ooze, olive gray (5Y4/2)
8	781 cm: foraminifera-bearing mud, with traces of sponge spicules, olive gray (5Y4/2)
9	867 cm: mud, with some foraminifera and traces of sponge spicules, dark gray (5Y4/1)
10	967 cm: foraminiferal clay, with traces of sponge spicules, olive gray (5Y4/2)
11	1067 cm: foraminifera-bearing mud, with traces of sponge spicules, olive gray (5Y5/2)
12	1167 cm: mud, with minor foraminifera, olive gray (5Y5/2)
	1267 cm: mud, with some foraminifera, olive gray (5Y4/2)

PS2064-1 (SL)

Lazarev Sea

ANT IX/3

Recovery: 0.82 m

69° 38.5'S, 00° 03.3'E

Water depth: 1501 m

Lithology	Description
0	0 cm: diatom-bearing sandy silt, with minor sponge spicules and some radiolaria, olive (5Y5/3)
	82 cm: diatom-bearing sandy silt, with some sponge spicules and traces of radiolaria, gray (5Y5/1)

PS2044-1 (SL)

Lazarev Sea

ANT IX/3

Recovery: 4.08 m + CC

69° 46.4'S, 00° 59.9'E

Water depth: 825 m

Lithology	Description
0	0 cm: mud, with traces of foraminifera, diatoms and sponge spicules, dark gray (5Y4/1)
1	68 cm: mud, with traces of foraminifera, diatoms and sponge spicules, olive gray (5Y4/2)
2	168 cm: foraminifera-bearing mud, with traces of diatoms, radiolaria and sponge spicules, dark gray (5Y4/1)
3	208 cm: foraminifera-bearing sandy mud, with traces of diatoms and sponge spicules, olive gray (5Y5/2)
4	308 cm: mud, with some diatoms and traces of foraminifera, radiolaria and sponge spicules, dark gray (5Y4/1)
4	408 cm: mud, with minor foraminifera and traces of diatoms and sponge spicules, dark gray (5Y4/1)

PS2047-3 (SL)

Lazarev Sea

ANT IX/3

Recovery: 3.24 m + CC

69° 29.4'S, 01° 12.7'E

Water depth: 2375 m

Lithology	Description
0	23 cm: foraminiferal mud, with traces of diatoms and sponge spicules, olive gray (5Y4/2)
1	124 cm: mud, with traces of diatoms and sponge spicules, olive gray (5Y4/2)
2	224 cm: mud, with some foraminifera and traces of diatoms and sponge spicules, olive gray (5Y4/2)
3	324 cm: mud, with some foraminifera and traces of diatoms and sponge spicules, olive gray (5Y4/2)

PS2049-4 (SL)

Lazarev Sea

ANT IX/3

Recovery: 2.19 m

69° 05.2'S, 00° 53.4'E

Water depth: 3264 m

Lithology	Description
0	0 cm: foraminifera-bearing mud, with some diatoms and traces of radiolaria and sponge spicules, dark gray (5Y4/1)
1	119 cm: mud, dark gray (5Y4/1)
2	219 cm: foraminiferal silt, dark gray (5Y4/1)

PS2045-3 (SL)

Lazarev Sea

ANT IX/3

Recovery: 10.84 m + CC

69° 41.0'S, 00° 55.6'E

Water depth: 1392 m

Lithology	Description
0	0 cm: diatom-bearing sandy silt, with some radiolaria and some sponge spicules, olive gray (5Y4/2)
1	93 cm: mud, with traces of foraminifera, diatoms and sponge spicules, dark gray (2.5Y4/0)
2	196 cm: foraminifera-bearing sandy mud, with traces of diatoms and sponge spicules, dark gray (5Y4/1)
3	294 cm: mud, with traces of diatoms, radiolaria and sponge spicules, dark gray (5Y4/1)
4	394 cm: mud, with minor diatoms and some sponge spicules, dark gray (5Y4/1)
5	494 cm: mud, with some foraminifera and traces of diatoms and sponge spicules, dark gray (5Y4/1)
6	594 cm: mud, with some foraminifera and traces of diatoms and sponge spicules, dark gray (5Y4/1)
7	685 cm: mud, with minor diatoms and traces of radiolaria and sponge spicules, dark gray (5Y4/1)
8	785 cm: sandy mud-bearing diatomaceous ooze, with minor sponge spicules and traces of radiolaria, dark gray (2.5Y4/0)
9	885 cm: mud, with traces of foraminifera, diatoms, radiolaria and sponge spicules, dark gray (5Y4/1)
10	985 cm: mud, with some foraminifera and some diatoms, traces of radiolaria and sponge spicules, dark gray (5Y4/1)
	1084 cm: mud, with some foraminifera, dark gray (2.5Y4/0)

PS2050-1 (SL)

Lazarev Sea

ANT IX/3

Recovery: 1.80 m + CC

68° 46.1'S, 00° 52.3'E

Water depth: 3903 m

Lithology	Description
0	0 cm: diatom-bearing mud, with traces of radiolaria and sponge spicules, olive gray (5Y4/2)
1	80 cm: foraminifera-bearing silt, with traces of sponge spicules, olive gray (5Y4/2)
	180 cm: sandy mud, olive gray (5Y4/2)

PS2046-1 (SL)

Lazarev Sea

ANT IX/3

Recovery: 7.09 m + CC

69° 37.2'S, 01° 02.6'E

Water depth: 1798 m

Lithology	Description
0	19 cm: clay, with minor diatoms and traces of sponge spicules, dark gray (5Y4/1)
1	119 cm: clay, with traces of foraminifera, diatoms, radiolaria and sponge spicules, dark gray (5Y4/1)
2	219 cm: mud, with some foraminifera and traces of diatoms, radiolaria and sponge spicules, dark gray (5Y4/1)
3	309 cm: clay, with traces of foraminifera, diatoms and sponge spicules, dark gray (5Y4/1)
4	409 cm: foraminifera-bearing mud, with traces of diatoms and sponge spicules, olive gray (5Y4/2)
5	509 cm: diatomaceous sandy mud, with some sponge spicules and traces of foraminifera and radiolaria, dark gray (5Y4/1)
6	609 cm: sandy mud, with some sponge spicules and traces of diatoms, dark gray (5Y4/1)
7	709 cm: mud, with traces of foraminifera, diatoms and sponge spicules, dark gray (5Y4/1)

PS2056-1 (SL)

Lazarev Sea

ANT IX/3

Recovery: 4.74 m + CC

68° 44.6'S, 06° 08.1'E

Water depth: 3060 m

Lithology	Description
0	0 cm: diatom-bearing foraminiferal ooze, with some radiolaria and some sponge spicules, olive gray (5Y5/2)
1	77 cm: foraminifera-bearing mud, with traces of diatoms and sponge spicules, olive gray (5Y5/2)
2	176 cm: diatom-bearing mud, with minor foraminifera and traces of radiolaria and sponge spicules, gray (5Y5/1)
3	276 cm: foraminiferal mud, with some diatoms and traces of radiolaria and sponge spicules, grayish brown (2.5Y5/2)
4	376 cm: diatomaceous mud, with traces of radiolaria and sponge spicules, olive (5Y5/3)
4	474 cm: diatomaceous ooze, with some radiolaria and traces of sponge spicules, gray (5Y6/1)

PS2055-2 (SL)

Lazarev Sea

ANT IX/3

Recovery: 10.79 m + CC

68° 17.4'S, 06° 14.9'E

Water depth: 3606 m

Lithology	Description
0	0 cm: diatomaceous silt, with some foraminifera and traces of radiolaria and sponge spicules, grayish brown (2.5Y5/2)
1	92 cm: mud, with minor diatoms and traces of foraminifera and sponge spicules, olive gray (5Y5/2)
2	192 cm: foraminifera-bearing mud, with some diatoms and traces of sponge spicules, olive gray (5Y4/2)
3	292 cm: diatom-bearing mud, with some radiolaria and traces of sponge spicules, olive gray (5Y5/2)
4	392 cm: diatomaceous mud, with some radiolaria and traces of sponge spicules, olive gray (5Y5/2)
5	491 cm: diatom-bearing mud, with traces of radiolaria and sponge spicules, olive gray (5Y5/2)
6	591 cm: mud, with traces of sponge spicules, olive gray (5Y5/2)
7	677 cm: diatom-bearing mud, with traces of radiolaria and sponge spicules, olive gray (5Y5/2)
8	777 cm: foraminifera-bearing diatomaceous mud, with traces of radiolaria and sponge spicules, olive gray (5Y5/2)
9	877 cm: diatomaceous mud, with minor sponge spicules and traces of radiolaria, olive gray (5Y5/2)
10	977 cm: foraminifera-bearing diatomaceous mud, with some radiolaria and traces of sponge spicules, olive gray (5Y5/2)
	1079 cm: sandy mud, with some diatoms and traces of radiolaria and sponge spicules, olive gray (5Y5/2)

PS2066-2 (SL)

Lazarev Sea

ANT IX/3

Recovery: 2.00 m + CC

70° 23.6'S, 05° 00.4'W

Water depth: 430 m

Lithology	Description
0	0 cm (GKG): diatom-bearing sandy silt, with some radiolaria and some sponge spicules, olive gray (5Y5/2)
1	100 cm: sandy mud, with some diatoms and traces of sponge spicules, dark gray (5Y4/1)
2	200 cm: sandy mud, with some diatoms and traces of sponge spicules, dark gray (5Y4/1)

PS2062-3 (SL)

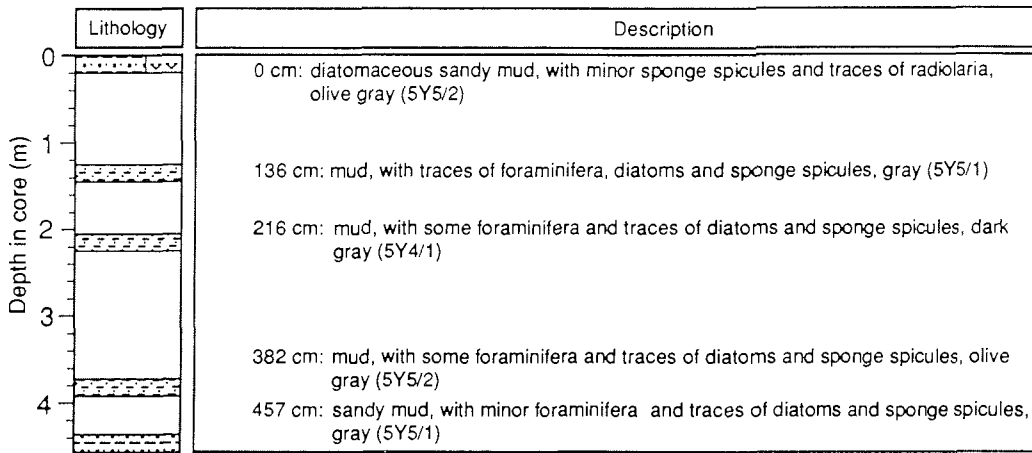
Lazarev Sea

ANT IX/3

Recovery: 4.57 m

69° 47.2'S, 01° 26.7'E

Water depth: 1602 m



PS2070-1 (KOL)

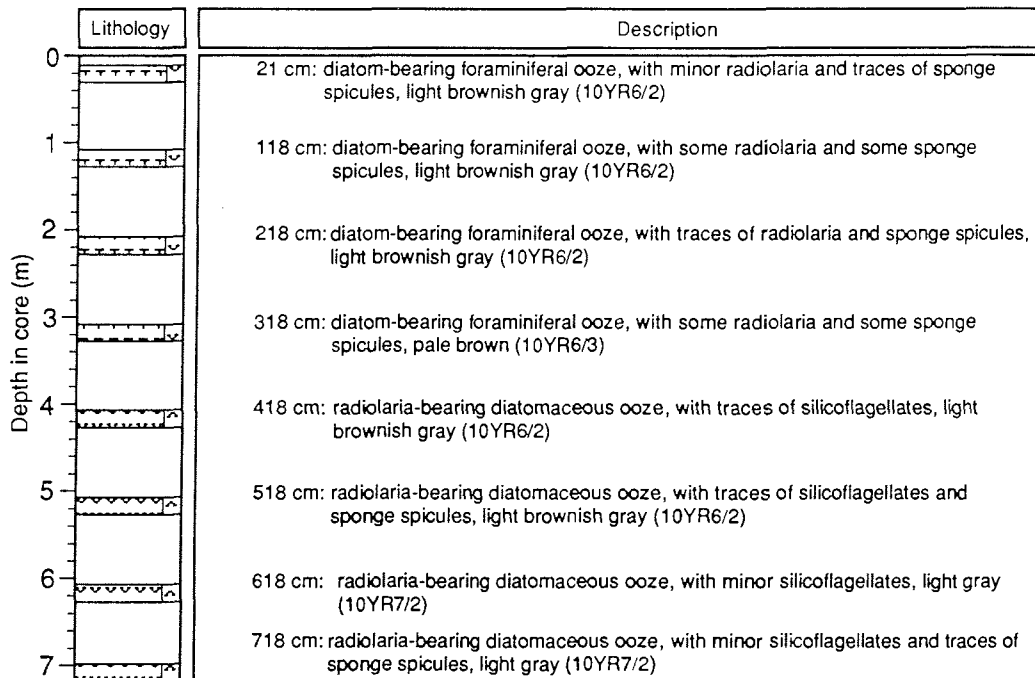
Maud Rise

ANT IX/3

Recovery: 7.18 m

65° 06.3'S, 03° 37.0'E

Water depth: 2611 m



PS2070-1 (KOL)

Maud Rise

ANT-IX/3

Recovery: 7.18 m

65° 06.3'S, 03° 37.0'E

Water depth: 2611 m

Depth in core (m)	Lithology	Struct.	Color	Description	Age
0				0-85 cm: foraminiferal ooze, diatom-bearing, pale brown, 22-26 cm: scattered small-sized dropstones 60-80 cm: burrows, light gray (10YR 7/2)	A. denticulata Quaternary
1			10YR 6/3	85-324 cm: foraminiferal ooze, diatom-bearing, light gray (85-170/175 cm), light gray and white (170/175-324 cm) 110-118 cm: distinct burrows at 196 cm: scattered dropstones 254 cm: dropstone with Mn-crust, ca. 1 cm in diameter	
2			10YR 8/2 10YR 7/2		S. universus Quaternary
3			10YR 6/3	324-365 cm: diatomaceous mud, foraminifera-bearing, pale brown with very pale brown (10YR 7/2) vertical burrow traces	E. calv. - S. circularis
4			10YR 7/3	365-446 cm: diatomaceous ooze, very pale brown	H. vema Pliocene
5			10YR 8/1 10YR 8/2	446-490 cm: diatomaceous ooze, white (<i>Ethmodiscus rex</i> -Layer), sharp contact at the base	
			10YR 8/1 10YR 8/2	471-474 cm: porcellanite, pale brown (10YR 6/3) and brown (10YR 5/3), broken in several pieces	
				490-520 cm: diatomaceous ooze, white (10YR 8/2) and light gray (10YR 7/2)	

PS2070-1 (KOL)

Maud Rise

ANT-IX/3

Recovery: 7.18 m

65° 06.3'S, 03° 37.0'E

Water depth: 2611 m

Depth in core (m)	Lithology	Struct.	Color	Description	Age
	5			10YR 8/2 10YR 7/2 10YR 6/3 10YR 8/2 10YR 7/2 10YR 8/2 10YR 6/2 10YR 6/3 10YR 7/3 10YR 8/2	520-545 cm: diatomaceous mud, pale brown, sharp contact at the base 545-595 cm: diatomaceous ooze, white, with distinct light gray vertical burrows 595-621 cm: diatomaceous ooze, light gray (595-609 cm), white (609-621 cm) 621-640 cm: diatomaceous mud, light brownish gray and pale brown, 632-645 cm: vertical burrow traces very pale brown 640-718 cm: diatomaceous ooze, very pale brown (640-664 cm), white (664-718 cm)
6					
7					

PS2074-1 (SL)

Cape Abyssal Plain

ANT-IX/4

Recovery: 13.03 m

39° 40.0'S, 14° 30.7'E

Water depth: 4644 m

Depth in core (m)	Lithology	Struct.	Color	Description	Age
0	[Lithology pattern]		10YR 7/3	0-2 cm: mud, grayish brown	
			2.5 Y 6/2	2-33 cm: calcareous mud, very pale brown (2-20 cm), light brownish gray (20-31 cm)	
1	[Lithology pattern]		2.5 Y 6/2	33-38 cm: mud, light brownish gray and light yellowish brown indurated layer	
			2.5 Y 7/2	38-53 cm: calcareous mud, light gray	
2	[Lithology pattern]		5Y 6/2	53-70 cm: mud, light olive gray	
			5Y 7/2	70-99 cm: calcareous mud, light gray	
3	[Lithology pattern]		2.5 Y 7/2	99-106 cm: mud, light gray and light brownish gray	
			2.5 Y 8/2	106-120 cm: calcareous mud, white	
4	[Lithology pattern]		2.5 Y 6/2	120-160 cm: mud, light brownish gray, 148-153 cm: indurated sediment, light brownish gray (2.5Y 6/2) and light yellowish brown (2.5Y 6/4)	
			2.5 Y 7/2	160-170 cm: calcareous mud, light gray, sharp contact at the top and the base	
5	[Lithology pattern]		2.5 Y 7/2	170-180 cm: mud, light gray and light brownish gray	
			2.5 Y 8/2	180-196 cm: calcareous mud, light gray	
6	[Lithology pattern]		5Y 6/2	196-207 cm: mud, light olive gray, sharp contact at the base	
			5Y 7/2	207-250 cm: calcareous mud, light gray, 215-216 cm and 225-228 cm: intercalated with pale olive	
7	[Lithology pattern]		5Y 6/2	250-255 cm: mud, light olive gray, sharp contacts at the base and the top	
			5Y 7/2	255-293 cm: calcareous mud, light gray (255-276 cm), gray (276-293 cm), 276 cm: sharp redox boundary (pyritized burrows occur throughout from 280 cm to the base of the core, 280-281 cm: gray (5Y 5/1) color lamination	
8	[Lithology pattern]		5Y 6/1	293-320 cm: mud, gray	
			5Y 7/1	320-360 cm: calcareous mud, light gray (320/325-340 cm), gray (340-360 cm), 346-360 cm: gray (5Y 6/1) color laminae	
9	[Lithology pattern]		5Y 6/1	360-408 cm: mud, gray mottled with dark gray (5Y 3/1) burrow traces	
			5Y 6/2	408-417 cm: calcareous mud, light olive gray with sharp contact at the base	
10	[Lithology pattern]		5Y 5/1	417-466 cm: mud, gray with very dark gray (5Y 3/1) burrows	
			5Y 6/1	466-473 cm: calcareous mud, light gray with distinct down core burrows and a sharp contact at the base	
11	[Lithology pattern]		5Y 5/1	473-509 cm: mud, gray with very dark gray (5Y 3/1) burrows	

NN 21
 A. denticulata
 Quaternary
 NN19-NN21

PS2074-1 (SL)

Cape Abyssal Plain

ANT-IX/4

Recovery: 13.03 m

39° 40.0'S, 14° 30.7'E

Water depth: 4644 m

Lithology	Struct.	Color	Description	Age		
5		5Y 5/1	509-515 cm: calcareous mud, light olive gray with a sharp contact at the base and lamination (Turbidite)	NN 19 ? <i>A. denticulata</i>		
		5Y 6/2				
		5Y 6/1	515-530 cm: mud, gray (5Y 5/1 = 515-518 cm; 5Y 6/1 = 518-525 cm), olive gray (525-530 cm)			
		5Y 5/2				
		5Y 6/1	530-546 cm: calcareous mud, light gray and gray (530-535 cm), gray (535-346 cm)			
		5Y 5/1				
		5Y 7/1	546-557 cm: mud, gray			
		5Y 6/1	557-585 cm: calcareous mud, light gray			
		5Y 6/1	572-575 cm: intercalated with mud, gray (5Y 6/1)			
		5Y 5/1	585 cm: 0.5 cm foraminiferal ooze layer			
	6		5Y 5/1		585-720 cm: mud, gray	NN 19 ? <i>A. denticulata</i>
			2.5Y 5/1			
			5Y 5/1		720-730 cm: calcareous mud, light olive gray, laminated with a sharp contact at the base (turbidite)	
		5Y 6/1				
		5Y 6/2	730-840 cm: mud, 730-740 cm: gray and light olive gray (5Y 6/2) color lamination 740-787/797 cm: light olive gray and gray 789/797-840 cm: gray, mottled with dark gray mostly at the base			
		5Y 6/1				
		5Y 6/2	840-878 cm: mud, gray and olive gray (840-860 cm), gray, mottled with dark gray (860-878 cm)			
		5Y 5/2				
		5Y 6/1	878-881 cm: foraminiferal ooze, light gray (5Y 7/1), laminated (turbidite)			
		5Y 6/0				
7		5Y 5/1	881-883 cm: mud, gray (5Y 6/1)	NN 19 <i>S. univertus</i>		
		5Y 6/1				
		5Y 6/1	883-886 cm: calcareous mud, light gray (5Y 7/1)			
		5Y 7/1				
		5Y 5/1	886-936 cm: mud, light gray			
		5Y 6/1				
		5Y 6/1	936-986 cm: mud, light gray and gray 940-941 cm: mottled with very dark gray (5Y 3/1)			
		5Y 5/1				
8		5Y 6/1	986-996 cm: mud, light gray and gray 940-941 cm: mottled with very dark gray (5Y 3/1)	NN 19 <i>S. circularis/E. calvertense</i>		
		5Y 6/2				
9		5Y 6/1	996-1000 cm: mud, light gray and gray 940-941 cm: mottled with very dark gray (5Y 3/1)	Quaternary		
		5Y 6/2				
10		5Y 6/1	1000-1003 cm: mud, light gray and gray 940-941 cm: mottled with very dark gray (5Y 3/1)	Quaternary		
		5Y 6/2				

PS2074-1 (SL)

Cape Abyssal Plain

ANT-IX/4

Recovery: 13.03 m

39° 40.0'S, 14° 30.7'E

Water depth: 4644 m

Depth in core (m)	Lithology	Struct.	Color	Description	Age
10	[Lithology pattern]		5Y 5/1 5Y 5/2	986-1073 cm: mud, gray and light olive gray (986-1040/1045 cm), gray and olive gray mottled with dark gray (1040/1045-1073 cm)	NN 19
			5Y 6/1 5Y 6/2	1073-1076 cm: calcareous mud, light gray, laminated with sharp contact at the base, partly graded bedding (turbidite)	
11	[Lithology pattern]		5Y 5/1	1076-1117 cm: mud, gray, partly mottled with dark gray	NN 19 ?
			5Y 6/1	1117-1127 cm: calcareous mud, gray,	
	[Lithology pattern]		5Y 5/1	1127-1177 cm: mud, gray and olive gray (5Y 5/2; 1127-1161 cm) light gray and gray (1161-1169 cm), light gray (1169-1177 cm)	S. circularis/E. calvertense Quaternary
			5Y 7/1+6/1 5Y 7/1		
12	[Lithology pattern]		5Y 6/2	1177-1252 cm: mud, light olive gray (1177-1203 cm), olive gray with dark gray (5Y 4/1) and light olive gray (5Y 6/2) color lamination (1203-1214), gray mottled with very dark gray (1214-1252 cm)	NN 19 ?
			5Y 5/2		
	[Lithology pattern]		5Y 6/1		NN 19 ?
			5Y 7/1 5Y 6/1	1252-1303 cm: mud, light gray and gray with very dark gray laminae (1252-1283 cm), olive gray (1283-1303 cm)	
13	[Lithology pattern]		5Y 5/2		

PS2076-3 (KOL)

Agulhas Ridge

ANT-IX/4

Recovery: 9.93 m

41° 08.9'S, 13° 28.2'E

Water depth: 2109 m

Depth in core (m)	Lithology	Struct.	Color	Description	Age
0			10YR 8/2 10YR 7/2	0-18 cm: foraminiferal mud, white and light gray	
1			10YR 8/2	18-194 cm: foraminiferal mud, white, homogeneous	NN21
2			10YR 8/1	194-242 cm: foraminiferal ooze, white	NN20 - NN21 <i>A. denticulata</i> Quaternary
			10YR 7/1 10YR 8/1	242-260cm: foraminiferal mud, light gray (242-250 cm), white (250-260 cm)	
			2.5Y 8/0	260-301 cm: nannofossil ooze, white	
3			10YR 8/1 10YR 7/1	301-342 cm: foraminiferal ooze, white and light gray (301-309 cm), white (309-342 cm) 336 cm: gray color lamination	NN19
			2.5Y 7/2	342-365 cm: foraminiferal mud, light gray	
			10YR 8/1 10YR 7/1	365-427 cm: foraminiferal ooze, white and light gray 427 cm: small dropstone 3 mm in diameter	
4			2.5Y 7/2 10YR 8/1 10YR 7/1	427-444 cm: foraminiferal mud, light gray (427-434 cm) with several light brownish gray (2.5Y 6/2) burrows, white and light gray (434-444 cm)	
			10YR 8/1	444-478 cm: foraminiferal ooze, white 460-480 cm: scattered sand grains	
5			2.5Y 7/2 10YR 8/1	478-490 cm: foraminiferal mud, light gray	

PS2076-3 (KOL)

Agulhas Ridge

ANT-IX/4

Recovery: 9.93 m

41° 08.9'S, 13° 28.2'E

Water depth: 2109 m

Depth in core (m)	Lithology	Struct.	Color	Description	Age
5		10YR 8/1		490-507 cm: foraminiferal ooze, white	A. denticulata
		2.5 Y 7/2		507-524 cm: foraminiferal mud, light gray	
6		10YR 8/1		524-560 cm: foraminiferal ooze, white	
		2.5 Y 7/2		560-594 cm: foraminiferal mud, light gray	
		2.5 Y 7/2		570-574 cm: light gray (2.5Y 7/2) and white (2.5Y 8/2)	
				582 cm: dropstone 0.5 cm in diameter	
7		10YR 8/1		594-637 cm: foraminiferal ooze, white	
		2.5 Y 7/2		637-645 cm: foraminiferal mud, light gray, with scattered dropstones	
		10YR 8/1		645-670 cm: foraminiferal ooze, white	
		2.5 Y 7/2		670-687 cm: foraminiferal mud, light gray, scattered sand grains	
		10YR 8/1		687-716 cm: foraminiferal ooze, light gray (687-689 cm), white (689-716 cm)	
		10YR 7/1 10YR 7/2		716-746 cm: foraminiferal mud, light gray	
8		2.5 Y 7/2		746-771 cm: foraminiferal ooze, white	S. universus
		10YR 8/1		771-779 cm: foraminiferal mud, light gray, 778-779 cm: color laminae, light gray (5Y 7/1)	
		10YR 8/1		779-817 cm: foraminiferal ooze, white 817 cm: very dark gray (5Y 3/1) burrow	
		5Y 8/1 5Y 7/1		817-842 cm: foraminiferal mud, white and light gray	
		10YR 8/1		842-890 cm: foraminiferal ooze, white	
		2.5 Y 7/2		890-897 cm: foraminiferal mud, light gray	
9		10YR 8/1		897-993 cm: foraminiferal ooze, white	NN 19
				913-916 cm: foraminiferal mud, light gray	
				924-935 cm: scattered dropstones	
10					Quaternary

PS2082-1 (SL)

Agulhas Basin

ANT-IX/4

Recovery: 13.91 m

43° 13.2'S, 11° 44.3'E

Water depth: 4610 m

Lithology	Struct.	Color	Description	Age
		10YR 8/3	0-6 cm: foraminifera-bearing mud, pale brown, 0-4 cm: disturbed sediment	<i>T. lentiginosa</i> <i>A. denticulata</i> Quaternary
		10YR 6/3	6-19 cm: foraminifera ooze, very pale brown	
		10YR 4/4	19-33 cm: foraminifera-bearing mud, pale brown contacts are strongly bioturbated	
		10YR 6/3	33-38 cm: Fe/Mn-rich mud, dark yellowish brown (33-36 cm)	
		2.5Y 5/2	37-38 cm: white (10YR 8/2) burrow	
		5Y 5/2	38-50 cm: foram-bearing mud, pale brown 50-56 cm: diatomaceous mud, light brownish gray at 56 cm: redox-boundary	
			56-237 cm: diatomaceous mud, olive gray dark gray (5Y 4/1) burrow traces occur throughout	
		5Y 6/1	237-270 cm: diatomaceous mud, gray 253-258 cm: olive gray (5Y 5/2) burrows	
		5Y 7/1	270-284 cm: nannofossil mud, light gray	
		5Y 6/1	284-328 cm: diatomaceous mud, gray with olive gray (5Y 5/2) and gray (5Y 5/1) burrow traces 305-306 cm: dark gray (5Y 4/1) color banding	
		5Y 7/1	328-362 cm: diatomaceous mud, light gray with gray (2.5Y 6/0; 2.5Y 5/0) burrow traces	
		5Y 5/1	362-412 cm: diatomaceous mud, gray with partly olive gray (5Y 5/2) burrows	
		5Y 6/1	412-452 cm: diatomaceous mud, gray (412-443 cm) with black (5Y 2.5/1) and olive gray (5Y 5/2) burrows, light gray (443-452 cm)	
		5Y 7/1 5Y 8/1	452-463 cm: nannofossil mud, white	
		5Y 7/1	463-512 cm: diatomaceous mud, light gray, between 564-486 cm: partly nannofossil mud, white (5Y 8/1) large burrow traces	

PS2082-1 (SL)

Agulhas Basin

ANT-IX/4

Recovery: 13.91 m

43° 13.2'S, 11° 44.3'E

Water depth: 4610 m

Lithology	Struct.	Color	Description	Age	
		5Y 7/1	512-545 cm: diatomaceous mud, gray (5Y 6/1) and light olive gray (5Y 6/2; 512-527 cm), light gray (5Y 7/1) and gray (5Y 6/1; 527-545 cm)	<p><i>T. lentiginosa</i></p> <p><i>H. karstenii</i></p> <p><i>A. denticulata</i></p> <p>Quaternary</p>	
		5Y 6/1			
		5Y 6/2			
		5Y 7/1	545-576 cm: nannofossil mud, light gray and white (545-562 cm), very pale brown (10YR 8/3), 563-665 cm: very pale brown (10YR 7/3) burrows 575-576 cm: grayish brown (10YR 5/2) burrows		
		5Y 6/1			
		10YR 7/2			
			10YR 8/2		576-599 cm: diatomaceous mud, light gray (576-579 cm), white and light gray (579-586 cm), light gray (586-599 cm) 185-186 cm: gray (7.5YR 6/0) color lamination
			10YR 8/3		
			10YR 7/2		
			5Y 7/1		599-800 cm: diatomaceous mud, gray with numerous light olive gray (5Y 6/2) and dark gray burrows, several haloburrows
		5Y 6/1			
		5Y 6/1			
		5Y 5/1	800-903 cm: diatomaceous mud, gray, with scattered dark gray burrow traces 860-690 cm: haloburrows		
		5Y 6/1			
		5Y 6/1	903-937 cm: diatomaceous mud, gray		
		5Y 5/1			
		5Y 6/1	937-951 cm: foraminifera and nannofossil-bearing, diatomaceous mud, light gray, bioturbated contact at the base		
		5Y 7/1			
		5Y 6/1	951-1009 cm: diatomaceous mud, gray 957-961 cm: gray (2.5Y 5/0) color laminae 677-678 cm: gray (2.5Y 5/0) burrows		
		2.5Y 5/0			
		5Y 6/1			

PS2082-1 (SL)

Agulhas Basin

ANT-IX/4

Recovery: 13.91 m

43° 13.2'S, 11° 44.3'E

Water depth: 4610 m

Depth in core (m)	Lithology	Struct.	Color	Description	Age	
10		5Y 6/1 2.5Y 5/0		1009-1027 cm: nannofossil mud, white with light gray burrows (1009-1017 cm), white and light gray with gray (2.5Y 5/0) burrows (1017-1027 cm) contact at the base is strongly bioturbated	T. lentiginosa A. denticulata Quaternary	
		5Y 8/1 5Y 7/1				
		5Y 6/1 5Y 6/1 5Y 5/1				
		5Y 6/1 5Y 6/2				1027-1140 cm: diatomaceous mud, gray and light olive gray, partly very dark gray (5Y 6/1) and light brownish gray (2.5Y 6/2), scattered haloburrows 1043 cm: light gray gray (5Y 7/2) burrow of nannofossil mud
		5Y 6/1				
11		7.5YR 3/3		1140-1226 cm: diatomaceous mud, gray 1176-1179 cm: gray and dark gray 1176 cm: very dark gray (7.5YR 3/3) burrow		
12		5Y 8/1 2.5YR 4/0		1226-1233 cm: nannofossil mud, white with gray burrows from sediment above,		
		5Y 5/2		1233-1260 cm: diatomaceous mud, light gray and gray (1233-1240 cm), olive gray (1240-1260 cm)		
		5Y 6/2 5Y 5/2		1260-1391 cm: diatomaceous mud, light olive gray and gray (1260-1300 cm), gray (1300-1391 cm) 1300-1368 cm: scattered dark gray burrow traces 1379 cm: very dark gray (5Y 3/1) haloburrow		
13		5Y 5/1				
14	5Y 6/1					

PS2083-3 (KOL)

Meteor Rise

ANT-IX/4

Recovery: 10.61 m

46° 21.9'S, 7° 02.3'E

Water depth: 1936 m

Lithology	Struct.	Color	Description	Age
	10YR 8/2		0-5 cm: foraminiferal mud, diatom-bearing, white	Quaternary <i>T. lentiginosa</i> <i>S. universus</i> <i>A. denticulata</i> <i>H. karstenii</i>
	10YR 8/1		5-24 cm: foraminiferal ooze, diatom-bearing, white	
	10YR 7/2		24-44 cm: foraminiferal mud, diatom-bearing; 24-30 cm: white (10YR 7/2) and sandy	
	10YR 8/2		30-44 cm: white (10YR 8/2); scattered clasts (>2 mm) occur between 19-44 cm	
	10YR 8/1		44-76 cm: foraminiferal ooze, diatom-bearing, white (44-54/57cm:10YR 8/1; 54/57-76 cm: 10YR 8/2)	
	10YR 8/2		76-102 cm: foraminiferal mud, diatom-bearing, mottled white (2.5Y8/2) very pale brown (10YR 7/3) and light gray (5Y 7/2)	
	2.5Y 8/2		102-111 cm: foraminiferal ooze, diatom-bearing, white	
	10YR 7/3		111-123 cm: foraminiferal mud, diatom-bearing, white, partly sandy	
	10YR 7/3		123-162 cm: foraminiferal mud, diatom-bearing, very pale brown (118/123-131 cm), white (131-136 cm), light gray (136-150/152) and white (5Y 8/1) light gray (5Y8/1) mottled, partly sandy between 146-150 cm and 158-162 cm; some foraminiferal ooze below 152 cm;	
	5Y 7/1		125 cm: mud clast, ca. 0.5 cm in diameter	
	5Y 8/1		162-225 cm: nannofossil ooze with minor foraminifera, white (118/123-131 cm), white (131-136 cm) in diameter of sandy foraminiferal mud, light gray (10Y 8/1)	
	5Y 7/1		225-238 cm: foraminiferal mud, diatom-bearing, light gray	
	5Y 8/1		238-245 cm: foraminiferal sandy mud, diatom-bearing, gray, fining upward sequence	
	10YR 8/1		143 cm: dropstone, 0.5 cm in diameter	
	10YR 8/3		245-351 cm: foraminiferal ooze, diatom-bearing, white (245-250), very pale brown (250-266 cm), light gray mottled with minor very pale brown (266-280 cm), pale olive (280-290 cm), light gray (290-311 cm), pale olive (311-351 cm),	
5Y 7/2		311-318 cm: foraminiferal mud, partly sandy,		
5Y 6/3		316 cm: dropstone, ca. 0.5 cm in diameter		
5Y 7/3		351-372 cm: foraminiferal mud, diatom-bearing, pale brown		
5Y 8/1		372-388 cm: foraminiferal ooze, diatom-bearing, white		
5Y 7/1		388-408 cm: foraminiferal mud, light gray		
5Y 6/3		408-417 cm: foraminiferal mud, diatom-bearing, pale olive some scattered sand grains between 412-424 cm		
5Y 7/3		417-487 cm: foraminiferal ooze, diatom-bearing, pale yellow partly mottled with light olive gray (5Y 6/2; 417-464 cm), light yellowish brown (464-468 cm), light gray (468-475 cm) and white mottled with light gray (2.5Y7/2)		
2.5Y 7/2				
2.5Y 7/2				
2.5Y 8/2				
10YR 8/1				

PS2083-3 (KOL)

Meteor Rise

ANT-IX/4

Recovery: 10.61 m

46° 21.9'S, 7° 02.3'E

Water depth: 1936 m

Depth in core (m)	Lithology	Struct.	Color	Description	Age
	10			2.5 Y 7/2 5Y 7/2 10YR 8/1	998-1010 cm: diatomaceous mud, foraminifera-bearing, light gray 1010-1028 cm: foraminiferal mud, diatom-bearing, light gray, partly sandy 1028-1046 cm: diatomaceous ooze, foraminifera-bearing, white mottled with light gray 1046-1061 cm: foraminiferal ooze, diatom-bearing, white and light gray (2.5Y 7/2) mottled
11					

PS2084-1 (KOL)

Meteor Rise

ANT-IX/4

Recovery: 9.94 m

47° 01.4'S, 07° 57.9'E

Water depth: 1667 m

Lithology	Struct.	Color	Description	Age
	10YR 8/1 10YR 7/1		0-28 cm: foraminiferal ooze, diatom-bearing, white and light gray	<p><i>T. lentiginosa</i></p> <p><i>A. denticulata</i></p> <p><i>S. universus</i></p> <p><i>A. ingens</i></p> <p>Quaternary</p>
	10YR 7/2		28-44 cm: foraminiferal mud, diatom-bearing, light gray, 37-41 cm: scattered small-sized dropstones	
	10YR 8/2		44-76 cm: foraminiferal ooze, diatom-bearing, white, 73-76 cm: scattered small-sized dropstones	
	10YR 7/3 10YR 7/2		76-99 cm: foraminiferal mud, diatom-bearing, very pale brown, (76-91 cm), light gray (91-99 cm)	
	10YR 8/1 2.5Y 6/2		99-118 cm: foraminiferal ooze, diatom-bearing, white 118-131 cm: foraminiferal mud, diatom-bearing, light brownish gray,	
	10YR 8/1 10YR 8/2		120-131 cm: scattered small sized dropstones 131 cm: dropstone, ca. 1 cm in diameter	
	10YR 7/1		131-169 cm: foraminiferal ooze, diatom-bearing, white (131-144/148 cm), light gray (144/148-169 cm) 151-169 cm: scattered small-sized dropstones	
	10YR 8/1		169-236 cm: nannofossil ooze, white 185-205 cm: large vertical burrow 218-225 cm: displaced sediment (flow in)	
	5Y 6/1		236-245 cm: foraminiferal sandy mud, diatom-bearing, gray (fining upward sequence) 242 cm: dropstone, ca. 1 cm in diameter	
	10YR 8/1 10YR 8/2		245-279 cm: foraminiferal ooze, diatom-bearing, white, some scattered small-sized dropstones	
	10YR 8/2 10YR 7/2		279-311 cm: foraminiferal mud, diatom-bearing, light gray and white	
	10YR 8/1 10YR 7/1		311-334 cm: foraminiferal ooze, diatom-bearing, white and light gray, 327-336 cm: scattered sand grains	
	5Y 6/3		334-406 cm: foraminiferal mud, diatom-bearing, pale olive 336-350 cm: scattered small-sized dropstones	
	5Y 7/1 5Y 7/2		406-422 cm: foraminiferal ooze, diatom-bearing, light gray	
	5Y 7/2 5Y 8/1 5Y 7/1		422-432 cm: foraminiferal mud, diatom-bearing, light gray 432-469 cm: foraminiferal ooze, diatom-bearing, white and light gray (432-444 cm), white (444-469 cm)	
	5Y 8/1 5Y 6/3 5Y 7/3		469-493 cm: foraminiferal mud, diatom-bearing, pale olive (469-476 cm) with some scattered sand grains, pale yellow (476-493 cm)	
	5Y 8/1+8/2		493-499 cm: foraminiferal ooze, diatom-bearing, white	

PS2084-1 (KOL)

Meteor Rise

ANT-IX/4

Recovery: 9.94 m

47° 01.4'S, 07° 57.9'E

Water depth: 1667 m

Depth in core (m)	Lithology	Struct.	Color	Description	Age
5			5Y 8/1+8/2	499-513 cm: foraminiferal ooze, diatom-bearing, white	A. ingens S. univertus Quaternary
			5Y 6/3	513-524 cm: foraminiferal mud, diatom-bearing, pale olive	
			5Y 7/2	524-545 cm: diatomaceous mud, foraminifera-bearing, light gray (524-529 cm), pale yellow (529-545 cm)	
			5Y 7/3	545-582 cm: foraminiferal ooze, diatom-bearing, light gray (545-554 cm), white and light gray (554-578 cm), white (578-582 cm)	
			10YR 8/1 10YR 7/1	579 cm: light gray (5Y 7/2) burrow	
			5Y 7/1	582-595 cm: foraminiferal sandy mud, light gray (582-590/595 cm), pale olive, (590/595-595)	
			5Y 6/1 5Y 7/3	595-606 cm: foraminiferal mud, diatom-bearing, pale olive, 598 cm: dropstone, ca. 1 cm in diameter	
			5Y 8/1+8/2		
			5Y 7/3	606-668 cm: diatomaceous mud, foraminifera-bearing, white (606-615 cm), pale yellow (615-636 cm), white (636-668cm)	
			5Y 8/1 5Y 8/2	668-700 cm: foraminiferal ooze, diatom-bearing, white (668-690), light gray (690-700 cm) with small scattered dropstones	
6			5Y 7/1+7/2	700-710 cm: foraminiferal mud, diatom-bearing, olive	A. ingens S. univertus Quaternary
			5Y 5/3	710-727 cm: foraminiferal sandy mud, pale olive	
			5Y 6/3	727-770 cm: foraminiferal ooze, diatom-bearing, white 745-746 cm: scattered small-sized dropstones	
			5Y 8/1	770-816 cm: foraminiferal mud, diatom-bearing, light gray (770-795 cm), white (795-809 cm), pale yellow (809-816 cm)	
7			5Y 8/1	816-880 cm: diatomaceous mud, foraminifera-bearing, white and light gray (816-856 cm), pale yellow (856-872 cm), pale olive (872-880 cm) 877-880 cm: scattered small-sized dropstones	A. ingens S. univertus Quaternary
			5Y 8/1 5Y 7/1		
			5Y 7/3		
			5Y 6/3		
			5Y 8/1 5Y 7/1		
			5Y 7/3		
8			5Y 8/1 5Y 7/1	880-925 cm: foraminiferal ooze, diatom-bearing, white and light gray (880-889 cm), white (889-920/930 cm)	S. circularis Quaternary
			5Y 7/3		
			5Y 6/3	925-994 cm: foraminiferal mud, diatom-bearing, pale yellow (920/930-948 cm), pale olive (948-960 cm), light gray (960-980 cm), pale yellow (980-994 cm)	
			5Y 7/2		
9			5Y 7/3		S. circularis Quaternary
			5Y 6/3		
10			5Y 7/2		S. circularis Quaternary
			5Y 7/3		

PS2086-1 (KOL)

South of Meteor Rise

ANT IX/4

Recovery: 3.87 m

48° 10.0'S, 07° 45.4'E

Water depth: 649 m

Lithology	Struct.	Color	Description	Age
		5Y 6/2	0-9 cm: foraminiferal ooze, light olive gray, gravel-bearing: 4-9 cm (high amount of dropstones)	<p><i>T. lentiginosa</i></p> <p><i>S. universus - A. denticulata</i></p> <p><i>A. ingens</i></p> <p>Quaternary</p>
		5Y 7/3	9-42 cm: foraminiferal ooze, pale yellow, 12 cm: dropstone, ca. 2 cm in diameter 20 cm: gneissic dropstone, ca. 2 cm in diameter	
		5Y 6/2	42-52 cm: foraminiferal ooze, light olive gray, with scattered small-sized dropstones	
		2.5Y 7/3	52-104 cm: foraminiferal ooze, pale yellow 74 cm: dropstone, ca. 0.5 cm in diameter	
		5Y 6/2	104-123 cm: foraminiferal ooze, light olive gray, with scattered small-sized dropstones 120 cm: gabbroid dropstone, 6 cm in diameter	
		2.5Y 7/3	123-175 cm: foraminiferal ooze, pale yellow, 153 cm: dropstone, 0.5 cm in diameter	
		5Y 6/3	175-243 cm: foraminiferal ooze, pale olive 223-226 cm: scattered small-sized dropstones	
		5Y 7/3	243-253 cm: foraminiferal ooze, pale yellow	
		5Y 6/3	253-287 cm: foraminiferal ooze, pale olive	
		5Y 7/3	287-300 cm: foraminiferal ooze, pale yellow	
		5Y 6/3	300-313 cm: foraminiferal ooze, pale olive 307-313 cm: scattered small-sized dropstones	
		2.5Y 8/2	313-343 cm: foraminiferal ooze, white	
		5Y 7/3	343-376 cm: foraminiferal ooze, pale yellow, scattered small-sized dropstones	
		5Y 7/2	376-387 cm: foraminiferal ooze, light gray	
			the core shows various stages of core deformation below 130 cm Core catcher (deformed) contains pieces of basaltic rocks	

PS2089-2 (KOL)

Southwest Indian Ridge

ANT-IX/4

Recovery: 10.46 m

53° 11.3'S, 05° 19.8'E

Water depth: 2618 m

Lithology	Struct.	Colour	Description	Age
			0-55 cm: diatomaceous sandy mud, light brownish gray, 10-13 cm: gravel-bearing 18-19 cm: light gray (2.5Y 7/2) burrows 53 cm: dropstone, ca. 0.5 cm in diameter	<i>T. lentiginosa</i> <i>A. denticulata</i> Quaternary
		2.5Y 6/2		
			55-108 cm: diatomaceous sandy mud, grayish brown, 84-86 cm: diatomaceous mud layer, light gray (2.5Y 7/2) and light brownish gray (2.5Y 6/2)	
		2.5Y 5/2		
			108-200 cm: diatomaceous sandy mud ligh brownish gray, very dark gray (2.5Y 3/0), sandy burrow traces between 130-131, 133-140, 138-140 cm and 155-158, 170-175 cm,	
		2.5Y 6/2		
			200-246 cm: diatomaceous sandy mud, light gray (2.5Y 7/2) and light brownish gray (2.5Y 6/2)	
		2.5Y 7/2 2.5Y 6/2		
			246-263 cm: diatomaceous mud, light gray (2.5Y 7/2) and light brownish gray (2.5Y 6/2), with scattered dropstones 257 cm: large burrow, very dark gray (2.5Y 3/0)	
		2.5Y 7/2 2.5Y 6/2		
		263-320 cm: diatomaceous sandy mud, light gray (2.5Y 7/2) and light brownish gray (2.5Y 6/2) between 263-297 cm, grayish brown (297-320 cm)		
	2.5Y 5/2			
		320-378 cm: diatomaceous ooze, white (2.5Y 8/2) and pale yellow (2.5Y 8/3), burrow from sediment above occurs at the top		
	2.5Y 8/2			
		378-397 cm: diatomaceous ooze, white (2.5Y 8/2) and light gray (2.5Y 7/2)		
	2.5Y 8/2 2.5Y 7/2			
		397-440 cm: diatomaceous ooze, white (2.5Y 8/2) and pale yellow (2.5Y 8/3)		
	2.5Y 8/2			
		440-521 cm: diatomaceous ooze, very pale brown (440-503 cm), white (503-521 cm), 502-503 cm: light gray (2.5 Y 7/2) burrows		
	10YR 8/2			

PS2089-2 (KOL)

Southwest Indian Ridge

ANT-IX/4

Recovery: 10.46 m

53° 11.3'S, 05° 19.8'E

Water depth: 2618 m

Depth in core (m)	Lithology	Struct.	Colour	Description	Age		
5			2.5Y 8/2	521-560 cm: diatomaceous ooze, 521-540 cm: white (2.5Y 8/2) and light gray (2.5Y 7/2), 540-550 cm: gray, 550-560 cm: white (2.5Y 8/2) and light gray (2.5Y 7/2) mottled with pure light gray (2.5Y 7/2)	Quaternary		
			2.5Y 8/2	560-585 cm: diatomaceous sandy mud, light brownish gray and very dark gray (2.5Y 3/0; 560-566 cm) 566-567 cm: very dark gray (2.5Y 3/0) sand layer, gravel-bearing 567-585 cm: light gray			
			2.5Y 7/2				
			2.5Y 7/2				
			10YR 8/2				
			10YR 7/2				
			2.5Y 8/2				
			2.5Y 7/2				
			2.5Y 8/4				
			2.5Y 8/2				
2.5Y 8/4	585-602 cm: diatomaceous ooze, pale yellow (2.5Y 7/2) and light gray with light gray burrows						
6			2.5Y 8/2	602-607 cm: Porcellanite, broken in numerous pieces	Quaternary		
			2.5Y 8/4	607-628 cm: diatomaceous ooze, white (2.5Y 8/2) and pale yellow (2.5Y 8/4) 628-649 cm: diatomaceous mud, light olive gray (5Y 6/2) intercalated with dark gray (5Y 4/1; 628-635 cm), pale olive (635-649 cm) 649-673 cm: diatomaceous sandy mud, olive gray (649-660 cm), gray (660-673 cm) 673-687 cm: diatomaceous sandy mud, gravel-bearing (673-677 cm), dark gray 687-712 cm: diatomaceous sandy mud, gray (5Y 5/1; 677-686/688 cm; 5Y 6/1: 686/688-712 cm) 712-714 cm: diatomaceous sandy mud, gravel-bearing, dark gray 714-736 cm: diatomaceous sandy mud, gray 736-750 cm: diatomaceous ooze, light gray 750-772 cm: diatomaceous sandy mud, gray			
			5Y 6/2				
			5Y 4/1				
			5Y 6/3				
			5Y 5/2				
			5Y 5/1				
			5Y 4/1				
			5Y 5/1				
			5Y 6/1				
5Y 4/1							
7			5Y 5/1	712-714 cm: diatomaceous sandy mud, gravel-bearing, dark gray	Quaternary		
			5Y 7/1	714-736 cm: diatomaceous sandy mud, gray 736-750 cm: diatomaceous ooze, light gray 750-772 cm: diatomaceous sandy mud, gray			
			2.5Y 8/2				
			2.5Y 8/4				
			2.5Y 8/2			772-895 cm: diatomaceous ooze, white (2.5Y 8/2) and light gray (2.5Y 8/2) strongly mottled (772-847 cm), pale olive (847-895 cm)	
			2.5Y 7/2				
			2.5Y 7/4				
			5Y 6/3				
			5Y 5/1				895-924 cm: diatomaceous sandy mud, gray, 903 cm: dropstone ca. 0.5 cm in diameter 924-945 cm: diatomaceous mud, gray 945-960 cm: diatomaceous sandy mud, gray with dark gray (2.5Y 3/0), burrow (947 cm) 960-962 cm: sand (volcanic ash), black (5Y 2.5/1), with large volcanic clast >2 cm
			5Y 6/1				
5Y 5/1							
5Y 5/1							
8			5Y 5/1	962-1046 cm: diatomaceous sandy mud, gray volcanic clasts at 1015 cm, 1028-1029 cm, core catcher: 1038-1046 cm	Quaternary		
			5Y 5/1	962-1046 cm: diatomaceous sandy mud, gray volcanic clasts at 1015 cm, 1028-1029 cm, core catcher: 1038-1046 cm			
			5Y 5/1				
			5Y 5/1				
			5Y 5/1				
			5Y 5/1				
			5Y 5/1				
			5Y 5/1				
			5Y 5/1				
			5Y 5/1				
5Y 5/1							

A. denticulata
T. lentiginosa
A. ingens
S. universus

PS2102-2 (SL)

Western Mid-Atlantic Ridge

ANT-IX/4

Recovery: 7.29 m

53° 04.4'S, 04° 59.7'W

Water depth: 2390 m

Lithology	Struct.	Color	Description	Age
		10YR 7/3 10YR 6/3 2.5Y 5/2	0-14 cm: diatomaceous ooze, very pale brown and pale brown (0-10 cm), grayish brown and light olive brown (2.5Y 5/4; 10-14 cm)	
		10YR 8/2 10YR 7/2	14-304 cm: diatomaceous ooze, white and light gray, partly mottled with pale yellow (5Y 7/3), light gray (2.5Y 7/2), light brownish gray (2.5Y 6/2) scattered small dropstones: 45-50 cm, 133-138 cm, 212-214 cm	
		2.5Y 6/2 10YR 8/2	304-324 cm: diatomaceous ooze, light brownish gray (304-318 cm), white (318-324 cm) 304-308 cm: scattered small dropstones	
		5Y 4/1	324-377 cm: diatomaceous mud, dark gray (324-335 cm), olive gray (335-377 cm)	
		5Y 5/2	377-384 cm: diatomaceous sandy mud, gray	
		5Y 5/1		
		5Y 6/1 5Y 5/1	384-455 cm: diatomaceous mud, gray, 436-437 cm: mottled with dark redish gray (10YR 4/1)	
		5Y 5/1 5Y 7/1		
		10YR 8/2 10YR 7/2	455-509 cm: diatomaceous mud, light gray (455-475/460 cm), white and light gray (475/460-509 cm), 491 cm: large burrow of sandy mud, black (5Y2.5/1)	
				<i>T. lentiginosa</i> <i>A. denticulata</i> Quaternary

PS2102-2 (SL)

Western Mid-Atlantic Ridge

ANT-IX/4

Recovery: 7.29 m

53° 04.4'S, 04° 59.7'W

Water depth: 2390 m

Depth in core (m)	Lithology	Struct.	Color	Description	Age	
	5				509-555 cm: diatomaceous ooze, pale olive (509-516 cm), white and light gray (516-533 cm), pale olive mottled with light olive gray (5Y 6/2) and white (10YR 8/2; 533-555 cm)	
				555-582 cm: diatomaceous ooze, light gray and very pale brown		
				582-618 cm: diatomaceous ooze, very pale brown (582-587 cm), white and light gray (587-594 cm), very pale brown (594-600 cm), pale yellow mottled with pale olive (5Y 7/3; 600-618 cm)		
6				618-633 cm: diatomaceous mud, dark gray	<i>T. lentiginosa</i> <i>A. denticulata</i> Quaternary	
				633-653 cm: diatomaceous sandy mud, dark gray with very dark gray (5Y 3/1) burrow traces		
				653-707 cm: diatomaceous mud, dark gray (653-682 cm), olive gray (682-707 cm)		
				707-712 cm: diatomaceous sandy mud, olive gray		
7				712-729 cm: diatomaceous mud, olive gray		

ANHANG 3: INSTITUTIONS**Participating Institutions**Argentina

ITBA Instituto Tecnológico de Buenos Aires
Avda Enardo Madero 351/99
1106 Buenos Aires

Belgium

VUB Vrije Universiteit Brussels
Laboratory for Analytical Chemistry
Pleinlaan 2
B-1050 Brussels

Brazil

CBM Centro de Biologia Marinha/UFPR
Av. Beira Mar,
Ponta do Sul
Paranagua 83200 Pr

Federal Republic of Germany

AWI Alfred-Wegener-Institut für
Polar- und Meeresforschung
Columbusstraße
2850 Bremerhaven

DWD Deutscher Wetterdienst
Seewetteramt
Bernhard-Nocht-Str. 76
2000 Hamburg 4

FBB Universität Bremen
Fachbereich Biologie FB2
Postfach 33 04 40
2800 Bremen 33

FGB Universität Bremen
Fachbereich Geowissenschaften FB5
Postfach 33 04 40
2800 Bremen 33

FiW Forschungsstelle für Wirbeltierforschung
Alfred-Kowalke-Str. 17
O-1136 Berlin

- FPB Universität Bremen
Fachbereich Physik FB1
Postfach 33 04 40
2800 Bremen 33
- HSW Helicopter-Service
Wasserthal GmbH
Kätnerweg 43
2000 Hamburg 65
- IfMG Johann Wolfgang Goethe-Universität
Institut für Meteorologie und Geophysik
Feldbergstr. 47
Postfach 11 19 32
6000 Frankfurt am Main 11
- IfMW Institut für Meereskunde
Akademie der Wissenschaften der DDR
Seestr. 15
O-2530 Rostock-Warnemünde
- IFUG Fraunhofer-Institut für
Atmosphärische Umweltforschung
Kreuzeckbahnstr. 19
8100 Garmisch-Partenkirchen
- IPÖ Universität Kiel
Institut für Polarökologie
Physikzentrum
Olshausenstraße 40-60
D-2300 Kiel 1
- KAE Krupp Atlas Elektronik GmbH
Seebaldsbrücker-Heerstr. 235
2800 Bremen
- RUB Ruhr-Universität Bochum
Fakultät für Chemie / Physikalische Chemie I
Postfach 10 21 48
4630 Bochum 1
- TA TERRAQUA
Indersdorfer Str. 16
8061 Arnbach
- UH Universität Heidelberg
Institut für Umweltphysik
Im Neuenheimer Feld 366
6900 Heidelberg

- ULP Universität Leipzig
Institut für Geophysik, Geologie
und Meteorologie
Talstr. 35
O-7010 Leipzig
- UR Universität Rostock
Informationstechnik
Albert-Einstein-Strasse 2
O-2500 Rostock
- UU Universität Ulm
Analytische Chemie
Postfach 40 66
7900 Ulm
- ZfM Zentrum für rohstofforientierte Meeresforschung
Universität Clausthal
Adolph-Roemer-Str. 2A
3392 Clausthal-Zellerfeld

France

- IEM Institut d'Etudes Marines
Université de Bretagne Occidentale
6 Avenue le Gorgeu
F-29287 Brest Cedex

Great Britain

- SPRI Scott Polar Research Institute
Cambridge

Netherlands

- RUU Rijksuniversiteit te Utrecht
Faculteit der natuur- en sterrenkunde
Princetonplein 5
NL-3508 TA Utrecht
- VUA Vrije Universiteit Amsterdam
Instituut voor Aardwetenschappen
Boelelaan 1085
NL 1081 HV Amsterdam

Switzerland

- AF Ariane Film AG
Postfach 835
CH-8025 Zürich

United States of America

OSU Oregon State University
 College of Oceanography
 Oceanography Admin. Bld. 104
 Corvallis, Oregon 97331-5503

Union of Socialistic Soviet Republics

AARI Arctic and Antarctic Research Institute
 38 Bering St.
 199226 Leningrad

ANHANG 4: SHIP'S CREW

<u>Dienstgrad</u>	<u>ANT IX/1</u>	<u>ANT IX/2</u>	<u>ANT IX/3</u>	<u>ANT IX/4</u>
Kapitän	Jonas	Jonas	Greve	Jonas
1. Offizier	Gerber	Gerber	Götting	Gerber
Naut. Offizier	Schwarze	Bürger	Bürger	Rodewald
1. Offz. Ladung	-	Fahje	Schwarze	-
Naut. Offizier	Varding	Rodewald	Varding	Schwarze
Arzt	Dr. Kohlberg	Dr. Kohlberg	Dr. Lademann	Dr. Lademann
Ltd. Ingenieur	Schulz	Schulz	Müller	Schulz
1. Ingenieur	Delff	Delff	Knoop	Delff
2. Ingenieur	Simon	Simon	Erreth	Simon
2. Ingenieur	Neugebauer	Neugebauer	E. Schuster	Neugebauer
Elektriker	Erdmann	Erdmann	G. Schuster	Erdmann
Elektroniker	Muhle	Humm	Husmann	Elvers
Elektroniker	Humm	Elvers	Hoops	Muhle
Elektroniker	Muttersbach	Muttersbach	Piskorzynski	Humm
Elektroniker	Elvers	Kampen	Pabst	Kampen
Funkoffizier	Müller	Müller	Geiger	Müller
Funkoffizier	Butz	Butz	Wanger	Butz
Koch	Klasen	Klasen	Kubicka	Köwing
Kochsmaat	Roggartz	Roggartz	Dutsch	Roggartz
Kochsmaat	Kästner	Kästner	Ströhlein	Kästner
1. Steward	Peschke	Peschke	Scheel	Peschke
Stewardess/Nurse	Teichmann	Teichmann	Lieboner	Teichmann
Stewardess	Hoppe	Hoppe	Hopp	Gorgas
Stewardess	Gorgas	Gorgas	Klemet	Hoppe
Stewardess	Gollmann	Gollmann	-	Meier
2. Steward	Mui	Mui	Lee	Lee
2. Steward	Lee	Lee	Yu	Yu
Wäscher	Yang	Chang	Chang	Chang
Bootsmann	Schwarz	Schwarz	Hopp	Schwarz
Zimmermann	Kassubeck	Kassubeck	Marowsky	Kassubeck
Matrose	Novo Loveira	Novo Loveira	Gil Iglesias	Novo Loveira
Matrose	Suarez Paisal	Reitz	Soage Curra	Meis Torres
Matrose	Prol Otero	Prol Otero	Abreu Dios	Pereira Portela
Matrose	Pereira Portela	Pereira Portela	Pousada Maratinez	Prol Otero
Matrose	Garcia Martinez	Reitz	Figueira Lemai	Carcia Martinez
Matrose	-	Carcia Martinez	Iglesias Bermudez	
Matrose	-	Papendorf	Winkler	
Matrose	Meis Torres	Meis Torres	Papendorf	Suarez Paisal
Lagerhalter	Barth	Barth	Schierl	Barth
Masch-Wart	Heurich	Heurich	Carstens	Buchas
Masch-Wart	Jordan	Jordan	Wittfoth	Heurich
Masch-Wart	Buchas	Buchas	Husung	Reimann
Masch-Wart	Reimann	Reimann	Dufner	Fritz
Masch-Wart	Fritz	Fritz	Reitz	Jordan

ANHANG 5: PARTICIPANTS**Fahrtteilnehmer / Participants:****ANT IX/1**

Bacher, Reiner	UU
Hamann, Hendrik	AWI
Helmers, Eckard,	AWI
Herber, A	AWI
Knappertsbusch, Michael	VUA
Köhler, Herbert	DWD
Kreher, Karin	UH
Langer, Eckhard	IFUG
Luxenhofer, Oliver	UU
Modersitzki, Jutta	AWI
Niewold, Muriel,	VUA
Oertel, Thomas	AWI
Papenbrock, Thomas,	RUB
Schäfer, Bettina	IFMG
Schreitmüller, Jörn	UU
Schulz-Baldes, Meinhard	AWI
Schwarz, Werner	KAE
Slemr, Franz,	IFUG
Staubes, Regina	IFMG

ANT IX/2

Baumann, Marcus	AWI
Behmann, Thomas	AWI
Bluszcz, Thaddäus	AWI
Brandini, Frederico	AWI
Brosin, Hans-Jürgen	IFMW
Buxhoeveden, Cristina Isabel	ITBA
Corradi, Pio Ante	AF
Dehn, Joachim	AWI
Dittrich, Birgit	AWI
Erdmann, Hilger	DWD
Fahrbach, Eberhard	AWI
Goeyens, Leo	VUB
Goldkamp, Ulrich	AWI
Harder, Markus	FPB
Heitmüller, Karl-Heinz	HSW
Hillebrandt, Oliver	HSW
Hinrichsen, Hans-Harald	FPB
Knoche, Martin	AWI
Köhler, Herbert	DWD
Krest, Jim	OSU
Kurbjeweit, Frank	AWI
Lengacher, Dieter	AF
Leynaert, Aude	IEM
Lindenmaier, Patrick	AF
Lindner, Louis	RUU
Markus, Thorsten	AWI
Monk, Jürgen	AWI
Papenbrock, Thomas	RUB
Pauls, Margarete	AWI
Pfeiffenberger-Pertl, Hans	AWI
Plugge, Rainer	AWI
Quéguiner, Bernard	IEM
Ragueneau, Olivier	IEM
Rauschert, Martin	FiW to K.G.I
Riewesell, Christian	HSW
Ross, Andy	OSU

Schäfer, Hartmut	FPB
Schlumpf, Hans-Ulrich	AF
Schmidt, Martin	IfMW
Schoch, Roland	FPB
Schöffmann, Erhard	FGB
Schrems, Otto	AWI
Schütt, Ekkehard	FPB
Segl, Monika	FGB
Simon, Bernd	FiW to K.G.I
Sonnabend, Hartmut	DWD
Staubes, Regina	IfMG
Sterr, Uta	FPB
Stiller, Michael	AWI to K.G.I
Strass, Volker	AWI
Tins, Wolfgang	TA
Vucelic, Sonja	AWI
Wasserthal, Claus	HSW
Weber, Michael	AWI
Wisotzki, Andreas	FPB
Zippel, Detlev	FiW from K.G.I

K.G.I. = King George Island

ANT IX/3

Arntz, Wolf	AWI
Bathmann, Ulrich	AWI
Beyer, Kerstin	AWI
Bönisch, Gerhard	AWI
Dreyer, Johannes	AWI
Ehrmann, Werner	AWI
Fahl, Kirsten	AWI
Gerdes, Dieter	AWI
Gerland, Sebastian	AWI
Gingele, Franz	AWI
Gleitz, Markus	AWI
Gorny, Matthias	AWI
Gradinger, Rolf	AWI
Griffith, Sabina	AWI
Großmann, Sönke	AWI
Gutt, Julian	AWI
Hain, Stefan	AWI
Hambrey, Michael	SPRI
Huasen, Manfred	HSW
Hinze, Heinrich	AWI
Höltzen, Heike	AWI
Janssen, H.-H.	AWI
Kringel, Robert	AWI
Kuhn, Gerhard	AWI
Kurbjeweit, Frank	AWI
Lahrmann, Uwe	HSW
Lochte, Karin	AWI
Lukin, Valery	AARI
Lundström, Volker	HSW
Maus, Bertram	AWI
Melles, Martin	AWI
Michel, Andreas	AWI
Munsch, Iris	AWI
Ochsenhirt, Wolf-Thilo	DWD
Pois, Hans-Arnold	DWD
Provorkin, Andrey	AARI
Rau, Ingo	AWI
Riemann, Franz	AWI
Rutgers v.d. Loeff, Michel	AWI

Schantz, Anja	AWI
Scharek, Renate	AWI
Schmiedl, Gerhard	AWI
Schrank, Wolfgang	HSW
Schröder, Michael	AWI
Schröder, Sabine	AWI
Smetacek, Victor	AWI
Steinmetz, Richard	AWI
Weissenberger, Jürgen	AWI
Wisotzki, Andreas	AWI
Witte, Hannelore	AWI
Wöhrmann, Andreas	IPÖ
Zimmermann, Christopher	IPÖ

ANT IX/4

Abelmann, A.	AWI
Bohrmann, G.	AWI
Gorny, M.	AWI
Hubberten, H.-W., Fahrleiter	AWI
Klindworth, C.	AWI
Knappertsbusch, M.	VUA
Köhler, H.	DWD
Krüger, T.	AWI
Kuhn, Th.	ZfM
Lensch, N.	AWI
Lorentzen-Schmidt, H.	AWI
Mackensen, A.	AWI
Niederjasper, F.	AWI
Oertel, Th.	AWI
Petschick, R.	AWI
Rehfeld, M.	UR
Röd, E.	DWD
Ruhland, G.	FGB
Schöne, T.	AWI
Schacht, M.	AWI
Schreitmüller, J.	UU
Vonhof, H.	VUA
Zielinski, U.	AWI

